# CATALOG OF APOLLO 16 ROCKS

## Part 1. 60015 - 62315

## Graham Ryder and Marc D. Norman

(Lunar Curatorial Laboratory, Northrop Services, Inc.)

CATALOG OF APOLLO 16 ROCKS

GRAHAM RYDER AND MARC D. NORMAN
(Northrop Services, Inc.)

September, 1980

# TABLE OF CONTENTS

# INTRODUCTION

This catalog characterizes each of 543 individually numbered rock samples
in the Apollo 16 collection, showing what each sample is and what is known
about it. Regolith samples are not included. The catalog is intended to
be used by both researchers requiring sample allocations and a broad
audience interested in Apollo 16 rocks. The sample descriptions are
arranged in numerical order, closely corresponding to the sample collection
stations.

Information on sample collection, petrography, chemistry, stable and radio-
genic isotopes, surface characteristics, physical properties, and curatorial
processing is summarized and referenced as far as it is known. In many
cases we found it necessary to reinspect samples in the laboratory and have
new thin sections of several rocks cut. Our intention has been to be
comprehensive--we have attempted to include all published studies of any
kind which provide information on a sample, as well as some unpublished
information. Exceptions are made where the same research group published
the same data and conclusions in two journals, in which case one reference
(usually the earlier) is chosen; if one is the Proceedings of the Lunar
Science Conference, this reference is selected. We have rarely included
references which are primarily bulk interpretations of existing data (such
as mixing models) or mere lists of samples. The references are complete
to early 1980. Foreign language journals were not scrutinized, but as far
as we can tell little data has been published only in such journals.

Much valuable information exists in the original Apollo 16 Sample Information
Catalog (1972). However, that catalog was compiled and published only three
months after the mission itself, from rapid descriptions of usually dust-
covered rocks, usually without anything other than macroscopic observations,
less often thin sections, and rarely some chemical data. Since that time,
the rocks have been extensively studied, analyzed, and split, with numerous
published papers. These make the original catalog inadequate, outmoded, and
in some cases erroneous, providing the motivation for this revision. However,
The Apollo 16 Sample Information Catalog (1972) contains more information on
macroscopic observations for most samples than does the present volume.
Early catalogs were produced specifically for those rocks collected by
raking the regolith: LM area and Station 5 (Keil, Dowty, Prinz); Stations
1, 4, and 13 (Phinney and Lofgren); and Stations 11 and 8 (Smith and Steele).
These samples are included in the present catalog.

# ACKNOWLEDGMENTS

# ABBREVIATIONS

The following abbreviations have been used in this catalog:

ppl. : plane polarized light (i.e. transmitted light)
xpl. : crossed polarizers
rfl. : reflected light

JSC : Johnson Spacecraft Center
TSL : Thin Section Laboratory
TS  : Thin Section
PM  : Probe Mount
P.I. : Principal Investigator

ANT : Anorthosite-norite-troctolite suite of rocks; a catch-all acronym for rocks usually with granoblastic, poikiloblastic, or cumulate textures, but sometimes brecciated, and with low abundances of incompatible elements.
KREEP : acronym for rocks high in potassium, rare earth elements, and phosphorus, and usually lower in alumina than other highlands rocks. The light rare earths are enriched over heavy rare earths, and a conspicuous negative Eu anomaly is present.

# THE APOLLO 16 MISSION

The Apollo 16 mission (April 1972) to the Descartes landing site in the central lunar highlands was the only Apollo mission restricted to highlands terrain (Figures i,ii). Hence, samples from the site are of fundamental importance in the understanding of lunar crustal evolution. Approximately 95 kg of rocks, mainly feldspathic breccias, and soils were collected during three periods of extravehicular activity. Using the Lunar Roving Vehicle, astronauts John W. Young and Charles M. Duke covered over 20 km of traverses, and samples were collected from 10 different stations (Figure iii).

The mission had two prime sampling objectives: the Cayley Formation, an example of highland plains; and the Descartes Formation, a rugged, hilly, and furrowed terrain. The consensus of premission photogeological interpretation was that both units were of probable volcanic origin; however, it became apparent even during the mission that the samples were not volcanic but predominantly impact-produced feldspathic breccias. The landing site included a portion of the Cayley Plain and two areas of mountainous terrain: Stone Mountain to the south and Smokey Mountain to the north. Traverses were selected to sample 1) the Cayley Plains around the Lunar Module, 2) Descartes material on Stone Mountain, 3) blocky debris around the rim of North Ray Crater, a 1 km wide, 230 m deep crater which lies on the boundary between Smokey Mountain and the Plains, and 4) blocky material from a ray of the younger South Ray Crater, an almost 1 km wide crater in the Cayley Plains. The exploration strategy was to use impact craters of various diameters as stratigraphic probes.

The great majority of samples collected are feldspathic breccias of varied characteristics. They include specimens chipped from boulders up to tens of meters in size, individually collected hand samples, samples raked from the regolith, and samples picked from regolith samples in the laboratory. In all, more than 500 rocks have been individually numbered in addition to the many regolith samples collected. The largest rock collected (61016) is 11,729 g; the smallest include many samples less than 1 g. The samples include friable breccias, coherent breccias, and varied impact melts; many of the latter have clast-free or near clast-free ophitic textures and were almost completely molten during their formation. Glass, glassy breccias, and glass coatings on breccias are common. A significant group are the cataclastic anorthosites, nearly pure plagioclase and certainly shocked igneous cumulates from the early lunar crust.

The Apollo 16 samples confirm that the highlands crust is feldspathic and formed by a process involving plagioclase accumulation. The details of variation between sampling sites have not yet been fully worked out; the most obvious distinction is that samples, including soils, from the North Ray Crater area are more aluminous ($\sim$28-30 wt% $Al_2O_3$) than those from other areas (26-28 wt% $Al_2O_3$), and include more friable, fragmental, light-colored breccias. North Ray Crater and South Ray Crater are about 50 m.y. and 2 m.y. old respectively.
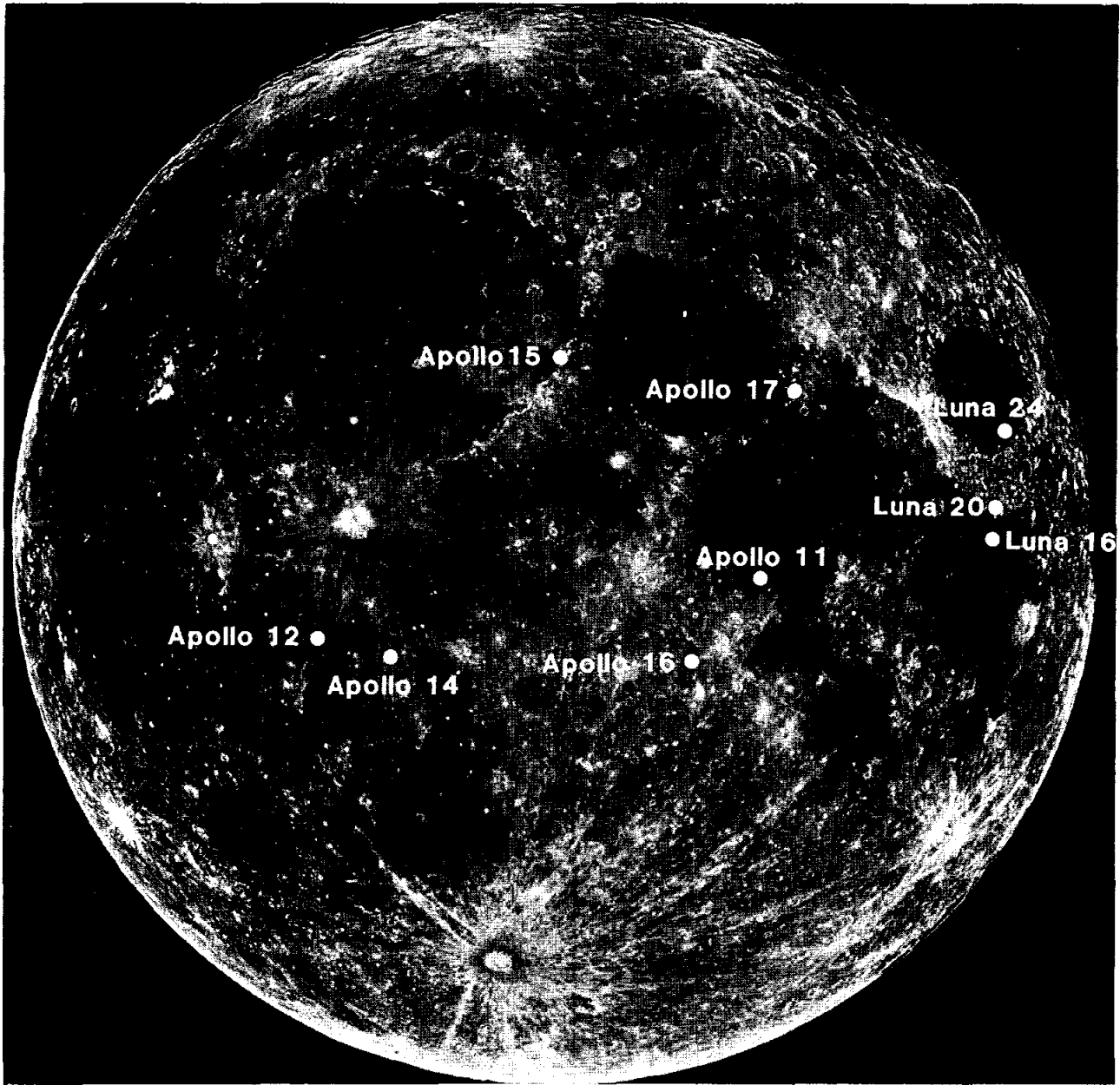
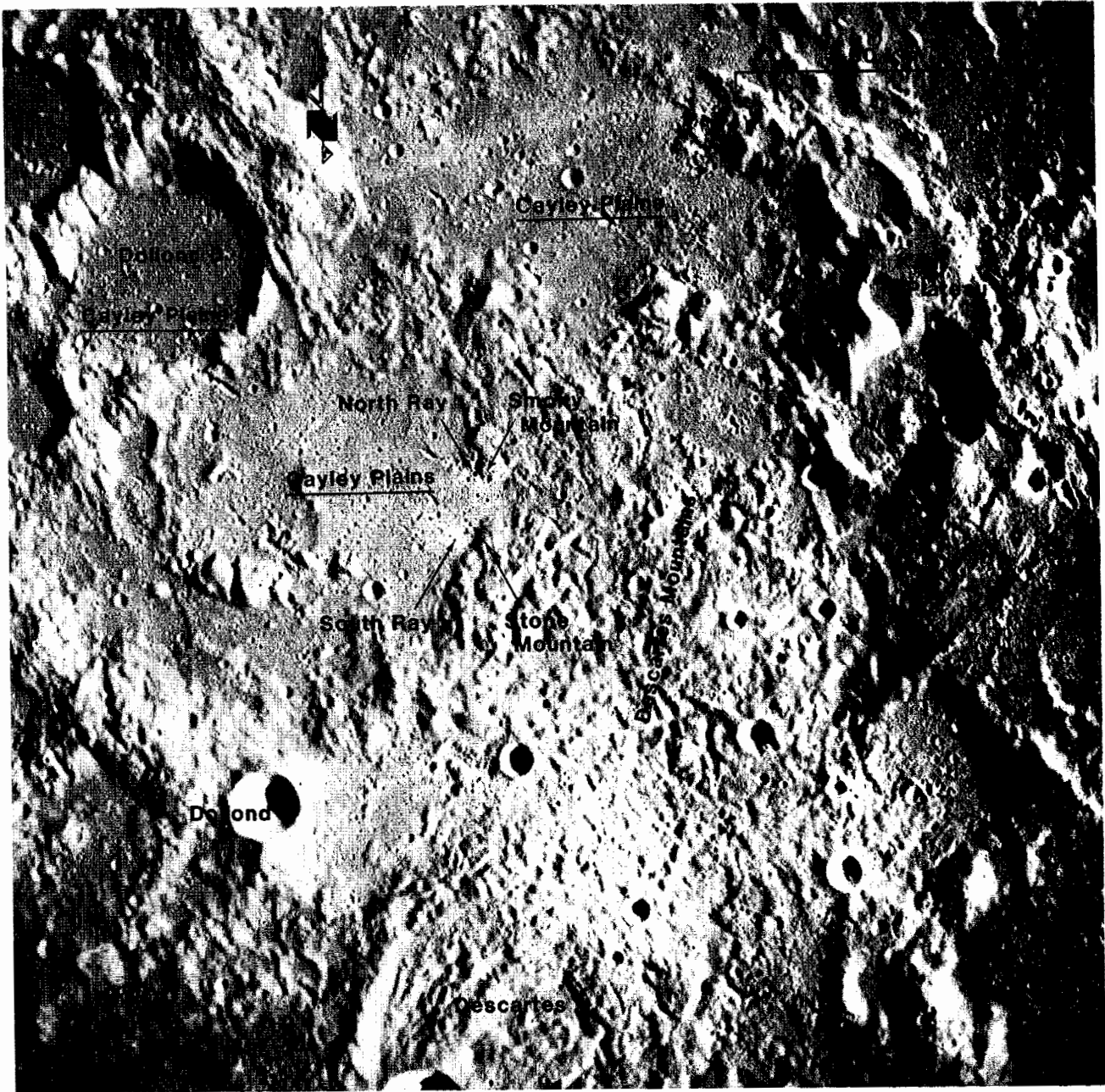Figure (i). Apollo and Luna sampling locations

Figure (ii).   Apollo 16 landing site area (Apollo 16 metric camera frame 439)

Figure (iii).   Apollo 16 traverses and sampling stations (Apollo 16 pan
                camera frame 4618)

References to detailed studies on the Apollo 16 samples are cited in the individual rock descriptions. The following list is a more general selected bibliography pertaining to the geological interpretation, and rock samples of the Apollo 16 landing site. The Proceeding of the Lunar Science Conferences, in particular the 4th, contain many other relevant papers.

AFGIT (Apollo Field Geology Investigation Team) (1973) Apollo 16 exploration of Descartes:  A geologic summary.  Science 179, 62-69.

AFGIT (in press) Geology of the Apollo 16 area, central lunar highlands (G.E. Ulrich, C.A. Hodges and W.R. Muehlberger, eds.).  U.S. Geol. Survey Open File Report No. 79-1091, 1128 pp.  (To be published as U.S. Survey Prof. Paper No. 1048).

Apollo 16 Preliminary Examination Team (1973) The Apollo 16 lunar samples: Petrographic and chemical description.  Science 179, 43-54.

Elston D.P., Boudette E.L., Schafer J.P., Muehlberger W.R. and Sevier J.R. (1972) Apollo 16 field trips.  Geotimes 17, 27-30.

Head J.W. (1974) Stratigraphy of the Descartes region (Apollo 16):  Implications for the origin of samples.  The Moon 11, 77-99.

Hinners N.W. (1972) Apollo 16 site selection.  Apollo 16 Prelim. Sci. Rep. NASA SP-315, p. 1-1.

Hodges C.A., Muehlberger W.R. and Ulrich G.E. (1973) Geologic setting of Apollo 16.  Proc. Lunar Sci. Conf. 4th, p. 1-25.

Hörz F., Carrier W.D., III, Young J.W., Duke C.M., Nagle J.S. and Fryxell R. (1972) Apollo 16 special samples.  Apollo 16 Prelim. Sci. Rep. NASA SP-315, p. 7-24 to 7-54.

LSAPT (Lunar Sample Analysis Planning Team) (1973) Fourth Lunar Science Conference.  Science 181, 615-622.

Milton D.J. (1968) Geologic map of the Theophilus Quadrangle of the Moon. U.S. Geol. Survey Misc. Geol. Inv. Map I-546 (LAC 78).

Milton D.J. and Hodges C.A. (1972) Geologic maps of the Descartes region of the Moon, Apollo 16 premission maps.  U.S. Geol. Survey Misc. Geol. Inv. Map I-748 (2 sheets).

Ulrich G.E. (1973) A geologic model for North Ray Crater and stratigraphic implications for the Descartes region.  Proc. Lunar Sci. Conf. 4th, p. 27-39.

Warner J.L., Simonds C.H., and Phinney W.C. (1973) Apollo 16 rocks:  Classification and petrogenetic model.  Proc. Lunar Sci. Conf. 4th, p. 481-504.

Wilshire H.G., Stuart-Alexander D.G., and Jackson E.D. (1973) Apollo 16 rocks: Petrology and classification.  J. Geophys. Res. 78, 2379-2392.

# NUMBERING OF APOLLO 16 SAMPLES

Five digit sample numbers were assigned each rock (coherent material greater than about 1 cm), the unsieved portion and each sieve fraction of scooped <1 cm material, the drill bit and each drill stem and drive tube section and each sample of special characteristic.  Rocks include samples chipped from boulders, individual hand samples, rake samples, and samples picked from regolith during laboratory processing.

The first digit (6) is the mission designation for Apollo 16 (previous missions used the first two digits).  The second digit indicates sampling site, as follows:

| Sampling Site | Initial Number |
|---|---|
| LM, ALSEP | 60000 |
| Stations 10 and 10 prime | 60000 |
| Station 1 | 61000 |
| Station 2 | 62000 |
| Station 4 | 64000 |
| Station 5 | 65000 |
| Station 6 | 66000 |
| Station 8 | 68000 |
| Station 9 | 69000 |
| Station 11 | 67000 |
| Station 13 | 63000 |

The only exceptions now known are 60017 which was collected at Station 13, and 61017 which could be from Station 2, not Station 1.

The first numbers for each area were used for drill stems, drive tubes, and special samples (surface samplers), with an omitted number to separate drive tube or drill stem strings.  (For example, at Station 9, 69001 is a single core tube and 69003 and 69004 are the two surface samplers.)  Drill stem sections and double drive tubes are numbered from the lower-most section upward.

The last digit denotes sample type.  Fines from a given documented bag are ascribed numbers according to:

| | |
|---|---|
| 6wxy0 | unsieved material (usually <1 cm) |
| 6wxy1 | <1 mm |
| 6wxy2 | 1-2 mm |
| 6wxy3 | 2-4 mm |
| 6wxy4 | 4-10 mm |

Rocks from a documented bag were numbered 6wxy5 - 6wxy9, usually in order of decreasing size.

Sample number decades were reserved for the contents of each documented bag. In the cases where the number of samples overflowed a decade the next available decade was used for the overflow. For example DB 11 contained soil, numbered 62280 - 62284, and 6 small rocks, numbered 62285 - 62289 and 62305.

Documented bags with predominantly soil samples were assigned even numbered decades and those with rock samples were assigned odd-numbered decades. The decades for rock samples usually only have an unsieved fines number for soil (adhering to the rock or scooped up with it) mixed in with any fragments that may have broken from the rock. For example, the 12 grams of soil and rock fragments in DB 362 are numbered 61130 and the 245 gram rock is 61135.

Paired soil and rake samples for each sampling area were assigned by centuries starting with 6x500. The soil sample documented bag has the first decade or decades of the century, in conformity with the last digit coding for rocks and fines (as explained above), and the rake sample documented bag uses the following decades. For example, 67700 - 67708 were used for the sieve fractions and four rocks from the soil sample in DB 388. Then for the companion rake sample in DB 423, 67710 - 67714 were used for the fractions of soil and the 32 >1 cm rake fragments were numbered 67715 - 67719, 67725 - 67729, ... , 67775, 67776.

As much as possible all samples returned loose in a sample collection bag or a sample return container were numbered in a decade. In the cases in which rocks from several stations were put into a single collection bag however, the soil and rock fragments were assigned a decade number that conforms to the site for the largest or most friable rock. The other rocks in the same bag have numbers for their own site, generally in the second or third decade of the thousand numbers for that site.

## APOLLO 16 ROCK SAMPLES: BASIC INVENTORY

The following pages are an inventory of all numbered Apollo 16 rock samples and are updated from the Apollo 16 Sample Information Catalog (1972); regolith and core samples are not included. Rock sample columns comprise the type of sample, its mass, a brief descriptive name, and the container (s) in which it was brought to earth.

Under SAMPLE TYPE, a blank indicates that the sample was an individually collected hand sample, in some cases chipped from boulders. An R indicates that the sample was collected with many others by raking the regolith. A P indicates that the sample was picked from a regolith sample during laboratory processing in Houston. Details on sample collection can be found in the Interagency Report: Astrogeology 51 (1972), the Apollo 16 Preliminary Science Report (1972), Bailey and Ulrich (1978), and AFGIT (in press).

The DESCRIPTION is not meant to be a formal classification nor to replace existing classifications. The descriptive names are not entirely mutually exclusive, because the categories are not precisely defined nor are all defined on similar bases, hence fail the criteria for formal classification. For samples for which thin sections have not been made the nature and genesis of a rock is far less well-known than for those for which thin sections do exist. Thus some of the rocks can be more specifically characterized than others, and this is partly reflected in the descriptive name. The descriptions contain few question marks, but actually in some cases are imprecise and may be altered following further study. The name given is not precisely the description given as the title line in the comprehensive descriptions in the main part of this catalog; the title line usually contains more information.

Early classifications of Apollo 16 rocks were given by Wilshire et al. (1973, and in AFGIT, in press) and Warner et al. (1973), and a general classification system for highlands rocks is presented and discussed by Stöffler et al. (1979, 1980).

The descriptive names used in the inventory are:

Basaltic impact melt: homogeneous, mainly subophitic to ophitic igneous texture, with clasts present in some but not all cases. Chemical data show meteoritic contamination.

Variolitic impact melt: homogeneous, igneous texture with radiating clusters of plagioclase, and interstitial glass and mafic minerals. Clasts are usually present, and chemical data show meteorite contamination.

Poikilitic impact melt: homogeneous, generally igneous texture with numerous tiny plagioclase grains embedded in larger oikocrysts of pyroxene (less commonly olivine). Interoikocryst areas contain ilmenite and glass. Clasts are usually conspicuous and more common than basaltic impact melts, and chemical data show meteorite contamination. (Some workers believe this texture to be metamorphic in origin).

The use of the above three terms usually requires that thin section study has been made. In cases where there is evidence that the sample is an impact melt and is not aphanitic, but the texture cannot be identified, we have used the more general term <u>crystalline impact melt</u>.

<u>Fine-grained impact melt</u>: numerous clasts in a seriate size distribution embedded in a fine-grained (<50 μm) melt matrix - the distinction between tiny clasts and the melt is usually difficult, but the melt includes laths of plagioclase and ilmenite.

<u>Glassy impact melt</u>: similar to the fine-grained impact melts but with more glass and larger laths of plagioclase.

The above two terms have been used for samples both with and without thin sections.

<u>Glass, cindery glass, glassy breccia</u>: these terms are used in a loose sense to split a gradational series, from near homogeneous glasses with few clasts through clearly polymict, clast-rich breccias with abundant glass in the matrix. The glassy impact melts are also gradational into this group; the distinction is that the glassy breccias may have several stages of glass production or distinct glass entities, whereas the glassy impact melts have glass produced in a single event. The glasses include both clear and devitrified glasses, and both spherical and irregular bodies.

<u>Fragmental polymict breccia</u>: polymict breccias characterized by angular, unequilibrated mineral and lithic clasts. They are mainly friable, although some are coherent and probably lightly sintered. They are a diverse group with variable colors and clast contents; most of the "light matrix breccias" in published studies are in this group.

<u>Coherent polymict breccia</u>: A catch-all phrase for mainly heterogeneous coherent polymict breccias with varied matrices from crystalline impact melt, to glassy, to those of unidentified character. Most of these are medium to dark gray in color.

<u>Dilithologic breccias</u>: Breccias which consist of two lithologies, one light-colored (cataclastic anorthosite or granoblastic material), the other dark-colored (usually fine-grained crystalline impact melt), generally referred to in published studies as "Black-and-White" breccias.

<u>Regolith breccia</u>: coherent to friable rocks which are lithified soils or at least contain abundant regolith-derived components such as glass beads, glass shards, and agglutuntic material; usually dark gray to brown.

<u>Friable regolith clod</u>: mainly disaggregated, often brown, clods which appear to have been loosely bound regolith.

<u>Cataclastic anorthosite</u>: near-monomineralic (plagioclase) rocks which are brecciated but commonly contain relict plagioclase grains a few millimeters across. If chemical or other data indicates a lack of meteoritic contamination the phrase <u>Pristine cataclastic anorthosite</u> is used. The modifiers <u>noritic</u> and <u>troctolitic</u> are also used.

Other sparsely-used descriptive names, for which explanation see the individual samples, are granoblastic anorthosite (60619), granoblastic troctolitic anorthosite (61577), poikiloblastic impactite (67955, 67746), granoblastic impactite (67566), and polymict granoblastic breccia (60035). They consist largely of materials with clearly metamorphic textures. Such lithic types are fairly common as smaller clasts in other polymict breccias. One sample (61576) is probably a single plagioclase crystal, and one sample (67667) is a pristine feldspathic lherzolite.

Finally, some of the descriptive names are combined forms (e.g. glassy impact melt/breccia) where two lithologies are conspicuous, and the prefix "meta-" is used in a few cases where a dominantly igneous texture has been modified by subsequent thermal effects.

The SAMPLE CONTAINER acronyms are:

| | |
|---|---|
| DB | Documented bag |
| PDB | Padded documented bag |
| SCB | Sample collection bag |
| SRC | Sample return container |

Further details of sample containers can be found in the Interagency Report: Astrogeology 51 (1972), and the Apollo 16 Sample Information Catalog (1972).

References Cited:

AFGIT (in press) Geology of the Apollo 16 area, central lunar highlands (G. E. Ulrich, C. A. Hodges and W. R. Muehlberger, eds.). U. S. Geol. Survey Open File Report No. 79-1091. 1128 pp. (To be published as U. S. Geol. Survey Prof. Paper No. 1048).

Apollo 16 Lunar Sample Information Catalog (1972). MSC 03210. Manned Spacecraft Center, Houston. 372 pp.

Apollo 16 Preliminary Science Report (1972). NASA SP-315. National Aeronautics and Space Administration, Washington, D.C.

Bailey N. G. and Ulrich G. E. (1975) Apollo 16 Voice Transcript. USGS-GD-74-030. United States Geological Survey, Flagstaff. 323 pp.

Interagency Report: Astrogeology 51 (1972) Prepared by the Geological Survey for the National Aeronautics and Space Administration. 252 pp.

Stöffler D., Knoll H.-D., Maerz U. (1979) Terrestrial and lunar impact breccias and the classification of lunar highlands rocks. Proc. Lunar Planet. Sci. Conf. 10th, p. 639-675.

Stöffler D., Knoll H.-D., Marvin U. B., Simonds C. H., and Warren P. H. (1980) Recommended classification and nomenclature of lunar highland rocks - a committee report. Proc. of the Conference on the Lunar Highlands Crust p. 51-70.

Warner J. L., Simonds C. H., and Phinney W. C. (1973) Apollo 16 rocks: Classification and petrogenetic model. _Proc. Lunar Sci. Conf. 4th_, p. 481-504.

Wilshire H. G., Stuart-Alexander D. G. and Jackson E. D. (1973) Apollo 16 rocks: Petrology and classification. _J. Geophys. Res. 78_, 2379-2392.

# APOLLO 16 ROCK INVENTORY

| SAMPLE NUMBER | SAMPLE TYPE | MASS g | DESCRIPTION * | SRC/DB OR SCB/DB |
|---|---|---|---|---|
| 60015 | | 5574.0 | Pristine cataclastic anorthosite (G) | SCB5/ |
| 60016 | | 4307.0 | Fragmental polymict breccia | SCB7/ |
| 60017 | | 2102.0 | Variolitic impact melt/breccia | SCB7/ |
| 60018 | | 1501.0 | Basaltic impact melt (G) | SCB7/ |
| 60019 | | 1887.0 | Glassy (regolith?) breccia (G) | SCB4/ |
| 60025 | | 1836.0 | Pristine cataclastic anorthosite (G) | SCB3/ |
| 60035 | | 1052.0 | Polymict granoblastic breccia (G) | SRC1/351 |
| 60055 | | 35.48 | Pristine cataclastic anorthosite | SRC1/355 |
| 60056 | | 16.07 | Cataclastic anorthosite (G) | SRC1/355 |
| 60057 | | 3.10 | Cataclastic anorthosite | SRC1/355 |
| 60058 | | 2.12 | Fragmental polymict breccia | SRC1/355 |
| 60059 | | 1.05 | Cataclastic anorthosite | SRC1/355 |
| 60075 | | 183.8 | Fragmental polymict breccia | SRC1/373 |
| 60095 | | 46.60 | Glass | SCB1/004 |
| 60115 | | 132.5 | Glassy breccia | SCB1/381 |
| 60135 | | 137.7 | Cataclastic anorthosite (G) | SCB6/430 |
| 60215 | | 385.8 | Pristine cataclastic anorthosite (G) | SCB6/13 |
| 60235 | | 70.13 | Basaltic impact melt | SCB6/15 |
| 60255 | | 871.0 | Regolith breccia (G) | SCB6/17 |
| 60275 | | 255.2 | Glassy breccia (regolith?) (G) | SCB7/18 |
| 60315 | | 787.7 | Poikilitic impact melt | SCB7/20 |
| 60335 | | 317.8 | Basaltic impact melt | SCB6/331 |
| 60515 | R | 16.74 | Cataclastic anorthosite | SCB4/349 |
| 60516 | R | 7.91 | Cataclastic anorthosite | SCB4/349 |
| 60517 | R | 1.23 | Cataclastic anorthosite | SCB4/349 |
| 60518 | R | 1.12 | Cataclastic anorthosite | SCB4/349 |
| 60519 | R | .50 | Cataclastic anorthosite | SCB4/349 |
| 60525 | R | 12.84 | Poikilitic impact melt | SCB4/349 |
| 60526 | R | 8.42 | Poikilitic impact melt | SCB4/349 |
| 60527 | R | 7.36 | Crystalline polymict breccia/glass(G) | SCB4/349 |
| 60528 | R | 2.94 | Glassy impact melt | SCB4/349 |
| 60529 | R | 1.24 | Basaltic impact melt | SCB4/349 |

* A (G) following the descriptive name indicates that the rock is at least partly coated with glass.

| SAMPLE NUMBER | SAMPLE TYPE | MASS g | DESCRIPTION | SRC/DB OR SCB/DB |
|---|---|---|---|---|
| 60535 | R | 7.23 | Fragmental polymict (regolith?) breccia (G) | SCB4/349 |
| 60615 | R | 32.97 | Basaltic impact melt (G) | SCB4/347 |
| 60616 | R | 3.40 | Poikilitic impact melt | SCB4/347 |
| 60617 | R | 2.77 | Crystalline impact melt (G) | SCB4/347 |
| 60618 | R | 21.67 | Basaltic impact melt/anorthosite | SCB4/347 |
| 60619 | R | 28.00 | Granoblastic anorthosite (G) | SCB4/347 |
| 60625 | R | 117.00 | Poikilitic impact melt | SCB4/347 |
| 60626 | R | 15.87 | Poikilitic impact melt | SCB4/347 |
| 60627 | R | 12.09 | Crystalline impact melt (G) | SCB4/347 |
| 60628 | R | 6.86 | Cataclastic anorthosite (G) | SCB4/347 |
| 60629 | R | 4.92 | Cataclastic anorthosite (G) | SCB4/347 |
| 60635 | R | 15.05 | Basaltic impact melt | SCB4/347 |
| 60636 | R | 35.65 | Basaltic/poikilitic impact melt (G) | SCB4/347 |
| 60637 | R | 7.98 | Fragmental polymict (regolith?) breccia | SCB4/347 |
| 60638 | R | .72 | Fragmental polymict breccia | SCB4/347 |
| 60639 | R | 175.1 | Fragmental polymict breccia (G) | SCB4/347 |
| 60645 | R | 33.5 | Fine-grained impact melt | SCB4/347 |
| 60646 | R | 3.39 | Fine-grained impact melt | SCB4/347 |
| 60647 | R | 1.76 | Glassy impact melt | SCB4/347 |
| 60648 | R | 2.84 | Glassy breccia | SCB4/347 |
| 60649 | R | 1.03 | Glassy breccia | SCB4/347 |
| 60655 | R | 8.63 | Glassy impact melt | SCB4/347 |
| 60656 | R | 11.23 | Glassy impact melt | SCB4/347 |
| 60657 | R | 6.05 | Fragmental polymict breccia (G) | SCB4/347 |
| 60658 | R | 5.47 | Glassy impact melt (G) | SCB4/347 |
| 60659 | R | 22.20 | Fragmental polymict breccia | SCB4/347 |
| 60665 | R | 90.1 | Glass | SCB4/347 |
| 60666 | R | 15.95 | Glassy impact melt | SCB4/347 |
| 60667 | R | 7.66 | Glassy/basaltic impact melt (G) | SCB4/347 |
| 60668 | R | 2.91 | Glassy impact melt | SCB4/347 |
| 60669 | R | 2.54 | Glass | SCB4/347 |
| 60675 | R | 1.30 | Fine-grained impact melt | SCB4/347 |
| 60676 | R | 8.92 | Glassy impact melt | SCB4/347 |
| 60677 | R | 5.23 | Glassy breccia | SCB4/347 |
| 60678 | R | 1.25 | Glassy impact melt | SCB4/347 |
| 60679 | R | 2.96 | Glassy impact melt | SCB4/347 |
| 61015 | | 1804.0 | Dilithologic breccia (G) | SRC1 |
| 61016 | | 11729.0 | Basaltic impact melt/pristine anorthosite (G) | BSLSS |
| 61017 | | 2.62 | Cataclastic anorthosite | SRC1/ |
| 61135 | | 245.1 | Fragmental polymict breccia | SRC1/362 |

| SAMPLE NUMBER | SAMPLE TYPE | MASS g | DESCRIPTION | SRC/DB OR SCB/DB |
|---|---|---|---|---|
| 61155 | | 47.59 | Glassy impact melt | SRC1/371 |
| 61156 | | 58.46 | Meta-poikilitic impact melt | SRC1/371 |
| 61157 | | 11.26 | Fragmental polymict breccia | SRC1/371 |
| 61158 | | 14.79 | Fragmental polymict breccia | SRC1/371 |
| 61175 | | 542.7 | Fragmental polymict breccia | SRC1/364 |
| 61195 | | 587.9 | Regolith breccia (G) | SRC1/002 |
| 61225 | | 3.52 | Crystalline impact melt | SRC1/357 |
| 61226 | | 1.53 | Cataclastic anorthosite (G) | SRC1/357 |
| 61245 | | 8.25 | Fine-grained impact melt | SRC1/352 |
| 61246 | | 6.05 | Fine-grained impact melt | SRC1/352 |
| 61247 | | 2.48 | Poikilitic impact melt | SRC1/352 |
| 61248 | | 1.71 | Fragmental polymict breccia | SRC1/352 |
| 61249 | | 1.17 | Basaltic impact melt | SRC1/352 |
| 61255 | | 1.13 | Cindery glass | SRC1/352 |
| 61295 | | 187.00 | Regolith breccia | SRC1/353 |
| 61505 | P | 1.651 | Fine-grained impact melt | SRC1/354 |
| 61515 | R | 2.00 | Fragmental polymict breccia | SRC1/372 |
| 61516 | R | 2.38 | Fragmental polymict breccia | SRC1/372 |
| 61517 | R | .47 | Fragmental polymict breccia | SRC1/372 |
| 61518 | R | .16 | Fragmental polymict breccia | SRC1/372 |
| 61519 | R | .33 | Fragmental polymict breccia | SRC1/372 |
| 61525 | R | 10.35 | Glassy breccia | SRC1/372 |
| 61526 | R | 4.08 | Fragmental polymict breccia | SRC1/372 |
| 61527 | R | .52 | Fragmental polymict breccia | SRC1/372 |
| 61528 | R | .24 | Fragmental polymict breccia (G) | SRC1/372 |
| 61529 | R | .28 | Fragmental polymict breccia | SRC1/372 |
| 61535 | R | .23 | Fragmental polymict breccia (G) | SRC1/372 |
| 61536 | R | 85.99 | Glassy breccia (G) | SRC1/372 |
| 61537 | R | 6.62 | Fragmental polymict breccia (G) | SRC1/372 |
| 61538 | R | 4.76 | Fragmental polymict breccia (G) | SRC1/372 |
| 61539 | R | 5.78 | Glassy breccia | SRC1/372 |
| 61545 | R | 3.61 | Fragmental polymict breccia (G) | SRC1/372 |
| 61546 | R | 110.7 | Glassy impact melt | SRC1/372 |
| 61547 | R | 17.93 | Basaltic impact melt (G?) | SRC1/372 |
| 61548 | R | 24.18 | Glassy impact melt | SRC1/372 |
| 61549 | R | 3.76 | Basaltic/poikilitic impact melt | SRC1/372 |

| SAMPLE NUMBER | SAMPLE TYPE | MASS g | DESCRIPTION | SRC/DB OR SCB/DB |
|---|---|---|---|---|
| 61555 | R | 3.46 | Glassy impact melt | SRC1/372 |
| 61556 | R | 2.23 | Glass | SRC1/372 |
| 61557 | R | .93 | Glassy impact melt | SRC1/372 |
| 61558 | R | 3.00 | Glass | SRC1/372 |
| 61559 | R | .62 | Glassy breccia | SRC1/372 |
| 61565 | R | .88 | Glassy breccia | SRC1/372 |
| 61566 | R | .66 | Glassy impact melt | SRC1/372 |
| 61567 | R | .19 | Glassy impact melt | SRC1/372 |
| 61568 | R | 19.32 | Basaltic/poikilitic impact melt | SRC1/372 |
| 61569 | R | 12.02 | Poikilitic impact melt | SRC1/372 |
| 61575 | R | 5.26 | Crystalline impact melt | SRC1/372 |
| 61576 | R | 5.87 | Plagioclase crystal (G) | SRC1/372 |
| 61577 | R | .21 | Granoblastic troctolitic anorthosite (G) | SRC1/372 |
| 62235 | | 319.6 | Poikilitic impact melt | SRC1/005 |
| 62236 | | 57.27 | Pristine noritic anorthosite | SRC1/005 |
| 62237 | | 62.35 | Pristine troctolitic anorthosite | SRC1/005 |
| 62238 | | 1.565 | Cataclastic anorthosite | SRC1/005 |
| 62245 | P | 6.03 | Crystalline impact melt | SRC1/006 |
| 62246 | P | 4.59 | Cataclastic anorthosite (G) | SRC1/006 |
| 62247 | P | 2.11 | Fragmental polymict breccia | SRC1/006 |
| 62248 | P | 1.61 | Fragmental polymict breccia (G) | SRC1/006 |
| 62249 | P | 1.41 | Fragmental polymict breccia | SRC1/006 |
| 62255 | | 1239.0 | Dilithologic breccia (G) | SRC1/007 |
| 62275 | | 443.0 | Cataclastic anorthosite | SRC1/009 |
| 62285 | P | 3.524 | Friable regolith clod | SRC1/011 |
| 62286 | P | 2.917 | Friable regolith clod | SRC1/011 |
| 62287 | P | 2.474 | Fine-grained impact melt | SRC1/011 |
| 62288 | P | 1.939 | Fragmental or crystalline polymict breccia | SRC1/011 |
| 62289 | P | 1.135 | Friable regolith clod | SRC1/011 |
| 62295 | | 250.8 | Basaltic impact melt | SRC1/010 |
| 62305 | P | .810 | Fragmental polymict breccia | SRC1/011 |
| 62315 | P | .77 | Fragmental polymict breccia | SRC1/006 |
| 63335 | | 65.4 | Fine-grained impact melt/breccia | SCB6/428 |
| 63355 | | 68.24 | Poikilitic impact melt | SCB6/429 |

| SAMPLE NUMBER | SAMPLE TYPE | MASS g | DESCRIPTION | SRC/DB OR SCB/DB |
|---|---|---|---|---|
| 63505 | P | 5.41 | Fine-grained impact melt | SCB4/346 |
| 63506 | P | 4.9 | Basaltic impact melt | SCB4/346 |
| 63507 | P | 2.78 | Fragmental regolith breccia (G) | SCB4/346 |
| 63508 | P | 2.61 | Fine-grained impact melt | SCB4/346 |
| 63509 | P | 2.05 | Fine-grained impact melt | SCB4/346 |
| 63515 | P | 1.32 | Fine-grained impact melt | SCB4/346 |
| 63525 | R | 6.68 | Fine-grained impact melt | SCB4/345 |
| 63526 | R | 2.91 | Fine-grained impact melt | SCB4/345 |
| 63527 | R | 6.10 | Basaltic impact melt (mafic) | SCB4/345 |
| 63528 | R | 4.12 | Fine-grained impact melt | SCB4/345 |
| 63529 | R | 23.48 | Fine-grained impact melt | SCB4/345 |
| 63535 | R | 6.85 | Basaltic impact melt | SCB4/345 |
| 63536 | R | 1.02 | Basaltic impact melt | SCB4/345 |
| 63537 | R | 4.78 | Basaltic impact melt | SCB4/345 |
| 63538 | R | 35.06 | Fine-grained impact melt/glass | SCB4/345 |
| 63539 | R | .39 | Fine-grained impact melt | SCB4/345 |
| 63545 | R | 15.95 | Basaltic impact melt | SCB4/345 |
| 63546 | R | 9.23 | Fine-grained impact melt | SCB4/345 |
| 63547 | R | 4.90 | Poikilitic impact melt | SCB4/345 |
| 63548 | R | 1.13 | Fine-grained impact melt | SCB4/345 |
| 63549 | R | 26.57 | Basaltic impact melt | SCB4/345 |
| 63555 | R | 3.38 | Fine-grained impact melt | SCB4/345 |
| 63556 | R | 18.10 | Poikilitic impact melt | SCB4/345 |
| 63557 | R | 7.53 | Fine-grained impact melt | SCB4/345 |
| 63558 | R | 7.09 | Poikilitic impact melt | SCB4/345 |
| 63559 | R | 6.04 | Glass | SCB4/345 |
| 63565 | R | .94 | Glass | SCB4/345 |
| 63566 | R | 19.61 | Glass | SCB4/345 |
| 63567 | R | 3.21 | Glass | SCB4/345 |
| 63568 | R | 4.06 | Glass | SCB4/345 |
| 63569 | R | .43 | Glass | SCB4/345 |
| 63575 | R | 4.72 | Glass | SCB4/345 |
| 63576 | R | 1.23 | Glass | SCB4/345 |
| 63577 | R | 12.41 | Crystalline polymict breccia | SCB4/345 |
| 63578 | R | 19.60 | Glassy/fine-grained impact melt breccia | SCB4/345 |
| 63579 | R | 11.35 | Fine-grained impact melt | SCB4/345 |
| 63585 | R | 32.62 | Basaltic/poikilitic impact melt | SCB4/345 |
| 63586 | R | 1.98 | Fine-grained impact melt | SCB4/345 |
| 63587 | R | 20.51 | Poikilitic impact melt | SCB4/345 |
| 63588 | R | 2.40 | Fragmental polymict breccia | SCB4/345 |
| 63589 | R | 13.51 | Fragmental polymict breccia | SCB4/345 |

| SAMPLE NUMBER | SAMPLE TYPE | MASS g | DESCRIPTION | SRC/DB OR SCB/DB |
|---|---|---|---|---|
| 63595 | R | 2.10 | Fragmental polymict breccia | SCB4/345 |
| 63596 | R | 6.40 | Poikilitic impact melt | SCB4/345 |
| 63597 | R | 5.67 | Poikilitic impact melt | SCB4/345 |
| 63598 | R | 12.66 | Poikilitic impact melt | SCB4/345 |
| 64425 | | 14.62 | Dilithologic breccia | SCB3/399 |
| 64435 | | 1079.0 | Fine-grained impact melt (G) | SCB1/394 |
| 64455 | | 56.68 | Basaltic impact melt (G) | SCB3/397 |
| 64475 | | 1032.0 | Dilithologic breccia | SCB3/398 |
| 64476 | | 125.1 | Dilithologic breccia | SCB3/398 |
| 64477 | | 19.32 | Glassy breccia | SCB3/398 |
| 64478 | | 12.34 | Poikilitic impact melt (G) | SCB3/398 |
| 64505 | P | 5.392 | Fragmental polymict breccia | SCB1/396 |
| 64506 | P | 5.079 | Basaltic impact melt (G) | SCB1/396 |
| 64507 | P | 4.474 | Dilithologic breccia | SCB1/396 |
| 64508 | P | 4.168 | Dilithologic breccia | SCB1/396 |
| 64509 | P | 3.150 | Fragmental polymict breccia | SCB1/396 |
| 64515 | P | 3.761 | Basaltic impact melt | SCB1/396 |
| 64516 | P | 2.929 | Cataclastic anorthosite | SCB1/396 |
| 64517 | P | 1.546 | Crystalline polymict breccia | SCB1/396 |
| 64518 | P | 1.490 | Fine-grained impact melt | SCB1/396 |
| 64519 | P | 1.124 | Cataclastic anorthosite | SCB1/396 |
| 64525 | P | 1.107 | Cataclastic anorthosite | SCB1/396 |
| 64535 | R | 256.6 | Dilithologic breccia | SCB1/395 |
| 64536 | R | 177.5 | Dilithologic breccia | SCB1/395 |
| 64537 | R | 124.3 | Dilithologic breccia | SCB1/395 |
| 64538 | R | 30.03 | Polylithologic breccia | SCB1/395 |
| 64539 | R | 17.76 | Dilithologic breccia | SCB1/395 |
| 64545 | R | 14.09 | Dilithologic breccia | SCB1/395 |
| 64546 | R | 12.80 | Dilithologic breccia | SCB1/395 |
| 64547 | R | 10.90 | Fragmental polymict or dilithologic breccia | SCB1/395 |
| 64548 | R | 8.49 | Dilithologic breccia | SCB1/395 |
| 64549 | R | 6.47 | Dilithologic breccia | SCB1/395 |
| 64555 | R | 5.29 | Fragmental dilithologic breccia | SCB1/395 |
| 64556 | R | 5.15 | Dilithologic or polymict breccia | SCB1/395 |
| 64557 | R | 4.790 | Fine-grained impact melt | SCB1/395 |
| 64558 | R | 3.130 | Dilithologic breccia | SCB1/395 |
| 64559 | R | 21.82 | Basaltic impact melt | SCB1/395 |

| SAMPLE NUMBER | SAMPLE TYPE | MASS g | DESCRIPTION | SRC/DB OR SCB/DB |
|---|---|---|---|---|
| 64565 | R | 14.73 | Glassy impact melt | SCB1/395 |
| 64566 | R | 14.13 | Fine-grained impact melt | SCB1/395 |
| 64567 | R | 13.86 | Poikilitic impact melt | SCB1/395 |
| 64568 | R | 9.379 | Poikilitic impact melt | SCB1/395 |
| 64569 | R | 14.32 | Poikilitic impact melt | SCB1/395 |
| 64575 | R | 6.837 | Poikilitic impact melt | SCB1/395 |
| 64576 | R | 6.916 | Basaltic impact melt | SCB1/395 |
| 64577 | R | 5.692 | Glassy breccia | SCB1/395 |
| 64578 | R | 5.596 | Fine-grained impact melt (G) | SCB1/395 |
| 64579 | R | 4.802 | Fine-grained impact melt | SCB1/395 |
| 64585 | R | 4.696 | Basaltic/poikilitic impact melt | SCB1/395 |
| 64586 | R | 3.337 | Fine-grained impact melt (G) | SCB1/395 |
| 64587 | R | 7.180 | Fragmental polymict breccia (G) | SCB1/395 |
| 64588 | R | 2.546 | Fragmental polymict breccia | SCB1/395 |
| 64589 | R | 4.039 | Cataclastic anorthosite | SCB1/395 |
| 64815 | R | 20.90 | Meta-poikilitic impact melt | SCB3/401 |
| 64816 | R | 3.83 | Poikilitic impact melt | SCB3/401 |
| 64817 | R | 8.98 | Basaltic impact melt | SCB3/401 |
| 64818 | R | 15.98 | Dilithologic breccia | SCB3/401 |
| 64819 | R | 11.76 | Pristine cataclastic anorthosite(G) | SCB3/401 |
| 64825 | R | 21.50 | Fragmental polymict breccia | SCB3/401 |
| 64826 | R | 11.33 | Fragmental polymict breccia | SCB3/401 |
| 64827 | R | 8.11 | Fragmental polymict breccia | SCB3/401 |
| 64828 | R | .97 | Fragmental polymict breccia | SCB3/401 |
| 64829 | R | 2.20 | Fragmental polymict breccia | SCB3/401 |
| 64835 | R | 2.32 | Fragmental polymict breccia | SCB3/401 |
| 64836 | R | 1.76 | Fragmental polymict breccia | SCB3/401 |
| 64837 | R | 2.18 | Fragmental polymict breccia (G) | SCB3/401 |
| 65015 | | 1802.0 | Poikilitic impact melt | SCB3/ |
| 65016 | | 21.02 | Glass | SCB1/ |
| 65035 | | 446.1 | Cataclastic anorthosite (G) | SCB1/404 |
| 65055 | | 500.8 | Basaltic impact melt | SCB3/337 |
| 65056 | | 64.78 | Variolitic impact melt | SCB3/337 |
| 65075 | | 107.9 | Basaltic impact melt (G) | SCB1/403 |
| 65095 | | 560.1 | Fragmental polymict (regolith?) breccia (G) | SCB3/336 |
| 65315 | | 300.4 | Pristine cataclastic anorthosite (G) | SCB1/405 |

| SAMPLE NUMBER | SAMPLE TYPE | MASS g | DESCRIPTION | SRC/DB OR SCB/DB |
|---|---|---|---|---|
| 65325 | R | 67.87 | Pristine cataclastic anorthosite (G) | SCB1/405 |
| 65326 | R | 36.40 | Cataclastic anorthosite | SCB1/405 |
| 65327 | R | 6.97 | Pristine cataclastic anorthosite (G) | SCB1/405 |
| 65328 | R | 1.28 | Cataclastic anorthosite (G) | SCB1/405 |
| 65329 | R | 1.92 | Cataclastic anorthosite | SCB1/405 |
| 65335 | R | 1.63 | Cataclastic anorthosite | SCB1/405 |
| 65336 | R | .60 | Cataclastic anorthosite (G) | SCB1/405 |
| 65337 | R | 11.57 | Fragmental polymict breccia | SCB1/405 |
| 65338 | R | 2.65 | Fragmental polymict breccia | SCB1/405 |
| 65339 | R | 1.62 | Fragmental polymict breccia | SCB1/405 |
| 65345 | R | .86 | Fragmental polymict breccia | SCB1/405 |
| 65346 | R | .80 | Fragmental polymict breccia | SCB1/405 |
| 65347 | R | .43 | Fragmental polymict breccia | SCB1/405 |
| 65348 | R | 11.66 | Glass | SCB1/405 |
| 65349 | R | 7.58 | Glassy impact melt | SCB1/405 |
| 65355 | R | 4.94 | Glassy impact melt | SCB1/405 |
| 65356 | R | 2.53 | Glassy impact melt | SCB1/405 |
| 65357 | R | 18.76 | Poikilitic impact melt | SCB1/405 |
| 65358 | R | 7.02 | Poikilitic impact melt | SCB1/405 |
| 65359 | R | 2.53 | Fragmental polymict breccia (G) | SCB1/405 |
| 65365 | R | 2.16 | Poikilitic impact melt | SCB1/405 |
| 65366 | R | 8.48 | Glass | SCB1/405 |
| 65515 | R | 50.25 | Fragmental polymict breccia (regolith clod) | SRC2/332 |
| 65516 | R | 10.49 | Fragmental polymict breccia (regolith clod) | SRC2/332 |
| 65517 | R | 11.85 | Fragmental polymict breccia (regolith clod) | SRC2/332 |
| 65518 | R | 9.477 | Fragmental polymict breccia (regolith clod) | SRC2/332 |
| 65519 | R | 10.58 | Fragmental polymict breccia (regolith clod) | SRC2/332 |
| 65525 | R | 7.483 | Fragmental polymict breccia (regolith clod) | SRC2/332 |
| 65526 | R | 3.545 | Fragmental polymict breccia (regolith clod) | SRC2/332 |
| 65527 | R | 2.890 | Fragmental polymict breccia (regolith clod) | SRC2/332 |
| 65528 | R | 3.082 | Fragmental polymict breccia (regolith clod) | SRC2/332 |
| 65529 | R | 2.555 | Fragmental polymict breccia (regolith clod) | SRC2/332 |

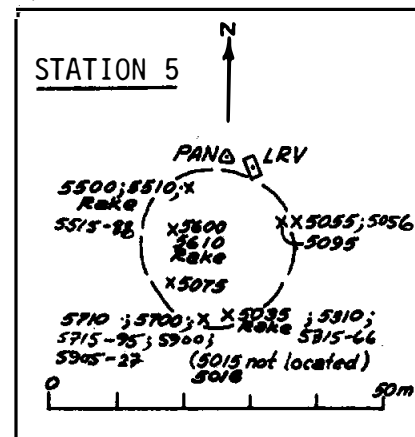| SAMPLE NUMBER | SAMPLE TYPE | MASS g | DESCRIPTION | SRC/DB OR SCB/DB |
|---|---|---|---|---|
| 65535 | R | 2.658 | Fragmental polymict breccia (regolith clod) | SRC2/332 |
| 65536 | R | 1.575 | Fragmental polymict breccia (regolith clod) | SRC2/332 |
| 65537 | R | 2.426 | Fragmental polymict breccia (regolith clod) | SRC2/332 |
| 65538 | R | 2.342 | Fragmental polymict breccia (regolith clod) | SRC2/332 |
| 65539 | R | 2.180 | Fragmental polymict breccia (regolith clod) | SRC2/332 |
| 65545 | R | 1.797 | Fragmental polymict breccia (regolith clod) | SRC2/332 |
| 65546 | R | 1.346 | Fragmental polymict breccia (regolith clod) | SRC2/332 |
| 65547 | R | 1.587 | Fragmental polymict breccia (regolith clod) | SRC2/332 |
| 65548 | R | 3.023 | Fragmental polymict breccia (regolith clod) | SRC2/332 |
| 65549 | R | 2.094 | Fragmental polymict breccia (regolith clod) | SRC2/332 |
| 65555 | R | 2.202 | Fragmental polymict breccia (regolith clod) | SRC2/332 |
| 65556 | R | 1.170 | Fragmental polymict breccia (regolith clod) | SRC2/332 |
| 65557 | R | 1.114 | Fragmental polymict breccia (regolith clod) | SRC2/332 |
| 65558 | R | 1.695 | Fragmental polymict breccia (regolith clod) | SRC2/332 |
| 65559 | R | 1.533 | Fragmental polymict breccia (regolith clod) | SRC2/332 |
| 65565 | R | .852 | Fragmental polymict breccia (regolith clod) | SRC2/332 |
| 65566 | R | 1.998 | Fragmental polymict breccia (regolith clod) | SRC2/332 |
| 65567 | R | 1.289 | Fragmental polymict breccia (regolith clod) | SRC2/332 |
| 65568 | R | .808 | Fragmental polymict breccia (regolith clod) | SRC2/332 |
| 65569 | R | .873 | Fragmental polymict breccia (regolith clod) | SRC2/332 |

| SAMPLE NUMBER | SAMPLE TYPE | MASS g | DESCRIPTION | SRC/DB OR SCB/DB |
|---|---|---|---|---|
| 65575 | R | .907 | Fragmental polymict breccia (regolith clod) | SRC2/332 |
| 65576 | R | .906 | Fragmental polymict breccia (regolith clod) | SRC2/332 |
| 65577 | R | .706 | Fragmental polymict breccia (regolith clod) | SRC2/332 |
| 65578 | R | .320 | Fragmental polymict breccia (regolith clod) | SRC2/332 |
| 65579 | R | .612 | Fragmental polymict breccia (regolith clod) | SRC2/332 |
| 65585 | R | 9.294 | Cindery glass | SRC2/332 |
| 65586 | R | 6.763 | Fragmental polymict breccia (regolith clod) (G) | SRC2/332 |
| 65587 | R | 2.141 | Fragmental polymict breccia (regolith clod) (G) | SRC2/332 |
| 65588 | R | 9.629 | Fragmental polymict breccia | SRC2/332 |
| 65715 | R | 31.36 | Fragmental polymict breccia | SCB1/334 |
| 65716 | R | 14.28 | Fragmental polymict breccia | SCB1/334 |
| 65717 | R | 7.415 | Fragmental polymict breccia | SCB1/334 |
| 65718 | R | 10.61 | Fragmental polymict breccia | SCB1/334 |
| 65719 | R | 7.04 | Fragmental polymict breccia | SCB1/334 |
| 65725 | R | 6.67 | Fragmental polymict breccia | SCB1/334 |
| 65726 | R | 5.19 | Fragmental polymict breccia | SCB1/334 |
| 65727 | R | 4.30 | Fragmental polymict breccia | SCB1/334 |
| 65728 | R | 4.22 | Fragmental polymict breccia | SCB1/334 |
| 65729 | R | 3.81 | Fragmental polymict breccia | SCB1/334 |
| 65735 | R | 4.26 | Fragmental polymict breccia | SCB1/334 |
| 65736 | R | 2.74 | Fragmental polymict breccia | SCB1/334 |
| 65737 | R | .85 | Fragmental polymict breccia | SCB1/334 |
| 65738 | R | 1.17 | Fragmental polymict breccia | SCB1/334 |
| 65739 | R | .95 | Fragmental polymict breccia | SCB1/334 |
| 65745 | R | 7.76 | Fragmental polymict (regolith?) breccia | SCB1/334 |
| 65746 | R | 4.19 | Regolith breccia | SCB1/334 |
| 65747 | R | .82 | Fragmental polymict (regolith?) breccia | SCB1/334 |
| 65748 | R | .97 | Fragmental polymict (regolith?) breccia | SCB1/334 |
| 65749 | R | .95 | Fragmental polymict (regolith?) breccia | SCB1/334 |
| 65755 | R | 1.42 | Glassy impact melt or regolith breccia | SCB1/334 |
| 65756 | R | .77 | Fragmental polymict breccia | SCB1/334 |
| 65757 | R | 26.20 | Glassy impact melt | SCB1/334 |
| 65758 | R | 5.95 | Dilithologic or crystalline polymict breccia | SCB1/334 |
| 65759 | R | 3.11 | Cataclastic anorthosite (G) | SCB1/334 |

| SAMPLE NUMBER | SAMPLE TYPE | MASS g | DESCRIPTION | SRC/DB OR SCB/DB |
|---|---|---|---|---|
| 65765 | R | 1.12 | Dilithologic breccia or melt-coated anorthosite (G?) | SCB1/334 |
| 65766 | R | 1.01 | Cataclastic anorthosite | SCB1/334 |
| 65767 | R | 17.51 | Glass | SCB1/334 |
| 65768 | R | 3.25 | Fragmental polymict breccia (G) | SCB1/334 |
| 65769 | R | 2.74 | Fragmental polymict breccia (G) | SCB1/334 |
| 65775 | R | 3.50 | Fragmental polymict breccia (G) | SCB1/334 |
| 65776 | R | 2.33 | Glassy impact melt | SCB1/334 |
| 65777 | R | 16.53 | Poikilitic impact melt (G) | SCB1/334 |
| 65778 | R | 12.22 | Poikilitic impact melt | SCB1/334 |
| 65779 | R | 12.71 | Basaltic impact melt | SCB1/334 |
| 65785 | R | 5.16 | Basaltic impact melt | SCB1/334 |
| 65786 | R | 83.02 | Glassy breccia (G) | SCB1/334 |
| 65787 | R | 8.28 | Crystalline polymict breccia (G) | SCB1/334 |
| 65788 | R | 9.32 | Glassy impact melt | SCB1/334 |
| 65789 | R | 12.24 | Cataclastic anorthosite (G) | SCB1/334 |
| 65795 | R | 6.84 | Basaltic impact melt | SCB1/334 |
| 65905 | P | 12.08 | Basaltic impact melt | SCB1/406 |
| 65906 | P | 6.584 | Basaltic impact melt (G) | SCB1/406 |
| 65907 | P | 4.658 | Fragmental polymict breccia | SCB1/406 |
| 65908 | P | 2.162 | Glass | SCB1/406 |
| 65909 | P | 2.024 | Cataclastic anorthosite | SCB1/406 |
| 65915 | P | 2.060 | Glassy or fine-grained impact melt | SCB1/406 |
| 65916 | P | 0.994 | Cataclastic anorthosite | SCB1/406 |
| 65925 | R | 3.82 | Fragmental polymict (regolith?) breccia | SCB1/335 |
| 65926 | R | 3.03 | Fragmental polymict (regolith?) breccia | SCB1/335 |
| 65927 | R | .72 | Fragmental polymict (regolith?) breccia | SCB1/335 |
| 66035 | | 211.4 | Fragmental polymict breccia (G) | SCB1/407 |
| 66036 | | 4.384 | Fragmental polymict breccia | SCB1/407 |
| 66037 | | 3.718 | Glassy breccia | SCB1/407 |
| 66055 | | 1306.0 | Polymict or dilithologic breccia | SCB1/408 |
| 66075 | | 347.1 | Fragmental polymict breccia | SRC2/409 |
| 66085 | | 3.66 | Fragmental polymict breccia | SRC2/339 |
| 66086 | | 2.027 | Fragmental polymict breccia | SRC2/339 |
| 66095 | | 1185.0 | Basaltic impact melt (G) | SCB1/410 |

| SAMPLE NUMBER | SAMPLE TYPE | MASS g | DESCRIPTION | SRC/DB OR SCB/DB |
|---|---|---|---|---|
| 67015 | | 1194.0 | Fragmental polymict breccia | SCB7/ |
| 67016 | | 4262.0 | Fragmental polymict breccia | BSLSS |
| 67025 | | 16.06 | Basaltic impact melt (G) | BSLSS |
| 67035 | | 245.2 | Fragmental polymict breccia | SCB7/382 |
| 67055 | | 221.9 | Fragmental polymict breccia | SCB7/383 |
| 67075 | | 219.2 | Cataclastic anorthosite | SCB7/384 |
| 67095 | | 339.8 | Basaltic impact melt (G) | SCB7/385 |
| 67115 | | 240.0 | Fragmental polymict breccia (G) | SCB7/386 |
| 67215 | | 276.2 | Fragmental (monomict granoblastic) breccia | SCB6/PDB1 |
| 67235 | | 937.2 | Poikilitic impact melt | SCB6/PDB2 |
| 67415 | | 174.9 | Cataclastic noritic anorthosite | SCB6/387 |
| 67435 | | 353.5 | Crystalline polymict breccia (G) | SCB6/415 |
| 67455 | | 942.2 | Fragmental polymict breccia | SCB6/416 |
| 67475 | | 175.1 | Glassy impact melt/breccia | SCB6/418 |
| 67485 | P | 6.55 | Fine-grained impact melt | SCB6/419 |
| 67486 | P | 5.80 | Glass | SCB6/419 |
| 67487 | P | 2.65 | Fine-grained impact melt | SCB6/419 |
| 64788 | P | 2.25 | Fine-grained impact melt | SCB6/419 |
| 67489 | P | 2.06 | Basaltic impact melt | SCB6/419 |
| 67495 | P | 1.34 | Fine-grained impact melt | SCB6/419 |
| 67515 | R | 60.8 | Fragmental polymict breccia | SCB6/420 |
| 67516 | R | 14.38 | Crystalline polymict breccia | SCB6/420 |
| 67517 | R | 9.65 | Fragmental polymict breccia | SCB6/420 |
| 67518 | R | 3.74 | Fragmental polymict breccia or cataclastic anorthosite | SCB6/420 |
| 67519 | R | 2.04 | Fragmental polymict breccia | SCB6/420 |
| 67525 | R | 2.52 | Cataclastic anorthosite | SCB6/420 |
| 67526 | R | 2.44 | Fragmental polymict breccia | SCB6/420 |
| 67527 | R | 2.40 | Fragmental polymict breccia | SCB6/420 |
| 67528 | R | 1.24 | Fragmental polymict breccia | SCB6/420 |
| 67529 | R | 1.13 | Cataclastic anorthosite | SCB6/420 |

| SAMPLE NUMBER | SAMPLE TYPE | MASS g | DESCRIPTION | SRC/DB OR SCB/DB |
|---|---|---|---|---|
| 67535 | R | .99 | Fragmental breccia or cataclastic anorthosite | SCB6/420 |
| 67536 | R | 1.20 | Fragmental breccia or cataclastic anorthosite | SCB6/420 |
| 67537 | R | 1.29 | Cataclastic anorthosite | SCB6/420 |
| 67538 | R | 1.77 | Fragmental polymict breccia | SCB6/420 |
| 67539 | R | 2.12 | Fragmental polymict breccia | SCB6/420 |
| 67545 | R | 1.88 | Fragmental polymict breccia | SCB6/420 |
| 67546 | R | 1.50 | Fragmental polymict breccia | SCB6/420 |
| 67547 | R | .83 | Fragmental polymict breccia | SCB6/420 |
| 67548 | R | 1.36 | Fragmental polymict breccia | SCB6/420 |
| 67549 | R | 43.1 | Fragmental polymict breccia | SCB6/420 |
| 67555 | R | 3.54 | Glassy breccia | SCB6/420 |
| 67556 | R | 82.1 | Basaltic impact melt | SCB6/420 |
| 67557 | R | 3.30 | Regolith breccia | SCB6/420 |
| 67558 | R | 2.56 | Fragmental polymict breccia | SCB6/420 |
| 67559 | R | 32.9 | Basaltic impact melt | SCB6/420 |
| 67565 | R | 10.43 | Poikilitic impact melt | SCB6/420 |
| 67566 | R | 4.31 | Granoblastic impactite | SCB6/420 |
| 67567 | R | 11.51 | Glass | SCB6/420 |
| 67568 | R | 11.05 | Glass | SCB6/420 |
| 67569 | R | 7.27 | Glass | SCB6/420 |
| 67575 | R | 4.47 | Glassy breccia | SCB6/420 |
| 67576 | R | 3.98 | Glassy breccia (regolith?) | SCB6/420 |
| 67605 | P | 44.52 | Fragmental polymict breccia | SCB6/422 |
| 67615 | R | 8.77 | Fine-grained impact melt | SCB6/421 |
| 67616 | R | 21.29 | Fine-grained impact melt | SCB6/421 |
| 67617 | R | 14.32 | Fine-grained impact melt | SCB6/421 |
| 67618 | R | 11.17 | Crystalline breccia (G) | SCB6/421 |
| 67619 | R | 6.15 | Fine-grained impact melt | SCB6/421 |
| 67625 | R | 6.72 | Fine-grained impact melt | SCB6/421 |
| 67626 | R | 19.19 | Crystalline polymict breccia | SCB6/421 |
| 67627 | R | 79.64 | Glass | SCB6/421 |
| 67628:renumbered 67685-88 | | | | |
| 67629 | R | 5.43 | Glass | SCB6/421 |
| 67635 | R | 9.12 | Pristine cataclastic anorthosite | SCB6/421 |
| 67636 | R | 3.23 | Pristine cataclastic anorthosite | SCB6/421 |
| 67637 | R | 2.34 | Pristine cataclastic anorthosite | SCB6/421 |
| 67638 | R | 7.23 | Fragmental/glassy polymict breccia | SCB6/421 |
| 67639 | R | 7.34 | Crystalline polymict breccia | SCB6/421 |

| SAMPLE NUMBER | SAMPLE TYPE | MASS g | DESCRIPTION | SRC/DB OR SCB/DB |
|---|---|---|---|---|
| 67645 | R | .84 | Fragmental polymict breccia | SCB6/421 |
| 67646 | R | 3.94 | Fragmental polymict breccia | SCB6/421 |
| 67647 | R | 47.72 | Regolith breccia | SCB6/421 |
| 67648 | R | 7.88 | Crystalline(?) polymict breccia | SCB6/421 |
| 67649 | R | 1.60 | Fragmental polymict breccia | SCB6/421 |
| 67655 | R | 4.11 | Crystalline polymict breccia | SCB6/421 |
| 67656 | R | 1.93 | Fragmental polymict breccia | SCB6/421 |
| 67657 | R | 1.70 | Fragmental polymict breccia | SCB6/421 |
| 67658 | R | 1.35 | Fragmental polymict breccia | SCB6/421 |
| 67659 | R | 1.62 | Crystalline or fragmental polymict breccia | SCB6/421 |
| 67665 | R | 5.88 | Fragmental polymict breccia | SCB6/421 |
| 67666 | R | 5.47 | Glassy breccia | SCB6/421 |
| 67667 | R | 7.89 | Pristine feldspathic lherzolite | SCB6/421 |
| 67668 | R | 3.58 | Poikilitic impact melt | SCB6/421 |
| 67669 | R | 12.54 | Fragmental polymict breccia | SCB6/421 |
| 67675 | R | 1.07 | Glass | SCB6/421 |
| 67676 | R | 2.33 | Variolitic impact melt | SCB6/421 |
| 67685 | R | 28.04 | Cindery glass | SCB6/421 |
| 67686 | R | 11.75 | Cindery glass | SCB6/421 |
| 67687 | R | 7.60 | Cindery glass | SCB6/421 |
| 67688 | R | 2.32 | Cindery glass | SCB6/421 |
| 67695 | R | 14.02 | Glass | SCB6/421 |
| 67696 | R | 7.85 | Glass | SCB6/421 |
| 67697 | R | 5.54 | Glassy breccia | SCB6/421 |
| 67705 | P | 5.82 | Glass | SCB4/388 |
| 67706 | P | 1.52 | Fragmental polymict breccia | SCB4/388 |
| 67707 | P | 1.42 | Fragmental polymict breccia | SCB4/388 |
| 67708 | P | 1.33 | Fragmental polymict breccia (G) | SCB4/388 |
| 67715 | R | 9.44 | Fine-grained impact melt | SCB4/423 |
| 67716 | R | 17.02 | Fine-grained impact melt | SCB4/423 |
| 67717 | R | 5.56 | Glassy breccia | SCB4/423 |
| 67718 | R | 41.05 | Fine-grained impact melt and fragmental breccia | SCB4/423 |
| 67719 | R | 2.13 | Fine-grained impact melt | SCB4/423 |
| 67725 | R | 5.85 | Crystalline polymict breccia (G) | SCB4/423 |
| 67726 | R | 4.53 | Crystalline polymict breccia | SCB4/423 |
| 67727 | R | 1.80 | Fine-grained impact melt | SCB4/423 |
| 67728 | R | 9.25 | Fine-grained impact melt | SCB4/423 |
| 67729 | R | 73.2 | Glassy breccia | SCB4/423 |

| SAMPLE NUMBER | SAMPLE TYPE | MASS g | DESCRIPTION | SRC/DB OR SCB/DB |
|---|---|---|---|---|
| 67735 | R | 13.30 | Glassy impact melt/breccia | SCB4/423 |
| 67736 | R | 14.92 | Crystalline impact melt | SCB4/423 |
| 67737 | R | 4.56 | Fine-grained impact melt | SCB4/423 |
| 67738 | R | 5.84 | Fine-grained impact melt | SCB4/423 |
| 67739 | R | 2.03 | Fine-grained impact melt | SCB4/423 |
| 67745 | R | 3.53 | Fine-grained impact melt | SCB4/423 |
| 67746 | R | 3.47 | Poikiloblastic inpactite | SCB4/423 |
| 67747 | R | 6.30 | Basaltic impact melt | SCB4/423 |
| 67748 | R | 4.74 | Fine-grained impact melt | SCB4/423 |
| 67749 | R | 11.47 | Fragmental polymict breccia | SCB4/423 |
| 67755 | R | 3.53 | Fine-grained impact melt | SCB4/423 |
| 67756 | R | 4.82 | Crystalline polymict breccia | SCB4/423 |
| 67757 | R | 4.83 | Basaltic/poikilitic impact melt | SCB4/423 |
| 67758 | R | 4.06 | Crystalline polymict breccia | SCB4/423 |
| 67759 | R | 4.56 | Fragmental polymict breccia | SCB4/423 |
| 67765 | R | 1.73 | Fine-grained impact melt | SCB4/423 |
| 67766 | R | 5.47 | Crystalline polymict breccia | SCB4/423 |
| 67767 | R | 1.67 | Fragmental polymict breccia | SCB4/423 |
| 67768 | R | .99 | Fragmental polymict breccia | SCB4/423 |
| 67769 | R | 3.05 | Poikilitic impact melt | SCB4/423 |
| 67775 | R | 6.58 | Fine-grained impact melt | SCB4/423 |
| 67776 | R | 3.10 | Fragmental polymict breccia | SCB4/423 |
| 67915 | | 2559.0 | Crystalline polymict breccia | SCB4/ |
| 67935 | | 108.9 | Basaltic impact melt | SCB4/389 |
| 67936 | | 61.82 | Basaltic impact melt | SCB4/389 |
| 67937 | | 59.67 | Basaltic impact melt | SCB4/389 |
| 67945 | | 4.37 | Basaltic impact melt (G?) | SCB4/390 |
| 67946 | | 3.20 | Variolitic impact melt | SCB4/390 |
| 67947 | | 2.43 | Basaltic impact melt | SCB4/390 |
| 67948 | | 1.59 | Basaltic impact melt | SCB4/390 |
| 67955 | | 162.6 | Poikiloblastic impactite | SCB4/390 |
| 67956 | | 3.70 | Basaltic impact melt | SCB4/390 |
| 67957 | | 1.73 | Glassy breccia | SCB4/390 |
| 67975 | | 446.6 | Fragmental polymict breccia (G) | SCB4/392 |
| 68035 | | 20.96 | Crystalline polymict breccia (G) | SCB3/413 |
| 68115 | | 1191.0 | Glassy breccia | SRC2/340 |
| 68415 | | 371.2 | Basaltic impact melt | SRC2/341-2 |
| 68416 | | 178.4 | Basaltic impact melt | SRC2/341 |

| SAMPLE NUMBER | SAMPLE TYPE | MASS g | DESCRIPTION | SRC/DB OR SCB/DB |
|---|---|---|---|---|
| 68505 | P | 1.30 | Poikilitic impact melt | SCB3/412 |
| 68515 | R | 236.1 | Dilithologic or polymict breccia(G) | SCB3/411 |
| 68516 | R | 34.04 | Fine-grained/glassy impact melt | SCB3/411 |
| 68517 | R | 13.13 | Crystalline of fragmental polymict breccia (G) | SCB3/411 |
| 68518 | R | 29.82 | Glass | SCB3/411 |
| 68519 | R | 10.56 | Basaltic impact melt (G) | SCB3/411 |
| 68525 | R | 38.96 | Poikilitic impact melt (G) | SCB3/411 |
| 68526 | R | 7.21 | Poikilitic impact melt | SCB3/411 |
| 68527 | R | 3.03 | Crystalline polymict breccia (poikilitic impact melt?) | SCB3/411 |
| 68528 | R | 1.08 | Crystalline polymict breccia | SCB3/411 |
| 68529 | R | 7.03 | Glass | SCB3/411 |
| 68535 | R | 8.04 | Glassy breccia | SCB3/411 |
| 68536 | R | 1.85 | Basaltic impact melt | SCB3/411 |
| 68537 | R | 1.41 | Fine-grained impact melt (G?) | SCB3/411 |
| 68815 | | 1826.0 | Glassy breccia | SRC2/343 |
| 68825 | P | 8.658 | Glassy impact melt | SCB1/375 |
| 68845 | P | 4.556 | Fine-grained impact melt | SCB1/344 |
| 68846 | P | 2.284 | Fine-grained impact melt | SCB1/344 |
| 68847 | P | 2.854 | Fine-grained impact melt | SCB1/344 |
| 68848 | P | 1.770 | Basaltic impact melt (G) | SCB1/344 |
| 69935 | | 127.6 | Glassy breccia | SCB3/378 |
| 69945 | | 6.88 | Poikilitic impact melt (G) | SCB3/377 |
| 69955 | | 75.94 | Cataclastic anorthosite | SCB3/380 |
| 69965 | | 1.12 | Fragmental polymict breccia (G) | SCB3/379 |

# PLANIMETRIC SKETCH MAPS AND SAMPLE LOCATIONS FOR APOLLO 16 SAMPLING SITES; MODIFIED FROM THE APOLLO 16 SAMPLE INFORMATION CATALOG (1972).

**STATION 1**

1500 ;1505
X 1510;1140 ; Rake
1515 - 77

NORTHEAST PAN

FLAG

X 1175 ;1160
X1140 ;1155-8;

X 1195 ;1195; 1180

X TRENCH 1240 ;1245 -49 ;
1255 ;1220 ;1225 ;1226.

LRV

PLUM

• 1016

1295 ; 1280
X LINEATION
PHOTOS
SOUTHWEST PAN

LRV TRACKS
N

• 1015
(1017 not located)

0          50m

**STATION 2**

BUSTER

PAN  X 2235 -39 ; 2240 ;2245-9;2315
2255

N

X 2275

X 2295 ; 2280 ;2285-9 ;2305

X LPM

LRV

PAN

0          50m

SPOOK

**STATION 4**

N

Pen4 x X DT 4002/4001

LRV X 4500 ;4505-9; Rake
X 4455        4515-89
X 4435

Pen3 x
Pen2 X x TRENCH 4420 ;4425 ;4475-78

NORTH PAN, 500mm
X Pen 1

X 4800 ; 4810 ,Rake 4815-37
SOUTH PAN

0          50m

**STATION 5**

N

PAN  LRV

5500;5510; X
Rake
5515-98      X X 5055;5056
X 5600       5095
5610
Rake
X 5075

5710 ;5700;X X 5035 ;5310;
5715-95; 5900;     Rake 5315-66
5905-27   (5015 not located)
5016

0          50m

xxx

STATION 6

N

6035-7;
6080; 6055; 6040

PAN

LRV

6080; 85-
86.

6075
6095

LRV Tracks

50m

STATION 8

N

8845-48;
X 8840

8815, 8880; 8820;
8825

LRV

X-8510; 8500, 8505, 8085
Rake 8515-37.

PAN

LRV

DT—X
8002/8001

8120; 8115

8415 ; 8416;

50m

STATION 9

LRV
PAN—

LRV Tracks

DT 9001—X

9003 ; 9004 ; 9920 ;
9940; 9945

9935; 9955, 9960, 9965

N

50m

LM/ALSEP-STATION 10

STATION 11

N

0      50m

"HOUSE ROCK"

E-W Split

7940;45-48

Area of
7935-97
7955-57
7960
7975
7915

Right polarization and
500mm photos

Area of
7055
7095
7115
7015
7075

Area of
7075

North Ray rim crest

Left polarization and
500mm photos

9235   Padded bag

Area of
7710   Rake
7700; 05-08 ;
7715 - 76

"White breccia boulders"   △ △ PAN
7455    7035-X
7475
7515-76    7605;
7490 ;7510 Rake   7610 ; Rake 7615-27 ; 7629-76 ; 7685-88 ; 7695-97
7485-95    7600;
X-7460
X     X   LRV
7415       7435     X   7215   Padded bag
7016
7020?
7023?    LRV Tracks

STATION 13

N

3520 ; 3500; 8505-09;
3515; Rake 3525-98.

3320 ;3340     3335 ;3355;
0017

☐ — LRV

△ PAN

X LPM

0      50m

INTRODUCTION:  60015 is a coherent, very light gray, shock-melted and cata-
clastic anorthosite which is probably chemically pristine.  It is largely
coated with a vesicular glass up to 1 cm thick (Fig. 1).  The glass contains a
few white inclusions and the glass-anorthosite contact is macroscopically sharp.

60015 was probably collected about 30 m west-northwest of the Lunar Module
but details of its collection, situation, and orientation are not known.
It is blocky with rare fractures.  Zap pits are common on two surfaces with
a few on the others.

FIGURE 1.
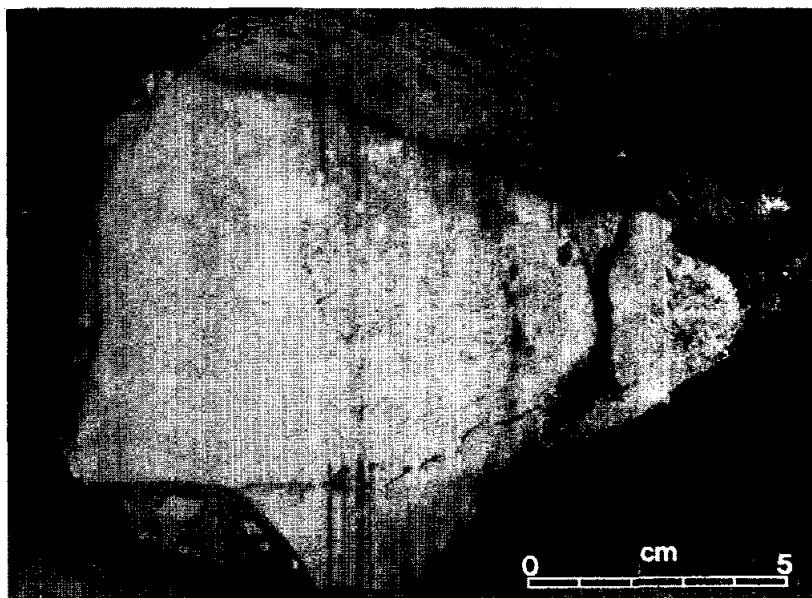


PETROLOGY:  Petrographic descriptions are given by Sclar et al. (1973), Sclar
and Bauer (1974), Dixon and Papike (1975) and Juan et al. (1974).  All note
the brecciation and intense shock damage to the anorthosite (Fig.2) which
took place prior to the emplacement of the glass coat.  The anorthosite
consists of more than 98% plagioclase ($An_{95-98}$) with 1-2% orthopyroxene
($En_{63}$) and augite (Fig. 3).  Ishii et al. (1976) calculate an equilibration
temperature of 987°C from the augite-orthopyroxene data of Dixon and Papike
(1975).  Olivine is absent, but ilmenite, Cr-spinel, troilite and minor Fe-metal
are present (Dixon and Papike, 1975).

There is a bimodal grain size with grains of plagioclase 1-3 mm in diameter set
in a finer-grained matrix.  Plagioclases are strained with undulose and patchy
extinction and some well-developed sets of shock lamellae exist.  Maskelynite
is not present.  The intergranular areas include colonnaded, feathery plagio-
clases (Fig. 2) interpreted as resulting from a rapidly cooled intergranular
shock melt.  No intergranular movement took place during the shock event and

1

a



b



c



FIGURE 2. 60015,120

a) anorthosite, xpl. width 2mm.
b) colonnades in anorthosite,
   xpl. width 0.5mm
c) glass coat, ppl. width 2mm.
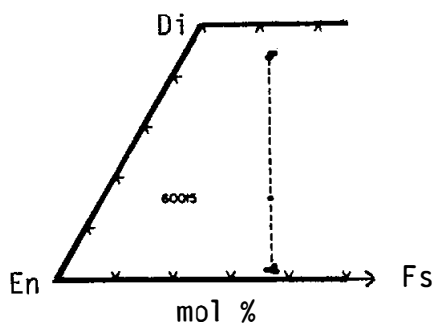
FIGURE 3. Pyroxenes; from Dixon and Papike (1975).
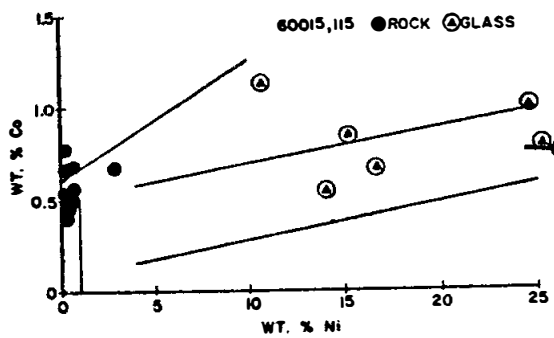


FIGURE 4. Metals; from Hewins and Goldstein (1975a).
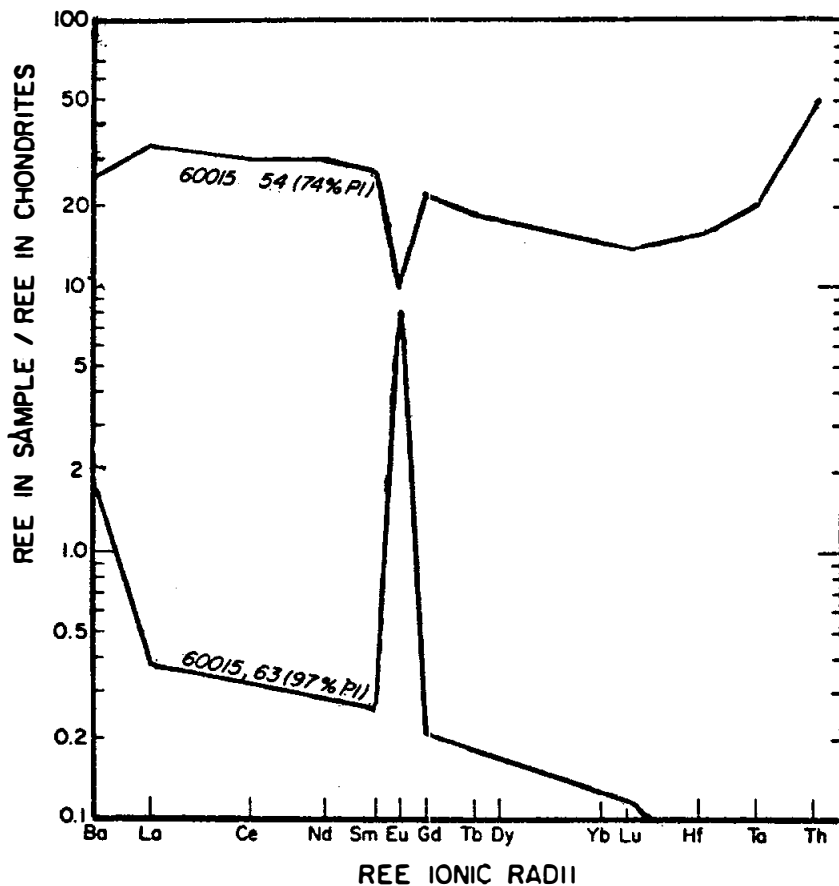


FIGURE 5. Rare earths; from Laul and Schmitt (1973).

3

temperatures are believed to have risen to over 1500°C. The progenitor was possibly porous (Sclar and Bauer, 1974). Fe-metal in the anorthosite contains little Co or Ni (Fig. 4) (Hewins and Goldstein, 1975a; Sclar and Bauer, 1974; Mao and Bell, 1976). The lowest values, which occur in the feathery plagioclase regions may be the result of shock reduction of $Fe^{2+}$ from plagioclase (Sclar and Bauer, 1974).

The glass coat is brown, vesicular and partly crystallized into skeletal microlites of plagioclase. The plagioclase-rich xenoliths and xenocrysts in the glass show no evidence of reaction with the glass, which is similar in composition to Apollo 16 soils (Table 2). Metal in the glass contains up to 30% Ni, in the meteoritic range (Fig. 4) (Hewins and Goldstein, 1975a; Mao and Bell, 1976). Mao and Bell (1976) show that metals are altered from their original meteoritic composition by reaction with the anorthosite, and that the higher Ni contents occur in metals associated with troilite and schreibersite.

The contact relationships of glass coat and anorthosite are described in detail by Sclar and Bauer (1974). The peripheral 6 mm of anorthosite lacks feathery plagioclase, but a 200 μm boundary layer of pure, colonnaded plagioclase exists, and is interpreted as quenched liquid derived by melting the surface of the anorthosite. Two distinct liquids, one the anorthosite surface, the other the glass coat, existed momentarily. The heat to melt the anorthosite surface must have been mainly from the shock event which produced the glass coat, not from the glass coat itself (Sclar and Bauer, 1974).

CHEMISTRY: Chemical studies are listed in Table 1 and summary chemistries of the anorthosite and of the glass coat in Table 2. Representative incompatible element patterns are shown as Figure 5.

For the anorthosite, Laul and Schmitt (1973) note that the REEs are low and identical to 15415 (Fig. 5). Volatile and light elements are very low in abundance (Jovanovic and Reed, 1973; Moore and Lewis, 1976; and others) as are Zr and Hf, with the lowest Zr/Hf of any sample (Garg and Ehmann, 1976). The level of meteoritic contamination, if any, is uncertain because Au, Ir (etc.) have not been measured. Co values are low (1 ppm or less) except for the analysis by Juan et al. (1974) which has 44 ppm Co, and 30 ppm Ni. The low Co contents and the Co/Ni ratios of the metal suggest that most of the anorthosite is uncontaminated. The glass coat was analyzed by Laul and Schmitt (1973) with results in agreement with microprobe data by Dixon and Papike (1975) and Sclar and Bauer (1974). Although similar to Apollo 16 soils, subtle chemical differences exist e.g. lower $TiO_2$ (Laul and Schmitt, 1973). The Ni/Au/Ir ratios suggest that the glass was created by the impact of an iron meteorite.

STABLE ISOTOPES: Clayton et al. (1973) reported $\delta O^{18}$ values of 5.67 for the anorthosite plagioclase and 5.68 for the glass coat, typical lunar values.

## TABLE 1
## Chemical studies of 60015

| Reference | Split # | Description | Elements analyzed |
|---|---|---|---|
| S.R. Taylor et al.(1973) | ,64 | anorthosite | majors, REEs, other trace |
| Janghorbani et al.(1973) | ,65 | " | majors |
| Laul and Schmitt (1973) | ,6 | " | majors, REEs, other trace |
| " | ,54 | glass coat | " |
| Juan et al. (1974) | ,67 | anorthosite | majors, some trace |
| Nunes et al. (1973) | ,50 | " | U, Th, Pb |
| Ehmann and Chyi (1974) | ,65B | " | Zr, Hf |
| Garg and Ehmann (1976) | ,65A | " | Eu, Zr, Fe, Cr, Sc, Co, Hf |
| Miller et al. (1974) | ,65B | " | Fe, Cr, Sc, Co, Eu |
| Schaeffer and Husain (1974) | ,22 ,69 | " | K, Ca |
| Jovanovic and Reed (1973) | ,60 | " | F, Cl, Br, I, Te, U, $P_2O_5$ |
| Moore et al. (1973) | ,61 | " | C |
| " | ,53 | glass coat | C |
| Cripe and Moore (1974) | ,61 | anorthosite | S |
| " | ,53 | glass coat | S |
| Moore and Lewis (1976) | ,61 | anorthosite | N |
| " | ,53 | glass coat | N |
| Phinney et al. (1975) | ? | " | K, Ca |
| Nyquist et al. (1975) | ,50I ,50II | " | Rb, Sr |
| Papanastassiou and Wasserburg (1976) | ,36 ,95 | " | Rb, Sr,K |
| Nunes et al. (1974) | ,46 | glass coat | Rb, Sr, K, U, Th |

## TABLE 2
## Summary chemistries of anorthosite and glass coat in 60015

| | Anorthosite | Glass Coat |
|---|---|---|
| $SiO_2$ | 44 | 44 |
| $TiO_2$ | 0.02 | 0.4 |
| $Al_2O_3$ | 36 | 27 |
| $Cr_2O_3$ | <0.01 | 0.1 |
| FeO | 0.35 | 5 |
| MnO | <0.01 | 0.05 |
| MgO | ~0.3 | 6 - 9 |
| CaO | 19 | 15 |
| $Na_2O$ | 0.4 | ~0.45 |
| $K_2O$ | <0.01 | 0.08 |
| $P_2O_5$ | 0.01 | |
| Sr | 178 | 157 |
| La | 0.13 | 11 |
| Lu | 0.003 | 0.49 |
| Rb | ? | 1.9 |
| Sc | 0.6 | 5.8 |
| Ni | | 900 |
| Co | 1 | 42 |
| Ir ppb | | 23 |
| Au ppb | | 8 |
| C | 20 | 59 |
| N | 23 | 50 |
| S | 27 | 890 |
| Zn | | |
| Cu | 2 | |

Oxides in wt%, others in ppm except as noted.

RADIOGENIC ISOTOPES AND GEOCHRONOLOGY: Rb-Sr data are summarized in Table 3. The low measured $^{87}Sr/^{86}Sr$ give calculated ratios at 4.6 b.y. close to BABI. Nyquist et al. (1975) calculate an isochron age from two whole rock samples as 3.8 ± 1.7 b.y. but because of the large error do not attribute significance to it. Two plagioclase clasts from the glassy rind have $^{87}Sr/^{86}Sr$ at 4.6 b.y. even lower than the anorthosite (Nunes et al., 1974).

TABLE 3. Summary of Rb-Sr data* for 60015

| Sample | Description | Rb/Sr | $^{87}Sr/^{86}Sr$ Measured | $^{87}Sr/^{86}Sr$ Calc. at 4.6 b.y. | Reference |
|---|---|---|---|---|---|
| ,50 I | Anorthosite | 0.00165 | 0.69934+4 | 0.69902 | Nyquist et al. 1975 |
| ,50 II | " | 0.00044 | 0.69915+5 | 0.69907 | " |
| ,50 | " | 0.00073 | 0.69904+6 | 0.69890 | Nunes et al. 1974 |
| ,36 | " | 0.00016 | 0.69903+3 | ⌐0.69900 | Papanastassiou and Wasserburg 1976 |
| ,95 | " | 0.00067 | 0.69908+4 | 0.69895 | " |
| ,46 | Plag. in glass | 0.00083 | 0.69900+7 | 0.69884 | Nunes et al. 1974 |
| ,46 | " | 0.00044 | 0.69887+3 | 0.69878 | " |
| ,46 | Glass coat | 0.01218 | 0.70120+6 | 0.69888 | " |

*Not corrected for interlaboratory bias.

Ar-Ar ages of 3.5 ± 0.05 b.y. (Fig.6) (Schaeffer and Husain 1974) and 3.54 ± 0.05 b.y. (Fig.7) (Phinney et al.,1975)demonstrate that the shock melting of the anorthosite was later than the ⌐4.0 b.y. cataclysm. These ages may just be lower limits but a good plateau was obtained by Schaeffer and Husain (1974).
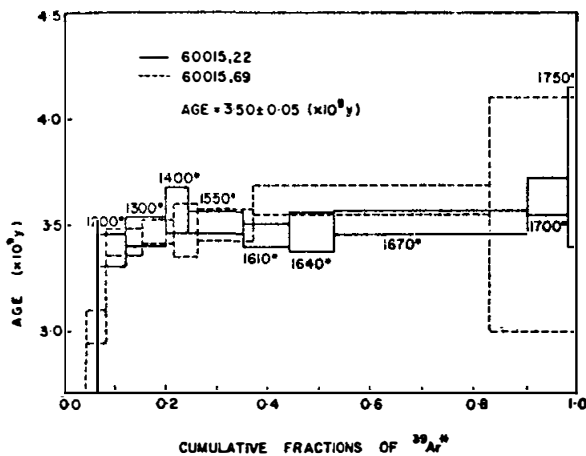


FIGURE 6. Ar release; from Schaeffer and Husain (1974).
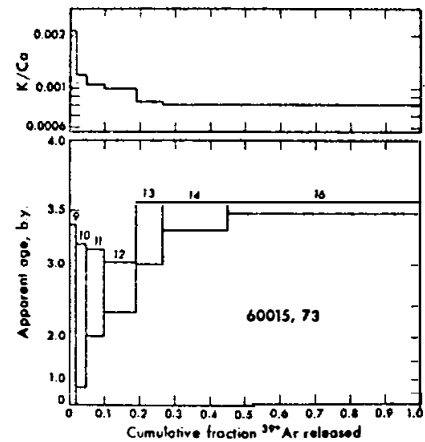


FIGURE 7. Ar release; from Phinney et al. (1975).

The U-Th-Pb data (Nunes et al.,1973, 1974) indicate an enrichment in Pb at
3.57 b.y. (2-stage model) or 3.8 b.y. (3-stage model). The Pb introduction
was presumably contemporaneous with the shock-melting event. These theoretically
valid model-dependent ages may not be as precise as first believed because up
to 3% of the Pb may be contamination (Nunes et al.,1974).

RARE GAS/EXPOSURE AGES: Leich and Niemeyer (1975) provide Xe, Ar and Kr isotopic
data and report an $^{81}$Kr-Kr exposure age of 1.96 ± 0.08 m.y., or 1.93 ± 0.08 m.y.
if the trapped xenon in the rock is terrestrial. The latter interpretation of
the origin of the trapped xenon is preferred following experiments (Niemeyer and
Leich,1976) which showed much more Ar, Xe and Kr in crushed samples, even though
temperatures greater than 1000° were required to release 75% of the trapped Kr
and Xe.

Phinney et al. (1975) and Schaeffer and Husain (1974) report Ar isotopic data
and calculate $^{38}$Ar-Ca exposure ages of 3 ± 1 m.y., and 4.6 ± 0.6 and 6.1 ± 0.5 m.y.
respectively. These are significantly higher than the $^{81}$Kr-Kr age which Leich and
Niemeyer (1975) consider more reliable.

MICROCRATERS AND TRACKS: Several studies of microcraters on the glass surface of
60015 have been made. The surface is in production, not equilibrium. Size-frequency
data is provided by Neukum et al. (1973), Hörz et al.(1974), Fechtig et al.
(1974), Mandeville (1976), and Hartung et al.(1977) (Fig.8). Neukum et al.(1973),
Nagel et al. (1975), and Mandeville (1976) provide measurements of pit characters.
Flavill et al. (1978) discuss some of the craters as being of secondary or tertiary
origin rather than of direct micrometeroid origin, and Hartung et al.(1977) note
that the data do not specify that there was a variation of the meteoroid flux with
time. Carey and McDonnell (1976) find no evidence for the build-up of sputtered
weld material on the surface. Storzer et al. (1973) plot the solar flare track
density against depth, as deduced from cratering statistics.
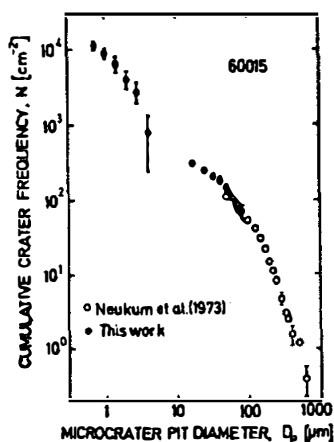


FIGURE 8. Microcraters; from Fechtig et al. (1974).

7

PHYSICAL PROPERTIES:  The remanent magnetism characteristics of the anorthosite have been studied by Runcorn's group (Collinson et al.,1973;Stephensen et al., 1974, 1975) using the anhysteretic remanent magnetization method (ARM). The rock does not appear to possess a measurable hard NRM, although grains capable of holding such an NRM are present.  This is probably due to the extremely low iron content.  The initial susceptibility and the saturation remanence are very low. Weeks (1973) studied electron paramagnetic resonance characteristics and noted that $Fe^{3+}$ and $Ti^{3+}$ are higher than in several other Apollo 16 rocks.

P and S wave velocities of the anorthosite from 0.5 to 7 kb are reported in Chung (1978) (Table 4, Fig.9).  Herminghaus and Berckhemer (1974) measured Q with ultrasonic absorption measurements at $10^{-4}$ torr and $+20^{\circ}C$ to $-180^{\circ}C$.  Q is quite low, independent of T, and at $20^{\circ}C$ only 20% higher than at atmospheric pressure.  The measurements suggest that the anorthosite has a high microcrack density.

TABLE 4.  Elastic wave velocities of anorthosite in 60015

| | Confining pressure (Kb) | | | | | | | | | |
|---|---|---|---|---|---|---|---|---|---|---|
| | 0.5 | 1.0 | 1.5 | 2 | 3 | 4 | 5 | 6 | 7 | 10* |
| P Km/s | 5.5 | 6.0 | 6.27 | 6.52 | 6.75 | 6.86 | 6.90 | 6.94 | 6.97 | 7.02 |
| S Km/s | 2.6 | 2.9 | 3.21 | 3.40 | 3.58 | 3.68 | 3.74 | 3.86 | 3.88 | 3.91 |

*Estimated by linear extrapolation.  Reference:  Chung (1973)

FIGURE 9. from Chung (1973).
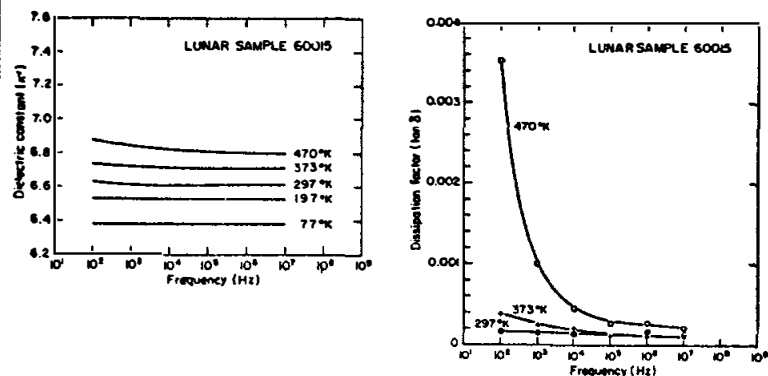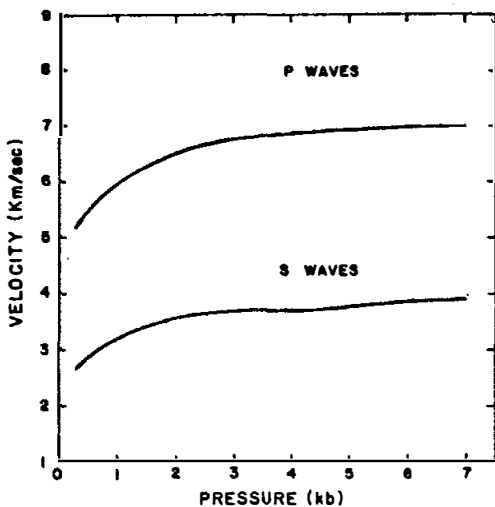




FIGURE 10.Dielectric properties; from Chung and Westphal (1973).

Dielectric constants and losses for the anorthosite are presented in Chung and Westphal (1973) (Fig.10).

Mandeville and Dollfus (1977) determined polarimetric properties of surface portions of 60015, one cratered and dust-free, others cratered and dust-covered.

PROCESSING AND SUBDIVISIONS: In 1972, 60015 was sawn into 5 main pieces (Fig.11). The large pieces ,1 and ,2 are preserved intact and ,3 was subdivided into 3 pieces for display purposes. All allocations are from the two slabs produced during sawing. The main subdivision of these slabs and the locations of the splits are shown in Figures 12 and 13. Several subsequent splits and renumbering of returned/consumed samples are not shown.
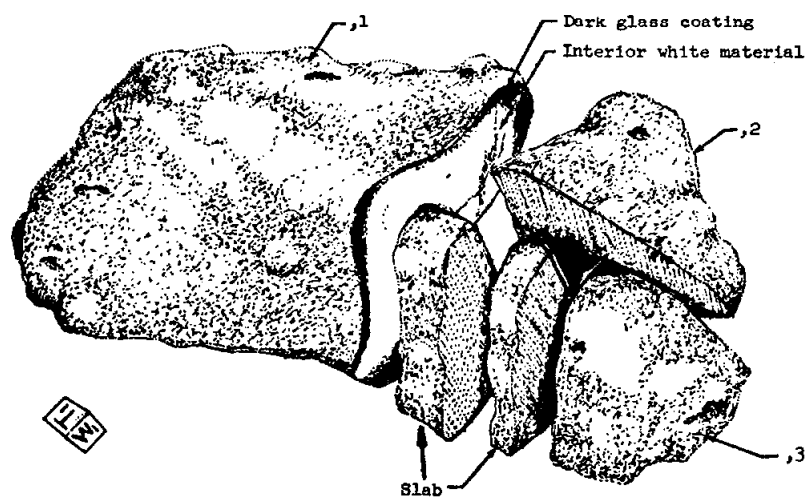


FIGURE 11.
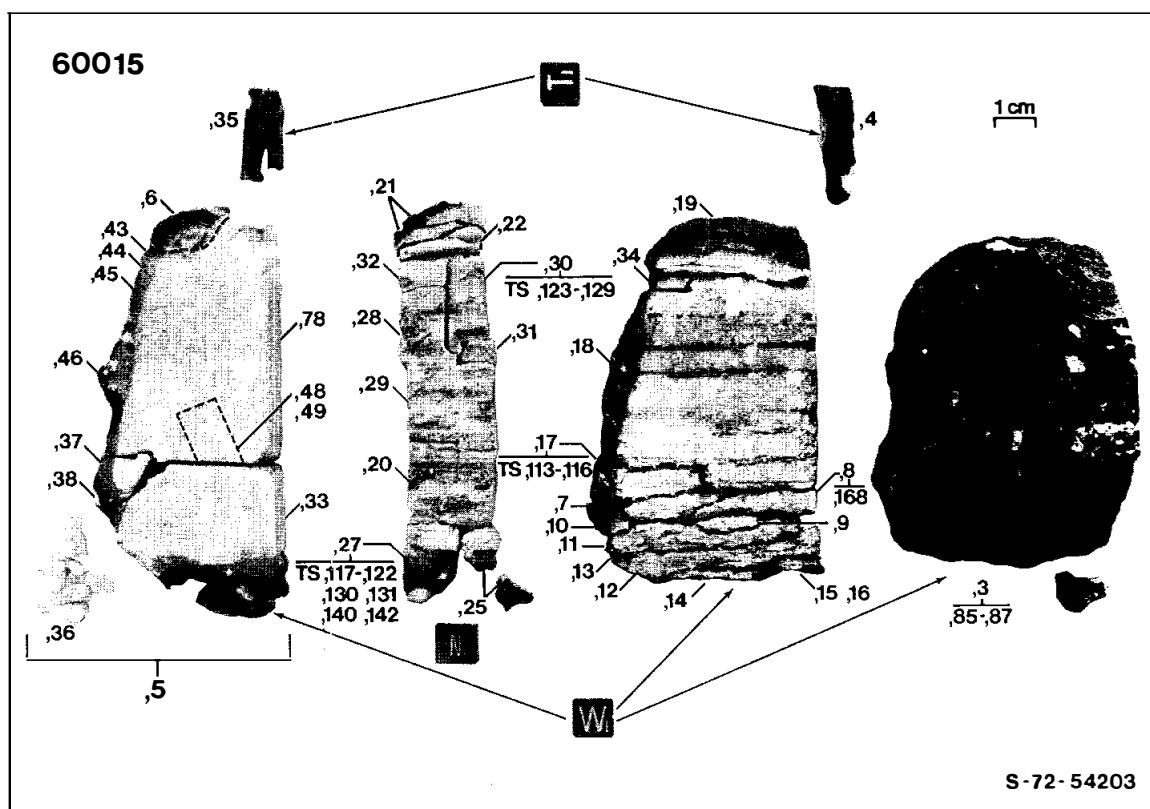


FIGURE 12.

FIGURE 13.
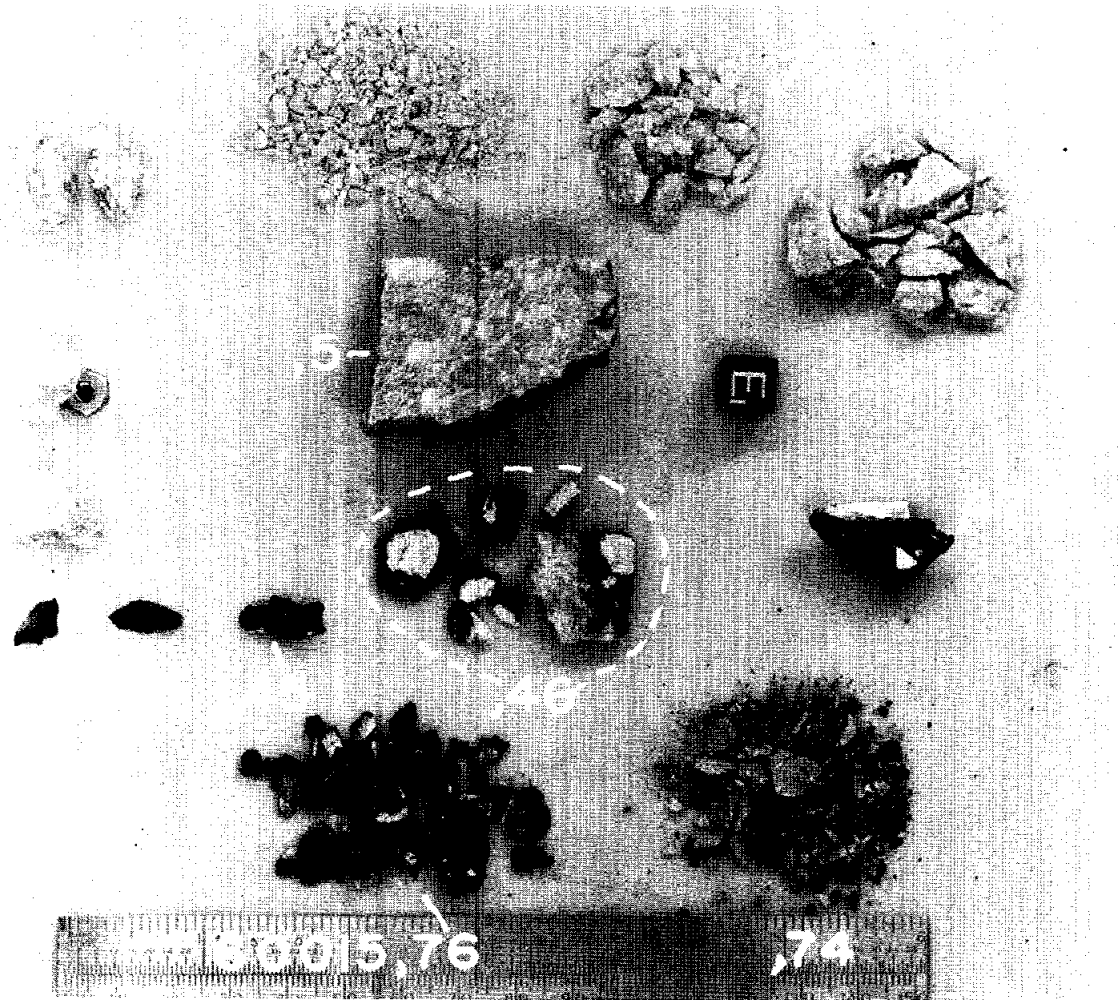


S-72-55505

INTRODUCTION:  60016 is a friable, medium gray breccia with a porous clastic matrix and abundant light and dark clasts of various sizes (Fig.1).

The sample was collected 14-15 m southwest of the Lunar Module where it had a poorly developed fillet.  Its orientation is known.  It is subrounded and zap pits are present on all surfaces.

FIGURE 1. S-78-34417.  Scale in mm.
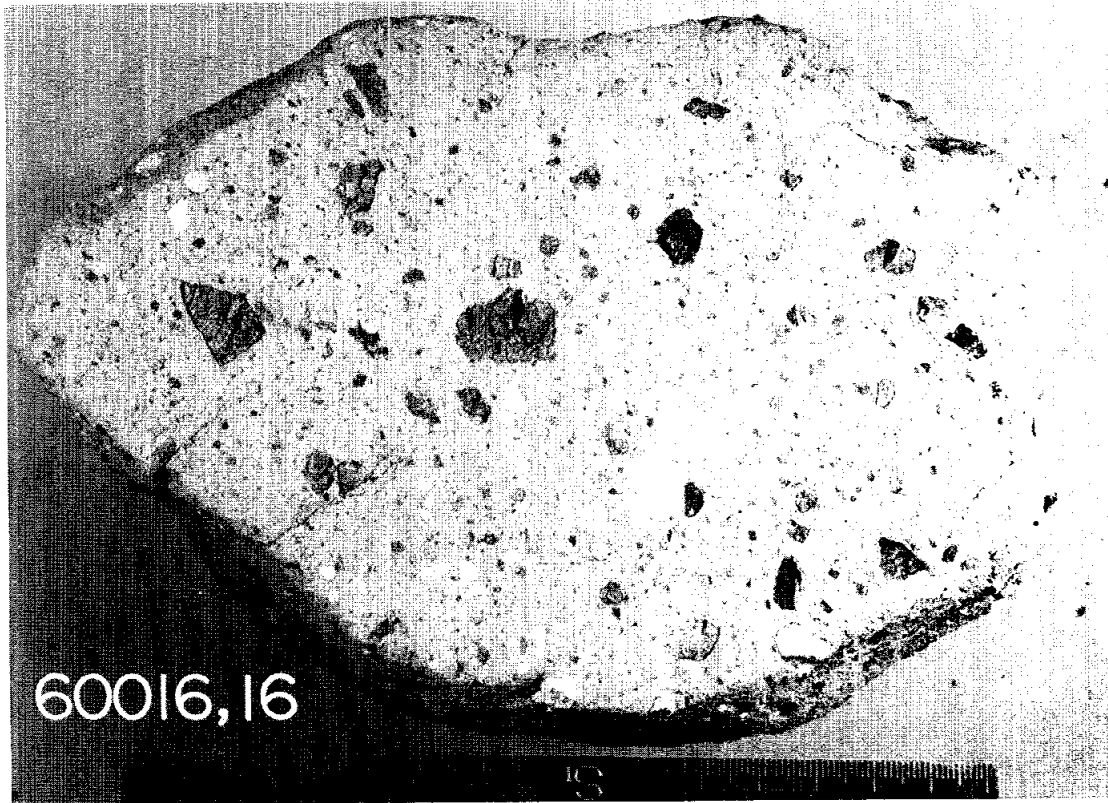


PETROLOGY:  Johan and Christophe (1974), Haselton and Nash (1975a,b), Takeda et al. (1979), Misra and Taylor (1975) and LSPET (1973) provide limited petrographic information.  The rock is polymict with a variety of clast types in a porous, unequilibrated matrix that is essentially free of glass (Fig.2).  Grain size is seriate from several mm downwards.  Some rust is present.

Mineral fragments of plagioclase, pyroxene, olivine, spinel and metal are present.  Lithic clasts include cataclastic and recrystallized anorthosite, coarse-and fine-grained poikilitic impact melt, granoblastic material, noritic

FIGURE 2.

a
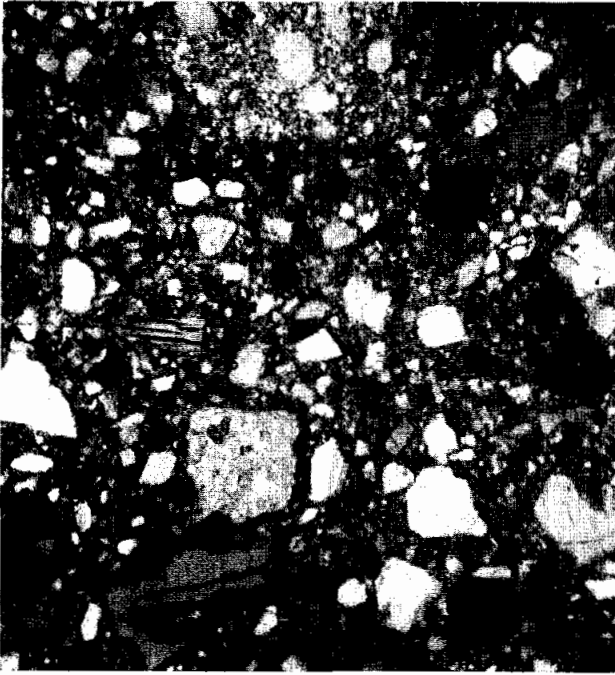


b
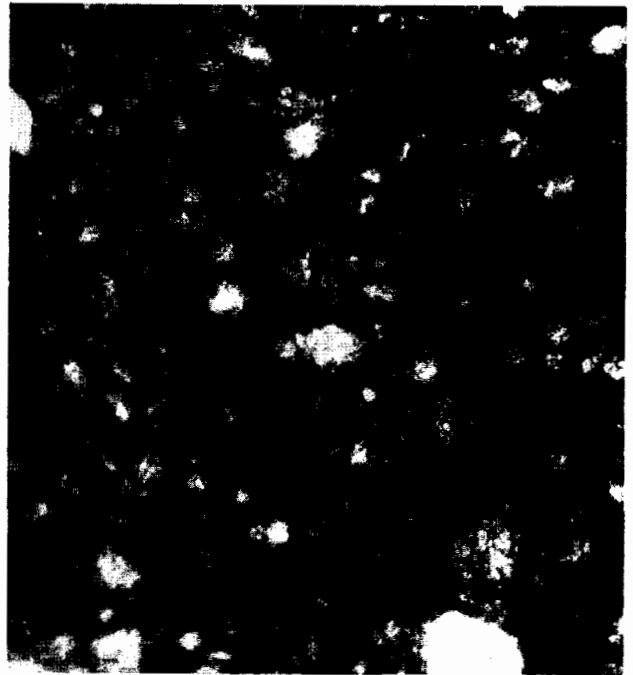


c
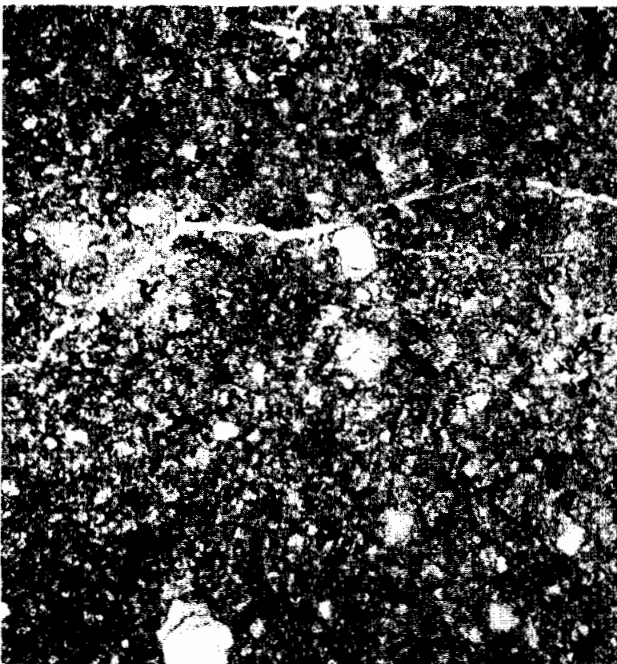


d



a) 60016,83. general matrix,ppl.
   width 2mm.

b) 60016,83. vitric breccia clast,
   ppl. width 0.5mm.

c) 60016,86. fine-grained poikilitic
   melt clast, ppl.  width 2mm.

d) 60016,98. feldspathic granoblastic
   impactite, xpl. width 2mm.

anorthosite with relict cumulate texture, dark-to-vitric matrix breccia and clast-bearing basaltic impact melt.  Also present are several types of glass beads and fragments in various stages of devitrification, and rare agglutinates. Most of the clasts show minimal effects of shock or thermal metamorphism.

Plagioclase in mineral and anorthosite clasts is of typical highlands composition ($An_{96-98}$, low Fe, Mg; Johan and Christophe, 1974).  These authors also report systematic variations of Fe, Mg and Na in plagioclase with respect to twin lamellae and associated intergrowths of exsolved pyroxene and silica (Fig.3). Pyroxene clast compositions are given in Figure 4.  One discrete grain of orthopyroxene ($En_{79}$) with ilmenite lamellae yielded an  equilibration temperature of 900-1000°C based on the coexisting mineral compositions (Fig.5) (Haselton and Nash, 1975a,b).  Metal grains in the matrix that are large enough to analyze by microprobe are homogeneous with 4-6% Ni (Fig.6) (Misra and Taylor, 1975).

Nearly all of the dark clasts (Fig.1) are aphanitic melts.  In thin section they are glassy with an obvious melt texture.  Most are packed with abundant plagioclase clasts and could also be called vitric matrix breccias (Fig.2). Poikilitic clasts occur as both coarse-and fine-grained varieties (Fig.2). They are very similar to typical Apollo 16 poikilitic rocks such as 60315 and 65015.  Macroscopically they appear as pale gray crystalline clasts.
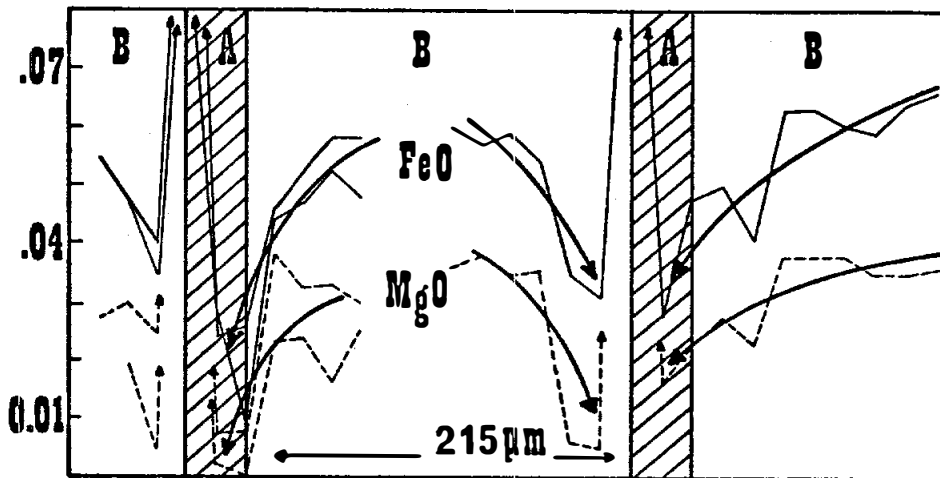


FIGURE 3.  Plagioclase; from Johan and Christophe (1974)
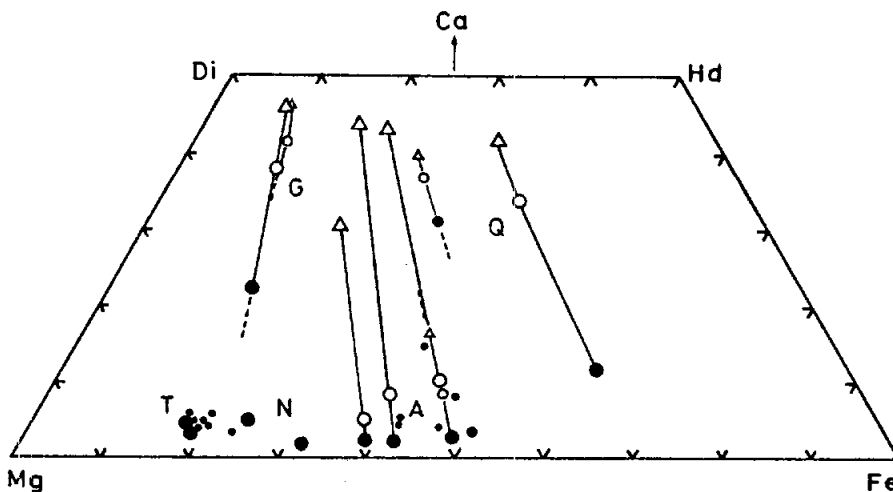


FIGURE 4. Pyroxenes; from Takeda et al. (1979).

13

$$FeSiO_3 + MgTiO_3 = FeTiO_3 + MgSiO_3$$

SKAERGAARD

60016

x DATA FROM CARMICHAEL
o COMPLEX ILMENITE-PYROXENE INTERGROWTHS

T°C/100
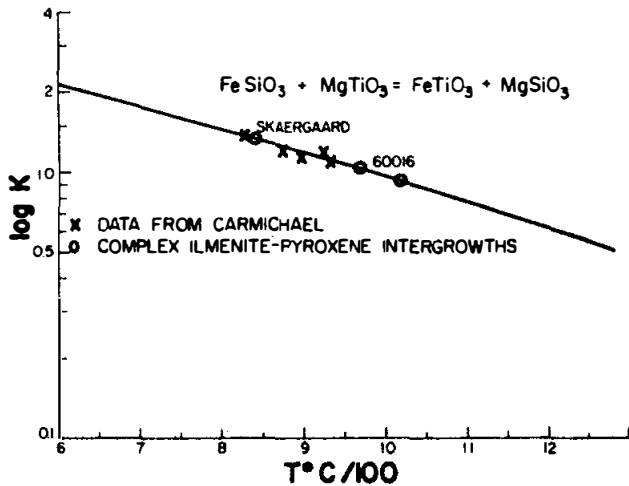
FIGURE 5. Equilibration temperature;
from Haselton and Nash (1975b).



60016
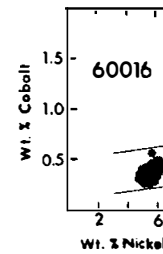
FIGURE 6. Metals; from
Misra and Taylor (1975).

CHEMISTRY: Bulk rock major element analyses are given by Janghorbani et al.
(1973) and S.R. Taylor et al.(1974).Bulk trace element data are provided by
these authors and Krähenbühl et al. (1973),Ganapathy et al. (1973), Garg
and Ehmann (1976), Jovanovic and Reed (1976a,b) and Goel et al. (1975). All
of these analyses are of splits of a single sample of chips and fines sub-
divided at the LCL. Wänke et al. (1975) give major and trace element chemistry
on an aphanitic clast, a poikilitic clast and a granoblastic impactite clast.
Goel et al. (1975) report nitrogen data on separated light and dark clasts.

The bulk rock is compositionally very similar to the local soils, but with
slightly lower $TiO_2$ and $Cr_2O_3$ (Table 1). Its REE pattern (Fig. 7) and Zr/Hf
ratio is typical of a highland breccia with trace element chemistry dominated
by KREEP (S.R. Taylor et al., 1974; Garg and Ehmann, 1976). Krähenbühl et al.
(1973) detect an enrichment of volatile relative to involatile elements (e.g.
high Tl/Cs and Tl/U) and conclude that the rock is probably enriched in a
fumarolic component.

Clast analyses by Wänke et al. (1975) are reproduced in Table 1. Both the
aphanite and the poikilitic clast are rich in KREEP and in siderophiles in-
dicating a probable impact origin. The granoblastic impactite has low levels
of incompatibles and may be low in siderophiles based on Co (Table 1). No other
siderophile data are available on this clast.

STABLE ISOTOPES: Clayton et al. (1973) report $\delta O^{18}$ values, listed in Table 2.
The uniform values indicate a dominant plagioclase component in all samples.

RADIOGENIC ISOTOPES AND GEOCHRONOLOGY: Weber and Schultz (1978) report K-Ar
gas retention ages of 3.8 ± 0.1 b.y. for both the poikilitic and the dark aphanite
clasts analyzed by Wänke et al. (1975).

FIGURE 7.



Figure showing REE plot for sample 60016, Sample/Chondrites versus La Ce Pr Nd Pm Sm Eu Gd Tb Dy Ho Er Tm Yb Lu. Labels: ,48 Poikilitic clast; ,22 Aphanitic clast; ,62 Bulk rock; ,51 Granoblastic clast; Wänke et al., 1975; S. R. Taylor et al., 1974; Wänke et al., 1975.
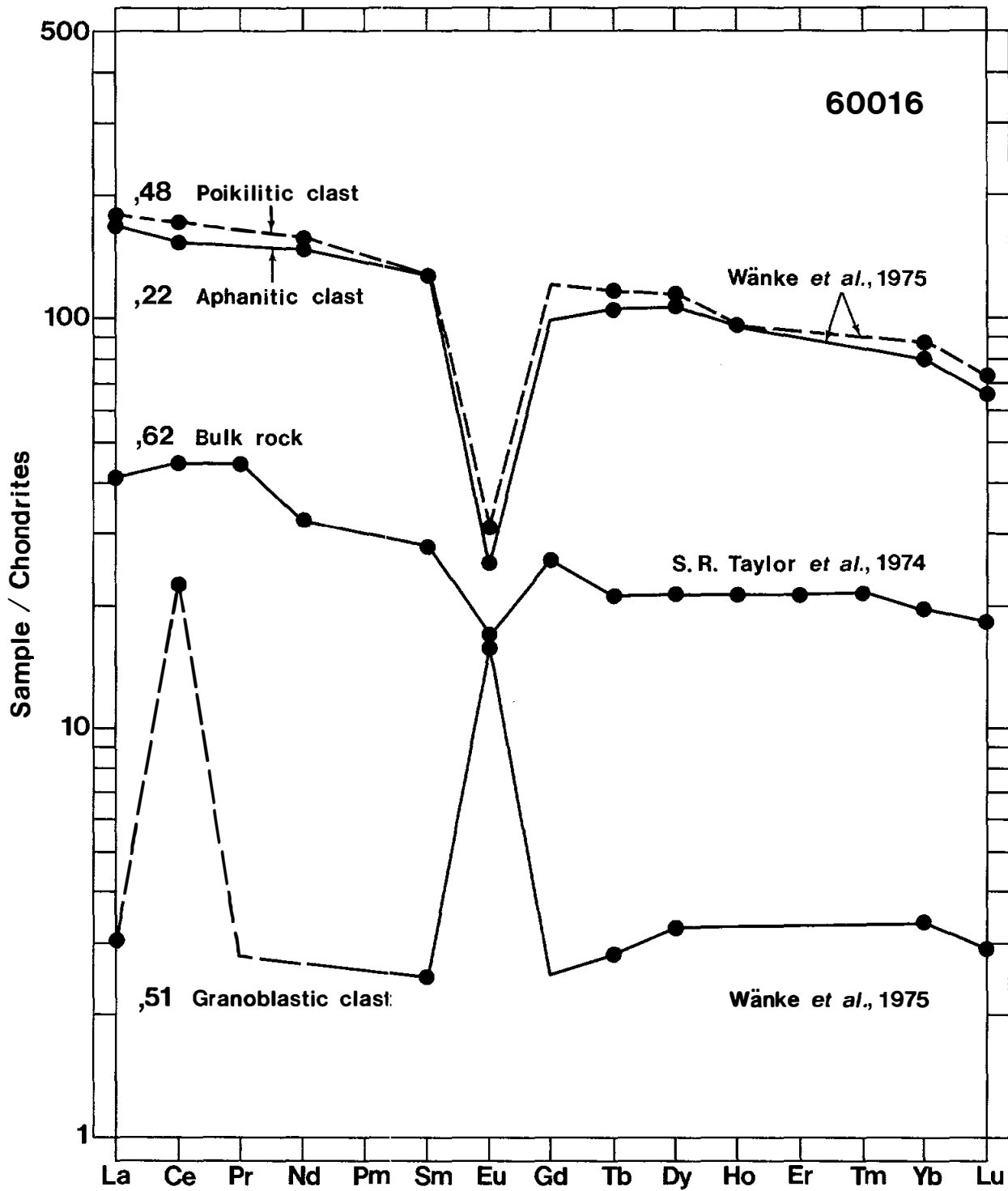
TABLE 1. Summary chemistry of 60016 bulk rock and clasts

| | Bulk rock | ,22.4 aphanite | ,48.4 poikilitic | ,51.4 granoblastic |
|---|---|---|---|---|
| $SiO_2$ | 45.5 | 43.0 | 44.7 | 44.3 |
| $TiO_2$ | 0.29 | | | 0.27 |
| $Al_2O_3$ | 27.4 | 20.03 | 15.88 | 29.48 |
| $Cr_2O_3$ | 0.07 | 0.15 | 0.21 | 0.09 |
| FeO | 4.8 | 7.42 | 11.5 | 4.0 |
| MnO | 0.057 | 0.09 | 0.12 | 0.63 |
| MgO | 6.2 | 7.64 | 12.45 | 3.82 |
| CaO | 15.2 | 11.9 | 10.8 | 17.2 |
| $Na_2O$ | 0.48 | 0.49 | 0.60 | 0.31 |
| $K_2O$ | 0.10 | 0.29 | 0.33 | 0.01 |
| $P_2O_5$ | | | | |
| Sr | | 160 | | 190 |
| La | 13.3 | 55.9 | 58.5 | 0.99 |
| Lu | 0.6 | 2.27 | 2.46 | 0.10 |
| Rb | 2.3 | | | |
| Sc | 8.2 | 13.6 | 15.6 | 7.43 |
| Ni | 300 | 740 | 1940 | |
| Co | 27 | 42.3 | 105 | 6.19 |
| Ir ppb | 5.7 | 15 | 36 | |
| Au ppb | 5.9 | 15 | 36 | |
| C | | | | |
| N | 28 | | | |
| S | | | | |
| Zn | 7.6 | | | |
| Cu | | | | |

All clast analyses by Wänke et al. (1975).
Oxides in wt%; others in ppm except as noted.

TABLE 2

$\delta O^{18}$ of various portions of 60016

| matrix | 5.73 |
|---|---|
| plagioclase | 5.78 |
| light clasts | 5.62 |
| dark clasts | 5.67 |

RARE GAS/EXPOSURE AGES: Bogard et al. (1973) and Weber and Schultz (1978) provide noble gas data for the bulk rock. The matrix of 60016 contains a large amount of trapped solar gas, probably indicating a significant regolith component.

Noble gas data and $^{21}Ne$ and $^{38}Ar$ exposure ages for clasts (Table 3) are also given by Weber and Schultz (1978).

TABLE 3.  $^{21}$Ne and $^{38}$Ar exposure ages (m.y.) of three clasts
from 60016

| | | $^{21}$Ne | $^{38}$Ar |
|---|---|---|---|
| ,22.4 | aphanite | 1.2 ± 0.2 | 3.0 ± 4.0 |
| ,48.4 | poikilitic | 3.5 ± 0.7 | 4.0 ± 1.5 |
| ,51.4 | granoblastic | 0.3 ± 0.1 | 1.2 ± 0.4 |



Crater diameter, μm
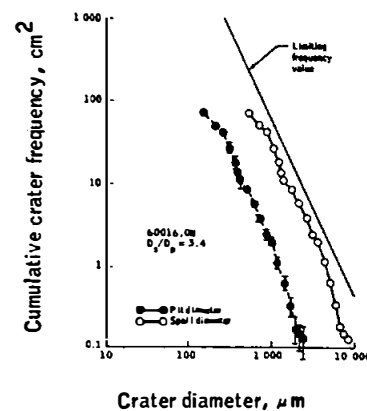
FIGURE 8. Microcraters;
from Morrison et al.
(1973).

MICROCRATERS: 60016 is subrounded in shape with microcraters on all sides. This suggests a complex exposure history that includes tumbling. The surface is probably in cratering equilibrium (Fig. 8) (Morrison et al. 1973; Neukum et al., 1973). Total exposure of the rock after lithification may have been on the order of 15-20 million years, assuming a constant micrometeoroid flux rate (Morrison et al., 1973).

PHYSICAL PROPERTIES:  Intrinsic and structure sensitive magnetic parameters and some characteristics of the natural remanent magnetization of 60016 were measured by Nagata et al. (1974,1975) and Cisowski et al. (1975). No significant NRM residue remains in the rock after 250 Oe·rms demagnetization. Therefore there is no magnetic component present which can be attributed to ordinary thermoremanent magnetization although the relatively stable component up to 250 Oe·rms may have some significance for lunar magnetism (Nagata et al., 1974).

The proportions of Fe-bearing phases, the $Fe^0/Fe^{2+}$ ratio and the average composition of the ferromagnetic metal component have also been determined by magnetic and Mossbauer techniques (Huffman et al., 1974; Nagata et al., 1974). Iron metal makes up ∿0.33 wt% of the rock. About 71% of this ferromagnetic metal can be attributed to a kamacite component averaging ∿5 wt% Ni (erroneously reported as 15 wt% Ni in Nagata et al., 1974). The remainder of the metal is apparently pure iron. This contrasts with the microprobe data of Misra and Taylor (Fig. 6) which show no metal with <4 wt% Ni. Nagata et al. (1975) conclude that this discrepancy can be resolved if the pure iron component exists as micron-size particles too small to analyze by microprobe and possibly forming by subsolidus reduction of oxide and silicate phases. FMR studies show that the metal was annealed at 700-900°C (Fig. 9) (Tsay and Bauman, 1975).

The reflectance (albedo) of the 60016 matrix has been measured by Adams and McCord (1973) and Charette and Adams (1977) (Fig. 10). Dollfus and Geake (1975) report polarimetric properties of both the poikilitic and the aphanite clast analyzed by Wänke et al. (1975).

17

60016
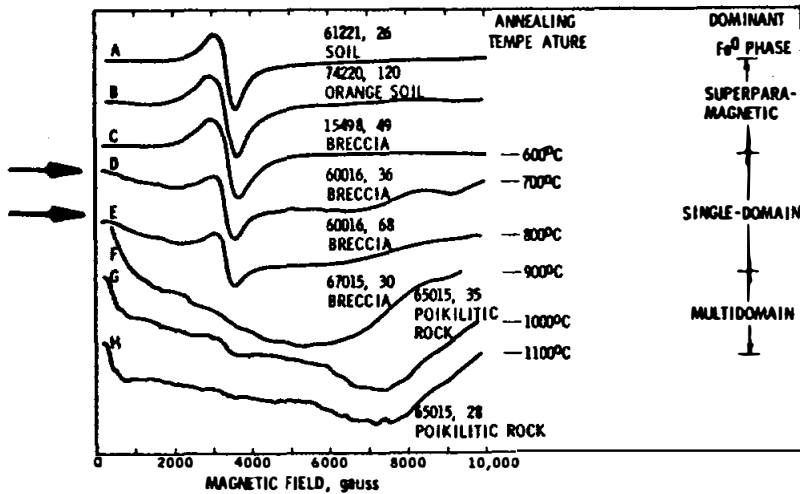


FIGURE 9. Correlation between ferromagnetic resonance and annealing temperature for metal phases; from Tsay and Baumann (1975)
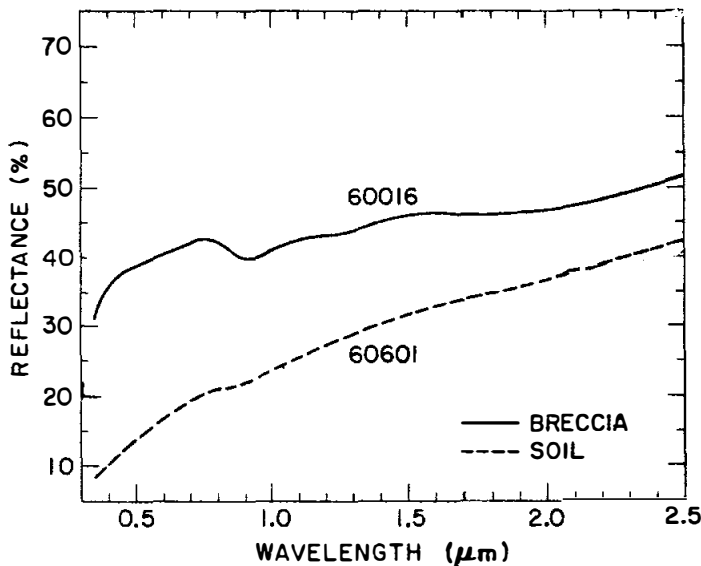


FIGURE 10. Spectral reflectance compared to mature soil; from Adams and McCord (1973).

PROCESSING AND SUBDIVISIONS: In 1972, 60016 was sawn into three main pieces and the slab extensively subdivided and allocated (Fig. 11). All of the various "whole rock" properties published so far were measured on splits of the slab. Bulk chemistry, the oxygen isotopes and rare gases were measured on splits of one undocumented sample of chips and fines (originally ,49-not shown on Fig. 11). The aphanite clast analyzed for chemistry, rare gases, exposure age and polarimetric properties was an interior clast (,48). The poikilitic clast also analyzed for the same properties was a pale gray exterior clast (,22 and ,23). The granoblastic clast was a large white exterior clast (,51 and ,53). Not all splits of the rock are shown in Figure 11.

FIGURE 11.

19
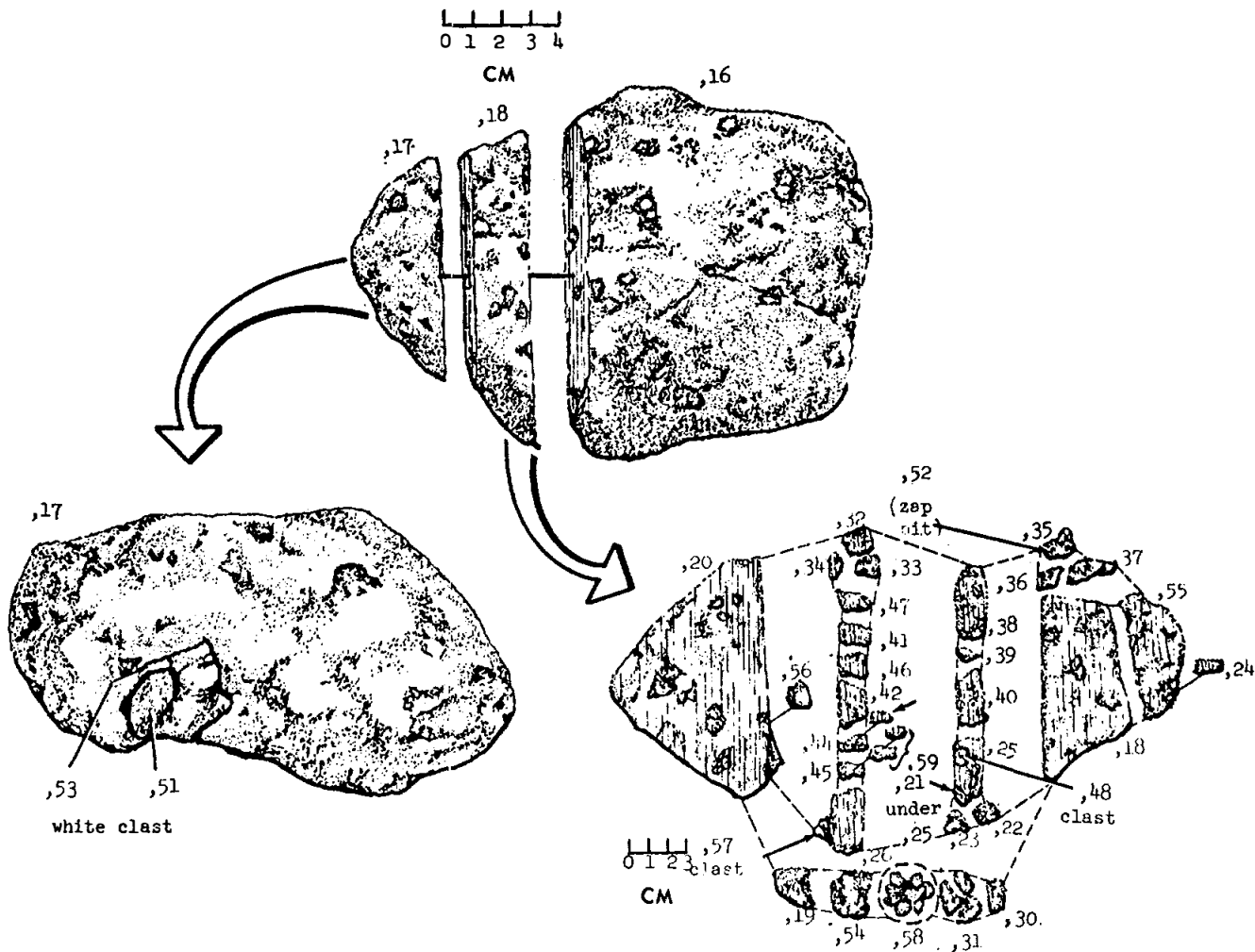
INTRODUCTION: 60017 is a crystalline, medium to dark gray, vesicular melt rock, containing clasts which are mainly dark melt breccia and macroscopically indistinct (Fig. 1). The melt, which has a variolitic texture, contains ~ 30% $Al_2O_3$.

Despite its number, 60017 was collected from Shadow Rock at Station 13 but its precise location on the boulder is unknown. Because it was broken from the boulder, one surface (B) is fresh while the others are subrounded. Few zap pits occur even on the surfaces that were exposed on the lunar surface.

FIGURE 1. Saw cut face. S-75-33756. Scale in mm.



PETROLOGY: The rock contains two dominant lithologies: ~70% variolitic melt and ~30% dark aphanitic clasts (Fig. 2). The rock is heterogeneous at the thin section scale such that some thin sections contain only variolitic melt whereas others contain very little of it. Petrographic information of various thin sections is provided by Kridelbaugh et al. (1973), Nord et al. (1975), Misra and Taylor (1975), Ganapathy et al. (1974), and Englehardt (1979). Cadenhead and Brown (1976) provide some details of a surface chip.

a

b
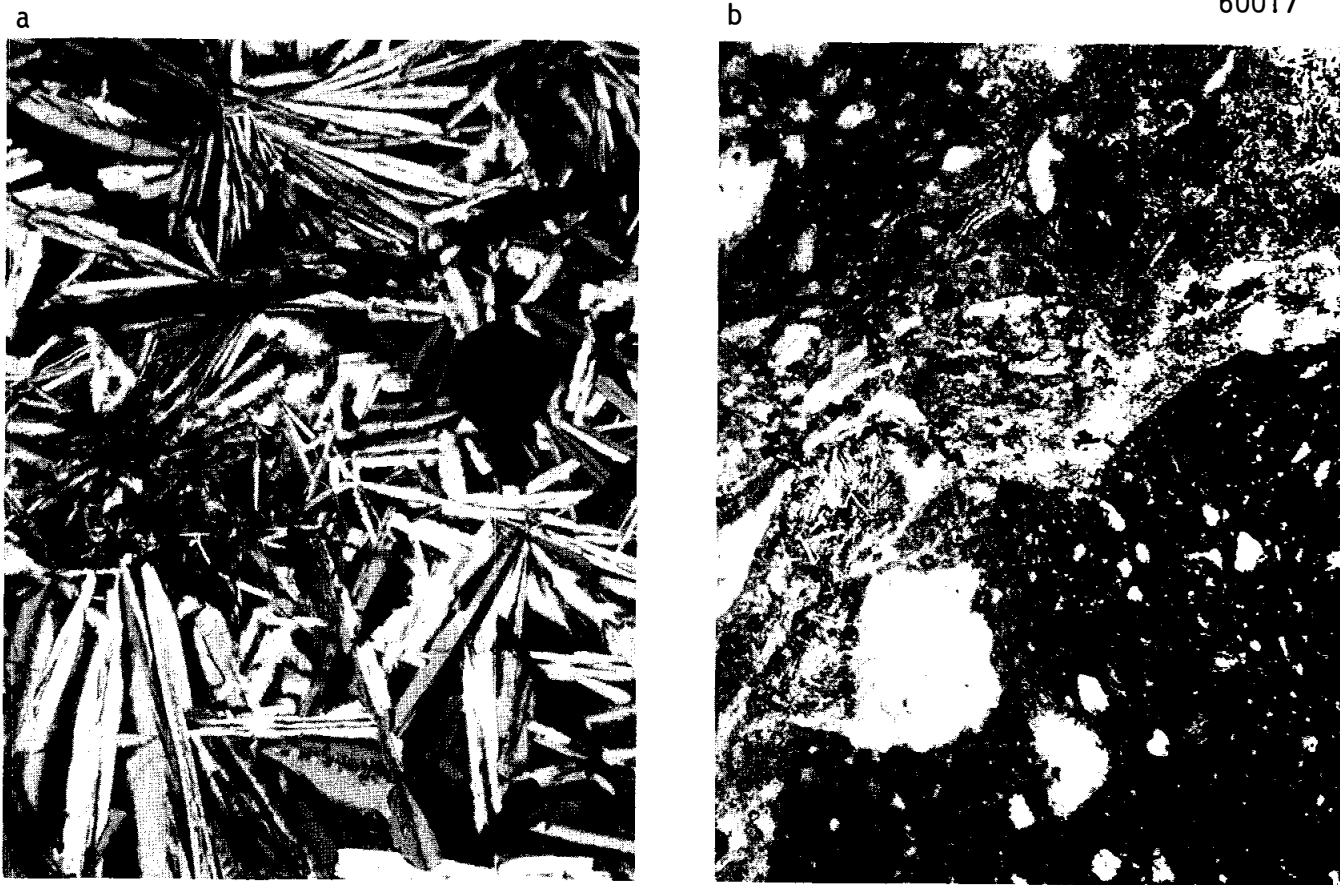


FIGURE 2.   a) 60017,116. variolitic melt, xpl.  width 2mm.
           b) 60017,119. aphanitic melts,ppl. width 2mm.

The variolitic melt consists of plagioclase laths with interstitial mafic
minerals, minor ilmenite and Fe-metal, and very rare troilite and cryptocrystal-
line material.  Although referred to as "devitrified glass" by Kridelbaugh et al.
(1973) and Misra and Taylor (1975) the evidence leading to this conclusion is not
stated.  The typical textures are shown in Figure 2.  The plagioclase laths which
are up to ~2mm long have compositions of $An_{93-95}$ (Kridelbaugh et al., 1973).
They are frequently skeletal and mainly untwinned.  Spherulites are often cored
by plagioclase xenocrysts.  Analyses of mafic minerals by Kridelbaugh et al. (1973)
show only olivine ($Fo_{68}$), although Nord et al. (1975) and Engelhardt (1979) refer
to the mafic mineral as pyroxene.  Analyses of metal by Misra and Taylor (1975)
have an average of 5.7% Ni, 1.3% Co, 0.05% P and 0.01% S.  Co shows a wide scatter
and is mainly out of the meteoritic range (Fig. 3).  Nord et al. (1975), in a high
voltage electron microscopy study, found no glass or evidence of deformation.

The variolitic melt is generally finer-grained towards the dark breccia clasts,
and contains rare xenocrysts of pink spinel and a few small lithic clasts,
including dunitic material.

FIGURE 3. Metals; from Misra and Taylor
          (1975).



21
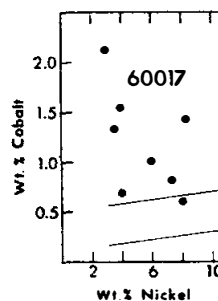
The dark breccia clasts are brown, aphanitic and inhomogeneous melt breccias. In places they are flow banded and deformed (Fig. 2). They are plagioclase-rich (>85%) and contain numerous plagioclase-rich xenocrysts and xenoliths which have various reaction rims. Petrographic descriptions are given by Kridelbaugh et al. (1973) and Nord et al. (1975). The former in particular note the bulk composition of "gabbroic anorthosite" and the variety of xenoliths, including shocked, re-crystallized anorthosite ($An_{94-96}$) and small "anorthositic gabbro" (actually basalt-textured)clasts(?) which have plagioclase laths ($An_{95}$), interstitial olivine ($Fo_{62-74}$) and thin dark rims. Nord et al. (1975) note the presence of some isotropic material and deformation with low dislocation densities within the dark breccia material.

The boundary between the variolitic melt and the dark breccia clasts is generally distinct, but in places it is diffuse and irregular, suggesting considerable digestion of the clasts. Cadenhead and Brown (1976) describe the characteristics of a surface chip ( ,43) using various methods. The petrography of the chip is not known but they find it to be heterogeneous, not porous at sub-micron scales, and of low density (2.78 g/cc). The surface is enriched in volatiles and surface iron is reduced more than the interior.

CHEMISTRY: Major and trace element analyses of bulk rock (Table 1) are presented by Janghorbani et al. (1973), Rose et al. (1973), Laul and Schmitt (1973), Laul et al. (1974), Morrison et al. (1973) and S.R. Taylor et al. (1973). Krahenbühl et al. (1973) and Ganapathy et al. (1974) report siderophile and other trace elements, Garg and Ehmann (1976) report trace elements, Tera et al. (1974) report U, Th, and Pb abundances, and Flory et al. (1973) report hydrocarbon and light element abundances. The latter suggest the presence of indigenous lunar methane. MacDougall et al. (1973) give a U abundance (∿0.2 ppm) from fission track mapping. These are probably mainly analyses of variolitic melt.

Although Morrison et al. (1973) state that they received and analyzed a white chip, photodocumentation demonstrates that they received a dark vesicular chip. Nonetheless their analysis is significantly different from other analyses, in particular being lower in alumina and higher in magnesia. Krähenbühl et al. (1973) and Ganapathy et al. (1974) give incorrect split numbers; they actually analyzed ,80.

60017 is significantly more aluminous than local soil compositions and has a positive Eu anomaly (Fig. 4). It is similar to sample 63335 taken from the same boulder. The trace siderophiles are low (although not at indigenous levels) as are many North Ray Crater samples. The siderophile element ratios place the sample in meteoritic Group 6 of Ganapathy et al. (1974). Rose et al. (1973) obtained higher Ni and Ni/Co than other analysts.

Defocussed beam microprobe analyses of the dark breccia and their included "anorthositic gabbro" clasts are reported by Kridelbaugh et al. (1973). The dark breccia is similar in composition to the bulk breccia analyses, while the "anorthositic gabbro" clasts are much less aluminous (Table 1).

TABLE 1. Summary chemistry of 60017

| | Bulk rock or variolitic melt | dark breccia* | "anorthositic gabbro"* |
|---|---|---|---|
| $SiO_2$ | 44 | 46 | 46 |
| $TiO_2$ | 0.3 | 0.2 | 1.1 |
| $Al_2O_3$ | 31.0 | 31.2 | 22.9 |
| $Cr_2O_3$ | 0.06 | | |
| FeO | 3 | 3.3 | 9.2 |
| MnO | 0.04 | | |
| MgO | 3 | 2.4 | 6.4 |
| CaO | 17.0 | 17.4 | 14.0 |
| $Na_2O$ | 0.53 | 0.03 | 0.76 |
| $K_2O$ | 0.07 | 0.43 | 0.05 |
| $P_2O_5$ | 0.02 | 0.02 | 0.06 |
| Sr | 140 ? | | |
| La | 3.0 | | |
| Lu | 0.16 | | |
| Rb | 0.8 | | |
| Sc | 6 | | |
| Ni | 50 | | |
| Co | 7 | | |
| Ir ppb | 1.4 | | |
| Au ppb | 0.4 ? | | |
| C | 30-105 | | |
| N | 7-24 | | |
| S | 120 | | |
| Zn | 5 | | |
| Cu | 2 | | |
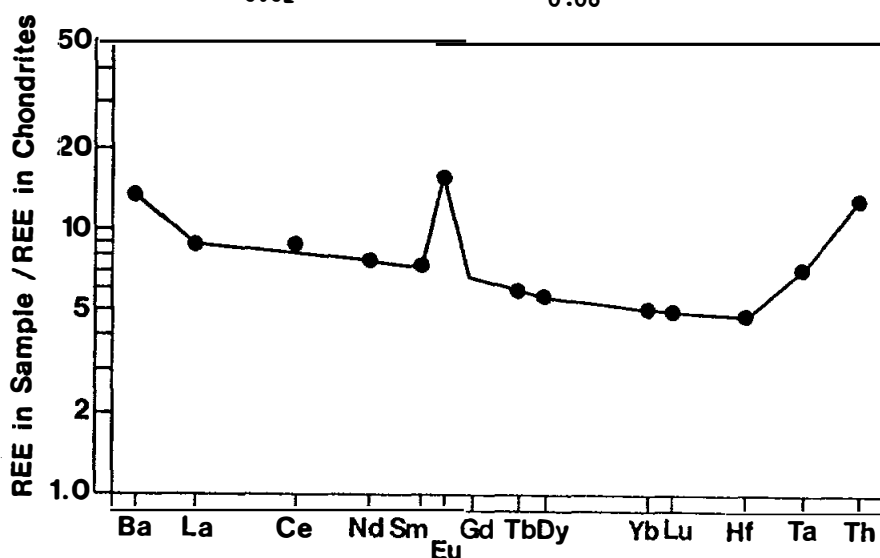
Oxides in wt%; others in ppm except as noted

*from DBA, Kridelbaugh et al.(1973)



FIGURE 4. Rare earths; from Laul and Schmitt (1973).

RADIOGENIC ISOTOPES AND GEOCHRONOLOGY: Murthy and Coscio (1977) and Murthy (1978) report $^{87}Sr/^{86}Sr$ for two hand-picked plagioclase clasts, which extrapolate to values close to BABI at 4.6 b.y. (Table 2)

Table 2. $^{87}Sr/^{86}Sr$ for plagioclase clasts in 60017,56

| | $^{87}Sr/^{86}Sr$ | $^{87}Sr/^{86}Sr$ at 4.6 b.y* |
|---|---|---|
| I | 0.69933+5 | 0.69900+5 |
| II | 0.69928+5 | 0.69899+5 |

* adjusted for bias by subtracting 0.00006 to be equivalent to Caltech data

Tera et al. (1974) report U, Th and Pb isotopic data for 60017,72, a bulk rock sample. The sample contains predominantly initial radiogenic lead rather than in situ -produced lead. The sample falls off a reference isochron which encompasses most other highlands samples on a $^{207}Pb/^{206}Pb$ v. $^{238}U/^{206}Pb$ evolution diagram (Fig. 5). The departure can be accounted for by assuming that the sample formed at ∿4.0 b.y.from a source ∿4.4 b.y.old or formed at ∿3.9 b.y.from a source 4.5 b.y. old.
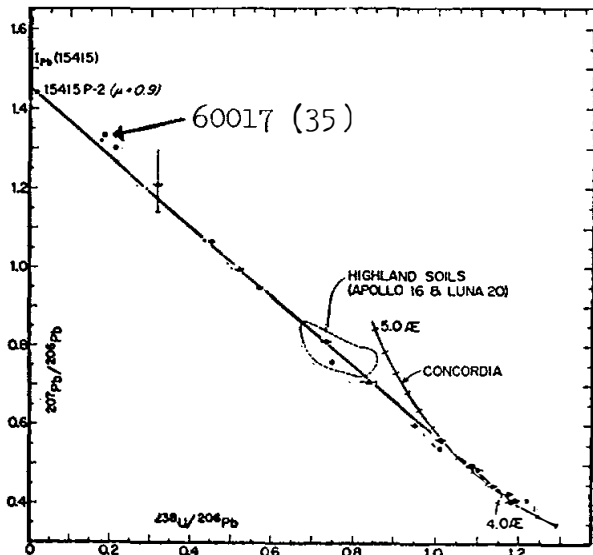


FIGURE 5. U-Pb evolution diagram. Reference isochron passes through total rock and plagioclase for rock 68415. Number in parentheses is μ value; from Tera et al.(1974).

TRACKS AND RELATED STUDIES : MacDougall et al. (1973) measured the U content from fission tracks, but found no solar flare tracks in olivine or feldspar. Fireman et al. (1973) report count rates for $^3H$, which is less abundant in the interior than the surface.

PHYSICAL PROPERTIES: Housley et al (1976) found that 60017,84 (bulk rock) has a very weak ferromagnetic resonance and is thus unlike either soils or soil breccias. Gold et al. (1974, 1975,1976a) used 60017 for calibration in Auger electron spectroscopy of samples. They found that the albedo (0.5) of 60017 does not decrease to highland soil albedo levels merely by crushing.

PROCESSING AND SUBDIVISIONS: A few small fragments were chipped off the samples prior to its sawing in late 1972. During sawing several fragments were produced (Fig. 6). The two largest pieces ,18 and ,52 and several small pieces are preserved intact. Slab A was dissected as shown in Figure 7, and ,17 was dissected to give splits ,53 through ,88 (Fig. 6). Most allocations have been made from the subdivisions of ,17.

Slab A

,18
Slab A
,15
,17
,52
,16
,35
,14
,13
,19
,11
,12

,70*  ,66
,17
,65  ,73  ,74
,85
,71  ,80
,57
,50
,55
,64  ,49
,79
,68*
,56*
,72*
,53
,67
,69
,75*
,60
,61
,54
,78
,59
,58
,63
,62

T₁
S₁

S₁
8

,61  ,65:

*Not oriented

,77  ,81  ,82  ,83  ,84  ,86 and
,87 undocumented chips

0  1  2  3  4
CM
Approx scale
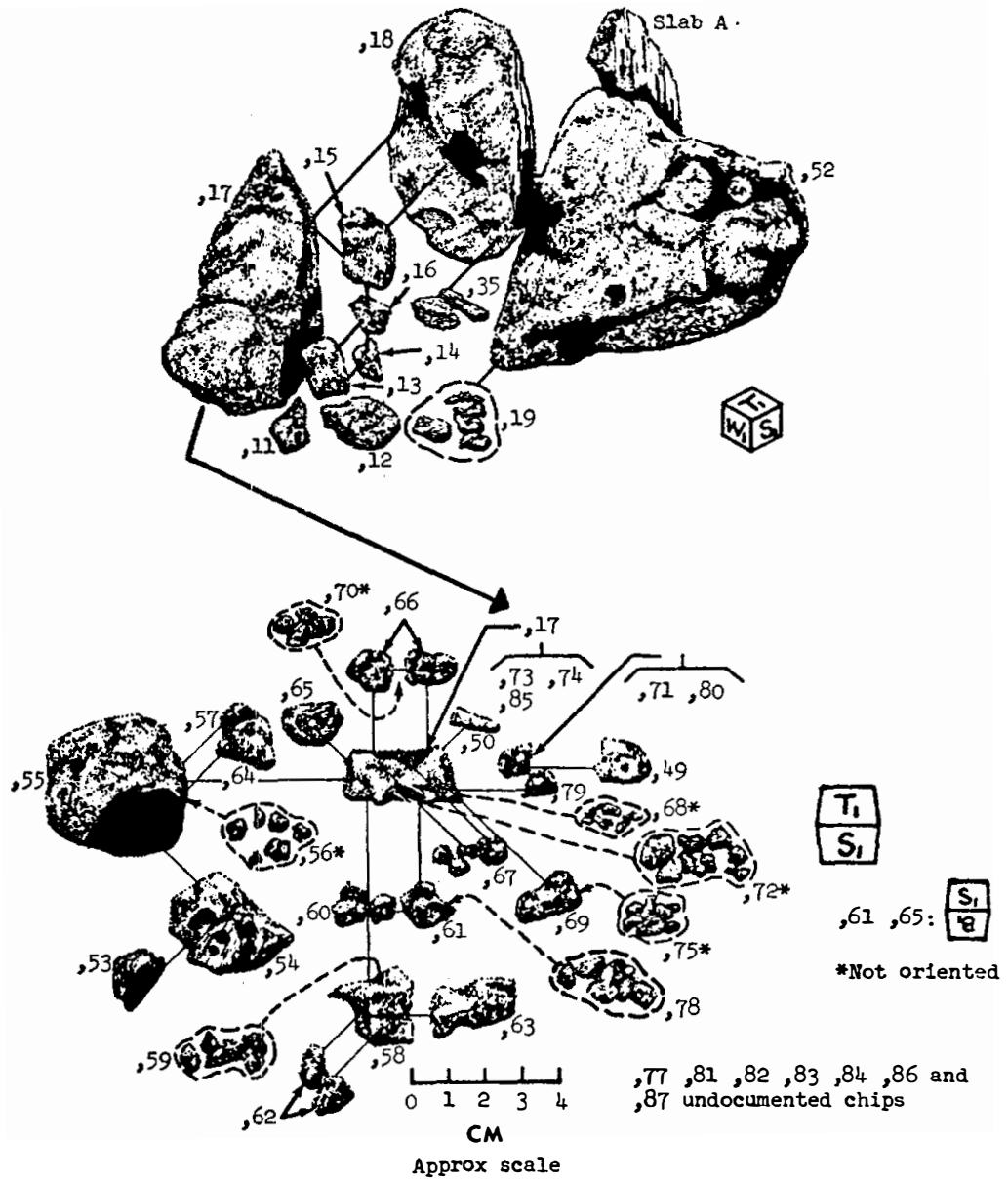
FIGURE 6. Cutting diagram

FIGURE 7. Subdivision of slab.
S-73-21544.



60017
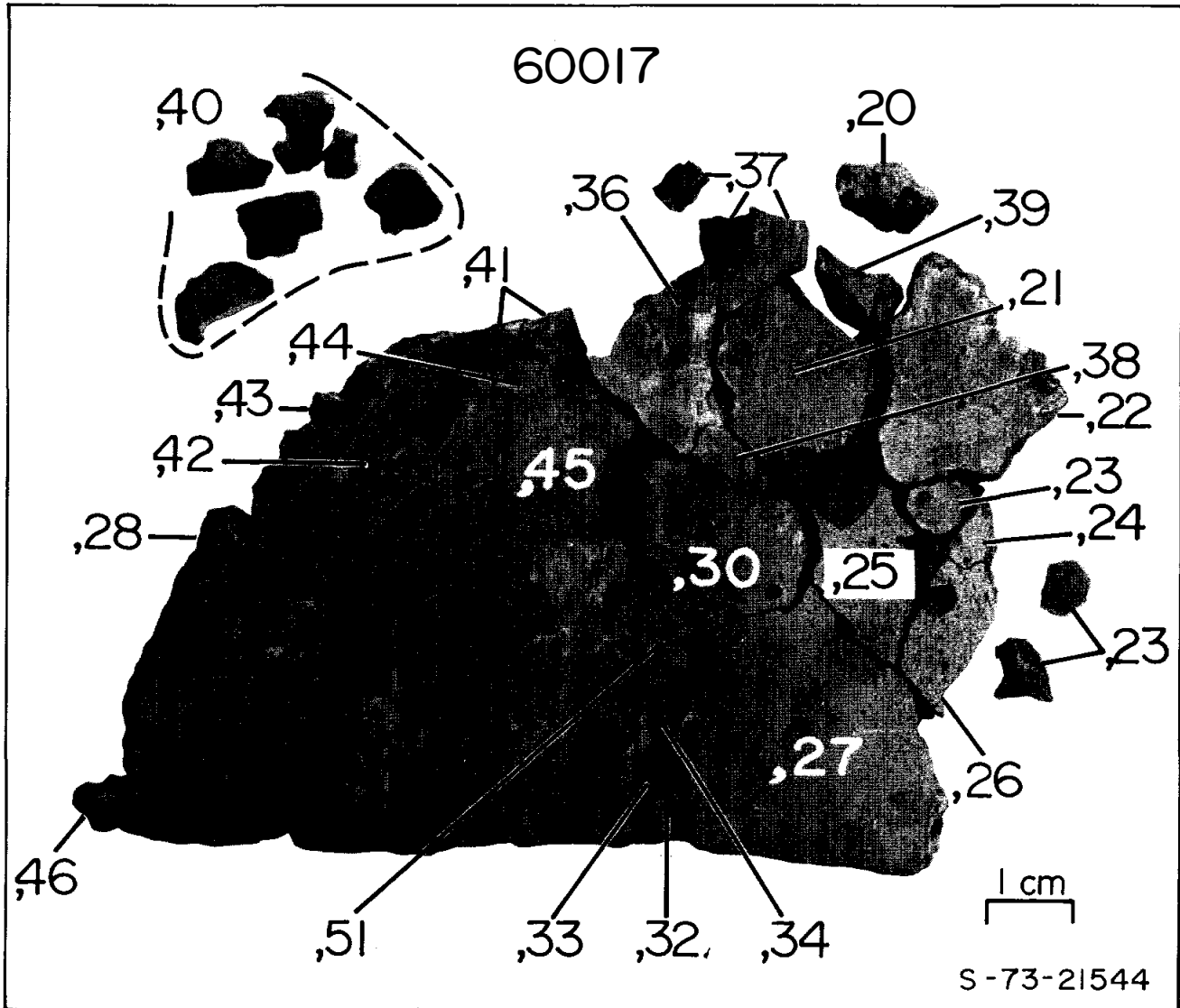
INTRODUCTION:   60018 is a coherent, medium gray, basaltic impact melt that
suffered a variety of shock effects after lithification.  Extensive fractures
and a network of glass veins penetrate the rock (Fig. 1).  A dark, vesicular
glass coats the exterior surfaces.

60018 was chipped from a 50 cm boulder 100 m southwest of the Lunar Module.
This boulder was perched and subrounded.  The location and orientation of
60018 are known.  Many zap pits are present on the lunar-exposed surface.

FIGURE 1. Saw cut face. S-78-31788. Scale in mm.



PETROLOGY:   Although intensely shocked, a relict melt texture is clearly
discernable over much of the rock.  An intergranular basaltic texture is
most common with plagioclase laths often forming radial clusters (Fig. 2).
Areas of fine-grained breccia and patches with a poikilitic to subophitic
texture are also present.  Grain size of the melt matrix varies dramatically
over short distances; maximum crystal length is ∿1 mm.
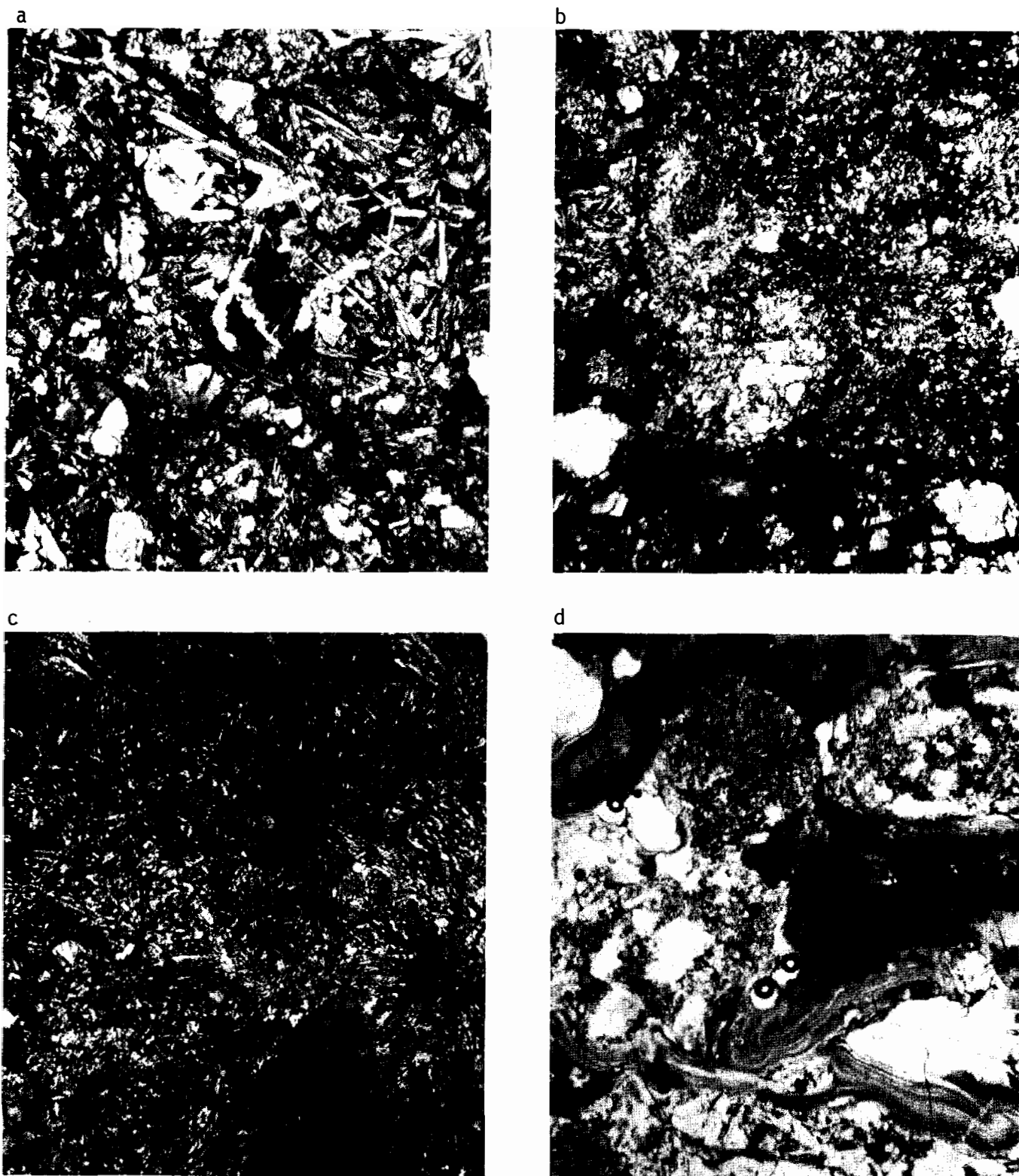
60018



FIGURE 2. a) 60018,53. general view, basaltic, xpl. width 2mm.
b) 60018,57. general view, poikilitic and glassy, xpl. width 2mm.
c) 60018,51. spherulitic, glassy, xpl. width 2mm.
d) 60018,51. glass veins, ppl. width 2mm.

Plagioclase xenocrysts are abundant.  Clasts of anorthosite and noritic.
anorthosite (up to ∿1 cm) are somewhat less common.  Metal fragments have Ni
and Co contents which plot within the "meteoritic field" (Reed and Taylor,
1974).  Troilite and schreibersite are occasionally associated with the metal.
Figure 3 shows that many of the kamacite particles not associated with schreiber-
site are nevertheless enriched in P relative to meteoritic metal.  Some rust is
also present. Late stage silicate-liquid immiscibility is apparent in some
interstitial areas.

Both the clasts and the host basalt show extreme shock effects.  Many of the
plagioclase laths and clasts have been converted to maskelynite or recrys-
tallized.  In the most severely altered zones interstitial mafics have been
converted to small rounded grains (Fig. 2).

A complex network of glass veins penetrates the rock and is probably related
to the glass coat.  In thin section these veins are green to brown, often con-
tain schlieren and debris, and seem especially common along clast-matrix
boundaries.  The intrusion of these glass veins appears to postdate the lithifi-
cation of the rock and is probably related to the event which caused the in-
tense shock metamorphism.
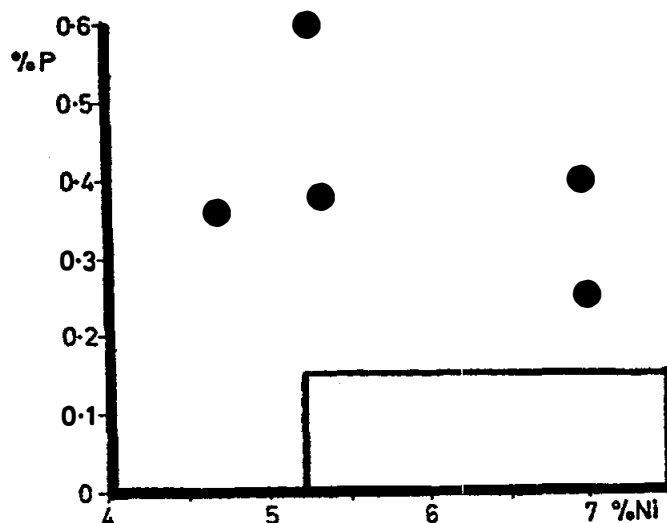
FIGURE 3. P v. Ni for metal; from Reed and Taylor (1974).

CHEMISTRY:  S.R. Taylor et al. (1973) and Haskin (unpublished) have analyzed bulk
rock samples for major and trace elements.  Haskin (unpublished) has also anal-
yzed clasts and glass samples.  Cripe and Moore (1974), Moore and Lewis (1976),
Moore et al. (1973) and Goel et al. (1975) provide carbon, nitrogen and sulfur
data.  Nunes et al. (1974) provide U, Th, and Pb abundances.

REEs in the basalt are high (Fig. 4). This, along with the high bulk Ni values
and metal compositions, indicates that the rock was a clast-laden impact melt with
significant KREEP and meteoritic components.  Also notable is the extreme en-
richment in sulfur relative to the other light elements (Table 1).

The glass veins are significantly more aluminous than the basalt and have lower
levels of incompatible elements (Table 1).  Thus the glass is not a whole rock

29

melt of the basalt.

White clasts analyzed by Haskin are virtually pure plagioclase or anorthosite based on their low contents of FeO and REEs (Table 1 ). One black clast, also analyzed by Haskin, is ultramafic with high FeO and very low levels of REEs (Table 1).

TABLE 1.  Summary chemistry of

the melt matrix (basalt), clasts and glass veins of 60018

|  | Basalt | Glass * | White clasts * | Black clasts * |
|---|---|---|---|---|
| $SiO_2$ | 45.7 | 44.9 | | |
| $TiO_2$ | 0.65 | 0.359 | | |
| $Al_2O_3$ | 24.0 | 28.5 | | |
| $Cr_2O_3$ | 0.11 | 0.086 | 0.006 | 0.04 |
| FeO | 5.6 | 4.60 | 0.3 | 34.8 |
| MnO | 0.07 | 0.048 | 0.015 | 1.07 |
| MgO | 8.9 | 4.83 | | |
| CaO | 13.8 | 16.6 | | |
| $Na_2O$ | 0.54 | 0.492 | 0.424 | 0.02 |
| $K_2O$ | 0.23 | 0.103 | | |
| $P_2O_5$ | | | | |
| Sr | | | | |
| La | 25 | 10.7 | 0.38 | (Sm=0.042) |
| Lu | 1.1 | 0.46 | 0.003 | |
| Rb | 7.7 | 3.1 | | |
| Sc | 9.1 | 6.0 | 0.44 | 7.1 |
| Ni | 400 | 520 | | |
| Co | 29 | 43 | 0.54 | 71 |
| Ir  ppb | | | | |
| Au  ppb | | | | |
| C | 32 | | | |
| N | 29 | | | |
| S | 2250 | | | |
| Zn | 2.2 | 2.6 | | |
| Cu | | | | |

Oxides in wt%; others in ppm except as noted.
*from Haskin (unpublished)

TABLE 2.  Oxygen isotope data

|  | $\delta O^{18}$ | $\delta O^{17}$ |
|---|---|---|
| Whole rock | 5.69 | |
| Light clast | 5.60 | |
| "Cataclastic anorthosite"* | 5.60 | 2.75 |

*Listed in Clayton and Mayeda (1975) as 60018,43.
Photodocumentation shows that this split is mostly basalt but also contains a large white clast.

FIGURE 4. Rare earths.
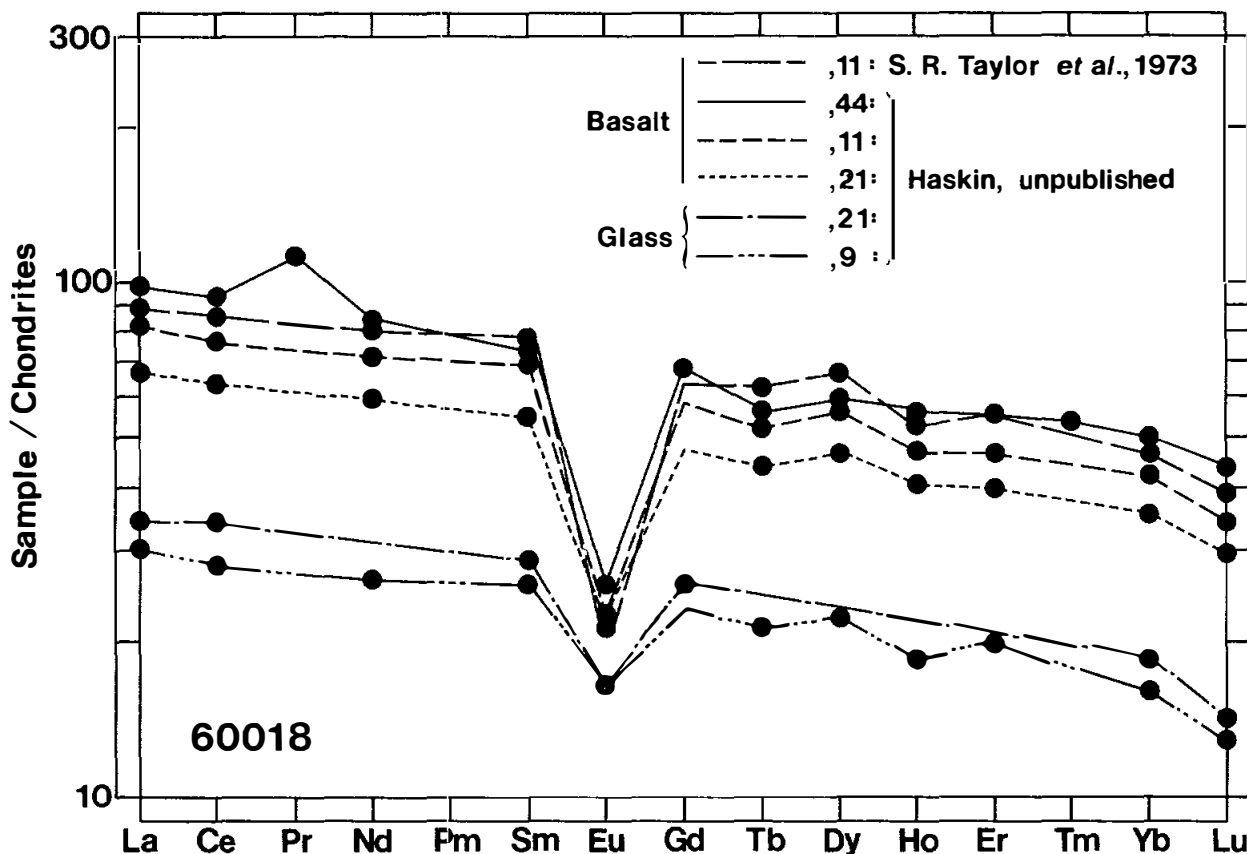


STABLE ISOTOPES: Clayton et al. (1973) and Clayton and Mayeda (1975) report $\delta O^{18}$ and $\delta O^{17}$ data for clasts and the bulk rock (Table 2).

RADIOGENIC ISOTOPES AND GEOCHRONOLOGY: Nunes et al. (1974, 1977) provide U-Th-Pb data for several splits of the rock. Many of their samples had sawn surfaces and were significantly (up to 77%) contaminated with terrestrial lead (Fig. 5). Only their "whole rock" and hand-picked glass samples do not appear to be contaminated. The "whole rock" analysis is nearly concordant at 4.2 b.y. but the glass contains excess Pb relative to U suggesting that the glass may be fused soil (Nunes et al., 1974,1977).

PHYSICAL PROPERTIES : Sugiura et al.(1978) report the results of paleontensity experiments performed while heating the sample under controlled $fo_2$ (Thellier's method) (Fig. 6). The natural remanent magnetization (NRM) of the rock is fairly strong and stable against AF-demagnetization although an ancient remanent magnetization probably is not present. As most of the NRM is thermally de-magnetized by 400° C, low temperature shock events may have been responsible for the remanent magnetization that is present. Some of the magnetic properties can also be accounted for by the chemical changes produced by heating.

Δ = 60018
1 = Whole rock
2 = <100 mesh (magnetics removed)
3 = Handpicked glass
4 = Magnetics
5 = Handpicked dark gray
6 = Handpicked light gray
7 = Handpicked white
M.T. = Modern terrestrial

Contamination line

Area of insert
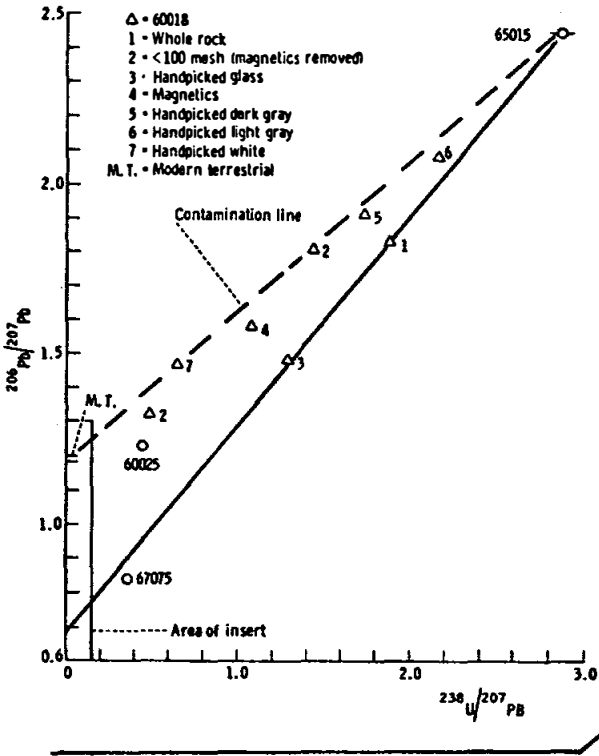
FIGURE 5. U-Pb data; from Nunes et al. (1977).
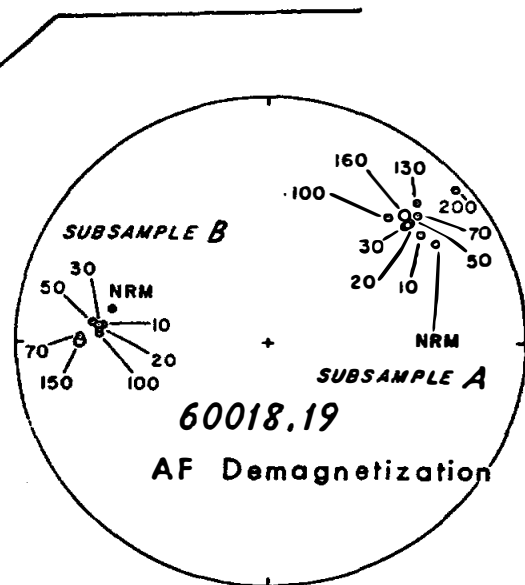


FIGURE 6. Demagnetization; from Sugiura et al. (1978).

SUBSAMPLE B

SUBSAMPLE A

60018,19

AF Demagnetization

Directional change of NRM during AF demagnetization for two pieces of 60018,19. Relative orientation of these two pieces is not known.

A(170 Oe, IRM)
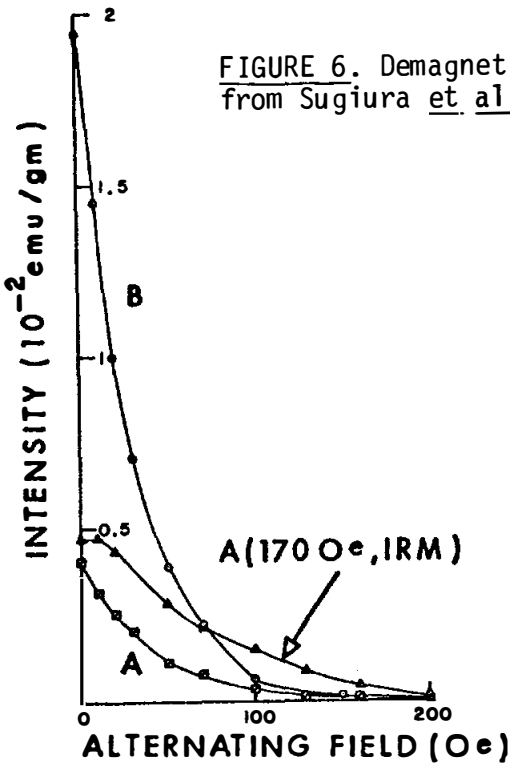
AF demagnetization of NRM for two pieces (A and B) of 60018,19 and of IRM for piece A.

Thermal Demagnetization
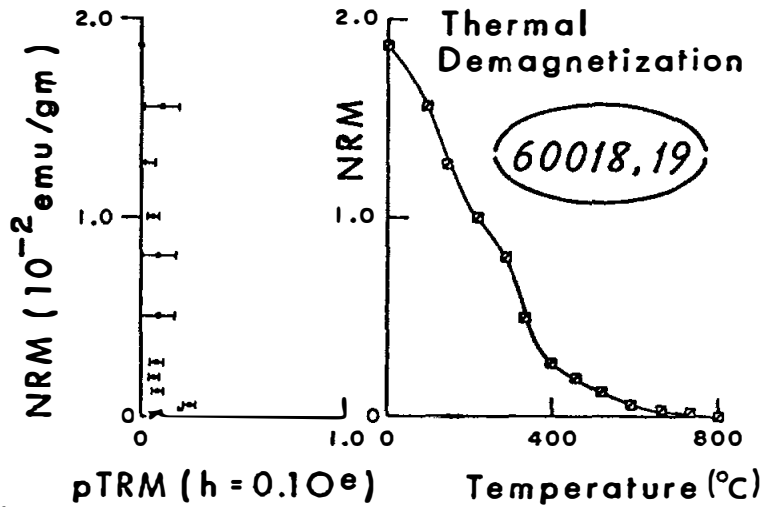
60018,19

NRM vs. pTRM plot and thermal demagnetization for 60018,19.

PROCESSING AND SUBDIVISIONS: In 1972 this rock was cut into three main pieces, one being a slab (Fig. 7). The slab was entirely subdivided with most of the allocations being taken from it. Not all splits are shown in the diagram.
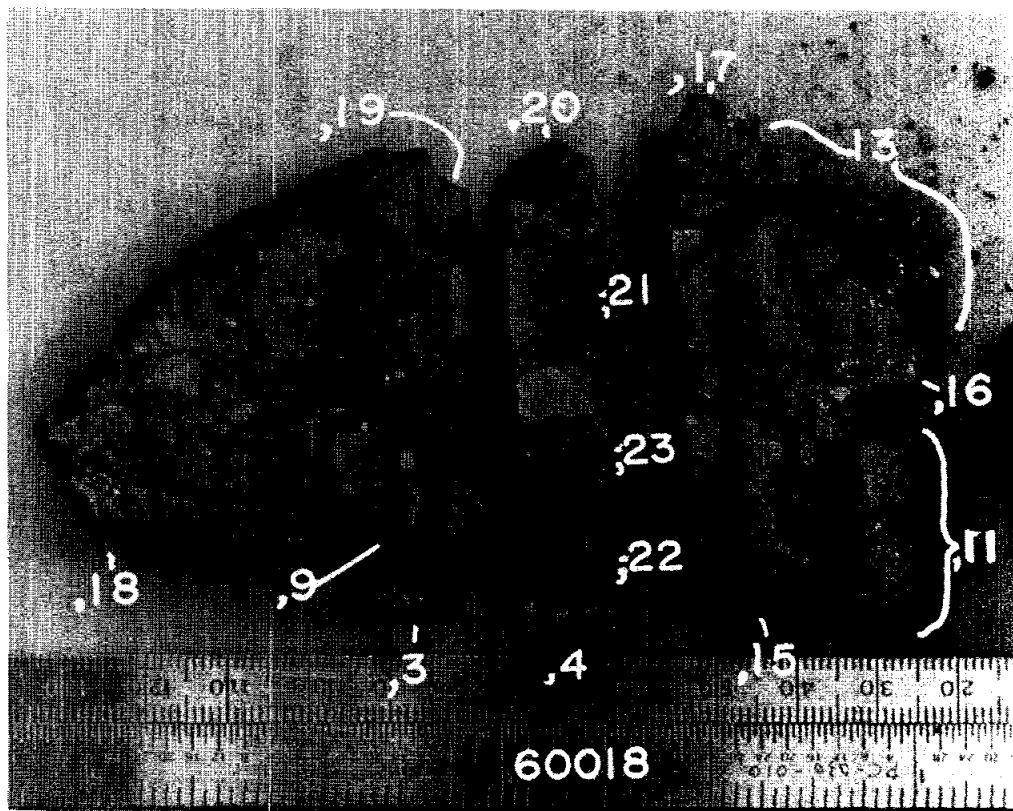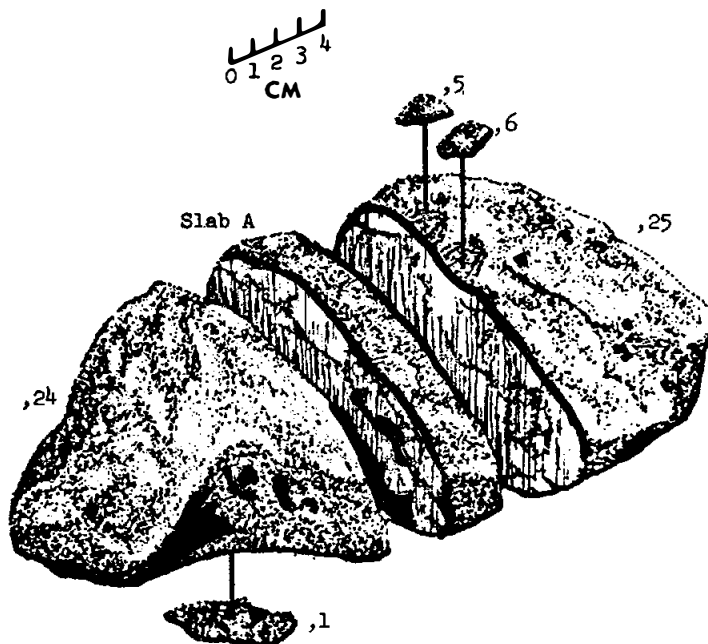


FIGURE 7. top: cutting diagram. bottom: slab dissection. S-73-21540.

33

INTRODUCTION:  60019 is a coherent, medium-gray glassy breccia containing
several large, light colored clasts (Fig. 1) which are mainly poikilitic and (more
rarely) basaltic impact melts.  Part of its surface has a rough glass coating.

The sample location is not known precisely but was approximately 115 m west south-
west of the Lunar Module.  It was partly buried (poorly developed fillet).  The
sample is subrounded.  The orientation is known and zap pits are present on some
surfaces.
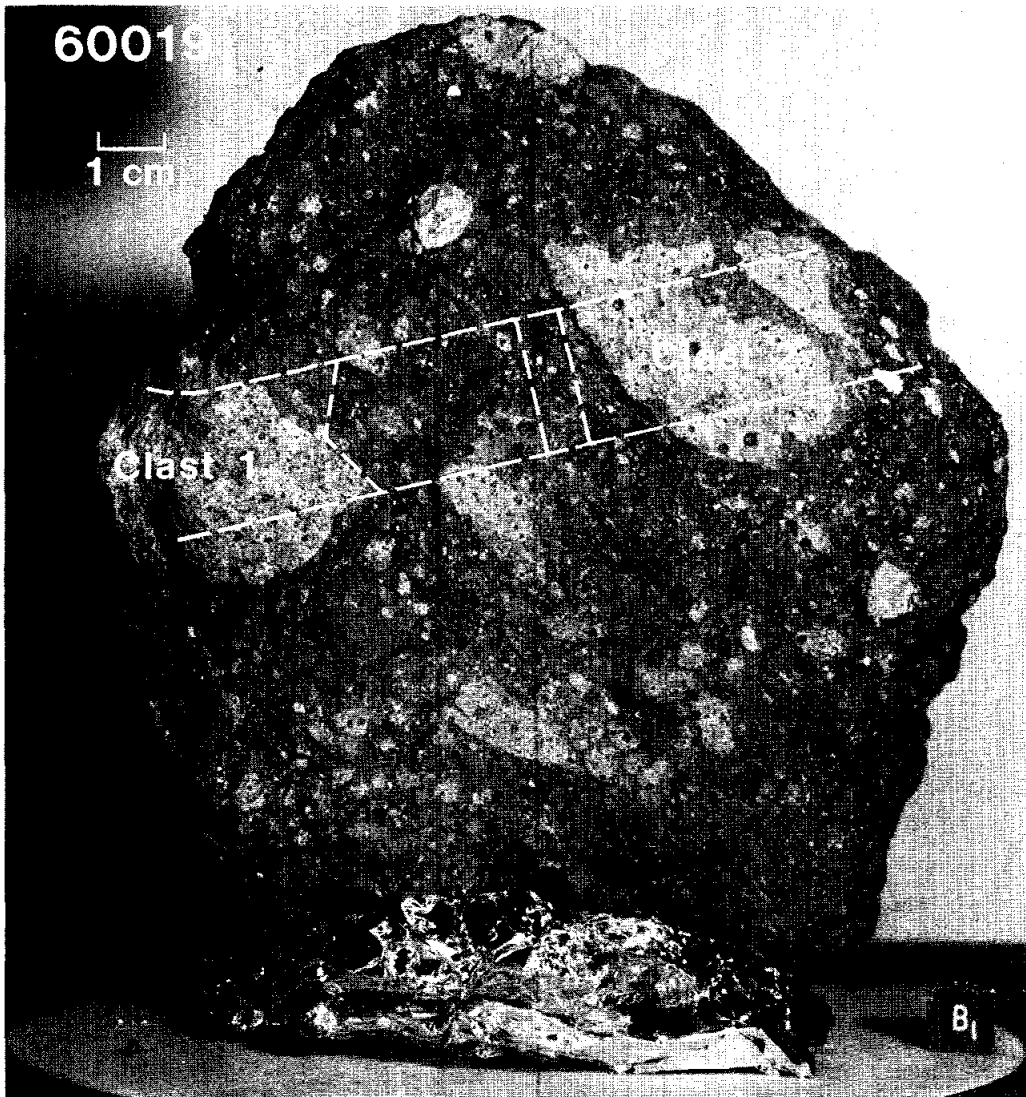


FIGURE 1.

PETROLOGY: Macroscopically the rock consists of a dark aphanitic matrix with abundant clasts up to 5 cm (Fig. 1). Clasts vary from fine-grained, crystalline lithic fragments to glass and mineral fragments. The matrix has glass-lined cracks and glassy veins. Rust patches occur in both the matrix and the larger clasts.

a                                          b
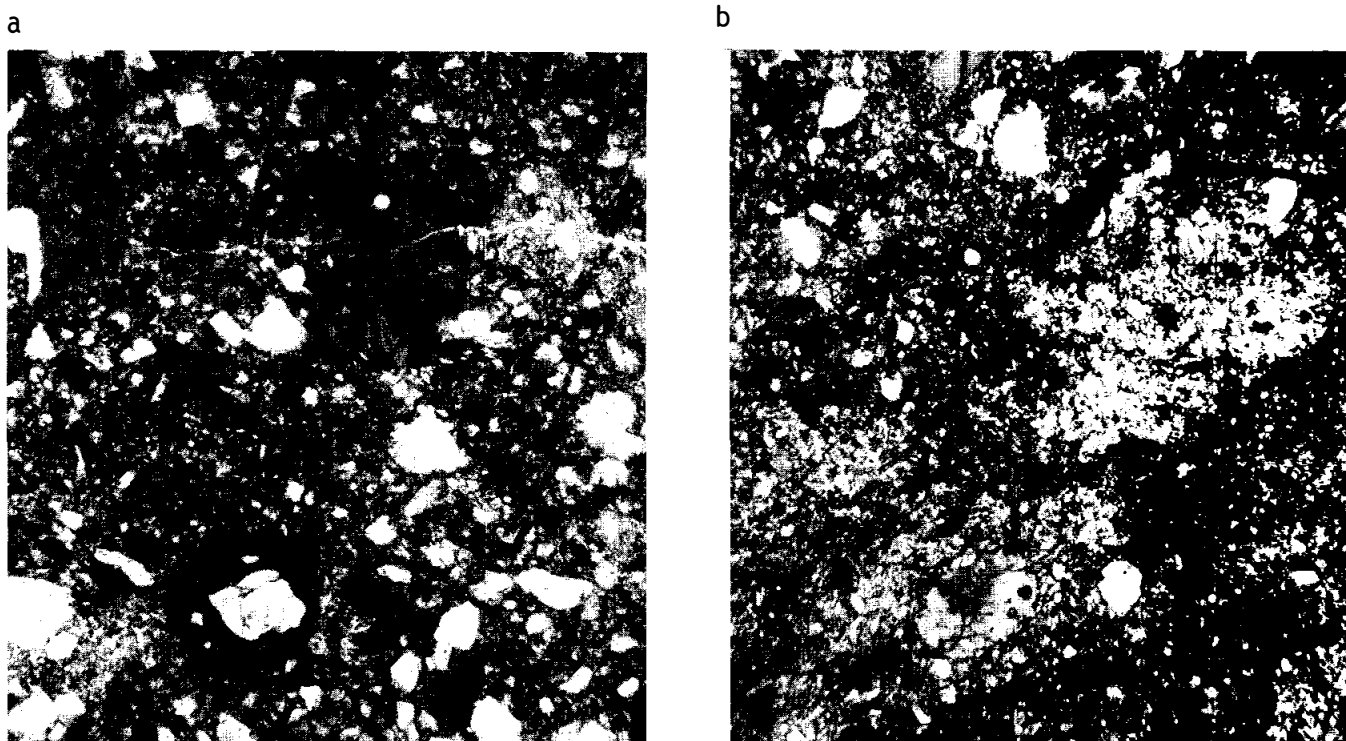


FIGURE 2. a) 60019,14. general view, ppl. width 2mm.
          b) 60019,77. Clast 1, poikilitic, xpl. width 2mm.

Thin sections show that the matrix is brown, glassy, partly vesicular and contains glass fragments (Fig. 2). These characteristics and its chemistry (below) suggest that 60019 is lithified regolith or is largely derived from regolithic material. Most of the large clasts (e.g. clasts 1 and 2, Fig. 1) are poikilitic impact melts. Clast 1 is poikilitic with abundant fragments (Fig. 2) including granoblastic impactites, cataclastic anorthosite, and aluminous basalt. In places the poikilitic texture, characterized by pyroxene oikocrysts up to 1 mm, grades into basaltic texture. Other smaller clasts in the matrix include coarse, aluminous, impact basalts, aluminous breccias, and plagioclase and mafic mineral grains. One small (2x3 mm) coarse basalt may be of mare affinity; it is mafic and has conspicuous ilmenite.

Hansen et al.(1979b and unpublished) investigated a granoblastic impactite clast in 60019. Plagioclase compositions show little dispersion of major ($An_{94-95}$) or minor ($K_2O$ 0.053%; FeO 0.098%; MgO 0.135%) elements. Olivine is $Fo_{79}$.

60019

CHEMISTRY: Rose et al. (1975) report
major and trace element analyses of
both the matrix and clast 1. Cripe
and Moore (1975) and Moore and Lewis
(1976) report light elements for these
same two lithologies. The matrix is
chemically indistinguishable from
Apollo 16 soils in all respects with
the exception of rare-earths which are
enriched in 60019. The poikilitic
clast is more aluminous and less
enriched in incompatible elements than
most other Apollo 16 poikilitic rocks;
this is at least in part a consequence
of its abundant clasts.

RARE GASES: Bernatowicz et al. (1978)
report xenon and krypton isotopic
abundances from heating studies of a
matrix sample. The sample contains
substantial excess fission xenon and
$^{129}$Xe, suggesting that excess fission
xenon is a global characteristic. The
sample is rich in solar wind components,
again suggestive of a significant regolith
component.

PROCESSING AND SUBDIVISIONS: In October,
1974, two end pieces (,4 and ,5) and a
slab were cut from 60019 (Figs. 1, 3).
The slab itself was subdivided leaving
two large pieces (,18 and ,23). Most
subdivisions were made from a column
down the center of the slab and from
the region of clast 1.

TABLE 1. Chemistry of 60019

| | Matrix | Clast 1 (Poikilitic) |
|---|---|---|
| $SiO_2$ | 45.3 | 45.3 |
| $TiO_2$ | 0.35 | 0.46 |
| $Al_2O_3$ | 26.3 | 23.2 |
| $Cr_2O_3$ | 0.10 | 0.14 |
| FeO | 5.3 | 6.9 |
| MnO | 0.06 | 0.08 |
| MgO | 6.7 | 9.5 |
| CaO | 14.9 | 13.6 |
| $Na_2O$ | 0.46 | 0.48 |
| $K_2O$ | 0.14 | 0.18 |
| $P_2O_5$ | 0.19 | 0.27 |
| Sr | 131 | 136 |
| La | 20 | 26 |
| Lu | | |
| Rb | 3.1 | 4.2 |
| Sc | 11 | 11 |
| Ni | 795 | 810 |
| Co | 49 | 45 |
| Ir ppb | | |
| Au ppb | | |
| C | 162 | 110 |
| N | 56 | 28 |
| S | 920 | 910 |
| Zn | 13 | <4 |
| Cu | 7.8 | 7.5 |

Oxides in wt %; others in ppm
except as noted.

36
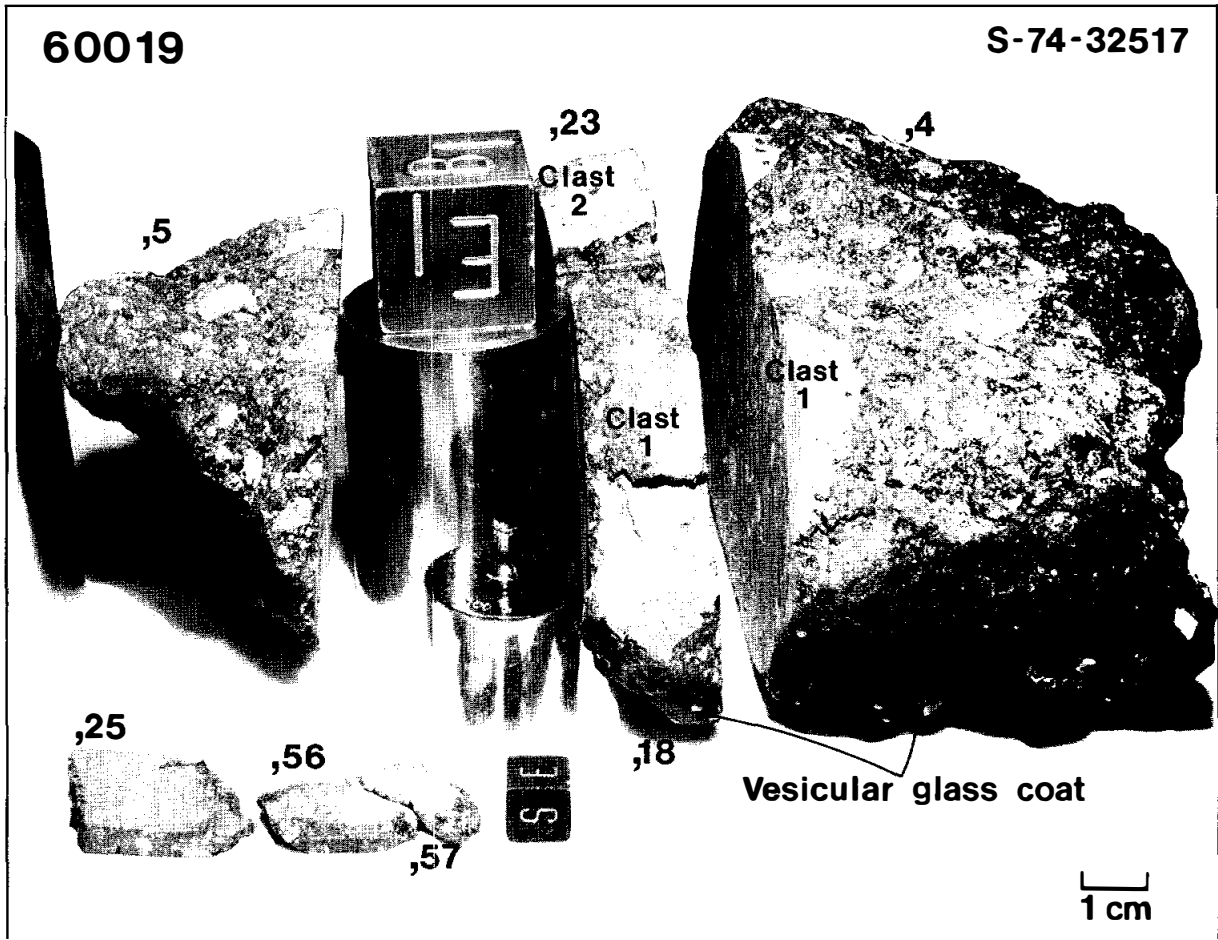
FIGURE 3. Saw cut subdivisions.

INTRODUCTION:  60025 is a coarse-grained, moderately shocked and cataclastic ferroan anorthosite which is monomict and is free of meteoritic siderophiles (i.e. chemically pristine).  A small patch of dark vesicular glass is present on one surface (Fig. 1).  60025 was collected 15 m southwest of the Lunar Module where it was perched.  It is moderately coherent with some penetrative fractures.  Its orientation is known and zap pits occur on all surfaces, though not equally distributed.

FIGURE 1. Saw cut slab.  S-72-49095. Scale in mm.
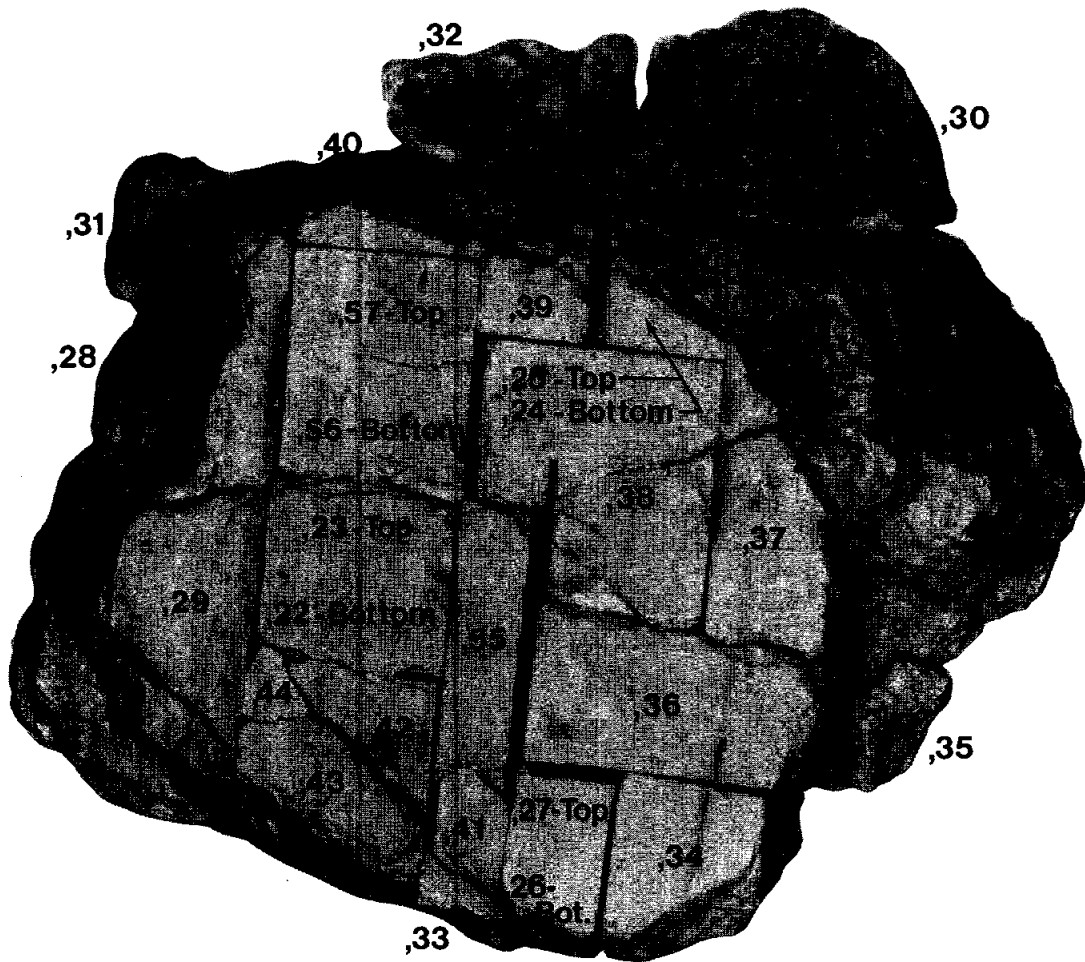


60025

PETROLOGY:   Walker et al. (1973), Hodges and Kushiro (1973), Dixon and Papike (1975), Warren and Wasson (1978) and LSPET (1973) provide general petrographic information.  Takeda et al. (1976) studied pyroxenes in detail and Longhi et al. (1976), Hansen et al. (1979a) and Meyer (1979) report data on minor elements in plagioclase.

The rock is a true anorthosite with > 90% plagioclase ($An_{94-98}$).   Shock-twinned and fractured clasts up to 4 mm long rest in a fine-grained and often recrystallized matrix of granulated plagioclase (Fig. 2).  Mafics are ferroan and irregularly distributed.  Walker et al. (1973), Hodges and Kushiro (1973) and Dixon and Papike (1975) report < 2% pyroxene and no olivine whereas LSPET (1973) indicates $\sim$ 10% olivine,and a "mafic-rich" portion described by Warren and Wasson (1978) contains 20% olivine ($Fo_{57-65}$) and 10% pyroxene.  A 2x2 mm optically continuous zone of pyroxene and a 4x4 mm zone of olivine attest to the coarse-grained nature of the rock prior to cataclasis (Warren and Wasson, 1978).Traces of silica, ilmenite, Cr-spinel and glassy inclusions in plagioclase are scattered throughout the rock.

Anhedral pyroxenes (most < 0.5 mm) are concentrated as discrete grains in the matrix but also occur as rods, stringers and irregular blotches along plagioclase twin planes and grain boundaries.  The dominant pyroxene is orthopyroxene.  Some grains show well developed exsolution lamellae of high-Ca pyroxene and were probably primary pigeonite.  Augite is also present as discrete grains.  Apparently three primary pyroxenes-orthopyroxene, pigeonite and augite - were present at the time of crystallization (Hodges and Kushiro, 1973).  Pyroxene compositions are shown in Figure 3.



FIGURE 2. 60025,130. general view,
xpl.  width 2mm.

a)

Co

CoMg

CoFe

Mg

50

Fe

Atomic per cent

b)

60025

ANORTHOSITE

50
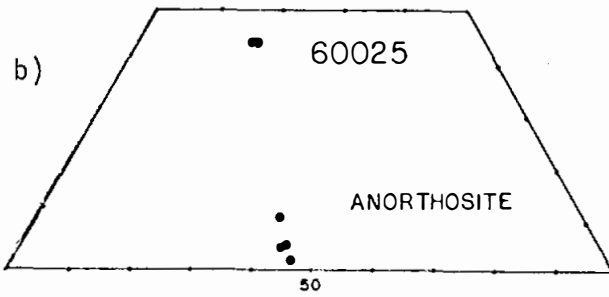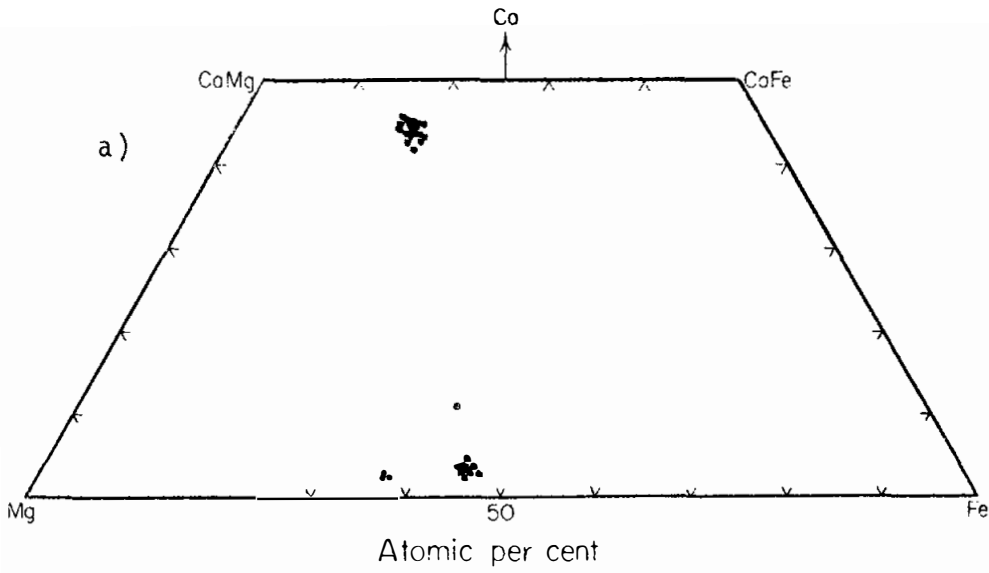
FIGURE 3. Pyroxenes.

a) from Hodges and Kushiro (1973).
b) from Walker et al. (1973).

SILICA

PSEUDOTERNARY
LIQUIDUS
RELATIONS AT
LOW PO2

SILICA

APOLLO 16 ROCKS

PYROXENE

PX

PLAGIOCLASE

OLIVINE

SPINEL

60025

OLIVINE

ANORTHITE
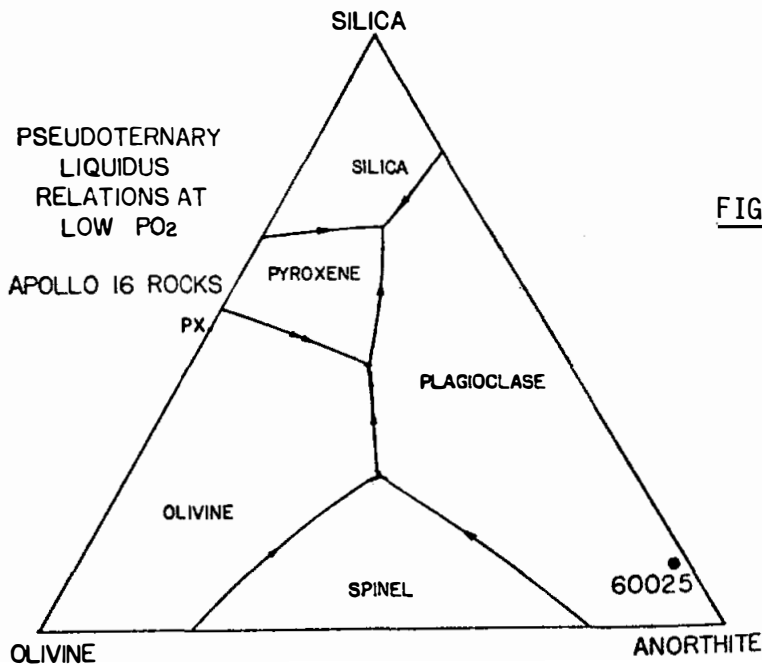
FIGURE 4. from Walker et al. (1973)

40

EXPERIMENTAL PETROLOGY: Ford et al. (1974) determined that plagioclase is the liquidus phase of a rock with the composition of 60025. The anhydrous liquidus occurs at temperatures > $1370^{o}C$. Moderate water vapor pressure lowers the liquidus temperature to below $1200^{o}C$. The anhydrous solidus is $\sim 1200^{o}C$.

CHEMISTRY: Chemical studies of 60025 are listed in Table 1 and a summary chemistry in Table 2. The splits analyzed were almost pure plagioclase (Table 2, Fig. 4); apparently none of the mafic rich portions were sampled for chemistry.

Rare earths are low with the large positive Eu anomaly typical of lunar anorthosites (Fig. 5). The REE pattern of 60025 parallels that of 15415 and 60015 but with absolute concentrations nearly twice as high. Zr and Hf and the Zr/Hf ratio are typical of lunar anorthosites and are among the lowest measured in any lunar material (Ehmann et al.,1975;Garg and Ehmann, 1976).

60025 is also low in siderophiles indicating a lack of meteoritic contamination. Its very high volatile to involatile ratios (e.g. Tl/Cs and Tl/U) however suggest that a fumarolic component is present (Krähenbühl et al., 1973). Sulfur is also enriched in 60025 relative to the other light gases (Table 2), its Fe content (Fig. 3 of Kerridge et al.,1975a) and other pristine anorthosites (e.g. 15415, 60015, 67075).

Flory et al. (1973) determined total amounts of hydrocarbons and other light gases and their release patterns upon heating. 60025 was the only rock analyzed by these authors to yield detectable methane, apparently produced by the hydrolysis of reactive, solar wind-deposited carbon.

Sato (1976) determined the oxygen fugacity of 60025 by the solid-electrolyte oxygen cell method and found it to have among the lowest $fo_2$ ever measured in lunar material. A self-reduction at high temperatures occurred during the first heating cycle. Reported values are given in Table 3.
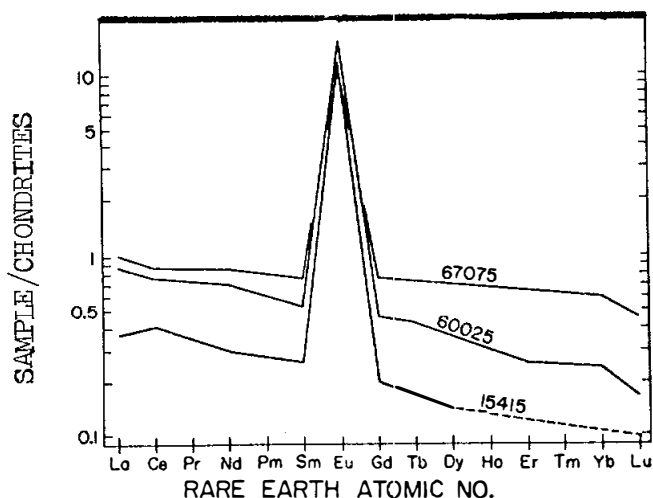


FIGURE 5. Rare earths; from Haskin et al.(1973).

TABLE 1. Chemical studies of 60025 anorthosite

| Reference | Split # | Elements analyzed |
|---|---|---|
| Janghorbani et al. (1973) | ,72 | majors |
| Rose et al. (1973) | ,95 | majors, trace |
| Haskin et al. (1973) | ,45 | majors, REEs, other trace |
| Laul and Schmitt (1973) | ,73 | majors, REEs, other trace |
| Nakamura et al. (1973) | ,76 | majors, REEs, Ba |
| Walker et al. (1973) | ,90 | majors* |
| Krähenbühl et al. (1973) | ,84 | meteoritic sids. and vols. |
| Ehmann and Chyi (1974) | ,72 | Zr, Hf |
| Ehmann et al. (1975) | ,72 | Zr, Hf, Sc, Co, Fe, Eu |
| Miller et al. (1974) | ,72 | Fe, Sc, Co, Eu |
| Cripe and Moore (1974) | ,82 | S |
| Moore et al. (1973) | ,82 | C |
| Moore and Lewis (1976) | ,82 | N |
| Schaeffer and Husain (1974) | ,86 | K, Ca |
| Nyquist et al. (1975) | ,268 | Rb, Sr |
| Papanastassiou and Wasserburg (1972b) | ,65 | Rb, Sr |
| Tera and Wasserburg (1972) Tera et al. (1973) | ,65 | U, Th, Pb |
| Nunes et al. (1974) | ?,9003 (from ,26) | U, Th, Pb, Rb, Sr, K |
| Nunes et al. (1977) | ,9003 (from ,26) | U, Th, Pb |

*Microprobe, fused powder

TABLE 2. Summary chemistry of anorthosite 60025

| | |
|---|---|
| $SiO_2$ | 44.2 |
| $TiO_2$ | 0.1 |
| $Al_2O_3$ | 35.3 |
| $Cr_2O_3$ | 0.02 |
| FeO | 0.6 |
| MnO | 0.014 |
| MgO | 0.2 |
| CaO | 19.0 |
| $Na_2O$ | 0.44 |
| $K_2O$ | 0.03 |
| $P_2O_5$ | 0.003 |
| Sr | 218 |
| La | 0.3 |
| Lu | 0.005 |
| Rb | 0.02 |
| Sc | 0.05 |
| Ni | ~1 |
| Co | 0.07 |
| Ir ppb | 0.006 |
| Au ppb | 0.007 |
| C | 35 |
| N | 56 |
| S | 240 |
| Zn | <2(?) |
| Cu | 8.4(?) |

Oxides in wt%; others in ppm except as noted.

TABLE 3. Oxygen fugacity of 60025 (Sato, 1976)

| T (°C) | $-\log f_{O_2}$ (atm) |
|---|---|
| 1000 | 16.9 |
| 1050 | 16.1 |
| 1100 | 15.4 |
| 1150 | 14.7 |
| 1200 | 14.1 |

STABLE ISOTOPES: Taylor and Epstein (1973) report $\delta O^{18}$ and $\delta Si^{30}$ values of +5.95 and -0.01 respectively for whole rock splits of 60025.

RADIOGENIC ISOTOPES AND GEOCHRONOLOGY: Rb-Sr data are summarized in Table 4. The very low measured $^{87}Sr/^{86}Sr$ extrapolates to very close to BABI at 4.0 and 4.6 b.y. Only whole rock data from the anorthosite are currently available although a mineral isochron could conceivably be obtained from the mafic-rich portions of the rock. Schonfeld (1976) constructed a Rb-Sr whole rock isochron from data on lunar anorthosites which gave an apparent age of 4.6 b.y. and an initial $^{87}Sr/^{86}Sr$ of 0.69905. 60025 lies on this isochron.

An Ar-Ar determination yielded a well defined plateau age of 4.19 ± 0.06 b.y. (Fig. 6) (Schaeffer and Husain, 1974). There was no increase in apparent age at high temperatures (Fig. 6) indicating no relict Ar in ancient plagioclase clasts (Schaeffer and Husain, 1974).

U-Th-Pb data show very low concentrations of all of these elements and essentially no initial radiogenic Pb (Tera and Wasserburg, 1972; Tera et al.,1973; Nunes et al., 1974,1977). The analyses are highly discordant (Fig. 7). Lead isotopes are not easily leachable and are highly evolved yielding a $^{207}Pb/^{206}Pb$ single stage model age of 4.64 b.y. (Tera and Wasserburg,1972). Nunes et al. (1974,1977) report serious terrestrial contamination in their samples with sawn surfaces. Interior chips without sawn surfaces do not show such contamination (Tera and Wasserburg, 1972).

TABLE 4. Summary of Rb-Sr data for anorthosite 60025

| Rb/Sr | $^{87}Sr/^{86}Sr$ measured | $^{87}Sr/^{86}Sr$ at 4.6 b.y | Reference |
|---|---|---|---|
| $1.16\times10^{-4}$ | 0.69896 ± 3 | 0.69894 | Papanastassiou and Wasserburg (1972b) |
| $9.44\times10^{-5}$ | 0.69908 ± 6 | 0.69906 | Nunes et al. (1974) |
| $1.34\times10^{-4}$ | 0.69905 ± 6 | 0.69902 | Nyquist et al.(1975) |
| $1.22\times10^{-4}$ | 0.69913 ± 3 | 0.69910 | Nyquist et al.(1979) |

Not corrected for interlaboratory bias
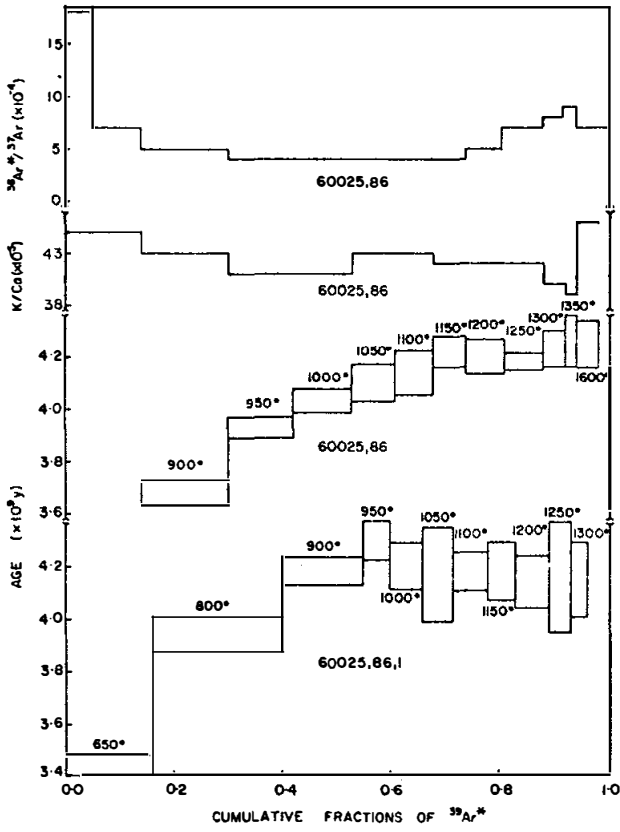
FIGURE 6. Ar release; from Schaeffer and Husain (1974).
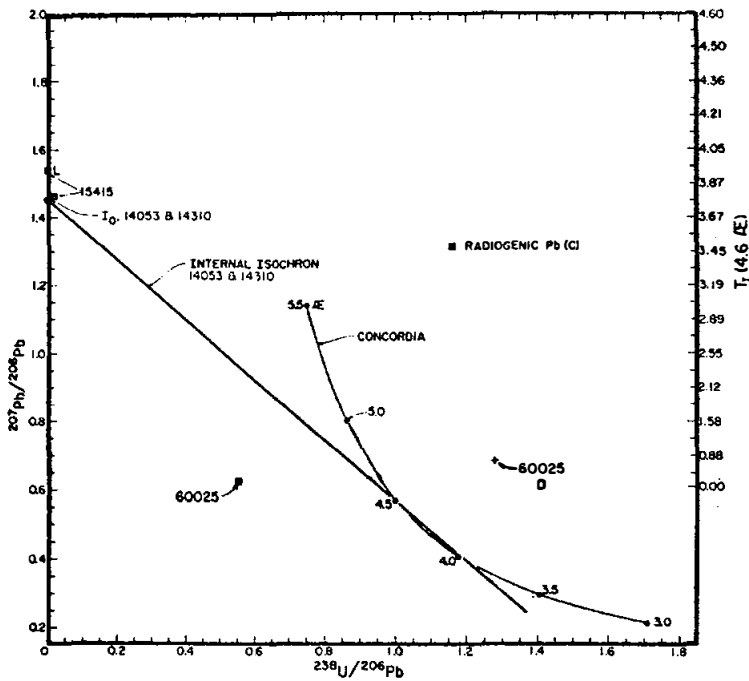


FIGURE 7. U-Pb evolution diagram; from Tera and Wasserburg (1972).

RARE GASES/EXPOSURE AGES: Lightner and Marti (1974a) and Leich and Niemeyer (1975) provide Xe, Kr and Ar isotope data. Significant amounts of trapped Xe not of solar or cosmic origin were found. It is however isotopically indistinguishable from terrestrial Xe and is believed to represent terrestrial contamination because experiments by Niemeyer and Leich (1976) showed that unexpectedly high temperatures (> 1000°C) were required to remove known terrestrial contamination.

Marti (pers. comm., 1975, referenced in Drozd et al.,1977) calculated a single stage $^{81}$Kr-Kr exposure age of 1.9 m.y., consistent with an excavation by the South Ray cratering event. Fruchter et al. (1977) and Kohl et al. (1977) report Mn and Al isotope data that confirm this 2 m.y. exposure age.

Schaeffer and Husain (1974) report Ar isotopic data and calculate $^{38}$Ar-$^{39}$Ar exposure ages which average 8.6 m.y., considerably higher than the $^{81}$Kr-Kr age which Leich and Niemeyer (1975) consider more reliable.

PHYSICAL PROPERTIES: Limited magnetic information is provided by Cisowski et al. (1976) who found that 60025 possesses high saturation isothermal remanent magnetization (IRMs) comparable to soil breccias and well above that of other cataclastic anorthosites (see their Fig. 6).

Katsube and Collet (1973a,b) and Gold et al.(1976b) report electrical characteristics of the anorthosite (Fig. 8).
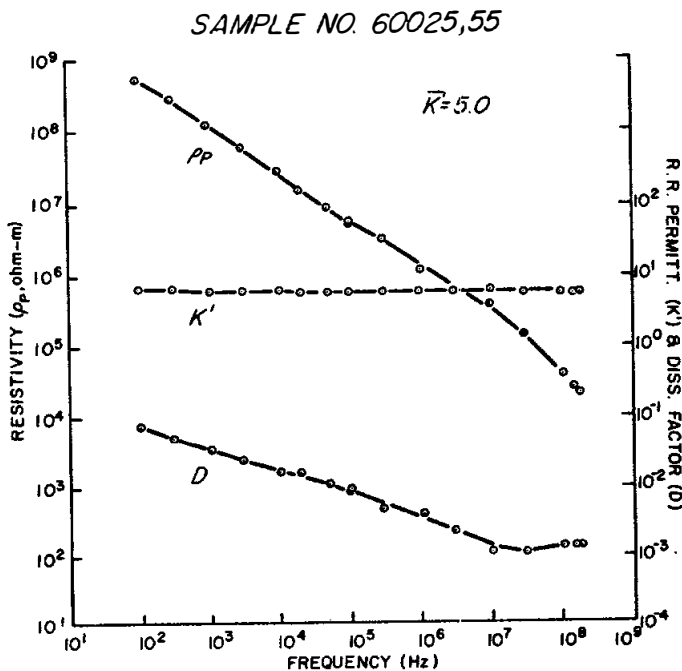


FIGURE 8. Electrical properties; from Katsube and Collett (1973b).

45

Sondergeld et al. (1979) measured compressional wave velocities on three per-
pendicular surfaces of a slab of the anorthosite. Measured velocities were
all < 1 km/sec and deviated up to 29% from the mean value of the three direc-
tions (0.66 km/sec). Neither variation in temperature (up to 90° C) nor vacuum
(down to $10^{-6}$ μm Hg) had any detectable effect on the velocities. These data
agree well with seismic wave data from the lunar surface at the Apollo 16 site.

Jeanloz and Ahrens (1978) determined shock wave, equation of state data for
the anorthosite over the pressure range 400-1000 kbar (Fig. 9). Porosity in
the rock (average ∿ 18%) induces smaller peak pressures and greater temper-
atures than experienced by non-porous rocks subjected to similar shock con-
ditions. Jeanloz and Ahrens (1979) extended the shock wave experiments to
higher and lower pressures (1160 and 270 kbar).
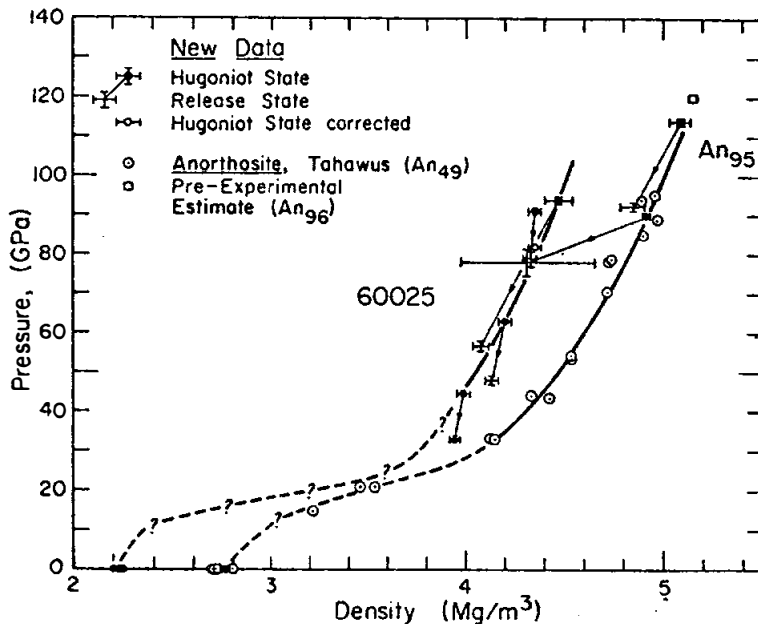


FIGURE 9. Hugoniot equation of
state data; from Jeanloz and
Ahrens (1978).

Microcracks were studied by Simmons et al. (1975) who found two sets of shock
induced cracks, possibly indicating separate shock events.

Hapke et al. (1978) provide ultraviolet reflectance data .

PROCESSING AND SUBDIVISIONS: In 1972, 60025 was sawn into three main pieces
(Fig. 10). The slab and the E butt end were extensively subdivided and
allocated. The mafic-rich thin sections described by LSPET (1973) and Warren
and Wasson (1978) are from an undocumented chip (60025,9) which is now a potted
butt. Processing notes in the data pack indicates that mafic-rich clumps may be
present on the N surface.
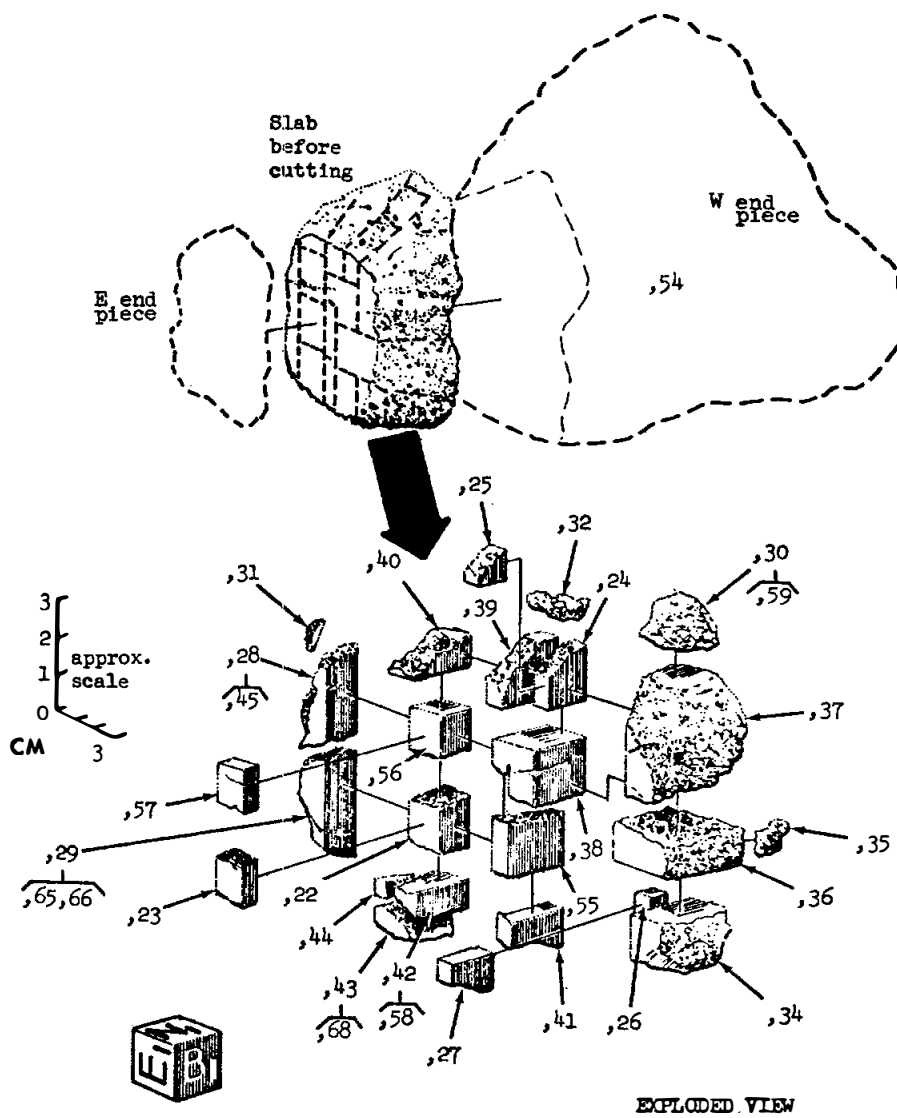
FIGURE 10. Cutting diagram.

INTRODUCTION:  60035 is a coherent, whitish breccia (Fig. 1) consisting mainly of a variety of feldspathic impactites with granoblastic and poikiloblastic textures (Fig. 2).  Macroscopically the breccia is homogeneous and cut by a few veins of dark glass.  It is partly coated with black glass which apparently once entirely coated the rock.

The sample was collected about 190 m south-southwest of the Lunar Module where it was partly buried.  Its orientation is known and zap pits are common on the "lunar up" surface, rare to absent on others.  60035 was originally set aside as a posterity sample and only recently made available for study.
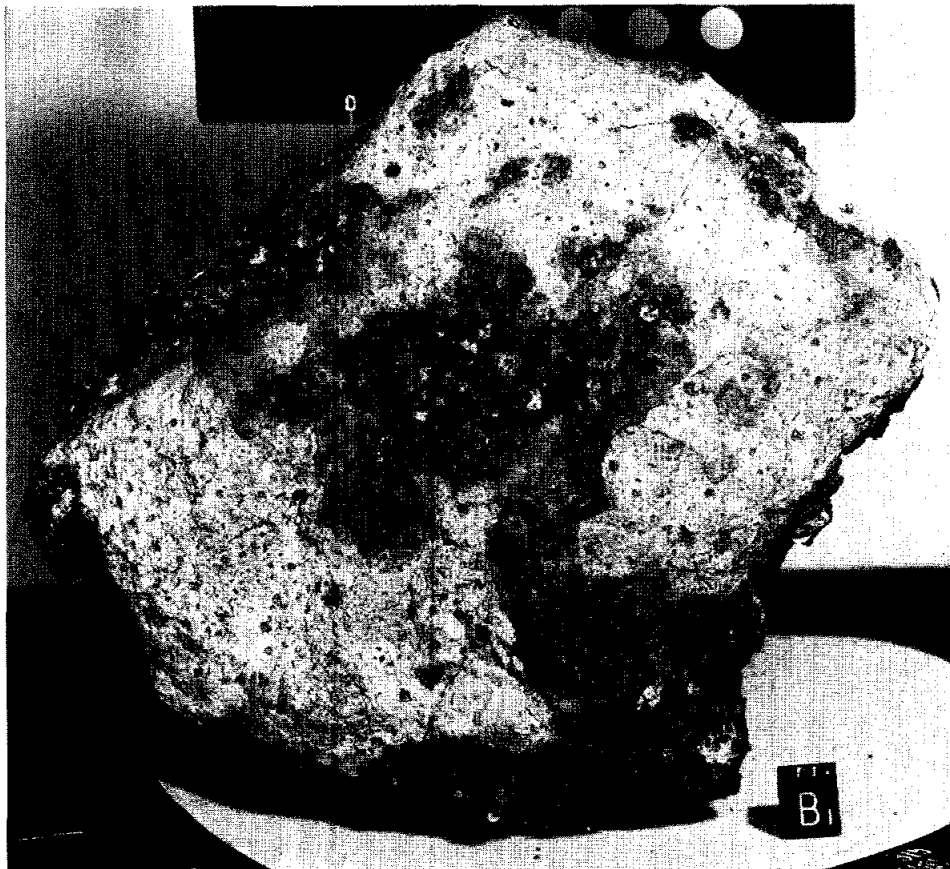


FIGURE 1. Cube is 1 cm.  S-72-38300.

PETROLOGY:  R. Warner et al. (1980) provide petrographic information.  Thin sections from widely separated portions of the rock consist of a variety of crystalline anorthositic, troctolitic, and noritic lithologies that grade in size from clasts to a finer-grained matrix.

a                                    b
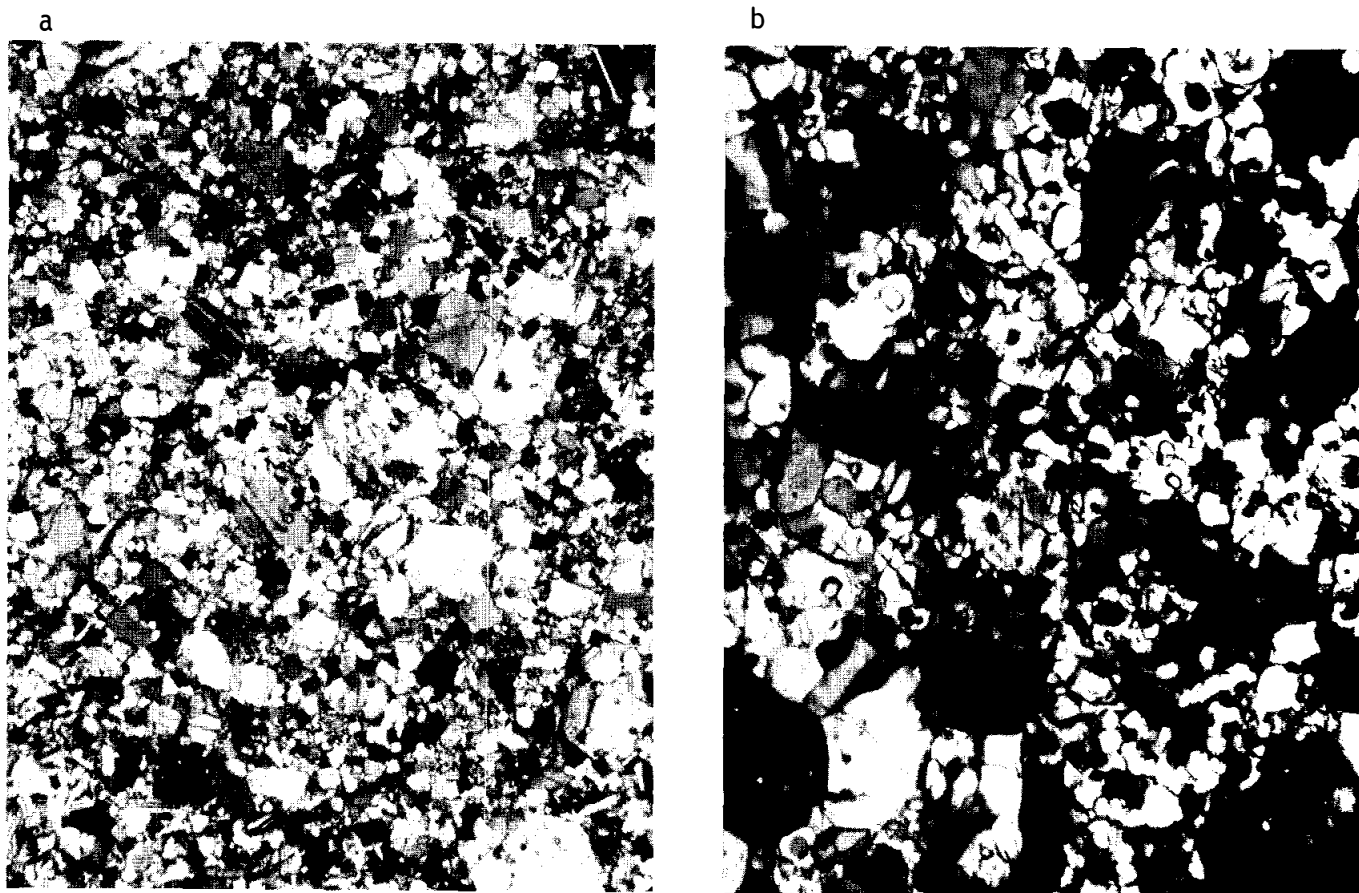


FIGURE 2. 60035,18.  a) granoblastic,xpl. width 2mm.  b) poikiloblastic,xpl. width 1mm.

The most common lithic type recognized by R. Warner et al. (1980) is poikiloblastic anorthositic norite (Fig. 2).  Low-Ca pyroxene oikocrysts enclose small rounded to subequant grains of plagioclase.  At least two distinct populations of pyroxene compositions were found:  one more Fe-rich than the other (Fig. 3).  More calcic plagioclases ($An_{97-98}$) are associated with the Fe-rich group.  Minor amounts of olivine are present.

Granoblastic anorthositic troctolite clasts (70-80% plagioclase) are also common (Fig. 2).  The grain size within these clasts is variable (0.05-0.25 mm).  Larger plagioclase grains typically show shock effects such as cataclasis or undulose extinction.  Olivine is $Fo_{76-82}$.

One large (4x8 mm) clast grades from fine-grained (0.05-0.25 mm) granular troctolite (~50% olivine, 50% plagioclase) through a coarser (up to 0.8 mm) zone with >60% plagioclase to another fine-grained (0.05 mm) area with low-Ca pyroxene more abundant than olivine.  The mafics in this clast are considerably more magnesian (olivine ~$Fo_{88}$; low-Ca pyroxene $Wo_3En_{86}$) than other mafics in this rock.

Other lithic types include cataclastic anorthosite, basaltic impact melt with lathy plagioclase, and mineral clasts of plagioclase, rare olivine, spinel and a variety of opaque phases including chromite, ilmenite, troilite and metal.  Most

metal grains analyzed by R. Warner et al. (1980) have ∿6% Ni and 0.8% Co (Fig. 4).
Metal in the magnesian granular troctolite is exceptional: 36-51% Ni and 1.2-1.9%
Co.
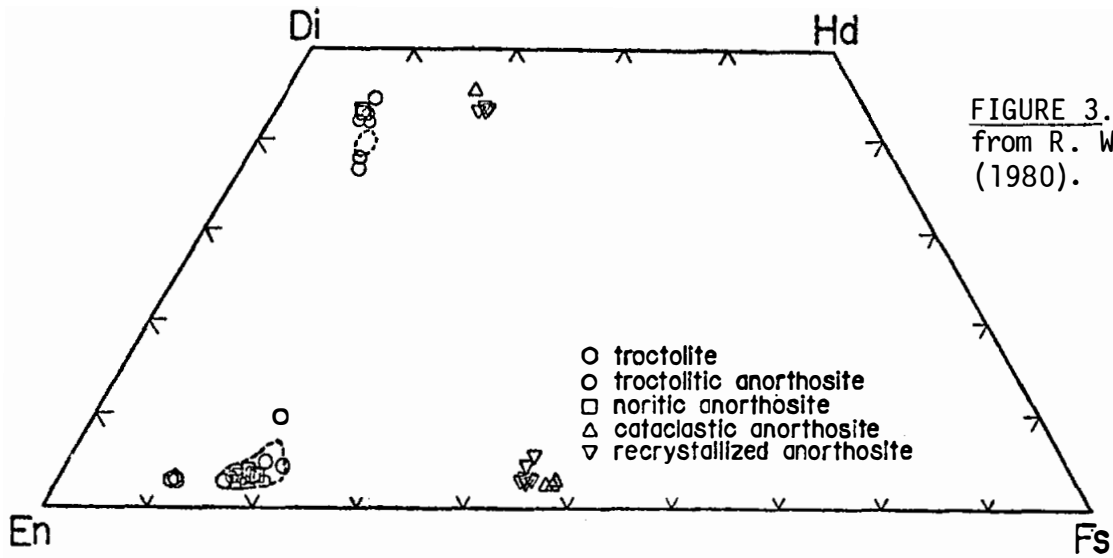


FIGURE 3. Pyroxenes;
from R. Warner et al.
(1980).

O troctolite
o troctolitic anorthosite
□ noritic anorthosite
△ cataclastic anorthosite
▽ recrystallized anorthosite
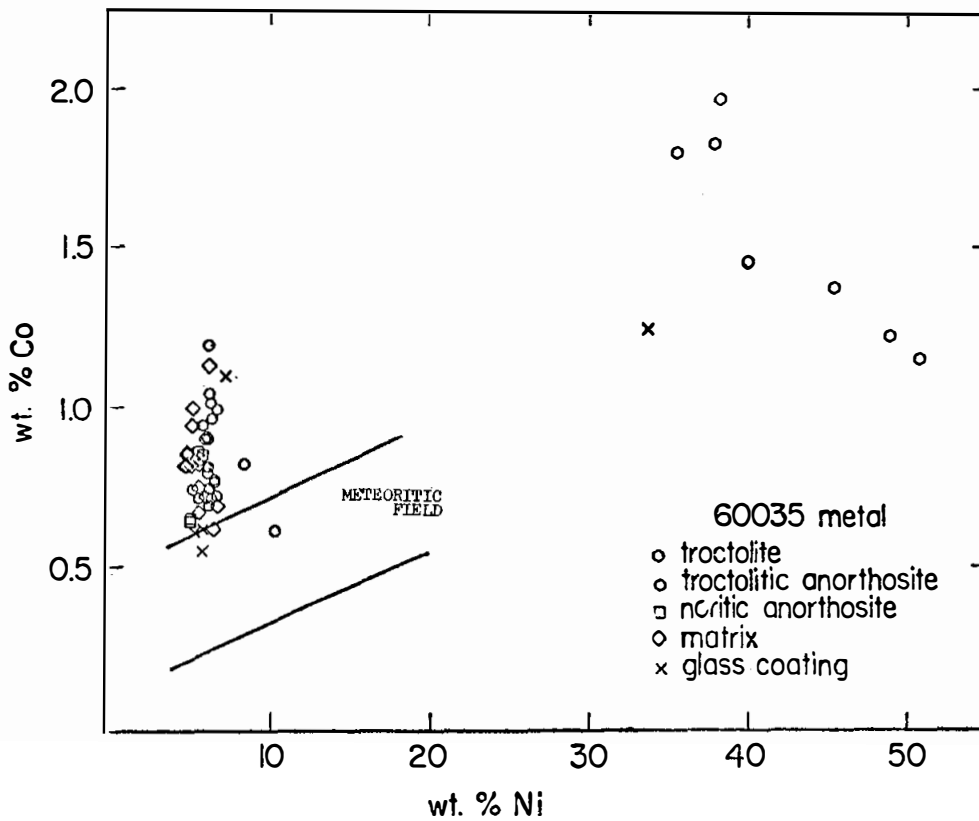


FIGURE 4. Metals;

from R.Warner et al.
(1980).

60035 metal

o troctolite
o troctolitic anorthosite
◻ noritic anorthosite
◇ matrix
x glass coating

CHEMISTRY: The only chemical analysis of 60035 is an average defocused electron beam analysis (DBA) of the glass coat presented in R. Warner et al. (1980), reproduced in Table 1.

### TABLE 1

#### Average DBA of 60035 glass coat

| | |
|---|---|
| $SiO_2$ | 44.3 |
| $TiO_2$ | 0.29 |
| $Al_2O_3$ | 29.4 |
| $Cr_2O_3$ | 0.12 |
| FeO | 5.1 |
| MnO | 0.04 |
| MgO | 5.7 |
| CaO | 15.8 |
| $Na_2O$ | 0.25 |
| $K_2O$ | 0.06 |
| $P_2O_5$ | 0.01 |

Oxides in wt%

PROCESSING AND SUBDIVISIONS: 60035 was initially set aside as a posterity sample, and has only recently been made available for study. Three small unlocated chips were used to make the first thin sections (,4 ,5 ,6) and then three chips (,8 ,10 ,13) from different areas of the rock were taken to make thin sections ,16 and ,17; ,18 and ,19; and ,20 and ,21 respectively. Subsequently a slab was cut (Fig. 5). The slab broke into several pieces, and the sawing produced many small chips. Some of these have been allocated to Schmitt for chemical analyses.

60035

FIGURE 5. Post sawing.  Scale in cm.  S-80 -35183.



52
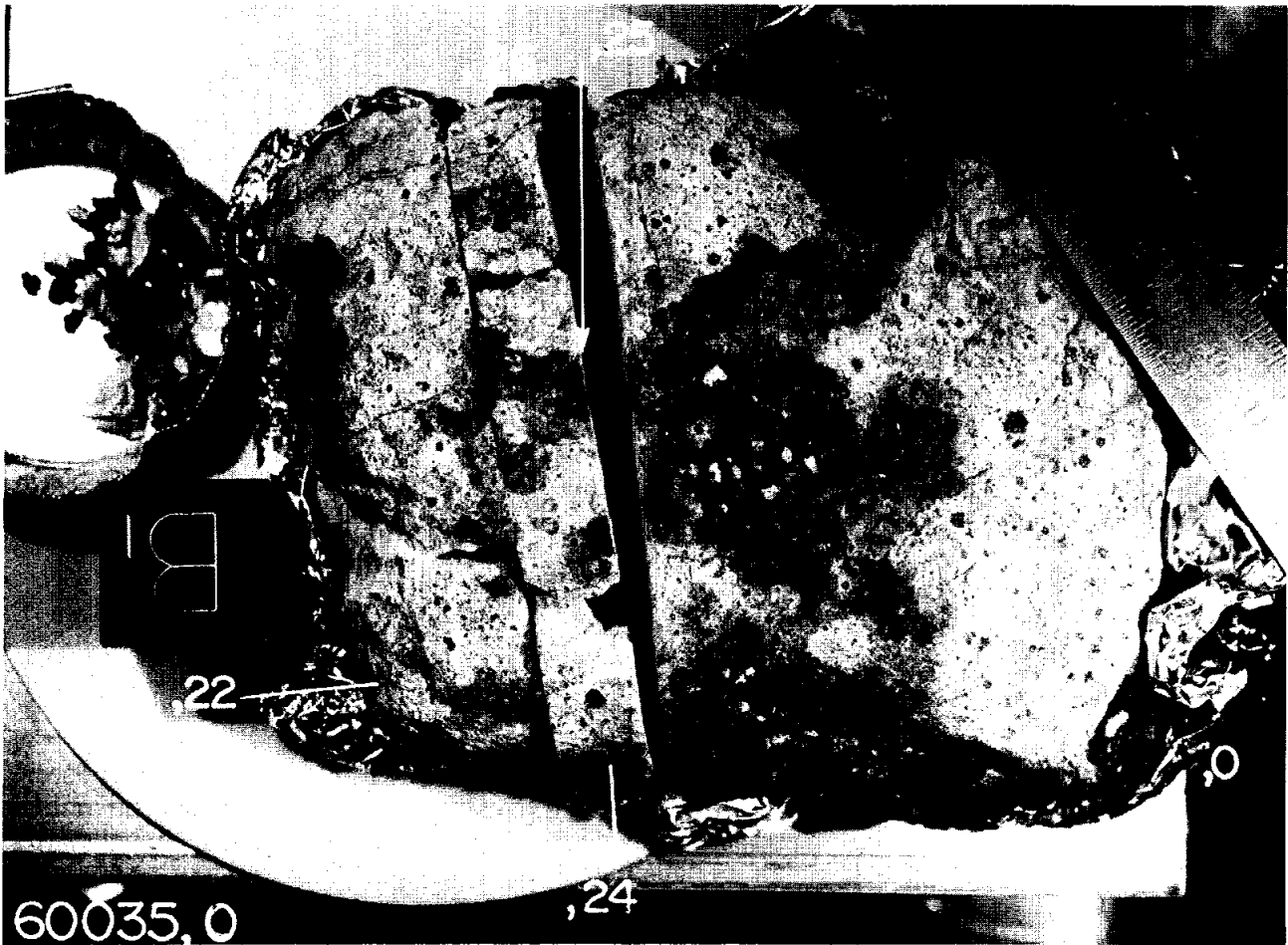
INTRODUCTION:   60055 is a homogeneous, friable, cataclastic anorthosite which
is chemically pristine.  Original surface features have been obscured due to
its friable, dusty nature (Fig. 1).  This rock was collected about 170 m south-
southwest of the Lunar Module.  The sample was disturbed prior to photographing,
hence burial and orientation data were lost.
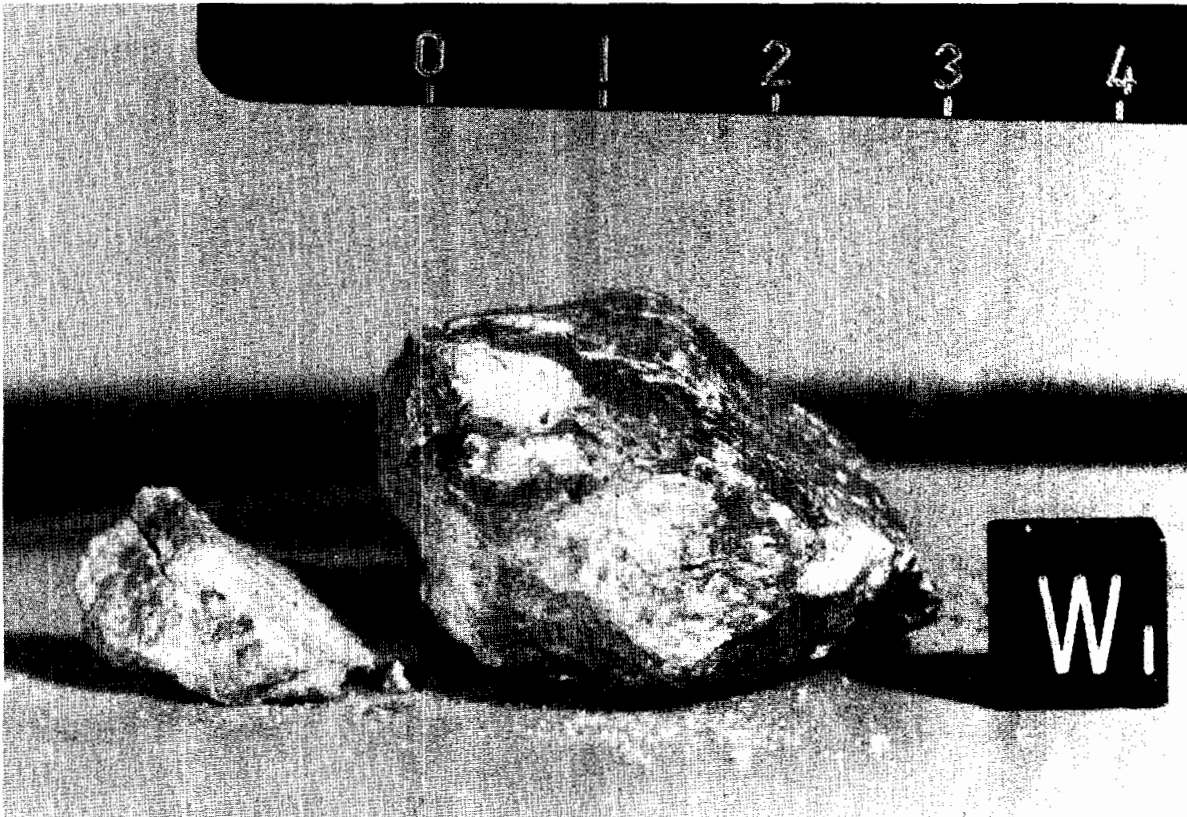


FIGURE 1.  Scale in cm.  S-72-41416.

PETROLOGY:  Warren and Wasson (1978) provide petrographic information.  They
describe a granular, unannealed anorthosite with 98% plagioclase ($An_{95-96}$)
and 2% high-Ca pyroxene ($Wo_{42-44}En_{42}$).  A single grain of exsolved low-Ca
pyroxene ($Wo_2En_{61}$) is also mentioned.  Original grain size was >2 mm.

Our own thin section observations confirm that the rock is a porous, cataclastic
anorthosite (Fig. 2) with traces of a silica mineral, rare grains of ilmenite
with exsolved rutile lamellae, and at least one other, more-poorly-reflecting
opaque phase.  Rare relict grain boundaries between mafics and plagioclase are
present.

CHEMISTRY:  Warren and Wasson (1978) report major and trace element data.  Their
analysis confirms the highly anorthosite nature of the rock and demonstrates that
the rock is free of meteoritic siderophiles and low in incompatible elements
(Table 1).
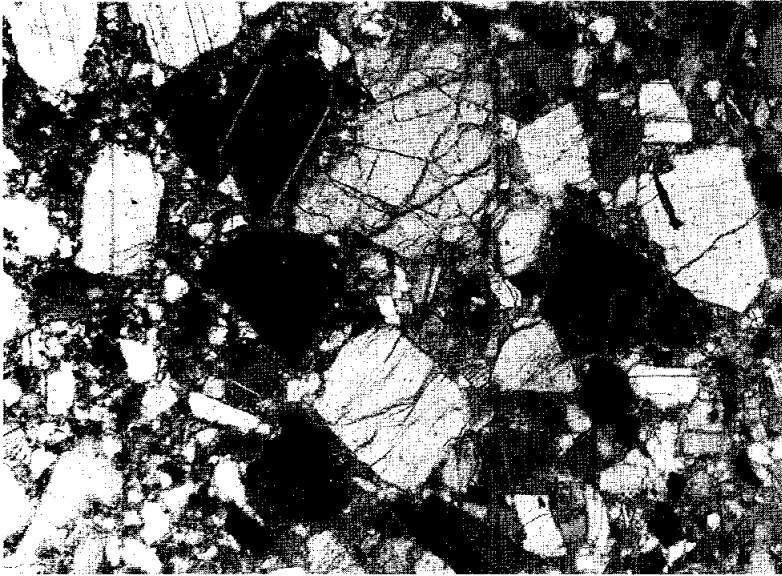
FIGURE 2. 60055,4.
general view, partly
xpl. width 2.3mm.

TABLE 1.  Summary chemistry of anorthosite 60055

| | |
|---|---|
| $SiO_2$ | 44.3 |
| $TiO_2$ | |
| $Al_2O_3$ | 34.0 |
| $Cr_2O_3$ | 0.005 |
| FeO | 0.34 |
| MnO | 0.096 |
| MgO | 0.33 |
| CaO | 19.04 |
| $Na_2O$ | 0.335 |
| $K_2O$ | 0.010 |
| $P_2O_5$ | |
| Sr | |
| La | 0.13 |
| Lu | 0.0038 |
| Rb | |
| Sc | 0.55 |
| Ni | 1.9 |
| Co | 0.84 |
| Ir ppb | 0.013 |
| Au ppb | 0.014 |
| C | |
| N | |
| S | |
| Zn | 0.60 |
| Cu | |

Oxides in wt%; others in ppm except as noted.

INTRODUCTION: 60056 is a friable, white rock (Fig. 1) that is probably a cataclastic anorthosite but may be a fragmental, polymict breccia.  A thin coat of dark glass is present on some pieces.  Apparently it was removed from its documented bag as a single piece but broke into many small fragments and fines during initial processing.  60056 was collected about 170 m southwest of the Lunar Module.  Zap pits are absent.
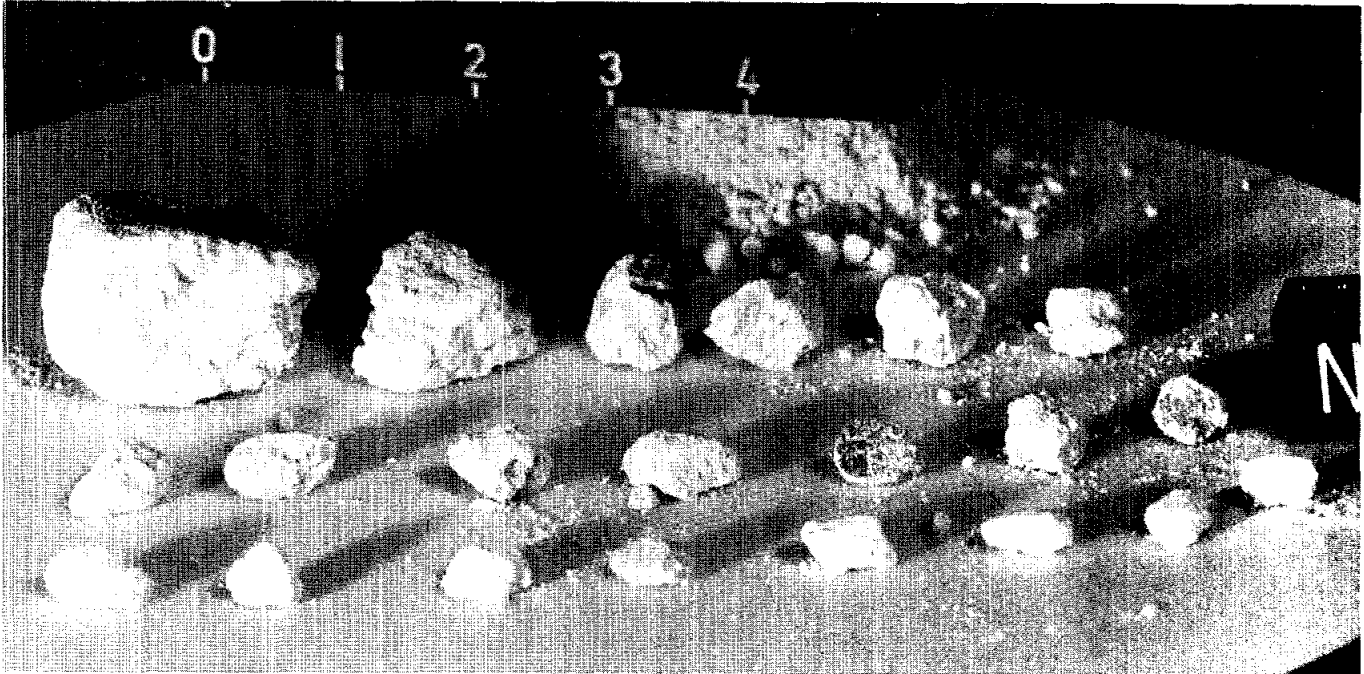


FIGURE 1. Scale in cm.  S-72-41420.

INTRODUCTION:  60057 is a friable, white rock (Fig. 1) that is probably a cata-
clastic anorthosite.  Some patina is present but zap pits are absent.  It was
collected ∿170 ᵐ southwest of the Lunar Module.
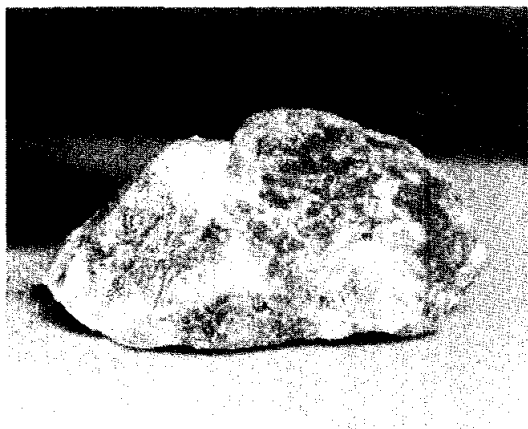


FIGURE 1.  Sample is about
2 cm. long.  S-72-41309.

<u>INTRODUCTION</u>:   60058 is a friable, light gray rock (Fig. 1) that is probably either a polymict or dilithologic clastic breccia.  Most of the rock is a white, friable matrix that supports a few (∿10% of the rock?) dark clasts.  It was collected ∿170 m southwest of the Lunar Module.  Zap pits are absent.
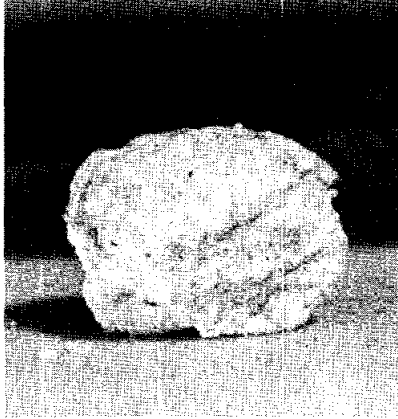


<u>FIGURE 1</u>. Sample is about 1.5 cm. long.  S-72-41309.

INTRODUCTION: 60059 is a friable, white rock (Fig. 1) that is probably a cataclastic anorthosite.  It was collected ∿170 m southwest of the Lunar Module. Zap pits are absent.
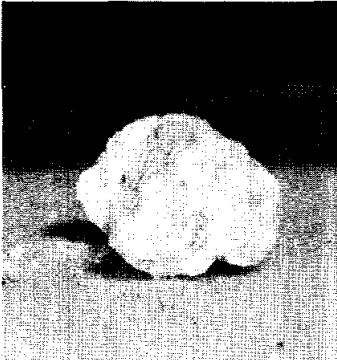


FIGURE 1.  Sample is about 1 cm. long.  S-72-41309.

INTRODUCTION:  60075 is a very friable clastic breccia; it was removed from its documented bag as 13 small pieces.  These pieces have been subsequently broken and powdered even more during processing and handling (Fig. 1).  A few zap pits on the largest fragment were reported in the original catalog description but the extremely dusty and friable nature of the rock has now obscured all original surfaces.  The rock was collected about 170 m south-southwest of the Lunar Module.  It was disturbed prior to photographing, hence burial and orientation data were lost.



FIGURE 1. Part of 60075.  Small scale units are mm.  S-75-33675

PETROLOGY:  Library thin sections are of a highly porous and fragmental breccia composed of abundant small (<2 mm) clasts in a fine-grained clastic matrix (Fig. 2).  Lithic clasts include granoblastic anorthosites, troctolites, and norites, cataclastic anorthosite, spinel-bearing basaltic impact melt and vitric matrix breccia.  Plagioclase, pyroxene and olivine clasts are also present as well as metal, troilite, oxide and devitrified brown glass fragments.  Pyroxene and plagioclase clasts occasionally contain parallel rods and stringers of exsolved opaques.

59

**TABLE 1**

Summary Chemistry of 60075

| | |
|---|---|
| $SiO_2$ | 45.47 |
| $TiO_2$ | 0.20 |
| $Al_2O_3$ | 32.55 |
| $Cr_2O_3$ | 0.03 |
| FeO | 1.73 |
| MnO | 0.02 |
| MgO | 1.87 |
| CaO | 17.63 |
| $Na_2O$ | 0.67 |
| $K_2O$ | 0.05 |
| $P_2O_5$ | 0.02 |
| Sr | 174 |
| La | <10 |
| Lu | |
| Rb | 1.0 |
| Sc | 5.1 |
| Ni | 50 |
| Co | 7.5 |
| Ir ppb | |
| Au ppb | |
| C | 4 |
| N | 66 |
| S | 630 |
| Zn | <4 |
| Cu | 3.4 |

Oxides in wt %; others in ppm
except as noted.
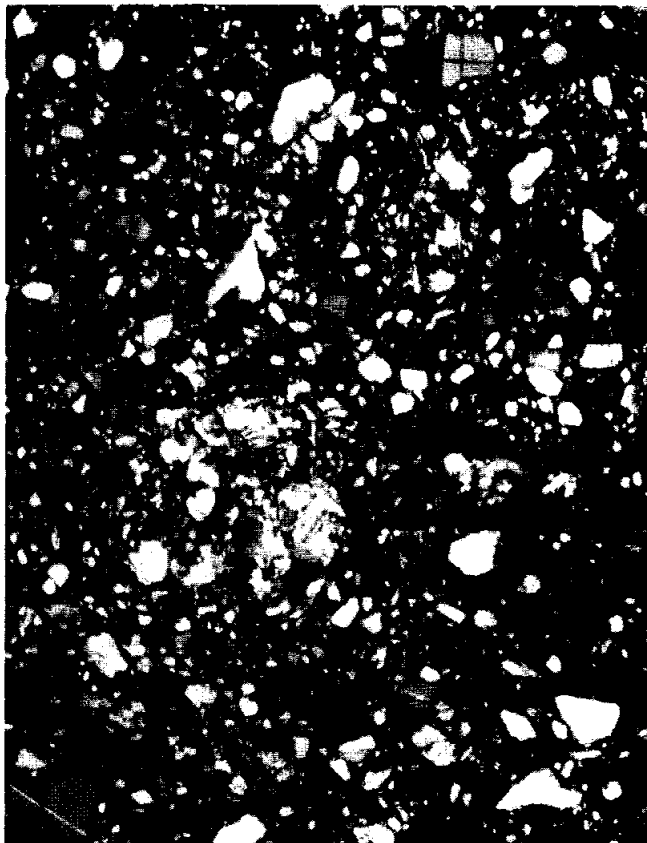


FIGURE 2. 60075,34. general view, xpl. width 2mm.

CHEMISTRY: Rose et al. (1975), Cripe and Moore (1975) and Moore and Lewis (1976) provide major and trace element data for the bulk rock (Table 1). Its reported composition is very aluminous and quite unlike that of the local soil. Despite the abundant metal seen in thin section, the split analyzed by Rose et al. (1975) was low in Ni and Co. Incompatible elements are also low indicating a very small KREEP component.

PROCESSING AND SUBDIVISIONS: All of the allocated splits came from a single 21 g fragment (60075,4) which was one of the original 13 pieces of the rock. During processing 60075,4 broke into a 2 cm fragment, two 1 cm fragments and many smaller chips and fines. Processing notes indicate that the portions analyzed for chemistry were typical fragments and fines that included both dark and light clasts.

INTRODUCTION: 60095 is a fractured spheroid of yellow-green to light brown
glass (Fig. 1).   Internal vesicles are numerous.  Cooling cracks and zap
pits are present but rare on all surfaces.  The sample was collected about 175 m
southwest of the Lunar Module at the heat flow hole site.
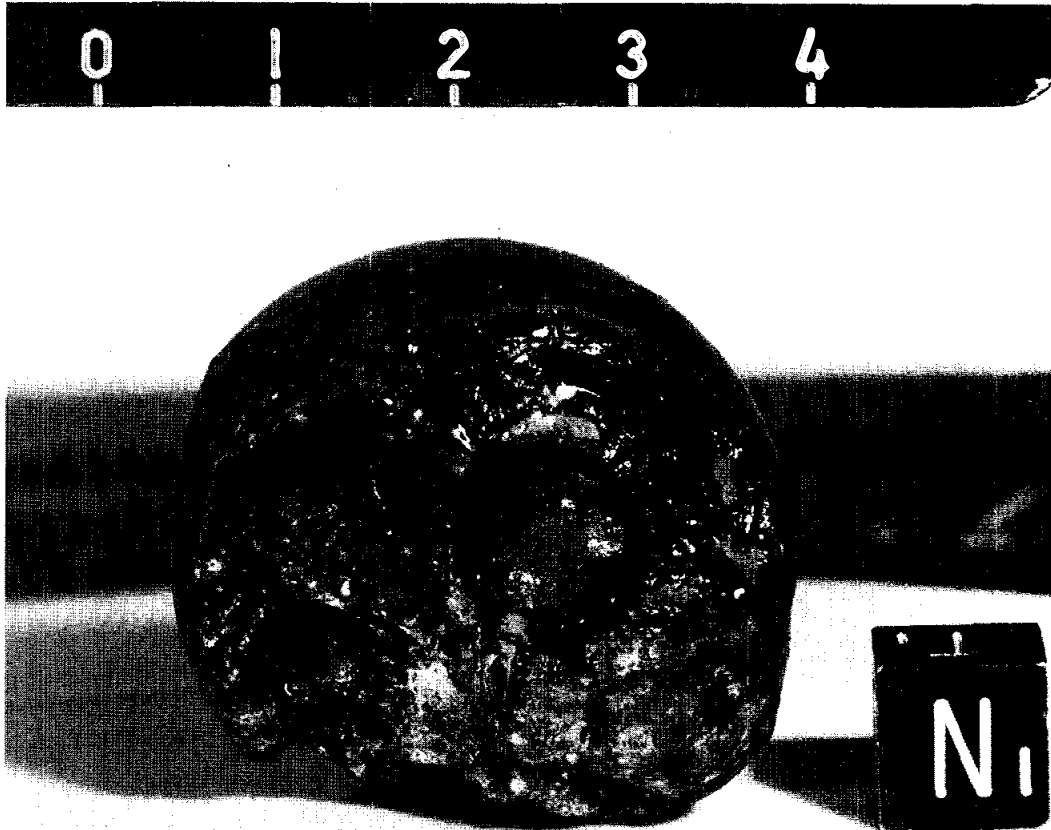


FIGURE 1. Scale in cm.  S-72-39424

PETROLOGY:    Schaal et al. (1979) and Mehta and Goldstein (1979) provide
petrographic information.  The sample is nearly holohyaline.  A few partially
digested and recrystallized clasts of plagioclase act as nucleation sites for
areas of devitrification and quench-crystal growth (Fig. 2).  Rounded blebs
of metal with associated troilite and schreibersite are abundant, ranging in
size from $\sim 50$ µm down to a few Ångstroms.  Submicron metal particles are
peppered through the glass, sometimes aligned in flow planes.  Mehta and
Goldstein (1979) provide detailed information on the metal in this rock.
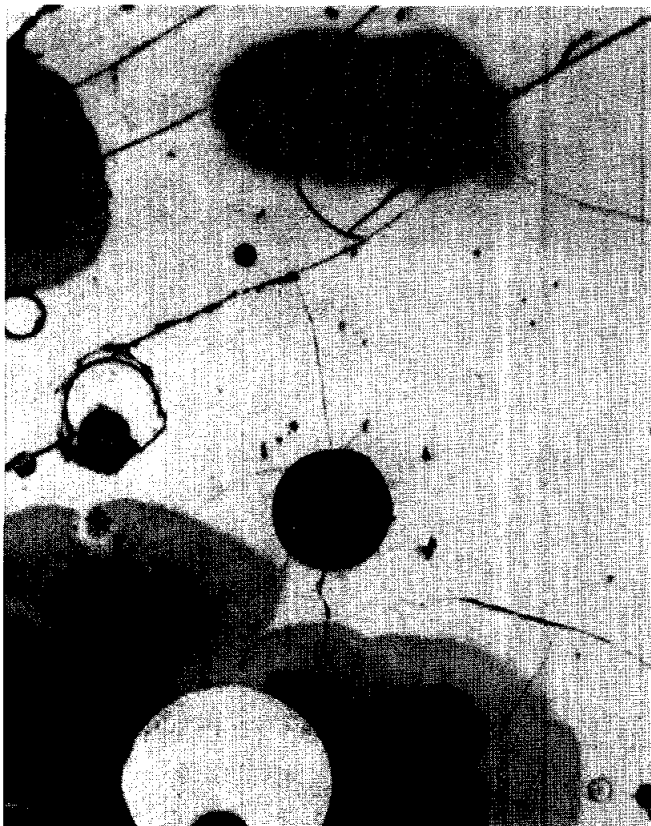
FIGURE 2. 60095,30. general view,ppl. width 2mm.

TABLE 1

Summary chemistry of 60095

| | |
|---|---|
| $SiO_2$ | 44.87 |
| $TiO_2$ | 0.51 |
| $Al_2O_3$ | 25.48 |
| $Cr_2O_3$ | 0.14 |
| FeO | 5.75 |
| MnO | 0.07 |
| MgO | 8.11 |
| CaO | 14.52 |
| $Na_2O$ | 0.28 |
| $K_2O$ | 0.09 |
| $P_2O_5$ | |
| Sr | |
| La | |
| Lu | |
| Rb | 1.67 |
| Sc | |
| Ni | 560 |
| Co | |
| Ir ppb | 25.4 |
| Au ppb | 7.11 |
| C | |
| N | |
| S | |
| Zn | 1.55 |
| Cu | |

Oxides in wt%; others in ppm except as noted.

CHEMISTRY: Schaal (unpublished) analyzed for major elements by defocussed electron beam (DBA) and Ganapathy et al. (1974) report siderophile and volatile abundances. In terms of major elements 60095 is equivalent to local Apollo 16 soil (Table 1). Siderophiles are very high. Hertogen et al. (1977) assigned this meteoritic component to group 5H, probably derived from the South Ray Crater projectile. Ganapathy et al. (1974) discuss other possibilities for the presence of this meteoritic group.

MICROCRATERS AND SURFACES: Neukum et al. (1973), and Brownlee et al. (1975) studied the microcraters on this sample (Figs. 3, 4 and 5). The surface has had a complex exposure history and is in production. Blanford et al. (1974) briefly mention glass droplets on the surface.
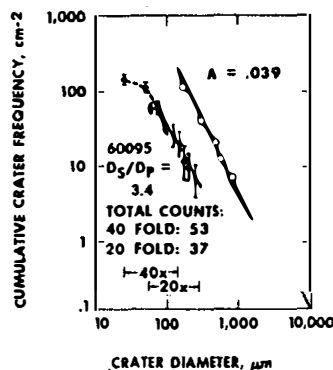
FIGURE 3. Microcraters; from Neukum et al.(1973).

FIGURE 4. Micro-craters; from Brownlee et al. (1975).
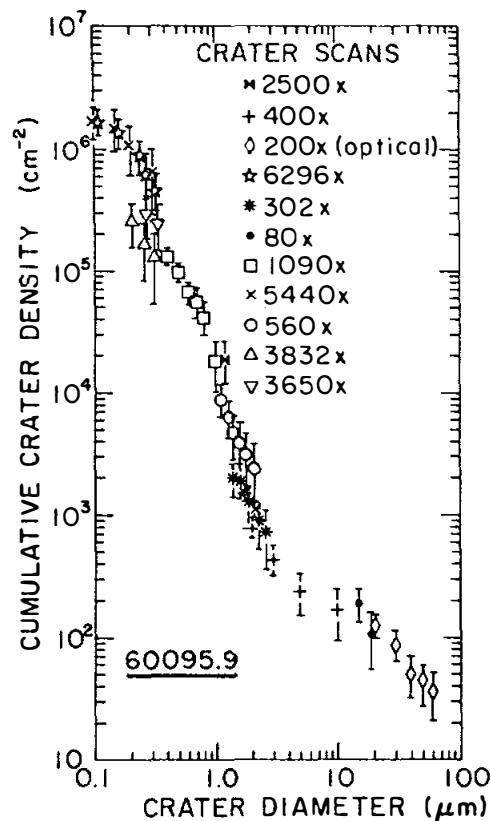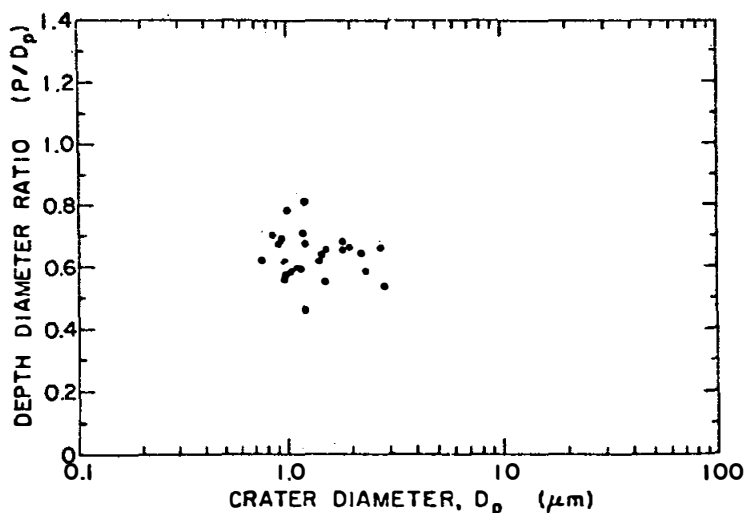


FIGURE 5. Microcraters; from Brownlee et al. (1975).

PHYSICAL PROPERTIES: Hopper et al. (1974), Uhlmann et al. (1974) and Klein and Uhlmann (1976) provide data relating to the glass forming process and discuss the kinetics of the transformation (Figs. 6,7,8,and 9). Theoretical con-siderations assuming a nucleation barrier of 50 kT predict that a sphere the size of 60095 should not be glassy. A somewhat higher nucleation barrier (60-65 kT) and very few heterogeneous nucleii are required to bring prediction in line with observation. The critical cooling rate of an object with the com-position of 60095 is 70 °C/sec; anhydrous liquidus temperature is 1270° C.

PROCESSING AND SUBDIVISIONS: In 1973, 60095 was cut into two pieces, the smaller being subdivided for allocations. The larger piece ($\sim$ 2/3 of the sample) pre-served the entire hemisphere with an intact exterior surface.
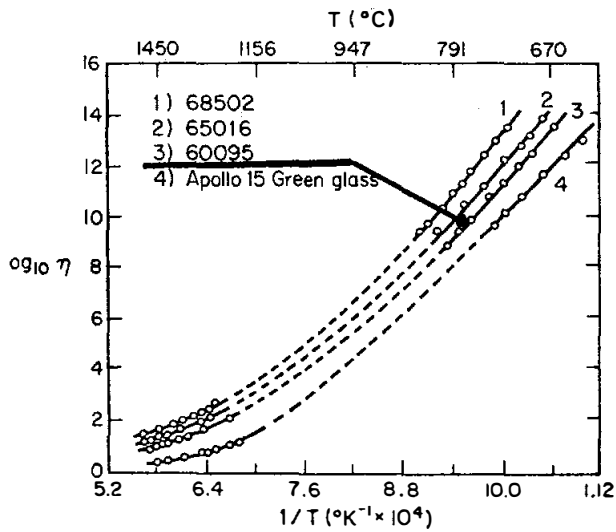
FIGURE 6. Viscosity v. temperature; from Uhlmann _et al._(1974).
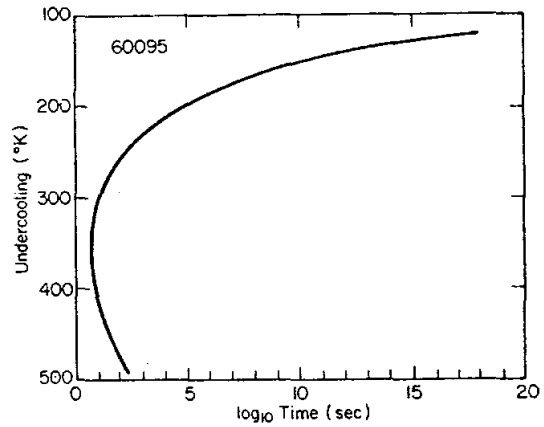


FIGURE 7. Time-temperature-transformation curve; from Uhlmann _et al._ (1974).
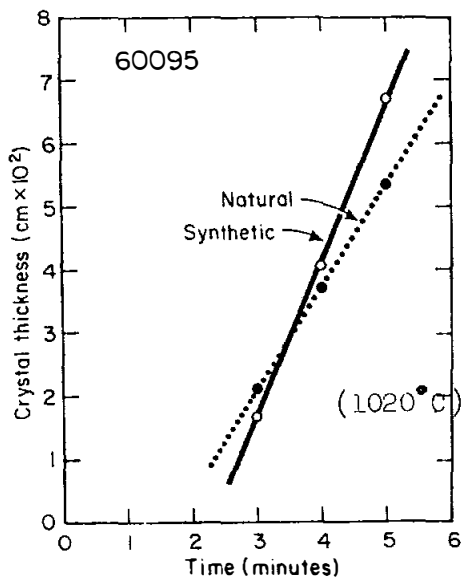


FIGURE 8. Crystal thickness v. time, from Klein and Uhlmann (1975).
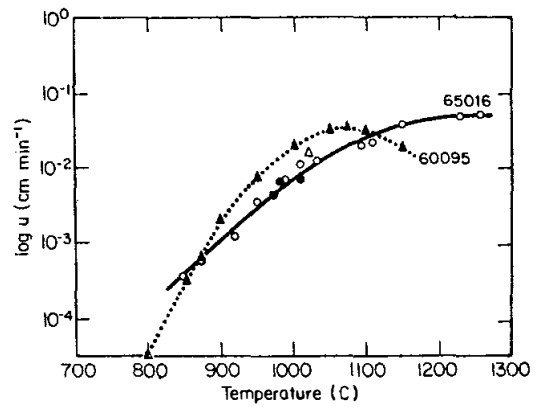


FIGURE 9. Crystal growth rate v. temperature, from Klein and Uhlmann (1975).

INTRODUCTION:  60115 is a tough, angular sample with many fractures (Fig. 1).  It
is dominantly glassy but complex.  The glassy matrix is variable in color  and
vesicularity, and glass veins cut it.  Plagioclase and light gray porphyritic
clasts are prominent as well as dark, glassy clasts.  Clasts boundaries are
commonly indistinct.

60115 was collected approximately 60 m southwest of the Lunar Module where it was
slightly buried.  Its orientation is known.  Very few zap pits are present.

S-72-40396

P - Porphyritic light gray clasts
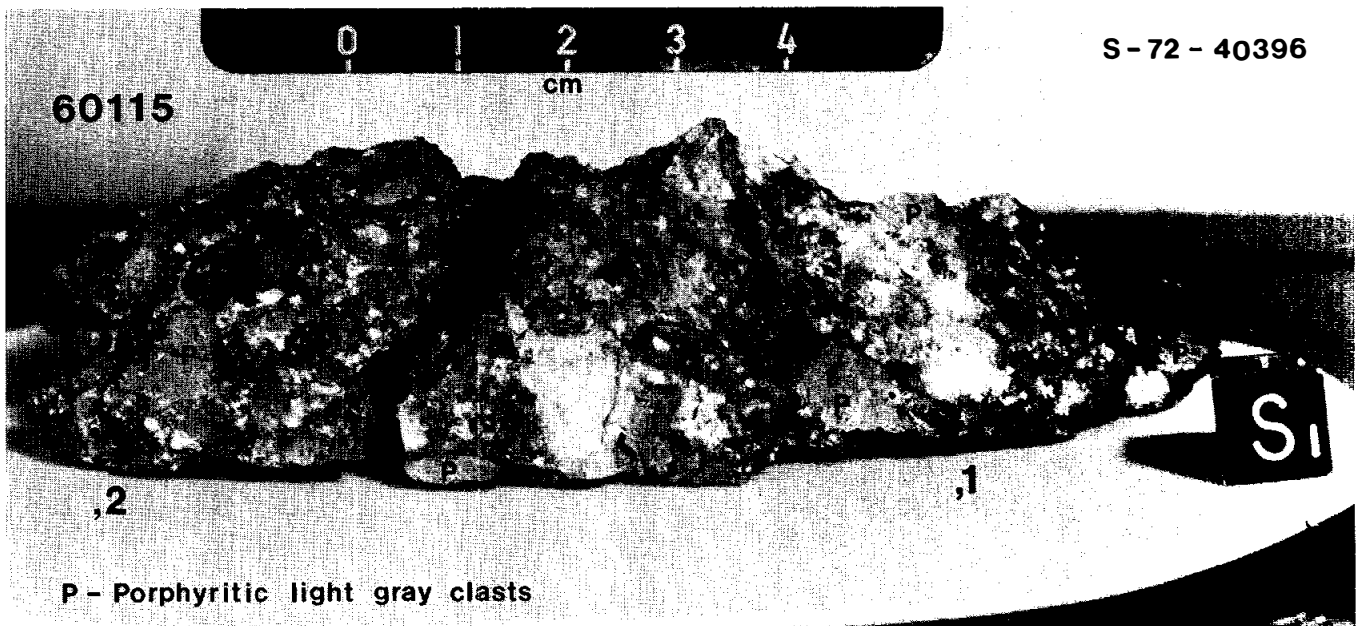
FIGURE 1.

PETROLOGY:  Thin sections dominantly show angular fragments of dark aphanitic
impact melt engulfed in a colorless shock-melted anorthosite (Fig. 2).   Relics
of shocked anorthosite, grading into the swirly glass, are abundant.  The glass
penetrates the dark clasts (Fig. 2).   In a few places the dark clasts are strung
out and melted, causing the host anorthositic glass to have a brown color.  The
dark aphanitic impact melts contain few clasts, but have metal grains。

The porphyritic clasts contain small (<500 μm) elongate mafic mineral phenocrysts
and some plagioclases set in a groundmass of spherulitic plagioclase laths, mafic
minerals, and glass (Fig. 2).   Metal is present.

CHEMISTRY:  Clark and Keith (1973) show that the bulk rock is low in K (0.054%),
Th (1.46 ppm) and U (0.35 ppm) from γ-ray counting.  Data on radionuclides ($^{26}$Al,
etc.) are also given, but it cannot be decided whether the surface is saturated
in $^{26}$Al or not (Yokoyama et al., 1974).

a


b


c


FIGURE 2.

a) 60115,8. shock-melted anorthosite and aphanitic clasts, ppl. width 2mm.
b) 60115,8. relict shocked anorthosite, xpl. width 2mm.
c) 60115,14. plagioclase porphyritic clast, ppl. width 2mm.

PROCESSING AND SUBDIVISIONS: 60115 has been split along a natural fracture into two main pieces, ,1 and ,2, and a few small pieces, but has not been extensively subdivided.

INTRODUCTION: 60135 is an oblate ellipsoidal rock with a core of shocked anorthosite partly coated with a smooth glass (Fig.1). The sample was collected from a level area 100 m southwest of the Lunar Module. It may have been perched and its orientation is not definitely known. Zap pits are present but areas on both the anorthosite and the glass are free of zap pits.
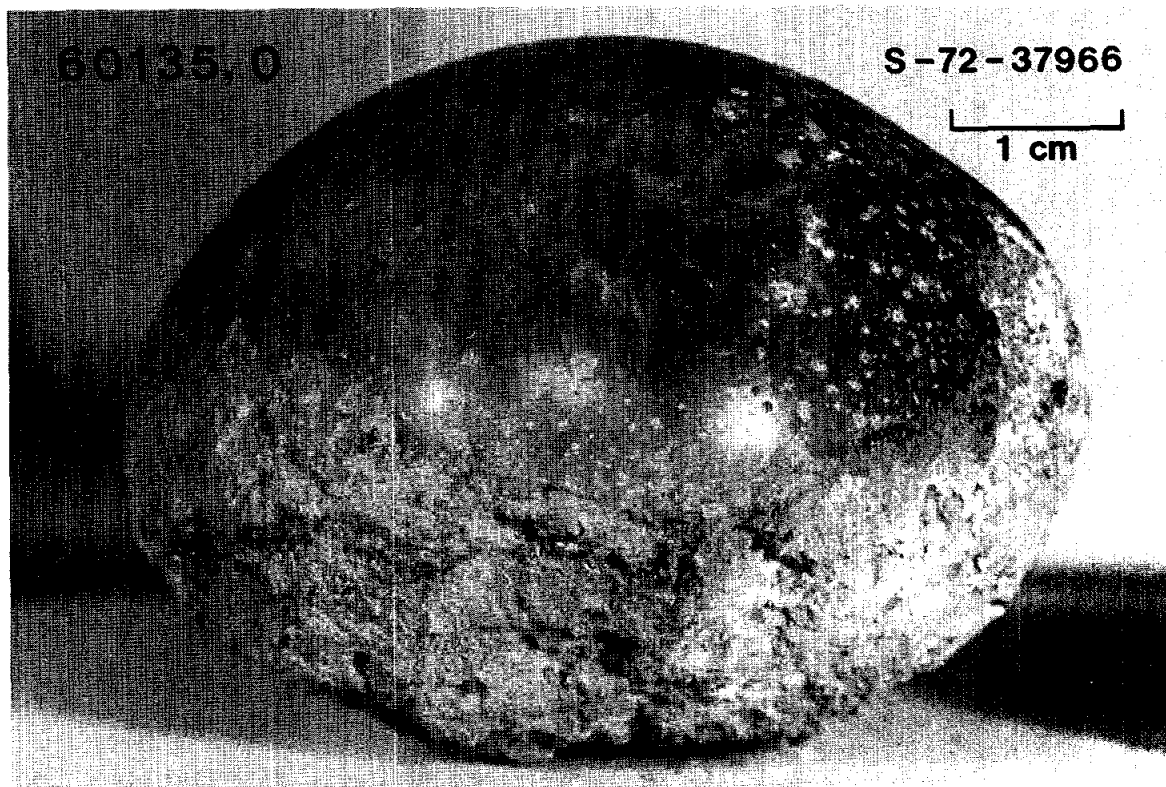


FIGURE 1.

PETROLOGY: A thin section of the anorthosite at the glass contact consists of three 3x3 mm patches of fine-grained shock mosaics of plagioclase (Fig.2) which probably represent original grains. A 500 µm deformed mafic grain (olivine?) occurs at their mutual junction. Brown vesicular, colonnaded de-vitrified glasses invade the anorthosite and surround the mafic grain. Macro-scopically the plagioclase is variably white, milky, cloudy and vitreous.

The vesicular coat varies from glass at the exterior, through spherulitic and bow-tie structures of plagioclase and mafic minerals to intergrown ragged plagioclase laths with interstitial glass in the interior (Fig.2). These laths can be seen macroscopically. The bulk is 90% or more of plagioclase. The glass coat makes small apophyses into the anorthosite but without ex-tensive veining.

a



b



c



FIGURE 2.
   a) 60135,6. anorthosite, shocked,
with mafic grain at junction, xpl.
width 2mm.
b) 60135,5. spherulitic coat, xpl.
width 1mm.
c) 60135,6. vesicular, basaltic-
spherulitic coat, xpl. width 2mm.

CHEMISTRY: Eldridge et al. (1973) measured K, U, Th, and cosmogenic radionuclides in the rock. The abundances of the incompatible elements are extremely low ($K_2O$ 0.017%, Th 0.27 ppm, U 0.068 ppm).

EXPOSURE AGE: The $^{26}$Al and $^{22}$Na abundances (Eldridge et al., 1973) indicate saturation values, hence an exposure long with respect to the half-life of $^{26}$Al.

MICROCRATERS: Size characteristics and cumulative size distributions of the crater population (Fig.3) on the glass surface of 60135 are presented by Neukum et al. (1973). This surface is a production surface and rock has a simple (i.e., un-tumbled) surface history.
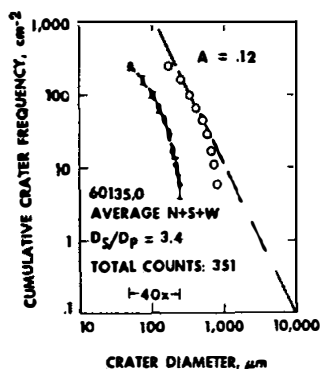
FIGURE 3. Microcraters; from Neukum et al.(1973).

PROCESSING AND SUBDIVISIONS: The rock is undivided except for chips taken for thin sections of the anorthosite and the coat.

INTRODUCTION:  60215 is a coherent, cataclastic anorthosite with very low porosity. A dark, vesicular glass coats ~15% of the rock's surface (Fig. 1).  The bulk of the rock is probably a monomict breccia although the presence of basaltic impact melt clasts indicates at least some mixing.  On the basis of very low Ni and Co concentrations the anorthosite has not been contaminated by meteoritic siderophiles.

Zap pits and patina are abundant on the lunar-up side.  The opposite surface is devoid of pits, indicating a simple exposure history.  The sample was collected about 115 m southwest of the Lunar Module.
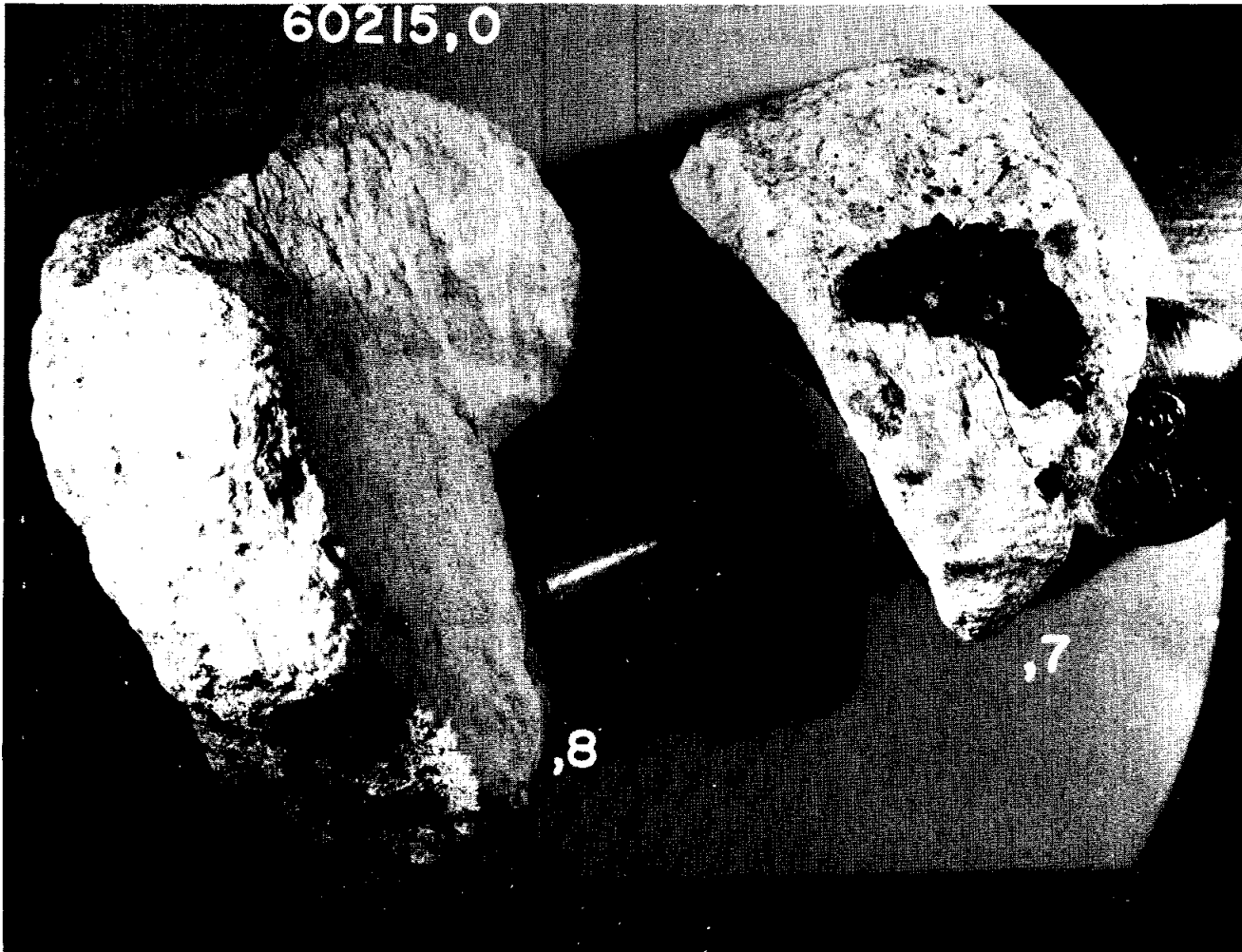


FIGURE 1. Scale in cm.  S-74-32059.

PETROLOGY:  Meyer and McCallister (1973), Dixon and Papike (1975), Ishii et al. (1976) and the Apollo 16 Lunar Sample Information Catalog (1972) provide petrographic information.  Seriate plagioclase mineral clasts ($An_{96}$) up to 4 mm long make up 97% of the rock (Fig. 2).  Small amounts of maskelynite are present and some grains have been recrystallized to a fibrous or microgranular texture. Accessory minerals include orthopyroxene ($En_{62-68}Wo_{1-2}$; Fig. 3), augite ($En_{44}Wo_{44}$), rare olivine ($Fo_{78}$), metal, troilite and ilmenite.  Pyroxenes occur as discrete grains without exsolution lamellae (Meyer and McCallister, 1973; Dixon and Papike, 1975).

a
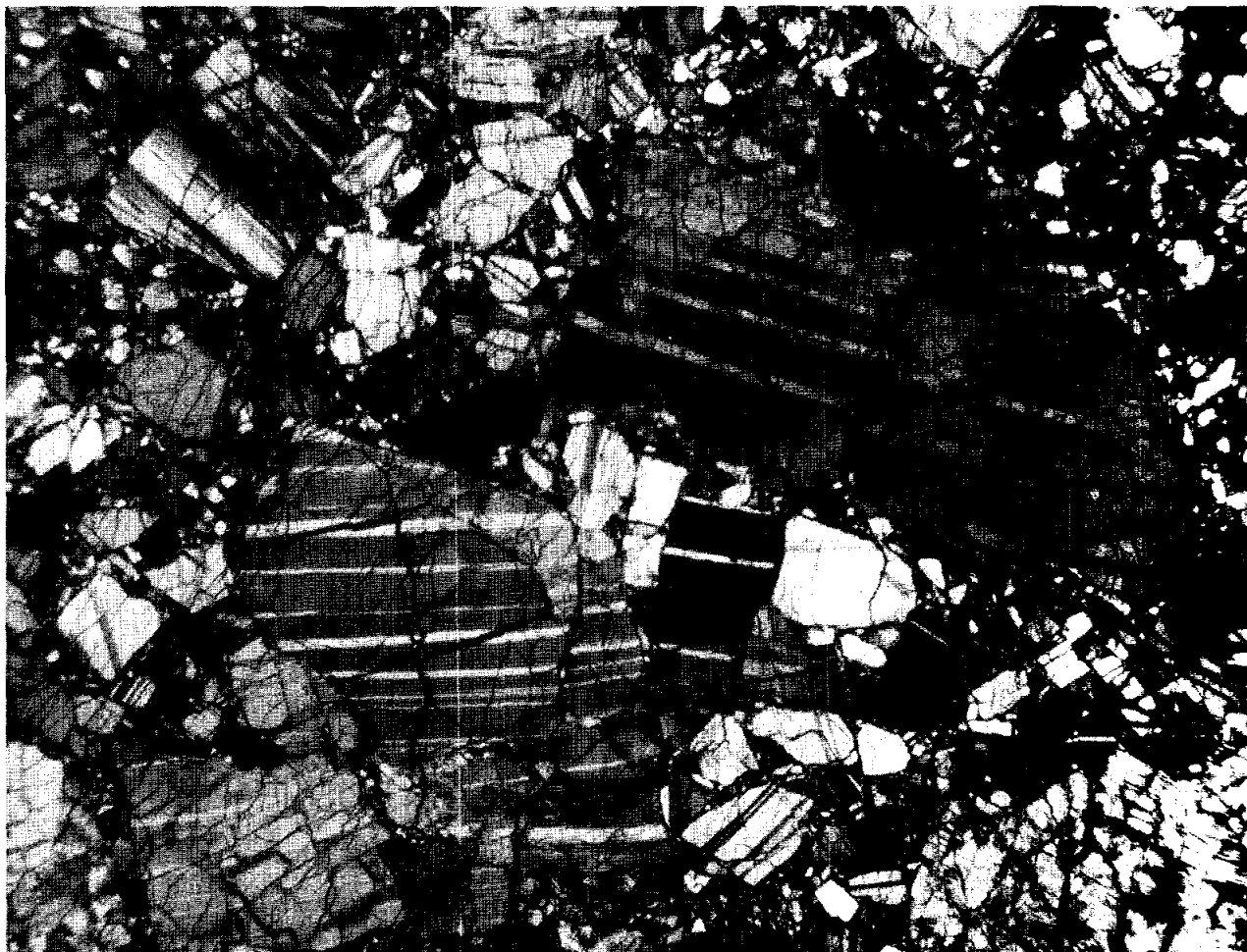


b



FIGURE 2. a) 60215 anorthosite, xpl.
width about 3mm.   S-72-43966.
b) 60215,14. basaltic clasts, partly
xpl.  width 1mm.

FIGURE 3. Pyroxenes; from
Dixon and Papike (1975).



60215
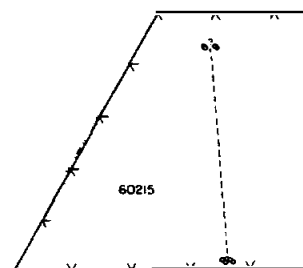
Lithic clasts are predominantly anorthositic, compositionally identical to the mineral clasts. One large anorthosite clast contains a nest of disaggregated orthopyroxene significantly more calcic than the mineral clasts ($En_{63}Wo_5$) and a single grain of Cr-spinel (Meyer and McCallister, 1973). Fragments of basaltic impact melt (troctolitic basalt; Meyer and McCallister, 1973) account for up to 3% of one thin section (,13). These clasts are small (<0.8 mm) and angular, and have subophitic to intersertal textures (Fig. 2). Plagioclase in these fragments is $An_{94}$ and olivine is $Fo_{80-90}$. Minor phases include interstitial glass and sulfides.

CHEMISTRY: Rose et al. (1975) (split ,30 erroneously published as ,33), Cripe and Moore (1975) and Moore and Lewis (1976) report chemical data for the anorthosite. Meyer and McCallister (1973) provide defocussed electron beam analyses (DBA) of two "troctolitic basalt" clasts. The anorthosite is nearly pure plagioclase with $Al_2O_3$ >35% (Table 1). The low Ni and Co contents indicate a lack of meteoritic contamination. Total sulfur is among the lowest ever measured in a lunar rock. The compositions of the two troctolitic basalt clasts are different (Table 1).

TABLE 1. Summary chemistry of 60215 lithic types

|  | Bulk anorthosite | Troctolitic basalt clasts(DBA) | |
|---|---|---|---|
| $SiO_2$ | 44.50 | 47.8 | 44.7 |
| $TiO_2$ | 0.0 | 0.15 | 0.83 |
| $Al_2O_3$ | 35.53 | 24.3 | 21.2 |
| $Cr_2O_3$ | 0.05 | 0.16 | <0.16 |
| FeO | 0.15 | 5.1 | 8.32 |
| MnO | 0.01 | 0.18 | 0.13 |
| MgO | 0.14 | 5.62 | 14.1 |
| CaO | 19.34 | 15.5 | 10.6 |
| $Na_2O$ | 0.40 | 0.45 | 0.63 |
| $K_2O$ | 0.02 | 0.01 | 0.22 |
| $P_2O_5$ | 0.0 | | |
| Sr | 121 | | |
| La | <10 | | |
| Lu | | | |
| Rb | <1 | | |
| Sc | <2 | | |
| Ni | 1.8 | | |
| Co | <2 | | |
| Ir ppb | | | |
| Au ppb | | | |
| C | 17 | | |
| N | 105 | | |
| S | <6 | | |
| Zn | <4 | | |
| Cu | 1.8 | | |

Oxides in wt%; others in ppm except as noted.

PROCESSING AND SUBDIVISIONS: In 1972, 60215 was cut into two main pieces (Fig. 1). Allocations were made from chips taken from both of these pieces. Several interior and exterior chips of both the anorthosite and the glass coat exist.

INTRODUCTION:  60235 is a vesicular, medium gray basaltic impact melt (Fig. 1).
The coherent rock has a soft, white, earthy coating, distinct from soil, in
places.  It was collected about 30 m south or southwest of the Lunar Module and
it was photographed prior to collection.  A few zap pits are present on all
surfaces.                                                                     .

/FIGURE 1. Scale in mm.
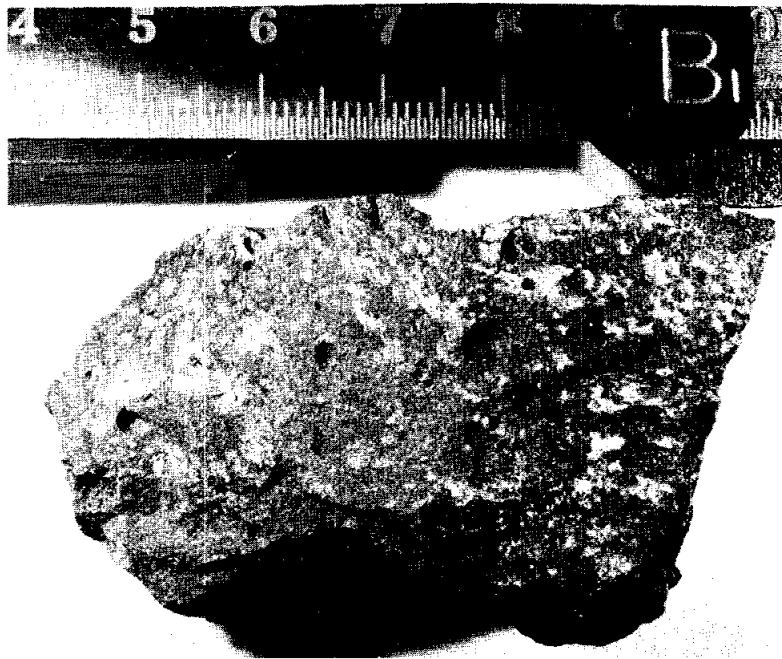


PETROLOGY:  A thin section cut for this study shows that 60235 is a plagioclase-
rich impact melt.  It consists of plagioclase laths 200-300 µm long (Fig. 2)
which are frequently hollow and have square cross-sections.  Interstitial
minerals are mainly pyroxene, with some mesostasis glass with opaque minerals and
cristobalite.  Clastic material consists of plagioclases and plagioclase-rich
breccias.

FIGURE 2. 60235,2. general
view, ppl. width 2mm.

PROCESSING AND SUBDIVISIONS: A single representative chip (,1) was used to make
thin section ,5.

INTRODUCTION:  60255 is a tough, dark, glassy matrix breccia with abundant and varied clasts.  A lineation of the clasts is apparent on sawn surfaces (Fig.1). In many respects 60255 is very similar to local soils but with a fairly large and stable magnetic component.  Splash glass coats part of the N  and E  surfaces.

This rock was probably collected 30-40 m southwest of the Lunar Module and was partially buried at the time of collection.  The lunar orientation is known.  Zap pits are rare to absent on all surfaces.

**60255, 45**                                                 S-79-34528
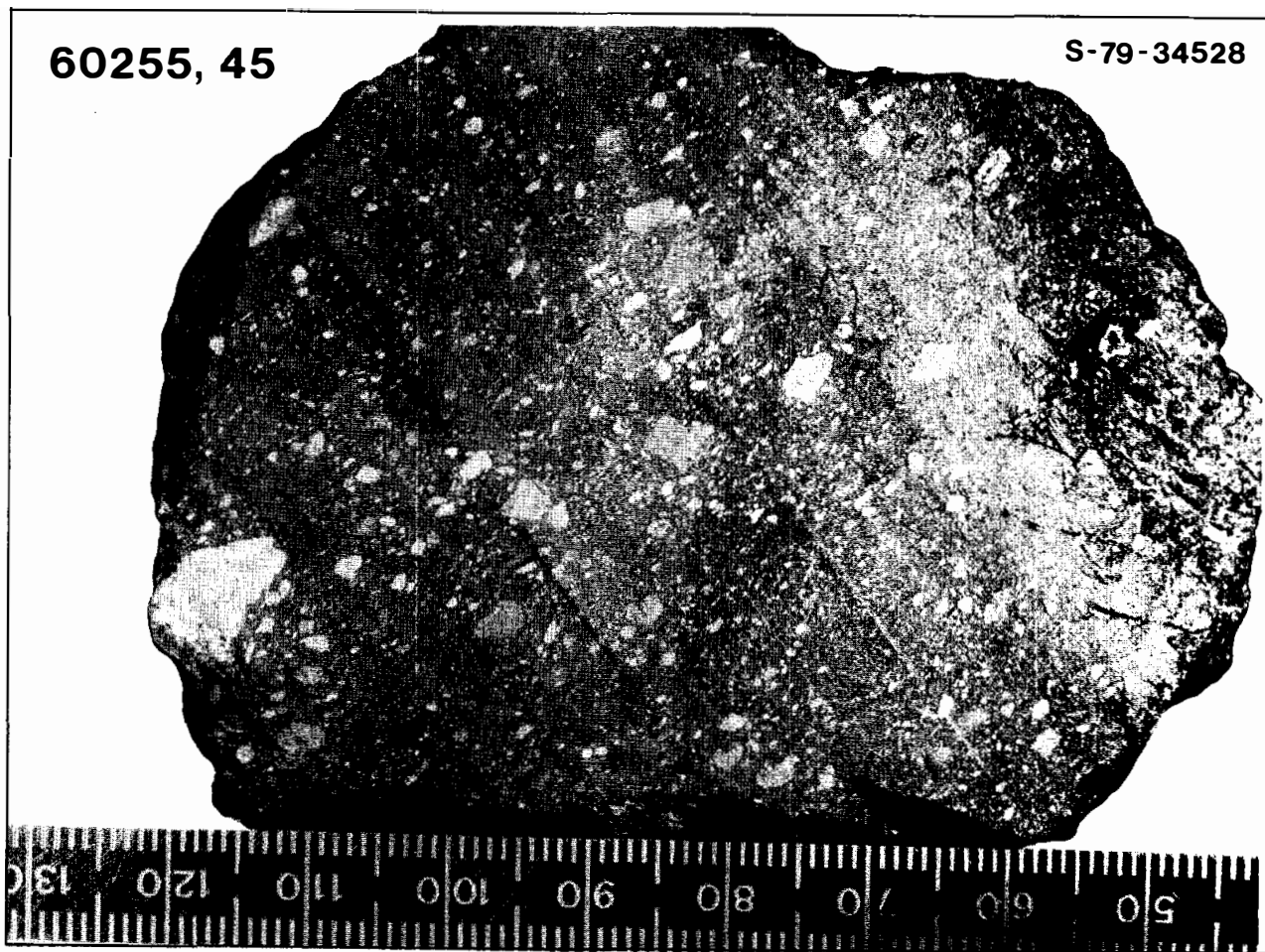
FIGURE 1. Saw cut face. Small scale division is mm.

PETROLOGY:  Petrographic descriptions are given by Schaeffer and Hollister (1975), James et al. (1975), Schaeffer (1974) and the Apollo 16 Lunar Sample Information Catalog (1972).  Many different lithic, mineral and glass clasts are welded together by a cryptocrystalline to glassy matrix.  All of the clasts show minute fractures and internal deformation indicative of mild shock.

75

a



b



c



d
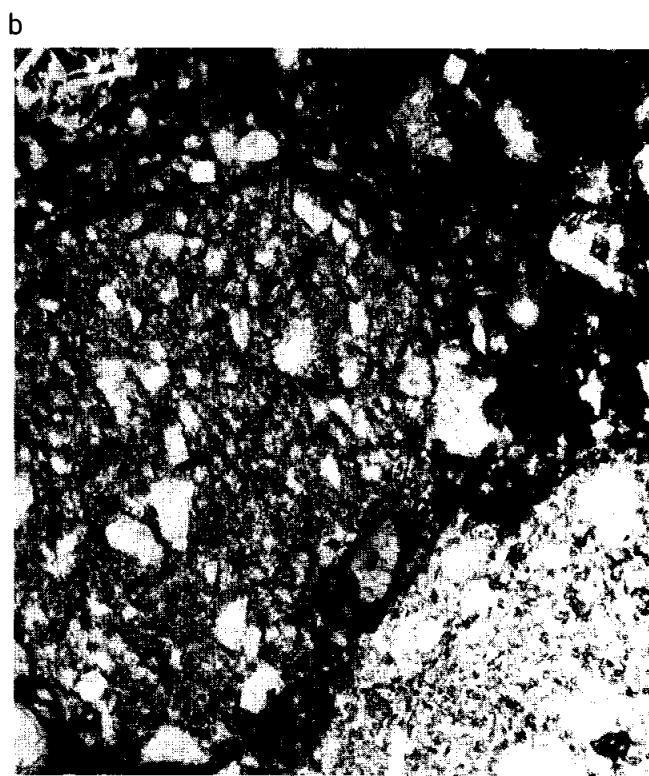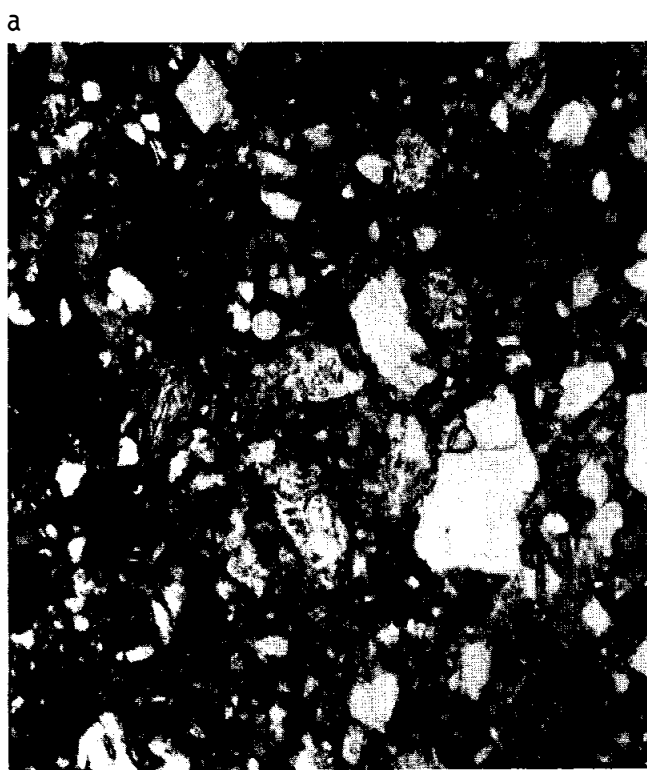


FIGURE 2. a) 60255,81. general view,ppl. width 2mm.

c) 60255,81. basaltic melt clast, xpl. width 2mm.

b) 60255,81. clasts,ppl. width 2mm.

c) 60255,75. vitrophyre (center), ppl. width 0.5mm.

Granoblastic and basaltic textured fragments are the most abundant of the lithic clasts (Fig.2). One of the basaltic textured impact melt clasts has homogeneous olivine ($Fo_{74}$), two zoned pyroxenes (augite and pigeonite) and plagioclase which is largely homogeneous ($An_{97}$) but with marked zoning (down to $An_{69}$) near contacts with mesostasis (Schaeffer and Hollister, 1975; Schaeffer, 1974).

A coarse-grained "gabbroic textured" clast (Fig. 2) with ~90% plagioclase and 10% poikilitic and exsolved pyroxene and olivine is sampled by several serial thin sections (,71-,76 and ,77-,82). The pyroxenes in this clast are ~$Wo_{3-8}En_{70-65}$ and $Wo_{30-35}En_{50-45}$, olivine is $Fo_{74}$ and plagioclase is $An_{92-95}$ (Schaeffer and Hollister, 1975; Schaeffer, 1974; Steele, unpublished). Fe-metal, troilite and ilmenite are accessory phases; mesostasis is absent.

Rare olivine vitrophyres are present in some sections (Fig. 2). No analyses are yet available. Clear, orange, yellow and brown glass beads and fragments are scattered throughout the rock. Some are partially crystalline. The presence of clean glass precludes any significant thermal event after the formation of this rock.

CHEMISTRY: Scoon (1974) reports major element data, Boynton et al.(1975) determined major and lithophile elements, Wasson et al. (1975) provide siderophile and volatile element analyses and Clark and Keith (1973) give K,U,Th and cosmic-ray induced nuclides determined by gamma-ray spectroscopy.

All of these data indicate that 60255 is compositionally indistinguishable from the local mature soils. Major elements indicate an anorthositic norite composition (Table 1) and REEs in the rock fall within the range of the REEs in the local mature soils (Fig.3). 60255 is also enriched in siderophiles and volatiles with absolute abundances and interelement ratios equivalent to those of the local soils.

TABLE 1. Summary chemistry of 60255

| | | | | |
|---|---|---|---|---|
| $SiO_2$ | 45.2 | Sr | | |
| $TiO_2$ | 0.69 | La | 12.6 | |
| $Al_2O_3$ | 26.1 | Lu | 0.70 | |
| $Cr_2O_3$ | 0.11 | Rb | | |
| FeO | 6.0 | Sc | 10.7 | |
| MnO | 0.07 | Ni | 391 | |
| MgO | 6.4 | Co | 35 | |
| CaO | 16.3 | Ir | ppb | 12.2 |
| $Na_2O$ | 0.49 | Au | ppb | 5.6 |
| $K_2O$ | 0.13 | C | | |
| $P_2O_5$ | 0.12 | N | | |
| | | S | | |
| | | Zn | 21.0 | |
| | | Cu | | |

oxides in wt.%; others in ppm except as noted.
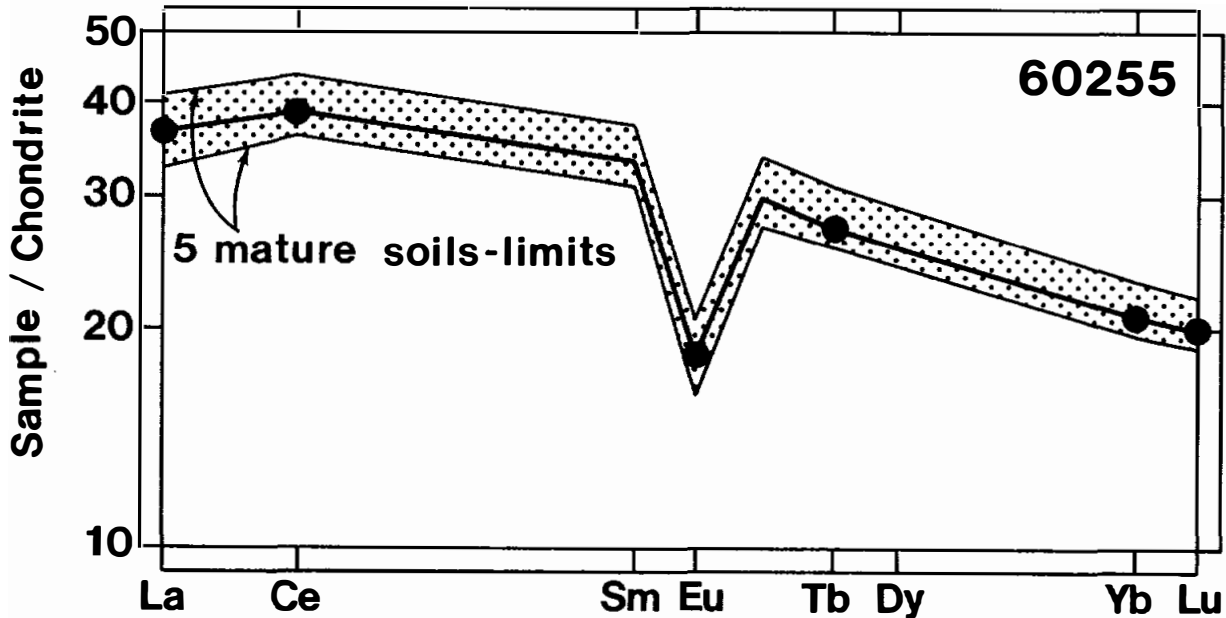
FIGURE 3. Rare earths; from Boynton et al. (1975).

RARE GAS/EXPOSURE AGE:  Clark and Keith (1973) provide data on cosmic-ray in-
duced nuclides as determined by gamma-ray spectroscopy.  Yokoyama et al.(1974)
discuss $^{22}$Na-$^{26}$Al chronology and conclude that 60255 is saturated in $^{26}$Al.
Bernatowicz et al. (1978) report Xe and Kr isotopic data. 60255 is rich in
trapped solar wind and a cosmogenic component but may or may not contain excess
fission Xe.

MICROCRATERS AND TRACKS:MacDougall et al. (1973) observe solar flare tracks
only in plagioclase grains and infer that the rock experienced a thermal event
which erased the tracks from some but not all components.  Estimated annealing
temperature was 700-800°C.  Uranium is concentrated in fine-grained areas but is
heterogeneously distributed throughout the rock (MacDougall et al., 1973).

PHYSICAL PROPERTIES: Magnetic characteristics of 60255 were studied by Nagata
et al. (1973) and Pearce et al. (1973) using standard alternating field (AF) and
thermal demagnetization techniques. A fairly large component of NRM (11x10$^{-6}$ emu/g)
is present that is quite stable with respect to intensity and direction of AF-
demagnetization between 100-400 Oe.rms (Fig.4).  This component is considered by
Nagata et al.(1973) to be a genuine natural remanent magnetization acquired on the
lunar surface.

Ferromagnetic metal accounts for 0.47 wt% of the rock and occurs as about equal amounts of pure iron and kamacite with $\sim$ 6 wt% Ni (Nagata et al.,1973). Fine-grained metal (30-150 Å) in 60255 averages 41 Å as determined by magnetic granulometry (Schwerer and Nagata, 1976). Mossbauer-determined distributions of iron among the various mineral phases are reported by Schwerer et al. (1973) and Huffman et al. (1974).

AF-DEMAGNETIZATION OF NRM AND IRM
SAMPLE : 60255
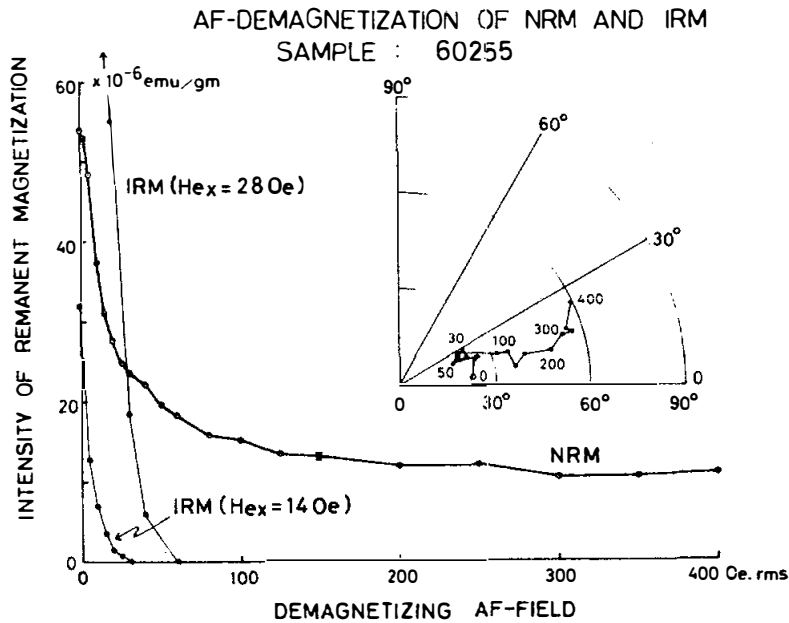


FIGURE 4. AF-demagnetization; from Nagata et al. (1973).

PROCESSING AND SUBDIVISIONS: In 1972, 60255 was slabbed and the slab subdivided (Fig.5). Allocations were made from the slab and from other chips. Thin sections from ,23 and ,30 (adjacent pieces from the slab) contain the basaltic and "gabbroic" clasts described in PETROLOGY. The largest single piece of 60255 remaining is ,45 (672.9 g).
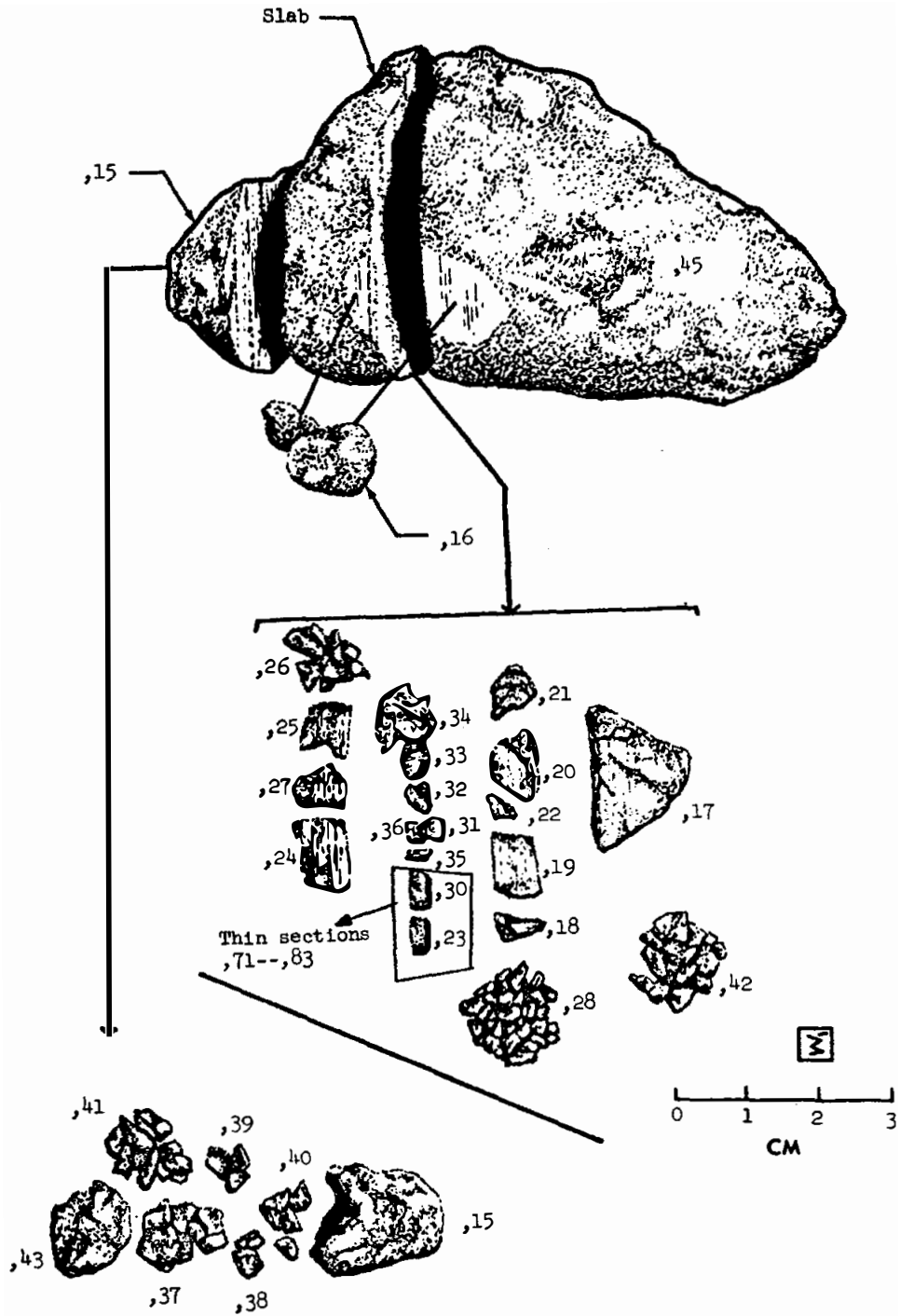
FIGURE 5. Cutting diagram.

INTRODUCTION:  60275 is a polymict, dark-colored breccia coated with a vesicular glass (Fig. 1).  The breccia matrix is glassy and mineral, lithic, glass, and devitrified glass fragments are common.

60275 was collected adjacent to the Lunar Module, where it was perched.  Its orientation is known.  It has a few zap pits on one surface.

a
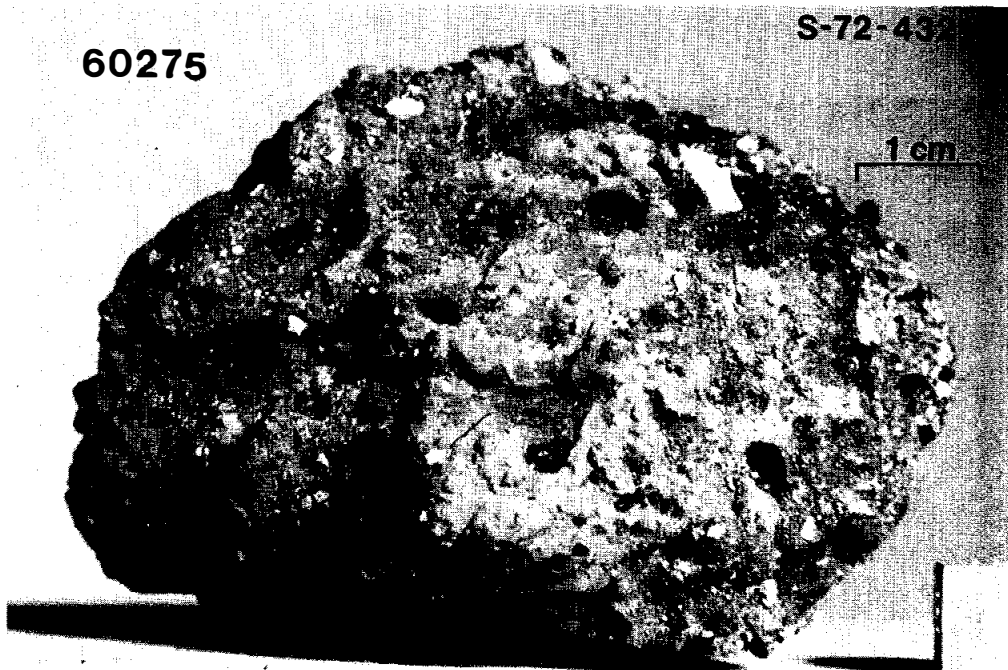


b
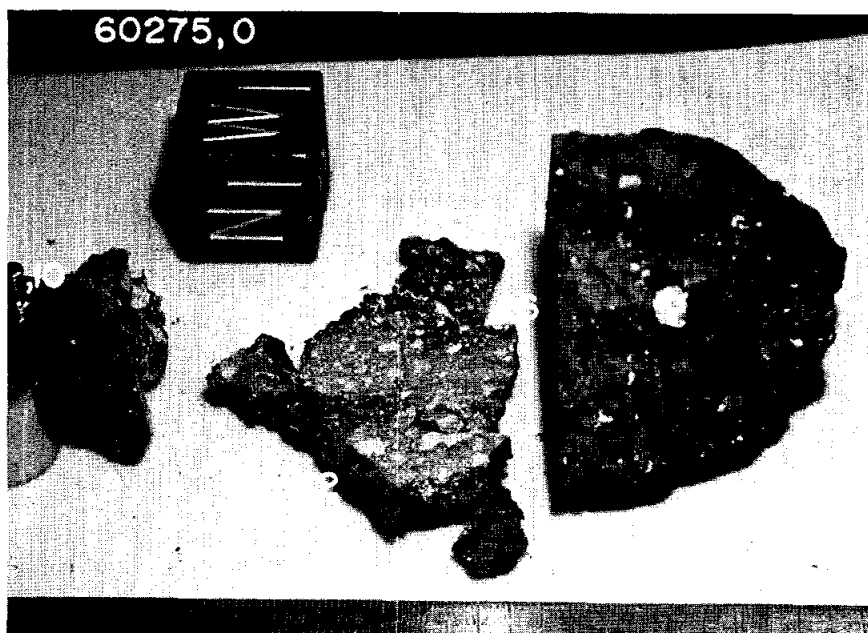


FIGURE 1.

b) is S-75-20527, cube is 2cm.

60275

PETROLOGY:  60275 consists of a variety of clasts apparently bonded with brownish glass (Fig. 2).  The lithic clast population includes poikilitic and basaltic-textured impact melts, cataclastic anorthosites, and feldspathic granulites.  Glass and brown  devitrified glass fragments are also common.  The sample may be a regolith breccia but it lacks glass beads and agglutinates. Hansen et al. (1979b and unpublished) report microprobe data for plagioclases and mafic minerals in granoblastic clasts in thin section ,47.  One clast has plagioclase $An_{95-96}$, pyroxene averaging $\sim En_{71}Wo_4$, and olivine $Fo_{57}$.  Two other analyzed clasts have similar plagioclases.

a
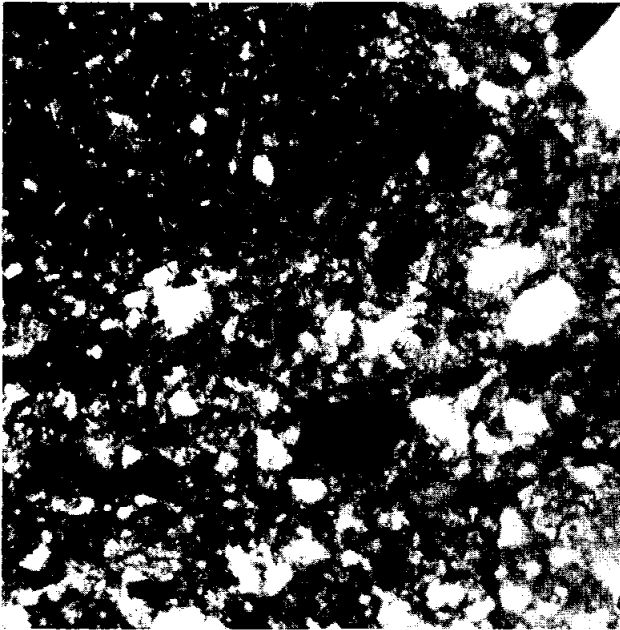


b
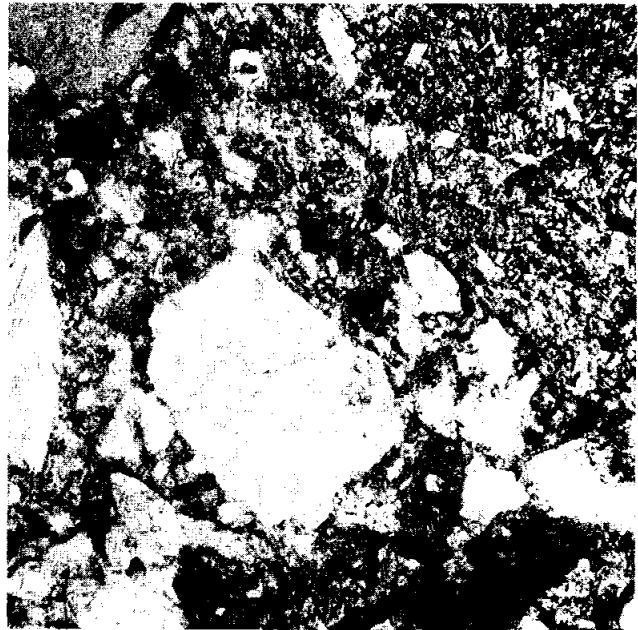


c



FIGURE 2.

a) 60275,51.  general view, ppl.  width 2mm.
b) 60275,13.  melt clasts, ppl.  width 2mm.
c) 60275,51.  glass, ppl. width 2mm.

82

CHEMISTRY: Christian et al. (1976) report major and some trace element analyses for a chip ,34, summarized in Table 1. Clark and Keith (1973) analyzed K, U, and Th in the bulk rock using gamma-ray spectroscopy; their K abundance is significantly lower than that of Christian et al. (1976). The analysis of Christian et al. (1976) is similar to local soil analyses.

TABLE 1. Summary chemistry of 60275

(from Christian et al., 1976)

| | | | |
|---|---|---|---|
| $SiO_2$ | 44.9 | Sr | 150 |
| $TiO_2$ | 0.62 | La | 14 |
| $Al_2O_3$ | 25.4 | Lu | |
| $Cr_2O_3$ | 0.10 | Rb | 3.2 |
| FeO | 5.8 | Sc | 9.8 |
| MnO | 0.06 | Ni | 250 |
| MgO | 7.6 | Co | 18 |
| CaO | 14.6 | Ir ppb | |
| $Na_2O$ | 0.46 | Au ppb | |
| $K_2O$ | 0.22 | C | |
| $P_2O_5$ | 0.26 | N | |
| | | S | |
| Oxides in wt%; others in | | Zn | 10 |
| ppm except as noted | | Cu | 5.4 |

RARE GASES AND EXPOSURE AGE: Bernatowicz et al. (1978) provide Xe and Kr isotopic data and conclude that 60275 contains significant amounts of solar wind components. It also has excess fission xenon. Clark and Keith (1973) report cosmic ray induced radionuclide data and the sample is saturated in $^{26}Al$ (Yokoyama et al., 1974).

PROCESSING AND SUBDIVISIONS: 60275 has been sawn and substantially split. The main post-sawing splits are shown in Figures 1 and 3. Earlier chips of the rock (,1 and ,2) were made into thin sections and clear glass fragments (,3) were made into grain mounts. ,12 (Fig. 3) was also made into a potted butt for thin sections.
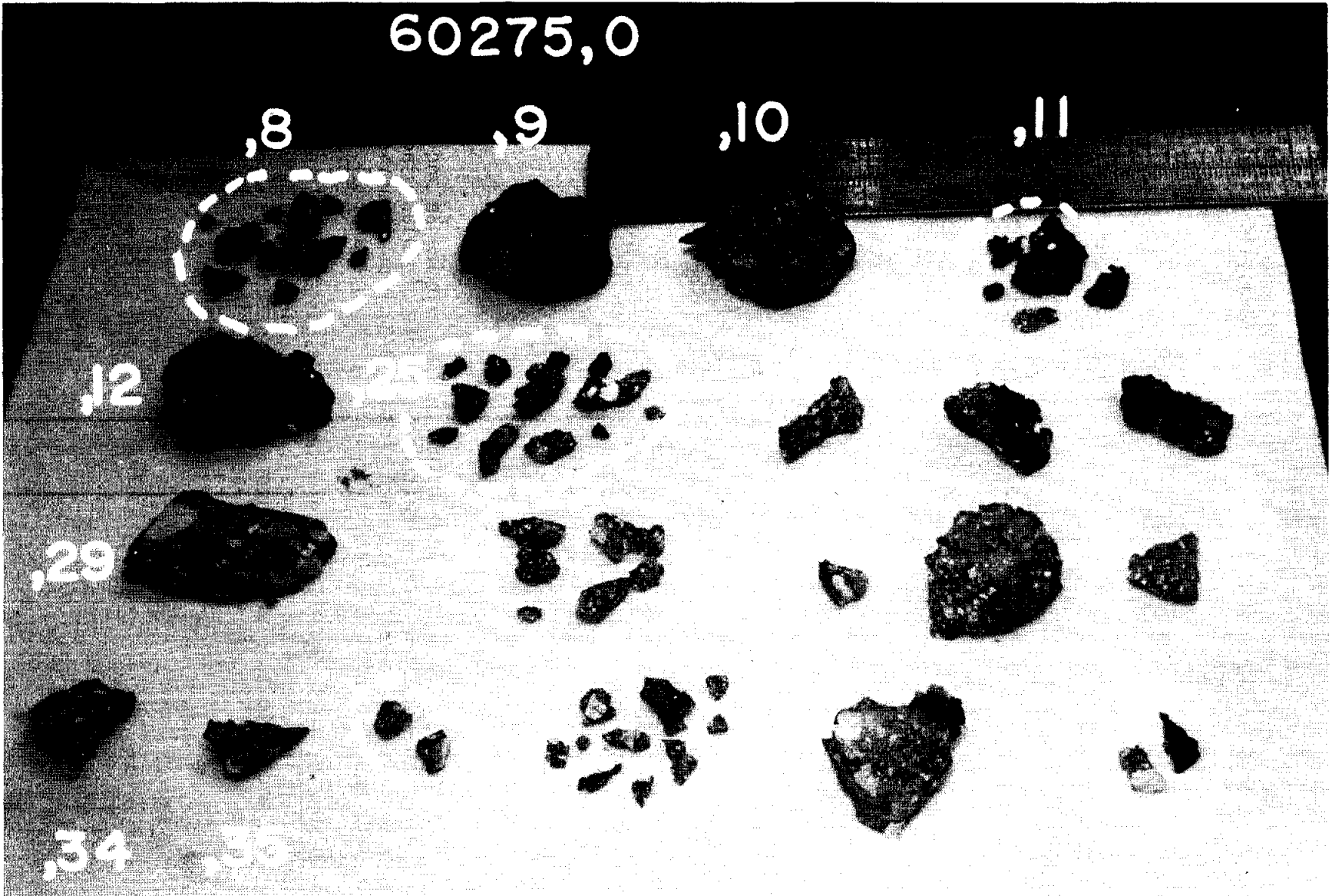
FIGURE 3. Rule is 15 cm. long.  S-75-20524.

INTRODUCTION: 60315 is a greenish-gray, very coherent poikilitic impact melt (Fig. 1) that is enriched in incompatible elements compared with most other Apollo 16 rocks. Its texture and major element chemistry is typical of Apollo 16 poikilitic rocks. Macroscopically the silicate phases are homogeneously distributed but the grain size is somewhat variable. The sample was collected 5 m north of the Lunar Module, where it was only slightly buried. Its orientation is known, and the exposed lunar surface has many zap pits, with few on other surfaces.



FIGURE 1. Scale in cm.   S-72-41572B

PETROLOGY: Bence et al. (1973), Simonds et al. (1973), Hodges and Kushiro (1973) and Walker et al. (1973) provide detailed petrographic descriptions of 60315. All note the anhedral orthopyroxene ($Wo_4$ $En_{80}$) oikocrysts up to 3 mm long which enclose abundant laths and clasts of plagioclase, rare olivines ($Fo_{74-77}$) and opaques (Fig. 2). Plagioclase clasts often have very calcic cores ($An_{95-97}$) and narrow, more sodic rims (down to $An_{89}$). Augite, olivine, ilmenite and armalcolite discontinuously rim some oikocrysts. Simonds et al. (1973) give a mode of 55% plagioclase + mesostasis, 34% orthopyroxene, 4% augite, 1% olivine and 1% opaques. Mineral compositions are shown in Figure 3. Similar data are presented by Vaniman and Papike (1981).

Areas interstitial to the oikocrysts have textures ranging from granular to subophitic and account for $\sim$ 10% of the rock. Most of the interstices are enriched in K, Na, Si, S, P and opaque minerals. Rounded vesicles are common. Bence et al. (1973) report one interstitial region with euhedral plagioclase crystals in a troilite matrix. In many places the oikocrysts grade into a fine-grained clastic matrix of plagioclase ($An_{71-80}$), olivine ($Fo_{71-80}$), pyroxene, opaques and lithic fragments. Plagioclase grains often show textural signs of reequilibration with the matrix. The small ($\sim$ 0.5 mm) subophitic patches consist of interlocking plagioclase laths ($An_{90-95}$) with interstitial olivine ($Fo_{71-73}$), zoned augite ($Wo_{35-41}$ $En_{53-48}$), orthopyroxene ($Wo_3$ $En_{82}$) and minor K-feldspar, ilmenite, armalcolite, phosphates, silica, metal and troilite.

Hewins and Goldstein (1975b), Ridley and Adams (1976) and Hodges and Kushiro (1973) calculated equilibration temperatures based on pyroxene, olivine and metal phase geothermometers. The silicate phases equilibrated at $\sim$ 1000-1200°C whereas the metallic phases record a temperature of $\sim$ 600°C. Metal compositions (Fig. 4) are

a   b
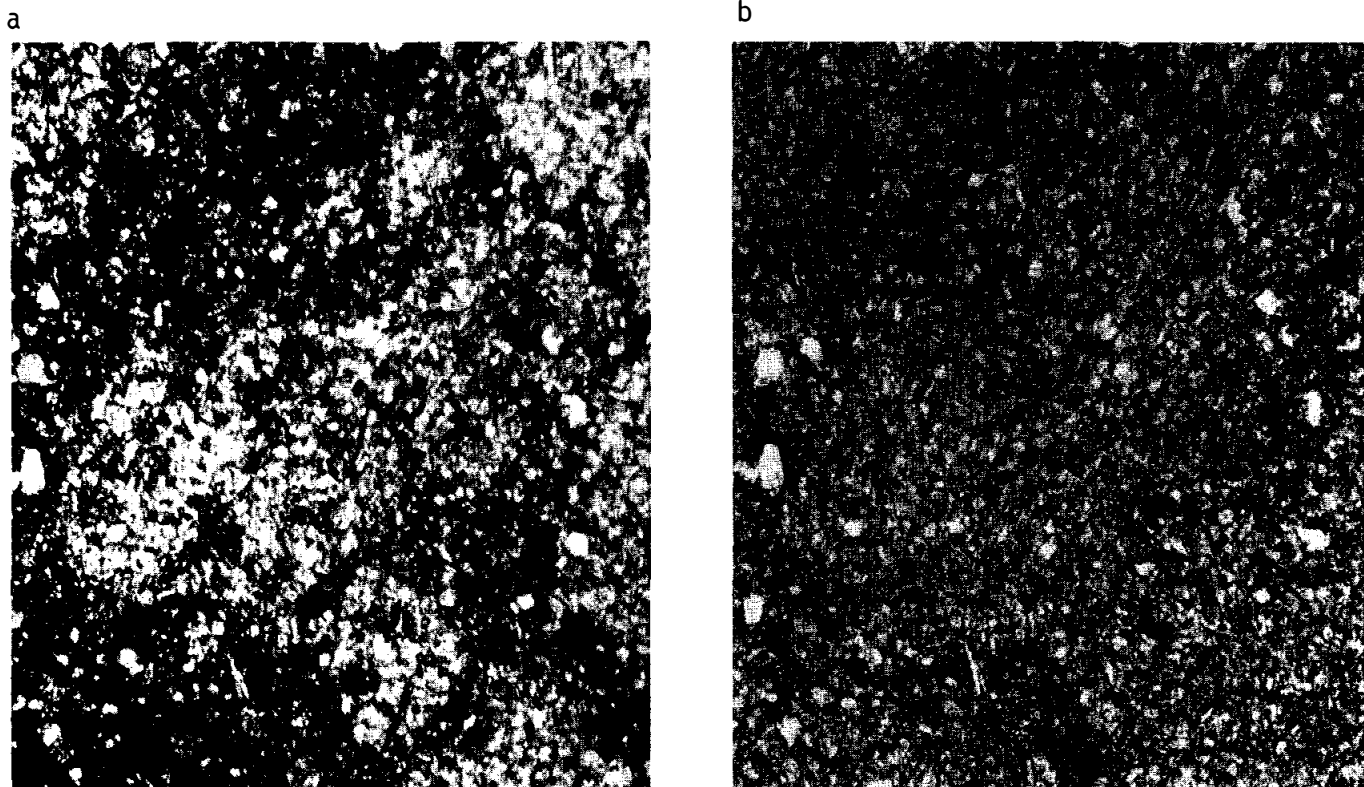


FIGURE 2. 60315,15. Same view, width 2mm. a)xpl. b)ppl.

given by L. Taylor et al. (1973a),Reed and Taylor (1974) and Misra and Taylor (1975). Meyer (1979) determined trace elements in plagioclase in 60315 using the ion microprobe.

EXPERIMENTAL PETROLOGY: Ford et al. (1974) experimentally determined the phase relations of 60315. Spinel is the equilibrium liquidus phase (1300°C) followed by olivine (1276°) and plagioclase (1256°). Pyroxene was not produced even at their lowest temperature (1200°). This is consistent with textural evidence which indicates that olivine and plagioclase preceeded pyroxene.
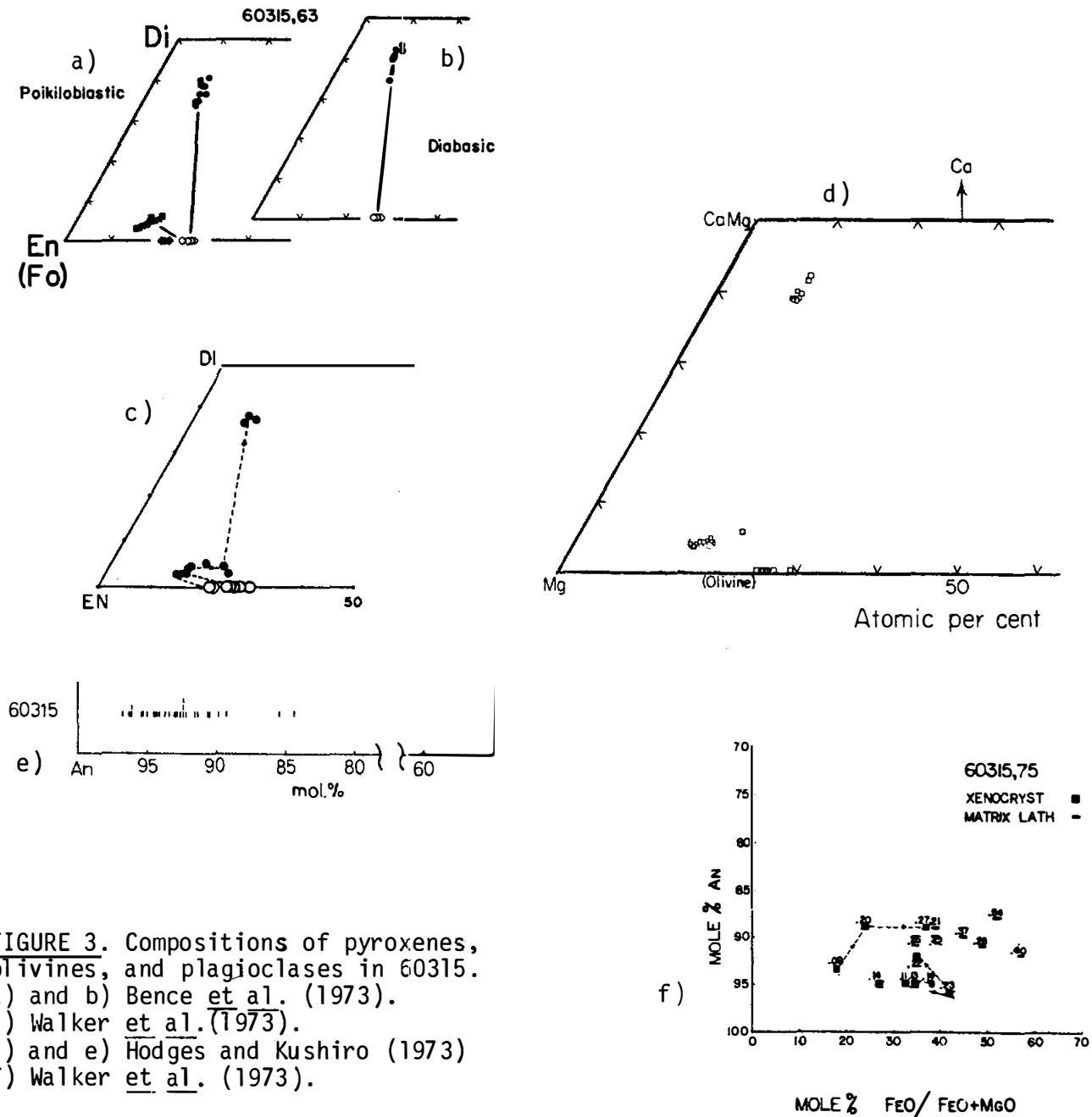
FIGURE 3. Compositions of pyroxenes, olivines, and plagioclases in 60315.
a) and b) Bence et al. (1973).
c) Walker et al.(1973).
d) and e) Hodges and Kushiro (1973)
f) Walker et al. (1973).

a) 60315,65

b) Poik 60315
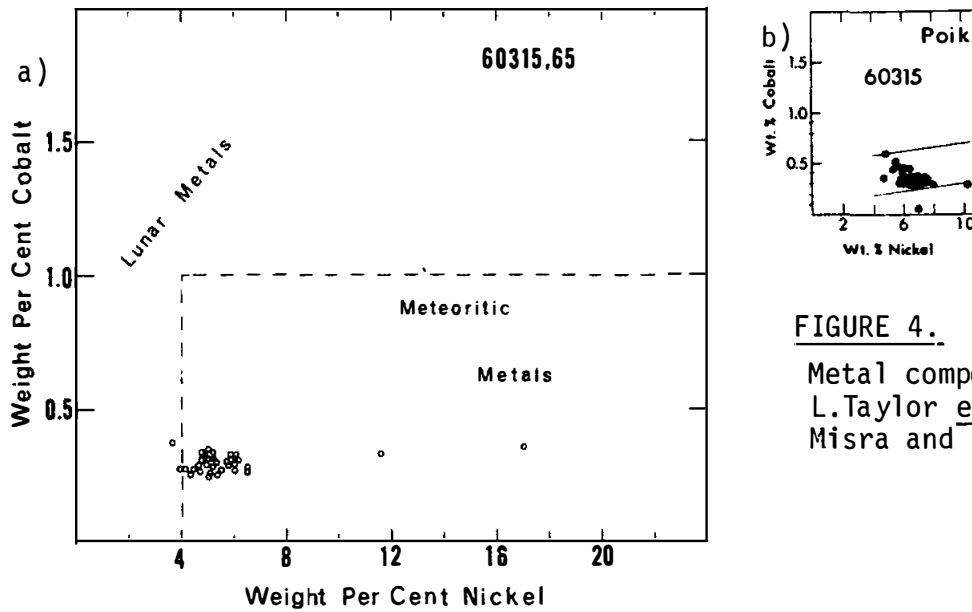
FIGURE 4.

Metal compositions; a) from
L.Taylor et al.(1973a). b) from
Misra and Taylor (1975).

CHEMISTRY: Chemical studies of 60315 are listed in Table 1 and a summary chemistry in Table 2. Rare earth element abundances and patterns are shown in Figure 5.

The major element chemistry of 60315 is very similar to Apollo 15 "Fra Mauro basalt" glasses, and it lies very near the olivine-plagioclase cotectic of the OL-AN-SI system (Fig. 6). Rare earth element abundances are among the highest measured in any Apollo 16 sample (see also 62235 and 65015) and have a KREEP pattern (Table 3 and Fig. 5). 60315 is not simply remelted local soil: it is much lower in $Al_2O_3$ and higher in rare earth elements. Siderophile abundances vary from split to split (e.g. reported Ni values range from 191-1400 ppm) but all indicate substantial amounts of meteoritic material. Hertogen et al. (1977) considered the anomalously low Ir/Au ratio indicative of a distinct meteoritic component and assigned 60315 to a new meteoritic signature, Group 1LL. Volatiles also vary by two orders of magnitude between different splits (e.g. reported Zn ranges from 0.3-12 ppm).

Sato (1976) measured the oxygen fugacity of 60315 directly using the solid-electrolyte oxygen cell method. Fugacity values at a series of temperatures are given in Table 3. Nash and Haselton (1975) calculated the equilibrium silica activity of a melt with the composition of 60315. They conclude that Apollo 16 crystalline rocks 60315 and 68416 have higher initial silica activities than Apollo 17 high-Ti mare basalts.

TABLE 1. Chemical studies of 60315

| Reference | Split # | Elements analyzed |
|---|---|---|
| Rose et al. (1973) | ,88 | majors, trace, incl. some REEs |
| Hubbard et al. (1973) | ,3 | majors, REEs, other trace |
| Hubbard et al. (1973) | ,57 | majors |
| Morrison et al. (1973) | ,53 | majors, REEs, other trace |
| LSPET (1973) | ,3 | majors, trace |
| S.R. Taylor et al. (1973) | ,58 | majors, REEs, other trace |
| Laul et al. (1974) | ,157 | majors, REEs, other trace |
| Wänke et al. (1976) | ,87; ,103 | majors, REEs, other trace |
| Wänke et al. (1977) | ,87 | V |
| Nyquist et al. (1973) | ,3 | Rb, Sr |
| Kirsten et al. (1973) | ,19 | K, Ca |
| Nunes et al. (1973) | ,81 | U, Th, Pb |
| Nunes (1975) | ,81 ? | U, Th, Pb |
| Eldridge et al. (1973) | ,0 | U, Th, K |
| Moore et al. (1973) | ,4 | C |
| Ganapathy et al. (1974) | ,79 | meteoritic sids. and vols. |
| Flory et al. (1973) | ,52 | volatile organogenic compounds |

TABLE 2. Summary chemistry of 60315

| | |
|---|---|
| $SiO_2$ | 46.5 |
| $TiO_2$ | 1.31 |
| $Al_2O_3$ | 17.2 |
| $Cr_2O_3$ | ˙0.21 |
| FeO | 9.3 |
| MnO | 0.11 |
| MgO | 13.2 |
| CaO | 10.2 |
| $Na_2O$ | 0.61 |
| $K_2O$ | 0.40 |
| $P_2O_5$ | 0.48 |
| Sr | 155 |
| La | 49 |
| Lu | 2.1 |
| Rb | 9.7 |
| Sc | 15 |
| Ni | ∿800 |
| Co | ∿50 |
| Ir ppb | ∿10 |
| Au ppb | ∿17 |
| C | ∿20 (?) |
| N | ∿20 |
| S | 1300 |
| Zn | ∿5 (?) |
| Cu | 11 |

Oxides in wt%; others in ppm except as noted.

TABLE 3. Oxygen Fugacity of 60315

| T (°C) | $-\log fo_2$ (atm) |
|---|---|
| 1000 | 16.2 |
| 1050 | 15.4 |
| 1100 | 14.6 |
| 1150 | 13.9 |
| 1200 | 13.2 |
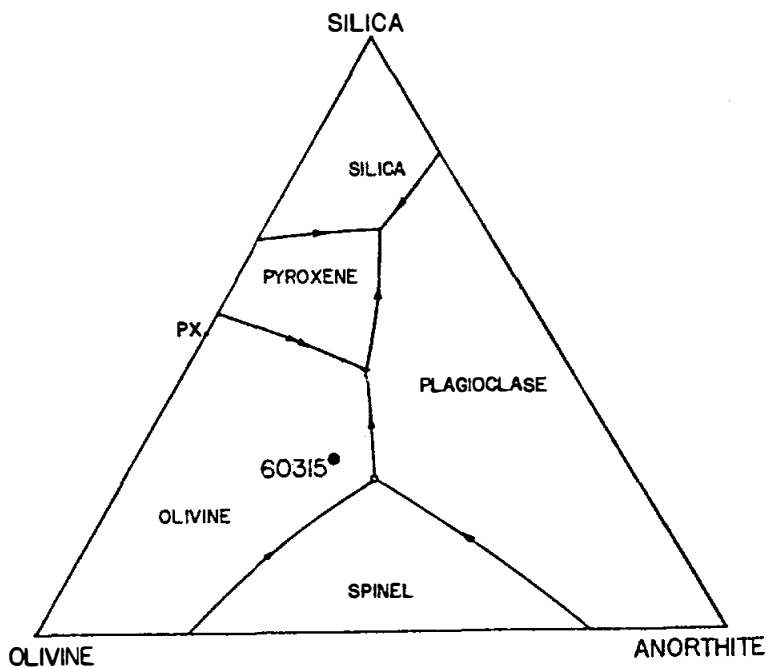
FIGURE 5. from Walker et al. (1973).
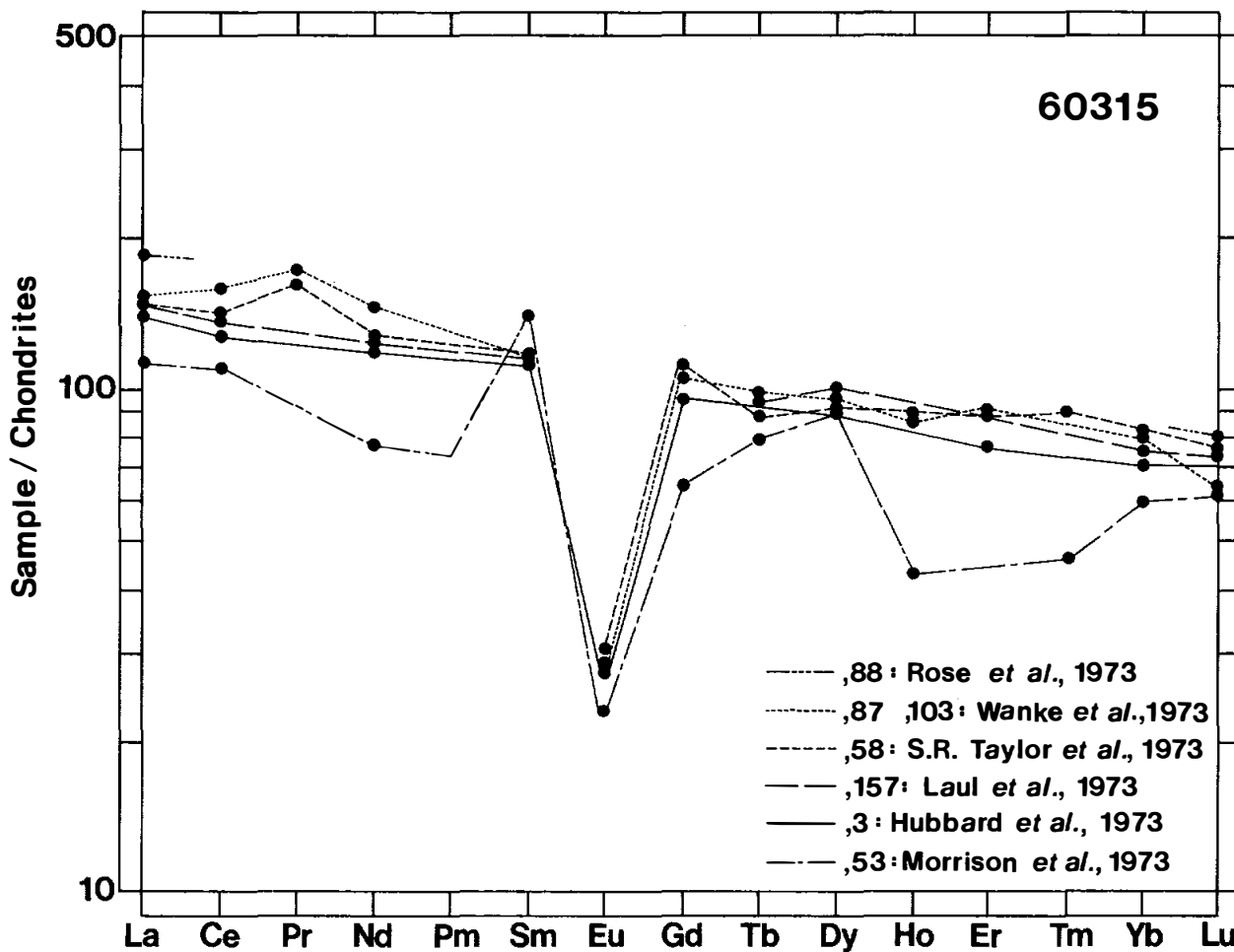


FIGURE 6. Rare earths.

GEOCHRONOLOGY AND RADIOGENIC ISOTOPES: Whole rock Rb-Sr data are presented by Nyquist et al. (1973). Model ages of $T_{BABI}$ = 4.41 ± 0.06 b.y. and $T_{LUNI}$ = 4.44 ± 0.06 b.y. were calculated. KREEP-rich rocks 60315, 62235, and 65015 define a whole rock Rb-Sr isochron of 4.42 ± 0.38 b.y. with initial $^{87}Sr/^{86}Sr$ = 0.6992 ± 9. Assuming a 3.9 b.y. age for these rocks yields an initial $^{87}Sr/^{86}Sr$ = 0.70040 ± 15 (Nyquist et al., 1973).

Well defined $^{39}Ar$-$^{40}Ar$ plateau ages of 4.03 ± 0.03, 3.94 ± 0.05 and 3.91 ± 0.02 b.y. were obtained by Kirsten et al. (1973), Husain and Schaeffer (1973) and Schaeffer et al. (1976) respectively (Fig. 7). Schaeffer et al. (1976) also report a K-Ar age of 3.69 ± 0.01 b.y.
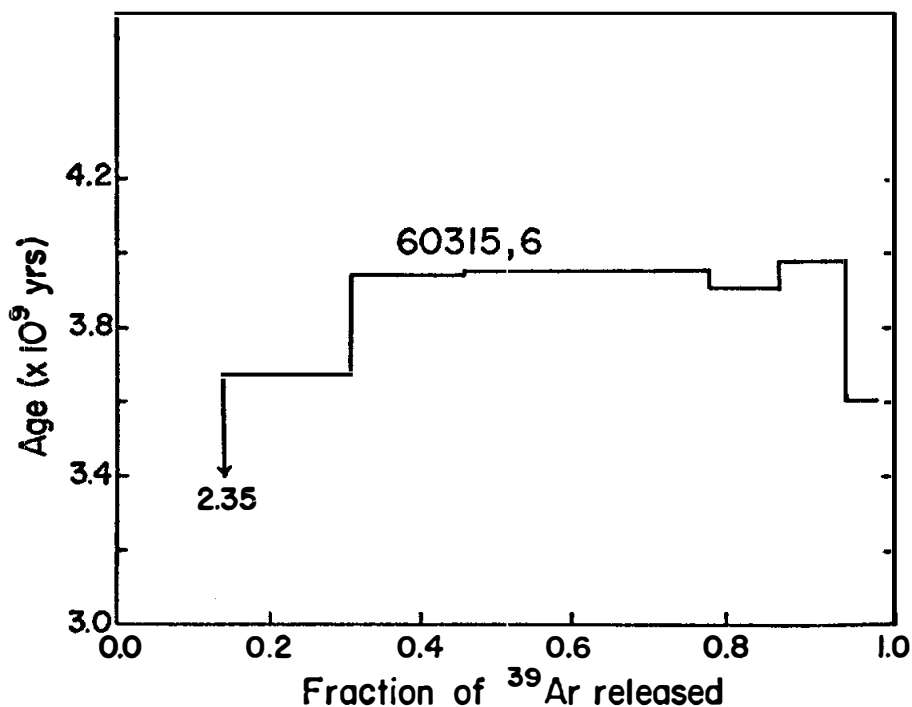


FIGURE 7a. Ar release; from Husain and Shaeffer (1973).
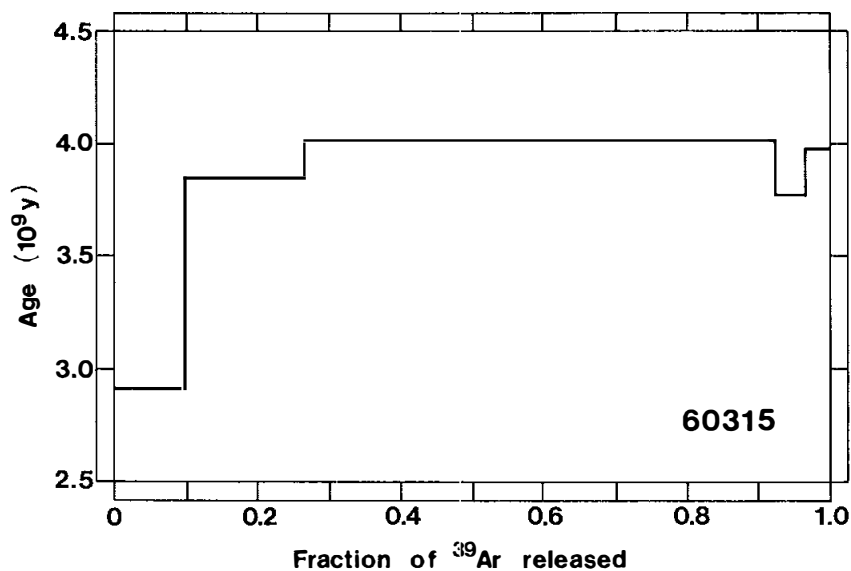


FIGURE 7b. Ar release; from Kirsten et al. (1973).

91

Nunes et al. (1973) and Nunes (1975) report U-Th-Pb data. 60315 is very enriched in in situ radiogenic lead ($^{206}Pb/^{204}Pb$, >10,000). Nearly all of the original lead was probably expelled during a period of intense heating. A Pb-Pb internal isochron yields an age of 3.99 ± 0.01 b.y. (Fig. 8). The bulk rock is concordant at 3.93 b.y. (Nunes, 1975) rather than slightly discordant at 3.99 b.y. as originally reported by Nunes et al. (1973).
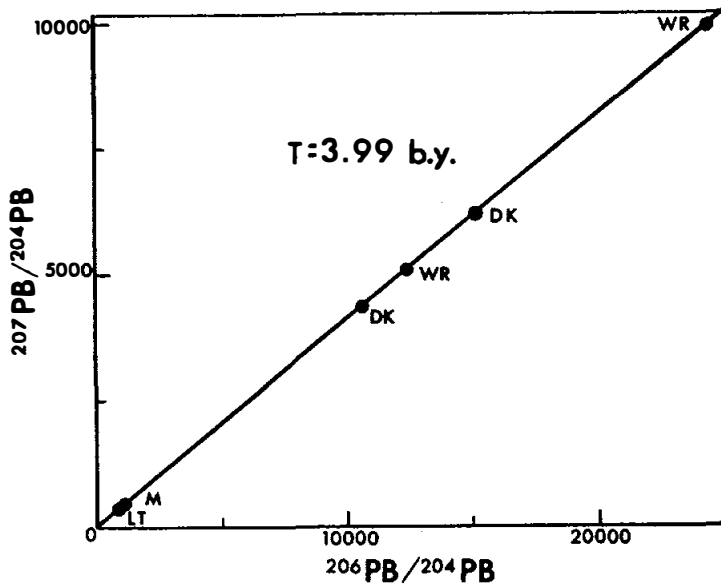


FIGURE 8. Pb-Pb isochron; from Nunes et al.(1973).

RARE GAS/EXPOSURE AGE: Kirsten et al. (1973) report a $^{38}Ar$ age of 4.5 ± 1 m.y. Schaeffer et al. (1976) determined a maximum $^{38}Ar$ age of 11 m.y. with a more probable age of 5 ± 3 m.y. Keith and Clark (1974) calculate a $^{26}Al$ maximum exposure age of 2.3 m.y. Eldridge et al. (1973) provide abundance data on cosmogenic radionuclides determined by γ-ray spectroscopy and Keith et al. (1975) discuss the saturated activities of specific short-lived, cosmogenic radionuclides.

MICROCRATERS AND TRACKS: Neukum et al. (1973), Fechtig et al. (1974) and Nagel et al. (1975) provide data on microcraters on 60315. The rock has had a simple exposure history and the surfaces are in production. Nagel et al. (1975) report small metallic spherules enriched in Fe, Ni and S suspended within some of the crater glass linings.

PHYSICAL PROPERTIES: Brecher et al. (1973), Nagata et al. (1973) and Schwerer and Nagata (1976) provide magnetic data and discussion (Figs. 9 and 10). Coarse multidomain grains predominate over a superparamagnetic fraction. About 40% of the metallic iron component in this rock is kamacite with ∿ 5% Ni. A very small component of NRM and IRM is stable against AF-demagnetization (Fig. 10). Measured magnetic parameters of 60315 vary from chip to chip by over an order of magnitude (see e.g. Brecher et al., 1973) possibly relating to the inhomogeneous distribution of metallic phases.

Mossbauer analyses are given by Brecher et al. (1973), Huffman et al. (1974) and Huffman and Dunmyre (1975) (Fig. 11). Tsay and Bauman (1977) studied paramagnetic iron using the electron spin reasonance (ESR) method. These spectra and the magnetic data referenced above indicate up to ∿ 4.5 wt% metallic iron in 60315.

## MAGNETIZATION CURVES
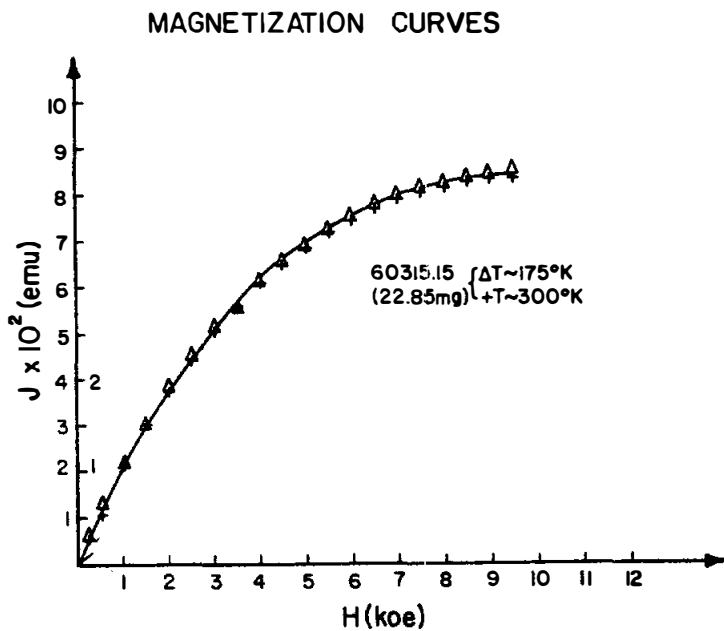


FIGURE 9. Magnetization; from Brecher et al.(1973).
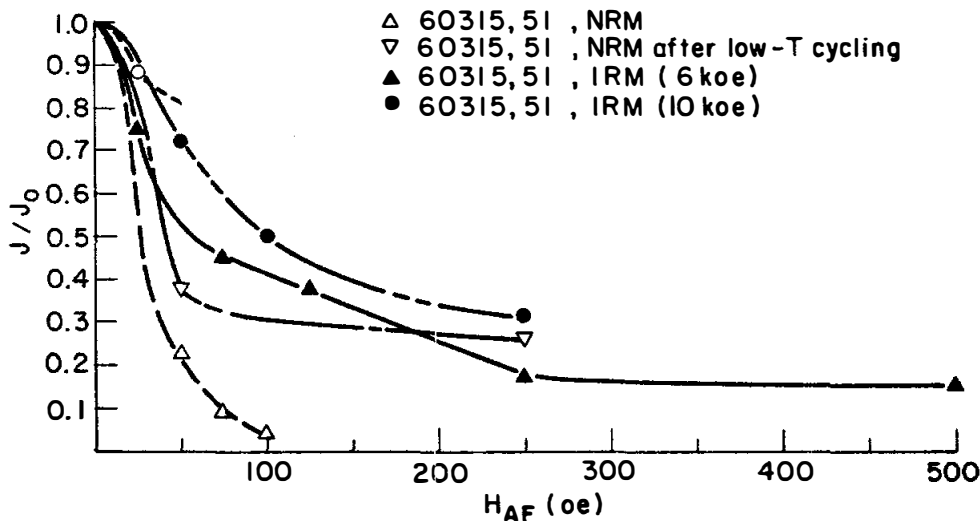


Normalized AF Demagnetization

FIGURE 10. AF-demagnetization; from Brecher et al. (1973).
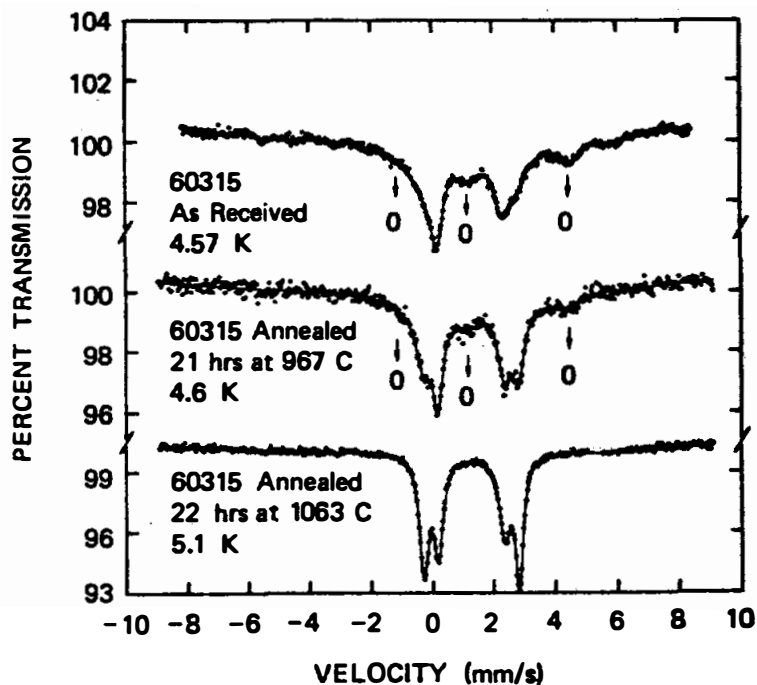
FIGURE 11. Liquid-helium spectra; from Huffman and Dunmyre (1975).

Elastic wave velocities at pressures up to 10 kb were measured by Mizutani and Newbigging (1973) (Fig. 12). These data closely match the seismic velocity profiles from 5-25 km depth in the moon.

Chung and Westphal (1973) note the unusual electrical properties of 60315. The dielectric constant, dielectric losses and conductivity are all high (Figs. 13 and 14) possibly owing to the high concentration of metallic iron in the rock.
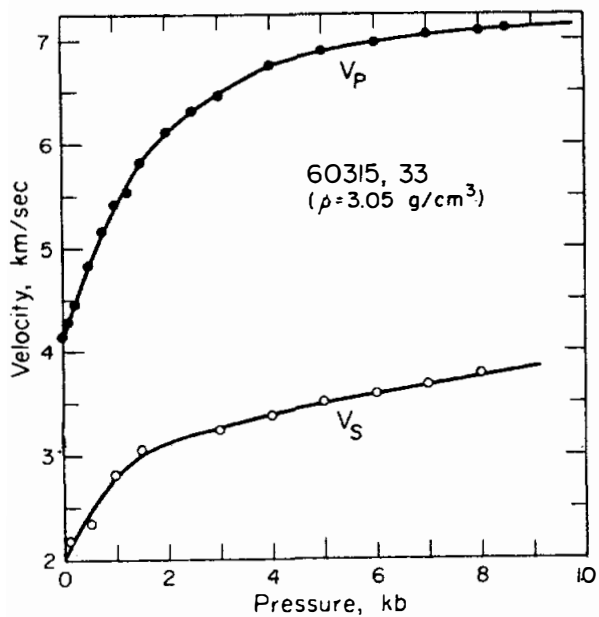


FIGURE 12. Elastic wave velocities; from Mizutani and Newbigging (1973).
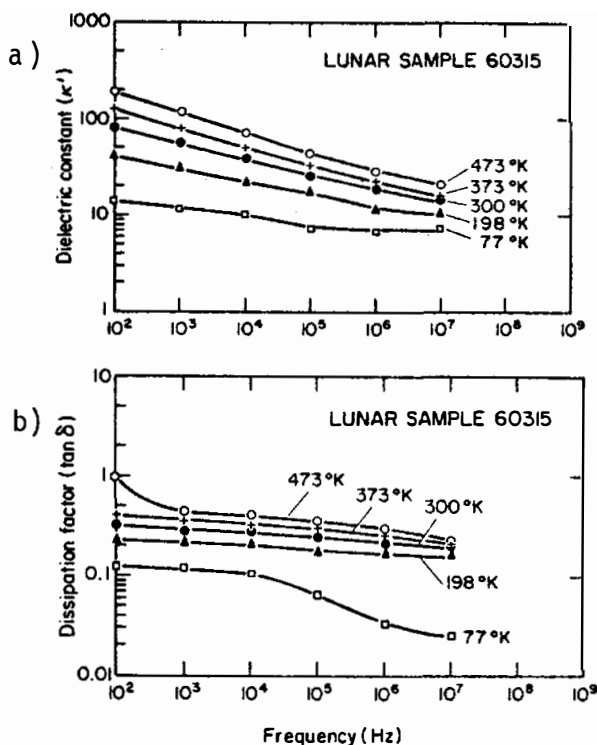


FIGURE 13. from Chung and Westphal (1973). a) dielectric constant b) dielectric losses.

94

T(°C)

LUNAR SAMPLE 60315

Conductivity, $\sigma$ (ohm-cm)$^{-1}$

1000/T(°K)

10 MHz

1 MHz

100 kHz

10 kHz

1 kHz

100 Hz
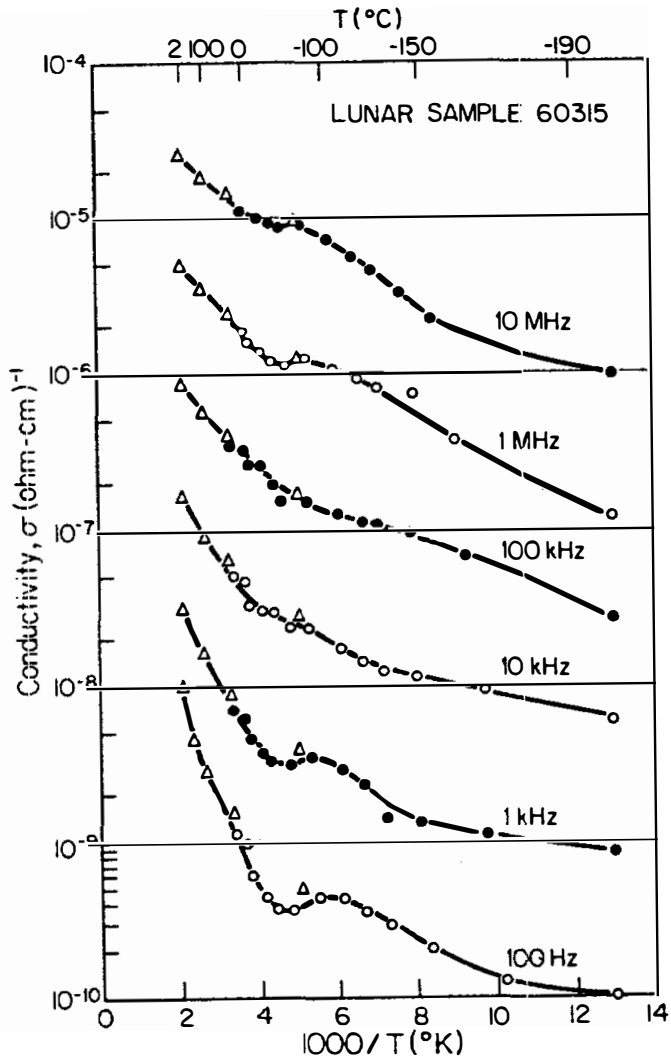
FIGURE 14. Electrical conductivity; from Chung and Westphal (1973).

Charette and Adams (1977) provide visible and near-infrared reflectance data.

PROCESSING AND SUBDIVISIONS: This rock has been extensively subdivided and widely allocated. In 1972, it was cut into four pieces, including a slab (Figs. 15,16). Allocations were primarily from the slab, from ,18 (entirely subdivided as ,47- ,59 and ,79- ,97) and from chips of ,0. The largest single piece remaining (,0 in Fig. 16) weighs 594.3 g and has been renumbered ,46. Serial thin sections were made from slab pieces ,20 and ,26. Thin sections also sample other portions of the rock. Many interior and exterior splits exist.

60315



FIGURE 15.

Cutting diagram.

,0

,17

,18

SLAB

,43

,42

,16

,41

,40

,38

,39



60315
Main slab dissections

S-72-51842

,28

,29

,26

,27

,37

,23

,44

,22

,21

,20

,19

,24

,33

,25

,35

,32

,36

,34

1 cm
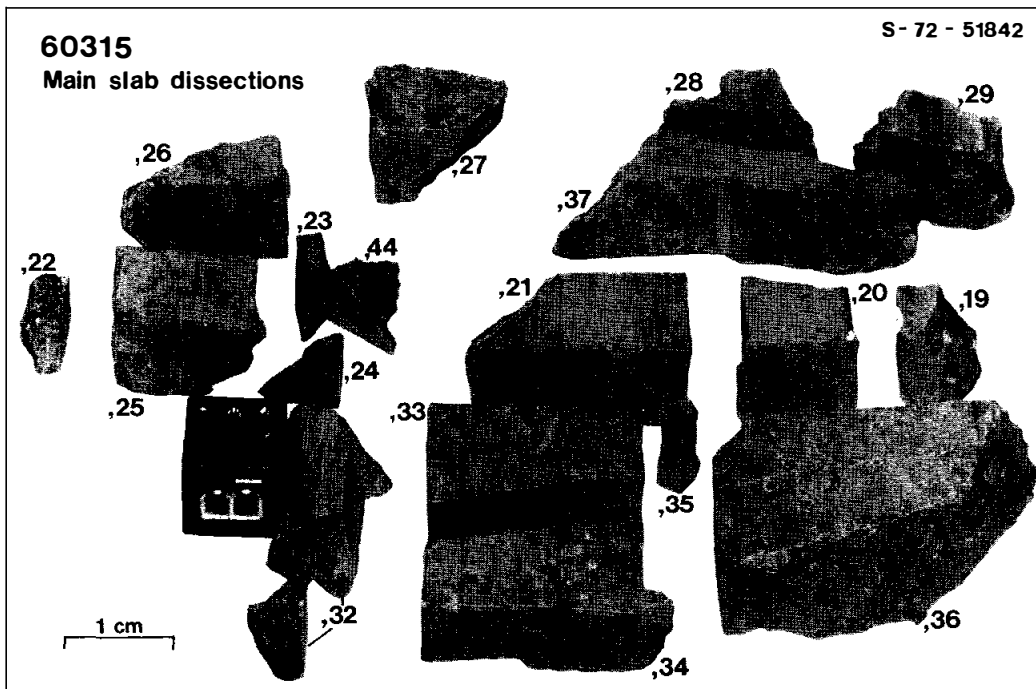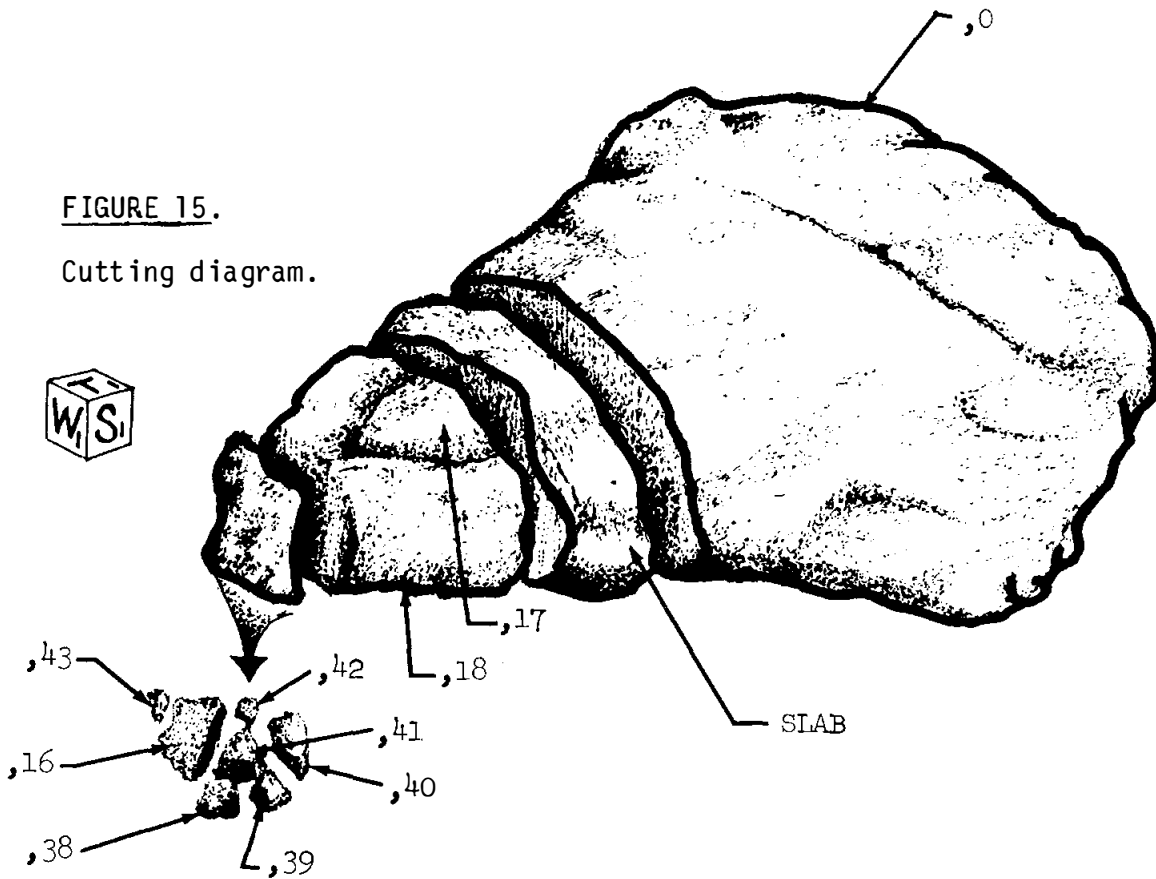
FIGURE 16.

96

INTRODUCTION:  60335 is a tough, medium gray, basaltic impact melt with a pro-
nounced vug population (Fig. 1).  The rock as a whole is homogeneous although the
grain size changes abruptly and color varies irregularly from dark to light areas.
Metal spherules (up to 5 mm) are abundant.

60335 was collected about 70 m east-northeast of the Lunar Module, where it was
1/3-1/2 buried with a moderately well-developed fillet.  Its orientation is known;
zap pits are present on all surfaces but one, although the densities vary
considerably from surface to surface.
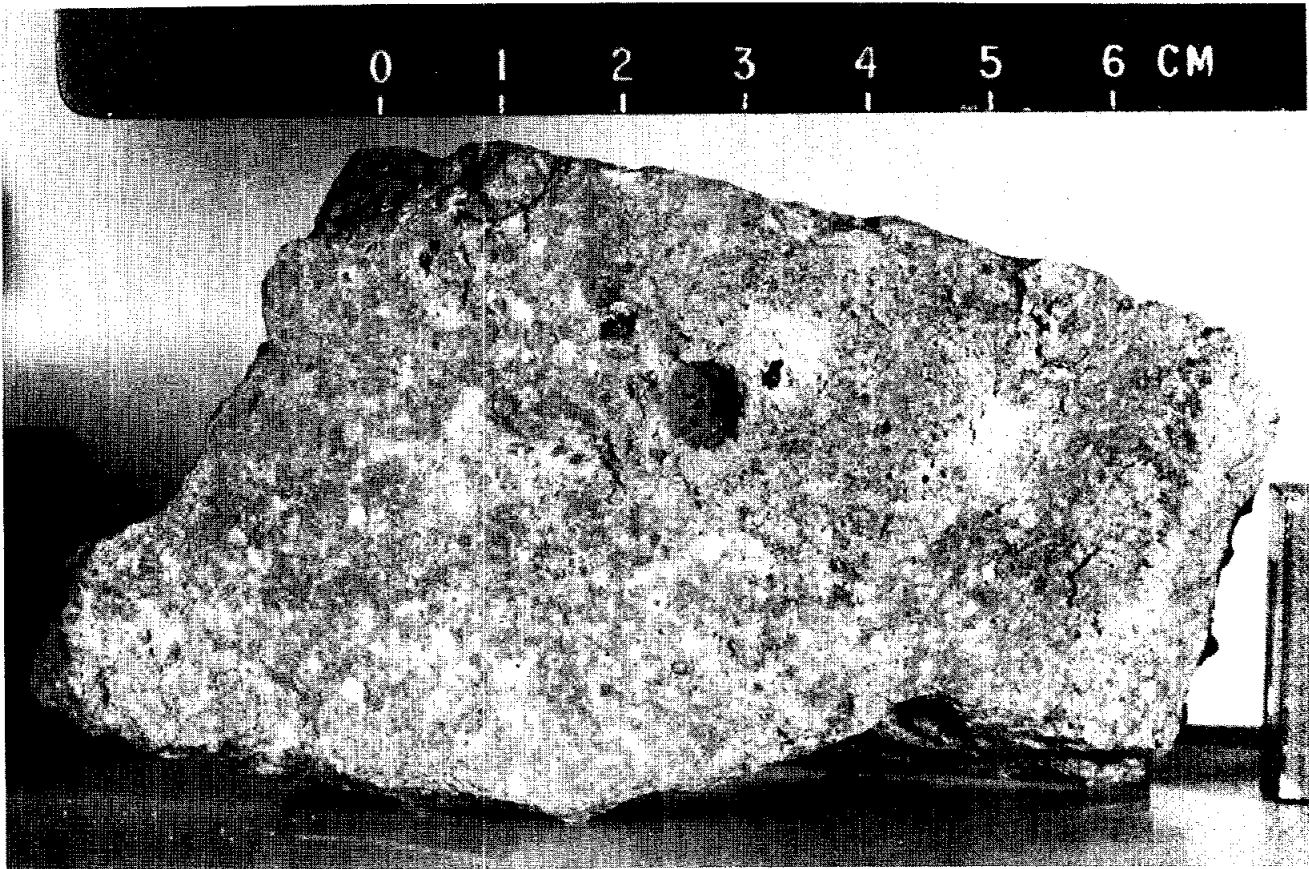


FIGURE 1.  S-72-38289

PETROLOGY:  Walker et al. (1973), Brown et al. (1973), Nord et al. (1973) and
Vaniman and Papike (1981) provide petrographic information.  Nord et al.(1973)
studied pyroxene exsolution using high-voltage transmission electron micro-
scopy.  Misra and Taylor (1975) report metal and schreibersite compositions.

60335 is a basaltic impact melt rock that exhibits a variety of melt textures
(Fig. 2).  Most commonly, normally zoned, subhedral plagioclase phenocrysts
(An$_{95-86}$) and shocked, anhedral plagioclase xenocrysts (An$_{97-95}$, up to 4 mm)
grade into a finer grained matrix of equant to lathy plagioclase partially
enclosed by olivine (Fo$_{85-79}$, single crystals up to 10 mm).  In other areas a
Si-K-rich glassy mesostasis fills the interstices.  Overgrowths of ortho-

a                                          b
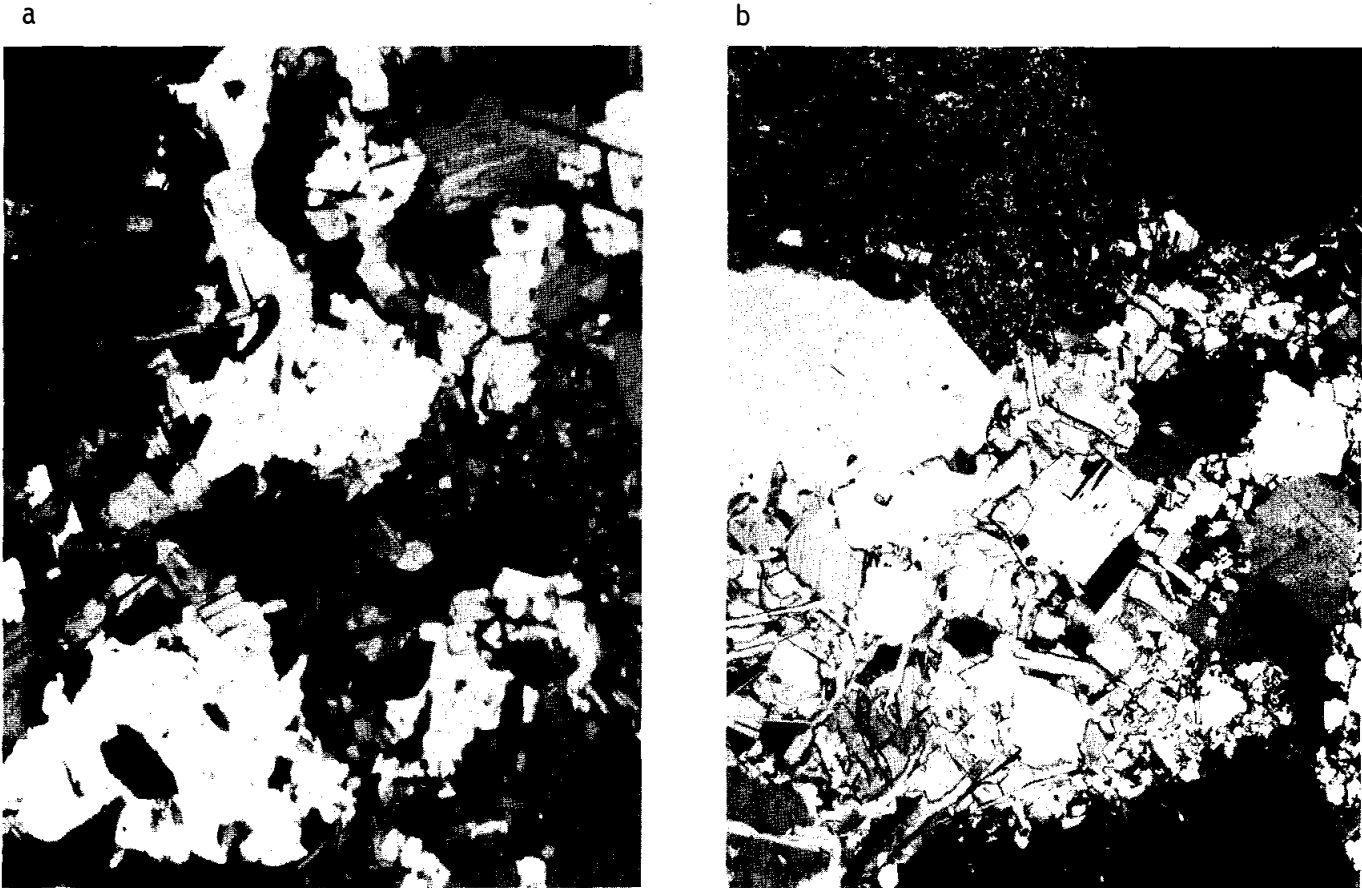


FIGURE 2. a) 60335,61. general basaltic, xpl. width 2mm. b) poikilitic area
(top left) and vesicle (top right) in general basaltic area, xpl. width 1mm.

pyroxene (Wo$_5$ En$_{76}$), pigeonite (Wo$_9$ En$_{68}$) and augite occasionally rim the olivines
and many of the plagioclase phenocrysts display a clear rim over a shocked core.
Pigeonite occasionally shows augite exsolution lamellae. A mode of the matrix
given by Walker et al. (1973) is reproduced as Table 1. Minor phases include
silica, phosphates, Zr-armalcolite, ilmenite, ulvöspinel, metal and schreiber-
site. Mineral compositions are given in Figures 3 and 4.

Less common melt textures in this rock include radiating clusters of plagioclase,
often cored by an incompletely digested clast and poikilitic patches in which
0.5 mm olivine encloses many small clasts and crystallites of plagioclase (Fig.2).
Although Walker et al. (1973) and the Apollo 16 Lunar Sample Information Catalog
(1972) interpret certain poikilitic areas as lithic clasts, an extensive survey
of library thin sections convinces us that these patches crystallized from the
same melt that produced the bulk of the rock. Evidence for this interpretation
includes the arcuate boundaries of the patches against vesicles (Fig. 2), the
tendency of the poikilitic patches to completely fill irregularly shaped areas
and the fact that some of the poikilitic olivines are single crystals with
olivines that are definitely a part of the ophitic matrix.

Lithic clasts include granoblastic anorthosite (2 mm) and granoblastic troctolite
(5 mm) with accessory ilmenite and metal. Most of the lithic clasts are shocked
with a well defined reaction rim of fine-grained, unshocked plagioclase.

a)

b) 60335

FELDSPATHIC
BASALT
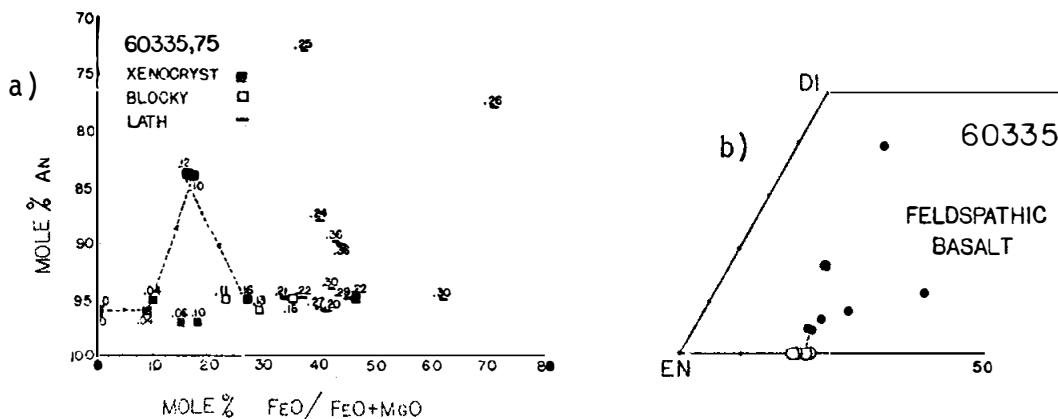
**FIGURE 3.** Mineral compositions;
a) plagioclases, from Walker et
al.(1973)
b) pyroxenes, from Walker et al.
(1973).
c) pyroxenes, from Vaniman and
Papike (1981).

c) 60335

**TABLE 1**

Mode of 60335 from Walker et al. (1973)

| | |
|---|---|
| Plagioclase | 64% |
| Olivine | 16% |
| Clinopyroxene | 10% |
| Opaques | 2% |
| Glassy mesostasis | 8% |
| Orthopyroxene | tr |
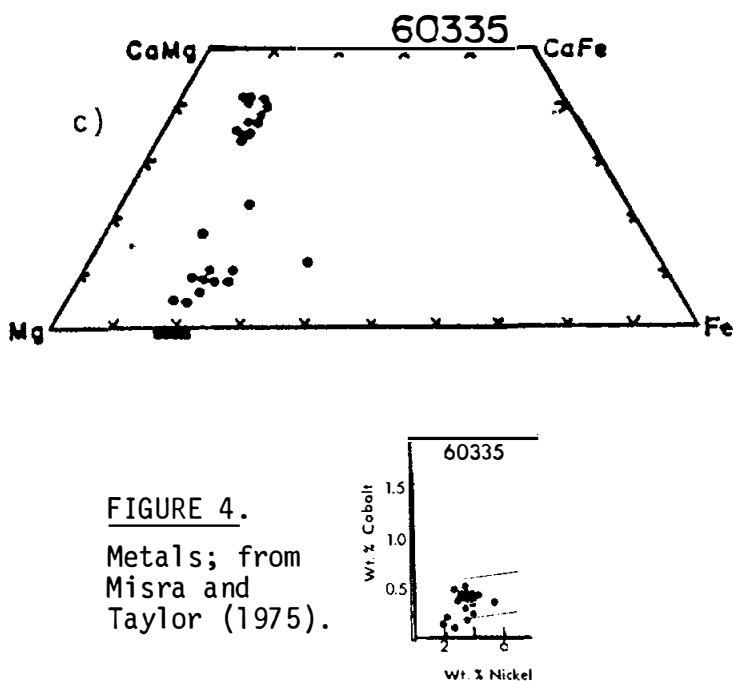
**FIGURE 4.**

Metals; from
Misra and
Taylor (1975).

60335

**EXPERIMENTAL PETROLOGY:** Muan et al. (1974) and Ford et al. (1974) report exper-
imentally determined equilibrium phase relations. At low pressure plagioclase is
the liquidus phase of 60335, followed by spinel, then olivine. Liquidus temper-
ature is >1370° C. Spinel becomes unstable between 1200-1216° C. At 1 kb pressure
with 10% water, spinel is the liquidus phase at temperatures >1250°C (Ford et al.,
1974).

L.A. Taylor et al.(1976) performed subsolidus heating experiments to observe changes
in metal grain morphology and chemistry. The most conspicuous textural change
observed was the development of euhedral metal crystals at the edges of the
annealed fragments. Observed changes in metal compositions are summarized in
Figure 5.
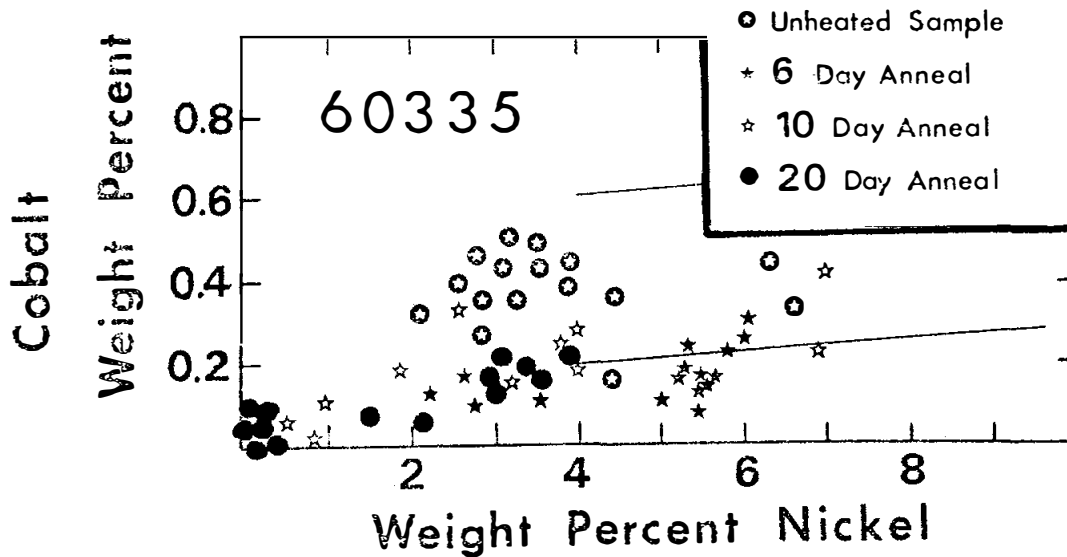
FIGURE 5. Subsolidus metal changes; from L. Taylor et al.(1976).

CHEMISTRY: Major and trace element data are given by Haskin et al. (1973), Rose et al. (1973), Miller et al. (1974), Fruchter et al.(1974)(of ,34 erroneously reported as ,4) Wänke et al. (1976) and LSPET (1973). Hubbard et al.(1974) and Ehmann and Chyi (1974) report trace elements, Clark and Keith (1973) provide data on natural and cosmogenic radionuclides and Barnes et al. (1973) present trace element and isotopic abundances (see also STABLE ISOTOPES and GEOCHRONOLOGY below). Walker et al. (1973) report major elements determined by electron microprobe analyses of natural rock powder fused to a glass.
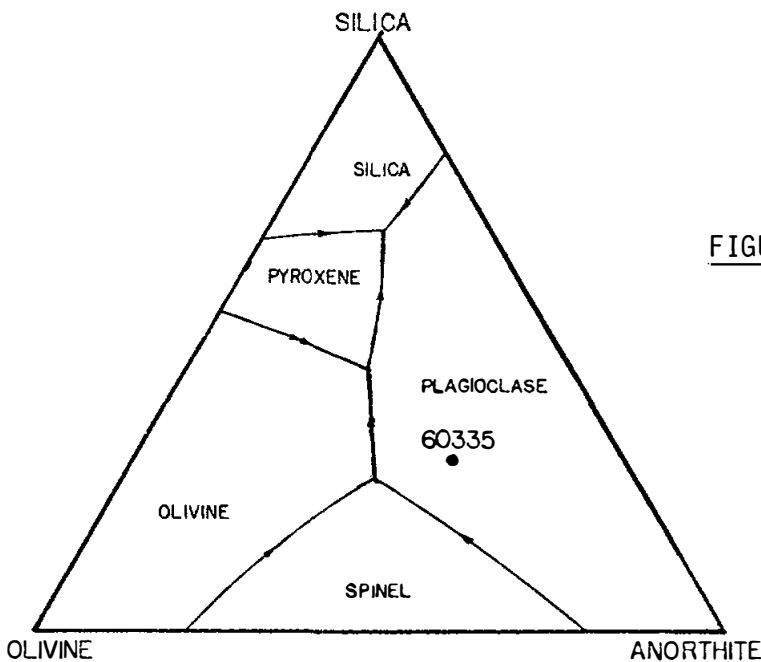


FIGURE 6. from Walker et al.(1973).

### TABLE 2

#### Summary chemistry of 60335

| | |
|---|---|
| $SiO_2$ | 46.0 |
| $TiO_2$ | 0.61 |
| $Al_2O_3$ | 24.9 |
| $Cr_2O_3$ | 0.13 |
| FeO | 4.7 |
| MnO | 0.07 |
| MgO | 8.1 |
| CaO | 14.3 |
| $Na_2O$ | 0.57 |
| $K_2O$ | 0.25 |
| $P_2O_5$ | 0.21 |
| Sr | 150 |
| La | 21 |
| Lu | 0.84 |
| Rb | 6.8 |
| Sc | 8.1 |
| Ni | 340 |
| Co | 20 |
| Ir ppb | 17 |
| Au ppb | 16.8 |
| C | |
| N | |
| S | |
| Zn | 2 |
| Cu | 8 |

**Oxides in wt%; others in ppm except as noted.**



FIGURE 7. Rare earths; from Haskin et al.(1973).
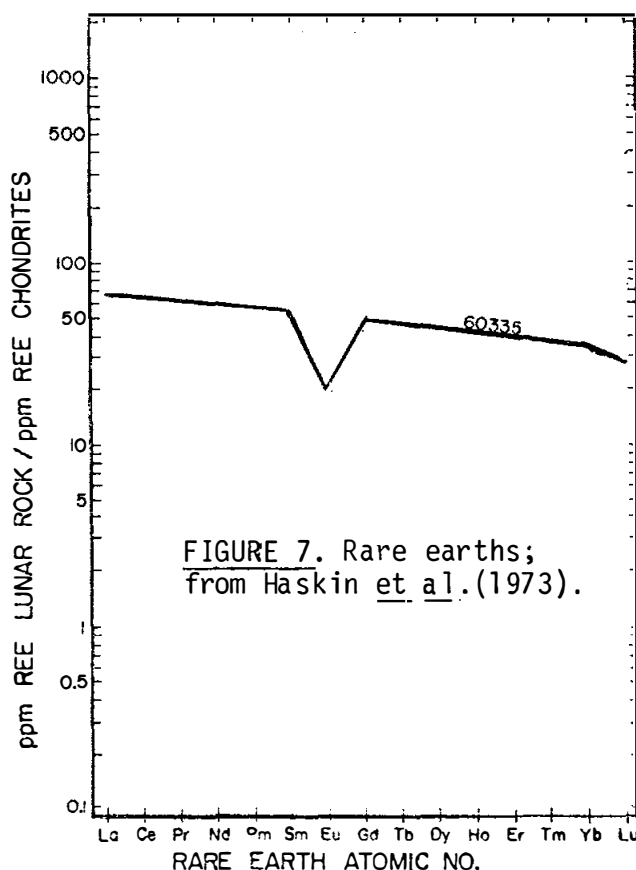
### TABLE 3

#### Average oxygen fugacity of 60335

| T ($^{o}$C) | $-\log f_{O_2}$(atm) |
|---|---|
| 1000 | 16.7 |
| 1060 | 15.6 |
| 1100 | 14.6 |
| 1150 | 13.7 |
| 1200 | 12.8 |

Chemically 60335 is a very homogeneous rock. Its major element composition is that of anorthositic norite (Table 2 and Fig. 6),very similar to the local mature soils. Rare earth elements (Fig. 7) are slightly higher in the rock (La $\sim$ 65 x chondrites) than in the local soils (La $\sim$ 45 x chondrites). The Zr/Hf is high, dominated by a KREEP component (Ehmann and Chyi, 1974). Siderophiles indicate a substantial meteoritic contribution (Table 2).

Sato (1976) measured the oxygen fugacity of 60335 directly using the solid-electro-lyte oxygen cell method. The low values (Table 3) are consistent with the equil-ibration of metallic iron with the silicate and oxide phases. A slight self-re-duction was noted during the first heating cycle.

STABLE ISOTOPES: Barnes et al. (1973) provide data on isotopes of Cr, Ni and K.

60335

RADIOGENIC ISOTOPES AND GEOCHRONOLOGY: Whole rock Rb-Sr data are provided by Barnes et al. (1973) and Nyquist et al. (1974). A model age of 4.055 b.y. was calculated by Barnes et al. (1973) assuming I = 0.6994 (sic.). Model ages of $T_{BABI}$ = 4.19 ± 0.06 b.y. and $T_{LUNI}$ = 4.23 ± 0.06 b.y. were calculated by Nyquist et al. (1974).

Whole rock U-Th-Pb isotopic data are reported by Barnes et al. (1973). Four model ages ranging from 4.059 - 4.081 b.y. and averaging 4.070 b.y. were calculated. 60335 is concordant at 4.075 b.y.

Relative isotopic compositions of $^{39}K$, $^{40}K$ and $^{41}K$ are given by Barnes et al.(1973).

RARE GAS/EXPOSURE AGE: Solar flare track data indicate that 60335 had a complex exposure history (Fig. 8) but allow an approximate burial (subdecimeter) age of 50 m.y. and a surface exposure age of $\sim$ 0.5 m.y. to be calculated (Bhandari et al., 1976). Bhandari (1977) reports a $^{26}Al$ surface exposure age of < 0.2 m.y. $^{26}Al$ and other cosmic-ray induced radionuclide abundance data are provided by Clark and Keith (1973).
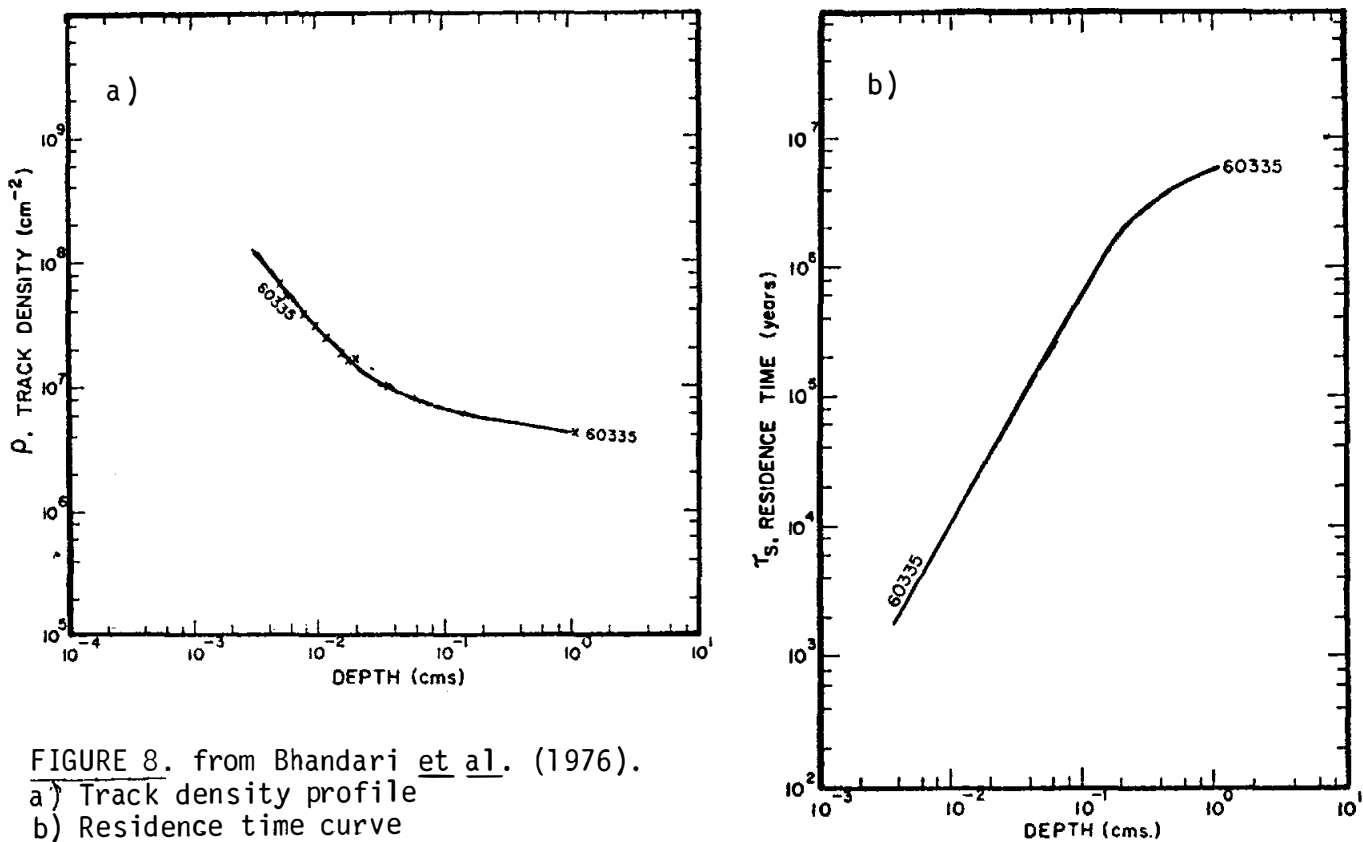


FIGURE 8. from Bhandari et al. (1976).
a) Track density profile
b) Residence time curve

MICROCRATERS AND TRACKS: Morrison et al. (1973) and Neukum et al. (1973) provide size-frequency data on microcraters. Morrison et al. (1973) note the exceptionally low frequency of craters on 60335 and calculate a "best estimate" exposure age of 0.6-0.8 m.y.

PHYSICAL PROPERTIES: 60335 is the "LPM" rock, chosen to measure the in situ remanent magnetization of a lunar sample using the Lunar Portable Magnetometer. Measurements made with the LPM on the lunar surface and in the laboratory did not detect any rock magnetization (Dyal et al., 1972). Pearce et al. (1973) report the total remanence of 60335 as $5.4 \times 10^{-6}$ emu/g, confirming that its intensity is well below the resolution of the LPM. Thus the amount of lunar-induced soft remanence in this sample could not be determined.

Intrinsic and remanent magnetic properties were measured on two chips of 60335 by Pearce et al. (1973) using room temperature hysteresis loops and AF-demagnetization techniques. Total metal content is 0.36 wt %, principally as multi-domain particles. The Curie temperature ($\theta = 760^{\circ}$C) is characteristic of iron with a few percent Ni. A low Curie temperature ($\theta' = 350^{\circ}$C) phase, possibly high-Ni metal, was also detected. Electron microprobe studies did not detect such a high-Ni metal phase (Misra and Taylor, 1975). Chou and Pearce (1976) note that 60335 has Ni/metal slightly higher than the local soils and interpret this as indicating that very little metal in the rock was produced by subsolidus reduction.

AF-demagnetization of the two chips revealed significant differences between the chip that was stored in field-free space (,30) and the chip that was not (,18) (Fig. 9). Apparently the rock acquired a non-lunar viscous remanence that is stable against AF-demagnetization but not against field-free storage (Pearce et al., 1973).
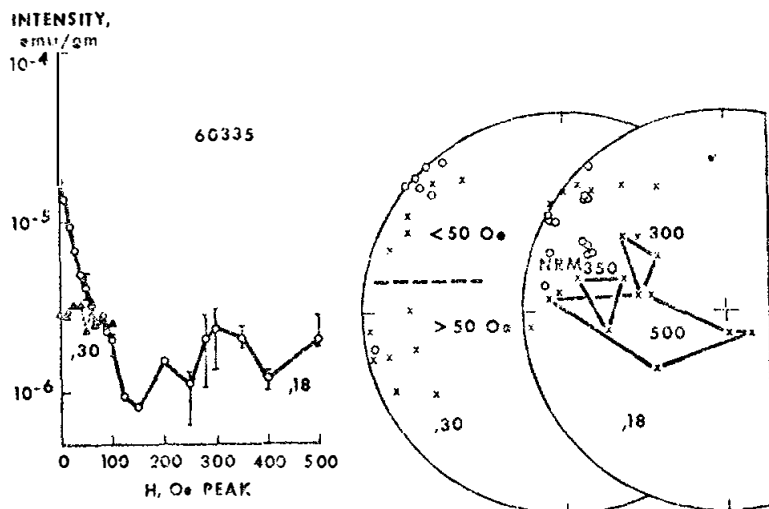


FIGURE 9. AF-demagnetization; from Pearce et al. (1973).

Velocity and linear strain data are provided by Warren et al. (1973) for hydro-static and uniaxial loading conditions (Fig. 10). Bulk elastic properties cal-culated from the density, bulk modulus and shear modulus of the silicate phases of the rock agree well with the measured values. These authors conclude that pore and crack effects exert an extreme control over bulk elastic properties.

Simmons et al. (1975) note the presence of healed cracks that displace twin lamellae in plagioclase xenocrysts.
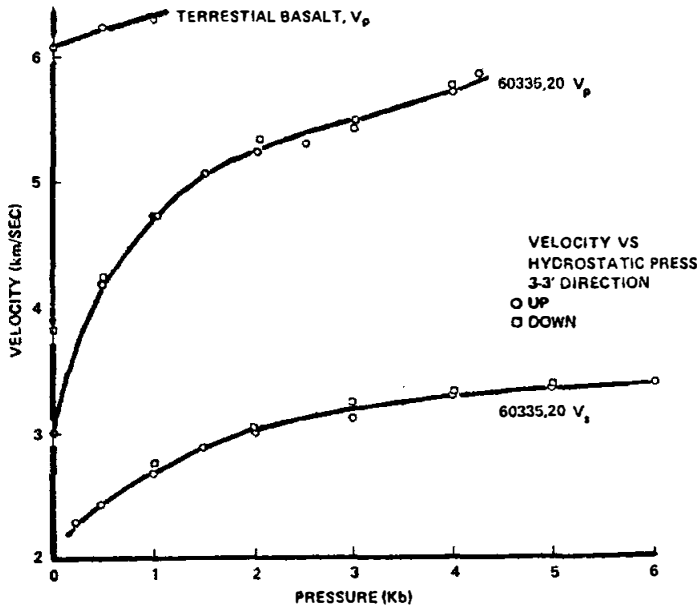
FIGURE 10. Velocity profiles; from Warren et al. (1973).

PROCESSING AND SUBDIVISIONS: In 1972, 60335 was cut into three main pieces, in-cluding a slab. All three of these pieces have been extensively subdivided as shown in Figure 11. Not all splits are shown. Allocations have been made from many portions of the rock.
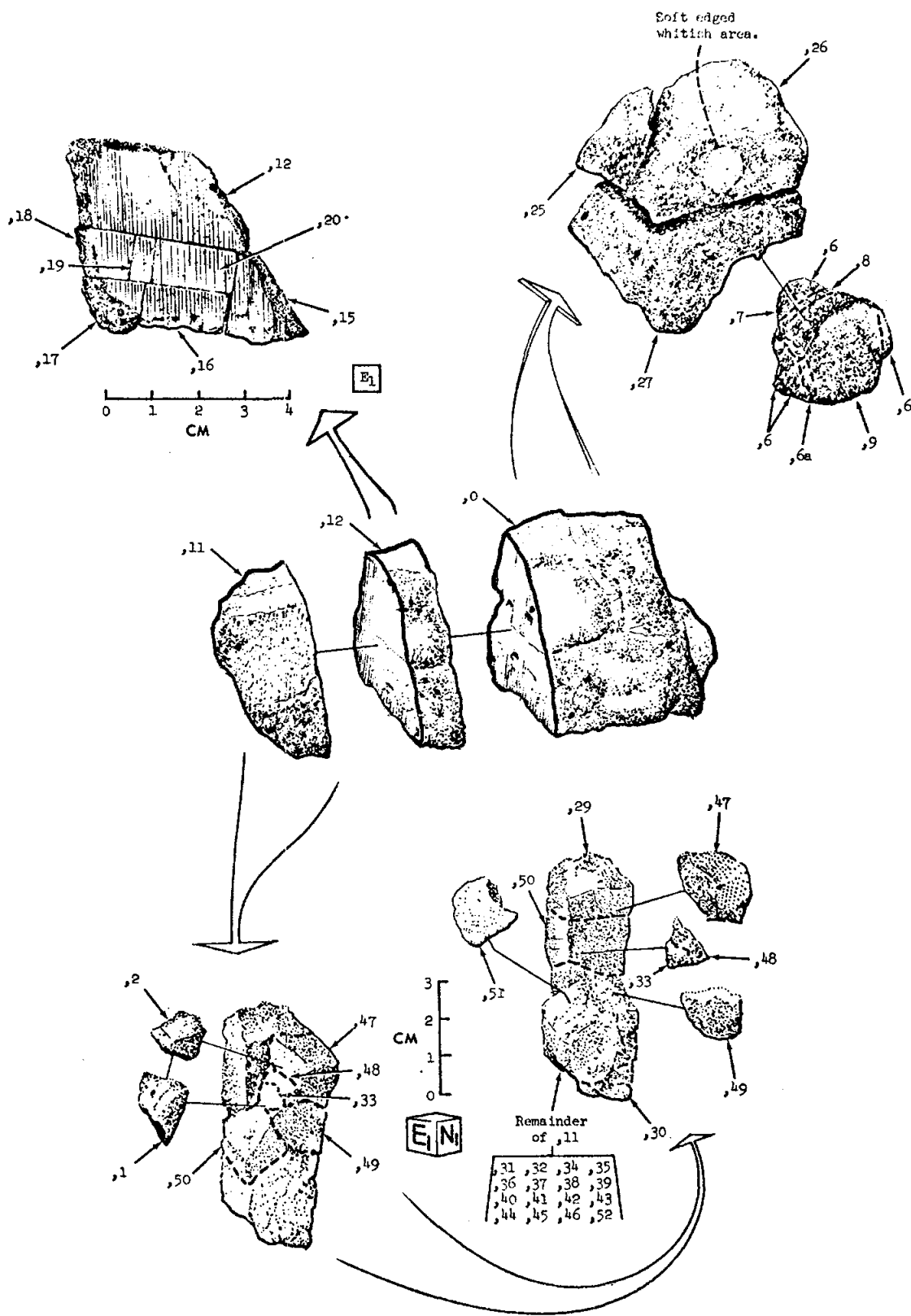
FIGURE 11. Cutting diagram.

INTRODUCTION: 60515 is a white, moderately coherent anorthosite with only minor mafic phases (Fig. 1).  It is rounded with a granular, finely comminuted appearance.  It is a rake sample collected 50 m southwest of the Lunar Module, and has abundant zap pits (Fig. 1).
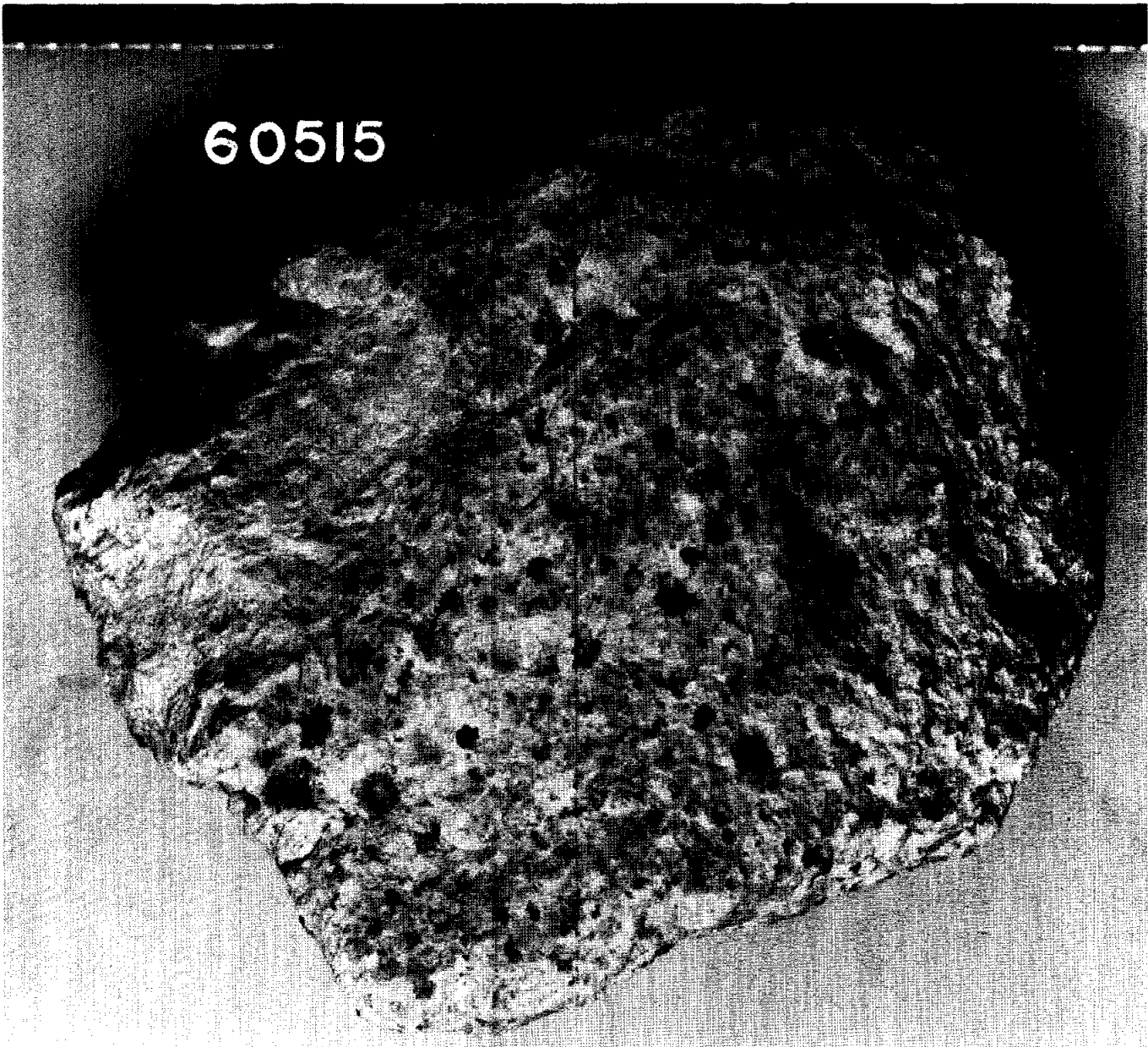


FIGURE 1.

S- 72-46333

Scale in mm.

INTRODUCTION:  60516 is a white, moderately coherent, cataclastic anorthosite (Fig. 1).  It is a rake sample collected about 50 m southwest of the Lunar Module.  Zap pits vary in abundance from few in some areas to many in others.

**60516**

1 cm

S-73-20461
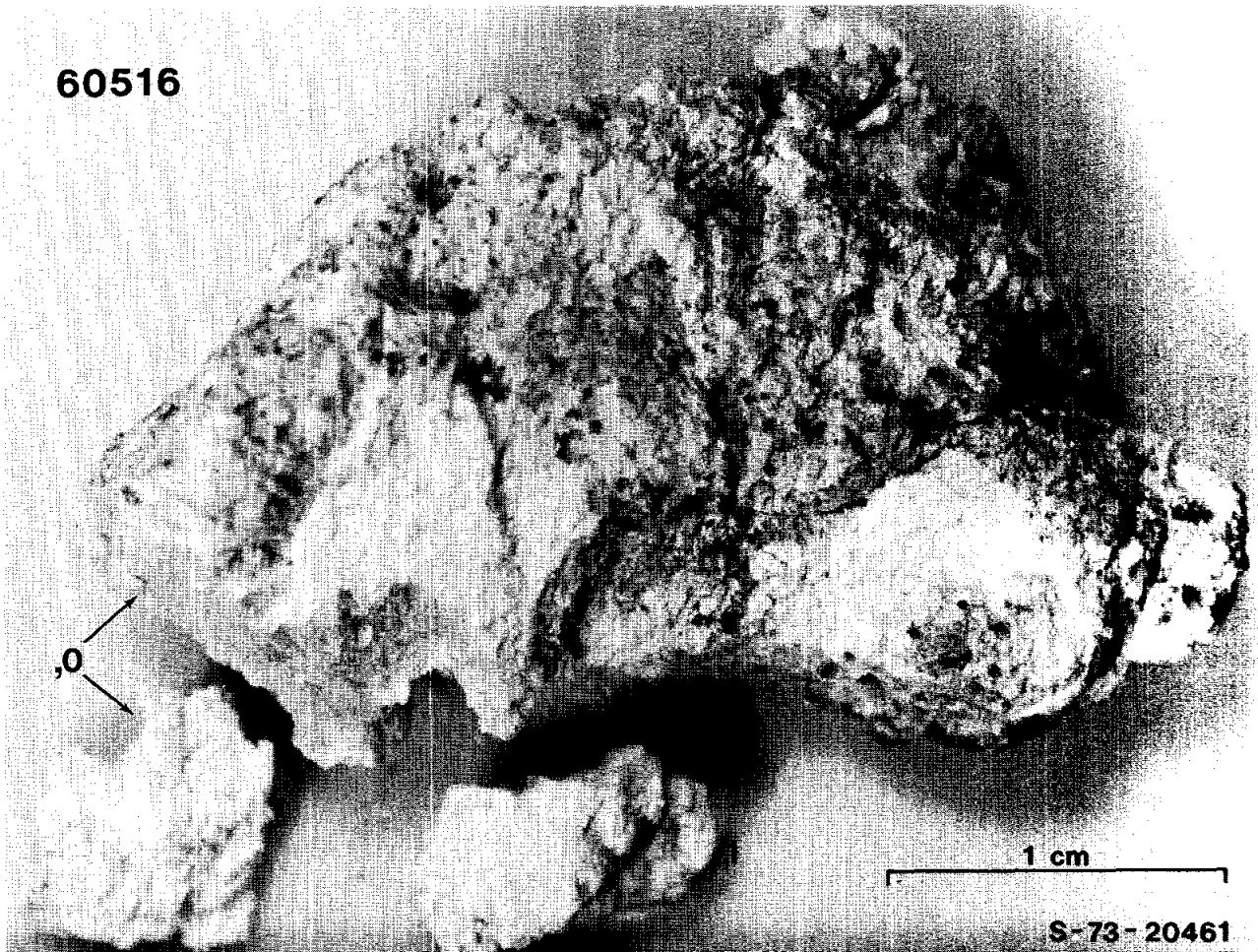
FIGURE 1.

PETROLOGY: A brief petrographic description is given by Warner et al. (1976b). 60516 is also included in a discussion of ferroan anorthosites by Dowty et al. (1974a).

The rock appears to be monomict.  Angular, moderately shocked clasts of plagioclase (up to 1.5 mm) rest in a granulated matrix, which is also dominantly plagioclase (Fig. 2).  Pyroxene is the only mafic mineral present and is very rare.  Mineral compositions are shown in Figure 3 and tabulated by Dowty et al. (1976).  The composition and equilibrated nature of the pyroxenes and the very calcic plagioclases are typical of lunar ferroan anorthosites.
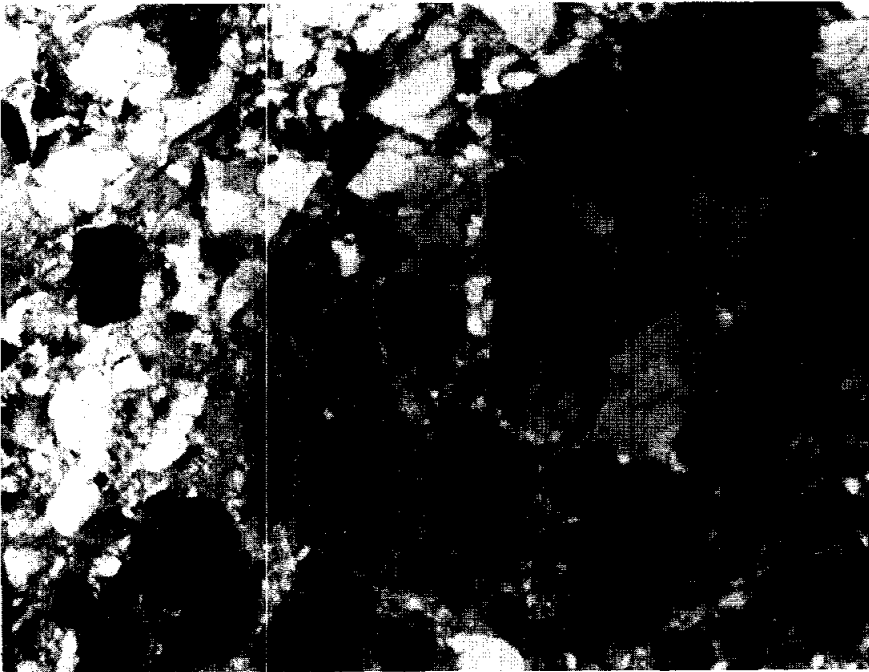
60516

CHEMISTRY: A defocussed beam analysis (DBA) is given by Dowty et al. (1974a) and reproduced by Warner et al. (1976b) and here as Table 1. This analysis shows 60516 to be nearly pure plagioclase.

TABLE 1. Summary chemistry of 60516

| (DBA, normalized to 100%) | |
|---|---|
| $SiO_2$ | 44.8 |
| $Al_2O_3$ | 35.2 |
| FeO | 0.28 |
| MgO | 0.05 |
| CaO | 19.2 |
| $Na_2O$ | 0.44 |
| $K_2O$ | 0.01 |
| $P_2O_5$ | 0.02 |

PROCESSING AND SUBDIVISIONS: In 1973 ,1 was removed for thin sections (Fig.1).

FIGURE 3. Mineral compositions; from R. Warner et. al. (1976b).

Di

Hd

En

Pyroxene composition (mole%)

Fs

NO OLIVINE

| 100 | 90 | 80 | 70 | 60 | 50 | 40 | 30 | 20 | 10 | 0 |

Forsterite content of olivine (mole%)

| 100 | 90 | 80 | 70 | 60 | 50 | 40 | 30 | 20 | 10 | 0 |
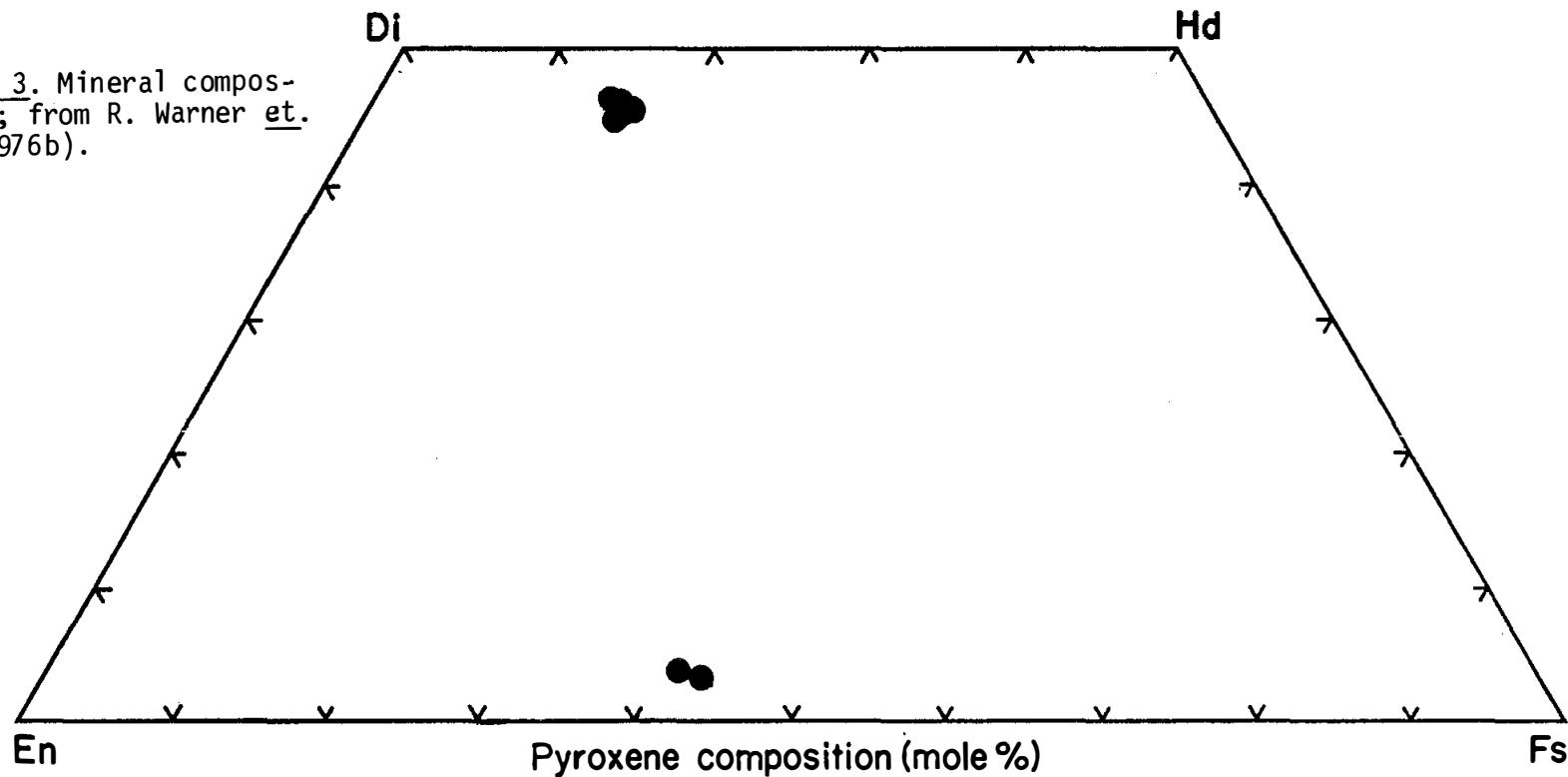
Anorthite content of plagioclase (mole%)
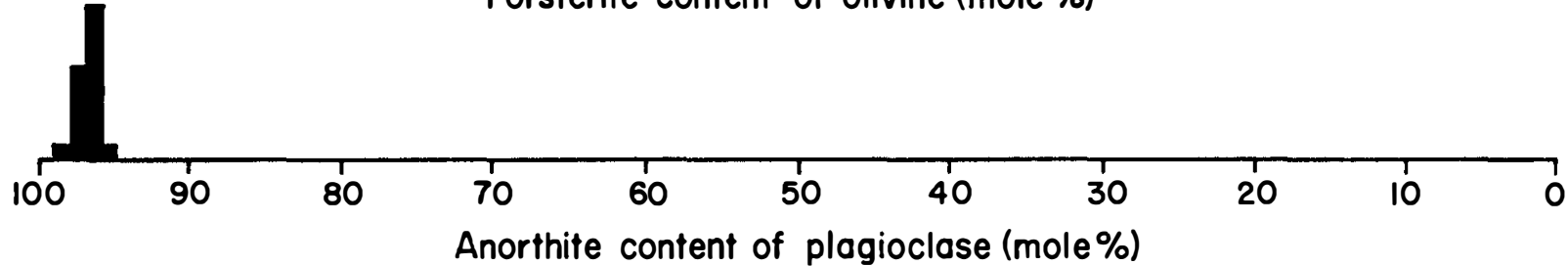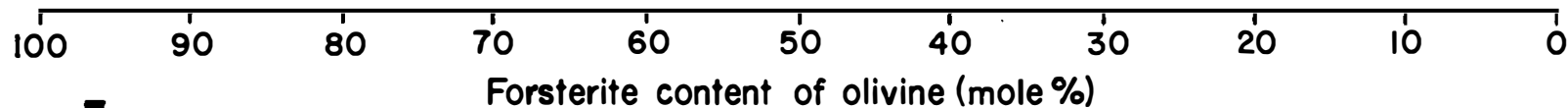
INTRODUCTION:  60517 is a white, moderately coherent anorthosite with minor mafic phases (Fig. 1).  It is subangular with a granular, finely commminuted appearance.  The tiny (<0.05 mm) black mafic specks are scattered through the rock.  It is a rake sample collected 50 m southwest of the Lunar Module.  Zap pits are heterogeneously distributed.
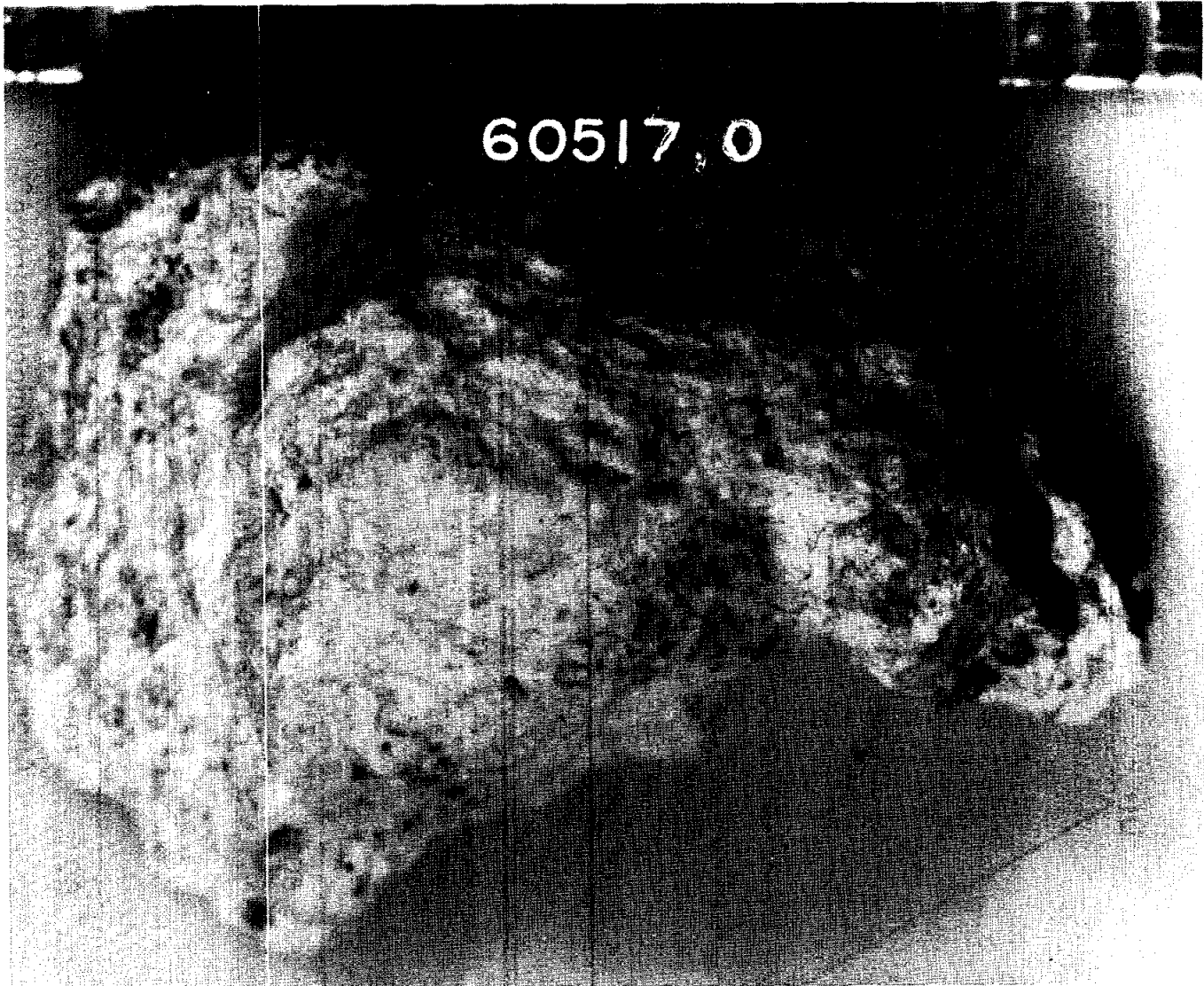
FIGURE 1.  Scale in mm.  S-72-46326

INTRODUCTION:  60518 is a white, moderately coherent anorthosite with only minor mafic phases (Fig. 1).  It is subangular with a granular, finely comminuted appearance.  The tiny (<0.05 mm) black mafic specks are scattered throughout the rock.  It is a rake sample collected 50 m southwest of the Lunar Module, and has a few zap pits.
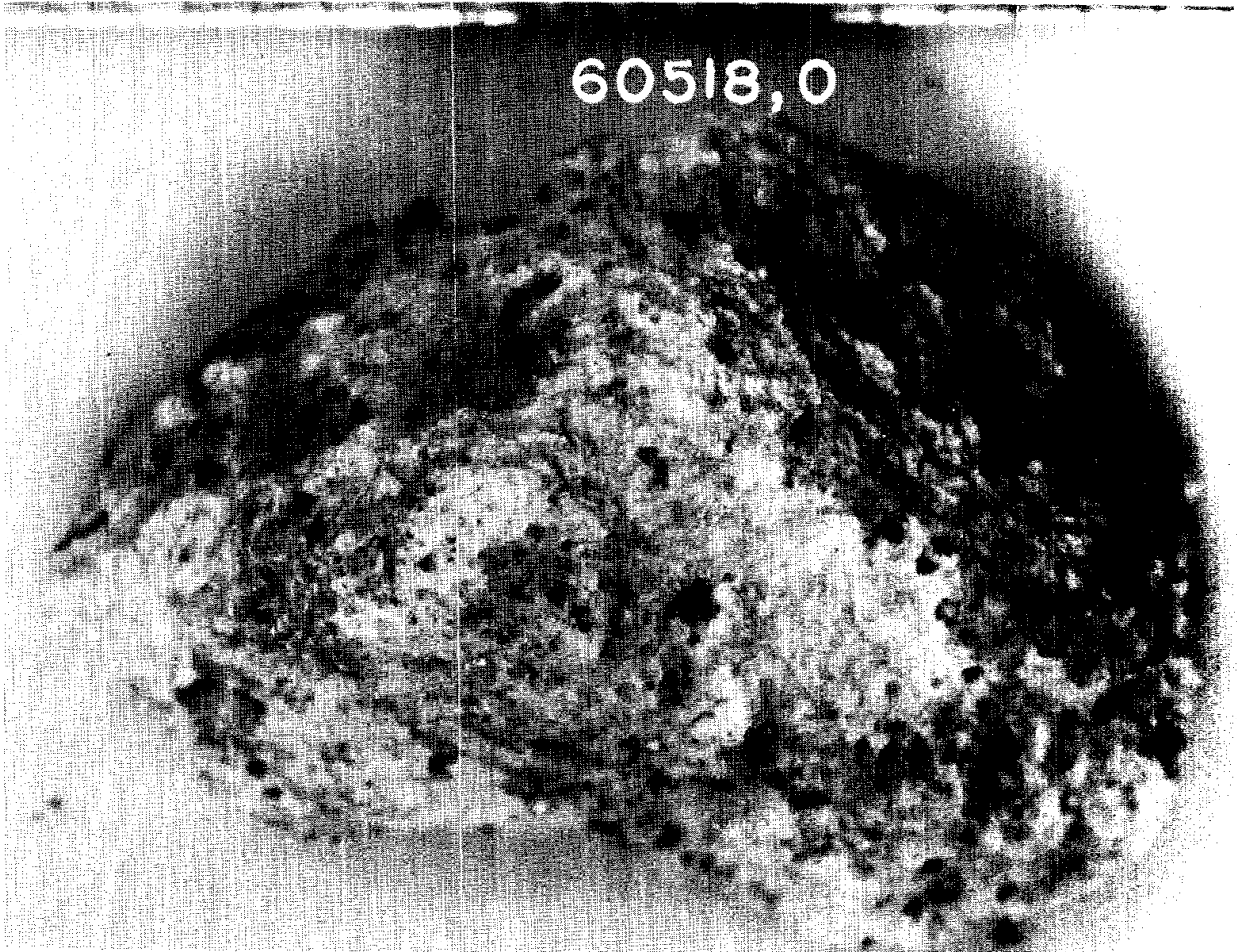


FIGURE 1. Scale in mm.  S-72-46330

INTRODUCTION:   60519 is a white, moderately coherent anorthosite with only minor mafic phases (Fig. 1).   It is subangular with a granular, finely comminuted appearance.  The tiny (<0.05 mm) black mafic specks are scattered throughout the rock.  It is a rake sample collected 50 m southwest of the Lunar Module.  Zap pits and patina are rare.
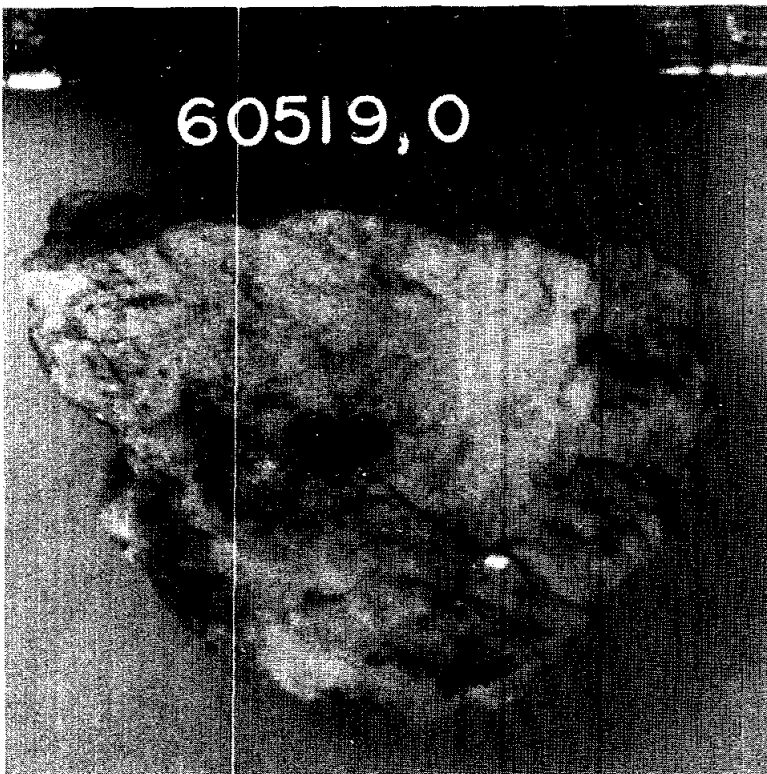
FIGURE 1. Scale in mm.
S-72-46324.

INTRODUCTION:  60525 is a medium gray, coherent, impact melt with a variable texture which is dominantly poikilitic or micropoikilitic (Fig. 1).  It is a rake sample collected about 50 m southwest of the Lunar Module and has a few zap pits.



FIGURE 1.

PETROLOGY; Warner et al. (1976b)  provide a brief petrographic description and mineral compositions.  60525 is texturally heterogeneous, grading from poikilitic (oikocrysts ∿ 0.1 mm) to subophitic over a single thin section (Fig.2). Clasts of plagioclase, minor olivine and several lithic fragments are present.  Mineral compositions are shown in Figure 3 and tabulated by Dowty et al. (1976). Minor phases include spinel, ilmenite, Fe-metal (5.7-9.1% Ni, 0.4-0.6% Co), zircon and a "K-rich phase" (8-14.8%, $K_2O$).

CHEMISTRY: A defocussed electron beam analysis (DBA) is given by Warner et al. (1976b) and reproduced here as Table 1.

PROCESSING AND SUBDIVISIONS:  In 1973 a single chip (,1) was removed for thin sections (Fig.1).
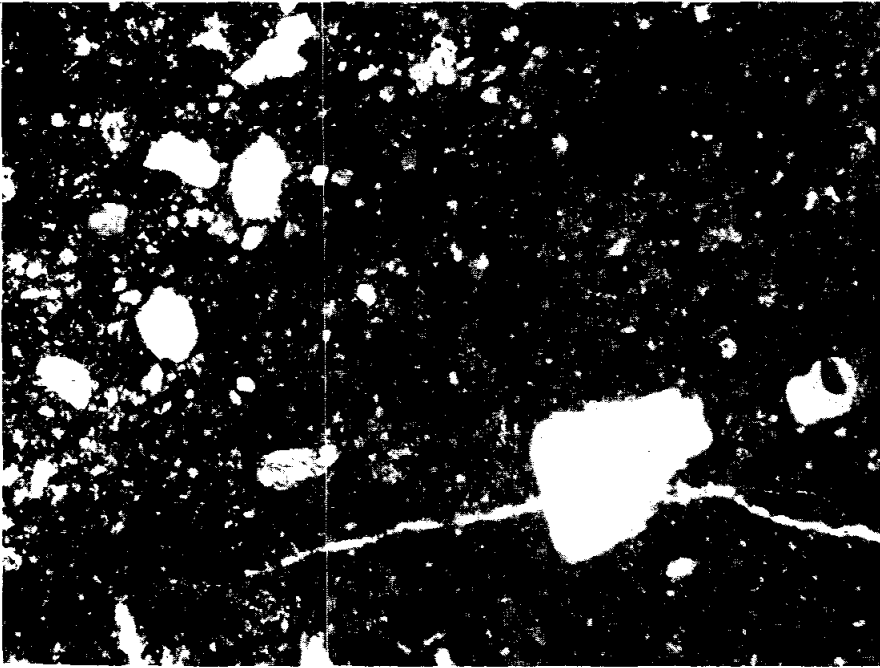
FIGURE 2. 60525,2. general view, ppl. width 3mm.



FIGURE 3. Mineral compositions; from R.Warner et al.(1976b).
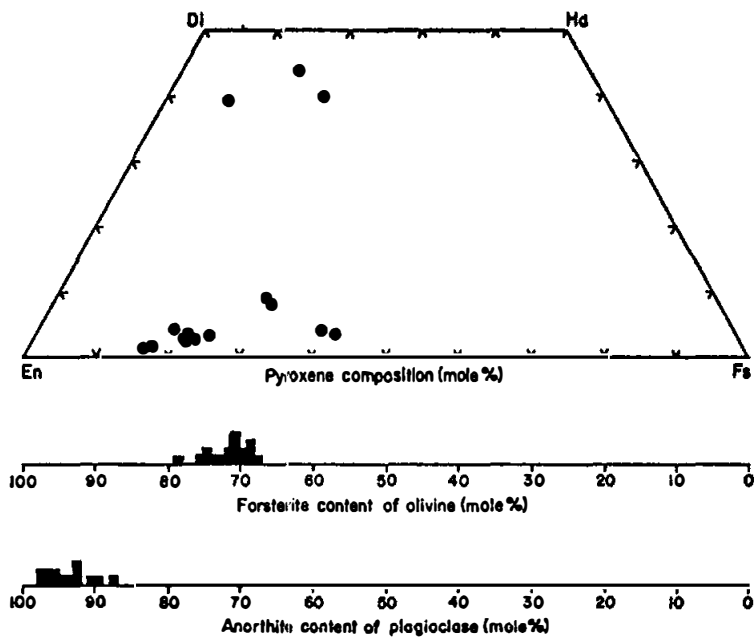
TABLE 1. Chemistry of 60525 (DBA)

| | |
|---|---|
| $SiO_2$ | 46.1 |
| $TiO_2$ | 1.05 |
| $Al_2O_3$ | 21.2 |
| $Cr_2O_3$ | 0.14 |
| FeO | 7.2 |
| MnO | 0.08 |
| MgO | 9.3 |
| CaO | 12.9 |
| $Na_2O$ | 0.64 |
| $K_2O$ | 0.27 |
| $P_2O_5$ | 0.26 |

INTRODUCTION:  60526 is a medium gray, coherent, poikilitic impact melt (Fig. 1).
It is a rake sample collected about 50 m southwest of the Lunar Module, and lacks
zap pits.  (The photograph labelled 60526 in Keil et al., 1972, p. 50 is actually
of 60527; the correct photograph is on p. 62).

PETROLOGY:  Warner et al. (1976b) provide a brief petrographic description and
mineral compositions.  Texturally 60526 is a typical fine-grained poikilitic
rock with oikocrysts (∿0.3 x 0.15 mm) of dominantly low-Ca pyroxene enclosing
abundant euhedral to subhedral plagioclase (Fig. 2).  Mineral compositions are
shown in Figure 3 and tabulated by Dowty et al. (1976).  Accessory phases include
ilmenite, armalcolite and Fe-metal (4.4-6.1% Ni, 0.3% Co).

CHEMISTRY:  A defocussed electron beam analysis (DBA) presented by Warner et al.
(1976b) is reproduced here as Table 1.  60526 is compositionally very similar to
the well-studied poikilitic rocks such as 60315.

PROCESSING AND SUBDIVISIONS:  In 1973 ,1 was removed for thin sections.  In 1978
,4 was allocated for chemistry (Fig. 1).
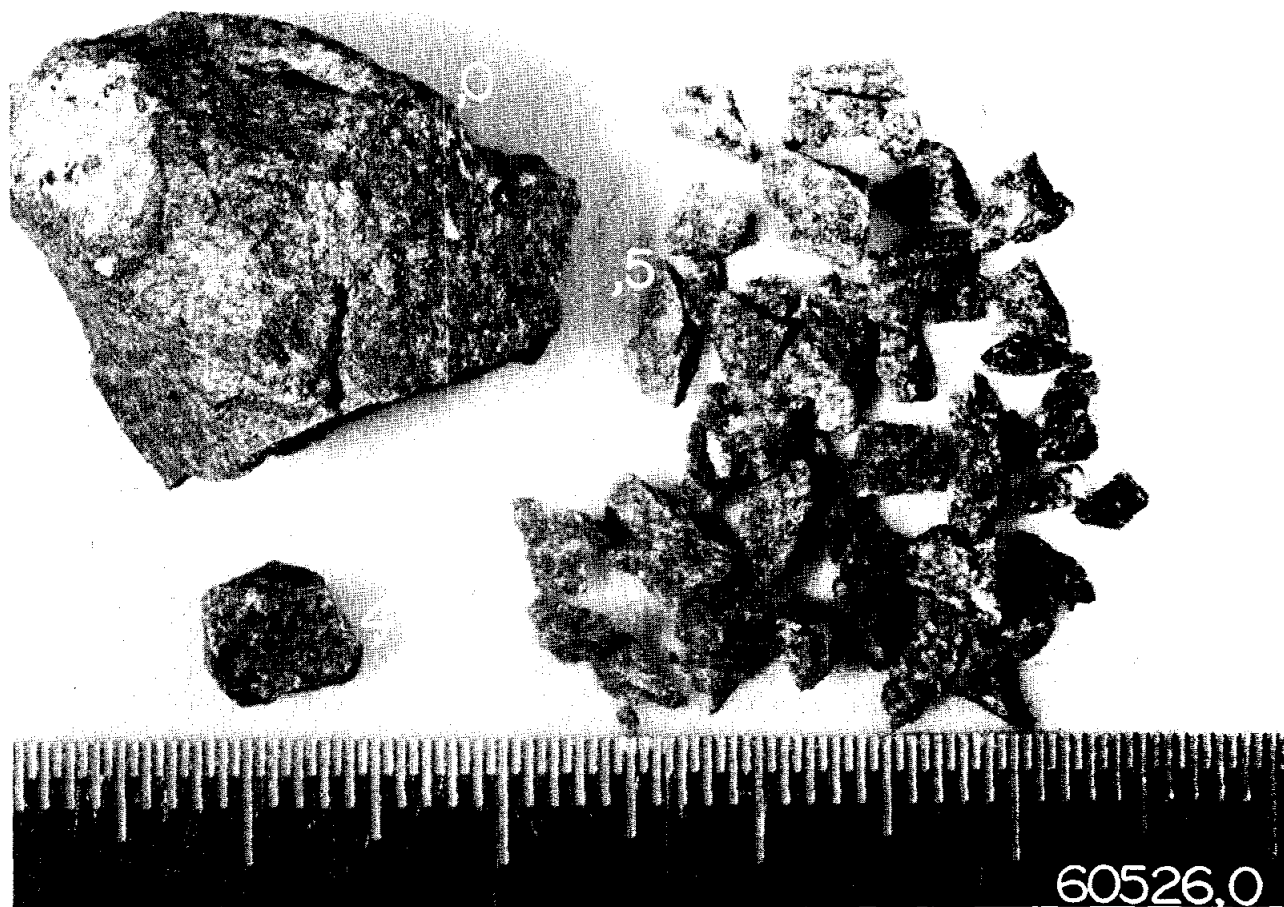


FIGURE 1. Large scale division in cm.  S-78-27394.

115
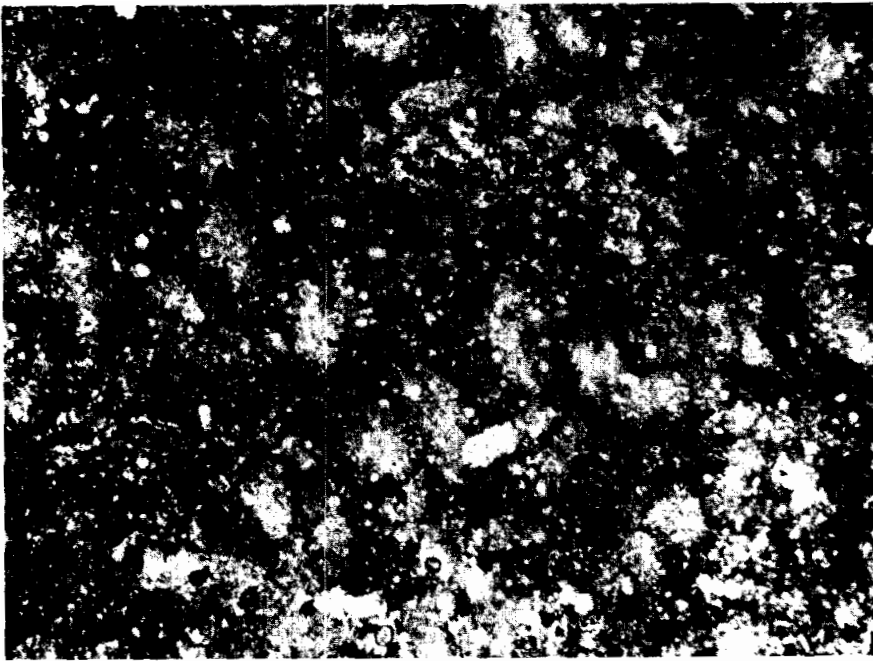
60526

FIGURE 2. 60526,3. general view, xpl. width 3mm.



FIGURE 3. Mineral compositions; from R. Warner et al. (1976b).
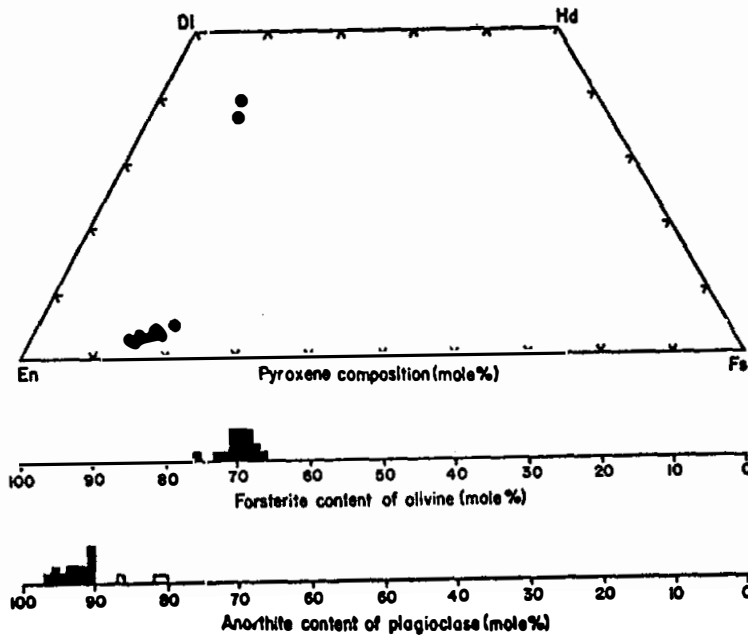
TABLE 1. Chemistry of 60526 (DBA)

| | |
|---|---|
| $SiO_2$ | 47.5 |
| $TiO_2$ | 1.40 |
| $Al_2O_3$ | 17.4 |
| $Cr_2O_3$ | 0.17 |
| $FeO$ | 8.9 |
| $MnO$ | 0.09 |
| $MgO$ | 13.5 |
| $CaO$ | 10.8 |
| $Na_2O$ | 0.71 |
| $K_2O$ | 0.45 |
| $P_2O_5$ | 0.44 |

116

INTRODUCTION:   60527 consists of a rectangular clast of coherent, crystalline rock thickly coated by highly vesicular, glassy impact melt and a separate piece of vesicular glass (Fig. 1).  The rectangular clast has ∿50% white material (in grains <0.05 mm long) embedded in dark material and is possibly a poikilitic impact melt.  The glassy coat contains rare white clasts (∿0.7 mm long).  It is a rake sample collected 50 m southwest of the Lunar Module and has rare zap pits.  (The photograph labelled 60527 in Keil et al., 1972, p. 40, is actually 60528; the correct photograph is on p. 50).

PROCESSING AND SUBDIVISIONS:  This rock was removed from its documented bag as two pieces which were numbered together as 60527.
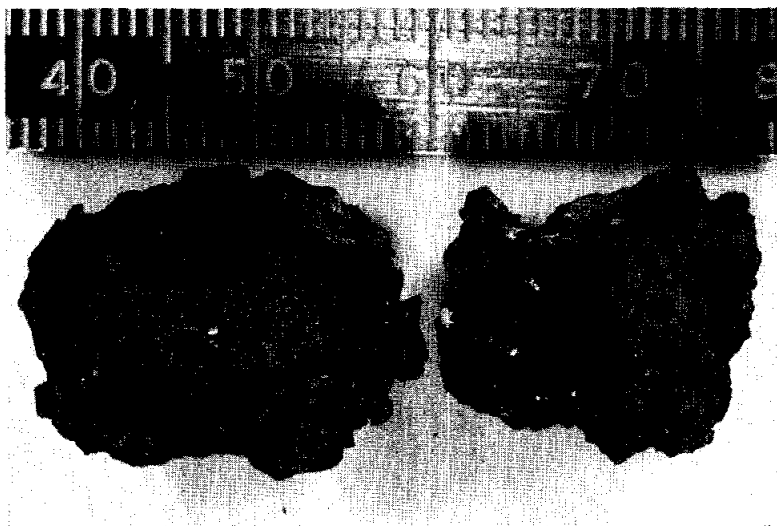


FIGURE 1.
Scale in mm.

INTRODUCTION:  60528 is a medium gray, coherent, glassy impact melt with several small (<1.5 mm) white clasts (Fig. 1).  This rake sample is very irregular in shape with abundant vesicles and rare zap pits and was collected about 50 m southwest of the Lunar Module.  (The photograph labelled 60528 in Keil et al., 1972, p. 61 is actually of 60529; the correct photograph is on p. 40).
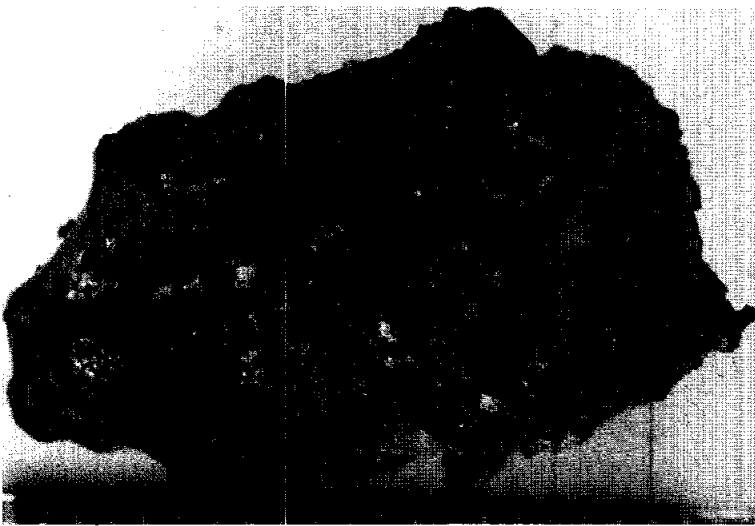


FIGURE 1.

Scale in mm.

INTRODUCTION: 60529 is a medium gray, coherent basaltic impact melt (Fig. 1).
It is angular with ~10% vesiscles. It is a rake sample collected about 50 m
southwest of the Lunar Module and has rare zap pits. (The photograph labelled
60529 in Keil et al., 1972, p. 62 is actually of 60526; the correct photograph
is on p. 61).
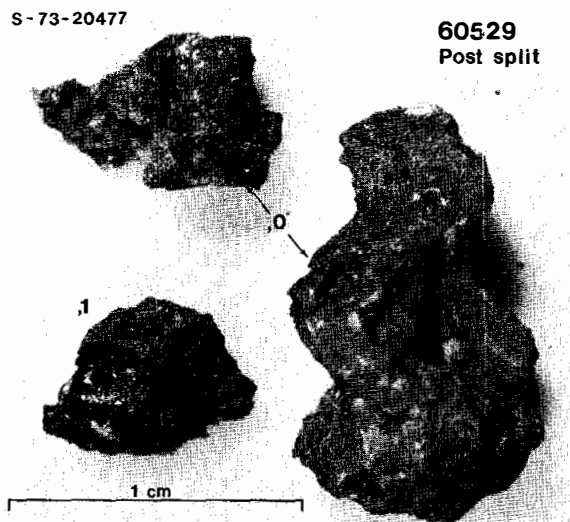


FIGURE 1.
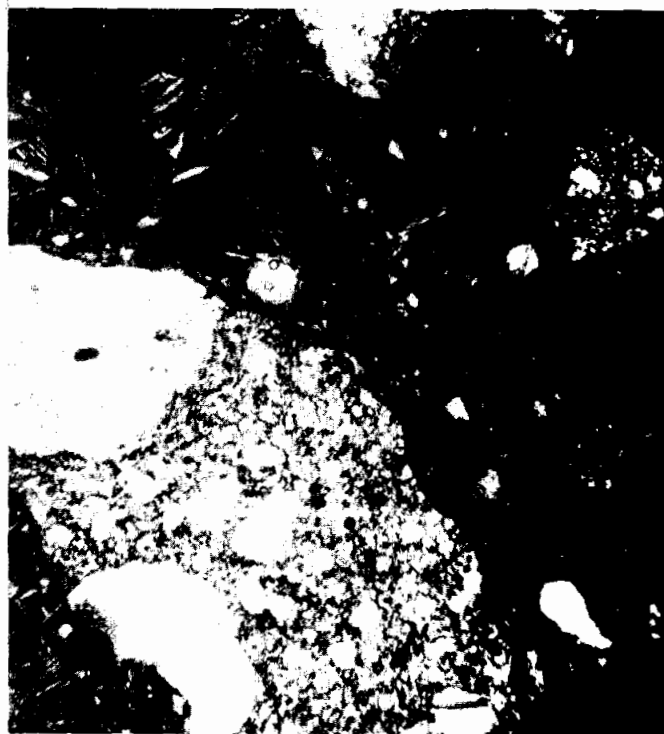


FIGURE 2.  60529,2.  general
view, ppl.  width 2mm.

PETROLOGY: Warner et al. (1976b) provide a brief petrographic description.
The matrix of 60529 is a very fine-grained impact melt with spherulitic
needles of plagioclase separated by a cryptocrystalline to glassy mesostasis
(Fig.2). Lithic clasts include breccia fragments and a few anorthosites, all
of which show evidence of assimilation into the melt. Mineral clasts are re-
latively rare and also show evidence of assimilation.

PROCESSING AND SUBDIVISIONS: In 1973 two small chips were removed from this
rock. One of these chips was allocated for thin sections as ,1 (Fig.1).

INTRODUCTION:  60535 is a medium gray, coherent, possibly regolith breccia (Fig. 1). One surface is coated with glass and another has a sheared appearance.  It is a rake sample collected 50 m southwest of the Lunar Module.  Zap pits are hetero- geneously distributed from abundant on one side to very few of the others.
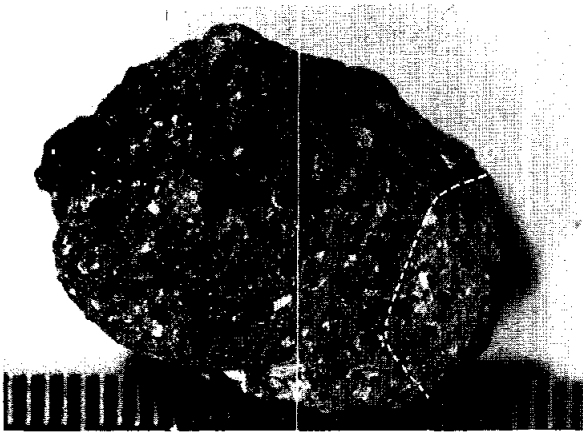


FIGURE 1.
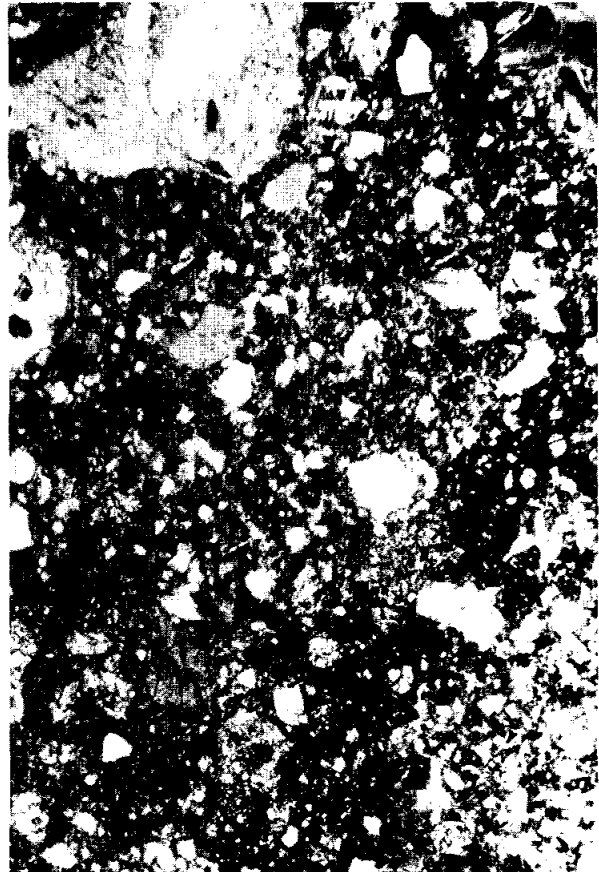


FIGURE 2. 60535,2.  general view, ppl.  width 2mm.

PETROLOGY:  Warner et al. (1976b)  provide a brief petrographic description. The matrix of 60535 is very porous and is composed of a heterogeneous mixture of mineral, lithic and glass fragments welded together by a small amount of glass.  Lithic clasts include a variety of breccias, several poikilitic rocks and several anorthositic fragments.  Numerous clasts of glass are also present including one 1.5 mm long shard noted by Warner et al. (1976b).

PROCESSING AND SUBDIVISIONS:  , In 1973, three small chips were pried from one end of the rock.  Two of these chips were allocated for thin sections as ,1 (Fig.1).

INTRODUCTION:  60615 is a light gray, coherent, basaltic impact melt.  Irregularly shaped vugs (up to 13 mm across) are common (Fig. 1).  Small, very thin areas of glass partially coat one surface.  It is a rake sample collected about 70 m west southwest of the Lunar Module.  Zap pits are heterogeneously distributed.



**60615**                                                    S-73-20458

FIGURE 1.

PETROLOGY:  Dowty et al. (1974b) and Warner et al. (1976b) provide petrographic descriptions.  Mineral analyses are tabulated by Dowty et al. (1976).  The texture of 60615 is predominantly intergranular with olivine and pyroxene confined to interstices between fine (∿0.1 mm) plagioclase laths (Fig. 2).  Mafic minerals are unusually magnesian (Fig. 3).  Plagioclase laths and xenocrysts are of the same composition.  Accessory phases include ilmenite, armalcolite, rutile, Fe-metal (4.3-13.6% Ni, 0.6-1.03% Co), schreibersite and troilite.  Angular xenocrysts of plagioclase account for ∿4% of the rock.  One "breccia" clast is noted by Warner et al. (1976b).

FIGURE 2. 60615,8. xpl. width 2mm.



FIGURE 3. Mineral compositions; from R.Warner et al. (1976b).

TABLE 1. Summary chemistry of 60615

| | |
|---|---|
| $SiO_2$ | 44.9 |
| $TiO_2$ | 0.52 |
| $Al_2O_3$ | 21,8 |
| $Cr_2O_3$ | 0.144 |
| FeO | 5.3 |
| MnO | 0.071 |
| MgO | 14.2 |
| CaO | 12.5 |
| $Na_2O$ | 0.386 |
| $K_2O$ | 0.13 |
| $P_2O_5$ | 0.09 |
| Sr | |
| La | 16.9 |
| Lu | 0.77 |
| Rb | |
| Sc | 9.0 |
| Ni | 490 |
| Co | 32 |
| Ir ppb | 9 |
| Au ppb | 8 |
| C | |
| N | |
| S | |
| Zn | |
| Cu | |

Oxides in wt%; others in ppm except as noted.

INTRODUCTION: 60616 is a medium gray, coherent, poikilitic impact melt (Fig.1). It is a rake sample collected about 70 m west southwest of the Lunar Module and lacks zap pits.



**60616**

S-73-20503

FIGURE 1.

PETROLOGY: Warner et al. (1976b)  provide a brief petrographic description and mineral compositions.  Oikocrysts are less abundant in 60616 than in most other poikilitic rocks, enclosing only ∿ 60-70% of the area of the section (Fig.2).  Inter-oikocryst areas have a subophitic texture. Clasts are predominantly plagioclase and are abundant.  Mineral compositions are shown in Figure 3 and tabulated by Dowty et al. (1976).  Minor phases include ilmenite and Fe-metal (6.1-8% Ni, 0.3-0.4% Co).

FIGURE 2. 60616,2. ppl. width 3mm.



Di    Hd

En    Pyroxene composition (mole %)    Fs

100  90  80  70  60  50  40  30  20  10  0
Forsterite content of olivine (mole%)

100  90  80  70  60  50  40  30  20  10  0
Anorthite content of plagioclase (mole%)
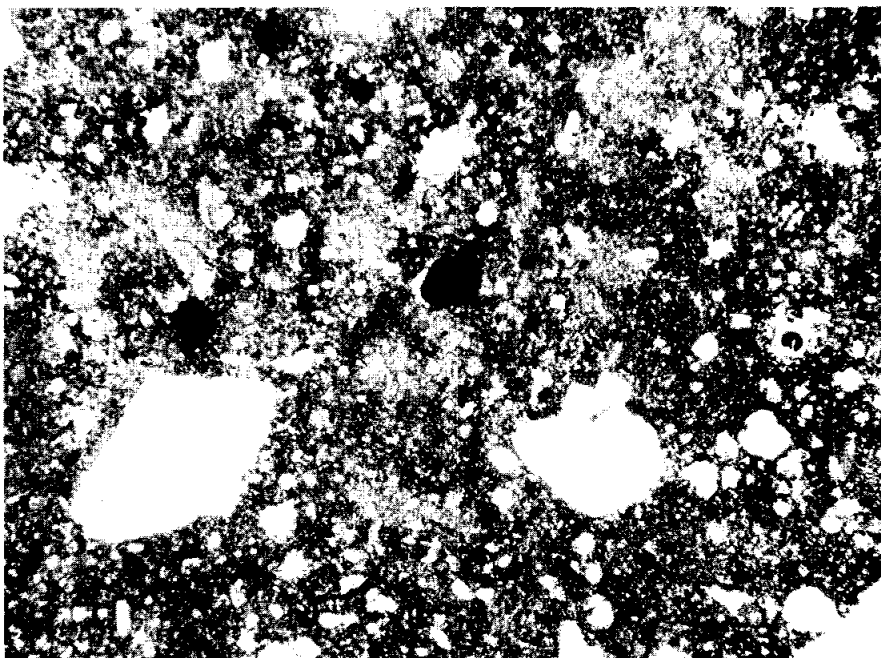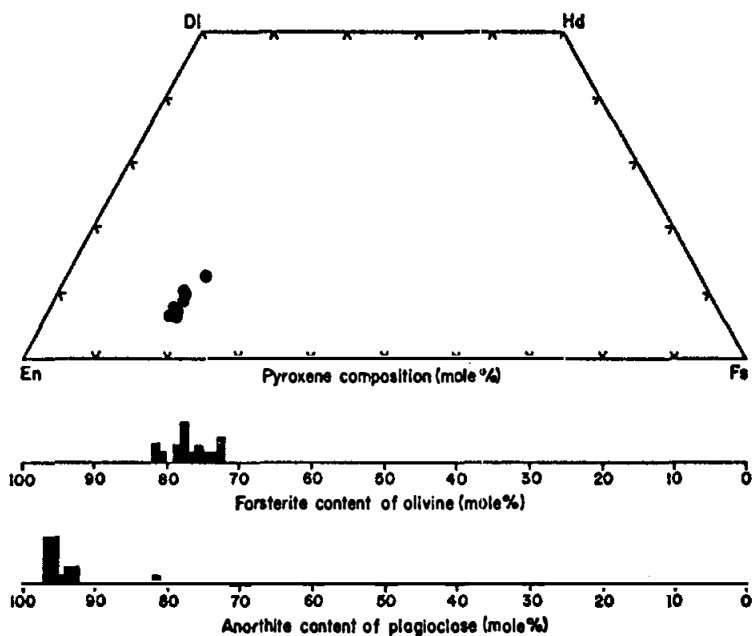
TABLE 1.  Chemistry of 60616 (DBA)

| | |
|---|---|
| $SiO_2$ | 45.5 |
| $TiO_2$ | 0.68 |
| $Al_2O_3$ | 24.5 |
| $Cr_2O_3$ | 0.11 |
| FeO | 5.9 |
| MnO | 0.06 |
| MgO | 8.3 |
| CaO | 14.3 |
| $Na_2O$ | 0.56 |
| $K_2O$ | 0.20 |
| $P_2O_5$ | 0.22 |

FIGURE 3. Mineral compositions; from R.Warner et al. (1976b).

CHEMISTRY: A defocussed electron beam analysis (DBA) is given by Warner et al. (1976b) and reproduced here as Table 1. 60616 is more aluminous than most other Apollo 16 poikilitic rocks.

PROCESSING AND SUBDIVISIONS: In 1973, two chips (,1) were allocated for thin sections (Fig.1).

INTRODUCTION:  60617 is a medium gray, coherent, impact melt (Fig. 1).  It is subangular with a few small areas of dark splash glass.  It is a rake sample collected about 70 m west southwest of the Lunar Module.  Zap pits are rare.
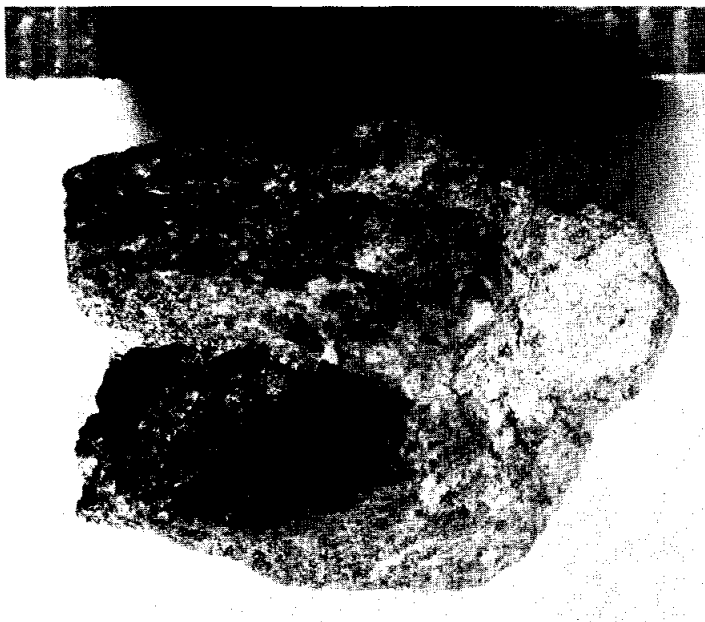


FIGURE 1.
Scale in mm.

INTRODUCTION:  60618 is a tough, light gray rake sample consisting of basaltic impact melt and cataclastic anorthosite (Fig. 1).  The anorthosite is not ferroan.  Possible clast-matrix relations have not been determined but the anorthosites are probably clasts in the basalt.  A few 2-3 mm vesicles are present, some of which appear to be lined with metal.

60618 is a rake sample collected about 70 m west southwest of the Lunar Module. Zap pits are rare.



FIGURE 1.

PETROLOGY:  Two distinct lithologies, a coarse-grained, cataclastic spinel-bearing anorthosite and a finer-grained basaltic melt have been recognized in this rock.  Petrographic descriptions are given by Dowty et al. (1974a,b) and Warner et al. (1976b).

The anorthosite described by Dowty et al. (1974a) and Warner et al. (1976b) consists of a single large (2x3 mm) plagioclase crystal in a granulated matrix of feldspar, minor olivine, spinel, pyroxene, ilmenite, metal (6.1% Ni, 1.3% Co),and schreibersite (Fig. 2).  Pyroxene occurs mainly in fine veins that cut both the large crystal and the matrix.  Mineral compositions are shown in Figure 3 and tabulated by Dowty et al. (1976), and show that the anorthosite has much more magnesian mafic minerals than typical ferroan anorthosites.

127

a



b
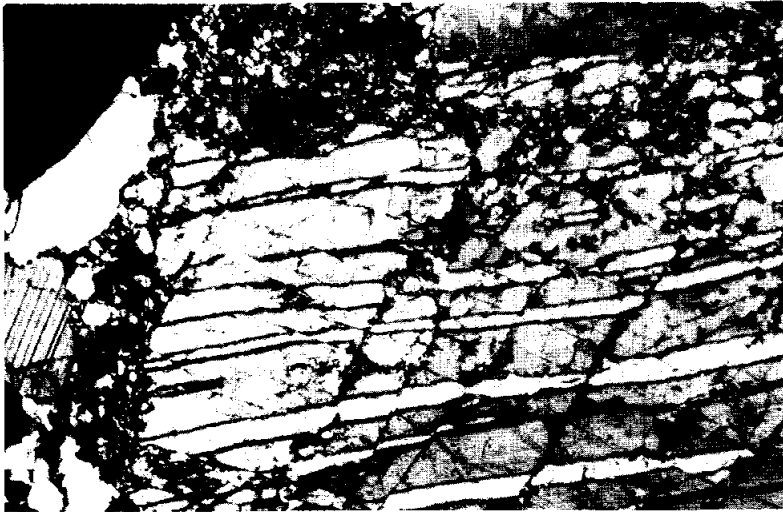
a) 60618,4. cataclastic anorthosite, xpl. width 3mm.
b) 60618,3. basaltic melt, xpl. width 3mm.
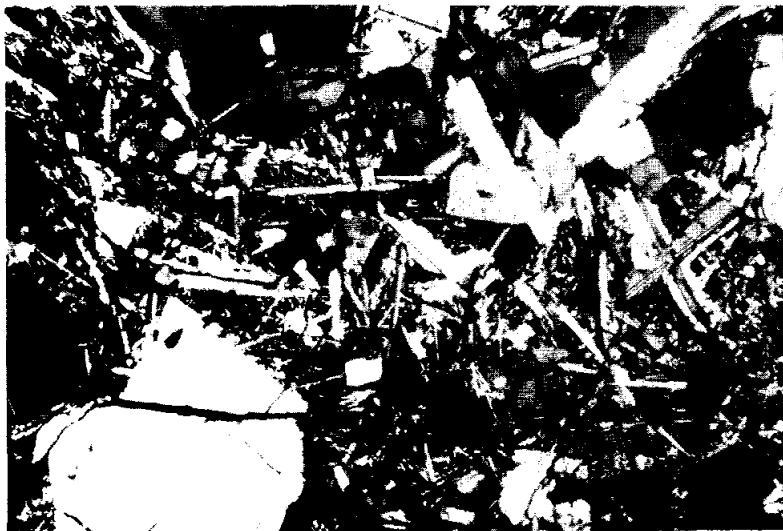
The basaltic impact melt portion consists of many equant, but somewhat irregular, relict plagioclase grains (~0.5 mm) in a subophitic melt matrix of plagioclase laths (up to 0.5 mm long), olivine, and pyroxene (Fig. 2). Mineral compositions are shown in Figure 4 and tabulated by Dowty et al. (1976). Accessory minerals include ilmenite, armalcolite, Fe-metal (2.5-6.9% Ni, 0.6-1.2% Co), schreibersite,and troilite.

Meyer (1979) reports ion probe analyses of minor elements in plagioclase from an unspecified section of the rock (Table 1).

TABLE 1

Minor elements in 60618 plagioclase (ppm) (Meyer, 1979)

| Li | Mg | Ba |
|----|-----|----|
| 4  | 800 | 16 |
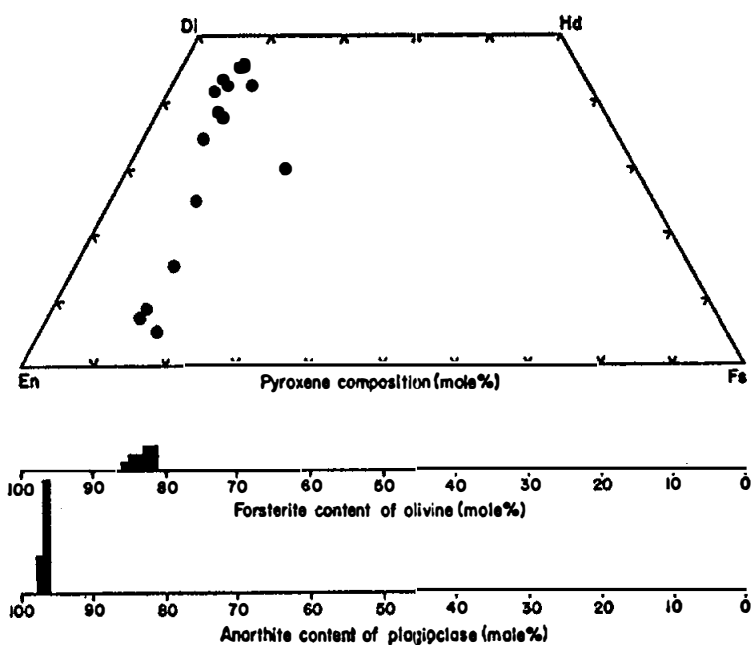
FIGURE 3. Anorthosite mineral compositions; from R. Warner et al. (1976b).
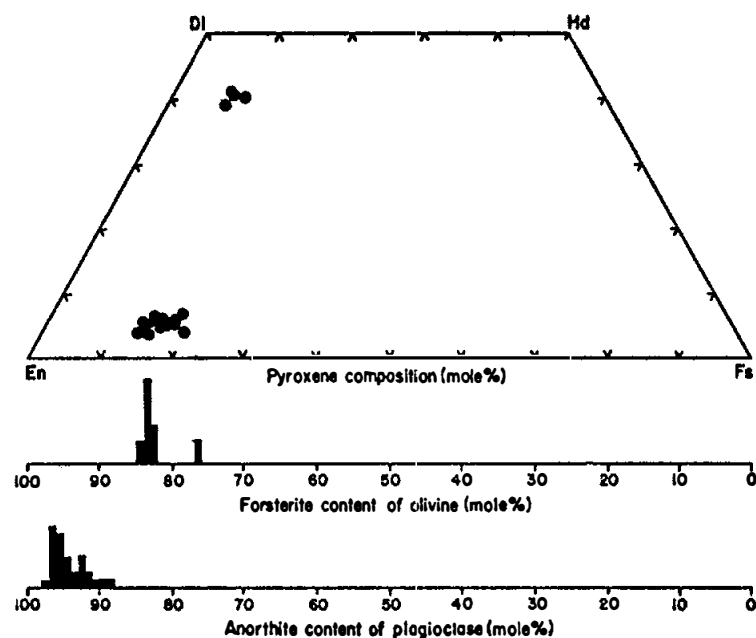


FIGURE 4. Basaltic melt mineral compositions; from R. Warner et al. (1976b).

CHEMISTRY: Major and trace element analyses of the anorthositic and the basaltic melt portions are given by Murali et al. (1977) and Ehmann et al. (1975). Eldridge et al. (1975) report whole rock abundances of natural and cosmogenic radionuclides. Jovanovic and Reed (1976b) provide halogen and other trace element abundances for a split probably rich in anorthosite. Microprobe defocussed beam analyses (DBA) of each lithology are reported by Dowty et al. (1974a,b) and Warner et al. (1976b). Ca and K abundances of an anorthosite-rich split are given by Schaeffer and Schaeffer (1977) in an Ar isotopic study.

Whole rock abundances of K, U, and Th show that the rock is very low in incompatible elements (K 670 ppm, U 0.28 ppm, Th 0.63 ppm). Eldridge et al. (1975) note the unusually low Th/U ratio (2.3) of this rock.

The anorthositic material is nearly pure plagioclase, with low abundances of incompatible elements (Table 2). Siderophile element abundances indicate meteoritic contamination.

The basaltic melt portions are less aluminous and have higher levels of incompatible elements than the anorthositic material (Table 2).

TABLE 2 Summary chemistry of 60618 lithologies

|  | Anorthosite | Basaltic impact melt |
|---|---|---|
| $SiO_2$ | 44.3 | 45.8 |
| $TiO_2$ | 0.03 | 0.27 |
| $Al_2O_3$ | 33.2 | 28.8 |
| $Cr_2O_3$ | 0.01 | 0.061 |
| FeO | 1.1 | 2.0 |
| MnO | 0.02 | 0.03 |
| MgO | 3.4 | 4.9 |
| CaO | 16.9 | 15.9 |
| $Na_2O$ | 0.40 | 0.49 |
| $K_2O$ | 0.047 | 0.15 |
| $P_2O_5$ | 0.009 | |
| Sr | | |
| La | 3.2 | 6.0 |
| Lu | 0.13 | 0.29 |
| Rb | | |
| Sc | 1.5 | 3.2 |
| Ni | 228 | 50 |
| Co | 12 | 4.1 |
| Ir ppb | 5 | |
| Au ppb | 3 | 15 |
| C | | |
| N | | |
| S | | |
| Zn | | |
| Cu | | |

Oxides in wt%; others in ppm except as noted.

RADIOGENIC ISOTOPES/GEOCHRONOLOGY:  Schaeffer and Schaeffer (1977) report an $^{40}Ar$-$^{39}Ar$ plateau age of 4.00±0.02 b.y. over the 900-1100°C temperature interval (Fig. 5).  Large losses of low temperature Ar with an age of ∿2.17 b.y. are also noted.
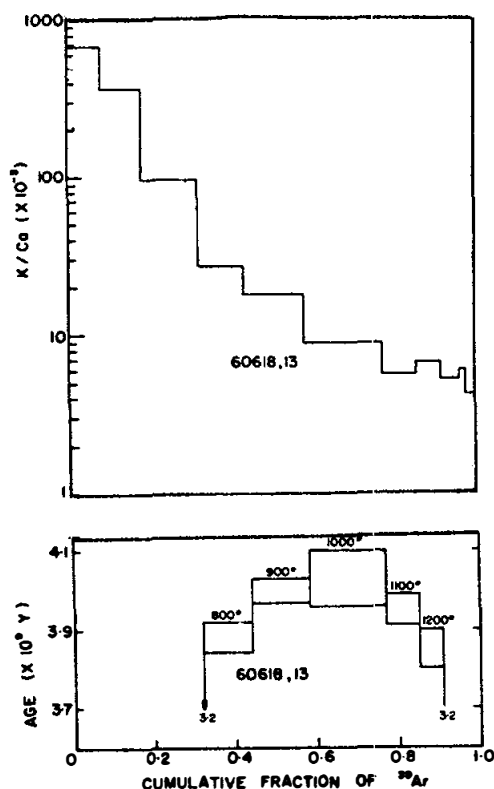
FIGURE 5. Ar release; from Shaeffer and Shaeffer (1977).

RARE GASES/EXPOSURE AGES:  Whole rock $^{22}Na$ and $^{26}Al$ data indicate that 60618 is probably saturated in $^{26}Al$ activity (Eldridge et al., 1975).  Excess $^{38}Ar$ at all temperatures preclude the calculation of an Ar exposure age (Schaeffer and Schaeffer, 1977).

PROCESSING AND SUBDIVISIONS:  In 1973, the pieces of 60618 were numbered ,8 - ,11 (Fig. 1).  The melt rock splits came from ,9.  The anorthosite splits were taken from ,10.

INTRODUCTION:   60619 is a coherent, light gray anorthosite that has been extensively recrystallized to a granoblastic texture.  A small amount of dark splash glass is present on some surfaces (Fig. 1).  60619 is a rake sample collected about 70 m west southwest of the Lunar Module.  Zap pits are heterogeneously distributed.
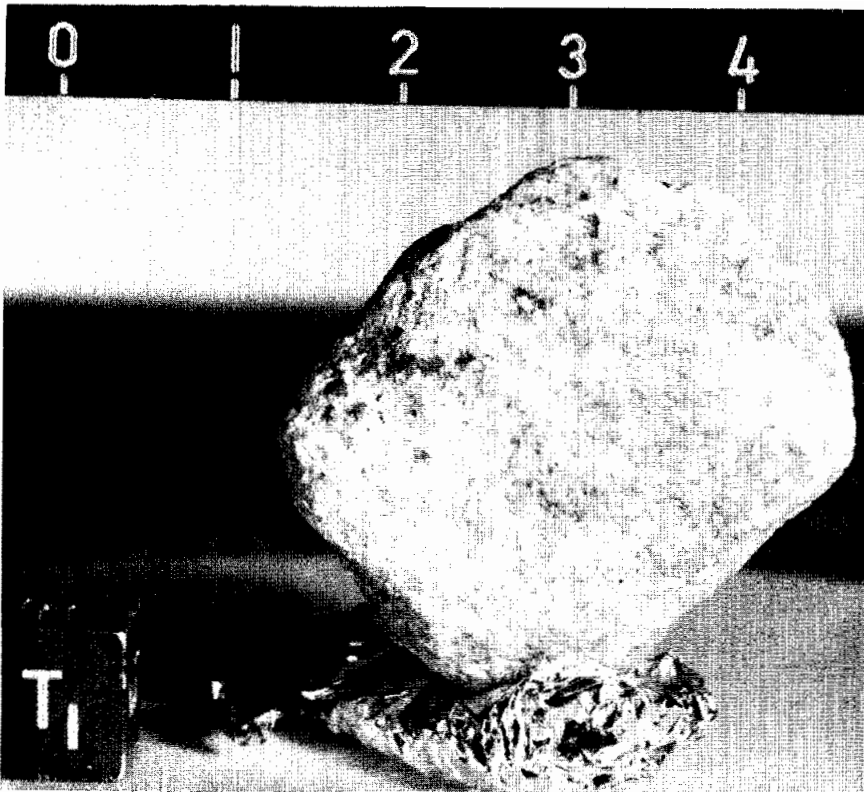


FIGURE 1.

S-72-43473. Scale in cm.

PETROLOGY:   Petrographic descriptions are given by Dowty et al. (1974a) and Warner et al. (1976b).  Accurate electron microprobe analyses of Na, Fe, Mg and K in 60619 plagioclases are given by Hansen et al. (1979a).

The granoblastic texture (Fig. 2) of 60619 is indicative of extensive recrystallization.  Small (<0.2 mm), anhedral grains of plagioclase have smooth boundaries and meet in triple junctions.  Anhedral mafic minerals occur (i) in these triple junctions, (ii) as inclusions in plagioclase, and (iii) as somewhat larger grains partially enclosing some plagioclase.  Mineral compositions are shown in Figure 3 and tabulated in Dowty et al. (1976).

FIGURE 2. 60619,2.
granoblastic anorth-
osite, partly xpl.
width 3mm.
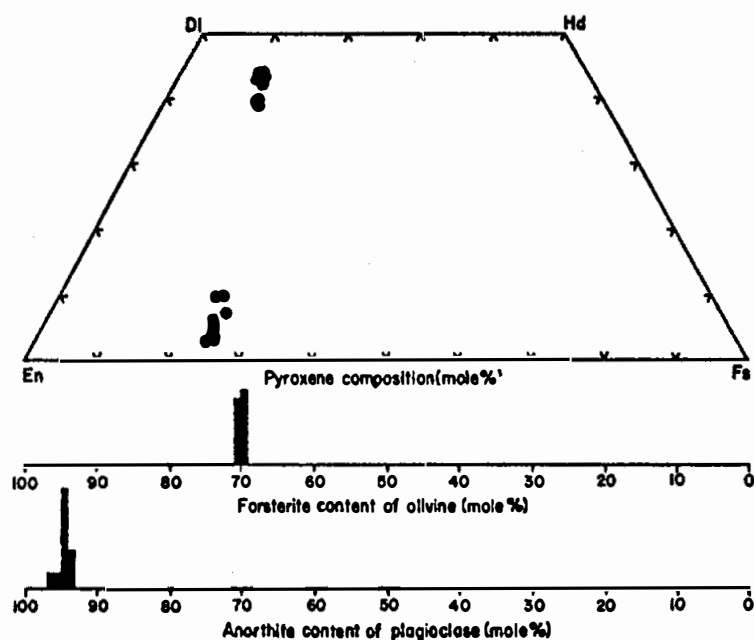


Figure 3. Mineral compositions,
from R. Warner et al. (1976b).

TABLE 1. Chemistry of 60619 (DBA)

| | |
|---|---|
| $SiO_2$ | 44.6 |
| $TiO_2$ | 0.06 |
| $Al_2O_3$ | 32.9 |
| $Cr_2O_3$ | 0.01 |
| FeO | 1.20 |
| MnO | 0.01 |
| MgO | 1.68 |
| CaO | 17.8 |
| $Na_2O$ | 0.63 |
| $K_2O$ | 0.04 |
| $P_2O_5$ | 0.03 |

CHEMISTRY: A defocussed electron beam analysis (DBA) is presented by Dowty et al. (1974a) and reproduced in Warner et al. (1976b) and here as Table 1.

PROCESSING AND SUBDIVISIONS: In 1973 two small chips (,1) were taken for thin sections (Fig. 1).

INTRODUCTION:  60625 is a light gray poikilitic rake sample with rusty patches.
It is fairly friable, rounded and covered with zap pits (Fig. 1).  Because it is
a rake sample, its orientation is unknown.  It was collected about 70 m west-
southwest of the Lunar Module.

## 60625, 0

S-72-43465

1 cm
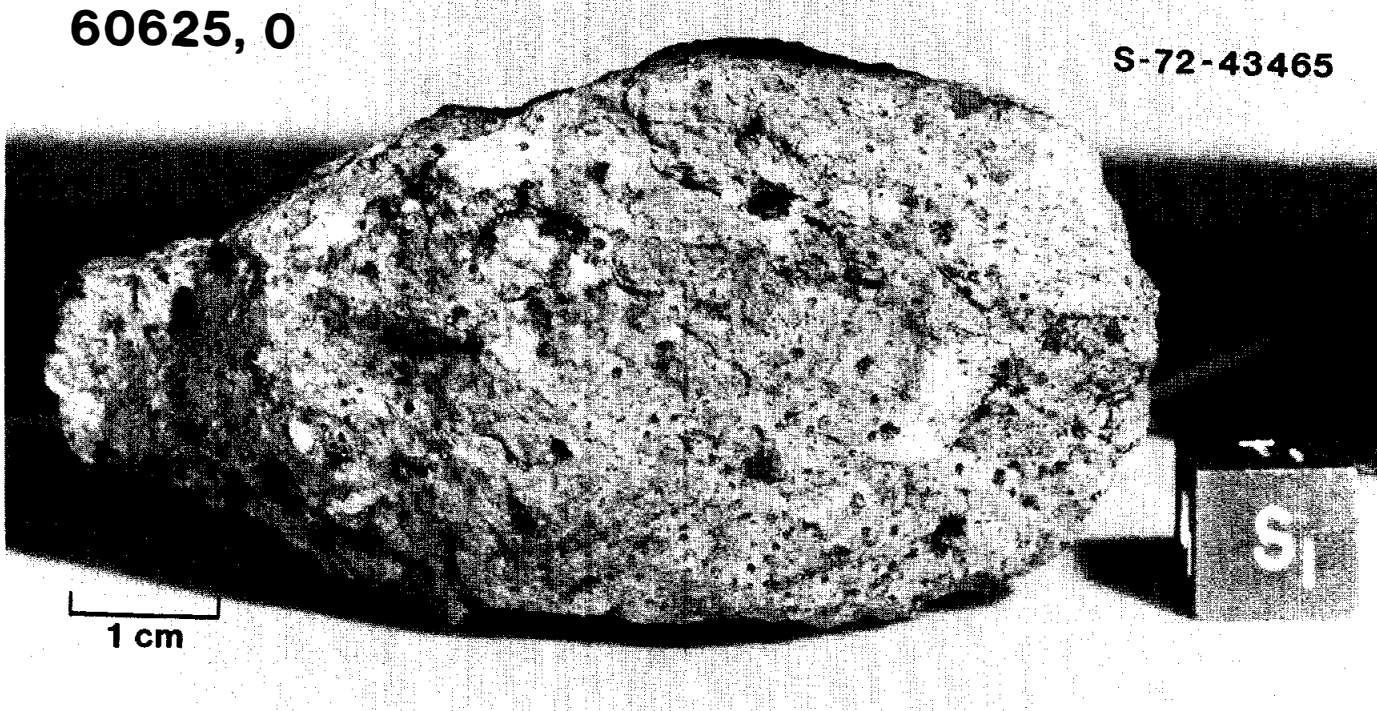
FIGURE 1.

PETROLOGY:  Mineral analyses and a brief petrographic description are provided by
Warner et al. (1976b).  60625 was listed as a rusty rock by L.A. Taylor et al.
(1973b).

60625 has a poikilitic texture (Fig. 2)  with most oikocrysts (mafic minerals) about
500 μm long and slightly elongated.  The oikocrysts enclose lathy plagioclase
chadacrysts (Fig. 2).   The overall texture is diffuse because the oikocrysts also
contain abundant glassy or cryptocrystalline areas, unlike the better-studied
poikilitic rocks such as 60315.  The interoikocryst areas are extremely narrow and
contain opaque minerals, plagioclase and glass.  Analyses of pyroxenes, olivines,
and plagioclases are summarized in Figure 3.   Warner et al. (1976b) also present
compositional data for ilmenite (∿9% MgO), armalcolite (∿9% MgO, ∿2% $ZrO_2$), Fe-
metal (∿0.45% Co, 3-10% Ni) and K-rich phases (8-14% $K_2O$).  A few lithic and
plagioclase clasts are present, most of which are shocked; mafic mineral clasts are
rare.

134
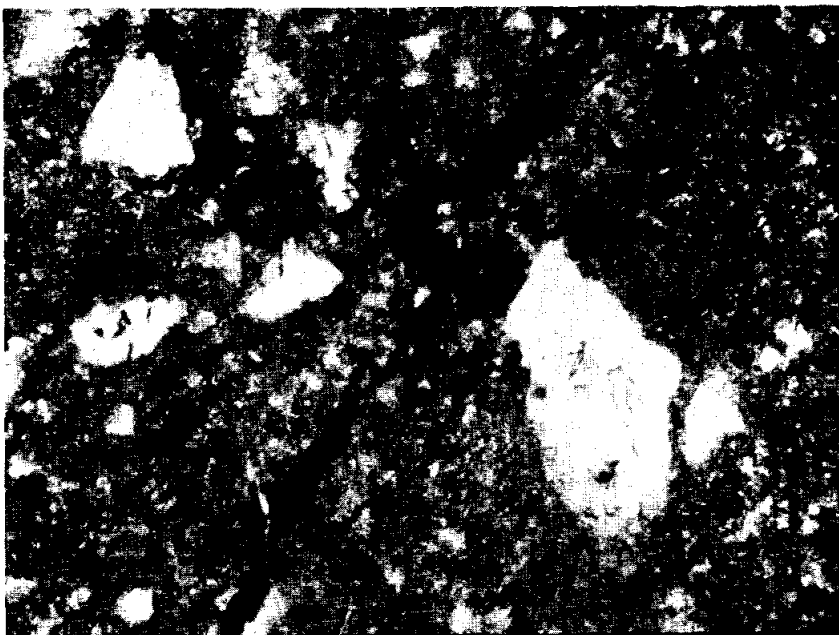
FIGURE 2. 60625,11.
general view, ppl.
width 3mm.



FIGURE 3. Mineral compositions; from R. Warner
et al.(1976b).

135

60625
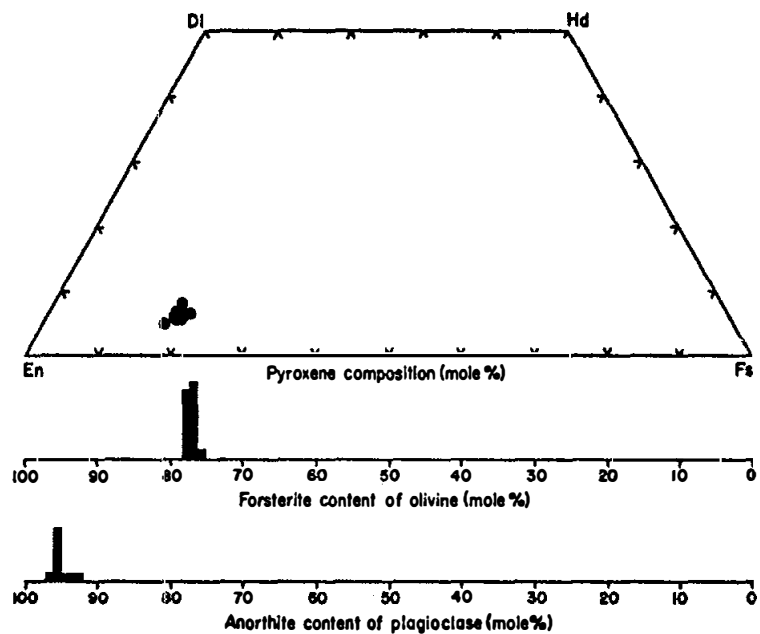
CHEMISTRY: Fruchter et al. (1974) present a partial major and trace element analysis without comment, and Warner et al. (1976b) present a defocussed beam analysis. These are summarized in Table 1.

TABLE 1.  Summary chemistry of 60625 poikilitic melt

|  | (i) | (ii) |
|---|---|---|
| $SiO_2$ |  | 44.7 |
| $TiO_2$ |  | 0.67 |
| $Al_2O_3$ | 25.9 | 22.6 |
| $Cr_2O_3$ | 0.12 | 0.11 |
| FeO | 5.4 | 7.8 |
| MnO |  | 0.06 |
| MgO |  | 9.8 |
| CaO |  | 13.2 |
| $Na_2O$ | 0.49 | 0.54 |
| $K_2O$ |  | 0.21 |
| $P_2O_5$ |  | 0.25 |
| Sr |  |  |
| La | 20.7 |  |
| Lu | 1.0 |  |
| Rb |  |  |
| Sc | 9.7 |  |
| Ni |  |  |
| Co | 27.0 |  |
| Ir ppb |  |  |
| Au ppb |  |  |

Oxides in wt%; others in ppm except as noted.
(i) from Fruchter et al. (1974).  (ii) DBA from Warner et al. (1976b).

PROCESSING AND SUBDIVISIONS: Only a few small pieces have fallen from or been separated from the parent ,0.

INTRODUCTION:   60626 is a light gray, coherent, poikilitic rock that has been extensively fractured.  Veins of dark glass cut the rock (Fig. 1).  It is a rake sample collected about 70 m west southwest of the Lunar Module.  It has zap pits which are heterogeneously distributed.

PETROLOGY:   Warner et al. (1976b) provide a brief petrographic description and mineral compositions.  60626 is poikilitic with irregularly shaped oikocrysts of dominantly low-Ca pyroxene.  Unlike most Apollo 16 poikilitic impact melts the plagioclase chadacrysts are anhedral and equant.  Clasts of plagioclase are abundant (Fig. 2).  Mineral compositions are shown in Figure 3 and tabulated by Dowty et al. (1976).  Accessory phases include titaniferous spinel (~21% $TiO_2$), ilmenite,and metal (1.0-1.7% Ni, 0.8% Co).

CHEMISTRY:   Major and trace element data are provided by Laul and Schmitt (1973). A defocussed electron beam analysis (DBA) is given by Warner et al. (1976b).

These data show that 60626 is much more aluminous than most Apollo 16 poikilitic impact melts, at least in part owing to its abundant clasts, and contains low levels of incompatible elements and siderophiles (Table 1).

PROCESSING AND SUBDIVISIONS:   In 1973 representative chips were allocated for petrography (,1), chemistry (,3) and Ar geochronological studies (,2).



S-73-20493
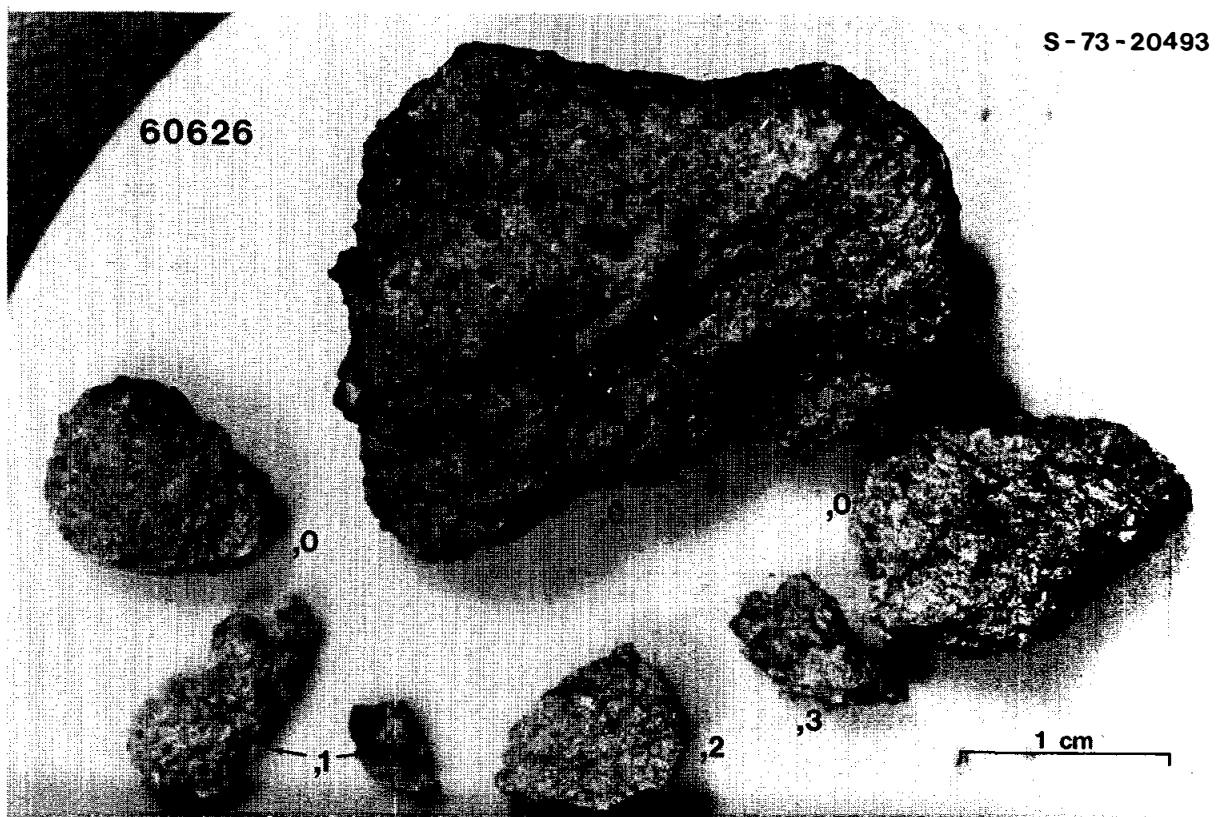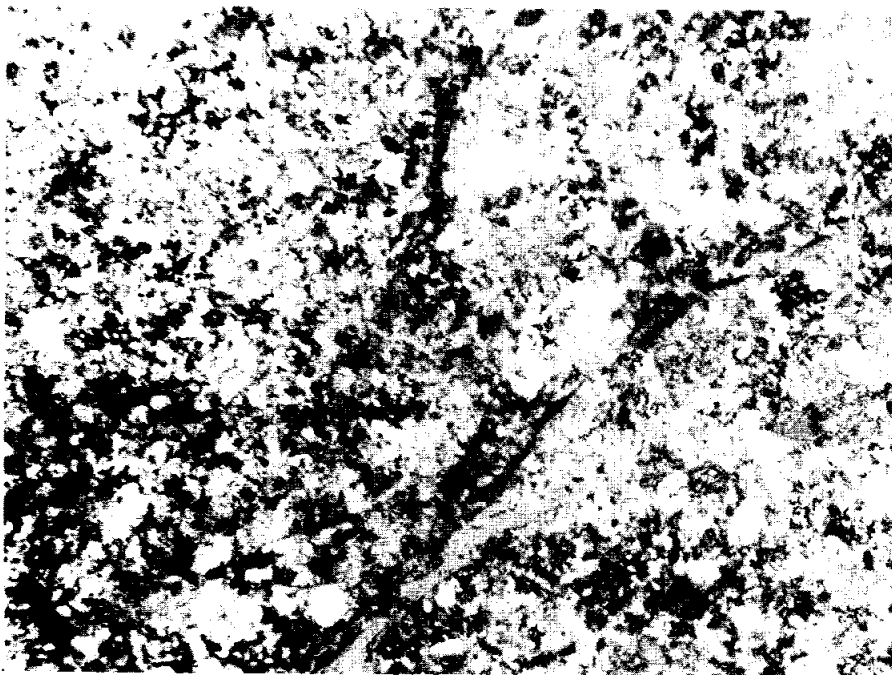
60626

FIGURE 1.

FIGURE 2. 60626,5.
general view, ppl.
width 3mm.



FIGURE 3. Mineral compositions; from R. Warner
et al. (1976b).

TABLE 1.  Summary chemistry of 60626
(mainly Laul and Schmitt, 1973)

| | |
|---|---|
| $SiO_2$ | 45.3 |
| $TiO_2$ | 0.35 |
| $Al_2O_3$ | 29.4 |
| $Cr_2O_3$ | 0.096 |
| FeO | 4.4 |
| MnO | 0.061 |
| MgO | 3.3 |
| CaO | 16.7 |
| $Na_2O$ | 0.444 |
| $K_2O$ | 0.10 |
| $P_2O_5$ | 0.04 |
| Sr | |
| La | 2.1 |
| Lu | 0.14 |
| Rb | |
| Sc | 10 |
| Ni | 30 |
| Co | 14 |
| Ir ppb | |
| Au ppb | |
| C | |
| N | |
| S | |
| Zn | |
| Cu | |
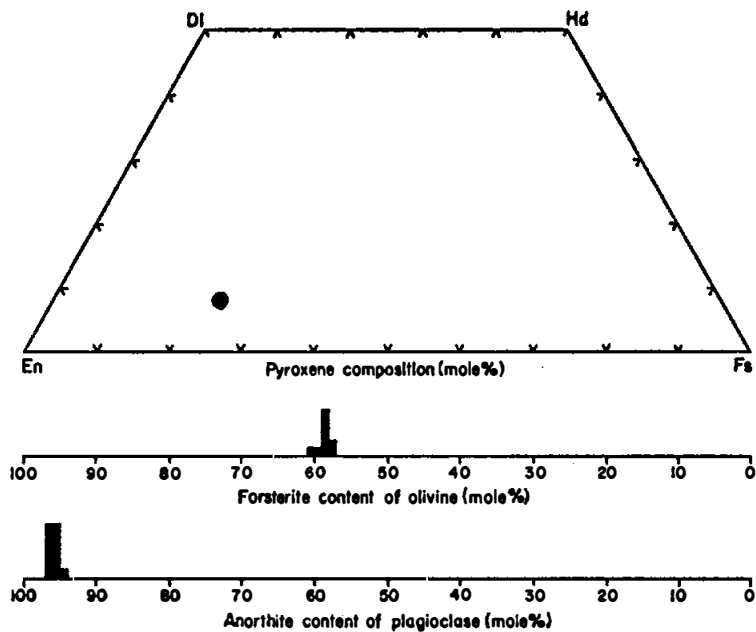
Oxides in wt%, others in ppm except as noted.

INTRODUCTION:  60627 is a light gray, coherent, impact melt with a very fine grain size (Fig. 1).  A few patches of dark splash glass are present on the surface of the smooth, sub-rounded sample.  It is a rake sample collected about 70 m west southwest of the Lunar Module.  Zap pits are abundant.



FIGURE 1. Small scale divisions in mm.

INTRODUCTION:  60628 is a white anorthosite of variable coherence (Fig. 1).  It
is subangular with a crushed appearance.  Plagioclase is of variable grain size
and ranges from clear to milky white.  A small amount of light colored splash
glass occurs on one surface; many zap pits also occur on this surface.  It is a
rake sample collected about 70 m west southwest of the Lunar Module.



FIGURE 1. Small scale
division in mm.
S-72-46822

INTRODUCTION:   60629 is a white, coherent, cataclastic anorthosite with a partial coating of dark glass (Fig. 1).  It is a rake sample collected about 70 m west southwest of the Lunar Module.  Many zap pits are present on all surfaces.



FIGURE 1.

PETROLOGY:  Petrographic descriptions are provided by Dowty et al. (1974a) and Warner et al. (1976b).   Angular clasts of plagioclase (up to 3 mm long, mostly <0.3 mm) rest in a granulated matrix which is also dominantly plagioclase (Fig.2).  Mafic minerals tend to occur as discrete grains in the matrix.  Mineral compositions are shown in Figure 3 and tabulated by Dowty et al. (1976).  Fe-metal is an accessory phase; the single analyzed grain has 5.17% Ni and 0.43% Co (Warner et al., 1976b).

CHEMISTRY:A defocussed electron beam analysis (DBA) is given by Dowty et al. (1974a) and reproduced by Warner et al. (1976b)  and here as Table 1.

141
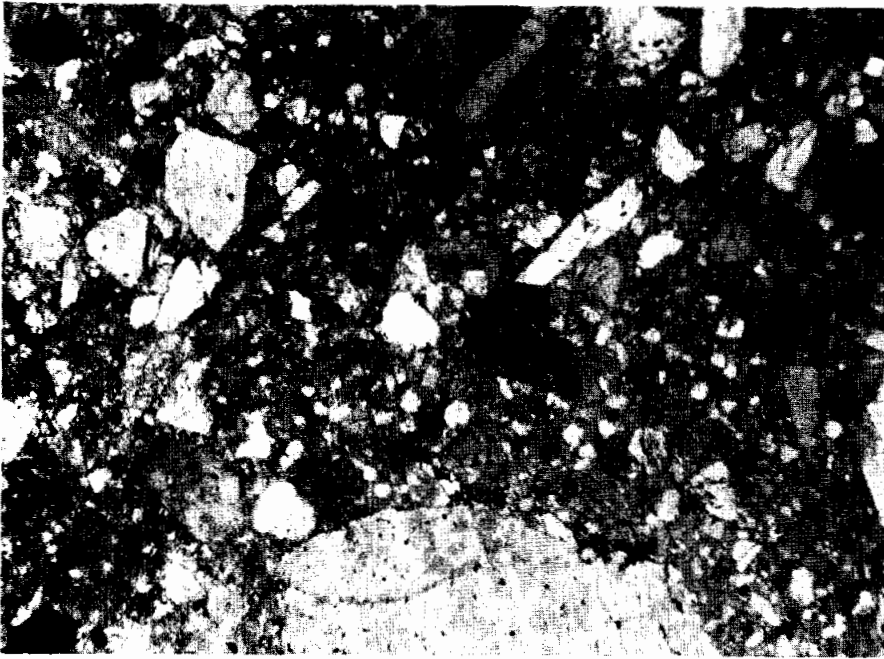
FIGURE 2. 60629,2.
general view, partly
xpl. width 3mm.



FIGURE 3. Mineral compositions; from R. Warner
et al. (1976b).
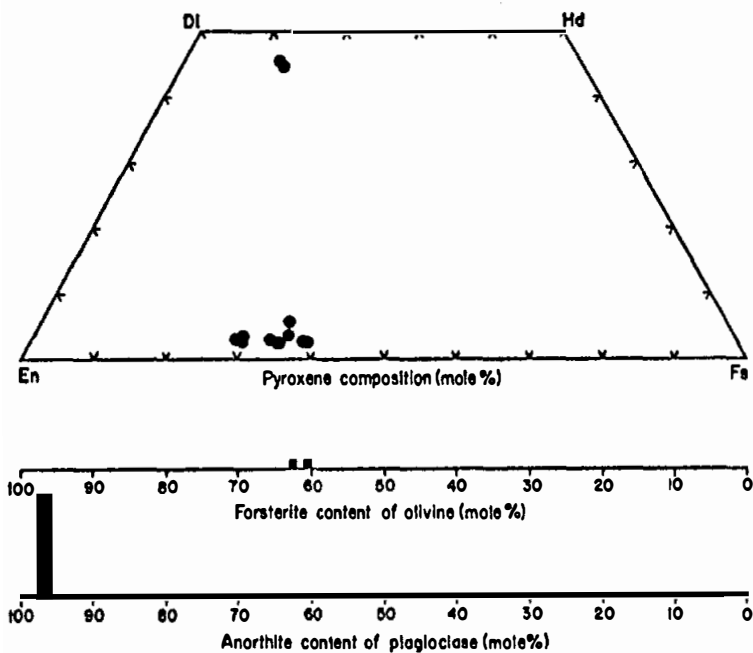
TABLE 1.  Chemistry of 60629
(DBA, normalized to 100%)

| | |
|---|---|
| $SiO_2$ | 44.6 |
| $TiO_2$ | 0.01 |
| $Al_2O_3$ | 35.1 |
| FeO | 0.36 |
| MgO | 0.26 |
| CaO | 19.2 |
| $Na_2O$ | 0.41 |
| $K_2O$ | 0.02 |
| $P_2O_5$ | 0.03 |

PROCESSING AND SUBDIVISIONS: In 1973 a chip of the anorthosite (,1) was taken
for thin sections.  During this processing a portion of the glass coat fell
off but has been kept with ,0 (Fig.1).

INTRODUCTION:   60635 is a medium gray, coherent, coarse-grained, basaltic impact melt (Fig. 1).   Vugs and vesicles are abundant.   It is a rake sample collected about 70 m west southwest of the Lunar Module.   Zap pits are rare.
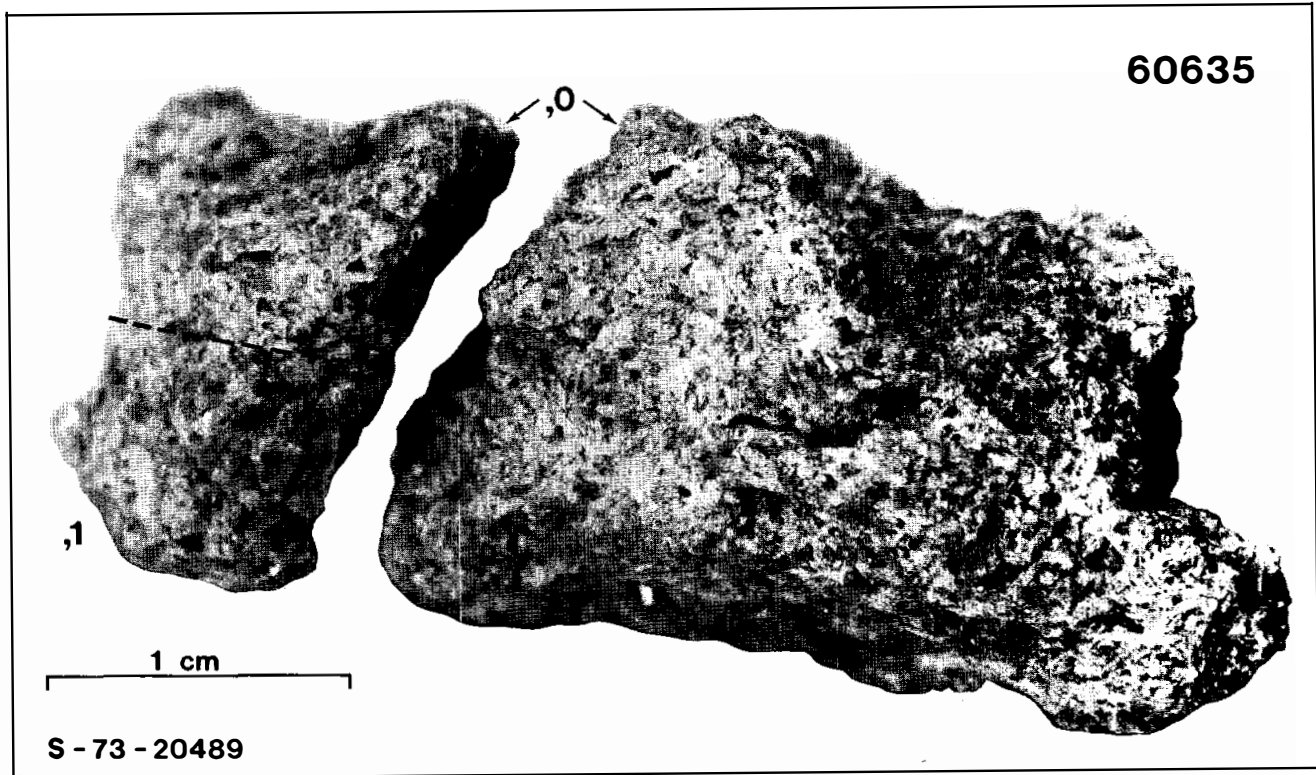


FIGURE 1.



FIGURE 2. 60635,2. general view, partly ppl. width 3mm.
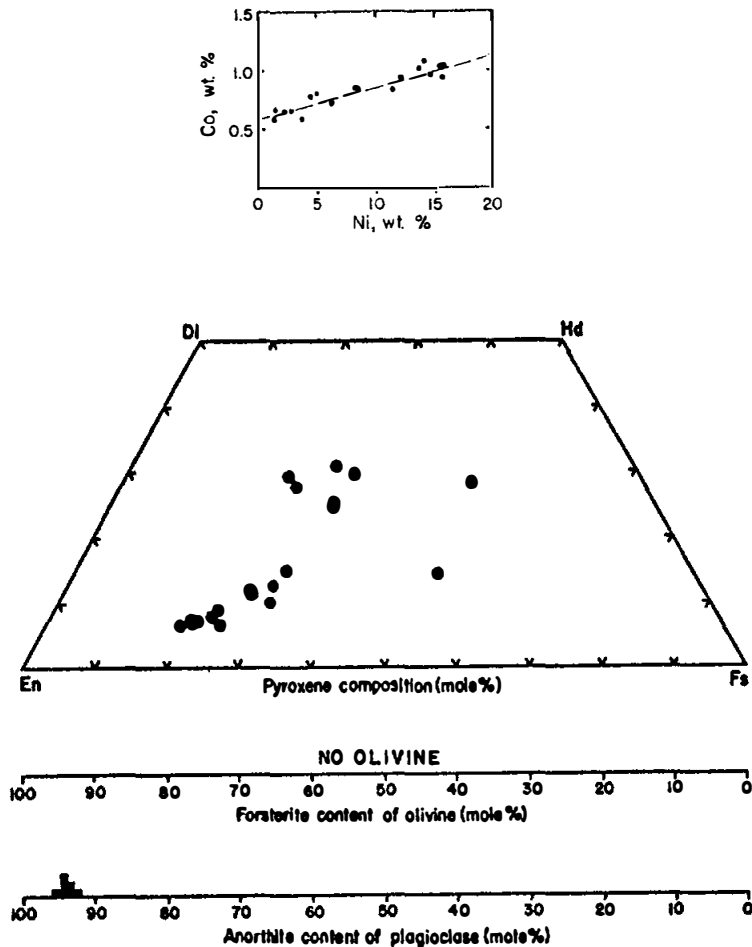
| | |
|---|---|
| $SiO_2$ | 45.8 |
| $TiO_2$ | 0.34 |
| $Al_2O_3$ | 27.6 |
| $Cr_2O_3$ | 0.07 |
| FeO | 4.7 |
| MnO | 0.04 |
| MgO | 4.1 |
| CaO | 15.8 |
| $Na_2O$ | 0.54 |
| $K_2O$ | 0.09 |
| $P_2O_5$ | 0.09 |

FIGURE 3. Mineral compositions; metals from Dowty et al. (1974b), silicates from R. Warner et al. (1976b).

PETROLOGY: Dowty et al. (1974b) and Warner et al. (1976b) provide petrographic descriptions. This is a coarse-grained rock with abundant phenocrystic laths and prisms of plagioclase (0.6-2.5 mm long) and smaller grains of plagioclase and pyroxene confined to interstices (Fig. 2). Olivine is absent and clasts are very rare. Mineral compositions are shown in Figure 3 and tabulated by Dowty et al. (1976). Minor phases include nearly pure ulvöspinel, Fe-metal, troilite and K-feldspar.

CHEMISTRY: A defocussed electron beam analysis (DBA) is presented by Dowty et al. (1974b) and reproduced by Warner et al. (1976b) and here as Table 1.

This analysis shows 60635 to be compositionally similar to local mature soils but with a higher Fe/Mg and lower $TiO_2$.

PROCESSING AND SUBDIVISIONS: During initial processing at JSC 60635 fell into two pieces. In 1973 a single chip (,1) was removed and allocated to Keil for petrography.

INTRODUCTION:  60636 is a medium gray, coherent impact melt with many crystal-
lined vugs (Fig. 1).  Some splash glass is present.  It is a rake sample collected
about 70 m west southwest of the Lunar Module.  Zap pits are rare.



FIGURE 1.

FIGURE 2. 60636,6. general view, partly ppl. width 2mm.
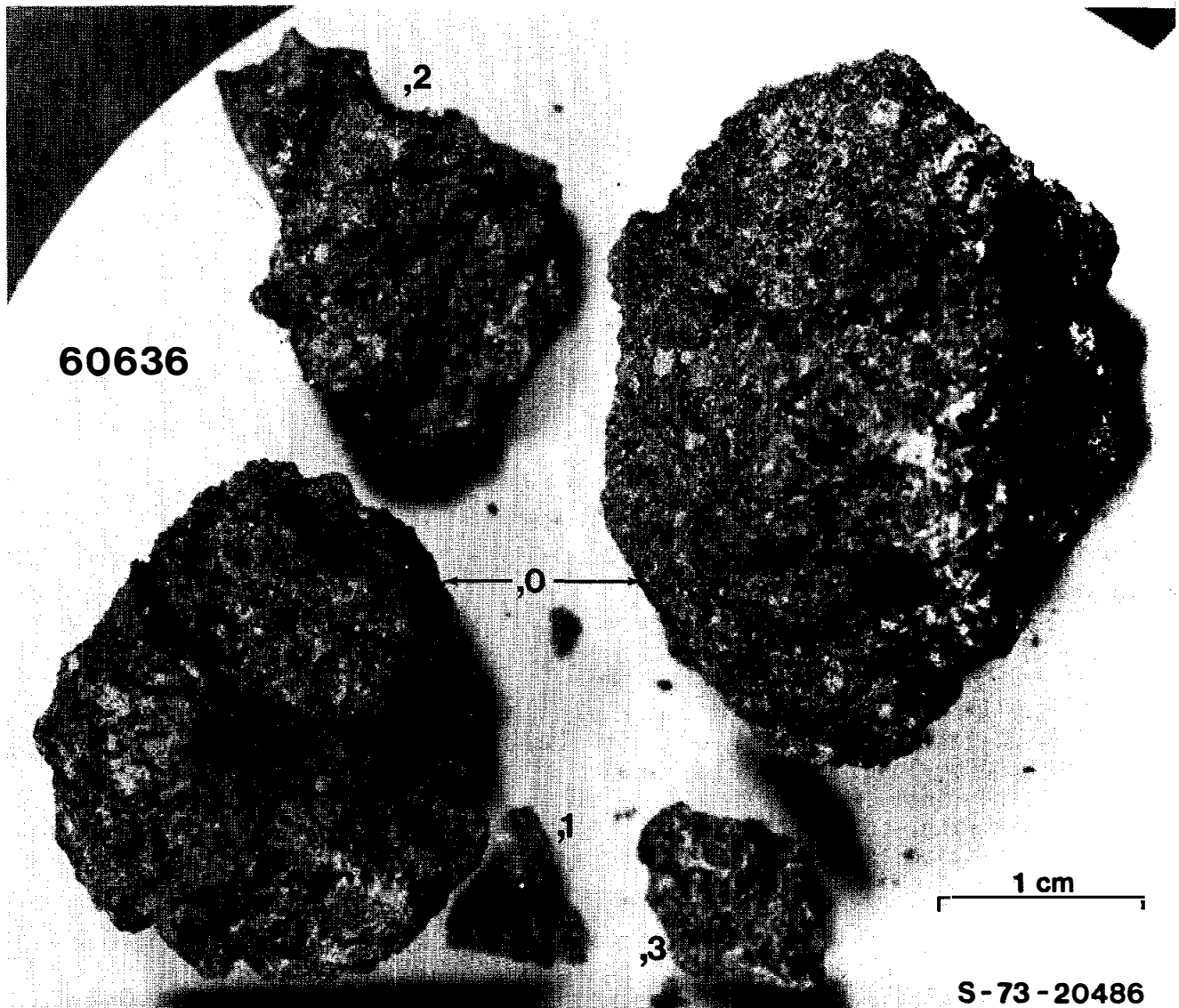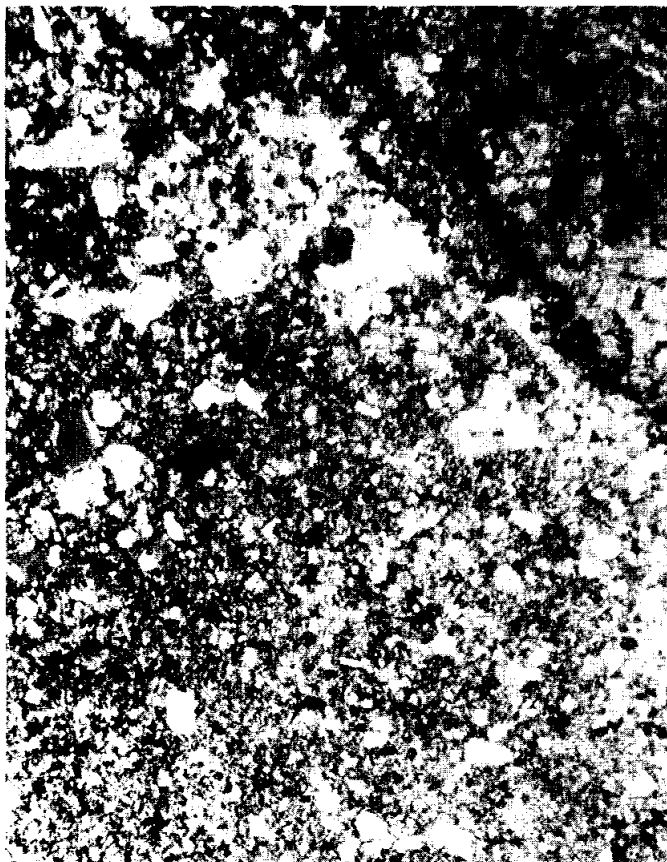
TABLE 1. Chemistry of 60636 (DBA)

| | |
|---|---|
| $SiO_2$ | 48.0 |
| $TiO_2$ | 0.93 |
| $Al_2O_3$ | 24.2 |
| $Cr_2O_3$ | 0.11 |
| FeO | 6.2 |
| MnO | 0.07 |
| MgO | 6.1 |
| CaO | 13.9 |
| $Na_2O$ | 0.79 |
| $K_2O$ | 0.73 |
| $P_2O_5$ | 0.40 |

PETROLOGY: A brief petrographic description is given by Warner et al. (1976b). 60636 is a clast-laden impact melt with tablet-shaped plagioclase grains (0.01 - 0.02 mm long) enclosed by subophitic to poikilitic pyroxene (Fig.2). Clasts of plagioclase and subordinate olivine are abundant. One fragment of plagioclase-rich, poikilitic breccia is noted by Warner et al. (1976b). Matrix and clast plagioclase grains are slightly rounded suggesting minor recrystallization or resorption.

CHEMISTRY: A defocussed electron beam analysis (DBA) is presented by Warner et al. (1976b) and reproduced here as Table 1. U, Th, and Pb data are provided by Tera et al. (1974) in a geochronological study. 60636 has very high levels of incompatible elements (Table 1).

GEOCHRONOLOGY: U, Th and Pb isotopic data are presented by Tera et al. (1974). These data are within error of concordia at $\sim$ 3.94 b.y. Virtually all of the radiogenic lead in 60636 has been produced by in situ decay, yielding model ages of 3.91 - 3.95 b.y.

PROCESSING AND SUBDIVISIONS: In 1972 representative chips were allocated for petrography (,1), chemistry (,3) and radiogenic isotope studies (,2).

INTRODUCTION: 60637 is a brownish gray, polymict breccia of variable coherence (Fig. 1). It is a rake sample collected about 70 m west southwest of the Lunar Module. Zap pits are rare.



FIGURE 1. Small scale divisions in mm.
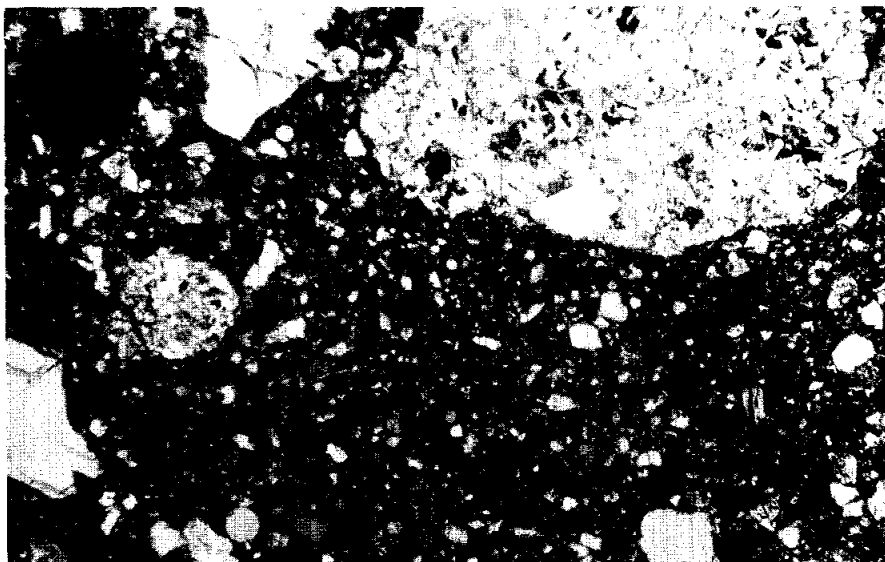


FIGURE 2. 60637,2. general view, partly ppl. width 3mm.

PETROLOGY: Warner et al. (1976b) provide a brief petrographic description. Various clasts, including a fragment of basaltic impact melt, numberous breccias and rare "chondrules," rest in a heterogeneous matrix of mineral and glass fragments welded together by a small amount of interstitial glass (Fig.2). Porosity of the matrix is high.

PROCESSING AND SUBDIVISIONS: In 1973 60637 was split into several fragments and one chip (,1) allocated for thin sections (Fig.1).

INTRODUCTION:   60638 is a brownish gray breccia of variable coherence (Fig. 1). Small white clasts are scattered through the angular sample.  It is a rake sample collected about 70 m west southwest of the Lunar Module.



FIGURE 1. Small scale divisions in mm.

INTRODUCTION:  60639 is a fragmental polymict breccia with a low porosity. A wide variety of clasts is present, a mare basalt and a pristine anorthosite (Fig. 1a) being of particular significance.  One side of the subangular rock is covered with a smooth dark glass (Fig. 1b).

The sample was a rake sample from an area 70 m west-southwest of the Lunar Module, hence its orientation is unknown.  Zap pits occur in a few areas.
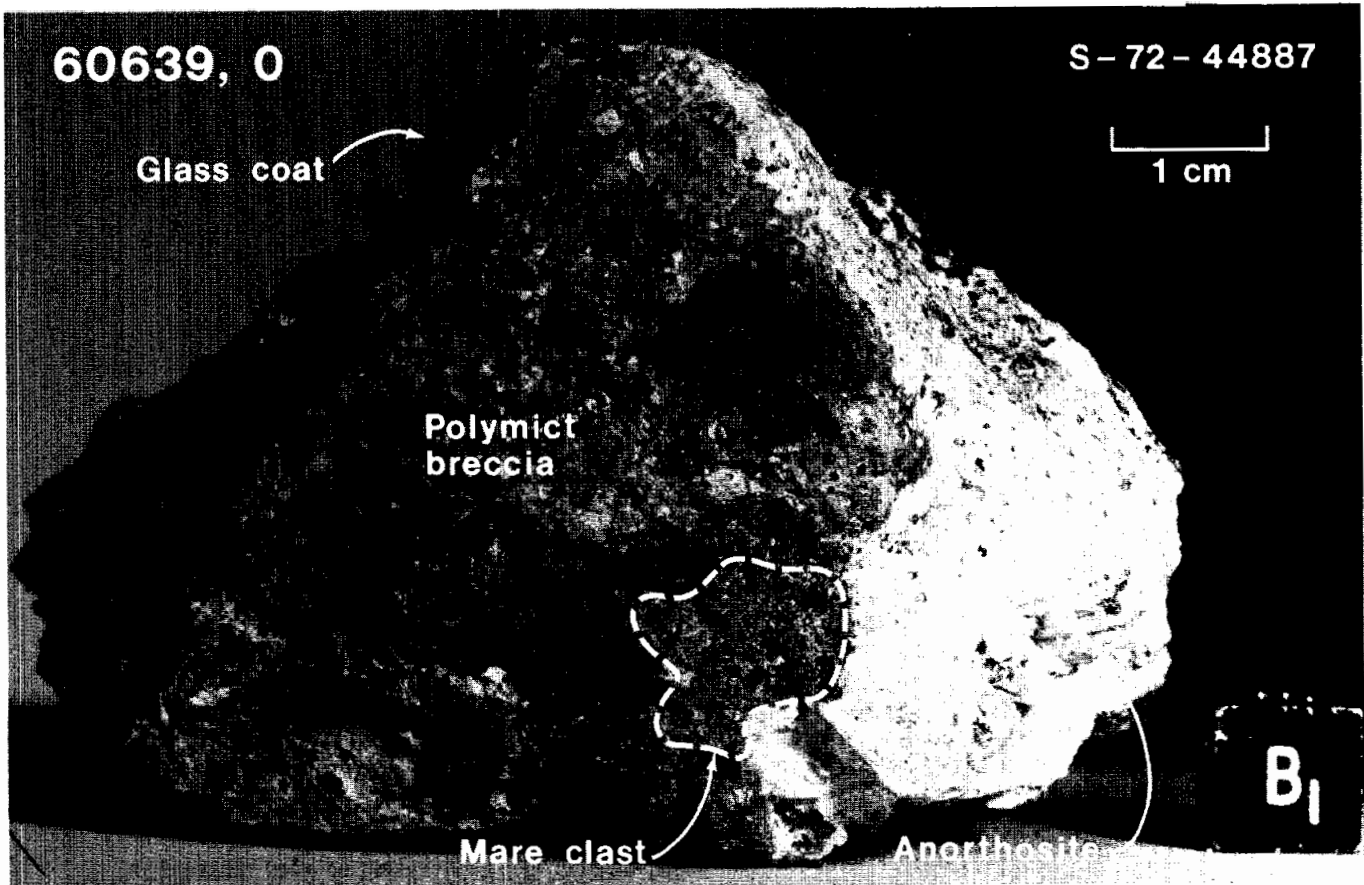


FIGURE 1a.

PETROLOGY:  The matrix is briefly described by Warner et al. (1976b).  The mare basalt clast is described, with mineral analyses, by Dowty et al. (1974b), Delano (1975) and Warner et al. (1976b).  The pristine anorthosite is briefly described, with mineral analyses, by Warren and Wasson (1978).

The matrix is fragmental (Fig. 2) with a low porosity.  Apart from the mare basalt and pristine anorthosite, lithic clasts include poikilitic, aphanitic, and glassy breccias.

## FIGURE 1b.

The <u>mare basalt</u> is subophitic,with plagioclase needles 300-500 μm long enclosed in clinopyroxene grains (Fig. 2). It contains ~5% olivine, ~35% plagioclase, ~50% pyroxene, ~5-10% ilmenite,and accessory spinels (Delano, 1975). Mineral data are shown in Figure 3. Modal mineralogy, zoning trends, and chemistry (below) are very similar to the intermediate-$TiO_2$ Luna 16 basalts.

The <u>anorthosite</u> is intensely cataclasized (Fig. 2), and consists almost entirely of plagioclase with a few tiny pyroxene grains. Mineral compositions have very narrow ranges (Warren and Wasson, 1978): plagioclases $An_{96.0-96.8}$; pyroxenes $En_{64-66} Wo_{1-2}$ and ~$En_{42} Wo_{43}$. Some other pyroxenes are incompletely exsolved pigeonites. These mineral compositions are typical of ferroan anorthosites.

a
b
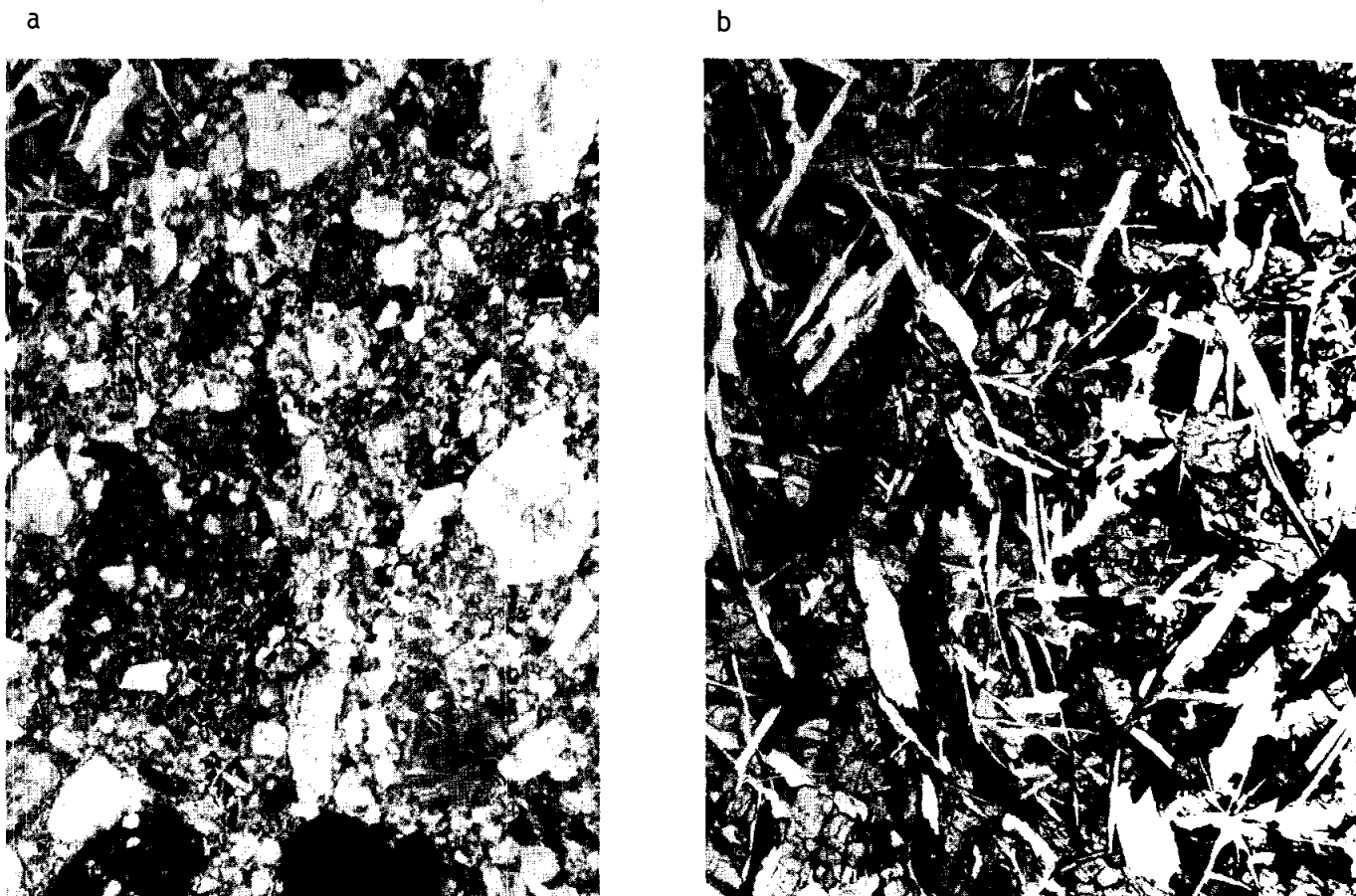
FIGURE 2. 60639,2. a) general view, partly ppl. width 2mm. b) mare basalt clast, partly ppl. width 2mm.
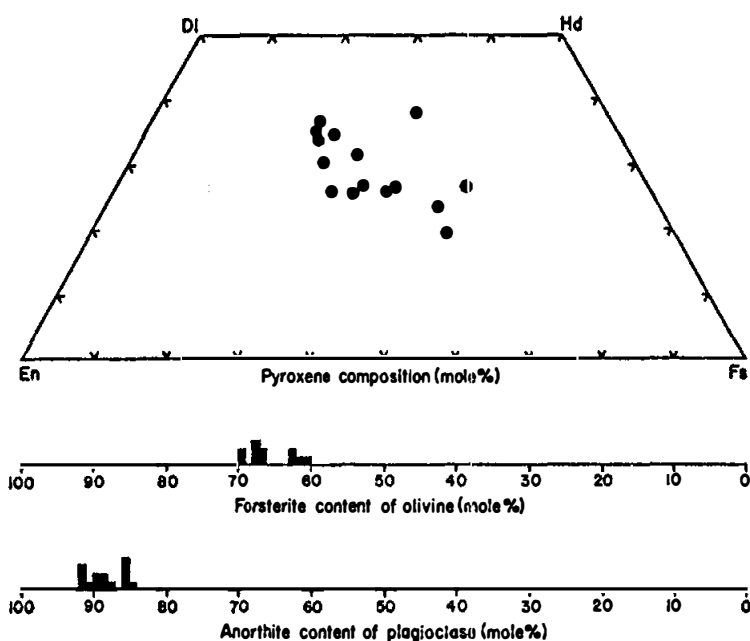


FIGURE 3a. Minerals in mare basalt clast; from R. Warner et al. (1976b).
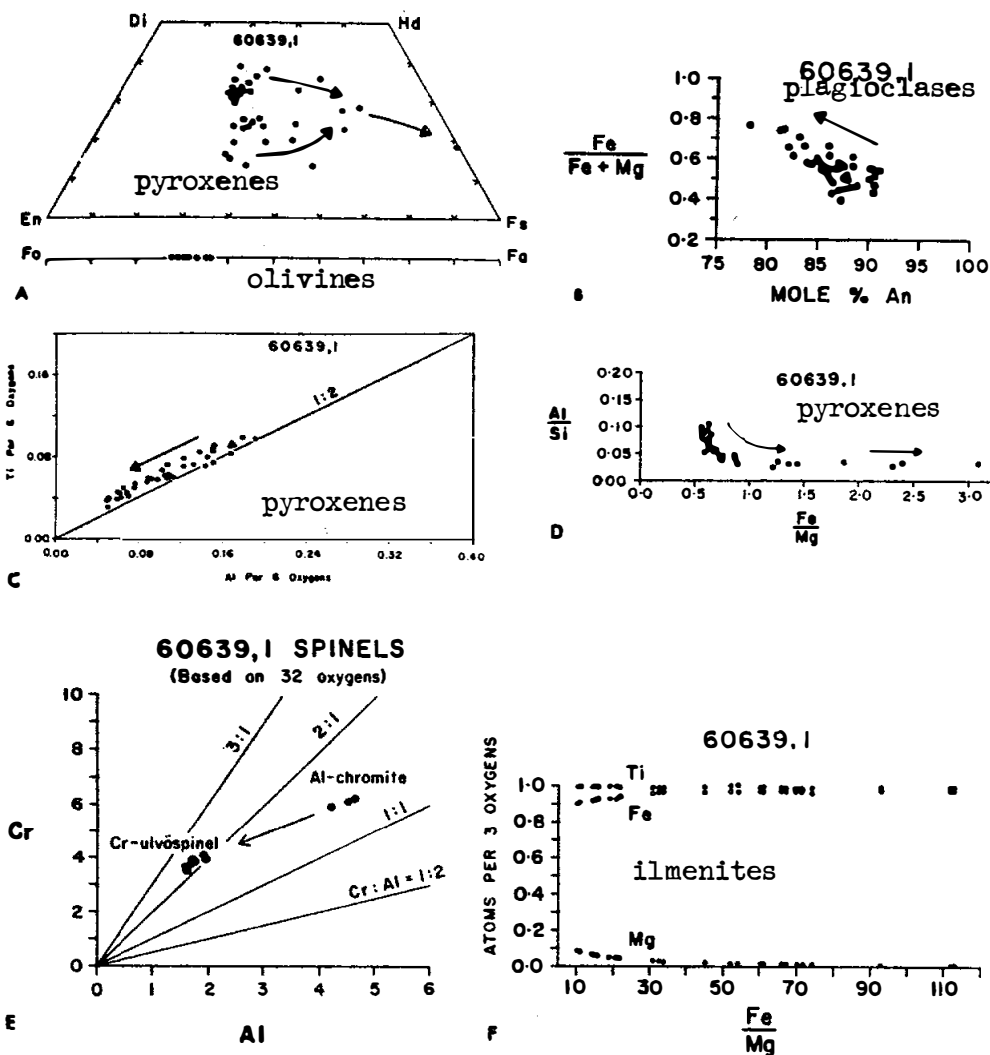
**FIGURE 3b**. Minerals in mare basalt clast; from Delano (1975).

CHEMISTRY: No matrix analyses are available. Data for the mare basalt (Murali et al., 1976; DBA in Warner et al., 1976b) and the anorthosite (Warren and Wasson, 1978) are summarized in Table 1.

The mare basalt is an intermediate-$TiO_2$, high-alumina basalt very similar to the Luna 16 mare basalts. The anorthosite is chemically pristine as shown by its low siderophiles, and is extremely low in mafic components and incompatible elements.

### TABLE 1

Summary chemistry of 60639 mare basalt and anorthosite clasts

|  | mare basalt | anorthosite |
|---|---|---|
| $SiO_2$ | (42) | 44.5 |
| $TiO_2$ | 7.4 | |
| $Al_2O_3$ | 12.4 | 35.1 |
| $Cr_2O_3$ | 0.30 | 0.006 |
| FeO | 20.0 | 0.34 |
| MnO | 0.25 | 0.01 |
| MgO | 6.5 | 0.35 |
| CaO | 10.6 | 19.4 |
| $Na_2O$ | 0.58 | 0.379 |
| $K_2O$ | 0.13 | |
| $P_2O_5$ | | |
| Sr | | |
| La | 15.5 | 0.11 |
| Lu | 1.8 | |
| Rb | | |
| Sc | 73 | 0.59 |
| Ni | | 0.72 |
| Co | 20 | 1.0 |
| Ir ppb | | ~0.02 |
| Au ppb | ~16 | 0.019 |
| C | | |
| N | | |
| S | | |
| Zn | | 2 |
| Cu | | |

mare basalt: Murali et al. (1976). anorthosite: Warren and Wasson (1978). Oxides in wt.%; others in ppm except as noted.

PROCESSING AND SUBDIVISIONS: No saw cuts have been made in 60639. All splits have been made by chipping and prying. Most of the original bulk of the rock (175 g) remains as ,0 (163 g).

INTRODUCTION:  60645 is a medium gray, coherent impact melt with a variable texture.  Vesicles are very abundant (Fig. 1).  It is a rake sample collected about 70 m west southwest of the Lunar Module and has rare zap pits.

PETROLOGY:  Warner et al. (1976b) provide a brief petrographic description. The matrix texture varies through very fine-grained poikilitic, subophitic, and granular (Fig. 2).  Minor amounts of a dark, cryptocrystalline mesostasis are present.  One large cataclastic anorthosite clast is noted by Warner et al. (1976b).

PROCESSING AND SUBDIVISIONS:  In 1973, three small chips were removed and allocated for thin sections as ,1 (Fig. 1).
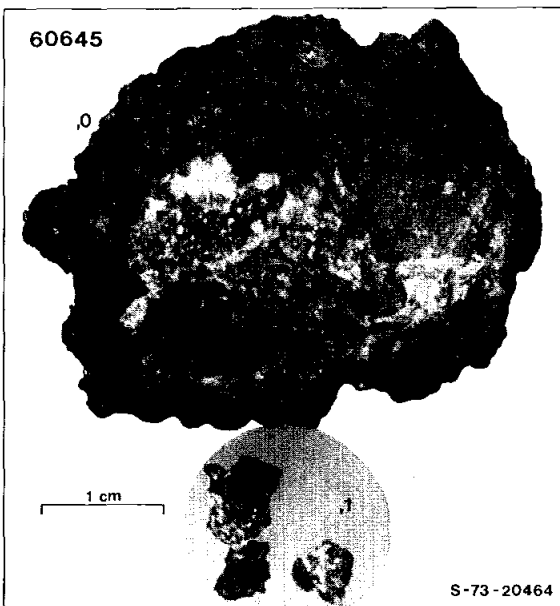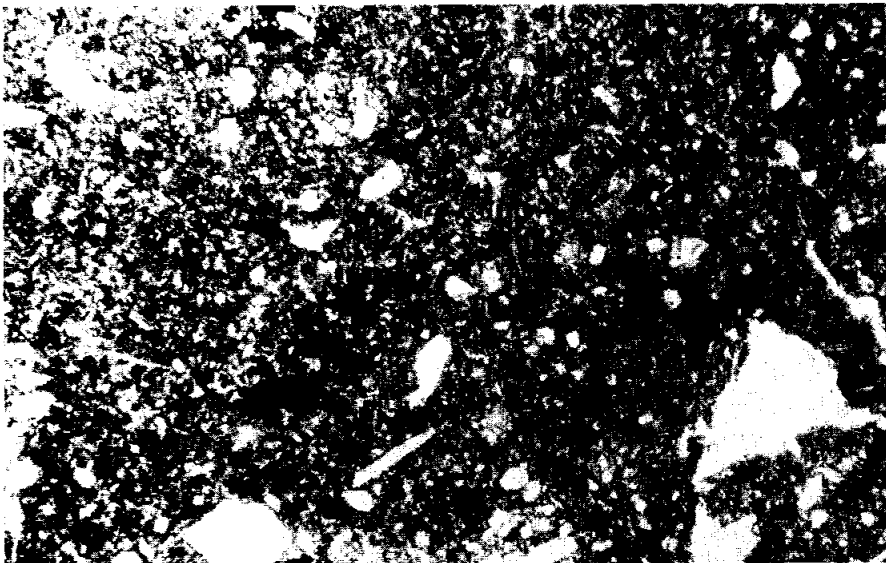


FIGURE 1.



FIGURE 2. 60645,3 general view, ppl. width 3mm.

154

INTRODUCTION:  60646 is a medium gray, coherent, glassy impact melt (Fig. 1). It is angular and highly vesicular.  A few small (<1 mm) white clasts are present.  It is a rake sample collected about 70 m west southwest of the Lunar Module and has only rare zap pits.



FIGURE 1. Small scale divisions in mm.

INTRODUCTION:  60647 is a medium gray, coherent, glassy impact melt (Fig. 1). Clasts include several white fragments (up to ∿4 mm) and a fragment of coherent, crystalline rock, probably basaltic impact melt.  It is angular and highly vesicular.  It is a rake sample collected about 70 m west southwest of the Lunar Module and has only rare zap pits.



FIGURE 1. Small scale divisions in mm.

INTRODUCTION:  60648 is a medium gray, coherent, glassy impact melt with abundant small (<3 mm) white clasts (Fig. 1).  It is angular and highly vesicular and one surface has a sheared appearance.  It is a rake sample collected about 70 m west southwest of the Lunar Module and lacks zap pits.
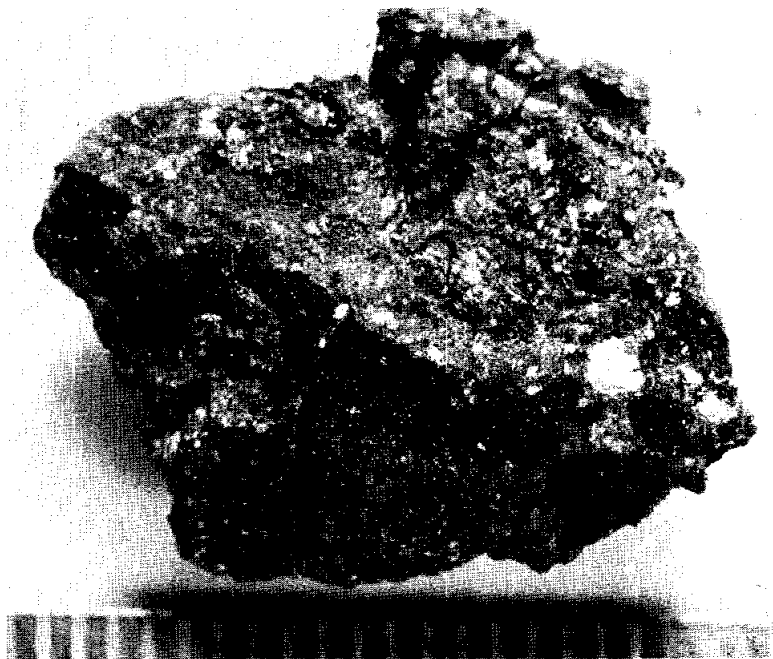


FIGURE 1. Small scale divisions in mm.

INTRODUCTION:   60649 is a medium gray, coherent, glassy breccia (Fig. 1).   Small (<1 mm) white clasts are abundant.   It is angular and slightly vesicular.   It is a rake sample collected about 70 m west southwest of the Lunar Module and lacks zap pits.
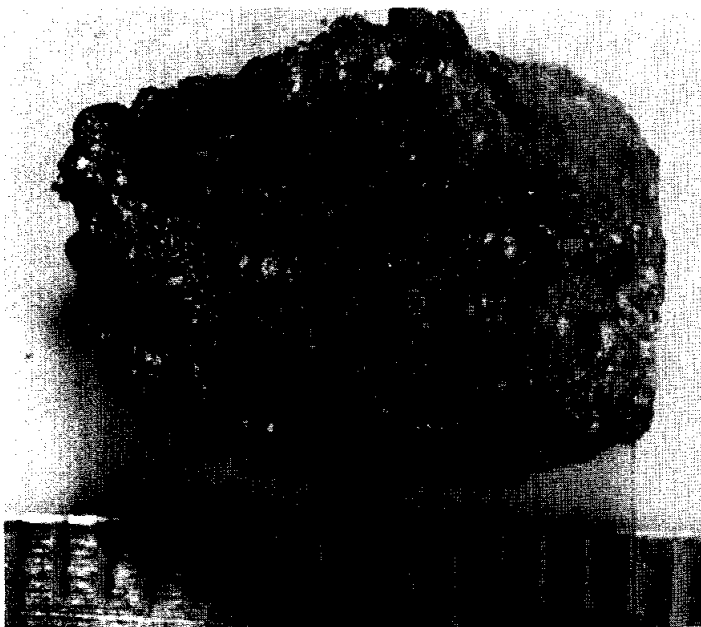


FIGURE 1. Small scale divisions in mm.

INTRODUCTION:  60655 is a medium gray, coherent, glassy impact melt (Fig. 1). Vesicles account for ~15% of the rock (Keil et al., 1972).  It is a rake sample collected about 70 m west southwest of the Lunar Module.  Zap pits are rare.

PETROLOGY:  Warner et al. (1976b) provide a brief petrographic description.  The matrix of 60655 consists of abundant glass containing angular mineral fragments (Fig. 2).  Various breccia clasts and a small number of glassy fragments are present.  Minor glassy veins intrude the matrix.

PROCESSING AND SUBDIVISIONS:  In 1973 this rock was subdivided into six pieces. One of these pieces was allocated for thin sections as ,1 and the other five grouped as ,0 (Fig. 1).



**60655**
**Post split**

**1 cm**

,1

S-73-20463
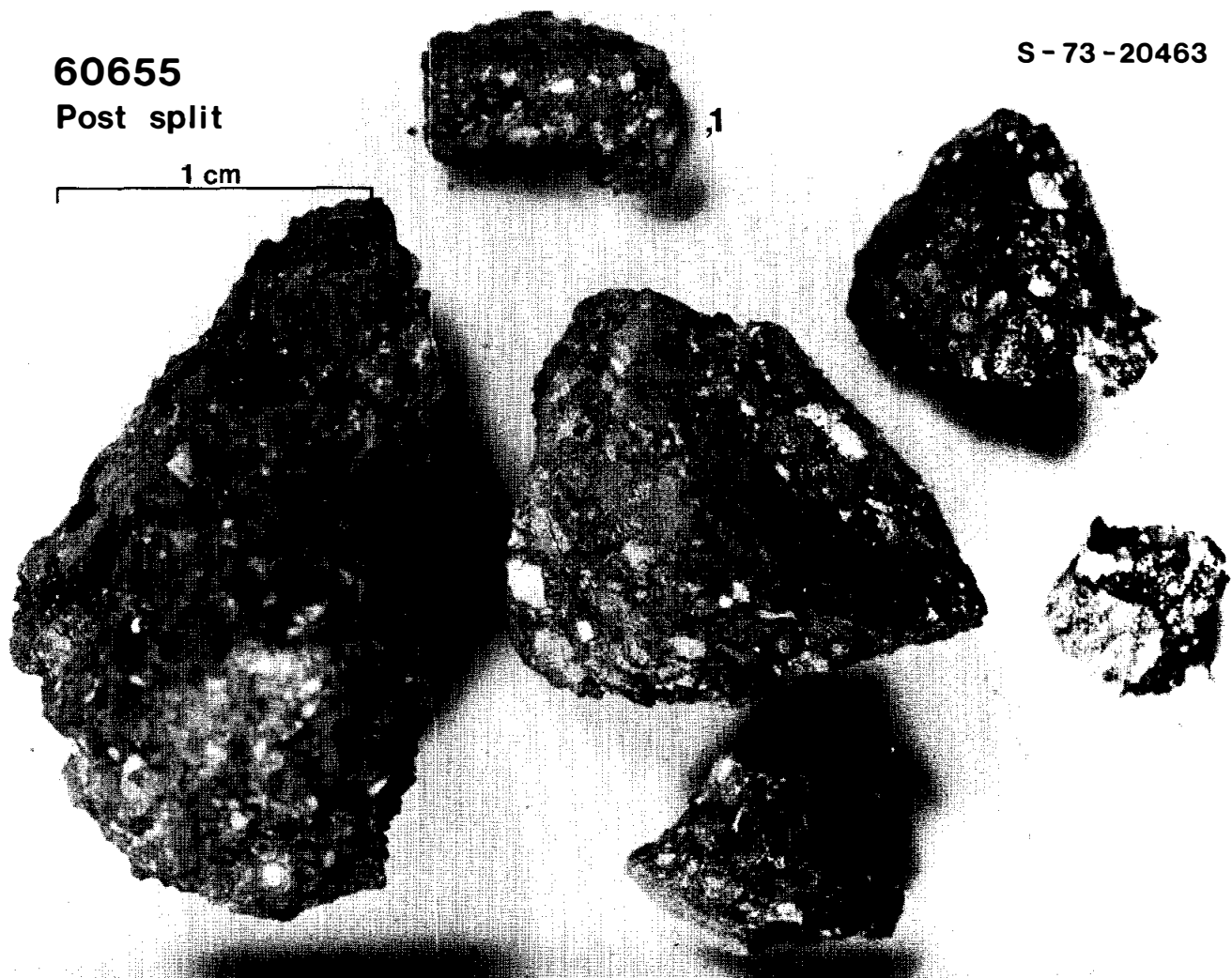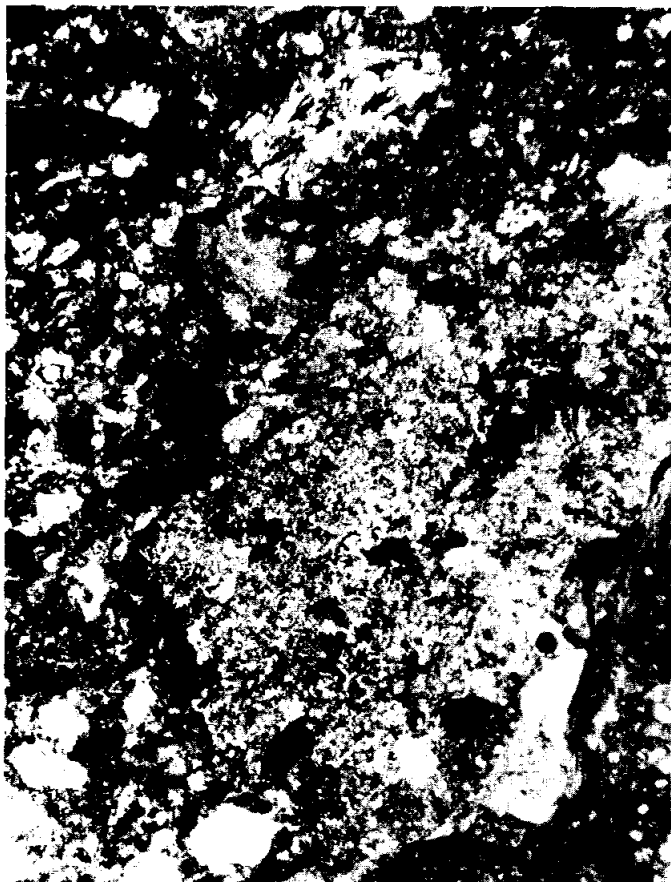
FIGURE 1.

FIGURE 2. 60655,2. general view, ppl. width 2mm.

INTRODUCTION:   60656 is a medium gray, coherent, glassy impact melt with several white clasts (Fig.1).  It is a rake sample collected about 70 m west southwest of the Lunar Module.  Zap pits are rare.

PETROLOGY: Warner et al. (1976b)  provide a brief petrographic description. Abundant mineral and lithic clasts reside in a glass-rich matrix (Fig.2).

PROCESSING AND SUBDIVISIONS: In 1973 four chips were removed from one end of the rock.  One of these chips was allocated for thin sections as ,1 (Fig.1).
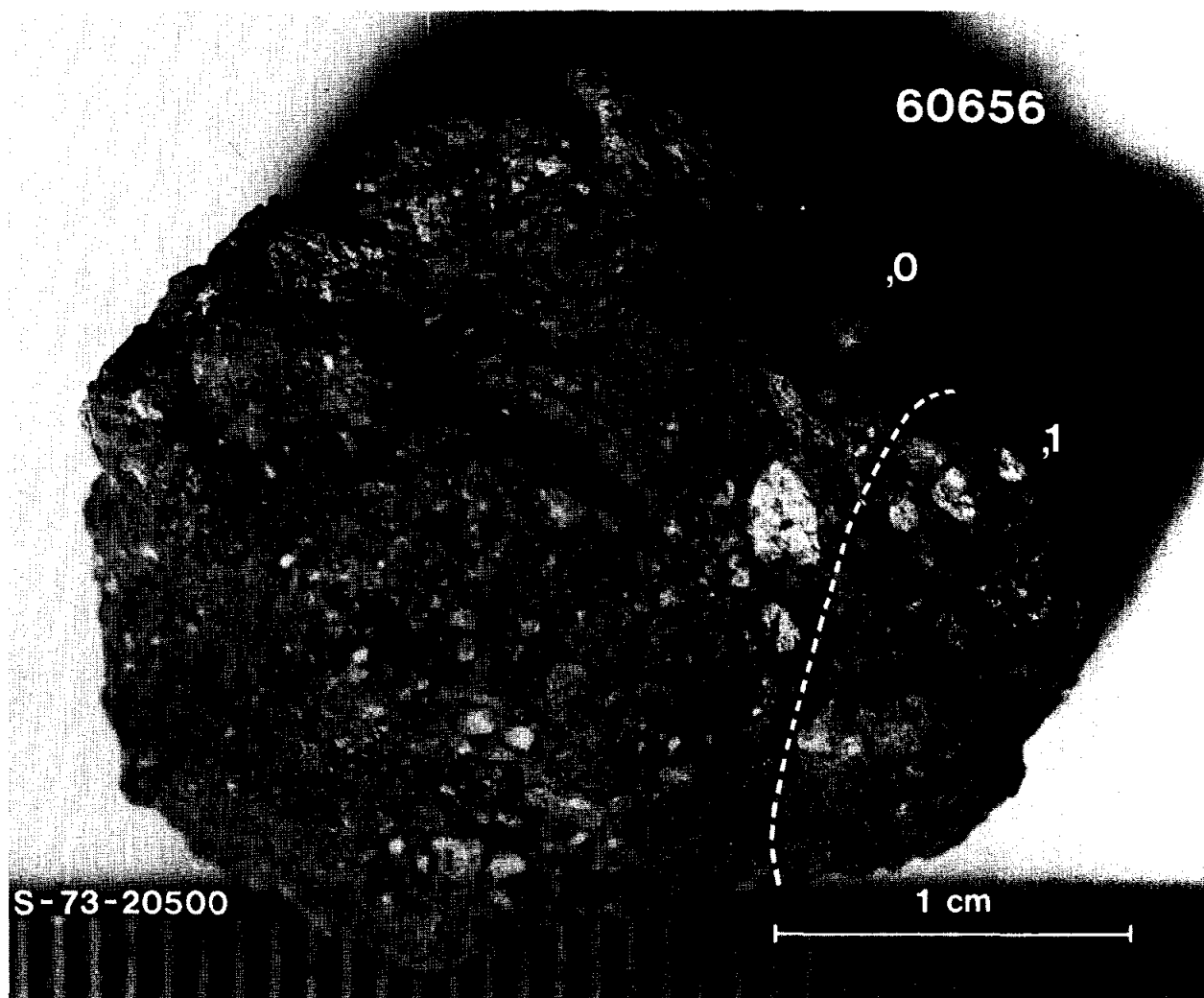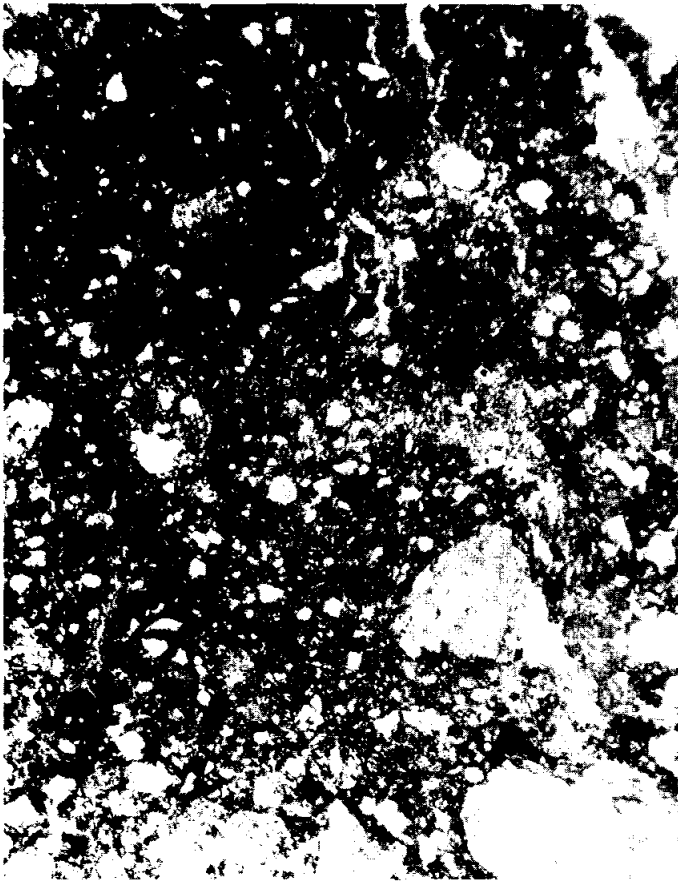


FIGURE 1.

60656



FIGURE 2. 60656,2. general
view, ppl. width 2mm.

162

INTRODUCTION:  60657 is a light gray, coherent breccia with dark, vesicular glass attached to two ends of the rock (Fig. 1).  White  anorthositic clasts are abundant in both the breccia and the glass coat.  It is a rake sample collected about 70 m west southwest of the Lunar Module.  Zap pits are rare.
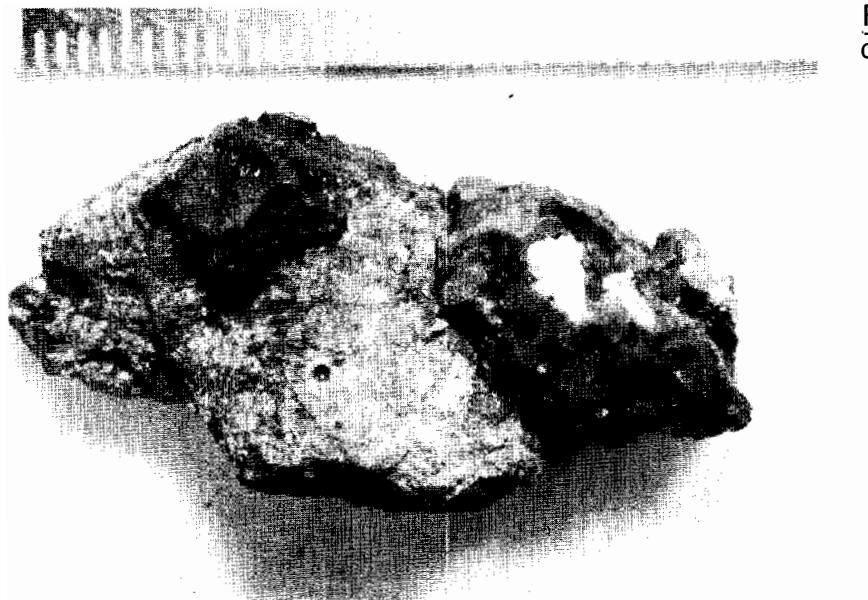


FIGURE 1. Small scale divisions in mm.

INTRODUCTION:  60658 is a light gray, coherent, glassy impact melt that was coated and intruded by dark, vesicular glass (Fig. 1).  It is a rake sample collected about 70 m west southwest of the Lunar Module.

PETROLOGY:  Warner et al. (1976b) provide a brief petrographic description. Abundant mineral and lithic clasts are welded together by glass (Fig. 2). Highly vesicular, flow-banded glass cuts the rock.

PROCESSING AND SUBDIVISIONS:  In 1973 a single chip was removed and allocated for thin sections as ,1 (Fig. 1).
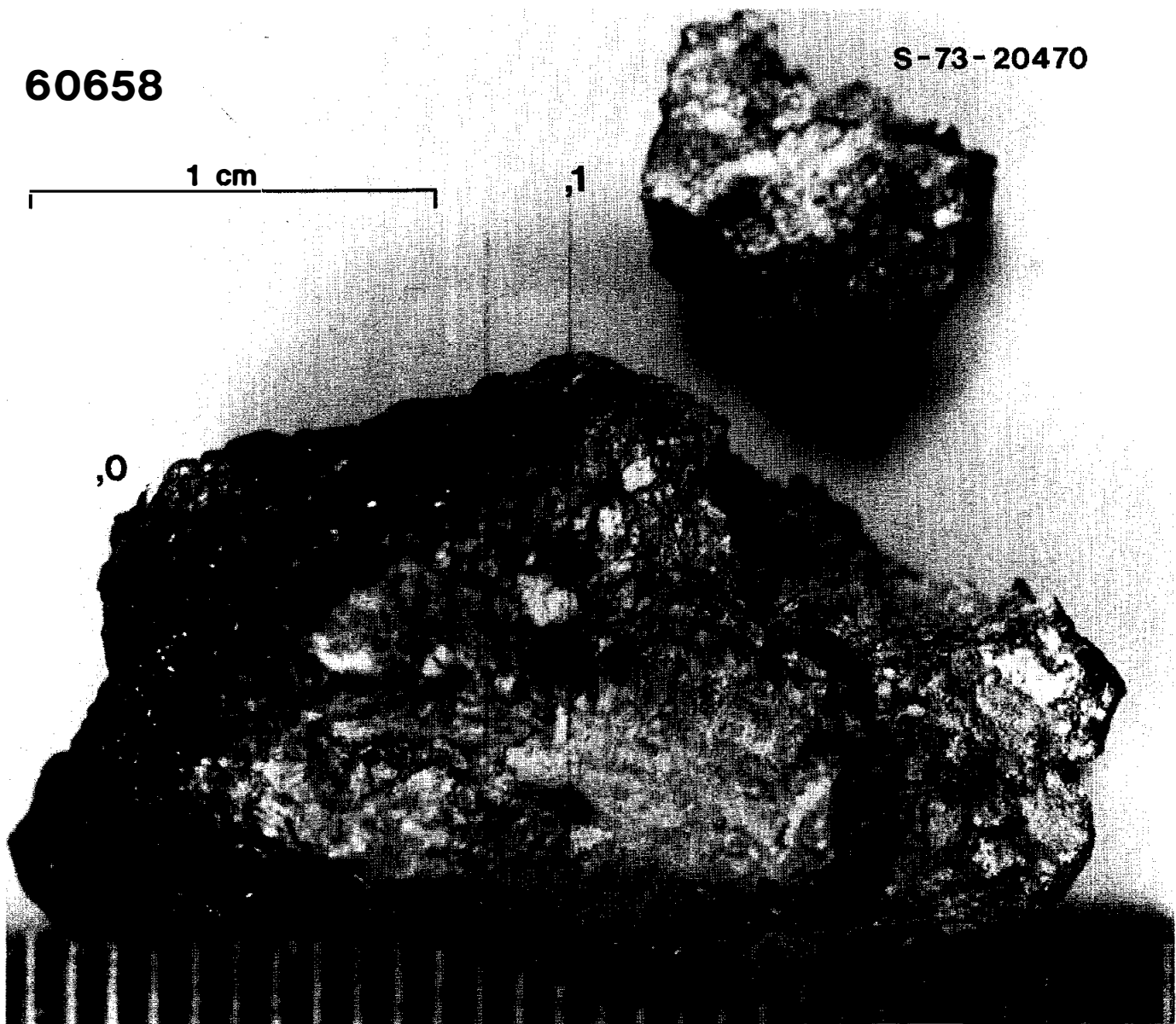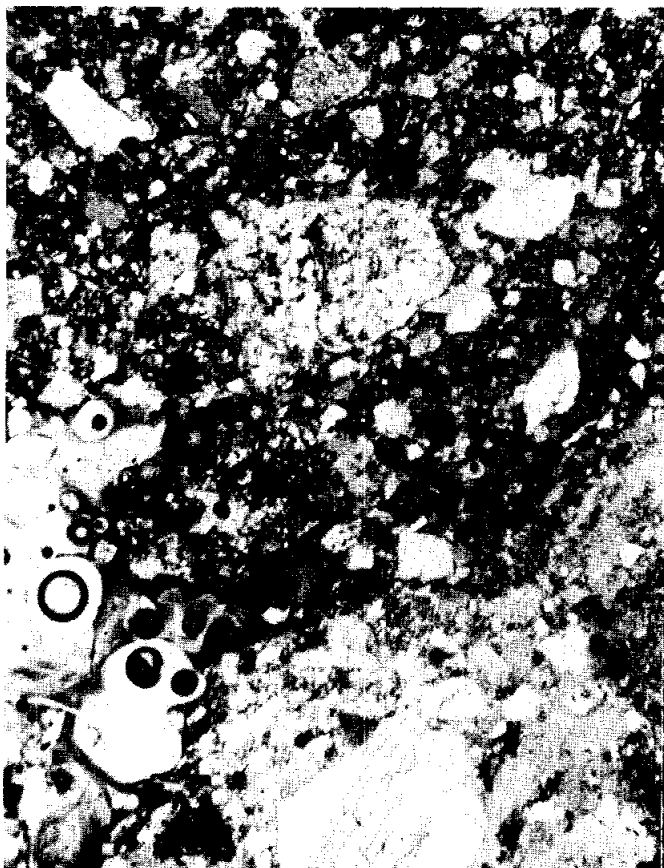


FIGURE 1.

FIGURE 2. 60658,2. general view, ppl. width 2mm.

INTRODUCTION:   60659 is a light gray, coherent breccia with many white clasts surrounded by a gray, fragmental matrix (Fig. 1).  It is a rake sample collected about 70 m west southwest of the Lunar Module.
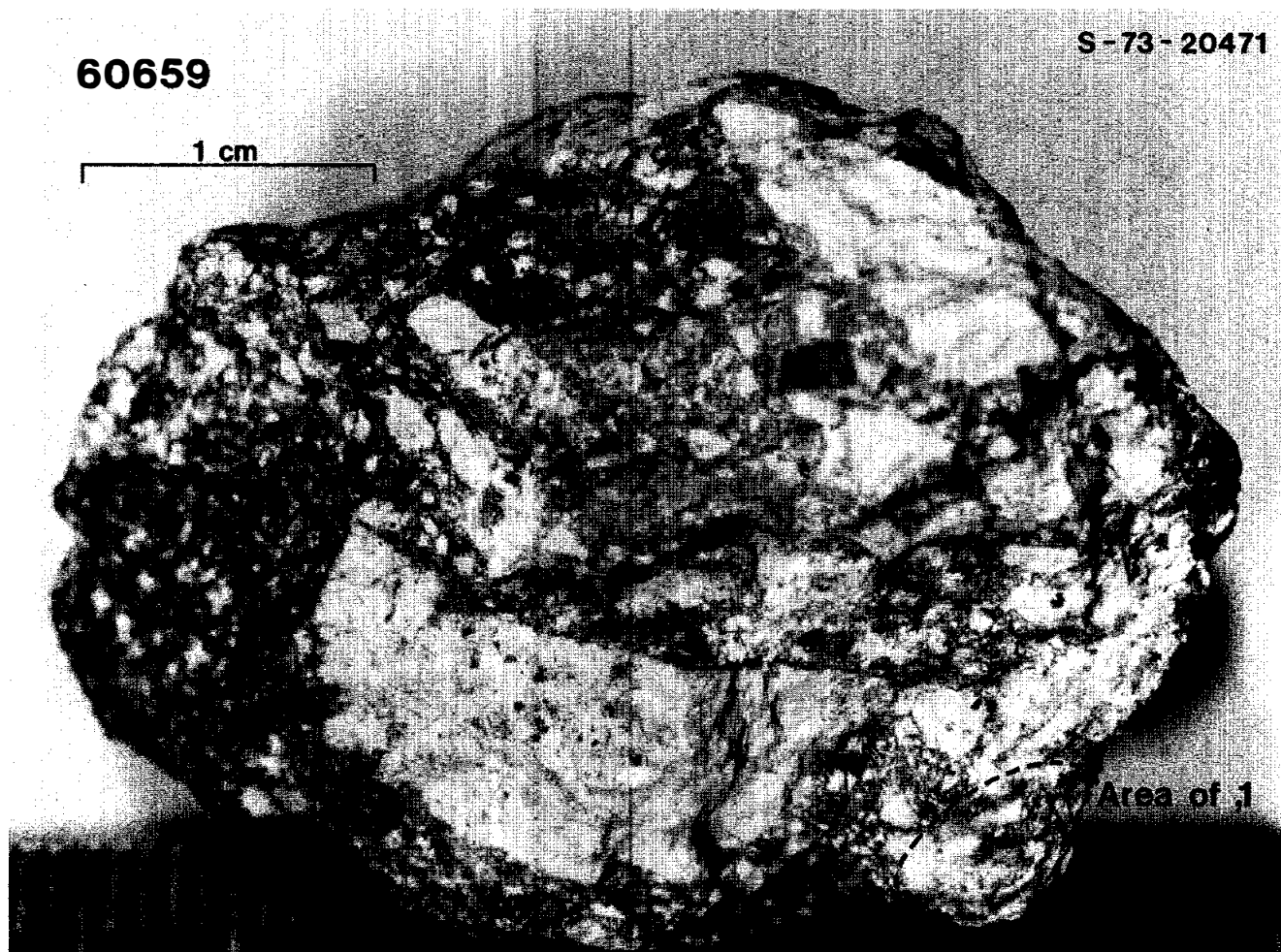


FIGURE 1.

PETROLOGY:  Petrographic descriptions of the matrix and a large cataclastic anorthosite clast are given by Warner et al. (1976b).  The anorthosite is included in a discussion of ferroan anorthosites by Dowty et al. (1974a).

The anorthositic clast has been severely granulated (Fig.2). Pyroxene is the only mafic mineral observed and occurs as small isolated grains in the matrix. Mineral compositions are shown in Figure 3 and tabulated by Dowty et al.(1976). Accessory phases include spinel and ilmenite.

The matrix is a fragmental breccia with low porosity (Fig.2).

a                                        b
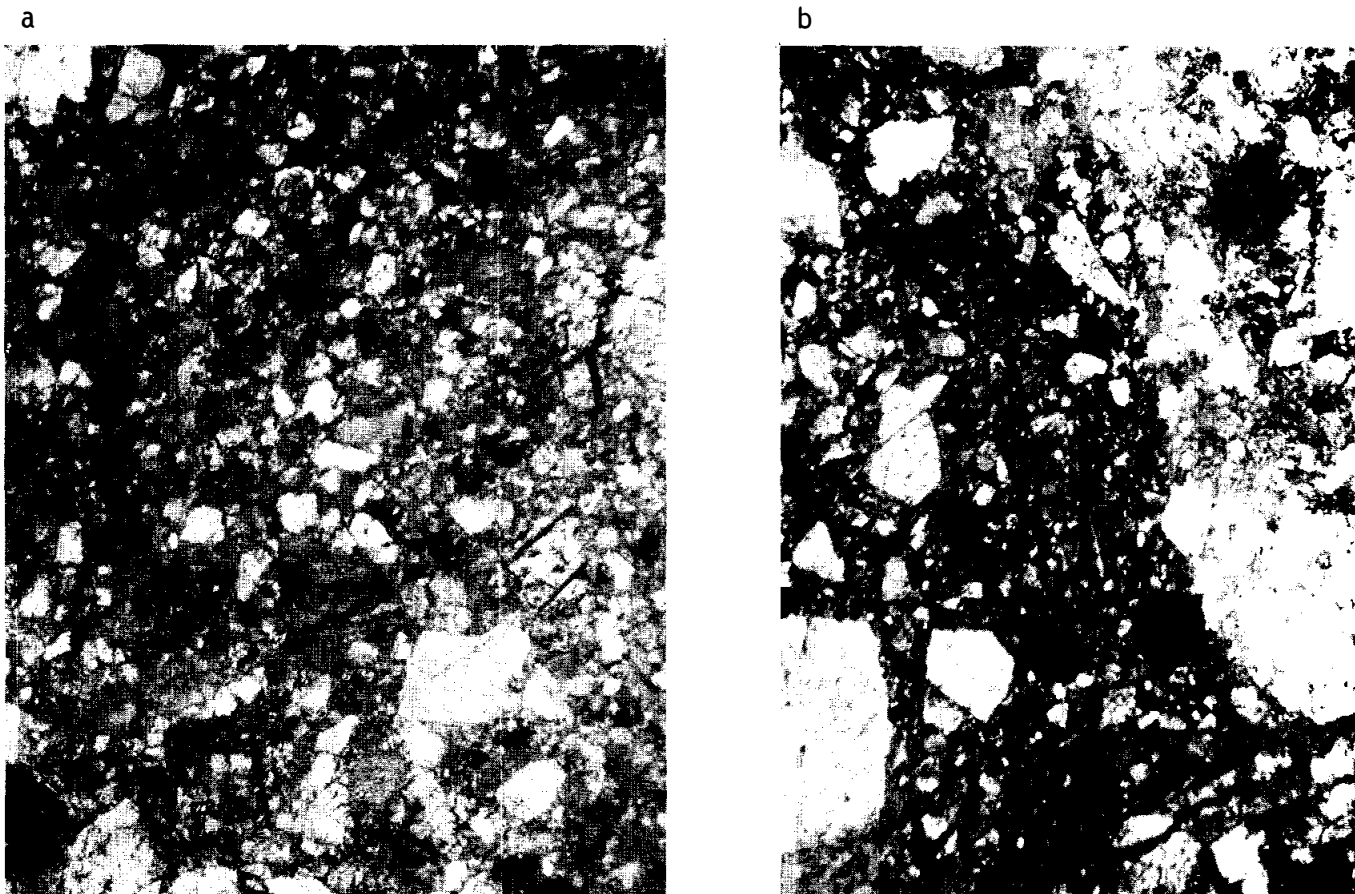
FIGURE 2. 60659,2.  a) anorthosite clast, partly ppl. width 2mm.

b) general matrix (top) and anorthosite clast (bottom),
partly xpl.  width 2mm.

FIGURE 3. Mineral compositions;
from R. Warner et al.(1976b).

NO OLIVINE

100  90  80  70  60  50  40  30  20  10  0
Forsterite content of olivine (mole%)

100  90  80  70  60  50  40  30  20  10  0
Anorthite content of plogioclose (mole%)

167
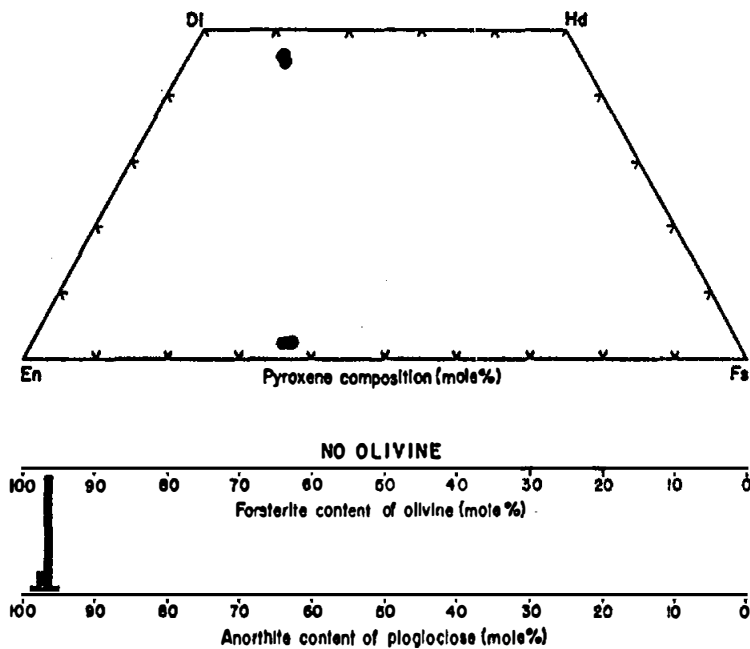
TABLE 1. Chemistry of 60659 anorthosite clast
(DBA, normalized to 100%)

| | |
|---|---|
| $SiO_2$ | 44.3 |
| $TiO_2$ | 0.02 |
| $Al_2O_3$ | 35.4 |
| FeO | 0.30 |
| MgO | 0.21 |
| CaO | 19.3 |
| $Na_2O$ | 0.43 |
| $P_2O_5$ | 0.03 |

CHEMISTRY: A defocussed electron beam analysis of the anorthosite clast is presented by Dowty et al. (1974a) and reproduced by Warner et al. (1976b) and here as Table 1. No analysis of the matrix is available.

PROCESSING AND SUBDIVISIONS: In 1973 two chips were removed from one end of the rock. One of these chips was allocated for thin sections as ,1 (Fig.1).

INTRODUCTION:  60665 is a vesicular glass containing small white clasts (Fig. 1), at least one of which is a cataclastic anorthosite.  60665 is a rake sample collected about 70 m west southwest of the Lunar Module.  It has a few small zap pits.



FIGURE 1. S-73-20497.  Larger pieces are about 6 cm across.

a                                                      b
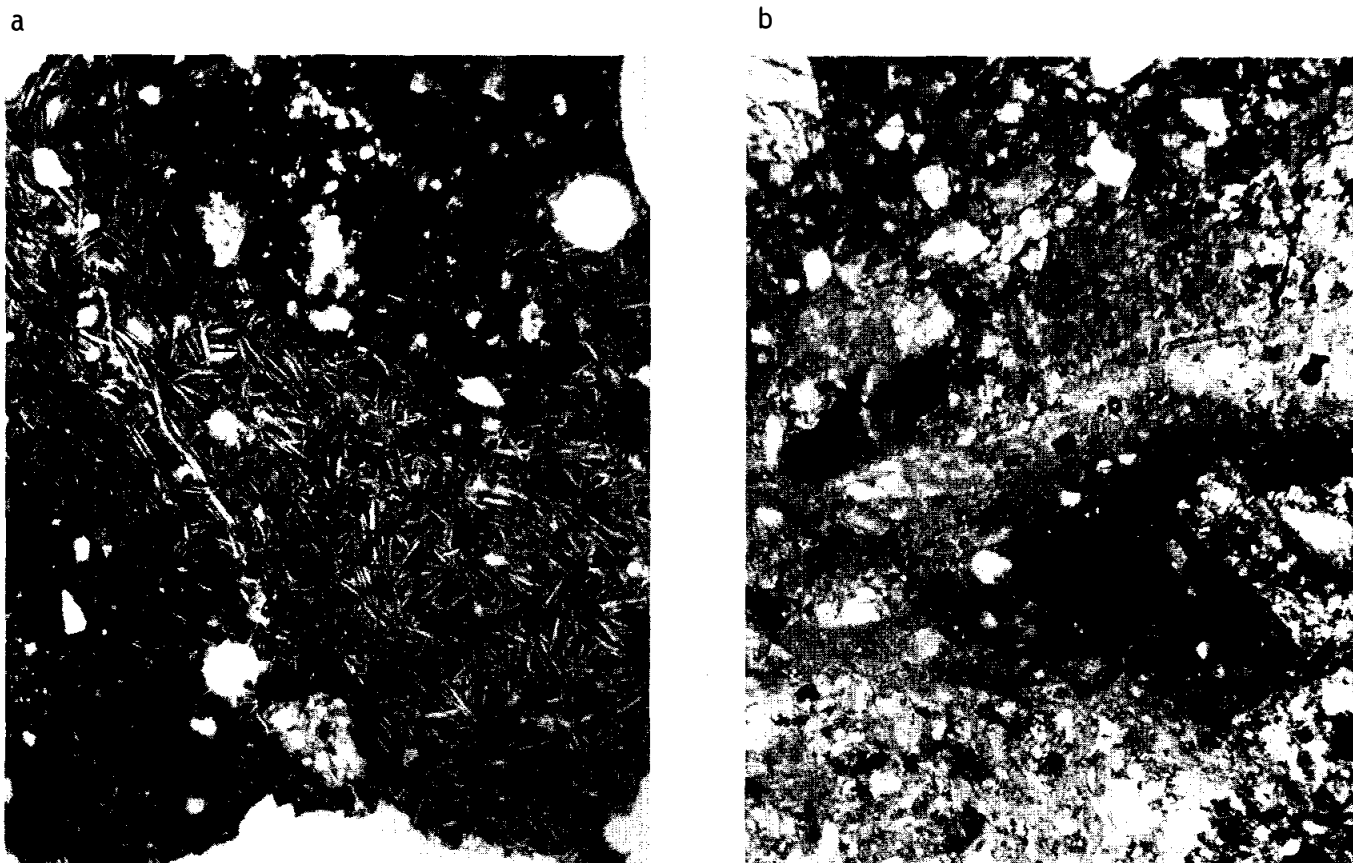


FIGURE 2. a) 60665,7.  devitrified glass, ppl.  width 2mm.
          b) 60665,3.  anorthosite clast, partly xpl.  width 2mm.


PETROLOGY:  60665 is a glass with many small clasts, and is largely devitri-
fied (Fig. 2).  Two white clasts are prominent macroscopically and one was
sampled for thin sections (Fig. 1).  Petrographic information on this clast
is provided by Dowty et al. (1974a) and R. Warner et al. (1976b); Hansen
et al. (1979a) report the abundances of minor elements in plagioclases and
the mg of orthopyroxene (Table 1).  The clast is an anorthosite (Fig. 2)
which is ferroan (Fig. 3).

TABLE 1.  Minor elements in plagioclase in anorthosite clast. (Hansen et al.
1979a)

| Ab mole% | MgO wt% | FeO wt% | $K_2O$ wt% | Opx mg |
|----------|---------|---------|------------|--------|
| 3.6      | 0.060   | 0.132   | 0.16       | 0.60   |
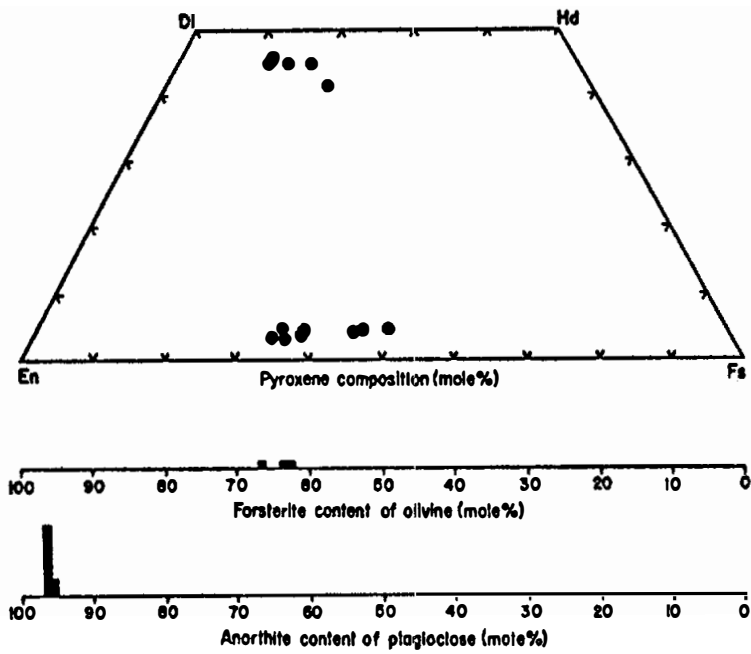
FIGURE 3. Mineral compositions for anorthosite clast; from R. Warner et al. (1976b).

PROCESSING AND SUBDIVISIONS: The sample has fallen into 2 pieces (Fig. 1). Part of one of the white clasts (,1) was removed for petrography (Fig. 1) and thin section ,3 cut from it. Two small white chips (,4) also exist. In 1979, two glass chips (,5) were made into a potted butt and thin section ,7 cut from it.

INTRODUCTION:  60666 is a dark gray, coherent, glassy to fine-grained impact melt with many clasts and vesicles and adhering dust.  A large fragment of lighter colored basaltic impact melt dominates the interior of the rock (Fig. 1). It is a rake sample collected about 70 m west southwest of the Lunar Module. Zap pits are rare.
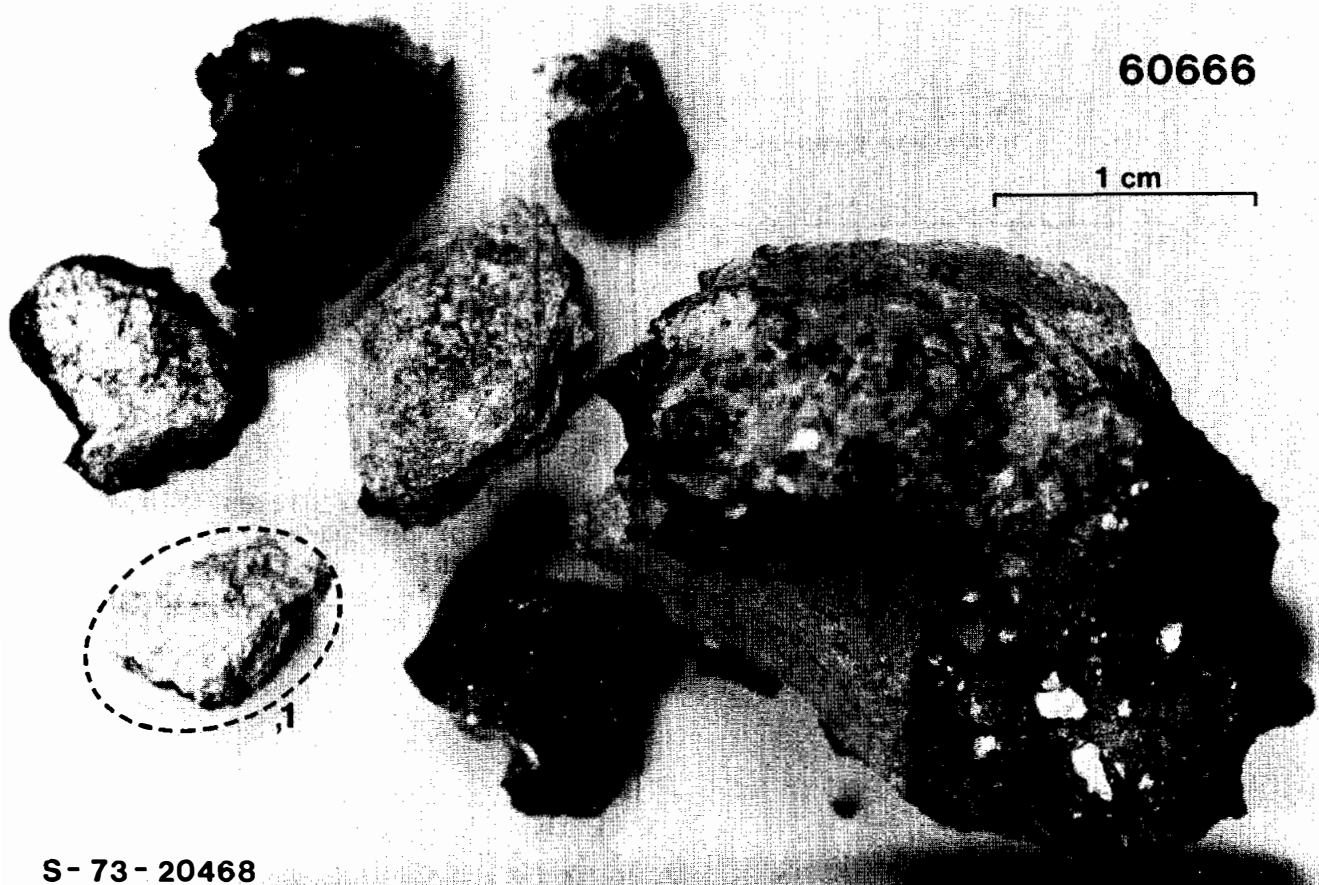


FIGURE 1.

PETROLOGY :  Dowty et al. (1974b)  and Warner et al. (1976b)  provide petrographic descriptions of the large basaltic clast. Xenocrysts of shocked plagioclase and olivine rest in a matrix of skeletal to feathery olivine and glassy to finely crystalline mesostasis (Fig.2).  Rare, very small needles of plagioclase occur interstitial to the matrix olivines.  A few grains of spinel appear to have grown from the melt.  The skeletal olivines are zoned (ranging from $Fo_{87-96}$) suggesting rapid growth from the melt. Plagioclase needles and xenocrysts are the same composition (Fig.3).  Intergrowths of Fe-metal (4-21% Ni, 0.4 - 1.3% Co), schreibersite and troilite and a few discrete grains of chromite are also present.  Mineral analyses are tabulated by Dowty et al. (1976).

FIGURE 2. 60666,2. general
view, partly xpl. width 2mm.
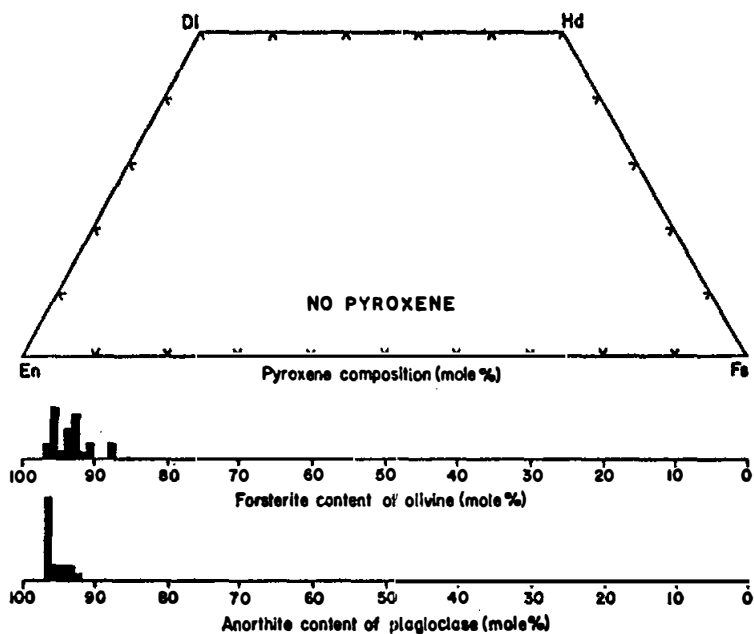


FIGURE 3. Mineral compositions;
from R. Warner et al. (1976b).

60666

TABLE 1.  Summary chemistry of 60666 lithologies

| | Dark,glassy melt (Wasson et al.,1977) | Basaltic clast,bulk (DBA, Dowty et al.,1974b) | Basaltic clast, excluding clasts) (DBA, Dowty et al.,1974b) |
|---|---|---|---|
| $SiO_2$ | | 42.7 | 45.1 |
| $TiO_2$ | 0.50 | 0.21 | 0.27 |
| $Al_2O_3$ | 29.7 | 20.8 | 18.9 |
| $Cr_2O_3$ | 0.12 | 0.11 | 0.14 |
| FeO | 5.57 | 4.2 | 5.0 |
| MnO | 0.07 | 0.05 | 0.05 |
| MgO | 6.5 | 18.6 | 19.0 |
| CaO | 15.4 | 11.7 | 11.0 |
| $Na_2O$ | 0.473 | 0.39 | 0.36 |
| $K_2O$ | 0.084 | 0.10 | 0.11 |
| $P_2O_5$ | | 0.04 | 0.06 |
| Sr | | | |
| La | 11.4 | | |
| Lu | 0.49 | | |
| Rb | | | |
| Sc | 6.5 | | |
| Ni | 800 | | |
| Co | 53 | | |
| Ir ppb | 28 | | |
| Au ppb | 9.0 | | |
| C | | | |
| N | | | |
| S | | | |
| Zn | <5.7 | | |
| Cu | | | |

Oxides in wt%; others in ppm except as noted.

CHEMISTRY: Major and trace element data on the dark,glassy melt are presented by Wasson et al. (1977). Dowty et al. (1974b) give major elements of the lighter colored, basaltic clast and of the melt portion only of this clast (excluding xenocrysts) by DBA.  The bulk DBA analysis of the basalt clast is reproduced by Warner et al. (1976b).

The two bulk analyses show that the basalt clast and the dark, glassy melt are not the same composition (Table 1).  The dark, glassy material analyzed by Wasson et al. (1977) is very similar to the local mature soils.  A significant meteoritic component is indicated by the siderophile data.  The basaltic clast analyzed by Dowty et al. (1974b) is much less aluminous and has a higher Mg/Fe than the dark, glassy material (Table 1).

PROCESSING AND SUBDIVISIONS:  In 1972 several chips were removed from the rock and a portion of the large basaltic clast (,1) allocated to Keil for petrography (Fig.1). In 1976, two small chips of dark glass (,3) were allocated to Wasson for chemistry.

INTRODUCTION:  60667 is a medium gray, coherent, basaltic impact melt (Fig. 1).
Many small white clasts and a few grains of metal are scattered through the
rock.  It is subangular with many vugs and some splash glass.  It is a rake
sample collected about 70 m west southwest of the Lunar Module.  Zap pits are
rare.
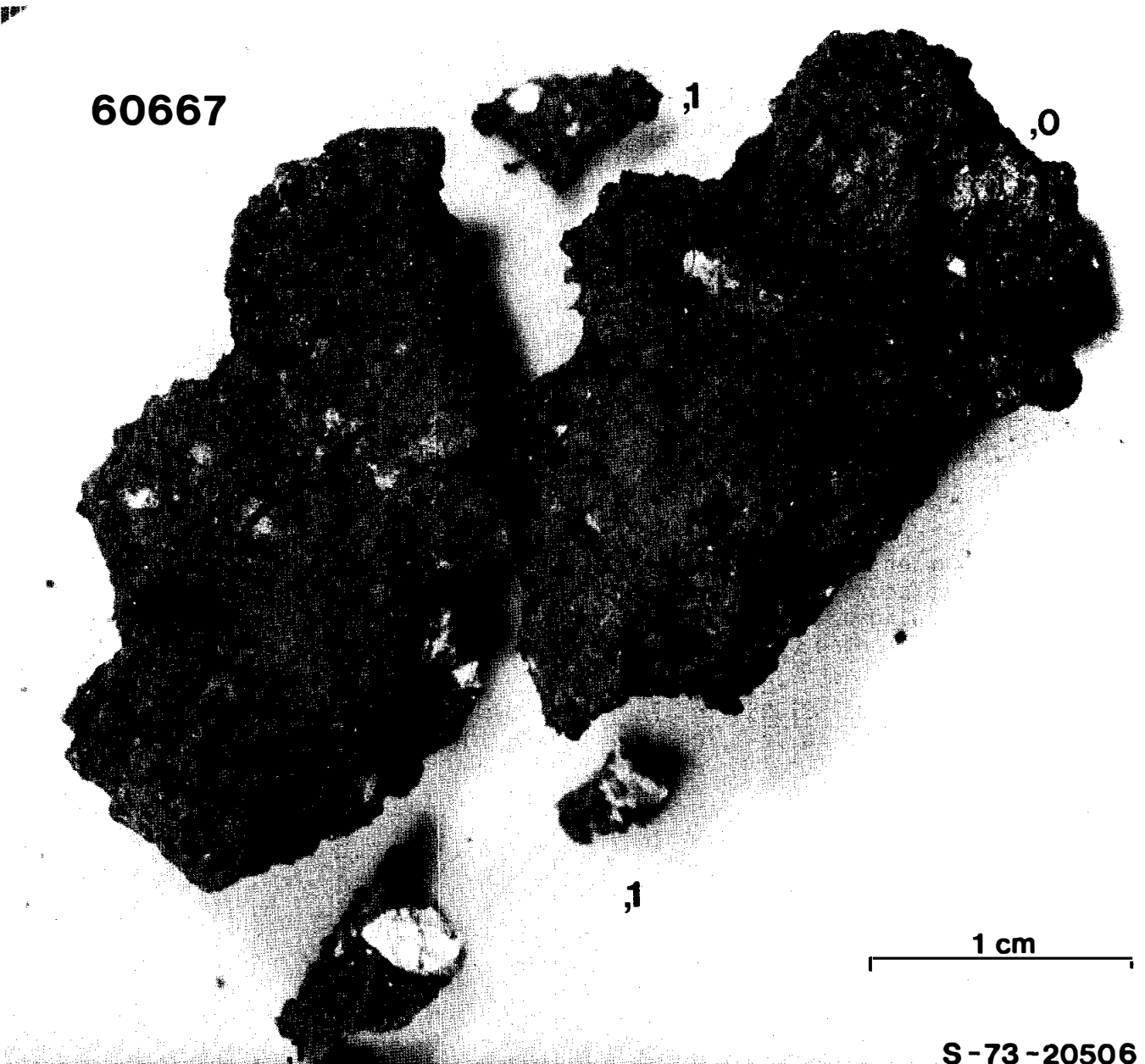


FIGURE 1.

60667



FIGURE 2. 60667,2. general view, partly xpl. width 2mm.

PETROLOGY: Warner et al. (1976b) provide a brief petrographic description. Abundant, cryptocrystalline to glassy mesostasis rests in interstices formed by many small plagioclase laths (Fig.2). One large, very fine-grained anorthosite clast is noted by Warner et al. (1976b).

PROCESSING AND SUBDIVISIONS: In 1972, the sample was split and three small chips (,1) allocated to Keil for petrography (Fig.1).

INTRODUCTION:   60668 is a dark gray, coherent, glassy impact melt (Fig. 1) which is angular and highly vesicular.  A considerable amount of dust is welded to the glass and a few white clasts are present.  It is a rake sample collected about 70 m west southwest of the Lunar Module and lacks zap pits.



FIGURE 1.  Small scale divisions in mm.

INTRODUCTION:  60669 is a dark gray, coherent, glassy impact melt (Fig. 1). It is angular and highly vesicular.  A few small (<1 mm) white clasts are scattered through the rock.  It is a rake sample collected about 70 m west southwest of the Lunar Module and lacks zap pits.



FIGURE 1. Small scale divisions in mm.

INTRODUCTION:   60675 is a coherent, dark gray, fine-grained impact melt with abundant vugs, vesicles and white clasts (Fig. 1).  It was collected as a rake sample about 70 m west southwest of the Lunar Module.  Zap pits are absent.



FIGURE 1. Small scale divisions in mm.

INTRODUCTION:  60676 is a dark gray, coherent, glassy impact melt (Fig. 1).
It is subangular and contains several large clasts.  Few vesicles are present
and most are filled with soil.  It is a rake sample collected about 70 m west
southwest of the Lunar Module.  Zap pits are absent.



**60676**
**Post split**

S-73-20474
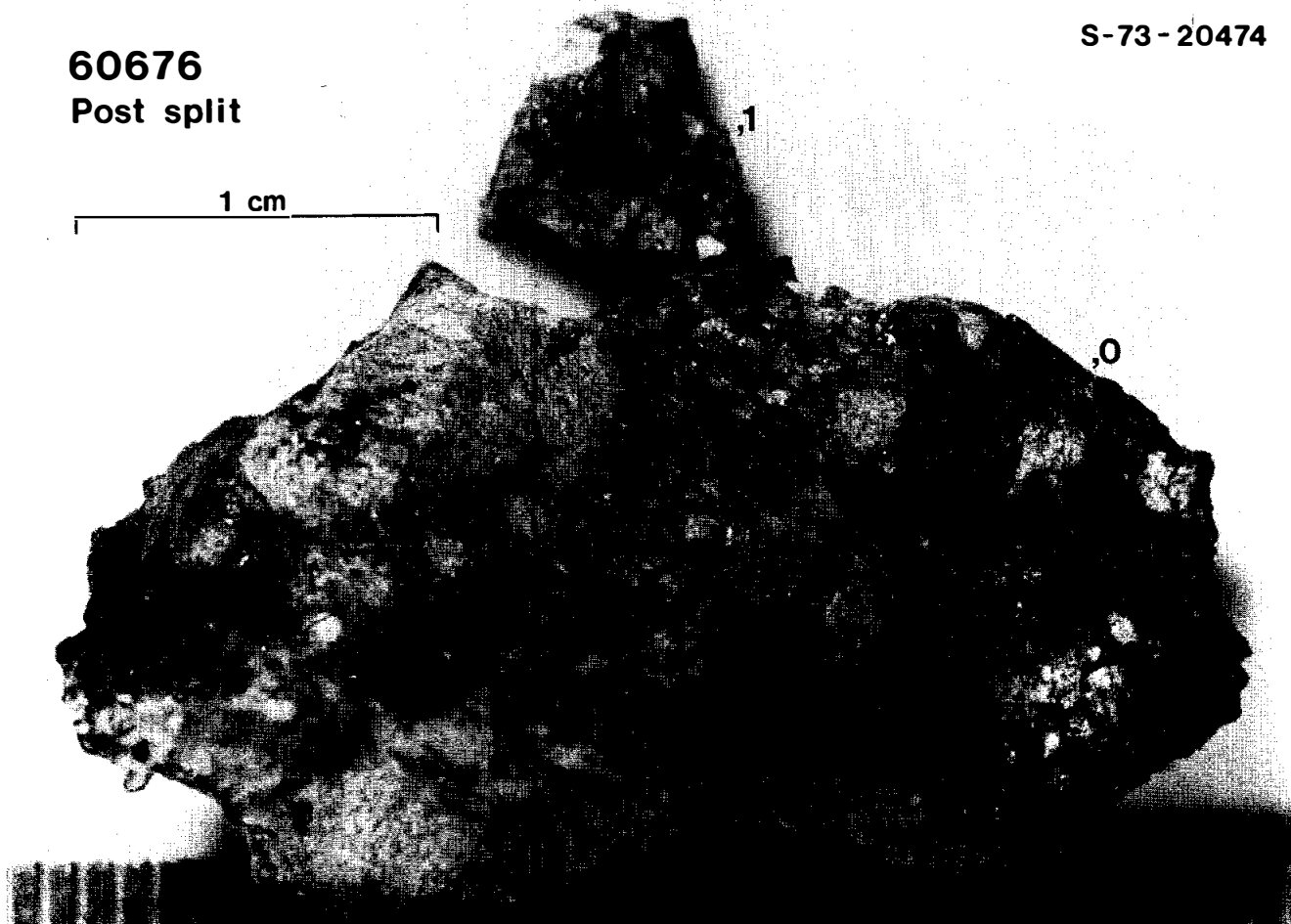
FIGURE 1.

PETROLOGY:  Warner et al. (1976b) provide a brief petrographic description and
mineral compositions.  Abundant dark, banded glass encloses a variety of clasts
(Fig. 2).  One large poikilitic rock fragment, several heavily shocked plagioclase
grains and a 0.1 mm pink spinel clast are noted by Warner et al. (1976b).  Mineral
compositions are shown in Figure 3 and tabulated by Dowty et al. (1976).  Other
minor phases include ilmenite, armalcolite, rutile and Fe-metal (5.4-6.5% Ni,
0.3-0.4% Co).

FIGURE 2. 60676,2.
general view, partly
xpl. width 3mm.
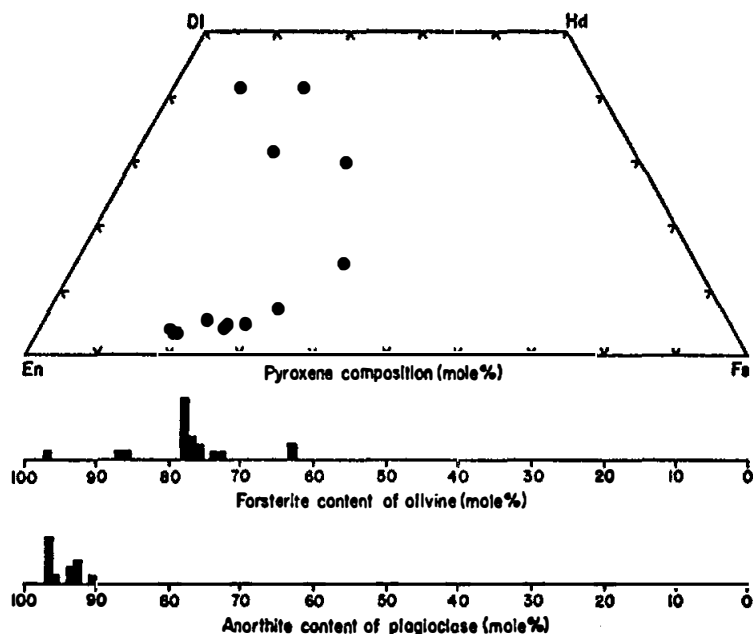


TABLE 1. Chemistry of 60676

| | |
|---|---|
| $SiO_2$ | 46.4 |
| $TiO_2$ | 0.70 |
| $Al_2O_3$ | 23.5 |
| $Cr_2O_3$ | 0.12 |
| FeO | 6.7 |
| MnO | 0.07 |
| MgO | 9.7 |
| CaO | 13.8 |
| $Na_2O$ | 0.55 |
| $K_2O$ | 0.18 |
| $P_2O_5$ | 0.24 |

FIGURE 3. Mineral compositions; from R. Warner
et al. (1976b).

CHEMISTRY: A defocussed electron beam analysis (DBA) is given by Warner et al.
(1976b) and reproduced here as Table 1.

PROCESSING AND SUBDIVISIONS: In 1973 a single chip (,1) was removed and allocated
to Keil for petrography (Fig. 1).

181

<u>INTRODUCTION</u>:   60677 is a coherent, dark gray, glassy breccia with several different clasts, including a large (14x2 mm), friable clast of granoblastic anorthosite (Fig. 1).  Many vesicles are present on all surfaces.  It is a rake sample collected about 70 m west-southwest of the Lunar Module and lacks zap pits.

S-73-20465

**60677**

1 cm
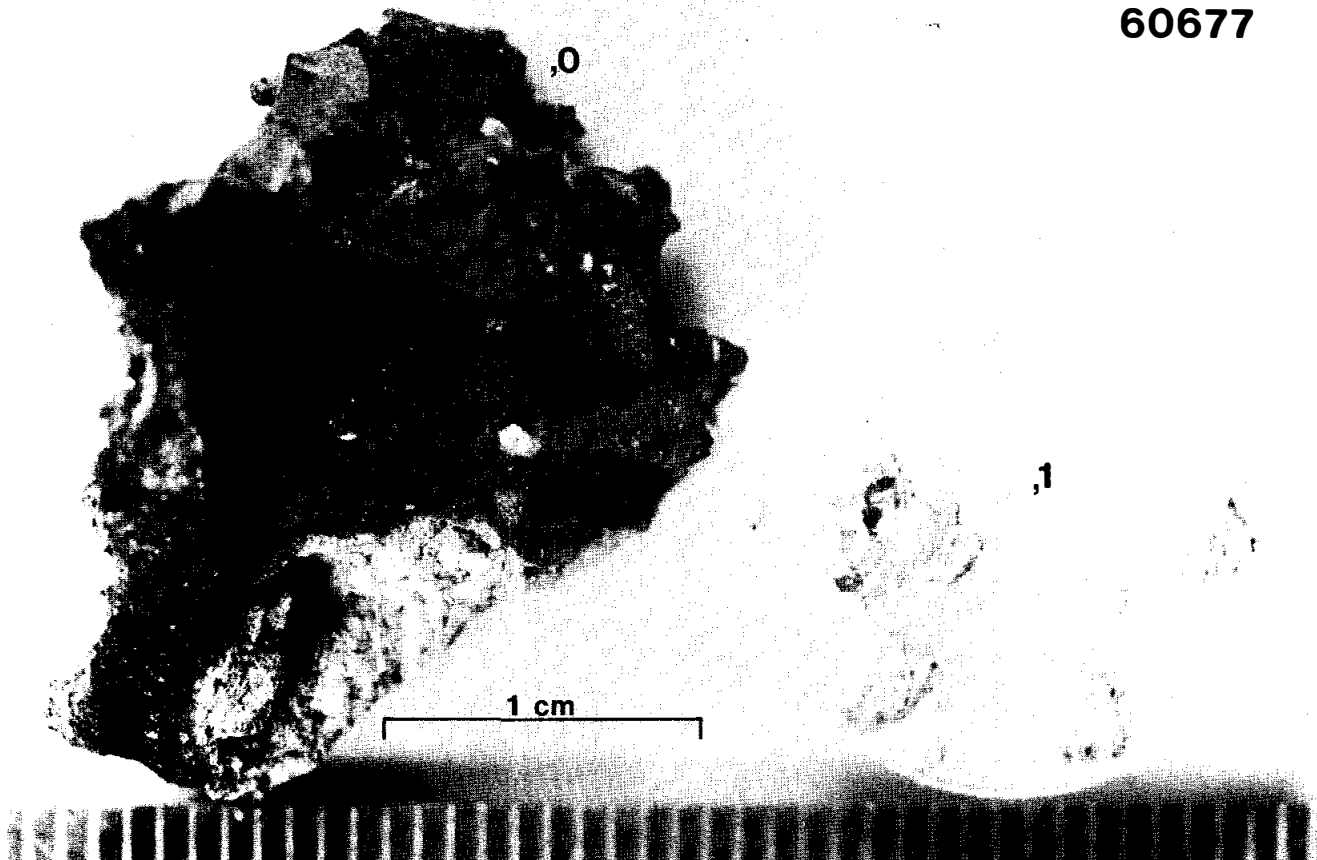
<u>FIGURE 1</u>.

<u>PETROLOGY</u>:  Warner <u>et al</u>. (1976b)  provide petrographic descriptions of both the glassy matrix and a granoblastic anorthosite clast.  Dowty <u>et al</u>. (1974a)  describe the same anorthosite clast.

The large white clast shown in Figure 1 is an annealed anorthositic breccia with a granoblastic texture (Fig.2).  Small, anhedral olivine grains reside in triple junctions formed by polygonal plagioclases.  Pyroxene is absent. Mineral compositions are shown in Figure 3 and tabulated by Dowty <u>et al</u>. (1976).  Ilmenite is an accessory phase.

The matrix of 60677 is a very porous mixture of mineral, lithic and glass clasts welded together by glass (Fig. 2).  Several breccia clasts and one poikilitic-textured clast are mentioned by Warner <u>et al</u>. (1976b).

a
b
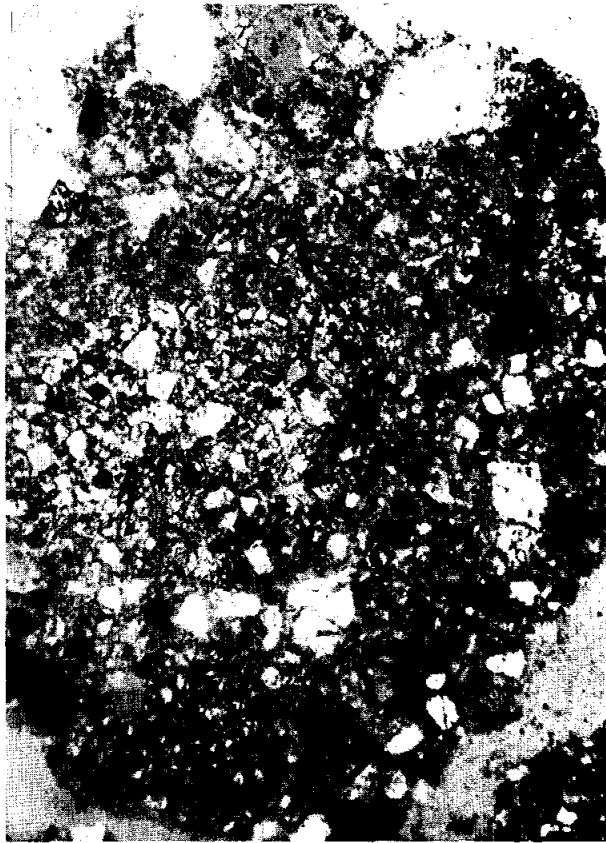


FIGURE 2. 60677,2. a) granoblastic anorthosite, partly xpl. width 2mm.
b) glassy breccia matrix, partly xpl. width 2mm.



NO PYROXENE

Pyroxene composition (mole%)

Forsterite content of olivine (mole%)

Anorthite content of plagioclose (mole%)
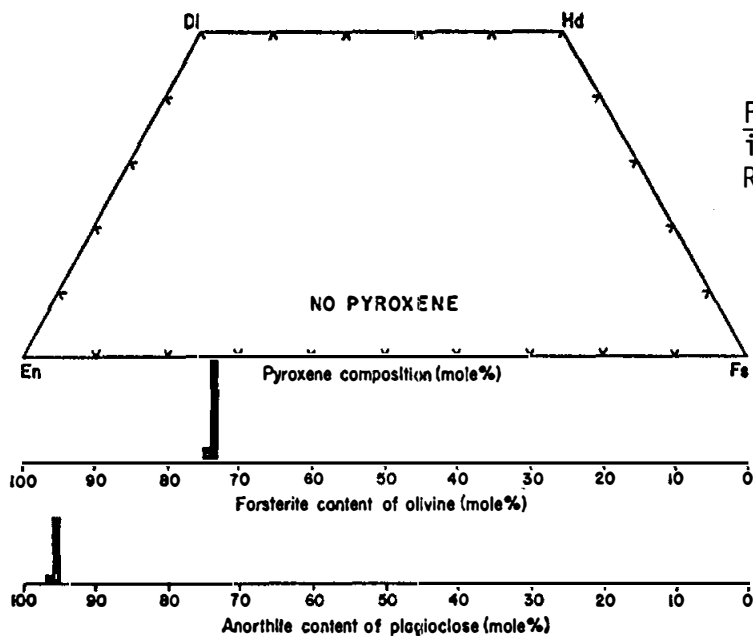
FIGURE 3. Mineral compositions
in granoblastic anorthosite; from
R. Warner et al. (1976b).

183

TABLE 1. Chemistry of 60677 anorthosite clast (DBA)

| | |
|---|---|
| $SiO_2$ | 44.3 |
| $TiO_2$ | 0.04 |
| $Al_2O_3$ | 34.2 |
| $Cr_2O_3$ | 0.01 |
| FeO | 1.04 |
| MnO | 0.01 |
| MgO | 1.40 |
| CaO | 18.3 |
| $Na_2O$ | 0.56 |
| $K_2O$ | 0.03 |
| $P_2O_5$ | 0.03 |

CHEMISTRY: A defocussed electron beam analysis (DBA) of the granoblastic anorthosite clast described above is presented by Dowty et al. (1974a) and reproduced by Warner et al. (1976b), and here as Table 1. No analysis of the glassy matrix is available.

PROCESSING AND SUBDIVISIONS: In 1973 four small chips (,1) were allocated to Keil for petrography (Fig.1).

INTRODUCTION:   60678 is a dark gray, coherent, glassy impact melt (Fig. 1). It is angular and highly vesicular.  Several small white clasts and a friable breccia clast (8 mm) are present.  It is a rake sample collected about 70 m west southwest of the Lunar Module and lacks zap pits.

FIGURE 1. Small scale divisions in mm.

INTRODUCTION:  60679 is a dark gray, coherent, glassy impact melt (Fig. 1). It is angular and highly vesicular.  Several white clasts and a friable breccia clast (13 mm) are present.  It is a rake sample collected about 70 m west south-west of the Lunar Module and lacks zap pits.
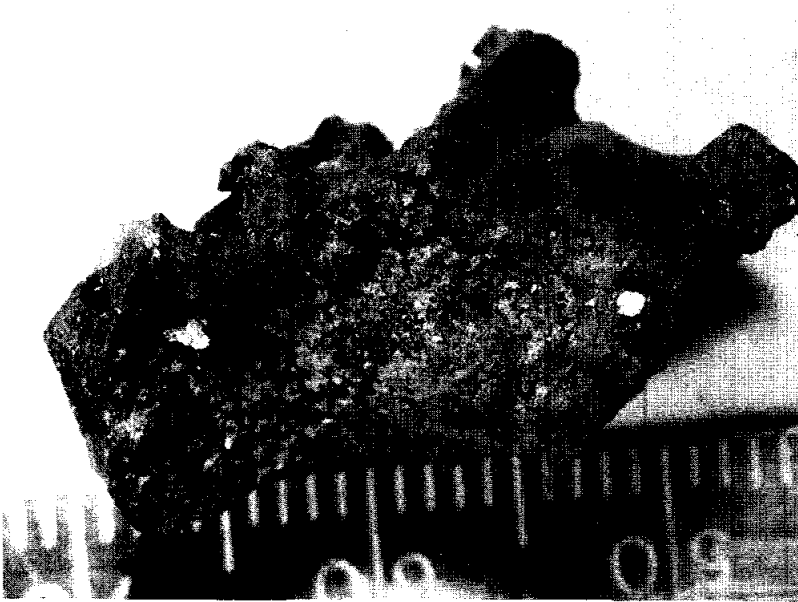
FIGURE 1. Small scale divisions in mm.

## 61015   DILITHOLOGIC (CATACLASTIC ANORTHOSITE AND BASALTIC IMPACT MELT)   1789 g
## BRECCIA, PARTLY GLASS COATED

INTRODUCTION:   61015 consists of ∿75% dark basaltic impact melt and ∿25% white anorthosite.  The melt/anorthosite contacts are sharp and form an unusual texture (Fig. 1).  A vesicular glass partially coats two sides.  The sample is tough and subangular.

61015 was collected 10 m south of Plum Crater and its orientation is known.  Zap pits on only half of its surface suggest a fairly simple exposure history.
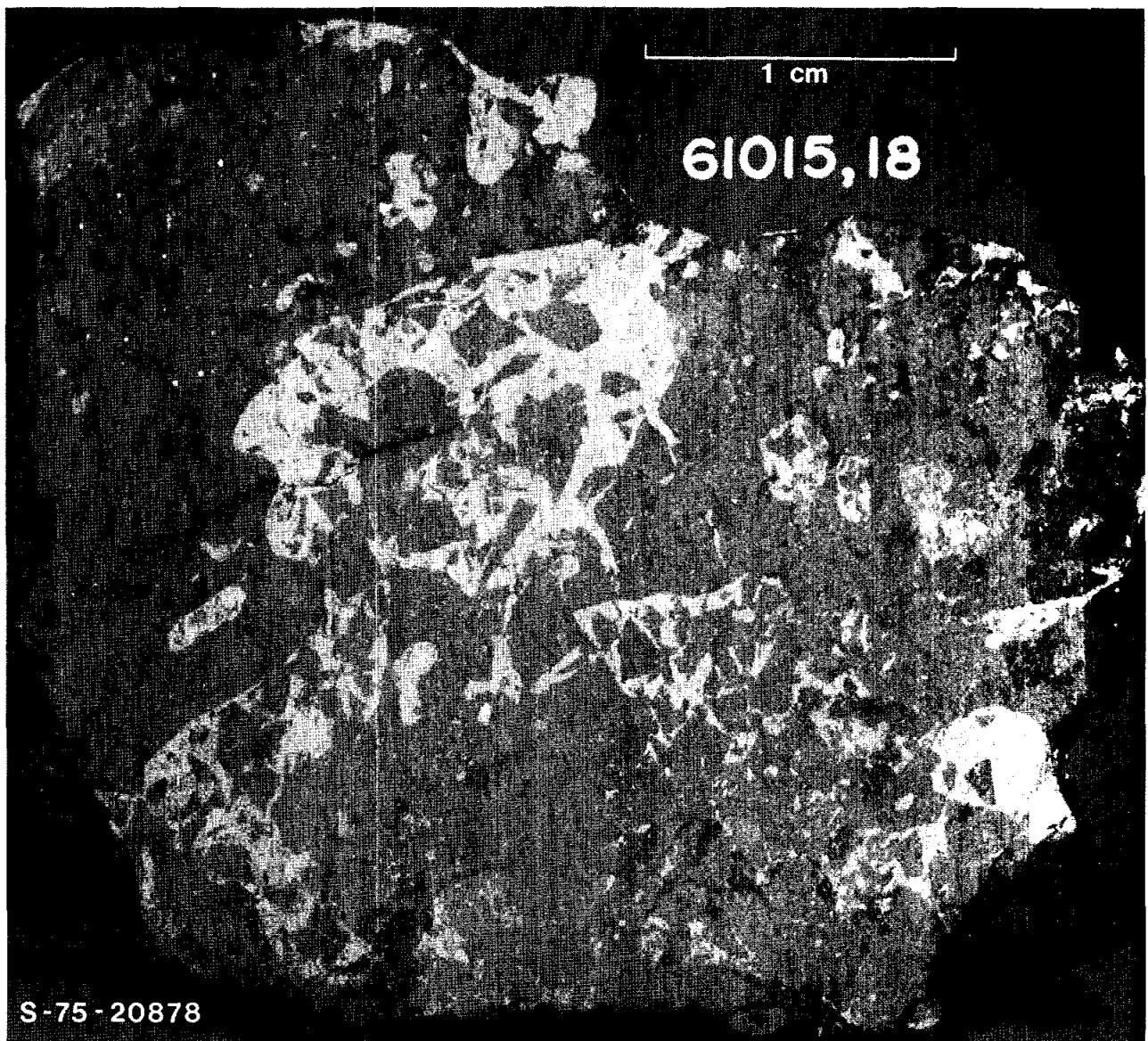


Figure 1. Saw cut face.

PETROLOGY:   A brief description is given by McGee et al. (1979) and 61015 is illustrated by LSPET (1973).

The basaltic impact melt (Fig. 2 ) is characterized by plagioclase laths less than 100 μm long subophitically embedded in small pyroxenes and abundant interstitial glass.  Engelhardt (1978) lists it as poikilitic, but a poikilitic texture is only poorly developed.  Clasts of shocked plagioclase are abundant.   Individual fragments of the basalt have different grain sizes; a few are aphanitic and some glassy.  No chilled margins are present.

The anorthosite is cataclastic and coarse--some plagioclases are 2 mm in diameter (Fig. 2).   A few pyroxenes (up to 300 μm) are present; some have either exsolution or shock lamellae.  Some opaques (chromite?),troilite, and Fe-metal are also present.  Except for the distinct dark fragments, the anorthosite appears pure i.e. it is not intimately mixed on a small scale with extraneous material.

The anorthosite probably intruded the basaltic impact melt in the rock-forming event.  The saw-cut faces (e.g. Fig. 1) show zones of white material whose boundaries with the main dark masses are mainly smooth and curving; within the white zones, angular black fragments are prominent.  In a few places the white forms small apophyses into the dark material.  The anorthosite must have been fluid (e.g. hot gas charged debris) though not a silicate liquid during its injection.  None the less, relationships between dark and white are not clearly established.

The glass coat (Fig. 2) is vesicular, brown-gray, and contains small metal blebs and plagioclase fragments.  Its thermal effects on the impact basalt are optically visible for 300 μm into the rock.  Thin (300 μm) veinlets of gray-brown, flow-banded glass penetrate the rock, apparently from the coat; these veinlets are opaque at their margins.

CHEMISTRY:   Chemical analyses of the basaltic impact melt and an impure sample of the anorthosite are presented in Palme et al. (1978).   Christian et al. (1976) present an analysis of the impact melt and of a mixed black-and-white split.   The analyses of the melt and the impure anorthosite are summarized in Figure 3 and Table 1.  The glass coat has not been analyzed.

The basaltic melt is aluminous, meteorite-contaminated and distinct from Apollo 16 soil compositions.  The impure anorthosite sample is meteorite-contaminated and the analyzed sample probably contained some of the basaltic impact melt.  The data indicate that the pure anorthosite is ferroan (FeO/MgO >1).

MICROCRATERS:  Microcrater frequency distribution data for the surface of 61015 are reported by Neukum et al. (1973) and Morrison et al. (1973) (Fig. 4).  Both papers note the rounded nature of the rock and that pits occur on only half of the surface, indicating a fairly simple exposure history.  While Morrison et al. (1973) do not believe that this rock has a steady-state surface, Neukum et al. (1973) consider that such equilibrium is likely.
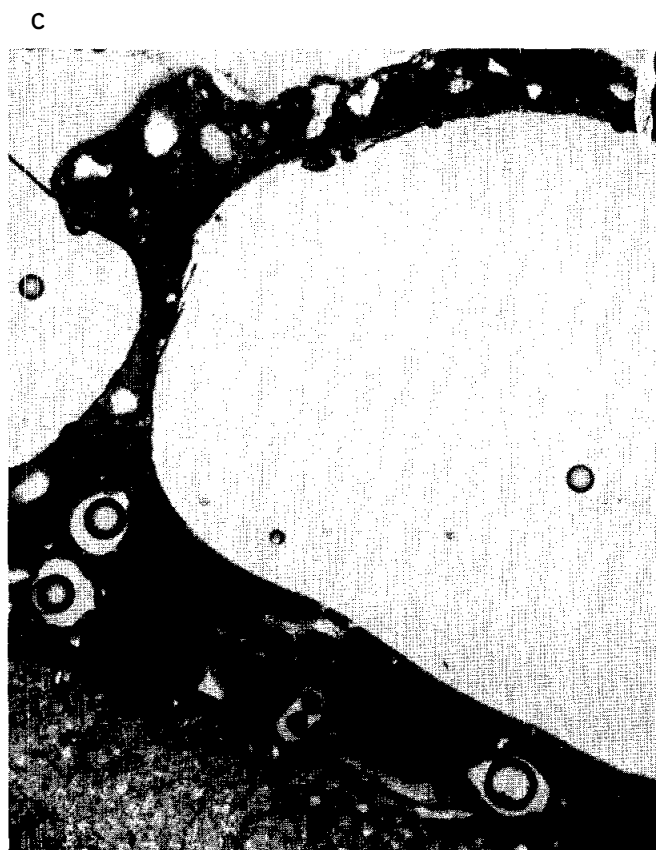
a



b



c



<u>Figure 2</u>. a) 61015,14. basaltic area,
ppl. width 2 mm.
b) 61015,14. anorthosite,
xpl. width 2 mm.
c) 61015,40. glass coat,
ppl. width 2 mm.

TABLE 1. Summary chemistry of basaltic impact melt
and impure anorthosite in 61015

| | Basaltic Melt | Impure Anorthosite |
|---|---|---|
| $SiO_2$ | 45.4 | 45.5 |
| $TiO_2$ | 0.70 | 0.27 |
| $Al_2O_3$ | 23. | 32.9 |
| $Cr_2O_3$ | 0.14 | 0.05 |
| FeO | 6.6 | 3.0 |
| MnO | 0.09 | 0.03 |
| MgO | 9.7 | 2.9 |
| CaO | 13.5 | 17.8 |
| $N_2O$ | 0.48 | 0.47 |
| $K_2O$ | ~ 0.17 | 0.047 |
| $P_2O_5$ | 0.19 | 0.087 |
| Sr | ~153 | 197 |
| La | 20. | 7.6 |
| Lu | 0.9 | 0.32 |
| Rb | 4.0 | |
| Sc | 10.5 | 3.9 |
| Ni | 540-1160 | 690 |
| Co | 30-61 | 39.5 |
| Ir ppb | 29 | 13 |
| Au ppb | 20 | 14 |
| C | | |
| N | | |
| S | 2150 | 470 |
| Zn | | |
| Cu | | |

Oxides in wt%; others in ppm except as noted.
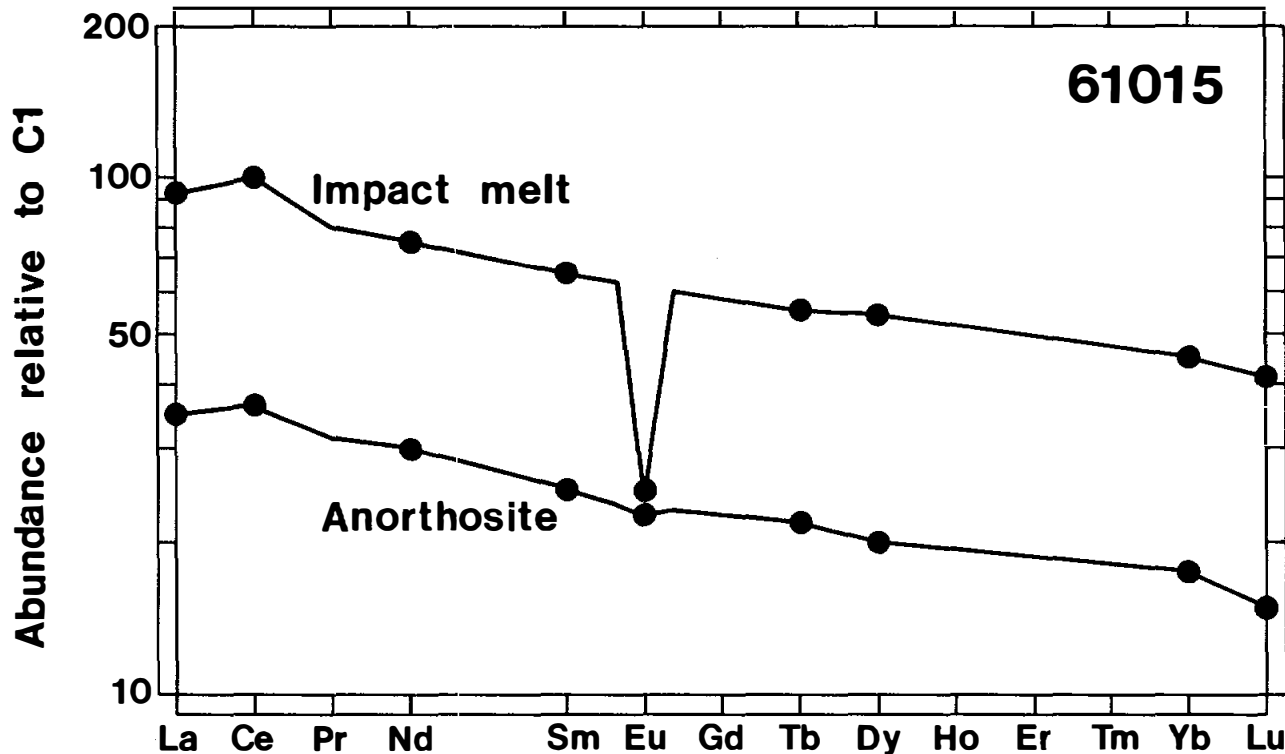
Figure 3. Rare earths; data from Palme et al. (1978).
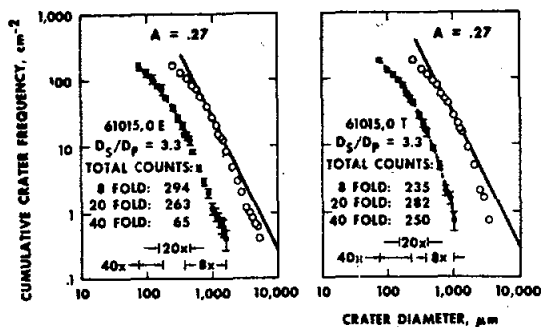


Figure 4. Microcraters; from Neukum et al. (1973).

PROCESSING AND SUBDIVISIONS: A few chips were removed from the rock prior to a saw cut being made to remove a butt end in 1973. Most of the sample remains as ,0 (1490 g). The butt end was split into ,18 (150 g); ,20 (93 g) and a number of other smaller pieces, some of which were further subdivided. Most of the allocations were from these latter chips.

INTRODUCTION:  "Big Muley" is the largest rock collected on the Apollo missions. The bulk of the sample is a fragment-laden aluminous impact melt in which all plagioclase has been shocked to diaplectic glass.  A chemically pristine but shocked and shock-melted anorthosite is a subordinate lithology.  The shock-melted portion of the anorthosite was liquid, not diaplectic and intrudes the basalt (Fig. 1).  Although the anorthosite has generally been referred to as a clast in the basalt, the contact of the non-melted anorthosite with the basalt is not in the thin sections and the relationships are obscure.  Much of the rock is coated with a thin aluminous glass (Fig. 1).  Warner et al. (1973) classify 61016 as a black-and-white rock:  cataclastic anorthosite plus mesostasis-rich basalt.

61016 was collected from the east rim of Plum Crater and its orientation is known.  Zap pits are absent from one side.  This side was exposed on the lunar surface, indicating that a recent, and only recent, rotation of the sample occurred.  Planar non-penetrative fractures are exposed on most surfaces.
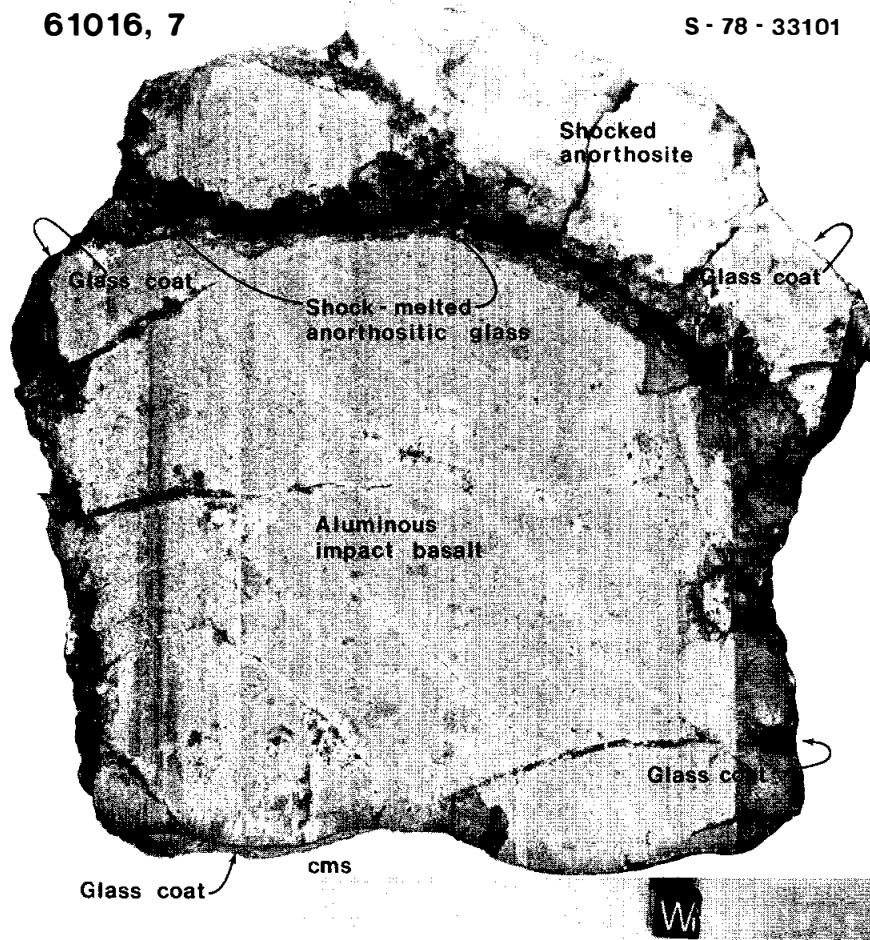


Figure 1.  Sawn face of 61016 showing main lithologies and the fractures.

61016 Slab                                    S-72-50692
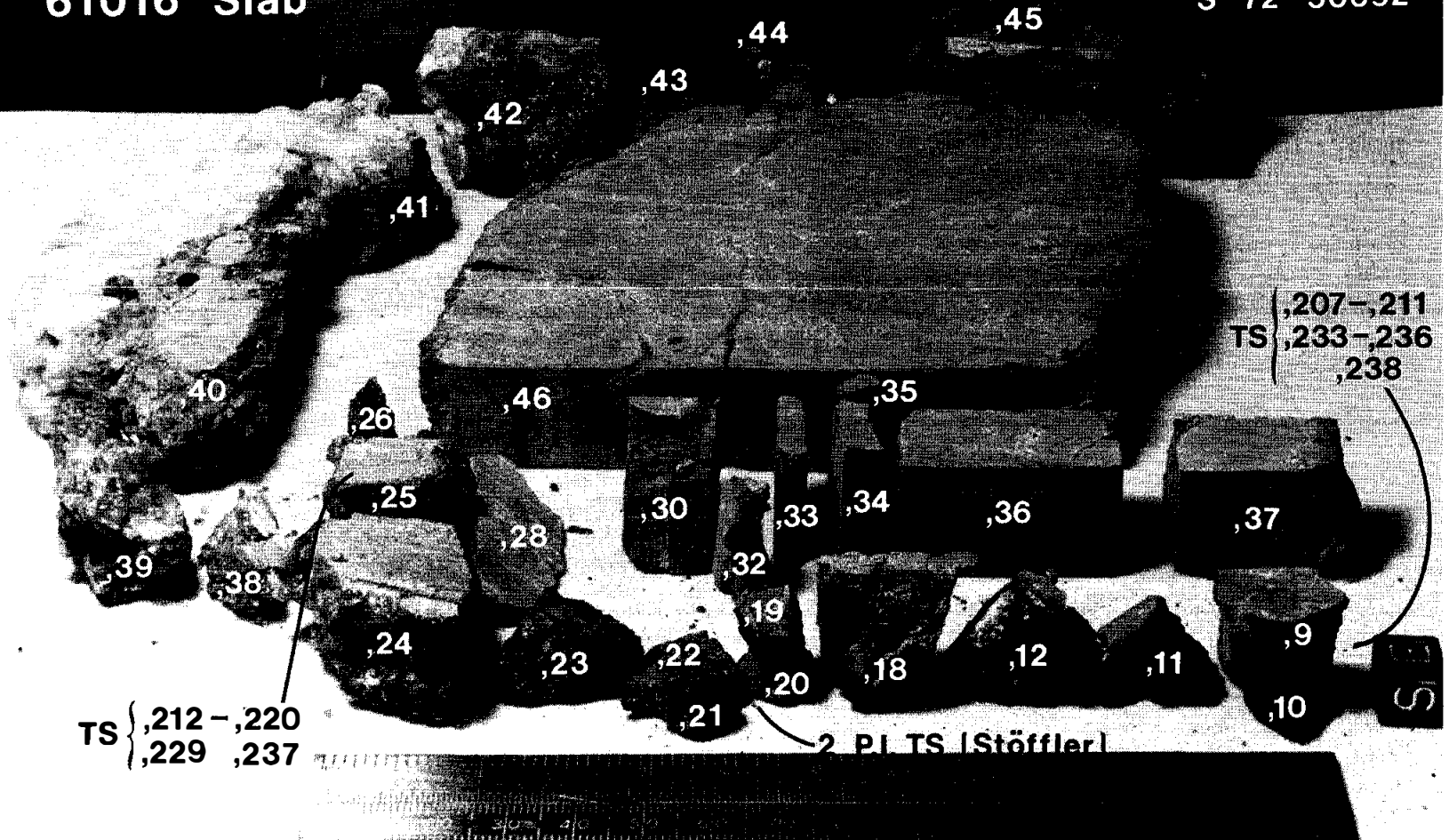
Figure 2. Slab subdivisions.

193
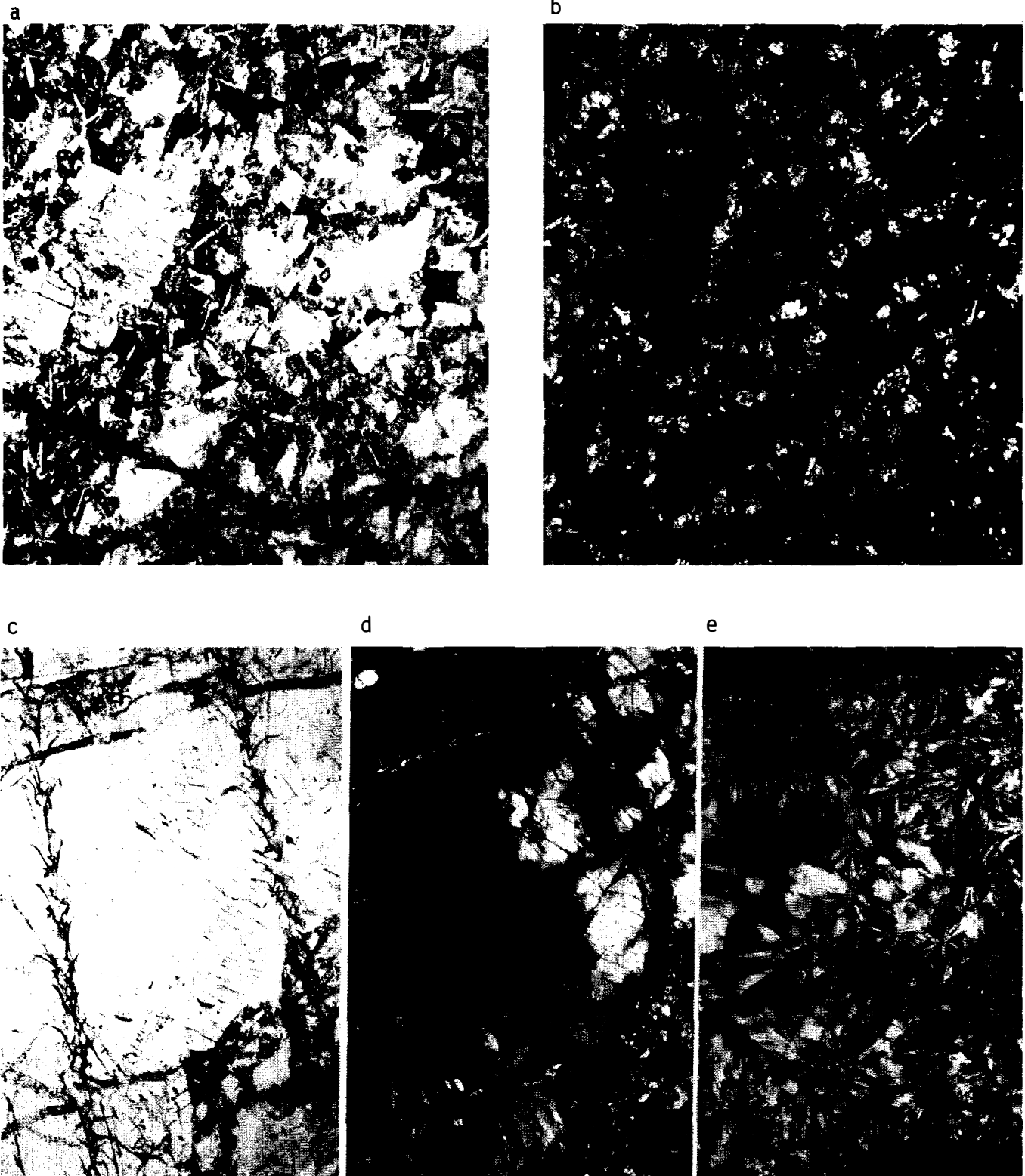
61016

61016



Figure 3. a) 61016,217, basaltic area, ppl. width 2 mm.
b) 61016,217, basaltic area, xpl. width 2 mm.
c) 61016,217, shock-melted anorthositic glass,
ppl. width 1.5 mm.
d) 61016,217, shock-melted anorthositic glass,
xpl. width 1.5 mm.
e) 61016,221, shocked anorthosite, xpl. width 1.5 mm.

194

PETROLOGY:   61016. consists of four lithologies (i) basaltic impact melt, (ii) shocked anorthosite, (iii) shock-melted anorthosite glass and (iv) glass coat (Figs. 1 and 3). A proper appreciation of the published petrographic descriptions requires an understanding of the location of the thin sections studied; these are shown in Figure 2, except for thin sections made from 2 chips of white anorthosite.

Stöffler et al. (1975) give an extensive description of the petrography and petrogenesis of 61016 with emphasis on the basaltic impact melt (referred to as "spinel troctolitic matrix") and the glass coat ("melt crust"). The paper provides microprobe analyses of minerals, metals, glasses, and xenoliths. Drake (1974), McGee et al. (1979) and Juan et al. (1974) describe thin sections which are composed of the impact melt and the anorthosite glass vein (from ,25).

The basaltic impact melt (Fig. 3) consists of anhedral to subhedral olivine (43%), equant to lath-shaped anorthite transformed to diaplectic glass (42%), some tiny spinels, Fe-Ni metal (1.5%) and an opaque mesostasis (14%) consisting of ilmenite, submicroscopic phases and glass (Stöffler et al., 1975). 16% of the basaltic lithology is xenolithic material. Olivine crystals are less than 200 μm and compositions range from $Fo_{79-93}$ (Stöffler et al., 1975; Drake, 1974). Plagioclases are $An_{92-98}$ (Stöffler et al., 1975). Fe-Ni metal (Fig. 4) has 4.24-7.48% Ni and 0.24-0.47% Co (Misra and Taylor, 1975; Stöffler et al., 1975). The compositions of one metal-schreibersite pair indicates equilibrium at ∿650°C (Misra and Taylor, 1975). Engelhardt (1979) notes that ilmenite occurs only in the mesostasis.
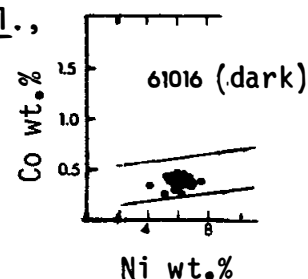


Figure 4. Metals, from Misra and Taylor (1975).

The chemically pristine shocked anorthisite is described by Steele and Smith (1973), Smith and Steele (1974), Stöffler et al. (1975), and Hansen et al. (1979a). It has a complex texture induced by shock metamorphism. Sub-rounded, fine-grained, polycrystalline anorthite "bodies" (Stöffler et al., 1975) are embedded in a mass of spherulitically crystallized anorthite (Fig. 3). Some pyroxene aggregates are present. Plagioclases are $An_{95-97}$ with low abundances of minor elements (Table 1) (Steele and Smith, 1973; Hansen et al., 1979a). Pyroxene blebs have two compositions, $En_{41}Wo_{44}$ and $En_{58}Wo_2$, lacking exsolution features on a 1 μm scale (Steele and Smith, 1973).

TABLE 1:  Minor Elements in 61016 Anorthosite Plagioclases
(Hansen et al., 1979a)

| Sample | Mol % Ab | FeO wt% | MgO wt% | $K_2O$ wt% |
|---|---|---|---|---|
| ,15 | 3.5 | 0.11 | 0.07 | 0.006 |
| ,27 melted | 3.8 | 0.231 | 0.17 | 0.022 |
| ,27 non-melted | 3.8 | 0.121 | 0.051 | 0.023 |

The shock-melted anorthosite glass is described by Juan et al. (1974), Drake (1974) and Dixon and Papike (1975) where it is referred to as the anorthosite. The confusion arises because the relevant thin sections have basaltic impact melt, shock-melted anorthosite, and a large diaplectic plagioclase which is probably a xenocryst in the basaltic melt rather than the anorthosite. The shock-melted anorthosite has the composition of nearly pure plagioclase (verified by our own partial analysis) ($An_{96}$; Drake, 1974; Dixon and Papike, 1975). Some low-Ca pyroxene grains are present with compositions $\sim En_{64}$ (Dixon and Papike, 1975) as well as high-Ca pyroxene and Cr-spinel. Ishii et al. (1976) use pyroxene data from Dixon and Papike (1975) to find an equilibration temperature of 983°C.

The glass crust is described by Stöffler et al. (1975). It contains unshocked anorthite crystals and is connected to glass veins penetrating the rock. In places the glass coat has penetrated and annealed plagioclase in the basaltic impact melt. A temperature gradient of 600°C within about 2 mm is inferred (Stöffler et al., 1975).

CHEMISTRY: Abundant chemical data for 61016 lithologies have been published. In a few cases the lithology analyzed has been erroneously or not specifically reported; Tables 2 and 3 list the references under the correct lithologies. In most cases the analyses are reported without specific comment.

The basaltic impact melt (Table 4) (61016 "dark") is aluminous and siderophile-rich. Ganapathy et al. (1974) place it in their meteorite Group 1. REEs are 45 (light)-20 (heavy) times chondrites i.e., a KREEP pattern (Fig. 5). Although roughly similar to local soils (Laul and Schmitt, 1973), in detail it differs significantly e.g., higher magnesium, lower nitrogen. The impact melt is volatile-enriched but when that enrichment occurred is not defined: Krähenbühl et al. (1973) note that both the impact melt and the anorthosite have similarly high Tl contents, suggesting post-formational enrichment. However, Cd and In are enriched in the impact melt as compared to the anorthosite (Krähenbühl et al., 1973; Wasson et al., 1975) suggesting pre-formational enrichment. While the impact melt has even higher contents of the volatiles Cl and Br than does 66095 (Jovanovic and Reed, 1973; and others), it has much lower abundances of Zn, even lower than local soils.

The anorthosite is almost pure plagioclase (Table 4) and is at least in part pristine (Krähenbühl et al., 1973); some analyses have slightly higher siderophile contents and may be contaminated. This would not be surprising in view of the shock-melting, if some of the analyzed samples include shocked glass. (The Ir content of 1620 ppb given by Hughes et al. (1973) is completely anomalous; because it is 3 times higher than chondrites whereas the corresponding Au, Re contents are $5 \times 10^{-4}$ times chondrites, it is probably erroneous). This pristine chemistry probably does not include volatiles, several of which (e.g., Tl, Cd) are enriched as compared with other ferroan anorthosites.

The glass coat (Table 4) has been analyzed only by the microprobe (Stöffler et al., 1975), thus no trace element data exist. Its major element composition distinguishes it from both local soil and the 61016 basaltic impact melt. It is similar to Station 11 soil.

TABLE 2.  Chemical work on 61016 basaltic impact melt

| REFERENCE | SPLIT ANALYZED | ELEMENTS ANALYZED |
|---|---|---|
| S.R. Taylor et al. (1973) | ,149 | major and traces |
| Duncan et al. (1973) | ,139 | major and traces |
| Janghorbani et al. (1973) | ,133 | majors |
| Rose et al. (1973) | ,150 | major and traces |
| Brunfelt et al. (1973) | ,145 | majors and traces |
| Hubbard et al. (1973) | ,143 | majors and traces |
| Nyquist et al. (1973) | | Rb, Sr |
| Laul and Schmitt (1973) | ,152 | major, traces, siderophiles |
| Nakamura et al. (1973) | ,148 | majors and traces |
| Wänke et al. (1973) | ,151 | majors, traces, siderophiles |
| Wänke et al. (1974) | ,151 | majors, traces, siderophiles |
| Wänke et al. (1977) | ,151 | V |
| Juan et al. (1974) | ,146 | majors and traces |
| Stettler et al. (1973) | ,4 | K, Ca |
| Jovanovic and Reed (1973) | ,131* | F, Cl, Br, I, Li, U, Te |
| Allen et al. (1974, 1975) | ,131* | 204Pb, Bi, Tl, Zn |
| Jovanovic and Reed (1976a) | ,131 | Ru, Os |
| Reed et al. (1977) | ,131 | Zn, Tl |
| Eldridge et al. (1973) | ,120 | K, U, Th |
| Ehmann and Chyi (1974) | ,133 | Zr, Hf |
| Miller et al. (1974) | ,133 | |
| Garg and Ehmann (1976) | ,133 | Zr, Hf, Fe, Co, Sc, Cr, REEs, Th |
| Des Marais (1978) | ,323 | N, S, C |
| Kerridge et al. (1975) | ,159 ,160 | C, S |
| Goels et al. (1975) | ,136 | N |
| Gibson and Moore (1975) | | Volatile gas compounds |
| Rees and Thode (1974) | ,137* | S |
| Krähenbühl et al. (1973) } Ganapathy et al. (1974) } | ,132 | Meteoritic siderophiles and volatiles |

* Erroneously referred to in paper as the anorthosite phase.
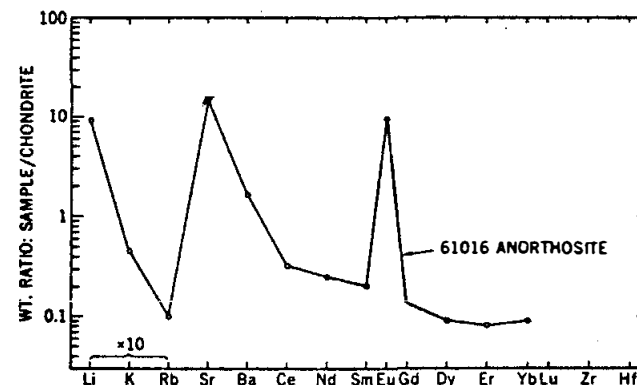


Figure 5. Incompatible elements, from Philpotts et al. (1973).

TABLE 3.  Chemical work on 61016 anorthosite

| REFERENCE | SPLIT ANALYZED | ELEMENTS ANALYZED |
|---|---|---|
| Nava (1974) | ,184 | Majors |
| Philpotts et al. (1973) | ,184 | REEs, Ba |
| Wrigley (1973) | ,173 | K, U, Th |
| Fruchter et al. (1974) | ,180 | Fe, Al, Co, Sc, Cr, REEs |
| Hubbard et al. (1974) | ,79 ,84 | Mg, REEs, other traces |
| Ganapathy et al. (1974) | ,156 | Siderophiles, volatiles |
| Wasson et al. (1975) Baedecker et al. (1974b) | ,161* | Siderophiles, volatiles |
| Hughes et al. (1973) | ,182 | Ni, Ir, Au, Re |
| Tera et al. (1973) | ,84 | K, Rb, Sr |
| Nyquist et al. (1973) | ,79 ,84 | Rb, Sr |
| LSPET (1973) | ,3** | Majors, traces |

* ,161 in data pack is a dark chip.  White chip intended for allocation to Wasson was ,183; the numbers evidently have become reversed.

** Mixed powder, severely contaminated with basaltic impact melt.

198

TABLE 4.  Summary chemistry of lithologies in 61016

| | Basaltic Impact Melt | Anorthosite | Glass Coat |
|---|---|---|---|
| $SiO_2$ | 43.3 | 45.0 | 44.5 |
| $TiO_2$ | 0.76 | 0.02 | 0.17 |
| $Al_2O_3$ | 25.1 | 34.6 | 29.8 |
| $Cr_2O_3$ | 0.10 | 0.01 | |
| FeO | 5.1 | 0.3 | 3.7 |
| MnO | 0.05 | <0.01 | |
| MgO | 10.7 | 0.2 | 4.9. |
| CaO | 14.3 | 19.6 | 15.6 |
| $Na_2O$ | 0.33 | 0.40 | 0.66 |
| $K_2O$ | 0.08 | 0.01 | 0.08 |
| $P_2O_5$ | 0.12 | 0.05 | 0.08 |
| Sr | 160 | 180 | |
| La | 15.3 | 0.1 | |
| Lu | 0.65 | 0.01 | |
| Rb | 2.0 | 0.1 | |
| Sc | 6.6 | 0.5 | |
| Ni | 443 | ∿1.0 | |
| Co | 36 | ∿1.0 | |
| Ir  ppb | 13 | 0.01 ? | |
| Au  ppb | 12 | 0.02 | |
| C | 35 | -- | |
| N | 19 | -- | |
| S | 538 | 100 | |
| Zn | ∿1 | 1.6 | |
| Cu | 4.4 | -- | |

Oxides in wt%; others in ppm except as noted.

STABLE ISOTOPES:  Stable isotope data are only available for the basaltic impact melt.  These data serve to emphasize that the melt is not melted soil.  Rees and Thode (1974) report S isotope data (erroneously referred to as for the anorthosite) showing that $\delta$ $^{34}$S is -0.1 $^o/_{oo}$, much lower than soils ($\sim$+8 $^o/_{oo}$).  Kerridge et al. (1975b) confirm the low value for $\delta$ $^{34}$S (+1.9, +1.3 $^o/_{oo}$).  These latter authors also report $\delta$ $^{13}$C results of -35.7, -32.8 $^o/_{oo}$ (soils +10 $^o/_{oo}$ or higher).  DesMarais (1978) reports $\delta$ $^{34}$C of -30.8 $^o/_{oo}$. Allen et al. (1974) report total $^{204}$Pb (considered stable because of its extremely long half-life) in the impact melt, and consider that non-leachable $^{204}$Pb is partitioned into fine metallic grains.

GEOCHRONOLOGY AND RADIOGENIC ISOTOPES: No Rb-Sr or Sm-Nd internal isochrons exist for any lithologies in 61016, but whole-rock Rb-Sr data are available for both the basaltic impact melt (Table 5) and the anorthosite (Table 6).  The anorthosite clearly was separated from high-Rb reservoirs very early in lunar history.

$^{40}$Ar-$^{39}$Ar data are available for the basaltic impact melt (Stettler et al., 1973) and the shocked anorthosite (Huneke et al., 1977).  A dark split ,4 gave an age of 3.65 ± 0.04 b.y. (Fig. 6) but a good plateau was not attained (Stettler et al., 1973).  Huneke et al. (1977) analyzed both clear and milky "diaplectic glasses" (Fig. 7).  The age spectra are anomalous, and the clear glass is shifted to younger ages, with an apparent age for the milky glass clearly defined at 4.1 b.y. Huneke et al. (1977) suggest that shock melting can result in glass with distinctly different age plateaus.  Neither glass records the true age of the anorthosite.
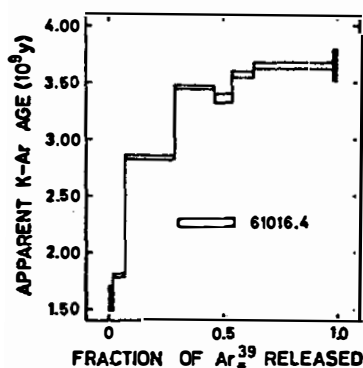


Figure 6. Ar releases of basaltic melt, from Stettler et al. (1973).
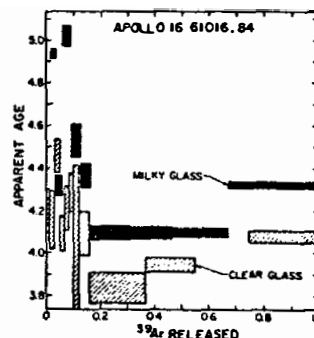


Figure 7. Ar releases of anorthositic glasses, from Huneke et al. (1977).

TABLE 5. Rb-Sr isotopic data for 61016 basaltic impact melt
(from Nyquist et al., 1973)

| Sample | Rb ppm | Sr ppm | $^{87}Sr/^{86}Sr$ | $T_{BABI}$(b.y.) |
|---|---|---|---|---|
| ,143 crystalline | 2.04 | 164.4 | 0.70139±8 | 4.50±0.16 |
| ,79 black glassy | 1.877 | 145.4 | 0.70151±10 | 4.49±0.33 |
| ,3 powder: mixed anorthosite & basalt | 0.446 | 177.9 | 0.69960±9 | 4.8±0.1 |

TABLE 6. Rb-Sr isotopic data for 61016 anorthosite

| Sample | Rb ppm | Sr ppm | $^{87}Sr/^{86}Sr$ | $^{87}Sr/^{86}Sr$* calc. at 4.6 b.y. | Reference |
|---|---|---|---|---|---|
| ,79 gray<br>gray, repeat | 0.017[a] | 179.0 | 0.69906±5[b]<br>0.69906±5[b] | 0.69892±5<br>0.69892±5 | Nyquist et al. (1793) |
| ,79 white<br>white, repeat<br>white, repeat | 0.0377 | 180.4 | 0.69924±40<br>0.69926±22<br>0.69906±4 [b,c] | -<br>-<br>0.69890±4 | Nyquist et al. (1973) |
| ,79 | 0.0250 | 184.7 | 0.69907±3 | 0.69892±3 | Nyquist et al. (1979) |
| ,84 | 0.040 | 181.7 | 0.69907±5[b] | 0.69891±5 | Nyquist et al. (1973) |
| ,84 | 0.032<br>0.044 | 178<br>180 | 0.69900±3<br>0.69900±4 | 0.69897±3<br>0.69895±4 | Tera et al. (1973) |

*Corrected for interlaboratory bias to conform with CalTech data where applicable.
a) Misprinted as 0.167 in original paper.
b) Corrected according to Nyquist et al. (1974, p. 1519) for error caused by tracer.
c) Preferred value for this sample (Nyquist, pers. comm.).

RARE GAS, EXPOSURE AGES AND SURFACES: Stettler et al. (1973) calculate a $^{37}Ar$-$^{38}Ar$ exposure age of <7 m.y. from a dark surface chip. This age is probably affected by $^{37}Cl$ because the Cl content of the rock is high and the exposure age is low. $^{38}Ar$ is produced from $^{37}Cl$ during pile irradiation and this effect is probably responsible for the unusual release curve observed (Stettler et al., 1973).

Rao et al. (1979) use quantitative techniques to isolate the solar cosmic ray-produced Ne and Ar components in three sampling intervals from ,287 (which contains anorthosite and glass surface material). A solar cosmic ray age of 1.7 ± 0.2 m.y. is derived, as well as a galactic cosmic ray age of 3.7 ± 0.3 m.y. An erosion rate of 5 mm/m.y. is assumed.

Fleisher and Hart (1974) studied the particle track record (heavy cosmic ray nuclei). Two dark chips were too heavily shocked to reveal tracks. An anorthosite surface chip has an unusual track density/depth profile suggesting recent loss of a 1 mm chip. Assuming negligible erosion, an exposure age of 20 m.y. is calculated; assuming 0.6 A/year erosion, an exposure age of 40 m.y. is calculated. This is consistent with $^{26}$Al data (Eldridge et al., 1973) which is saturated in the surface indicating exposure of more than a few million years. Bhattacharya and Bhandari (1975), evaluating erosional effects on the track record, derive an exposure age of 1.5 m.y. for the surface chip ,287. Bhandari et al. (1975) calculate an age of 1.2±0.4 m.y. based on large craters, and 0.5 m.y. based on craters less than 80 μm in diameter. They suggest a simple one-stage exposure history. Bhandari et al. (1975, 1976) also measured $^{26}$Al with depth and conclude that there has been little variation in the average solar flare proton production over the last 1.5 m.y.

MacDougall et al. (1973) found no solar flare tracks in either olivine or feldspar in an anorthosite sample.

Mandeville (1976) studied the size distribution of microcraters on a chip of impact melt (,23). The sample has fewer craters than the sample studied by Bhandari et al. (1975) which was on the lunar top of the sample (Fig. 8). Depth/pit diameters are also reported.

Gold et al. (1976a) report auger spectrometer analyses for Fe, Ti, Ca and Si (normalized to 60017 values) for a chip of basaltic impact melt. Fe is enriched in the surface.
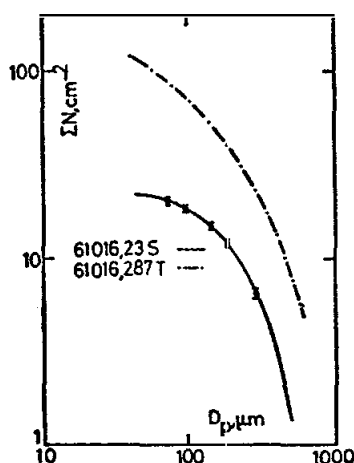


Figure 8. Microcraters, from Mandeville et al. (1976).

PHYSICAL PROPERTIES: Stephenson et al. (1977) tabulate, without comment, magnetic data for a glass chip from 61016. Housley et al. (1976) found that the ferromagnetic remanence (FMR) of a chip of basaltic impact melt (,27) was extremely weak.

Chung and Westphal (1973) provide dielectric constant, dielectric losses, and electrical conductivity data as a function of frequency and temperature. These data (Fig. 9) are for a chip of basaltic impact melt. The seismic data of Chung (1973) are for the same chip. Elastic wave (P-and S-) velocities were measured as a function of pressure as received and in both "dry" and "wet" modes (Table 7, Fig. 10). At low pressures, water increases velocities and drying the sample decreases velocities; this effect is greatest for P-waves. Warren and Trice (1975) use Chung's (1973) data to plot dynamic compressional modulus/density against pressure. They erroneously refer to the data as being for the anorthosite.

Dollfus and Geake (1975) report polarimetric and photometric characteristics of light reflected from a sample of dust-covered, surface basaltic impact melt (,23). The polarization curves resemble lunar fines.
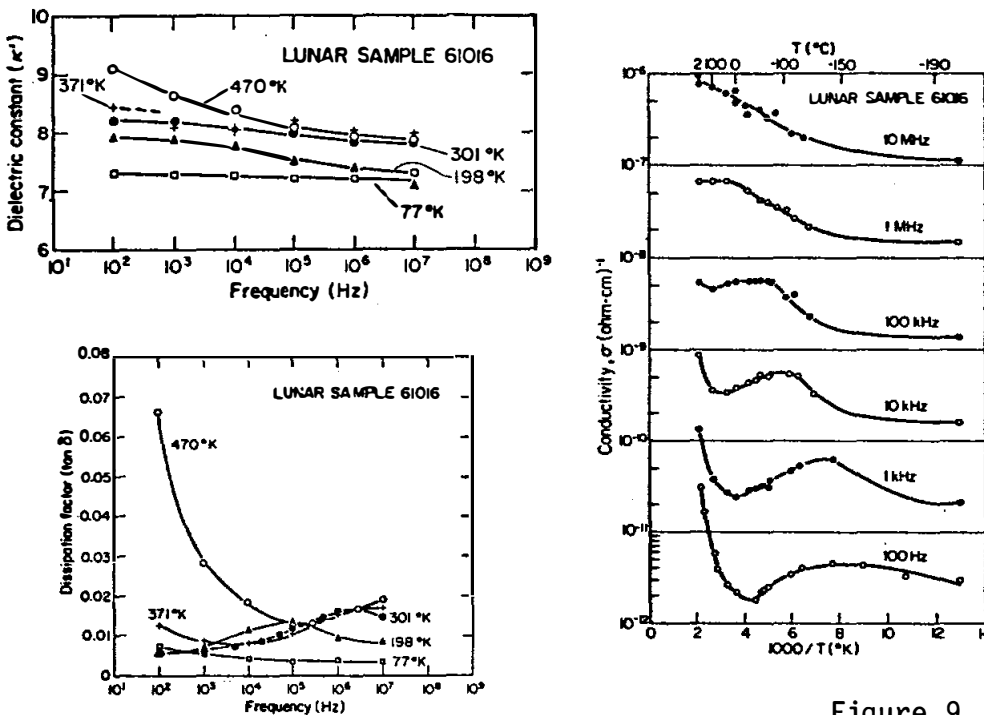


Figure 9. Electrical data, from Chung and Westphal (1973).

| Condition of Sample | Mode | 0.5 | 1.0 | 1.5 | 2 | 3 | 4 | 5 | 6 | 7 | (10)* |
|---|---|---|---|---|---|---|---|---|---|---|---|
| As Received | P | 5.6 | 6.2 | 6.30 | 6.60 | 6.77 | 6.87 | 6.91 | 6.96 | 6.99 | 7.02 |
| (from Table 2) | S | 2.4 | 3.1 | 3.22 | 3.36 | 3.58 | 3.69 | 3.74 | 3.86 | 3.88 | 3.90 |
| | $V_p/V_s$ | 2.3 | 2.0 | 1.96 | 1.96 | 1.89 | 1.86 | 1.84 | 1.80 | 1.80 | 1.80 |
| "dry" (1) | P | 3.75 | 5.23 | 5.32 | 5.72 | 6.23 | 6.41 | 6.70 | 6.97 | 7.00 | 7.02 |
| | S | 2.23 | 3.04 | 3.09 | 3.25 | 3.52 | 3.64 | 3.72 | 3.86 | 3.88 | 3.90 |
| | $V_p/V_s$ | 1.68 | 1.72 | 1.72 | 1.76 | 1.77 | 1.76 | 1.80 | 1.80 | 1.80 | 1.80 |
| "wet" (2) | P | 6.5 | 6.70 | 6.73 | 6.75 | 6.78 | 6.88 | 6.91 | 6.97 | 6.99 | 7.03 |
| | S | 2.4 | 3.10 | 3.23 | 3.36 | 3.58 | 3.69 | 3.74 | 3.86 | 3.88 | 3.90 |
| | $V_p/V_s$ | 2.7 | 2.16 | 2.09 | 2.01 | 1.89 | 1.86 | 1.84 | 1.80 | 1.80 | 1.80 |

TABLE 7. Seismic data, from Chung (1973).

*Estimated by a linear extrapolation of high-pressure velocity data.

(1) The term "dry" refers to the state of sample 61016 as it was heated in vacuum at 400°C for 10 hours and slowly cooled down to ambient temperature.

(2) The term "wet" refers to a water-saturated sample 61016.
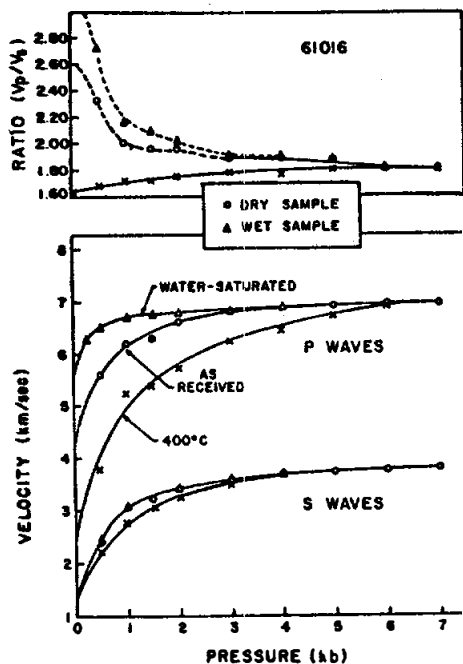
Figure 10. Seismic data, from Chung (1973).

PROCESSING AND SUBSIVISIONS: 61016 has been extensively subdivided. In 1972 a slab was cut from the rock producing two end pieces ,7 and ,8 (Figs. 1 and 11). ,7 remains essentially intact. The slab has been extensively dissected (Figs. 2 and 11) and ,8 has been totally subdivided into numerous daughters (not shown).
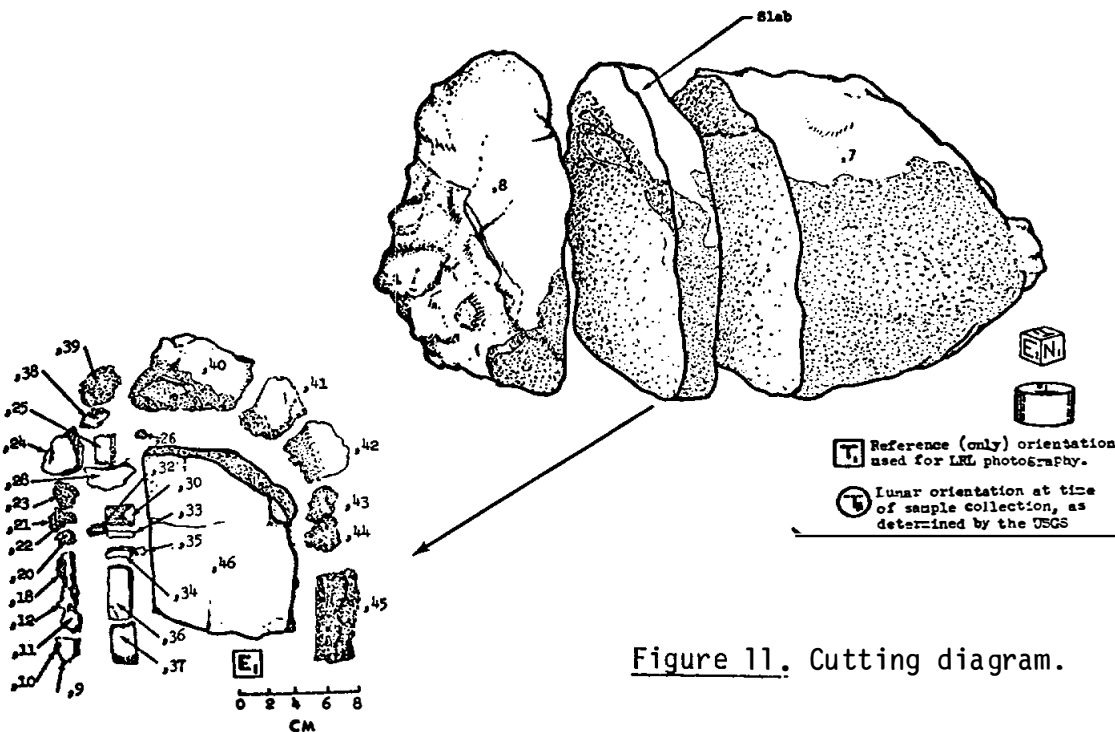


Figure 11. Cutting diagram.

INTRODUCTION:  61017 is a friable, fractured piece of cataclastic anorthosite
(Fig. 1).  It is almost pure white with rare black and yellow flecks.  61017
was a loose sample in the sample return container from the first extravehicular
activity on the mission.  Its lunar location is unknown and it could be from
Station 1, 2, or from the ALSEP (Apollo Lunar Surface Experiments Package)
site.  At least one zap pit is present and part of the surface either has a
patina or adhering soil.



Figure 1. 61017,0. Smallest scale division 0.5mm.

INTRODUCTION:   61135 is a friable, light gray breccia (Fig. 1) containing a diverse population of mineral and lithic fragments.

This sample was collected from the northeast rim of Plum Crater.   Lunar orientation is known.   A few zap pits are present on some surfaces.
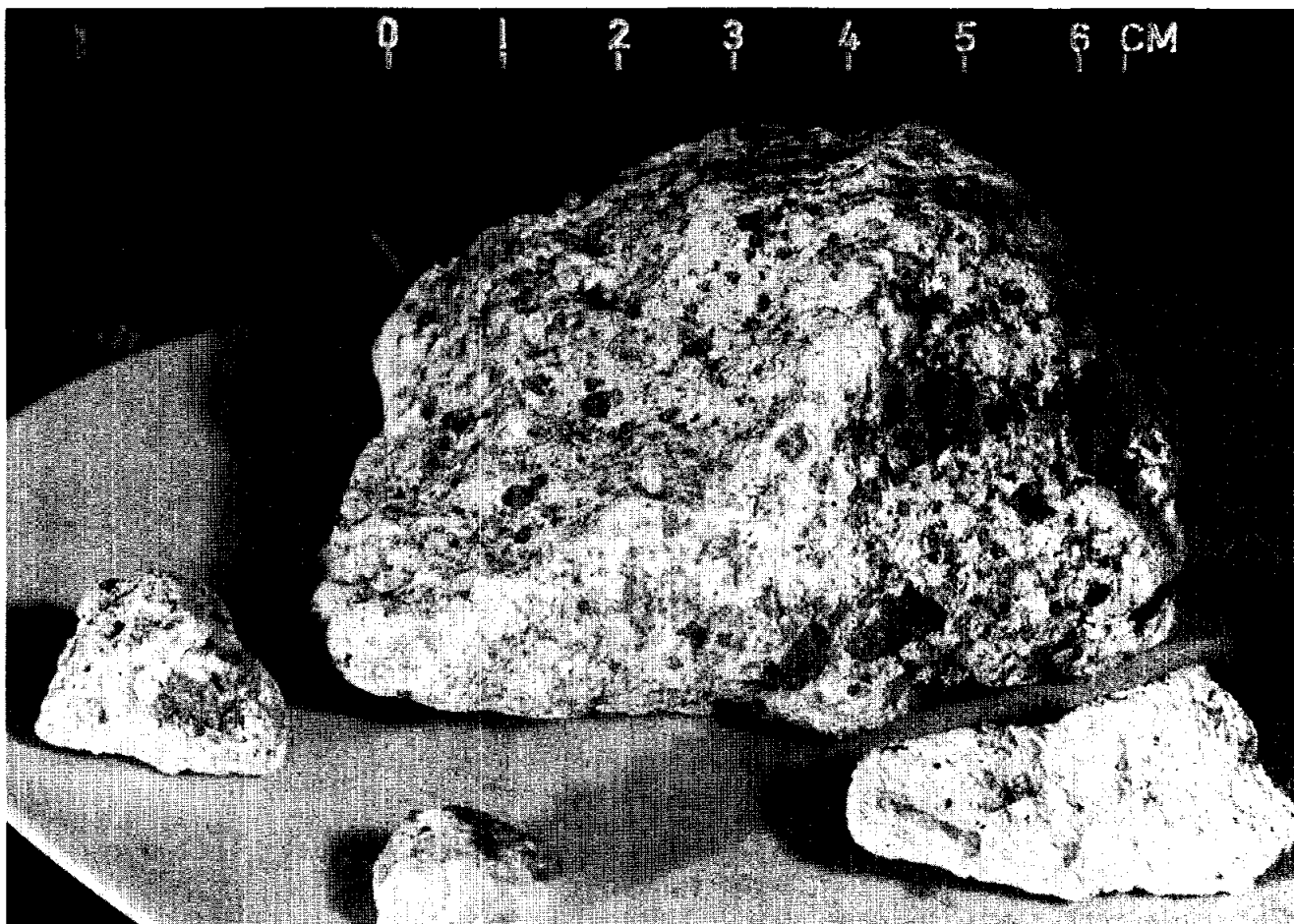


Figure 1.  61135,0.  S-72-38316.

PETROLOGY: 61135 is a clastic, unrecrystallized breccia composed of various mineral and lithic fragments welded together by a small amount of glass (Fig.2). Angular grains of both shocked and unshocked plagioclase dominate the mineral fragment population.   Mafic minerals, Fe-metal, troilite and ilmenite clasts are much less common.   Lithic fragments include granoblastic anorthosite and noritic anorthosite (up to $\sim$3 mm), basaltic and poikilitic impact melts, and clast-rich, glassy matrix breccia.   Brown and clear glass beads and fragments are abundant and indicate a significant regolith component in this rock.
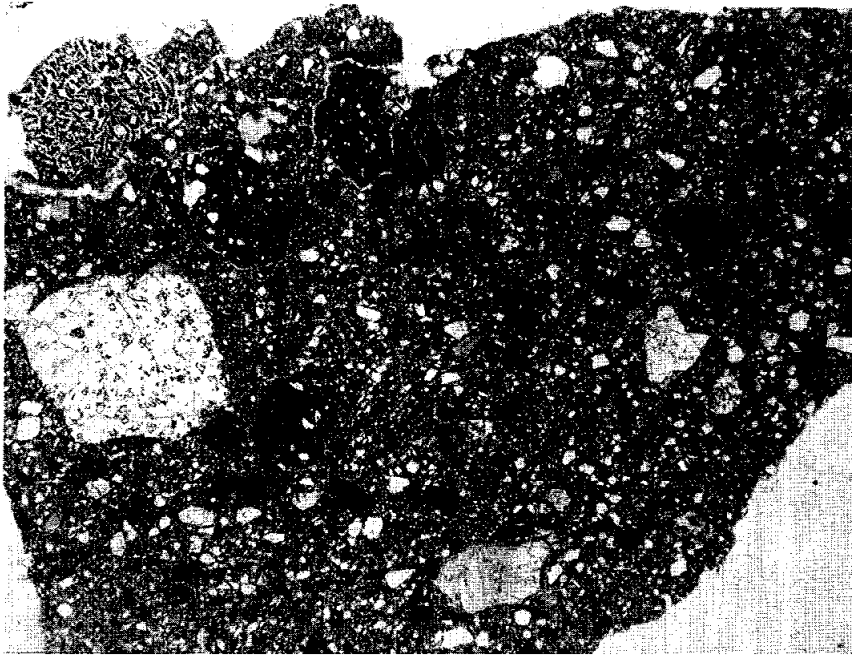
61135



Figure 2. 61135,7, general view, ppl. width about 15mm.

CHEMISTRY:    Eldridge et al. (1973) report whole rock K-U-Th and cosmogenic radionuclide abundances.  Ca and K data for three splits are provided by Schaeffer and Schaeffer (1977) in a K-Ar geochronological study.  Total N and C in a bulk sample are given by Moore and Lewis (1976).

The whole rock gamma ray data show 61135 to be poor in natural radionuclides (690 ppm K, 0.38 ppm U, 1.39 ppm Th). A randomly-picked sample and a split of fine powder analyzed by Schaeffer and Schaeffer (1977) show K abundances very similar to the whole rock value of Eldridge et al. (1973) and Ca levels indicative of nearly pure plagioclase (Table 1). The third split analysed by Schaeffer and Schaeffer (1977) was a single coherent fragment considerably enriched in K and depleted in Ca relative to the other samples (Table 1).  No further information on the nature of these samples is available.

RADIOGENIC ISOTOPES/GEOCHRONOLOGY:  Schaeffer and Schaeffer (1977) give K-Ar data for three splits.  Two of the samples, a randomly-picked split and a split of fine powder, contain considerable amounts of trapped gas and did not give $^{40}Ar$-$^{39}Ar$ plateaus.  The third sample, a single coherent fragment, yielded a plateau age of 3.90 ± 0.10 b.y.

TABLE 1. Summary chemistry of 61135 lithologies

|        | Bulk rock | K-rich fragment |
|--------|-----------|-----------------|
| CaO    | 18.9      | 11.8            |
| $K_2O$ | 0.088     | 0.58            |
| C      | 54        |                 |
| N      | 55        |                 |

Oxides in wt%; others in ppm.

RARE GAS/EXPOSURE AGES: [26]Al-[22]Na whole rock data are provided by Eldridge et al. (1973). From these data Yokoyama et al. (1974) could not decide whether 61135 is saturated in [26]Al or not.

Ar data are given by Schaeffer and Schaeffer (1977) for three splits: a randomly picked sample, a split of fine powder, and a single coherent fragment. The first two samples contained considerable trapped gas, probably residing in the fine matrix of the rock. [38]Ar exposure ages of these two splits are given as 61 m.y. and 44 m.y. (Schaeffer and Schaeffer, 1977, Table 6 ). The third split gave an average [38]Ar exposure age of 28 m.y., but due to the extreme variability of the exposure age measured over the [40]Ar-[39]Ar plateau temperature range (1800 m.y. at 400°C to 4 m.y. at 1150°C), the average age reported probably has little significance. A trapped [38]Ar component is also suggested by Schaeffer and Schaeffer (1977)

PROCESSING AND SUBDIVISIONS: 61135 was removed from its Documented Bag in 1972 as one large piece (,1) plus three smaller pieces (,2-,4) and some fine residue (,5). Schaeffer received 1 g of chips from ,5 in 1973. In 1975 ,2 and ,3 were subdivided for further allocations. The large piece ,1 (221.96 g) remains in stock at JSC.

INTRODUCTION: 61155 is a moderately coherent, medium gray, glassy impact melt with abundant white clasts (Fig. 1). At least two sets of perpendicular fractures and a series of thin, short (~5 mm) glass veins cut the rock. A slickenside is present on the B surface.

61155 was collected ~25 m northeast of Plum Crater. Zap pits are abundant on two surfaces, rare to absent on the other surfaces.

PETROLOGY: 61155 is a glassy impact melt that is very clast-rich (Fig. 2). In places the matrix texture approaches poikilitic. Oikocrysts (~0.3 mm) are separated from one another by a concentration of relatively large clasts of plagioclase. Glassy mesostasis is abundant. Clasts include fragments of basaltic impact melt and cataclastic anorthosite. Fe-metal, troilite and ilmenite are accessory phases.



Figure 1. 61155,0. Scale is cm. S-72-38371.
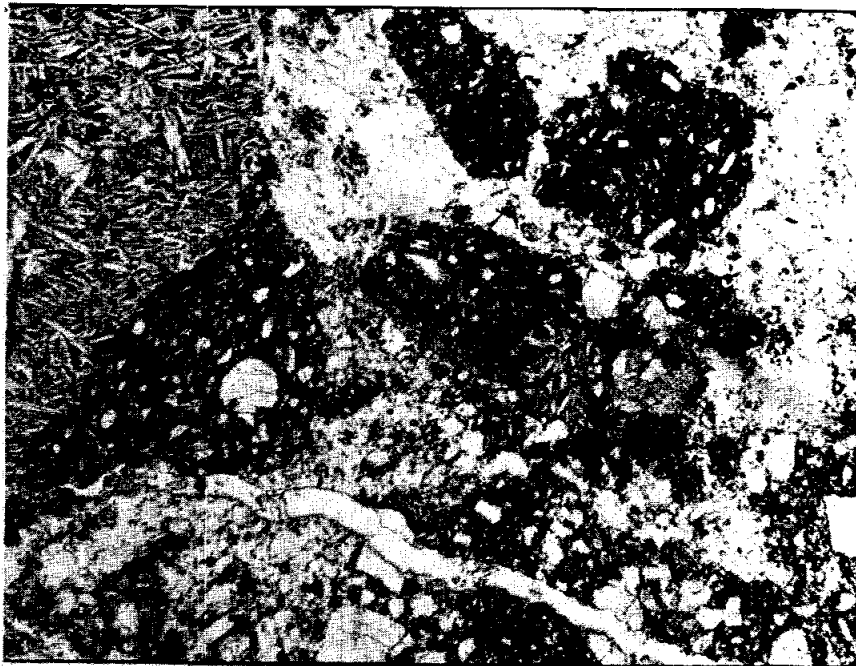
Figure 2. 61155,7, general view, ppl. width 3mm.

CHEMISTRY: Eldridge et al. (1973) provide whole rock K(445 ppm), U(0.31 ppm) and Th(1.12 ppm) abundances by gamma ray spectroscopy.

EXPOSURE AGE: Eldridge et al. (1973) provide $^{26}$Al and $^{22}$Na data. From these data Yokoyama et al. (1974) conclude that 61155 is saturated in $^{26}$Al, indicating an exposure age of at least a few million years.

PROCESSING AND SUBDIVISIONS: In 1972 several chips were removed and one of these (,3) allocated for thin sections.

INTRODUCTION: 61156 is a tough, medium gray, poikilitic impact melt rock that has been thermally metamorphosed. Macroscopically the rock is blocky and angular; few clasts are apparent (Fig.1). Metal spherules and small vugs (<0.5 mm) are inhomogeneously distributed throughout the rock. There are many zap pits on the "lunar up" surface, few on other surfaces. This sample was collected 25 m northeast of Plum Crater.
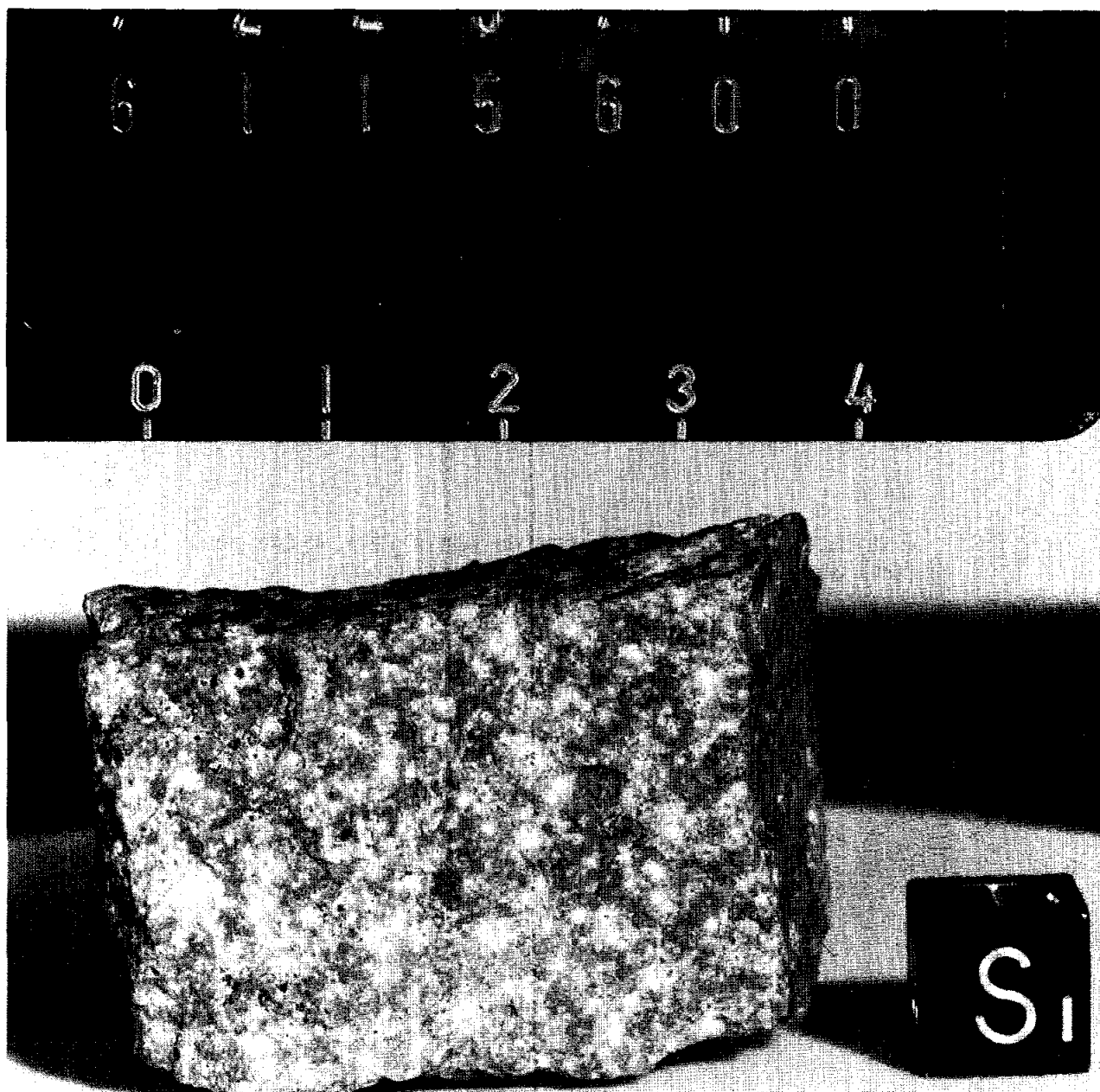


Figure 1. 61156,0. Scale is cm. S-72-38391.

PETROLOGY: Petrographic information is given by Albee et al. (1973), Simonds et al. (1973),and the Apollo 16 Lunar Sample Information Catalog (1972). Haggerty (1973) provides detailed microprobe analyses and descriptions of armalcolite and other oxides. Meyer et al. (1974) determined trace elements in plagioclase xenocrysts by ion microprobe. Metal compositions from an anorthositic clast and the poikilitic host are reported by Hewins and Goldstein (1975a)

61156 is a fine-grained, meta-poikilitic rock with several small (50-200 μm) plagioclase and pyroxene xenocrysts and at least one large (>10 mm) clast of anorthositic breccia. Modal data are presented by Albee et al. (1973) and the Apollo 16 Lunar Sample Information Catalog (1972) and reproduced here as Table 1. In the poikilitic host,mineral grains are anhedral and granular (Fig. 2) suggesting that the rock has undergone a period of extensive subsolidus annealing. Two types of poikilitic texture are randomly distributed throughout the rock. Most commonly, anhedral orthopyroxene oikocrysts (up to ~1 mm, averaging ~100 μm) enclose small, rounded, elongate to equant plagioclase crystals (20-50 μm). Pyroxene oikocrysts, however, are not as abundant in 61156 as in most of the other Apollo 16 poikilitic rocks. The second, less common poikilitic texture in this rock is characterized by an interlocking network of anhedral plagioclase grains (usually <50 μm) intergrown with small, equant grains of olivine and (rarely) high-Ca pyroxene (up to ~50 μm). Many of these mafic grains are optically continuous over an area generally <0.5 mm. Olivine and high-Ca pyroxene are not included within the orthopyroxene oikocrysts. K-rich patches are scattered throughout the rock but are never found within oikocrysts. Minerals are homogeneous and largely equilibrated (Fig. 3). Ridley and Adams (1976) calculate a termperature of equilibration of 1010°C for coexisting olivine and augite.



a

b
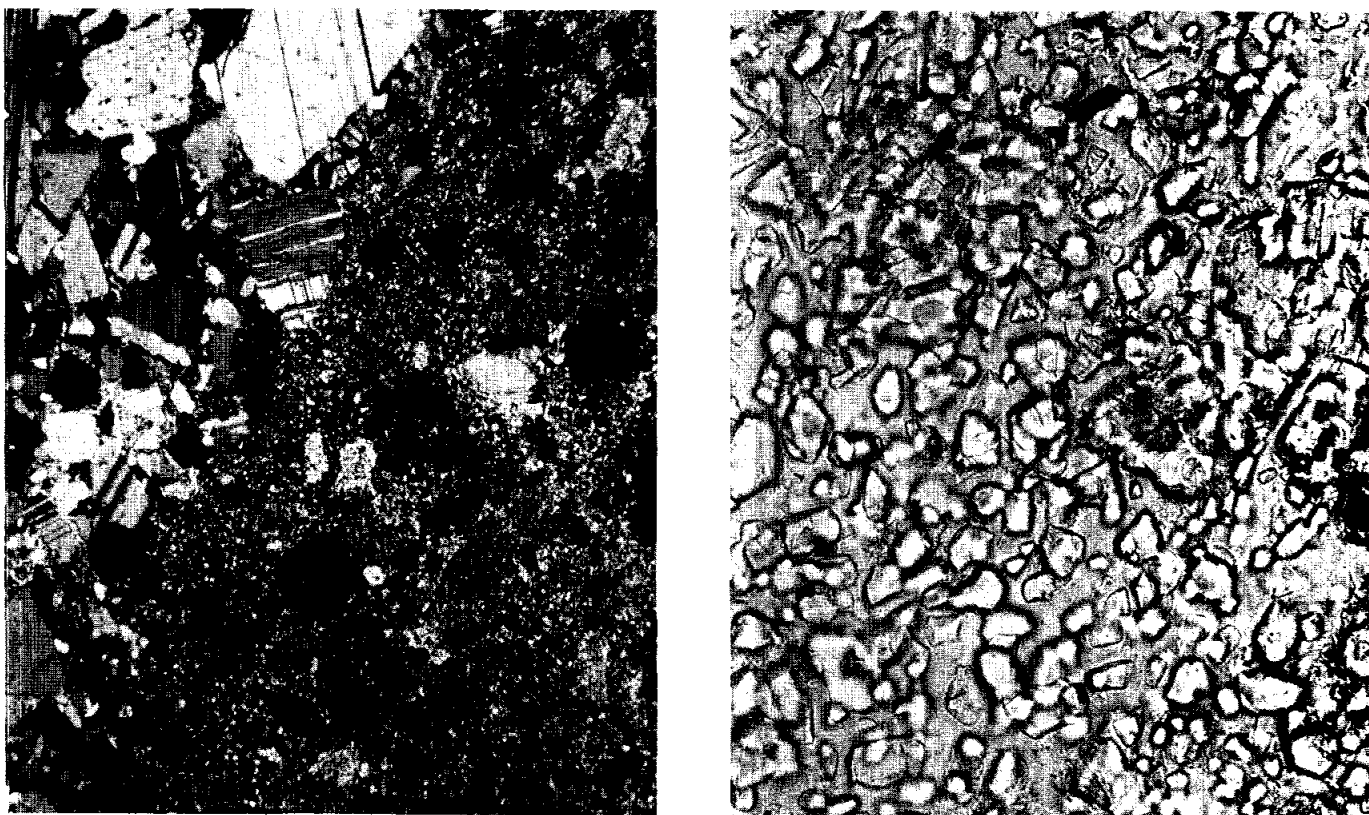
Figure 2. 61156,30. a) general view, xpl. width 2mm.
b) poikilitic area, ppl. width 0.2mm.

TABLE 1

Modal data for 61156

| | 61156,5 (1300 pts; Apollo 16 Lunar Sample Information Catalog,1972) | 61156,31 (1990 pts; Albee et al., 1973) vol% | wt% |
|---|---|---|---|
| orthopyroxene | 25.9 | 20.6 | 23.0 |
| oikocryst | 18.4 | | |
| xenocryst | 7.5 | | |
| plagioclase | 59.5 | 62.1 | 55.4 |
| in oikocrysts | 15.0 | | |
| surrounding olivine | 38.0 | | |
| xenocryst | 6.5 | | |
| olivine | 11.7 | 10.2 | 12.9 |
| high-Ca pyroxene | | 5.1 | 5.6 |
| metal | 1.0 | 0.3 | 0.9 |
| other opaques | 1.9 | 0.6 | 1.2 |
| phosphates | | 0.3 | 0.3 |
| K-rich interstices | | 0.6 | 0.5 |

A wide variety of opaque and other accessory phases occur within the poikilitic portions of 61156, including ilmenite, armalcolite, Cr-spinel, rutile, baddelyite, metal, troilite and schreibersite. Oxides often form complex associations, probably representing the decomposition of some pre-existing oxide phase (Albee et al., 1973; Haggerty, 1973). Ilmenite plates are apparently not related to the development of oikocrysts. Metal occurs principally as 100-400 μm globules and is very homogeneous in composition (Fig.4).

Xenocrysts of plagioclase and low-Ca pyroxene account for $\sim$ 15% of the rock. Many of these plagioclase clasts have calcic cores ($An_{95-97}$) rimmed by overgrowths of the same composition as in the poikilitic host ($An_{87-93}$). Trace elements in plagioclase clasts as determined by ion microprobe (Meyer et al., 1974) are presented in Table 2. Ba in these clasts is significantly below the initial Ba expected by in situ crystallization.

TABLE 2

Trace elements in plagioclase xenocrysts in 61156

| | | |
|---|---|---|
| $Na_2O$ | 0.39 | wt% |
| Li | 5 | |
| Mg | 400 | |
| K | 760 | |
| Ti | 110 | |
| Sr | 150 | |
| Ba | 18 | |

All data in ppm except as noted (from Meyer et al., 1974)

61156- PLAGIOCLAS

KAlSi₃O₈

$BaAl_2Si_2O_8$ +
$FeAl_2Si_2O_8$ +
$MgAl_2Si_2O_8$

Or₅

NaAlSi₃O₈   An₈₅   An₉₀   An₉₅   CaAl₂Si₂O₈
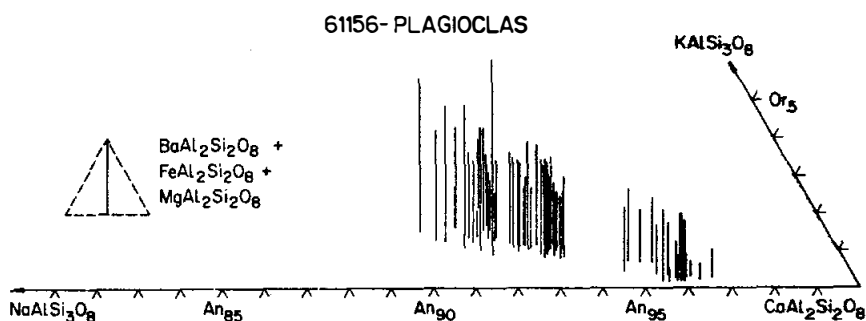
**Figure 3.** Mineral compositions, from Albee *et al*. (1973).

CaMgSi₂O₆   Ca(Fe, Mn)Si₂O₆

61156 - PYROXENE

$NaAlSi_2O_6$ + $CaTiAl_2O_6$
+ $CaCrAlSiO_6$ + $CaAlAlSiO_6$

Mg₂Si₂O₆   (Fe, Mn)₂Si₂O₆

Number
of analyses   20
10

OLIVINE

ARMALCOLITE

ILMENITE

Mg   Fe+Mn
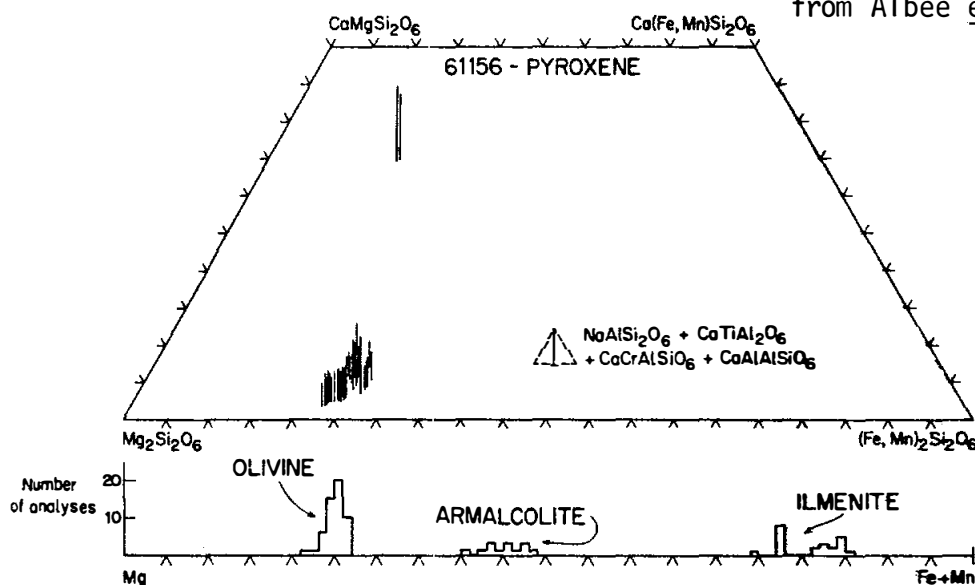
At least one large (>10 mm) clast of anorthositic breccia is also found in 61156. It consists of angular, well-twinned plagioclase (An₉₅; up to 1 mm) which has been coarsely crushed. Interstitial mafics are rare but, where present, tend to show a poikilitic texture around smaller plagioclase grains within the clast. The clast-matrix boundary is irregular with matrix sometimes penetrating along grain boundaries of the clast. Metal in the clast is of the same composition as that in the poikilitic host (Fig.4) (Hewins and Goldstein, 1975a).

CLAST IN
61156,30

61156,30
POIKILITIC HOST
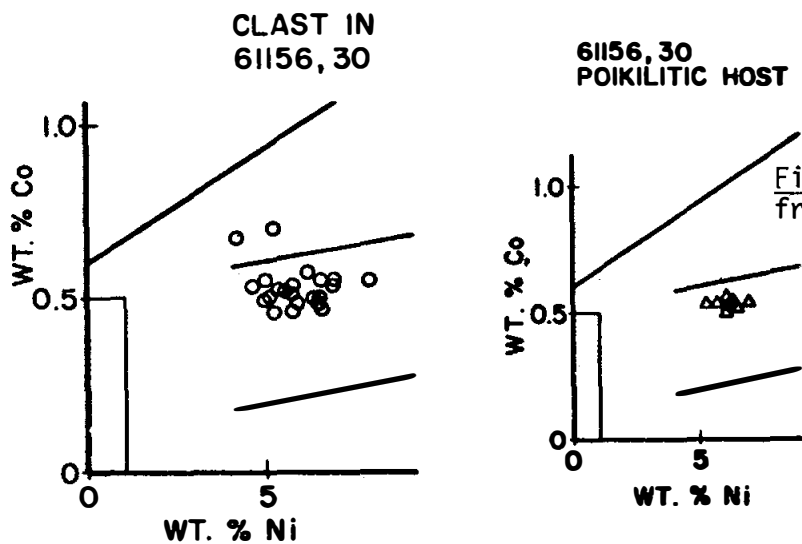
**Figure 4.** Metal compositions. from Hewins and Goldstein (1975a).

CHEMISTRY: Major and trace element analyses are given by Hubbard et al.(1973), Wänke et al. (1974) and LSPET (1973). Albee et al. (1973) calculate a major element bulk composition based on a mode and mineral analyses. Eldridge et al. (1973) provide data on natural and cosmogenic radionuclides. Rb, Sr and U, Th, Pb data are presented by Nyquist et al. (1973) and Tera et al. (1974) respectively.

Compositionally, 61156 is more similar to Apollo 16 basaltic melt rocks than to the other poikilitic melt rocks. It is more aluminous than most other poikilitic rocks (Table 3), plotting on the plagioclase-spinel cotectic in the system olivine-anorthite-silica (Fig. 5). Rare earth elements (Fig. 6) are moderately enriched over local soils but are significantly less than in the KREEP-rich poikilitic rocks such as 62235 and 60315. Siderophiles indicate a significant, though variable, meteoritic content (Table 3). This variation in levels of siderophiles is almost certainly due to the inhomogeneous distribution of metal.

TABLE 3. Summary chemistry of 61156

| | |
|---|---|
| $SiO_2$ | 45.0 |
| $TiO_2$ | 0.64 |
| $Al_2O_3$ | 23.0 |
| $Cr_2O_3$ | 0.13 |
| FeO | 7.8 |
| MnO | 0.11 |
| MgO | 9.7 |
| CaO | 13.5 |
| $Na_2O$ | 0.40 |
| $K_2O$ | 0.108 |
| $P_2O_5$ | 0.22 |
| Sr | 154 |
| La | 21.5 |
| Lu | 0.90 |
| Rb | 2.43 |
| Sc | 9.36 |
| Ni | 184-1190 (?) |
| Co | 59.4 |
| Ir ppb | 23 |
| Au ppb | 22 |
| C | |
| N | |
| S | 1200 |
| Zn | 5.0 |
| Cu | 6.6 |
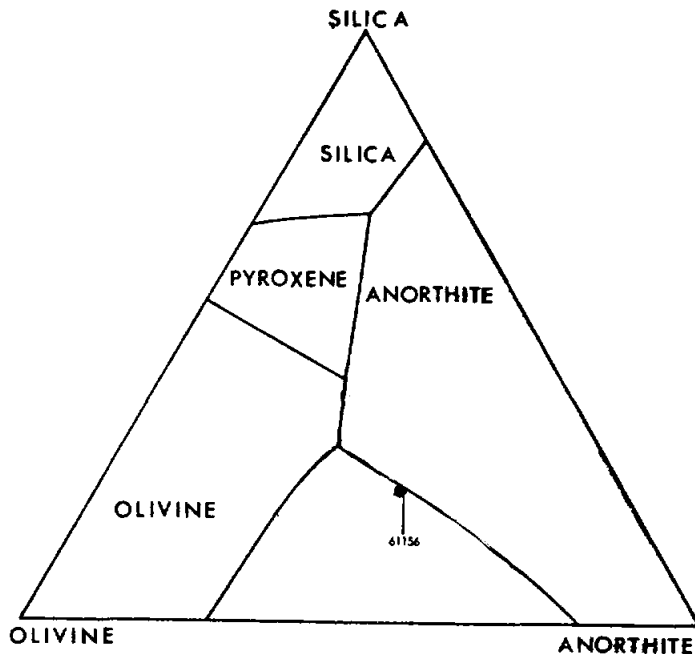


Figure 5. From Simonds et al. (1973).

Oxides in wt% ; others in ppm except as noted.

**61156**

Wänke *et al.*, 1974

Hubbard *et al.*, 1973

,35

,2

La Ce Pr Nd Pm Sm Eu Gd Tb Dy Ho Er Tm Yb Lu
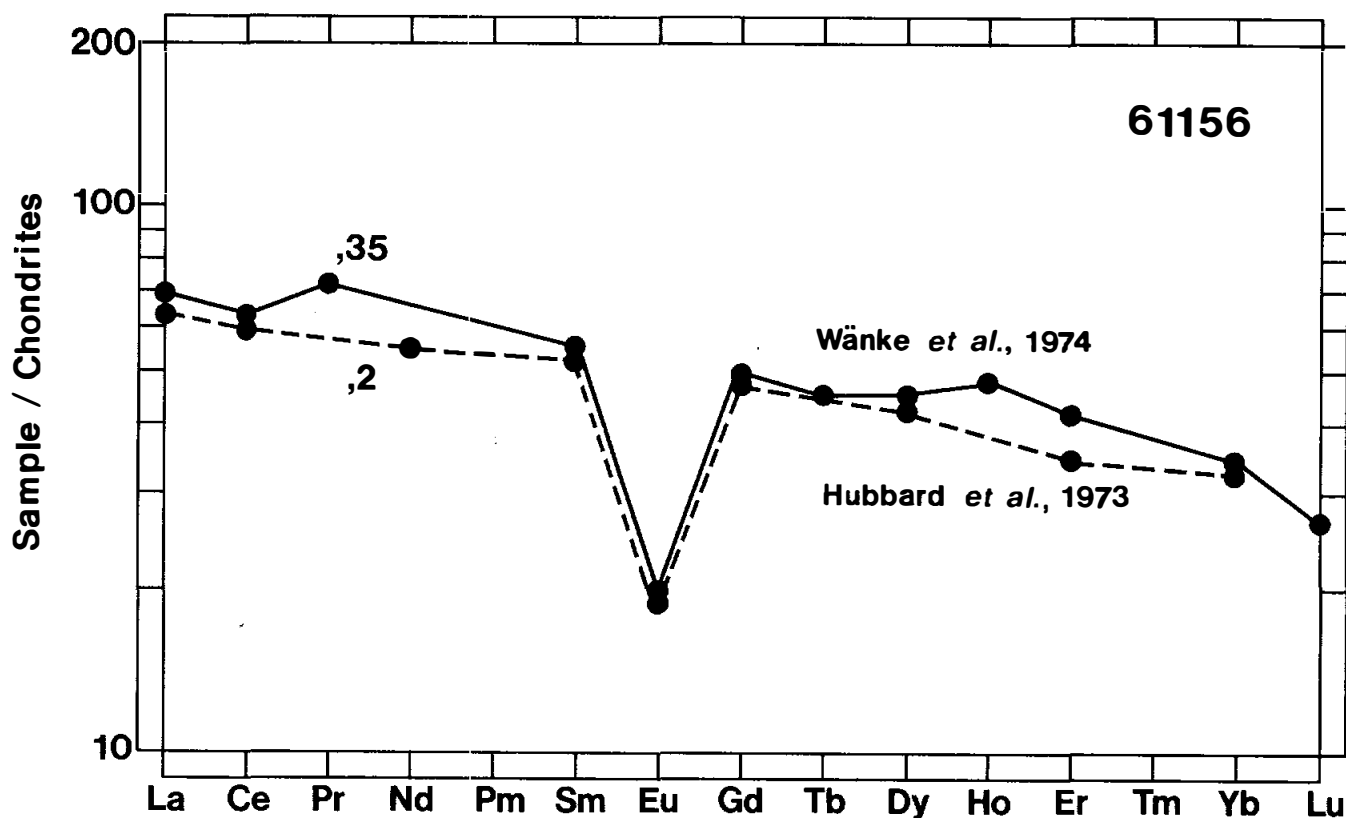
Figure 6. Rare earths.

TABLE 4. Summary of isotopic data on 61156

| $^{87}Rb/^{86}Sr$ | $^{87}Sr/^{86}Sr$ measured | $^{87}Sr/^{86}Sr$ at 4.6 b.y.* | $T_{BABI}$ (b.y.) | $T_{LUNI}$ (b.y.) | Reference |
|---|---|---|---|---|---|
| 0.0451 | 0.70202+8 | 0.69949 | 4.66+.12 | | Tera et al.(1974) |
| 0.0462+4 | 0.70217+5 | 0.69948 | 4.63+.11 | 4.77+.11 | Nyquist et al.(1973) |

*extrapolated from 3.9 to 4.6 b.y. and corrected for interlaboratory bias by Nyquist (1977)

U-Th-Pb model ages (b.y.)

| $^{207}Pb/^{206}Pb$ | $^{206}Pb/^{238}U$ | $^{207}Pb/^{235}U$ | $^{208}Pb/^{232}Th$ | Reference |
|---|---|---|---|---|
| 4.24 | 4.21 | 4.23 | 3.88 | Tera et al. (1974) |

RADIOGENIC ISOTOPES AND GEOCHRONOLOGY: Nyquist et al. (1973) report whole rock Rb-Sr isotopic data. Tera et al. (1974) provide whole rock Rb-Sr and U-Th-Pb isotopic data.

The data are summarized in Table 4. Notable are the old model ages calculated from Rb-Sr systematics. U-Pb isotopes do not show such old model ages. The whole rock analysis of Tera et al. (1974) is within error of concordia at 4.24 b.y.

MICROCRATERS: Neukum et al. (1973) provide size-frequency data (Fig.7). They conclude that the surface of 61156 is in production.
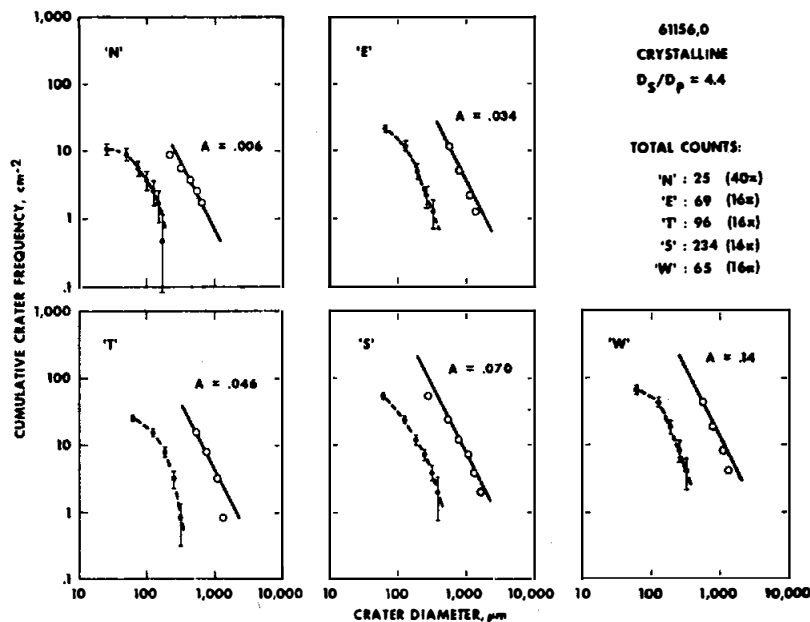


Figure 7. Microcraters, from Neukum et al. (1973).

PHYSICAL PROPERTIES: Intrinsic and remanent magnetic parameters were measured on two splits of 61156 by Nagata et al. (1974) using hysteresis and AF-demagnetization techniques. They find no significant residue of NRM after 150 Oe-rms demagnetization. Greater than 90% of the metal in 61156 is kamacite with 4-6% Ni. Schwerer and Nagata (1976) determined size distribution data for metallic particles in the 0.003-0.15 μm (30-150 Å) size range using magnetic granulometry. The mean grain size of fine-grained metal in this rock is 37 Å.

Huffman et al. (1974) present Mossbauer and magnetic analyses of the same two splits studied by Nagata et al. (1974) These results are summarized in Table 5.

TABLE 5

Distribution of Fe in the mineral phases of 61156*(Huffman et al.,1974)

| Sample | pyroxene | olivine | ilmenite | troilite | metal | wt% metal |
|---|---|---|---|---|---|---|
| 61156,11 | 57.9 | 34.2 | 2.8 | 2.8 | 2.2 | 0.70 |
| 61156,12 | 49.3 | 43.9 | 2.0 | 1.8 | 2.9 | 1.76 |

*percentage of total Fe

PROCESSING OF SUBDIVISIONS: In 1972, 61156,0 was chipped to produce ,1 ,2 and ,4 from the N surface. In 1973, the largest piece remaining (61156,0) was entirely subdivided to produce ,3 and ,9-,13 (Fig.7). ,9-,12 came from the W half of ,0. ,13 is the E end of ,0 and is now the largest single piece remaining (43.4 g). Other splits have since been made from the chips.
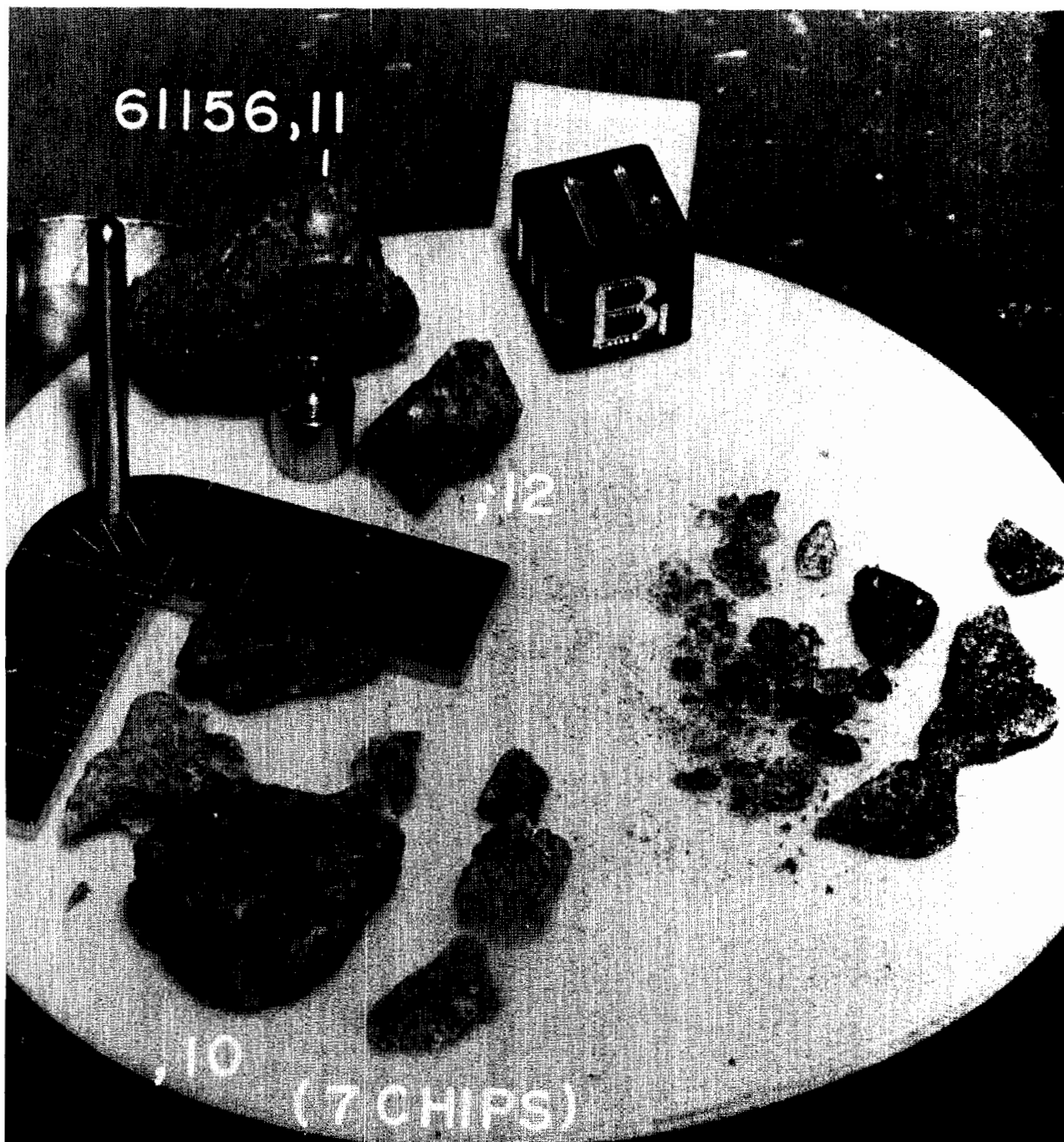


Figure 8. S-72-53534.

INTRODUCTION:  61157 is an irregularly shaped fragment of pale medium gray,
fragmental breccia (Fig. 1).  It is fairly coherent and fractured with some
planar surfaces.  It contains dark and light colored angular clasts, all of
which are small.  61157 was taken from the regolith 25 m northeast of
Flag Crater.  Its surfaces have some patina and zap pits.



Figure 1. 61157,0. Smallest scale subdivision 0.5mm

INTRODUCTION:   61158 is a pale gray, friable, polymict breccia (Fig. 1).   It contains small dark and light-colored fragments.   The sample was taken from the regolith 25 m northeast of Flag Crater.   It has rare zap pits.

PROCESSING AND SUBDIVISIONS:   A part of 61158 has been numbered separately as ,1 (4.00 g).



Figure 1. 61158,0



61158,1. Smallest scale subdivision 0.5mm.

INTRODUCTION:  61175 is a friable, gray matrix breccia (Fig. 1) with a wide variety of clast types.  It is subrounded in shape,and homogeneous in color and texture.

61175 was collected near the northeast rim of Plum Crater, and its orientation is known.  Zap pits are abundant on the "lunar up" surface and rare to absent on other surfaces.
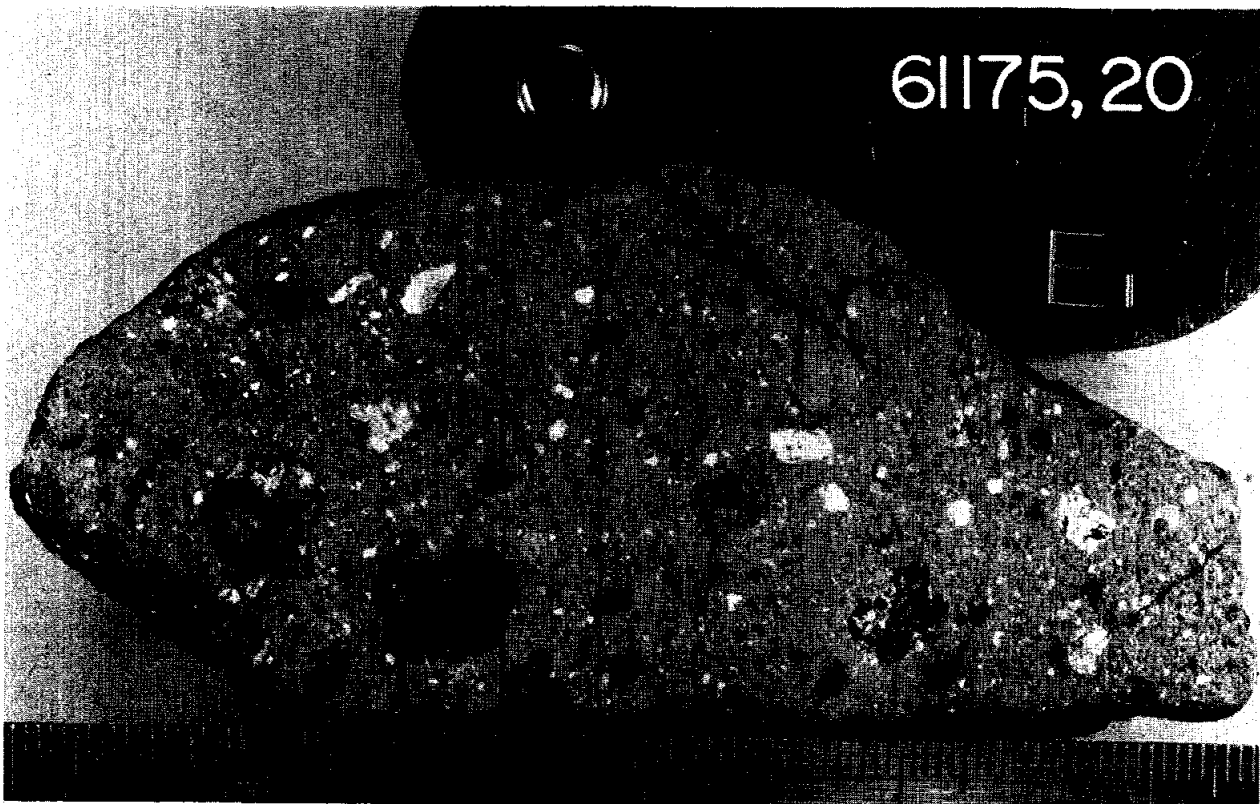


Figure 1. S-78-31342, mm scale.

PETROLOGY: Winzer et al. (1977) provide detailed petrographic information. A variety of mineral and lithic clasts rest in a friable, clastic matrix sinter- ed by a small amount of alkali-rich glass (Fig. 2). Modal data are presented by Winzer et al. (1977) and reproduced here as Table 1. Grain size of the matrix is seriate from several millimeters down to a few microns. A significant rego- lith component is suggested by the several types of glass beads and fragments present in the matrix. Glass compositions are plotted in Figure 3. A mare com- ponent is present in the glasses and as a glassy breccia clast (Winzer et al. 1977; Delano, 1975). Coarse spinel fragments (up to several mm) are scattered through the matrix but are not present in any of the lithic clasts, suggesting that at least one rock type not present as clasts has contributed to the matrix (Winzer et al., 1977).

Lithic clasts include, in approximately decreasing order of abundance, basaltic melt rocks (clast-free and clast-bearing), coarse-grained annealed rock(granu- lite), fine-grained annealed rocks (hornfelses), and cataclastic anorthosites.

Basaltic melt rock clasts (Fig. 2) have textures ranging from vitrophyric to diabasic. Most are holocrystalline with plagioclase, clinopyroxene, ortho- pyroxene, olivine, ilmenite and a complex mesostasis as the principal constit- uents. Minerals are zoned and compositions from all textural varieties overlap. Olivine and pyroxene compositions are shown in Figures 4 and 5. Plagioclase is $An_{95-83}$. Some of the basaltic clasts carry xenocrysts of olivine and plagioclase and rare lithic fragments. Accessory minerals, normally associated with the mesostasis but also occuring as xenocrysts, include Mg-spinel, chromite, troilite, metal (up to 9% Ni), schreibersite, ilmenite, armalcolite, rutile and a Zr-min- eral.

Coarse-grained granoblastic clasts (granulites of Winzer et al., 1977) include anorthositic, noritic and troctolitic lithologies with the anhedral minerals, smooth grain boundaries and triple junctions indicative of extensive subsolidus annealing (Fig. 2). Mafic minerals are unzoned and largely equilibrated within any single clast (Fig.6). Some large plagioclase grains have calcic cores ($An_{95-97}$) and narrow, more sodic rims. Some of the noritic clasts have anhedral orthopyroxene poikiloblasts (up to ∿1 mm) which enclose anhedral plagioclase and rare ilmenite. Several of the poikiloblasts show exsolution lamellae (up to 0.1 mm) of high-Ca pyroxene. Anhedral,magnesian ilmenites are found in some granoblastic clasts.

Fine-grained granoblastic clasts (hornfelses of Winzer et al.,1977) are character- ized by an interlocking mass of anhedral plagioclase plus olivine and/or py- roxene with smooth grain boundaries and triple junctions. Grain size is typical- ly ∿ 50μm or less. Many of these clasts are rich in xenocrysts. Minerals are un- zoned and largely equilibrated (Fig. 5); glass is absent. Xenocrysts of plagio- clase often have calcic cores ($An_{95}$) and thin rims of the same composition as the groundmass plagioclase (down to $An_{88}$). Metal (4.5-9% Ni), troilite, ilmenite, apatite and schreibersite occur as accessory minerals. Several of the fine-grain- ed annealed clasts have a poikiloblastic texture that ranges from poorly to well developed (Fig. 2). These poikiloblastic clasts are texturally distinct from the typical Apollo 16 poikilitic rocks (such as 60315) which usually show a melt tex- ture characterized by euhedral crystallites of plagioclase enclosed by anhedral pyroxene oikocrysts.
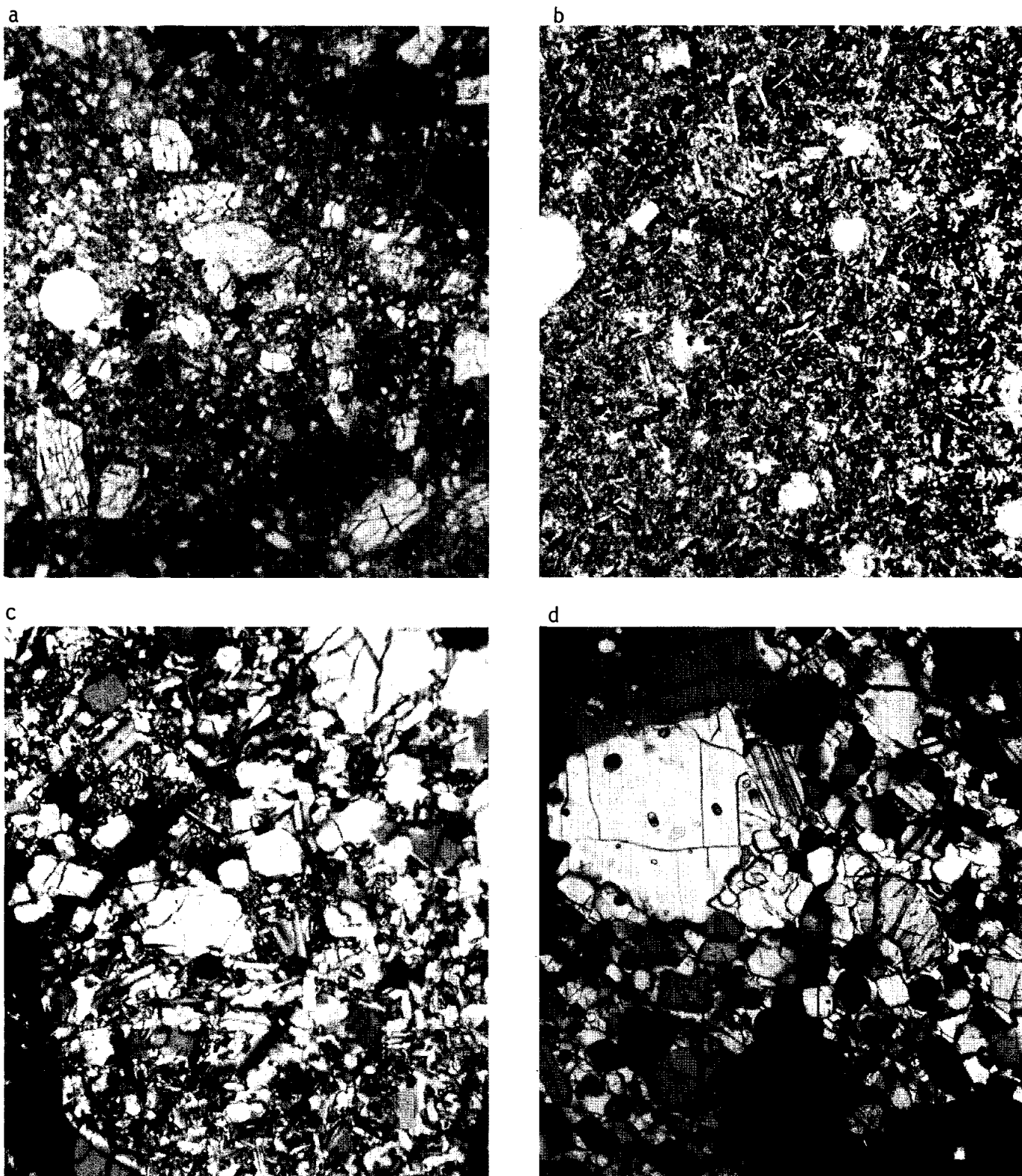
61175



Figure 2. a) 61175,108, general view, ppl. width 2mm.
b) 61175, 97, basaltic clast, ppl. width 1mm.
c) 61175, 108, fine-grained granoblastic clast, xpl. width 2mm.
d) 61175, 97, coarse- grained granoblastic clast, xpl. width 2mm.

222

Cataclastic anorthosites occur as larger clasts (up to 2 cm) which have been moderately to severely shocked and brecciated. Maskelynite is abundant and melting has occurred in some clasts. Original grain size of the plagioclase (An95-100) was several millimeters. Minor phases include olivine, orthopyroxene, and rare ilmenite and spinel.
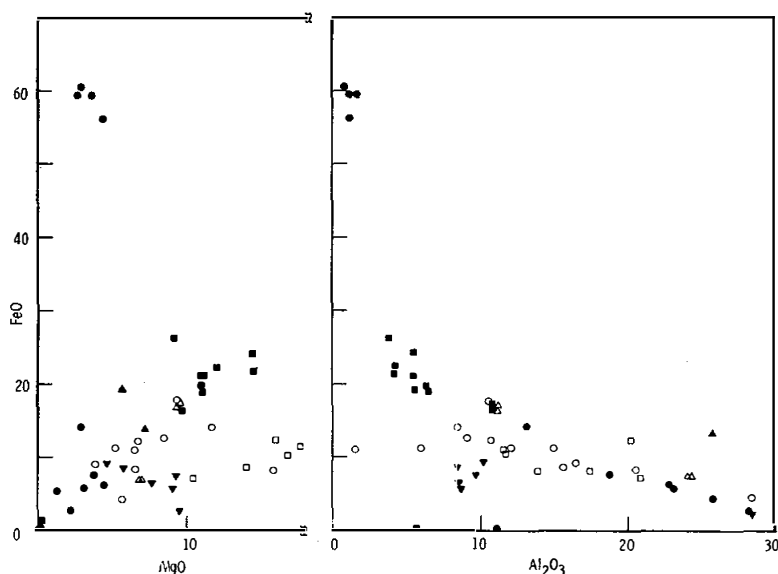
Figure 3. Glass compositions, from Winzer et al. (1977).
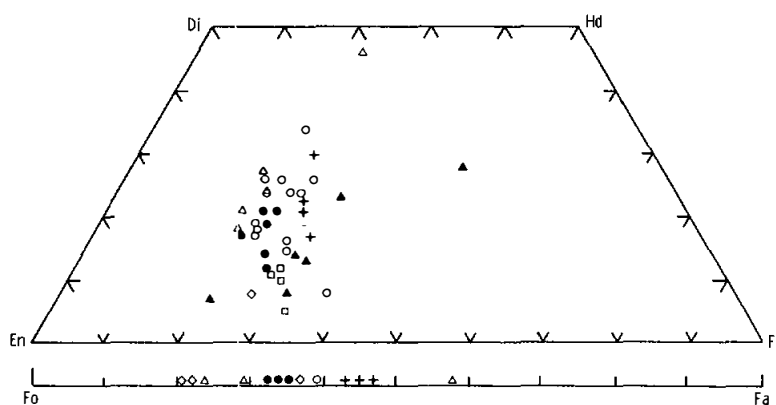
Figure 4. Pyroxene, olivine compositions in clast-free basaltic clasts, from Winzer et al. (1977).

223
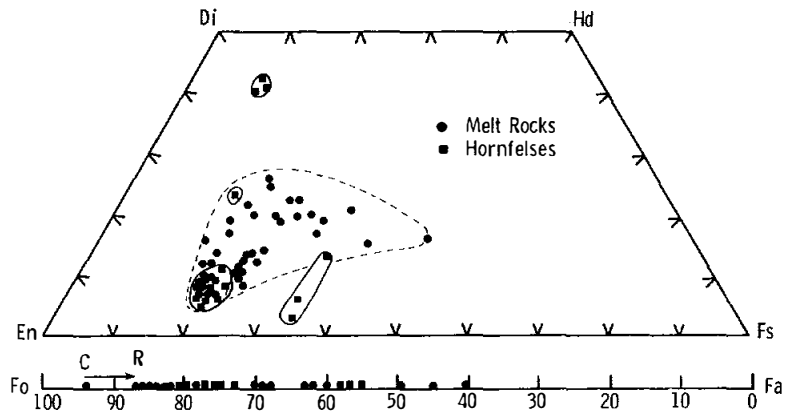
Figure 5. Pyroxene, olivine compositions in clast-bearing melt clasts and fine-grained granoblastic clasts, from Winzer et al. (1977).
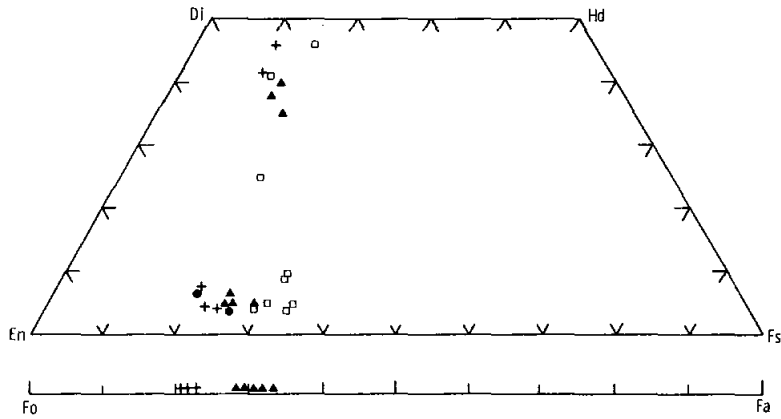


Figure 6. Pyroxene, olivine compositions in coarse-grained granoblastic clasts, from Winzer et al. (1977).

CHEMISTRY: Winzer et al. (1977) provide major and trace element data for matrix and various clast samples. S.R. Taylor et al. (1974) report major and trace element analyses on a plagioclase-rich separate of a whole rock sample. Cripe and Moore (1974) report bulk sulfur and Moore and Lewis (1976) give bulk carbon and nitrogen data. Eldridge et al. (1973) determined K, U, and Th by gamma-ray spectroscopy.

Analyses by Winzer et al. (1977) show the matrix of 61175 to be somewhat more mafic than its clasts (Table 2). Compared to the local soils, the 61175 matrix has the same Fe/Mg but is depleted in absolute abundances of ferromagnesian elements and REEs.

None of the rock types classified on the basis of texture can be singled out as chemically distinct. Figure 7 shows that the major element chemistry of all of the clast types overlap although some clustering is apparent. Coarse-grained clasts tend to plot near the anorthite apex while the fine-grained annealed rocks have compositions similar to other Apollo 16 poikilitic melt rocks and plot near the olivine-plagioclase-spinel peritectic. Basaltic textured clasts cluster between these two groups.
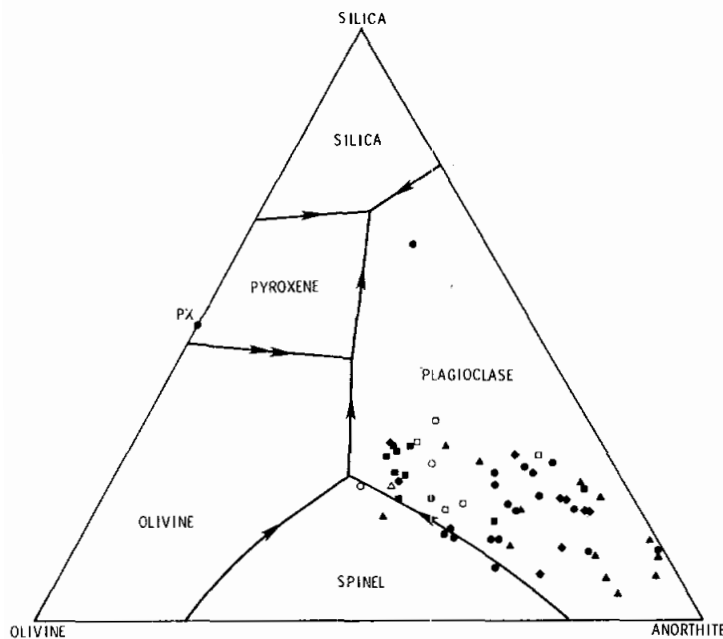


Figure 7. From Winzer et al. (1977).

▲—ANT, ■—hornfels, ●—impact melts, and ◆—basalts. Unfilled symbols mark clasts whose classification is uncertain.

TABLE 1. Summary chemistry of 61175

| | |
|---|---|
| $SiO_2$ | 45.5 |
| $TiO_2$ | 0.53 |
| $Al_2O_3$ | 27.8 |
| $Cr_2O_3$ | 0.06 |
| FeO | 4.3 |
| MnO | 0.06 |
| CaO | 16.2 |
| $Na_2O$ | 0.51 |
| $K_2O$ | 0.10 |
| $P_2O_5$ | |
| Sr | 201 |
| La | |
| Lu | 0.5 |
| Rb | 2.3 |
| Sc | |
| Ni | |
| Co | |
| Ir ppb | |
| Au ppb | |
| C | 69 |
| N | 91 |
| S | 570 |
| Zn | |
| Cu | |

Oxides in wt%; others in ppm except as noted.
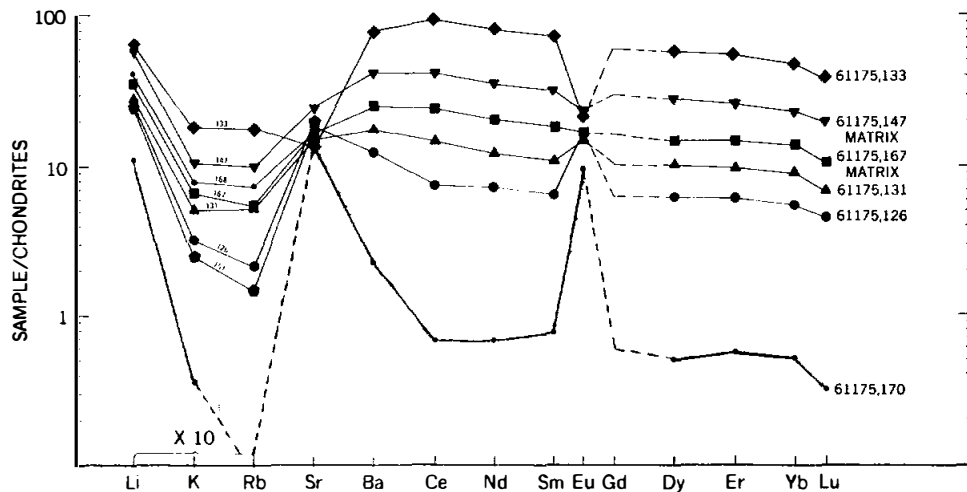
Lithophile trace element abundances from clasts and matrix of 61175. 61175,133 and ,126 are dark clasts and are probably melt rocks. 61175,131 and ,170 are white clasts, and are moderately shocked anorthosites.

**Figure 8.** From Winzer **et al.** (1977).

Rare earth elements (Fig. 8) also show the diversity of clast compositions although too few clasts have been analyzed to show definite trends. Apparently the clasts have a range of REE abundances which bracket that of the matrix. Of particular interest is split 61175, 170 which sampled a small anorthosite clast. This clast has very low REE abundances and may represent a pristine lithology although no siderophile data are available. Other anorthositic clasts from this rock have significantly higher REEs (,131 on Fig. 8) and have probably been contaminated with KREEP. Basaltic clasts may be either poor or rich in a KREEP component (e.g. ,126 and ,133 respectively, Fig. 8).

STABLE ISOTOPES: Clayton et al. (1973) determined a whole rock $\delta\ O^{18}$ value of 5.78°/oo, typical of Apollo 16 breccias.

EXPOSURE AGE: A maximum track exposure age of 10 m.y. is reported by Crozaz et al. (1974, reference to Fleisher and Hart, 1974, unpublished). Crozaz et al.(1974) also calculate a surface exposure age of > 1.5 m.y. from the cosmogenic radio- nuclide data of Eldridge et al. (1973).

MICROCRATERS: Morrison et al. (1973) and Neukum et al. (1973) report size-frequency data for microcraters on 61175 (Fig. 9). From the subrounded shape of the rock and its crater distribution, both authors conclude that 61175 is probably in equi- librium.

Schaal et al. (1976) provide detailed petrography and microprobe analyses of a thin section cut through a 3.6 mm, glass-lined microcrater as an example of an impact into a complex, polymict host. Preferential assimilation of plagioclase over py- roxene and small scale flow and mixing was observed. The glass lining is inhomo- geneous (30-37% $Al_2O_3$) and significantly enriched in a plagioclase component relative to the host matrix. Shock effects in the host progressively diminish away from the crater through a zone $\sim$ 1.5 mm into the rock.
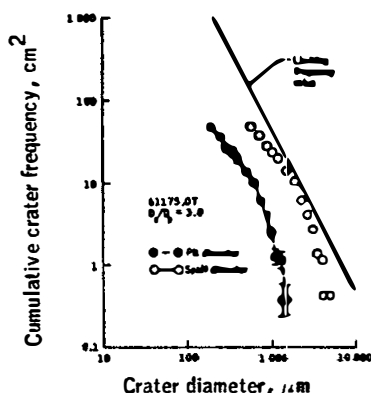


Figure 9. Microcraters, from Morrison et al. (1973).

PHYSICAL PROPERTIES: Compressional and shear wave velocities at pressures up to 10 kb were measured by Mizutani and Osako (1974) (Fig.10). The porous nature of 61175 results in velocities significantly less than those determined for the lunar crust.

PROCESSING AND SUBDIVISIONS: In 1972, 61175 was chipped into six main pieces (,0-,5). In 1973 the largest of these (,0) was cut into three pieces (,16 ,19 and ,20) one of which was a slab (,19). The slab was subsequently divided for allo- cations (Fig. 11). All of the Winzer et al. (1977) allocations came from the slab with most of them being taken from ,21 and ,30. The large white clast shown in ,30 is a moderately shocked anorthosite and was analyzed as ,151 (see CHEMISTRY). The anorthosite clast with very low REEs (,170) was a small clast from ,21. It was not the large white clast seen in ,21 in Figure 14. S.R. Taylor et al. (1974) received several whole rock chips from butt end ,16 but the analysis (,80) is unlike any of the other matrix analyses and looks more like a plagioclase-rich separate.

Figure 10. Wave velocity profile, from Mizutani and Osako (1974).
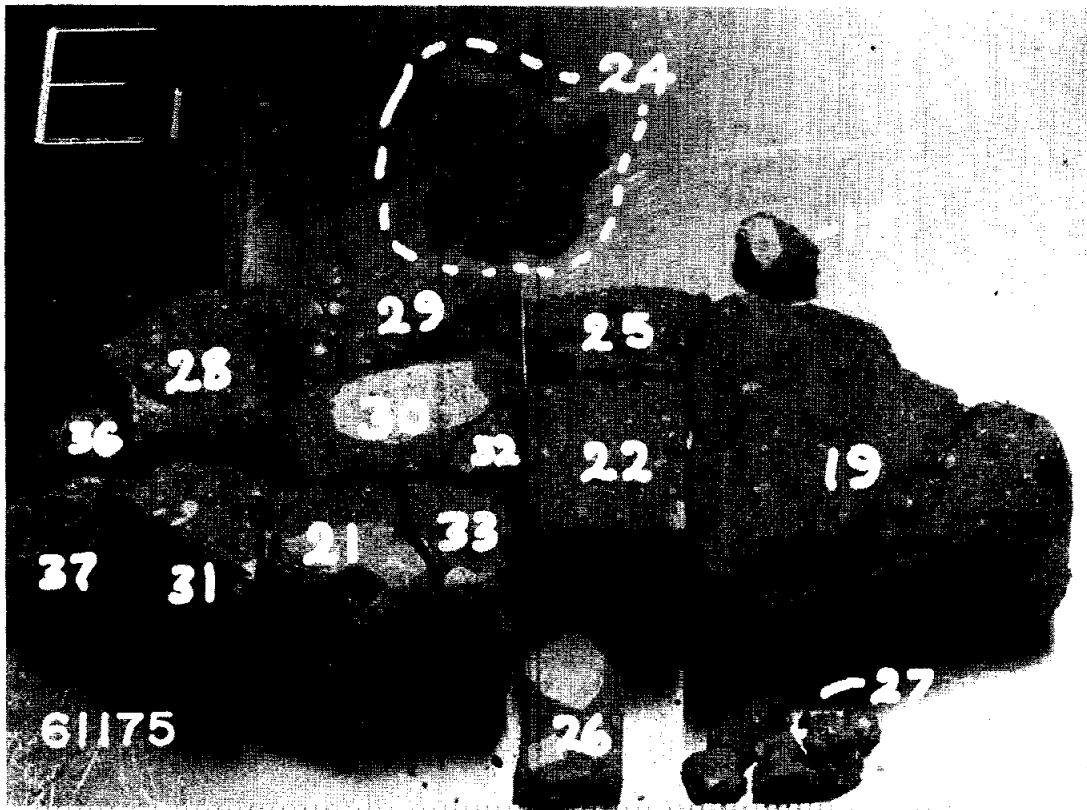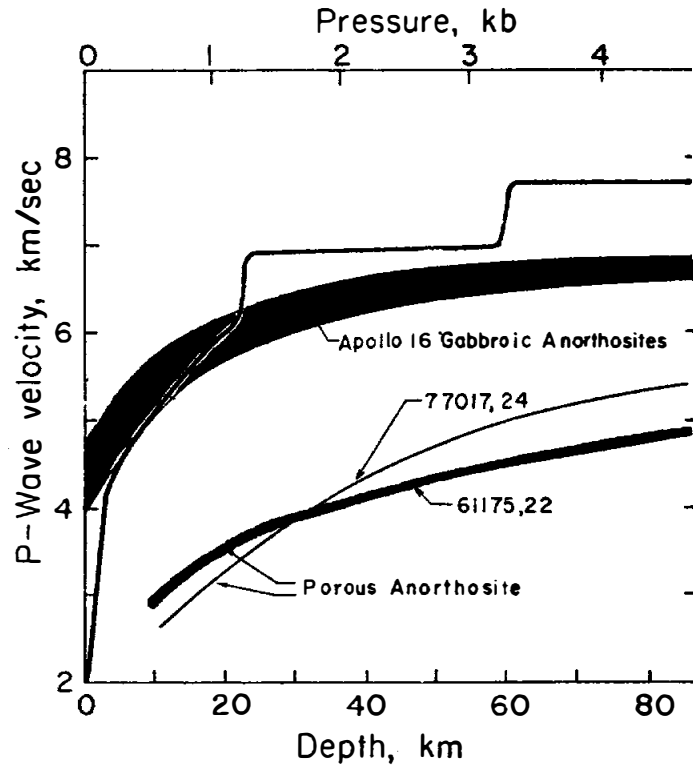


Figure 11. Slab subdivisions, mm scale. S-73-25605.

INTRODUCTION:  61195 is a coherent, medium gray breccia with a glassy matrix and abundant clasts (Fig. 1).  A significant regolith component is indicated by the petrography and chemistry.  A dark, vesicular glass coats 80-90% of the exterior surface and intrudes the rock as small veins.

This sample was collected from the northeast rim of Plum Crater, where it was about ¼ buried.  Its orientation is known.  Zap pits are common on the "lunar up" surface, rare to absent on other surfaces.
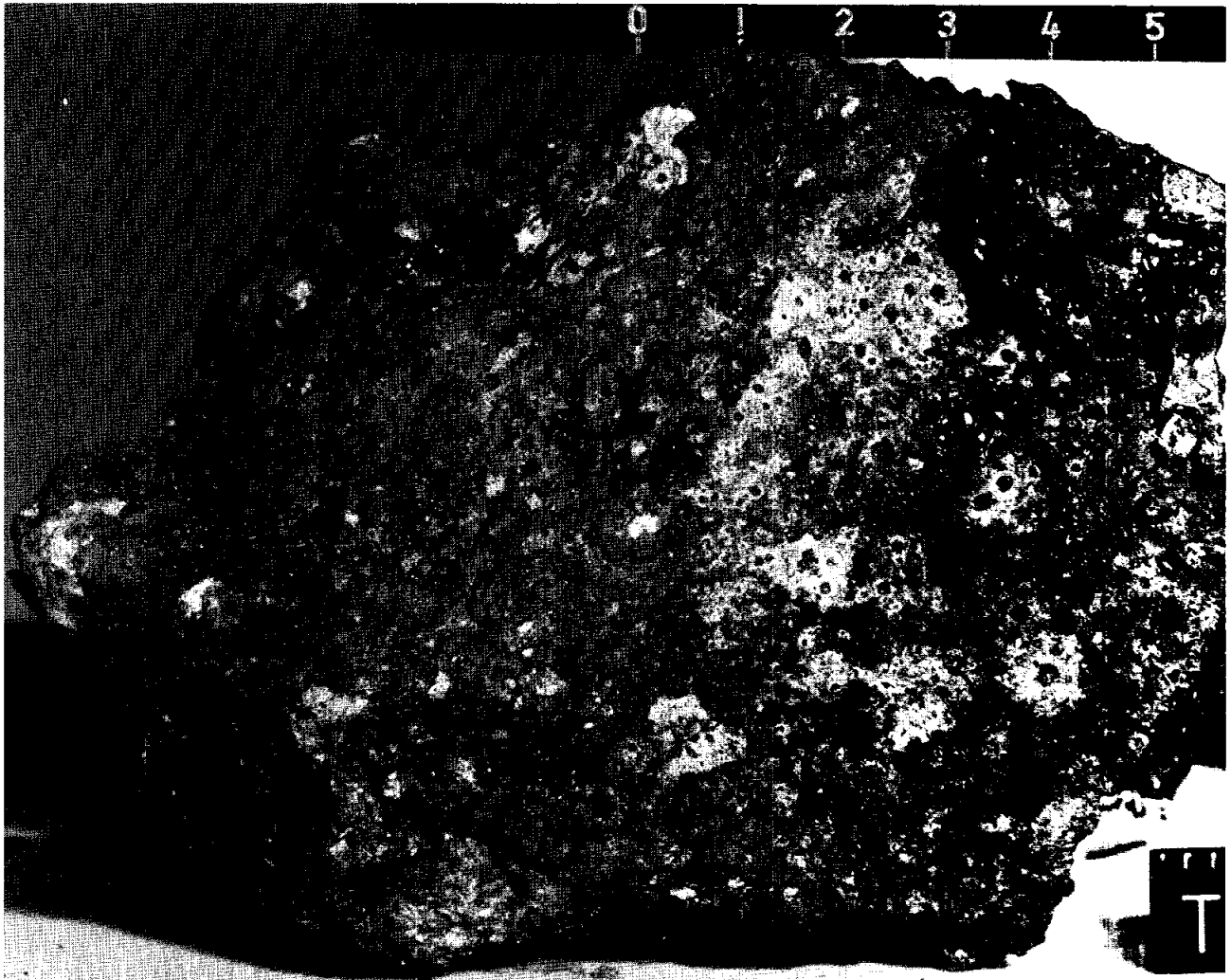


Figure 1. S-72-37972, cm scale.

61195

PETROLOGY:   61195 is a glassy matrix breccia with an abundant and diverse clast population (<0.1-3 mm) (Fig. 2) and a low porosity.  Two sets of nearly perpendicular fractures cut the rock and cross clast-matrix boundaries.

Homogeneous and partly crystalline glass beads and fragments are common, and indicate a regolith component.  Mineral clasts include plagioclase, pyroxene and olivine, nearly all of which have been shocked or recrystallized.  Lithic clasts include rounded to angular fragments of granoblastic anorthosite and anorthositic norite, cataclastic anorthosite, spinel- and clast-bearing basaltic impact melt, fine-grained poikilitic impact melt, clast-rich vitric matrix breccia,and plagioclase vitrophyre.  Fe-metal, troilite, schreibersite and rare ilmenite are accessory phases in both the matrix and some clasts.

Figure 2. 61195,36, general view, ppl. width 2mm.

CHEMISTRY:   Wänke et al. (1975) provide bulk major and trace element data. Eldridge et al. (1973) report whole rock data for K, U, and Th determined by gamma-ray spectroscopy.  The major and lithophile element abundances (Table 1, Fig. 3) are identical to those of local mature soils.  Siderophile element abundances in the rock are slightly lower than in the soils.

230

TABLE 1. Summary chemistry of 61195

| | |
|---|---|
| $SiO_2$ | 45.5 |
| $TiO_2$ | 0.50 |
| $Al_2O_3$ | 26.8 |
| $Cr_2O_3$ | 0.099 |
| FeO | 5.13 |
| MnO | 0.06 |
| MgO | 5.56 |
| CaO | 15.4 |
| $Na_2O$ | 0.46 |
| $K_2O$ | 0.088 |
| $P_2O_5$ | 0.17 |
| Sr | 166 |
| La | 14.6 |
| Lu | 0.64 |
| Rb | 3.86 |
| Sc | 8.53 |
| Ni | 410 |
| Co | 27.1 |
| Ir ppb | 11.3 |
| Au ppb | 6.1 |
| C | - |
| N | - |
| S | 660 |
| Zn | 9.71 |
| Cu | 3.76 |

Oxides in wt%; others in ppm except as noted.

Figure 3. Rare earths.



231
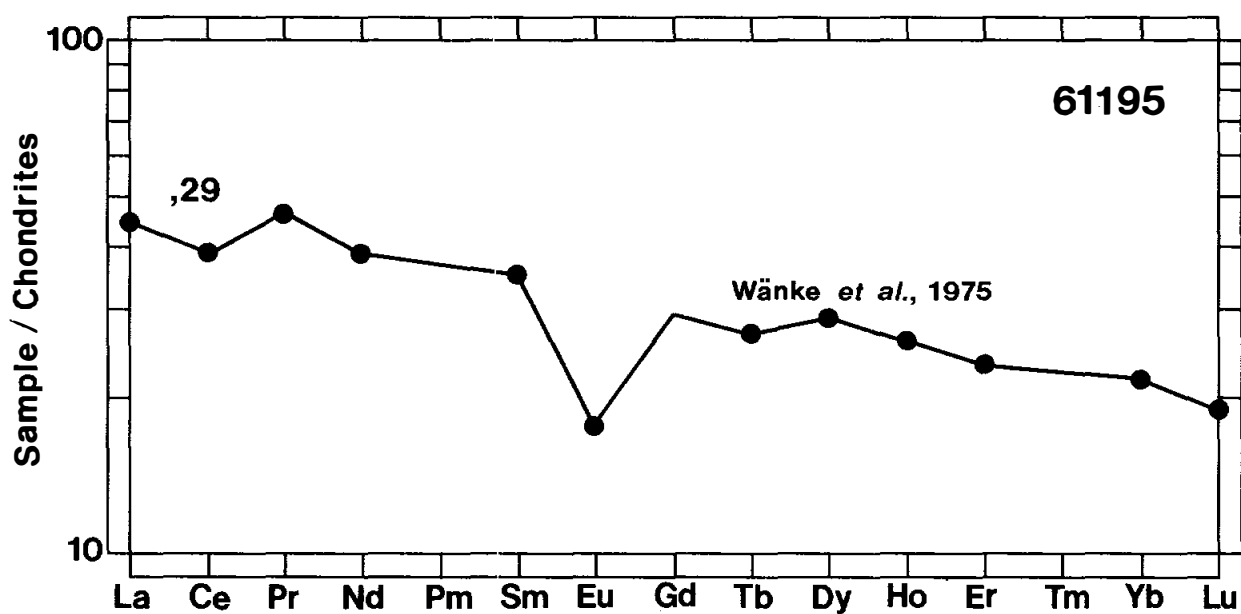
EXPOSURE AGE: Eldridge et al. (1973) report cosmogenic radionuclide data and conclude that the rock is unsaturated in $^{26}$Al. The very low $^{26}$Al/$^{22}$Na indicates a surface exposure age of <1 m.y.

PROCESSING AND SUBDIVISIONS: In 1973, 61195 was cut into three main pieces including a slab. The slab was entirely subdivided into smaller chips (Fig. 4). Allocations for thin sections were made from two chips of the slab (,7 and ,9). Wänke et al. (1975) analyzed a collection of small chips (,29) for chemistry. Other chips were also taken from butt end ,4.
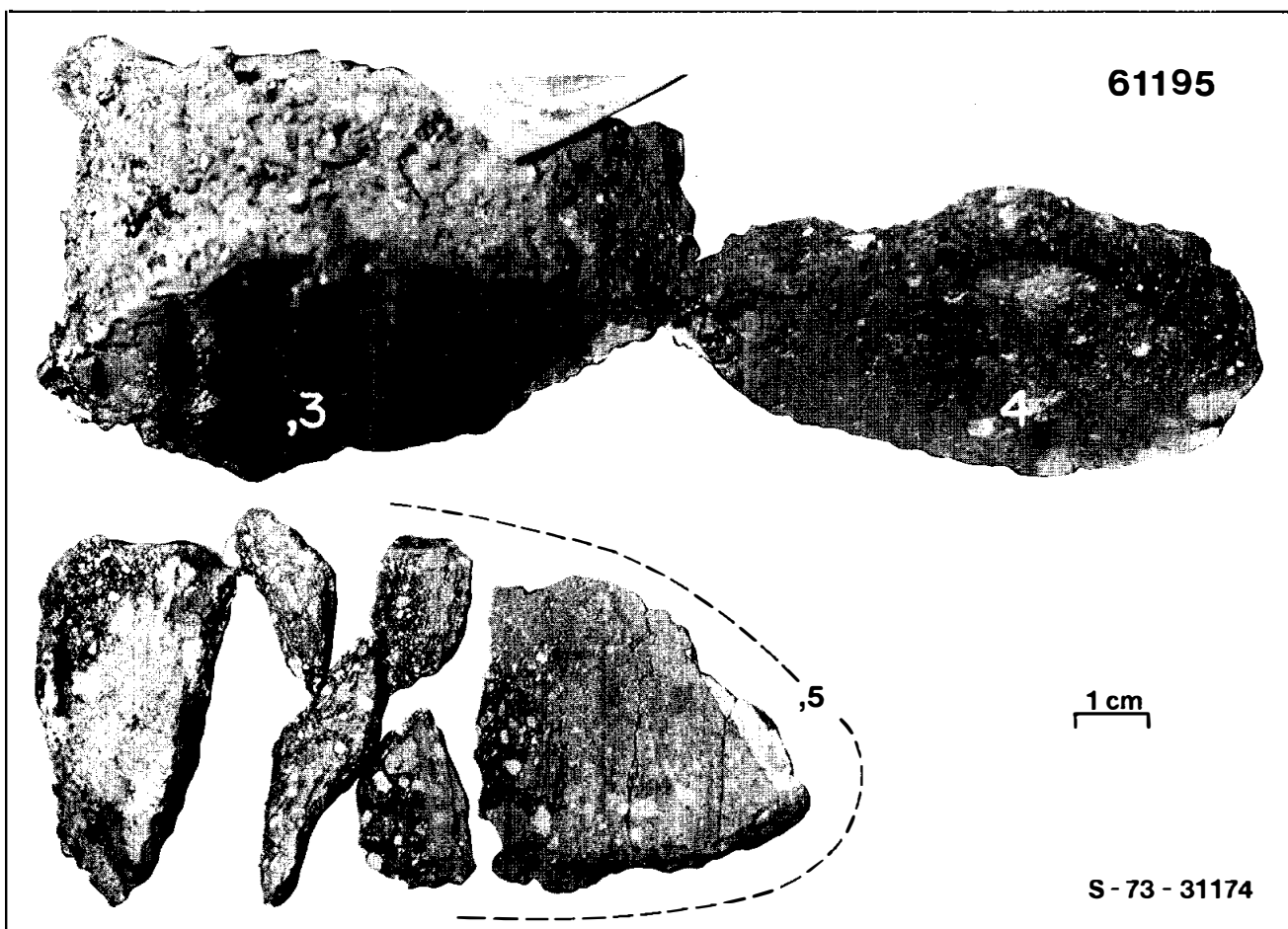


Figure 4.

INTRODUCTION:   61225 is a coherent, medium gray, crystalline rock that is
probably an impact melt (Fig. 1).  Vugs and vesicles are heterogeneously
distributed and all but one of the surfaces are covered with thick, white dust.
The N surface is clean and appears to be fresh.  This rock was taken from the
soil sample from the bottom of the trench on the east rim of Plum Crater. Zap
pits are absent.
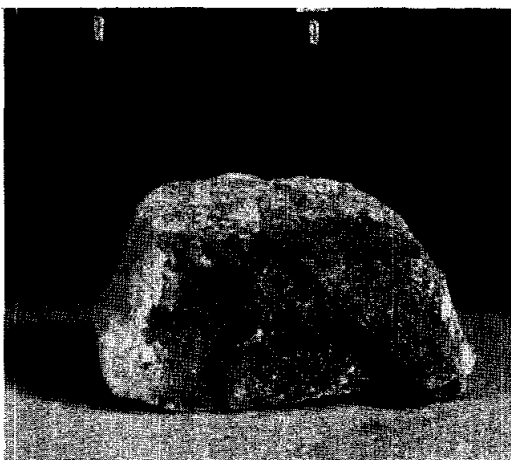


Figure 1. S-72-41306, cm scale.

INTRODUCTION:  61226 consists of coherent, white anorthosite separated by a zone of crushed, pale gray breccia (Fig. 1).  The latter may be a crushed version of the anorthosite, although it contains small black specks.  A thin ($\sim$ 1 mm) black glass coats part of the surface.

61226 was taken from a soil sample collected from the bottom of a trench dug on the east rim of Plum Crater.  It lacks zap pits.



Figure 1. Smallest scale subdivision 0.5mm.

INTRODUCTION:   61245 is a fine-grained or glassy, dark gray, crystalline rock (Fig. 1).  It contains vesicles, both round (up to 2 mm across) and elongate (up to 1 cm long).  It contains a few percent rounded white clasts. 61245 was taken from a soil sample collected from the top of a trench dug on the east rim of Plum Crater.  It lacks zap pits.



Figure 1. Smallest scale subdivision 0.5mm.

INTRODUCTION:  Most of 61246 is a fine-grained or glassy, gray or greenish impact melt.  It contains rare vesicles, some of which are soil filled, and is angular and coherent (Fig. 1).  One side has a rind of fragmental (though coherent) breccia which is firmly attached and may have been welded on while the melt was still hot.  This fragmental rind consists of tiny black fragments in a pale-colored matrix.

61246 was taken from a soil sample collected from the top of a trench dug on the east rim of Plum Crater.  It lacks zap pits.
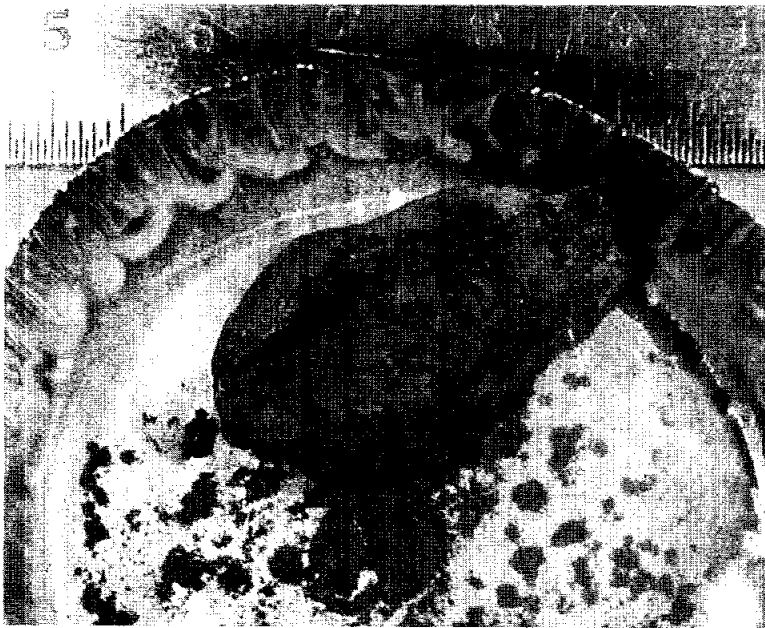


Figure 1. Smallest scale subdivision 0.5mm.

INTRODUCTION:  61247 is a coherent, angular sample (Fig. 1).  It is macro-
scopically similar to the poikilitic impact melt 65015, with pale-colored
pyroxene oikocrysts (?) about 1 mm across enclosing gray (plagioclase?)
grains.  Some of the plagioclases are quite lath-shaped but most very
angular.  Between these areas are distinctive dark chains.  The sample con-
tains a few vugs.

61247 was taken from a soil sample collected from the top of a trench dug
on the east rim of Plum Crater.  It lacks zap pits.
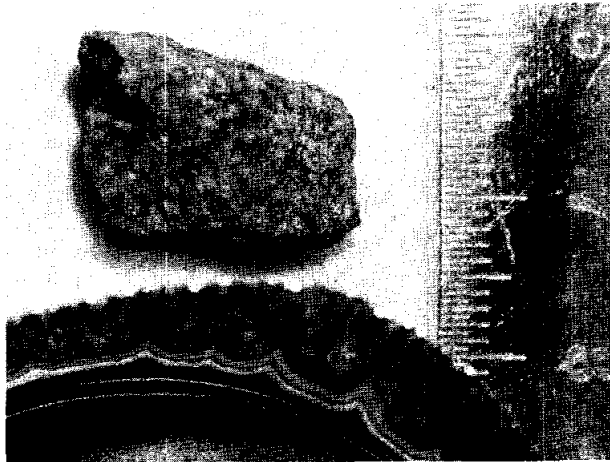
Figure 1. Smallest scale subdivision 0.5mm.

INTRODUCTION:  61248 is an extremely friable, polymict breccia (Fig. 1).  It
is pale-colored with several small, dark, coherent clasts.  61248 was taken
from a soil sample collected from the top of a trench dug on the east rim of
Plum Crater.  It is far too friable to have retained zap pits.



Figure 1. mm scale.

INTRODUCTION:  61249 is a slabby coherent sample (Fig. 1).  It is crystalline with yellowish/gray and white minerals, and ilmenite forms distinct laths. A basaltic texture is not well-developed, although the plagioclases appear to be ∿ 1 mm long.  The sample lacks vugs or vesicles.

61249 was taken from a soil sample collected from the top of a trench dug on the east rim of Plum Crater.  It has several zap pits.
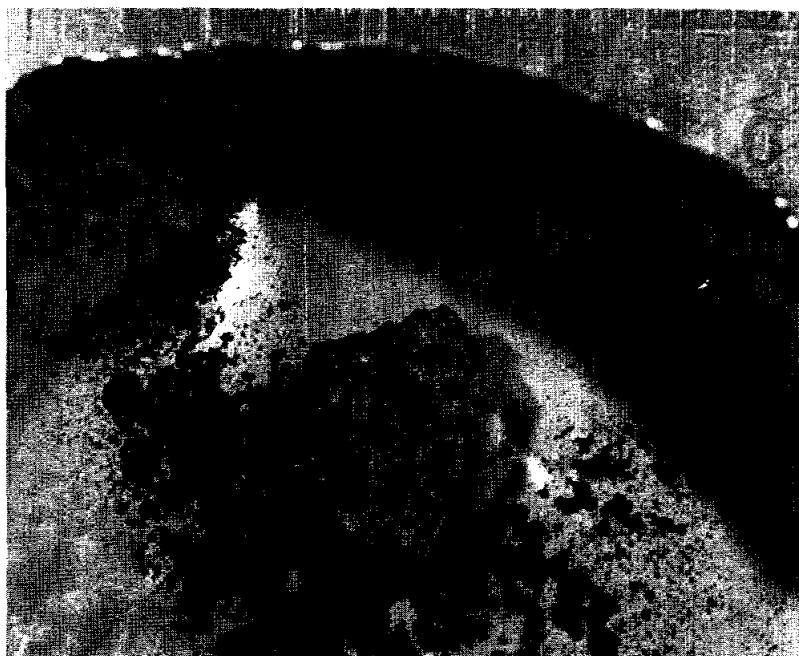


Figure 1. mm scale.

INTRODUCTION:  61255 is a vesicular, cindery black glass (Fig. 1), containing one prominent pure white clast.  The glass has several broken surfaces.  61255 was taken from a soil sample collected from the top of a trench dug on the east rim of Plum Crater.  It lacks zap pits.



Figure 1. Smallest scale subdivision 0.5mm.

INTRODUCTION:  61295 is a moderately coherent polymict breccia (Fig. 1) containing a wide variety of clasts.  Glass shards, glass beads, and agglutinates are present; some of the glasses appear to be of mare derivation.  Only about 10% of the clasts are larger than 1 mm, and most are angular.

61295 was removed from an unburied portion of a 2 m boulder on the southwest rim of Plum Crater, and its orientation is known.  Its exposed surface is rounded and has many zap pits.
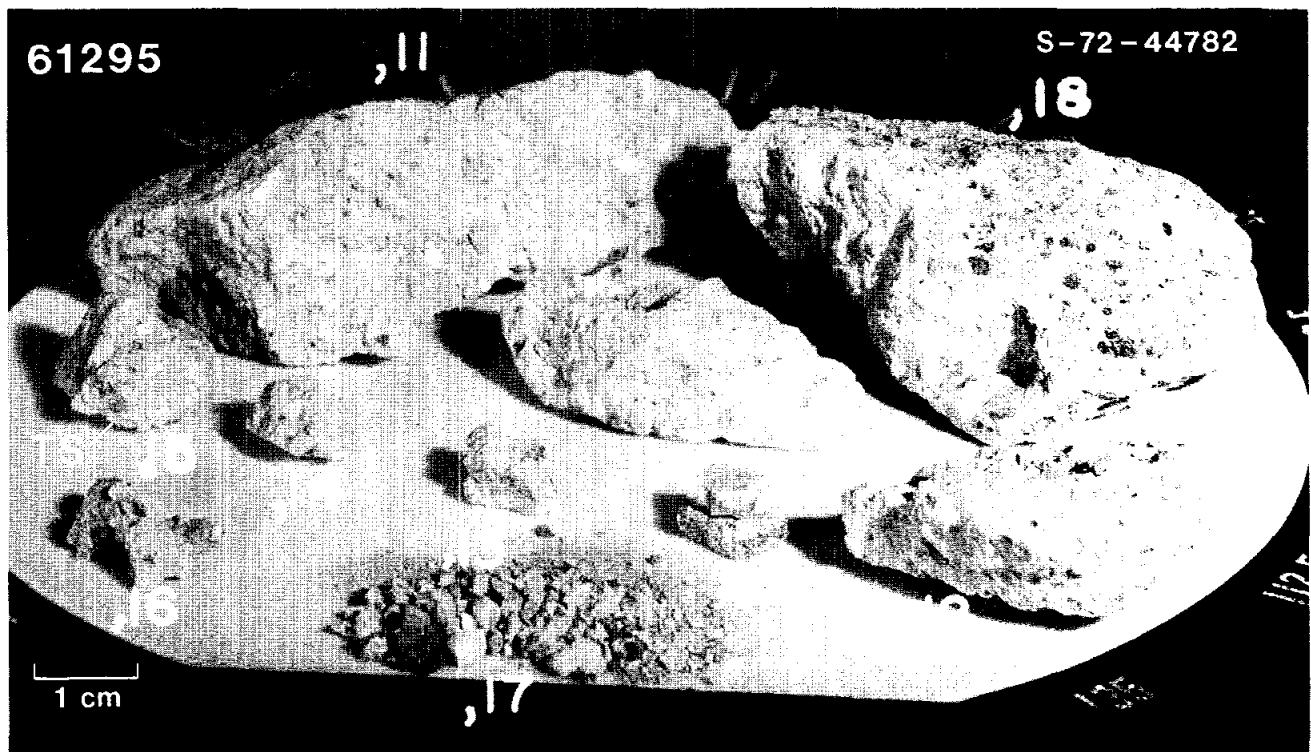
61295

PETROLOGY: LSPET (1973) depicts 61295 as typical of those polymict, light-gray, moderately friable breccias which have essentially glass-free matrices.

Thin sections are of a polymict breccia containing abundant lithic clasts (Fig. 2). 25% of the rock consists of fragments larger than 200 μm. The matrix is extremely porous and most fragments, including the smallest, are angular (Fig. 2). The lithic clasts include feldspathic impact basalts, feldspathic granulites, aphanitic breccias, and poikilitic impact melts. Plagioclase and mafic mineral fragments are common. Regolith-derived materials--orange glass shards, clasts and pale green glass balls, and agglutinate fragments--are common. Some of the glasses are evidently of mare origin: Delano (1975) refers to mare components in 61295 but does not detail specific analyses.
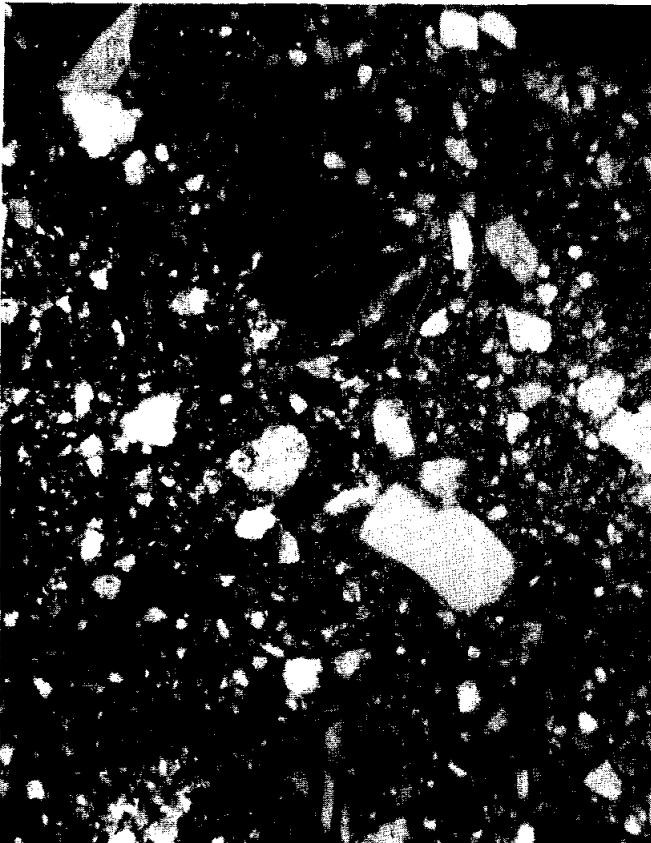


Figure 2. 61295,37, general view,pppl. width 2mm.

CHEMISTRY: For bulk rock samples, LSPET (1973) presents major and some trace element abundances. Hubbard et al. (1974) present abundances of trace elements including rare-earths. Eldridge et al. (1973) present K, U, Th, and radio-nuclide data, and Moore et al. (1973) present carbon contents. Nyquist et al. 1974) present Rb, Sr abundances. Little specific comment is made by these authors.

The chemistry is summarized in Table 1 and Figure 3. Although the rock contains regolith-derived fragments, it differs from local soils in its high $Al_2O_3$, and its C content (55 ppm) is significantly lower than most soils (100+ ppm).

242
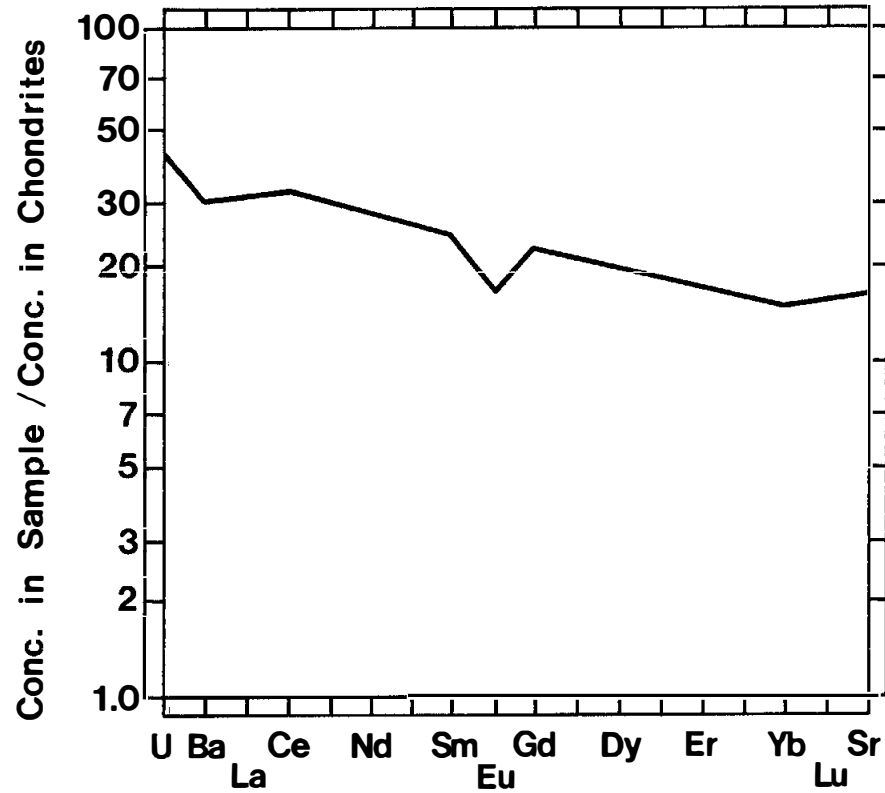
Figure 3. Rare earths, from Hubbard et al. (1974).

TABLE 1. Summary chemistry of 61295 bulk rock

| | |
|---|---|
| $SiO_2$ | 45.2 |
| $TiO_2$ | 0.56 |
| $Al_2O_3$ | 28.3 |
| $Cr_2O_3$ | 0.08 |
| FeO | 4.5 |
| MnO | 0.06 |
| MgO | 4.7 |
| CaO | 16.2 |
| $Na_2O$ | 0.46 |
| $K_2O$ | 0.09 |
| $P_2O_5$ | 0.10 |
| Sr | 186 |
| La | 10.4 |
| Lu | |
| Rb | 2.3 |
| Sc | |
| Ni | 114 |
| Co | |
| Ir ppb | |
| Au ppb | |
| C | 55 |
| N | |
| S | 600 |
| Zn | |
| Cu | |

Oxides in wt%; others in ppm except as noted.

RADIOGENIC ISOTOPES AND GEOCHRONOLOGY: The only radiogenic isotope data published on 61295 are Rb-Sr whole rock data by Nyquist et al. (1974),summarized in Table 2.

TABLE 2. Whole rock Rb-Sr isotopic data (Nyquist et al.,1974)

| Rb ppm | Sr ppm | $^{87}Sr/^{86}Sr$ | $T_{BABI}$* b.y. | $T_{LUNI}$* b.y. |
|--------|--------|-------------------|-----------------|-----------------|
| 2.308 | 186.0 | 0.70130±6 | 4.28±.15 | 4.41±.15 |

*BABI and LUNI adjusted for interlaboratory bias.

EXPOSURE AGES: Yokoyama et al. (1974) assess the radionuclide data of Eldridge et al.(1973) as indicating that 61295 is saturated with $^{26}Al$. Thus the exposure age of 61295 is long in relation to the half-life of $^{26}Al$.

PROCESSING AND SUBDIVISIONS: 61295 has main subdivisions as shown in Figure 1, but many small pieces also exist. A poikilitic impact melt clast was removed from ,12 and part made into a potted butt for thin sections. Bulk matrix ,3 (not shown) was also made into thin sections.

INTRODUCTION:  61505 is a medium dark gray, angular fragment (Fig. 1) which is fine-grained and coherent.  It lacks obvious clasts or vesicles.  It is probably a fine-grained or glassy impact melt.  It was taken from a regolith sample collected 30 m east of Flag Crater.  Zap pits are common on most surfaces and have white or colorless glass linings.
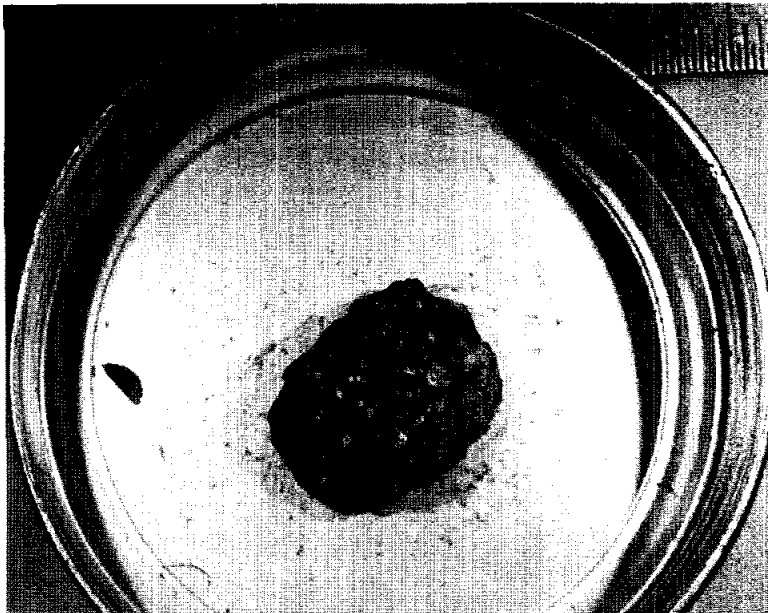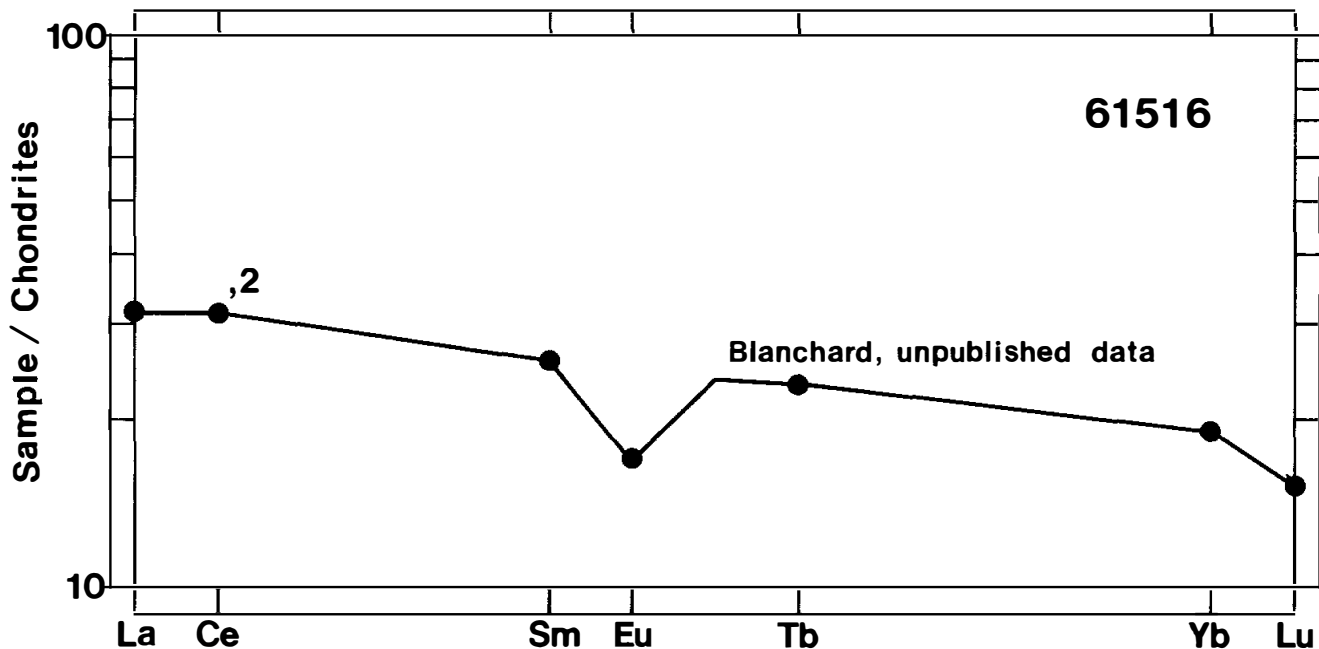


Figure 1. Smallest scale subdivision 0.5mm.

INTRODUCTION: 61515 is a friable, light gray clastic breccia with many small, white to gray clasts (Fig. 1). It is a rake sample collected about 45 m northeast of Plum Crater. Zap pits are rare.



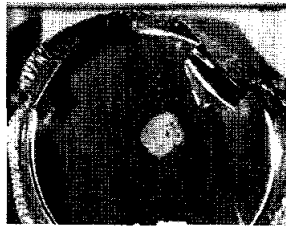Figure 1. S-72-43347.

INTRODUCTION:  61516 is a friable, light gray, clastic breccia (Fig. 1).  It is a rake sample collected ~45 m northeast of Plum Crater.  Zap pits are present.

PETROLOGY:  Warner et al. (1973) include  61516 in a general petrographic discussion of Apollo 16 rake samples and provide  a photomicrograph.  Phinney et al. (1976) studied the matrix characteristics using SEM techniques.
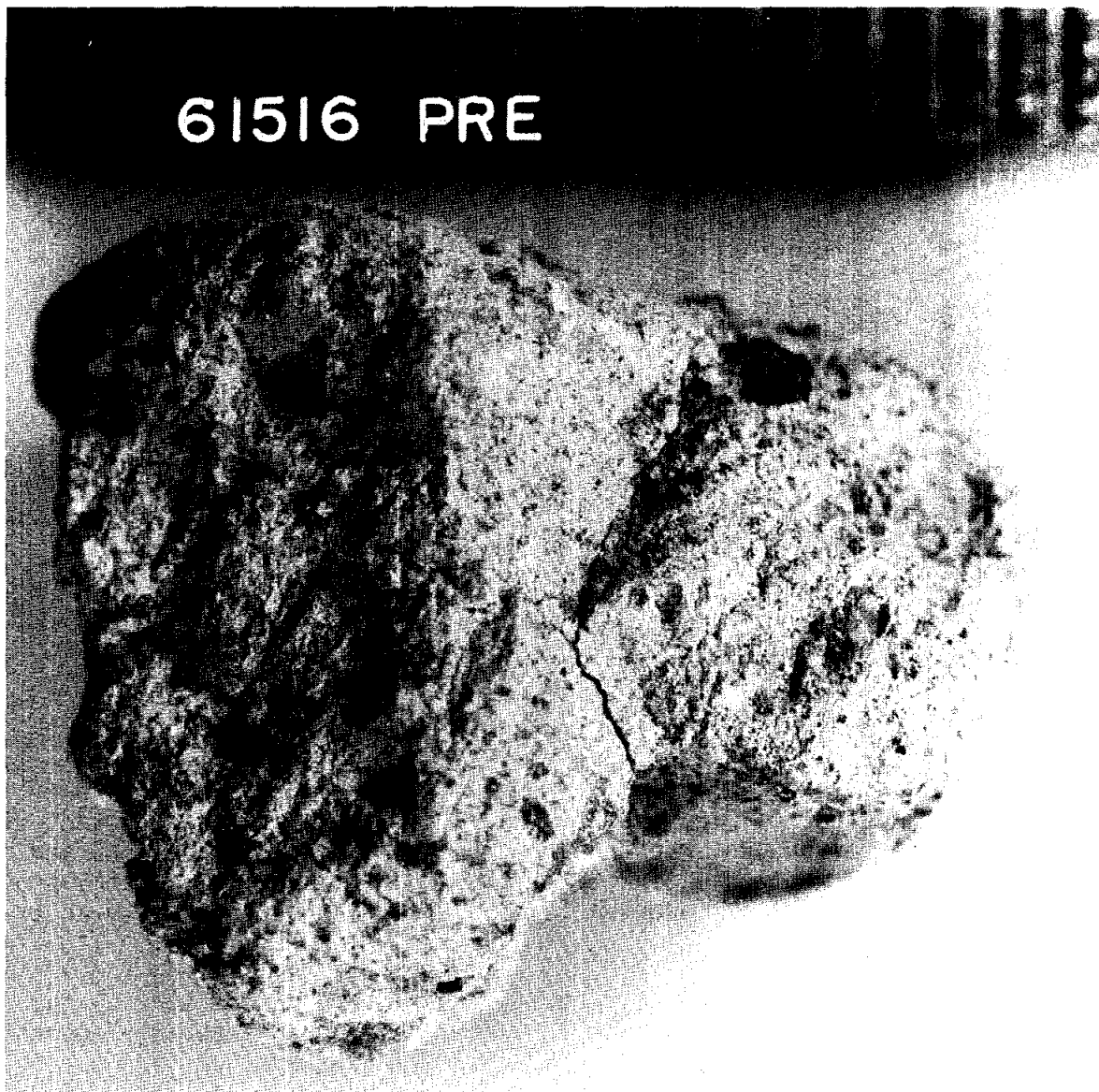


Figure 1. S-72-55331, mm scale.

Abundant mineral and lithic clasts rest in a porous, unequilibrated matrix (Fig. 2). Plagioclase fragments are the dominant clast type. A few large (up to ∿0.5 mm) grains of mafic silicate are present. Lithic clasts include grano-blastic anorthosite, basaltic impact melt, coarse-grained poikilitic impact melt,and recrystallized, granoblastic breccia. Phinney et al. (1976) find that the matrix contains 2-3% glass with traces of sintering and ∿35% porosity.



Figure 2. 61516,4, general view, ppl. width 1mm.

CHEMISTRY: Floran et al. (1976) present major element data obtained by electron microprobe analysis of natural rock powder fused to a glass (except FeO and $Na_2O$, by instrumental neutron activation). Blanchard (unpublished data) pro-vides a trace element analysis and the FeO and $Na_2O$ data quoted by Floran et al. (1976).

These data show that 61516 is similar in its major element chemistry to the local mature soils,but contains slightly lower levels of rare earth elements as compared to the soils (Table 1, Fig. 3).

248

TABLE 1.  Summary chemistry of 61516

| | |
|---|---|
| SiO$_2$ | 45.58 |
| TiO$_2$ | 0.42 |
| Al$_2$O$_3$ | 27.24 |
| Cr$_2$O$_3$ | 0.102 |
| FeO | 4.61 |
| MnO | |
| MgO | 6.05 |
| CaO | 15.35 |
| Na$_2$O | 0.538 |
| K$_2$O | 0.12 |
| P$_2$O$_5$ | |
| Sr | |
| La | 10.4 |
| Lu | 0.52 |
| Rb | |
| Sc | 7.16 |
| Ni | 195 |
| Co | 18.1 |
| Ir ppb | |
| Au ppb | |
| C | |
| N | |
| S | |
| Zn | 29 |
| Cu | |

Oxides in wt%; others in ppm except as noted.
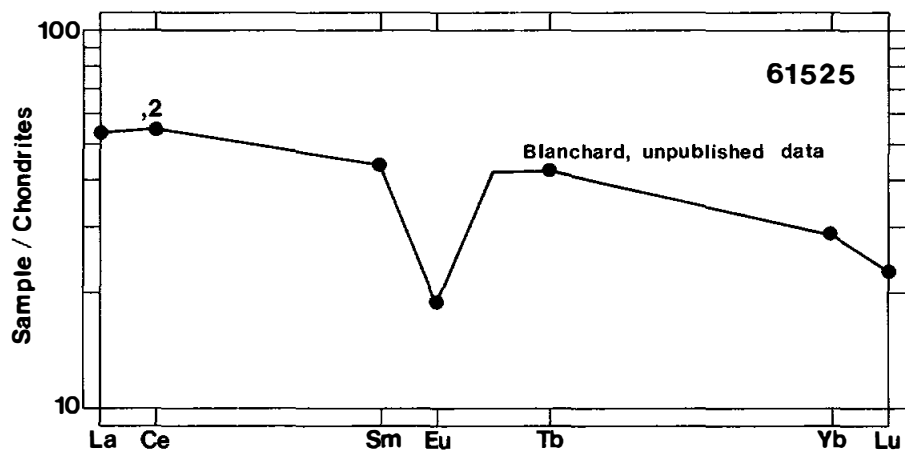
PHYSICAL PROPERTIES: Pearce and Simonds (1974) report the results of a room temperature hysteresis curve determination on 61516. The very small saturation remanence to saturation magnetization ratio ($J_{RS}/J_S$ = 0.005) indicates that virtually all of the ferromagnetic phases in this sample are multidomain particles. $Fe^O/Fe^{2+}$ is 0.0949 and total $Fe^O$ is 0.24 wt%.

PROCESSING AND SUBDIVISIONS: During processing in 1972 the rock broke into many pieces. One of these (,1) was allocated to Phinney for thin sectioning and petrography. In 1975 a set of eleven small chips (,2) was allocated for chemistry; the analyses of Floran et al. (1976) and Blanchard (unpublished) are both of portions of this split. The magnetic studies were done on the potted butt of ,1. The rest of the rock remains at JSC as ,0 (2.09 g).



Figure 3. Rare earths.

INTRODUCTION:  61517 is a friable, light gray, clastic breccia with several white to gray clasts (Fig. 1).  It is a rake sample collected about 45 m northeast of Plum Crater.  Zap pits are rare or absent.



Figure 1. S-72-43349.

INTRODUCTION:  61518 is a friable, light gray, clastic breccia with several white to gray clasts (Fig. 1).  It is a rake sample collected about 45 m northeast of Plum Crater.  Zap pits are rare or absent.



Figure 1. S-72-43349.

INTRODUCTION:  61519 is a friable, light gray, clastic breccia with several small, white to gray clasts (Fig. 1).  It is a rake sample collected about 45 m northeast of Plum Crater.  Zap pits are rare to absent.
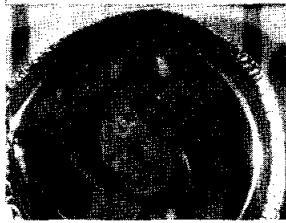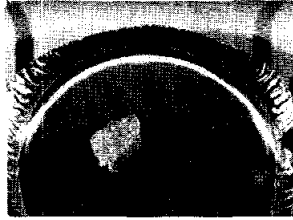


Figure 1. S-72-43349.

INTRODUCTION:    61525 is a moderately friable, medium gray, polymict breccia with considerable glass in the matrix (Fig. 1).  It is a rake sample collected ∿45 m northeast of Plum Crater.  Zap pits are abundant on one surface, absent on others.



61525

S - 72 - 55332
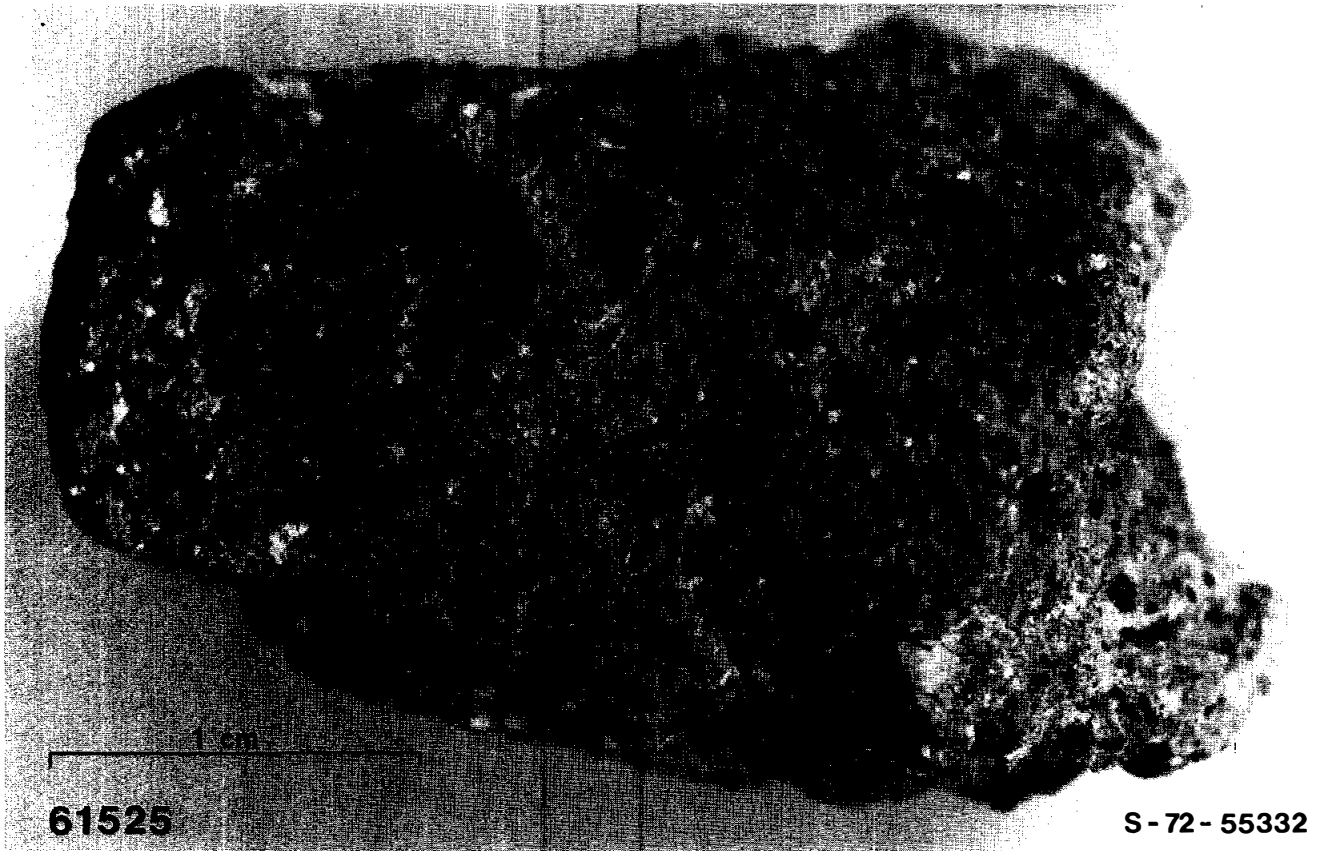
Figure 1.

PETROLOGY:  Warner et al. (1973) include  61525 in a general petrographic discussion of Apollo 16 rake samples and classify it as a "glassy breccia".  Phinney et al. (1976) studied the matrix characteristics using SEM techniques.

61525 consists of shocked mineral and lithic clasts,and occasional beads and fragments of clear glass,in a chaotic, glassy matrix (Fig. 2).  Phinney et al. (1976) report that the matrix contains ∿25% glass and variable (1-10%) porosity. Fe-metal compositions are provided by Gooley et al. (1973) and reproduced here as Table 1.

TABLE 1. Metal Compositions of 61525 (wt %)

| | Ni | Co | P | S |
|---|---|---|---|---|
| Metal | 5.6-6.6 | 0.5 | 0.0-0.2 | 0.02 |

CHEMISTRY: Floran et al. (1976) report major element data obtained by electron microprobe analysis of natural rock powder fused to a glass (except FeO and $Na_2O$, by instrumental neutron activation). Blanchard (unpublished data) provides a trace element analysis and the FeO and $Na_2O$ data quoted by Floran et al. (1976)

These data show that 61525 is similar to the local mature soils in major element composition, but is somewhat enriched in rare earth elements compared to the soils (Table 2, Fig. 3).

TABLE 2. Summary Chemistry of 61525

| | |
|---|---|
| $SiO_2$ | 45.85 |
| $TiO2$ | 0.55 |
| $Al_2O_3$ | 26.19 |
| $Cr_2O_3$ | 0.120 |
| FeO | 5.27 |
| MnO | |
| MgO | 5.57 |
| CaO | 15.12 |
| $Na_2O$ | 0.591 |
| $K_2O$ | 0.23 |
| $P_2O_5$ | |
| Sr | |
| La | 17.6 |
| Lu | 0.776 |
| Rb | |
| Sc | 9.24 |
| Ni | 190 |
| Co | 17.8 |
| Ir ppb | |
| Au ppb | |
| C | |
| N | |
| S | |
| Zn | 50 |
| Cu | |

Oxides in wt %; others in ppm except as noted.
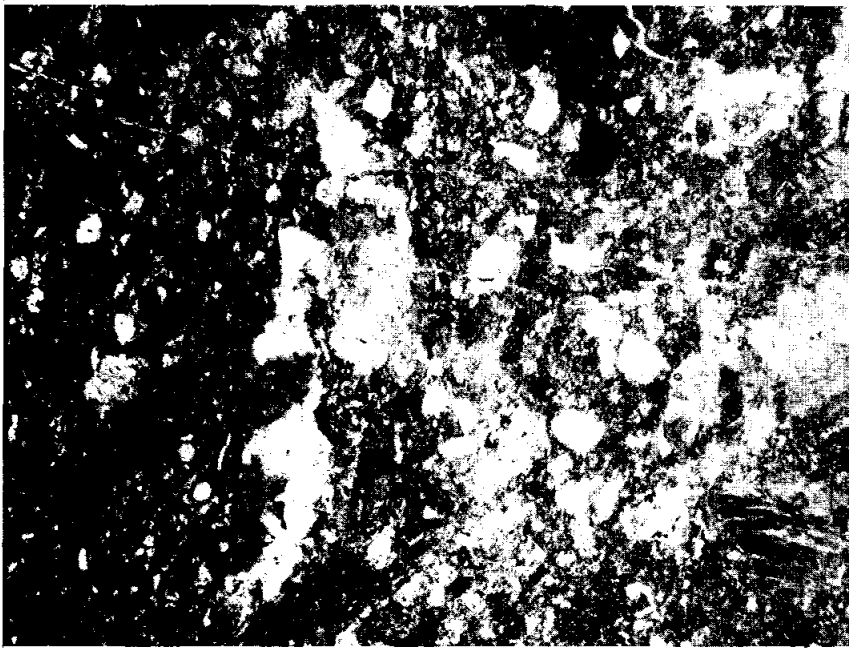
61525

Figure 2. 61525,4, general
view, ppl. width 2mm.

Figure 3. Rare earths.

61525

Blanchard, unpublished data

,2

256

PHYSICAL PROPERTIES: Pearce and Simonds (1974) report the results of a room temperature hysteresis curve determination on 61525. The saturation remanence to saturation magnetization ratio ($J_{RS}/J_S$ = 0.014) indicates that 3-6% of the ferromagnetic phases in this sample are single domain particles and the rest are multidomain. $Fe^O/Fe^{2+}$ is 0.0654 and total FeO is 0.25 wt%.

PROCESSING AND SUBDIVISIONS: In 1972 a single chip (,1) was removed and allocated to Phinney for thin sectioning and petrography. In 1975 a set of three small chips (,3) were allocated for chemistry; the analyses of Floran et al.(1976) and Blanchard (unpublished) are both portions of this split. The magnetic studies were done on the potted butt of ,1.

INTRODUCTION:  61526 is a moderately coherent, light gray, clastic breccia with many small white to gray clasts (Fig. 1).  It is a rake sample collected about 45 m northeast of Plum Crater.  Zap pits are rare or absent.



Figure 1. S-72-43349.

INTRODUCTION:  61527 is a moderately coherent, medium gray, clastic breccia with many small white to gray clasts (Fig. 1).  It is a rake sample collected about 45 m northeast of Plum Crater.  Zap pits are rare or absent.



Figure 1. S-72-43349.

INTRODUCTION:  61528 is a moderately coherent, mediu  gray, clastic breccia with many small, white to gray clasts and a small patch of glass coat (Fig. 1).  It is a rake sample collected about 45 m northeast of Plum Crater.  Zap pits are rare or absent.



Figure 1. S-72-43349.

INTRODUCTION:   61529 is a moderately coherent, medium gray, clastic breccia with many small white to gray clasts (Fig. 1).   It is a rake sample collected about 45 m northeast of Plum Crater.   Zap pits are rare or absent.



Figure 1.  S-72-43349.

INTRODUCTION:  61535 is a moderately coherent, light gray, clastic breccia with a thin coat of dark glass on one surface (Fig. 1).  It is a rake sample collected about 45 m northeast of Plum Crater.  Zap pits are rare or absent.
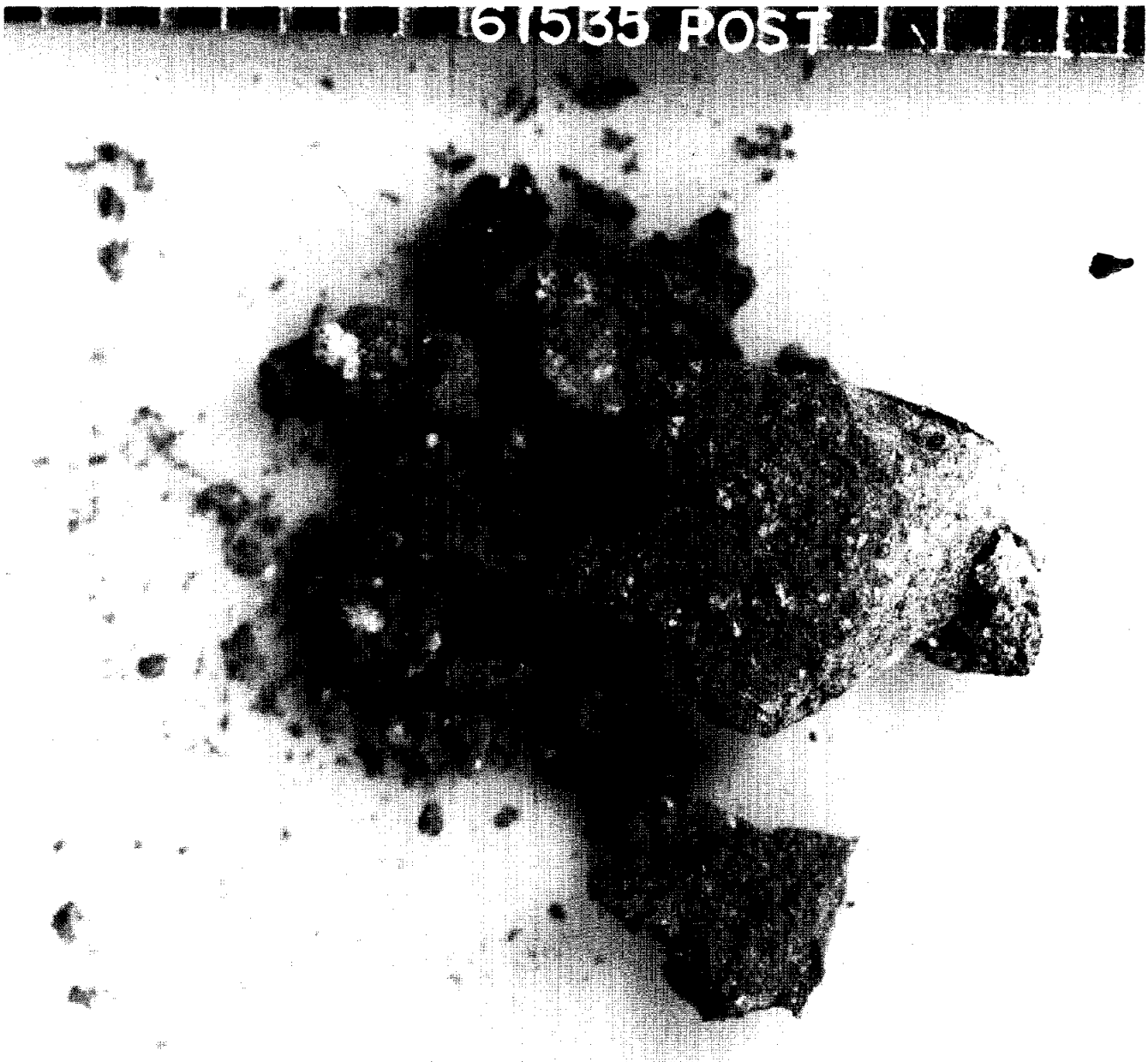


Figure 1. S-72-55318, mm scale.

PETROLOGY:  The thin section of 61535 is entirely of a highly vesicular and clast-laden, glassy impact melt, presumably the glass coat (Fig. 2).  This lead Warner et al. (1973) to classify this rock as a "glassy breccia".

PROCESSING AND SUBDIVISIONS:  During processing in 1972 the rock crumbled to many pieces.  Two of these (,1) were allocated to Phinney for thin sectioning and petrography.  From data pack photos these pieces appear to have been representative of the bulk rock although photo documentation is not complete. Apparently only the glass coat made it into the thin section.



Figure 2. 61535,4, general view, ppl. width 2mm.

INTRODUCTION:   61536 is a coherent, glassy breccia with light-colored clasts
(Fig. 1).  A vesicular, debris-filled green glass coats portions of the surface.
The large white clast in Figure 1 is a granoblastic troctolitic(?) anorthosite.
61536 is a rake sample collected from the rim of Flag Crater.
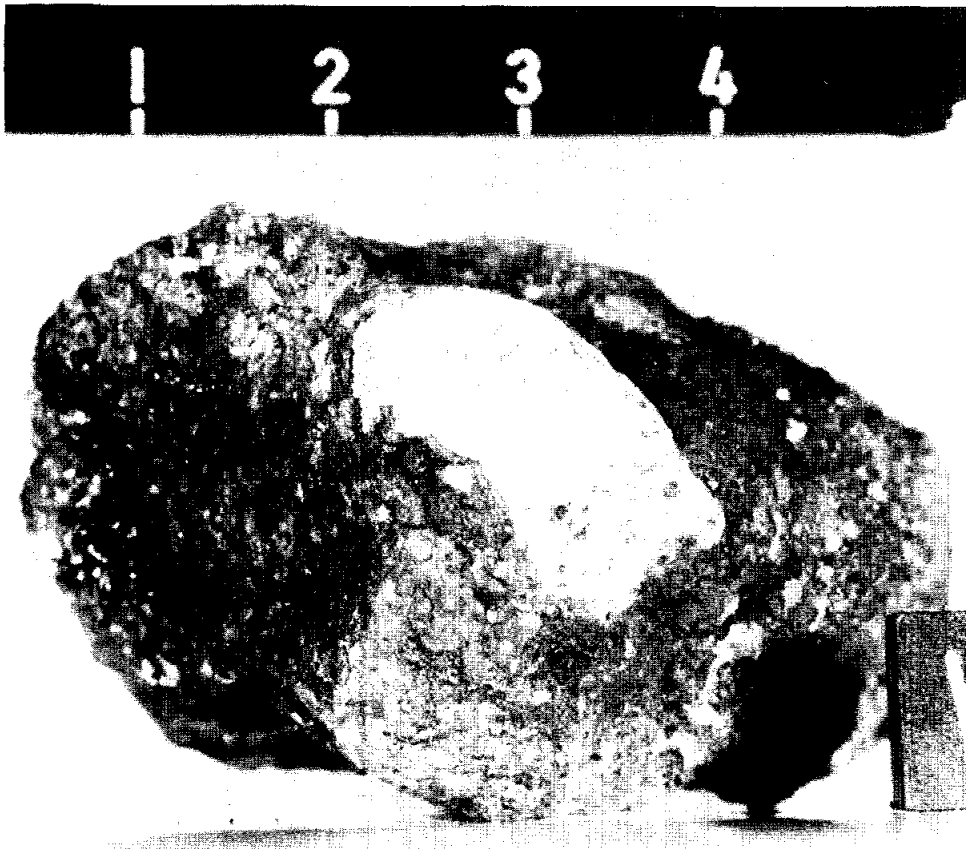


Figure 1. S-72-43398, cm scale.

PETROLOGY:   Thin sections cut for this study show that the matrix of 61536 is
glassy to cryptocrystalline.  Angular clasts of mildly shocked plagioclase,
mafic minerals, basaltic and poikilitic impact melts, brown glassy breccia or
devitrified glass, and orange-brown glass shards are common (Fig. 2).  Many of
the clasts exhibit reaction rims with the matrix.  Metal, troilite, and glass
beads are also present but not common.  Several of the metal particles are
rusty.

The large white clast seen in Figure 1 is a granoblastic troctolitic (?) anortho-
site (Fig. 2), composed of anhedral to elongate plagioclase (∿85%) and rounded
mafic minerals (∿15%). Many grains meet in triple junctions. Plagioclases are
much larger (200-400 μm) than the mafic minerals (25-50 μm). Trace amounts of
ilmenite, troilite and metal are scattered through the clast. The clast in
thin section ,7 is cut by a brown glassy vein containing lithic clasts. The
vein is more uniform and contains fewer clasts than the general breccia matrix
and is clearly intrusive.

PROCESSING AND SUBDIVISIONS: Thin section ,5 was made from a chip of matrix.
The large white clast was designated ,2 most of which remains part of ,0. Two
chips (,3 and ,4) were taken from ,2 and thin sections ,6 and ,7, respectively,
cut from them. ,3 was entirely used up.

a     b     c
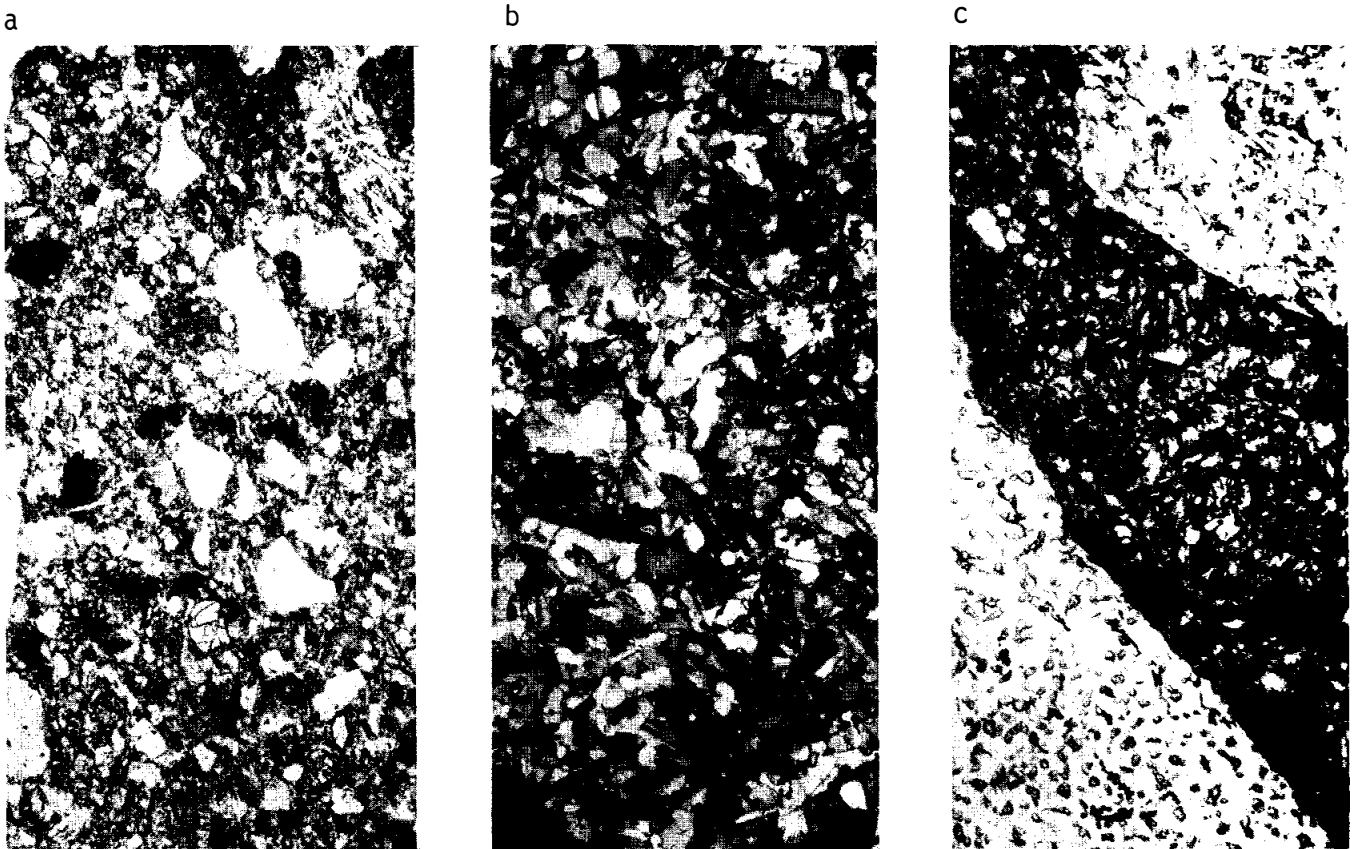


Figure 2. a) 61536,5, matrix, ppl. width 2mm.
          b) 61536,6, granoblastic clast, xpl. width 2mm.
          c) 61536,7, granoblastic clast, ppl. width 2mm.

INTRODUCTION:  61537 is a moderately coherent, medium gray breccia with a few small white clasts and coated by a dark vesicular glass (Fig. 1).  Several cracks penetrate the breccia but the rock is held together by the glass coating.  This is a rake sample collected about 45 m northeast of Plum Crater. Zap pits are rare or absent.



Figure 1. S-72-43349.

INTRODUCTION: 61538 is a light gray, moderately coherent breccia with a few small white clasts and coated with highly vesicular glass (Fig. 1). Many of the vesicles in the glass coat are filled with soil. This is a rake sample collected about 45 m northeast of Plum Crater. Zap pits are rare or absent.
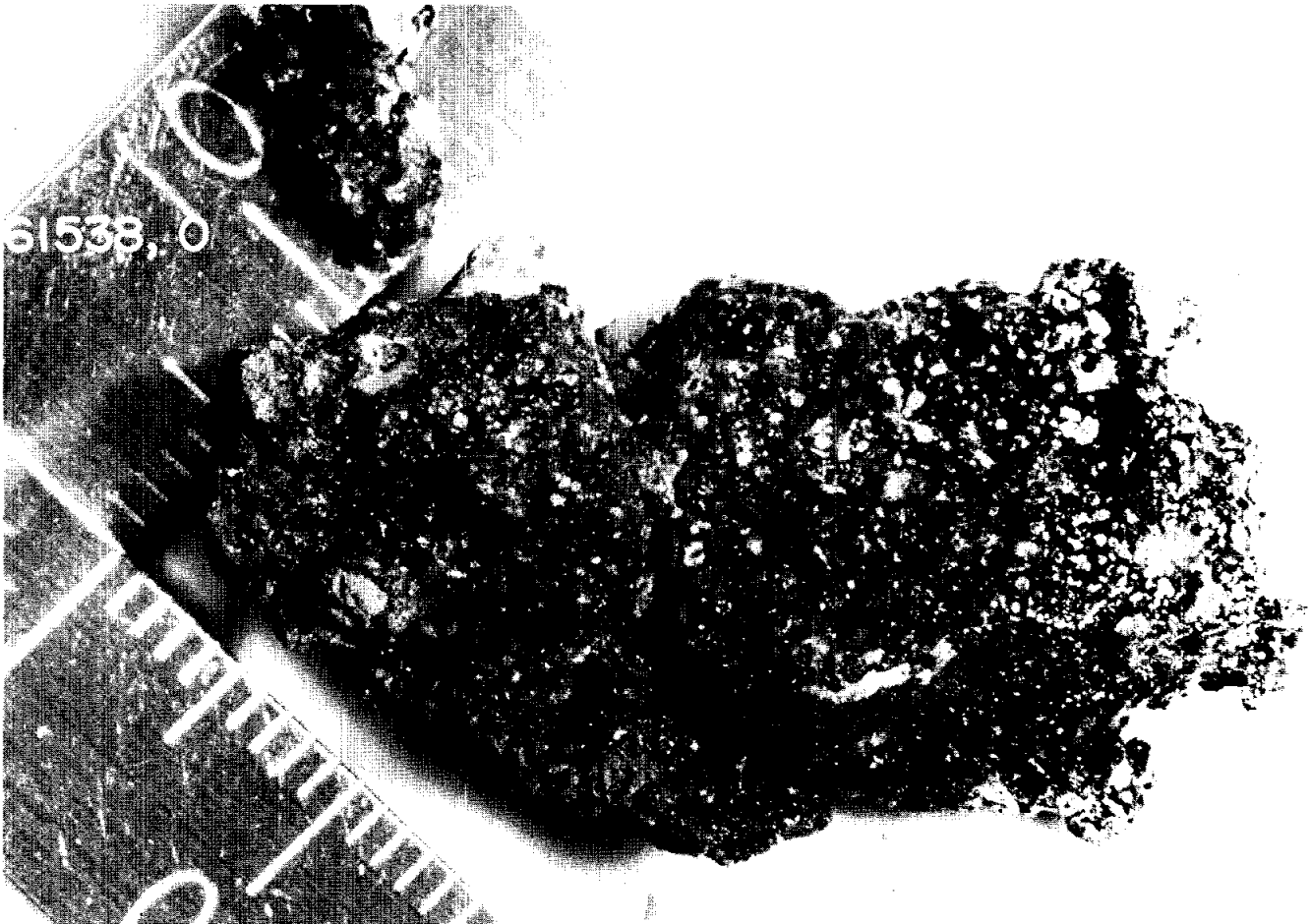


Figure 1. S-73-17119, mm scale.

PETROLOGY: The only thin section of this rock shows a glassy, vesicular impact melt with abundant fragments of plagioclase and anorthositic breccia (Fig. 2). Portions of the glass have crystallized to clusters of elongate tablets and needles of plagioclase separated by a fine-grained mesostasis.

PROCESSING AND SUBDIVISIONS: In 1973 a single chip of glass with some adhering breccia (,1) was allocated to Phinney for thin sectioning and petrography.
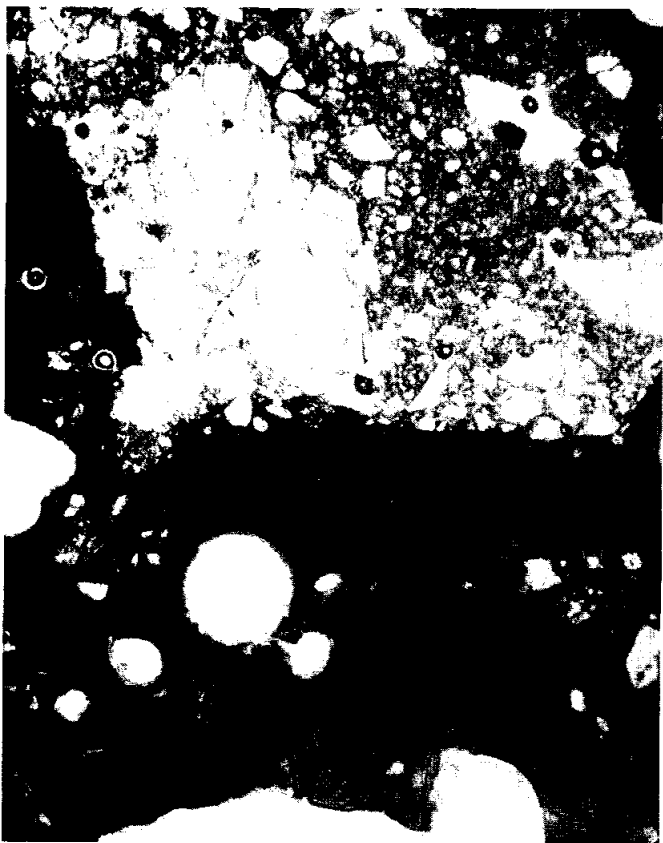


Figure 2. 61538,4, general view, ppl. width 2mm.

INTRODUCTION:  61539 is an aggregate of several fragments of moderately coherent, medium gray breccia welded together by dark, vesicular glass (Fig. 1).  Considerable dust adheres to the glass.  This is a rake sample collected about 45 m northeast of Plum Crater.  Zap pits are rare or absent.



Figure 1. S-72-43349.

INTRODUCTION:  61545 is a moderately coherent, medium gray breccia coated with dark glass (Fig. 1).  Several light clasts are present in the breccia and many smaller fragments of breccia are adhering to the glass.  This is a rake sample collected about 45 m northeast of Plum Crater.  Zap pits are rare or absent.
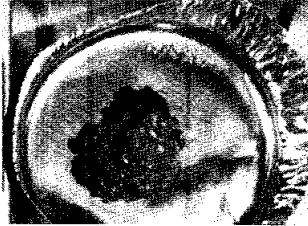


Figure 1. S-72-43349.

<u>INTRODUCTION</u>:  61546 is a coherent, dark gray, glassy impact melt with several large white clasts (Fig. 1).  Vesicles account for ∿25% of the dark matrix. This is a rake sample collected about 45 m northeast of Plum Crater.  Zap pits are abundant on one surface, absent on other surfaces.



<u>Figure 1</u>. S-72-43422, cm scale.

PETROLOGY:   The texture of the matrix varies from aphanitic to nearly basaltic, often over short distances (Fig. 2).  Glass or very fine-grained mesostasis is abundant throughout the rock.  Clasts of plagioclase, mafic minerals and cataclastic anorthosite are abundant and often show diffuse boundaries with the matrix.  Spherules of Fe-metal, often intergrown with troilite and schreibersite, are scattered through the matrix.

PROCESSING AND SUBDIVISIONS:   In 1973 two small chips (,1) were allocated to Phinney for thin sectioning and petrography.



Figure 2. 61546,4, general view, ppl. width 1mm.

INTRODUCTION: 61547 is a coherent, medium gray, crystalline impact melt with a few large vesicles (Fig. 1). It is angular and may be coated by dark glass. It was collected as a rake sample about 45 m northeast of Plum Crater. Zap pits are rare or absent.
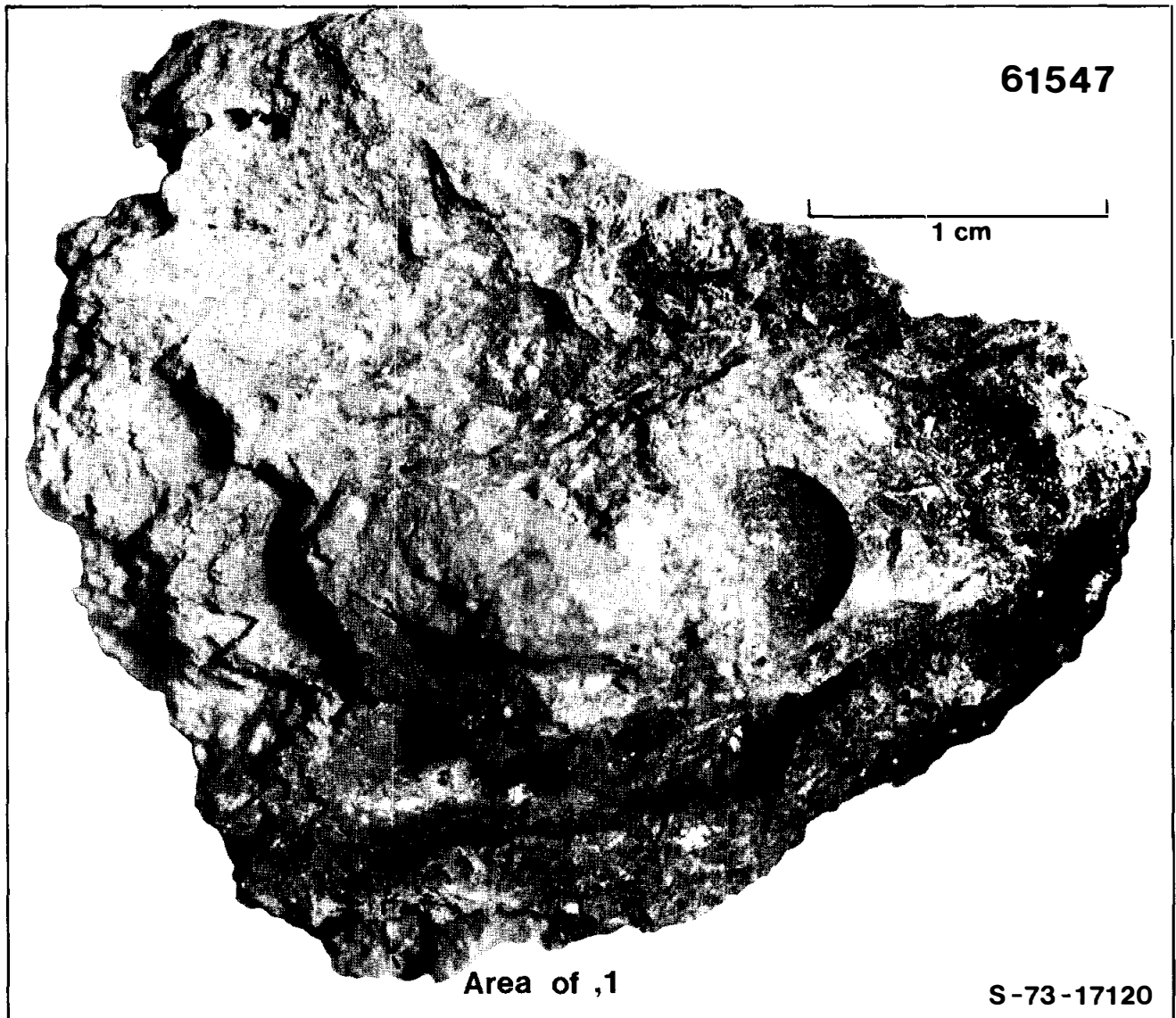


Figure 1.

PETROLOGY:  The thin section of 61547 is dilithologic, showing a fine-grained, basaltic impact melt in sharp contact with a cryptocrystalline to glassy impact melt (Fig. 2).  Clasts of the basalts are present in the glassy material indicating that the latter is probably a coat or vein.

PROCESSING AND SUBDIVISIONS:  In 1973 four small chips (,1) were removed and allocated to Phinney for petrography.
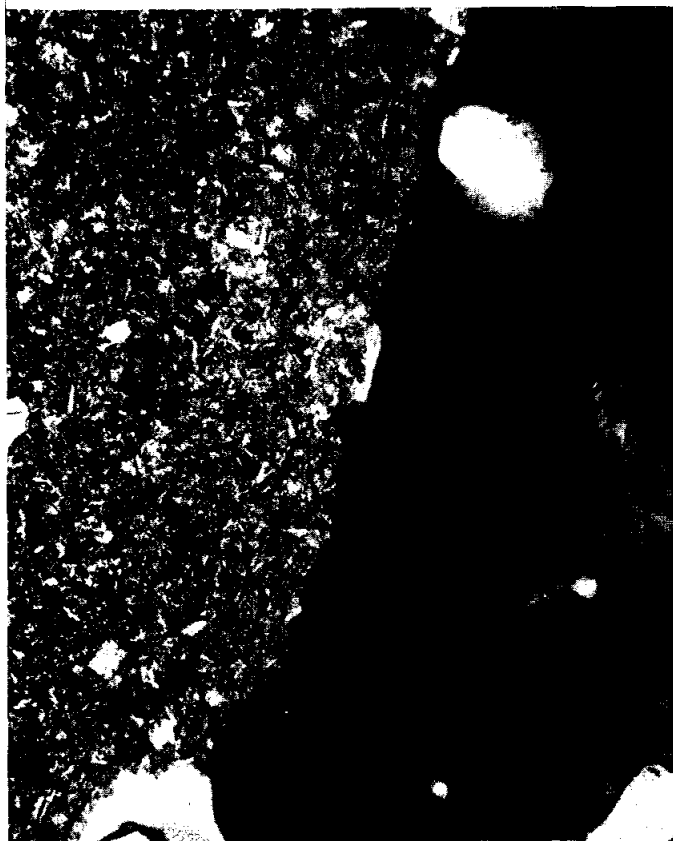


Figure 2. 61547,4, general view, ppl. width 1mm.

INTRODUCTION:  61548 is a coherent, medium gray, glassy impact melt with abundant clasts and vesicles (Fig. 1).  It is subrounded and was collected as a rake sample about 45 m northeast of Plum Crater.  Zap pits are rare.



Figure 1. S-72-55319, mm scale.

PETROLOGY: Warner et al. (1973) include this rock in a general discussion of Apollo 16 rake samples and provide a photomicrograph. Abundant monomineralic clasts of plagioclase, mafic minerals and spherules of Fe-metal rest in a chaotic, glassy matrix that approaches a basaltic texture in places (Fig. 2).

PHYSICAL PROPERTIES: Pearce and Simonds (1974) report the results of a room temperature hysteresis curve determination on 61548. The very small saturation remanence to saturation magnetization ratio ($J_{RS}/J_S = 0.0015$) shows that most of the ferromagnetic phases in this rock occur as relatively large (>300Å), multidomain particles. The magnetically-determined $Fe^0/Fe^{2+}$ (0.0659) and total $Fe^0$ (0.024 wt%) are also given by Pearce and Simonds (1974).

PROCESSING AND SUBDIVISIONS: In 1972 a small piece (,1) was removed and allocated to Phinney for thin sectioning and petrography. The potted butt was used for the magnetic determinations.



Figure 2. 61548,4, general view, ppl. width 1mm.

INTRODUCTION:  61549 is a coherent, medium gray, crystalline impact melt with
several large clasts (Fig. 1).  It is subangular and was collected as a rake
sample about 45 m northeast of Plum Crater.  Zap pits are absent.



Figure 1. S-72-55347, mm scale.

PETROLOGY: Warner et al. (1973) provide a petrographic description and mineral compositions. 61549 is texturally intermediate between a basalt and a fine-grained poikilitic impact melt. Skeletal olivine phenocrysts and laths of plagioclase rest in a fine-grained, faintly poikilitic matrix of plagioclase and pyroxene (Fig. 2). Abundant clasts of plagioclase and lesser amounts of relict spinel and granoblastic norite are present. Mineral compositions are very homogeneous (Fig. 3) suggesting equilibration. Warner et al. (1973) classify this rock as a metamorphosed basalt.

PROCESSING AND SUBDIVISIONS: In 1972 three pieces were broken from the rock and one of these (,1) allocated to Phinney for thin sectioning and petrography.



Figure 2. 61549,4, general view, ppl. width 1mm.
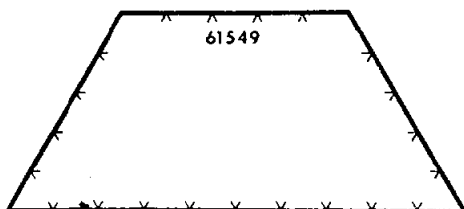


Figure 3. Mafic mineral compositions, olivine plotted along base, from Warner et al. (1973).

<u>INTRODUCTION</u>:  61555 is a coherent, dark gray, glassy impact melt with several <u>white clasts</u> and vesicles (Fig. 1).  It is a rake sample collected about 45 m northeast of Plum Crater.  Zap pits are rare.



<u>Figure 1</u>. S-72-43350.

INTRODUCTION: 61556 is a coherent, medium gray fragment of devitrified (?) impact glass (Fig. 1). It is angular and somewhat vesicular. Clasts are relatively rare. It is a rake sample collected about 45 m northeast of Plum Crater.
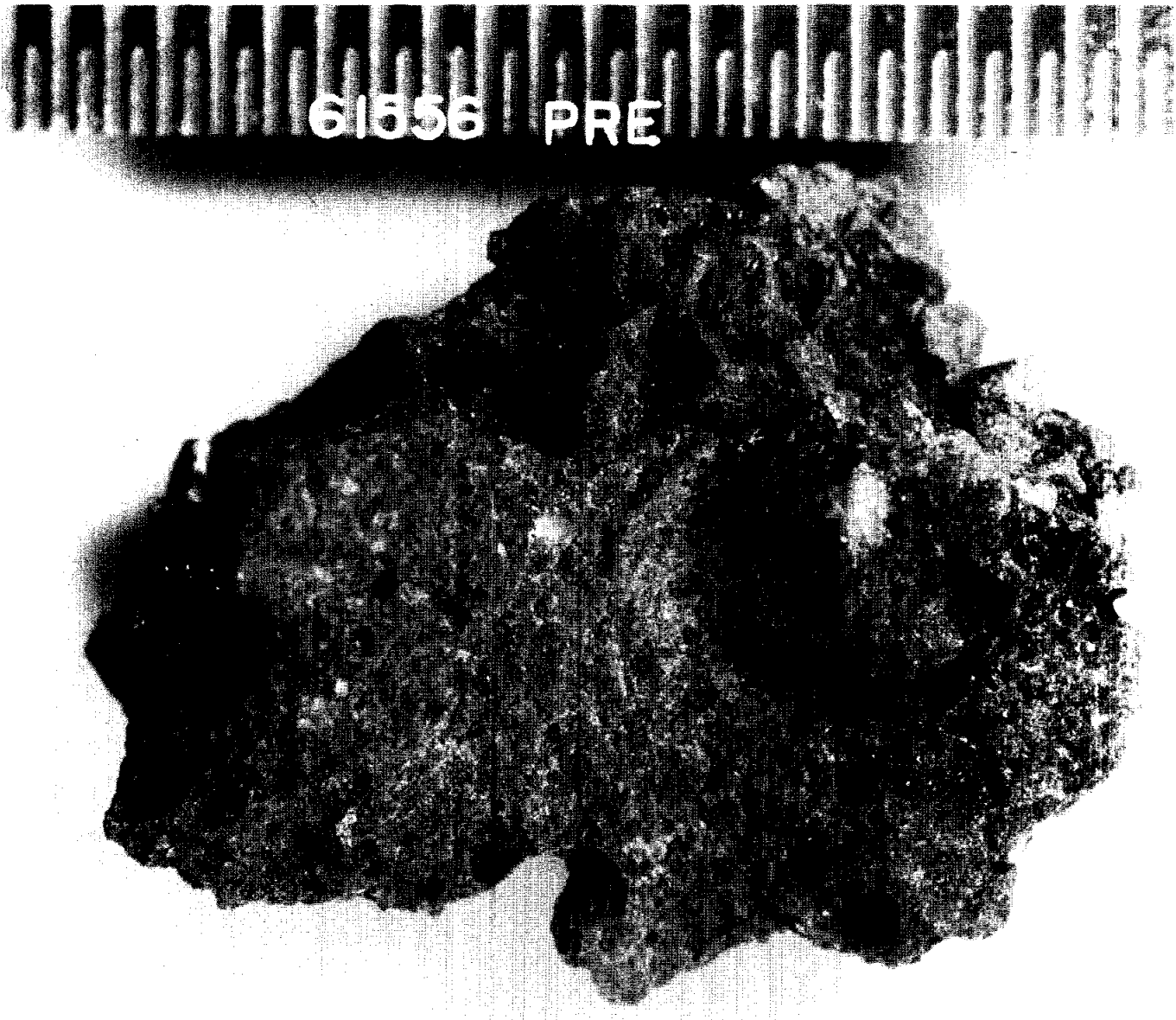


Figure 1. S-72-55349, smallest scale subdivision 0.5mm.

PETROLOGY:  Warner et al. (1973) include  this rock in a general petrographic
study of Apollo 16 rake samples.  61556 is characterized texturally by sets of
closely packed plagioclase tablets separated by thin regions of olivine and/or
mesostasis (Fig. 2, and photomicrograph in Warner et al., 1973).  The rock is
virtually entirely crystalline; very little, if any, clean glass remains.
Mineral compositions of 61556 presumably fall within the range cited by Warner
et al. (1973) for devitrified glass samples, i.e. plagioclase $An_{94-97}$, olivine
$Fo_{75-79}$, with high-Ca pigeonite ($\sim Wo_{15}En_{65}$), Fe-Ti oxide and Fe-metal as
accessory phases.  Fe-metal is 4.9-5.5% Ni, 0.5% Co, 0.4-0.6% P and 0.02% S
(Gooley et al., 1973) and occurs as large (up to $\sim 0.5$ mm), rounded grains (Fig.
2, and photomicrographs in Gooley et al., 1973) and as small spherules disseminated
throughout the rock.  Metal-troilite intergrowths are common.

PROCESSING AND SUBDIVISIONS:  In 1972 a small piece (,1) was removed and
allocated to Phinney for thin sectioning and petrography.



Figure 2. 61556,4, general
view, ppl. width 2mm.

INTRODUCTION:  61557 is a coherent, dark gray, glassy impact melt with a few clasts and vesicles (Fig. 1).  It is a rake sample collected about 45 m north-east of Plum Crater.  Zap pits are rare or absent.



Figure 1. S-72-43350.

INTRODUCTION:  61558 is a coherent, medium gray, impact melt with abundant clasts and vesicles (Fig. 1).  It is a rake sample collected about 45 m northeast of Plum Crater.
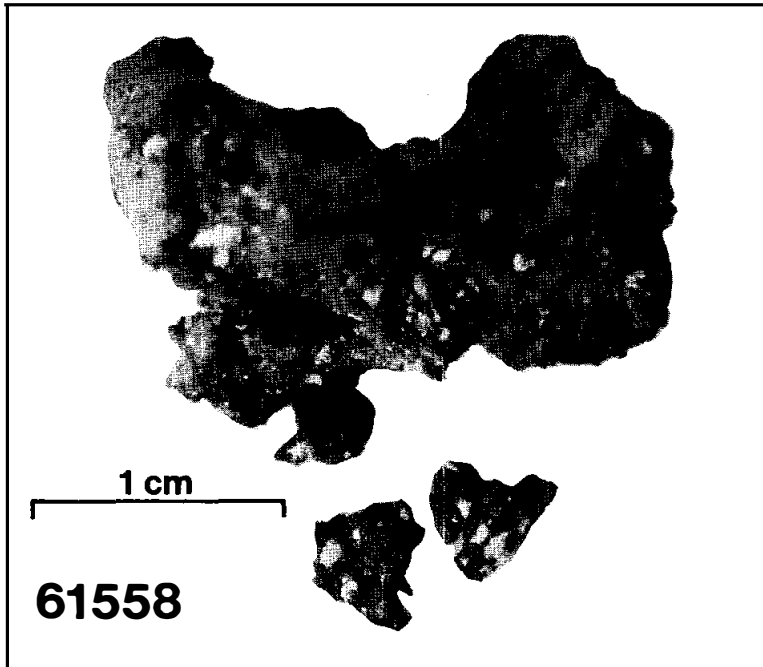


Figure 1.

**61558**

PETROLOGY:  Warner et al. (1973) include  this rock in a general petrographic discussion of Apollo 16 rake samples.  Although 61558 may have been very glassy at one time, it is now almost completely crystalline.  "Quench" crystals surround clasts, but the texture away from the clasts is dominated by a series of interlocking spherulites (Fig. 2, and photomicrograph in Warner et al., 1973). Fragments of plagioclase and cataclastic anorthosite and spherules of Fe-metal, often intergrown with troilite and schreibersite, are scattered through the rock. Compositions of coexisting metal and metal/phosphide intergrowths are given by Gooley et al. (1973) and are reproduced here as Table 1.

TABLE 1.  Coexisting metal and metal/phosphide intergrowth compositions (wt%)

|  |  | Ni | Co | Fe | P | S |
|---|---|---|---|---|---|---|
| a) | Metal | 18.9 | 1.0 | 77.4 | 1.0 | 0.05 |
|  | Eutectic intergrowth | 28.8 | 0.8 | 56.2 | 12.2 | 0.4 |
| b) | Metal | 22.4 | 1.0 | 74.0 | 1.0 | 0.02 |
|  | Eutectic intergrowth | 29.2 | 0.9 | 56.5 | 12.1 | 0.5 |

61558



Figure 2. 61558,4, general view, ppl. width 2mm.

PHYSICAL PROPERTIES: Pearce and Simonds (1974) report the results of a room temperature hysteresis curve determination on 61558. The very small saturation remanence to saturation magnetization ratio ($J_{RS}/J_S$ = 0.009) indicates that most of the ferromagnetic phases in this rock occur as relatively large (>300 Å), multidomain particles. Total $Fe^O$ is 0.037 wt% and $Fe^O/Fe^{2+}$ is 0.0858 (Pearce and Simonds, 1974).

PROCESSING AND SUBDIVISIONS: In 1972 three small chips were removed and one of these (,1) was allocated to Phinney for thin sectioning and petrography. The magnetic studies were done on the potted butt made from ,1.

INTRODUCTION:   61559 is composed of several fragments of gray breccia and abundant dust welded together by dark, vesicular glass (Fig. 1).  It is a rake sample collected about 45 m  northeast of Plum Crater.  Zap pits are absent.

PETROLOGY:   Abundant clasts of plagioclase, mafic minerals, cataclastic anorthosite and basaltic impact melt rest in a matrix of dark, vesicular glass (Fig. 2).

PROCESSING AND SUBDIVISIONS:   In 1973 three small pieces (,1) were allocated to Phinney for thin sectioning and petrography.
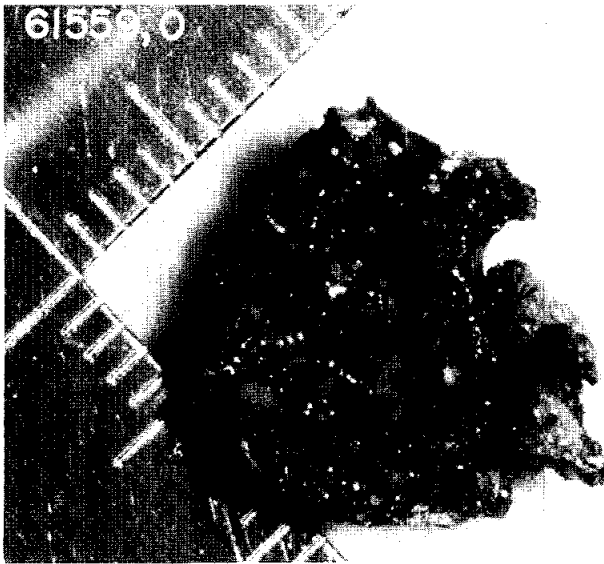


Figure 1. S- 73-17115, mm scale.
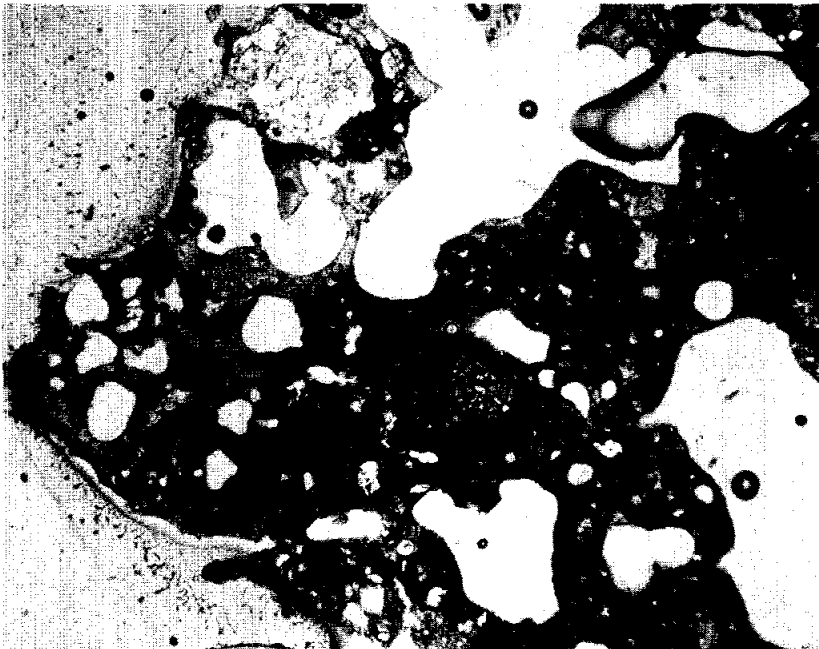


Figure 2.   61559,4, general view, ppl. width 2mm.

INTRODUCTION:  61565 is an aggregate of several fragments of gray breccia welded together by dark, vesicular glass (Fig. 1).  Some dust adheres to the smooth surfaces of the glass.  It is a rake sample collected about 45 m northeast of Plum Crater.  Zap pits are absent.



Figure 1. S-72-43350.

INTRODUCTION:  61566 is a coherent, dark gray, glassy impact melt (Fig. 1).  It is angular with several clasts and many vesicles and was collected as a rake sample about 45 m northeast of Plum Crater.  Zap pits are absent.



Figure 1.  S-72-43350.

INTRODUCTION:  61567 is a coherent, dark gray, glassy impact melt (Fig. 1).
Some white clasts and vesicles are present.  It is a rake sample collected
about 45 m northeast of Plum Crater.  Zap pits are absent.



Figure 1. S-72-43350.

INTRODUCTION:  61568 is a coherent, medium gray, crystalline impact melt with few vesicles (Fig. 1).  It is a rake sample collected ~45 m northeast of Plum Crater.  Zap pits are abundant.



Figure 1. S-72-55324.

PETROLOGY: The only thin section of this rock is dilithologic, showing a fine-grained basaltic impact melt in sharp contact with a poikilitic lithology (Fig. 2). Warner et al. (1973) include 61568 in a general petrographic discussion of Apollo 16 rake samples and provide mineral compositions for the basaltic lithology. Simonds et al. (1973) give a brief petrographic description and mineral compositions of the poikilitic material. Clast/matrix relations cannot be determined from this thin section.

The basaltic lithology is fine-grained with grains of olivine and pyroxene filling interstices between plagioclase laths. Relatively large and angular clasts of plagioclase are abundant (Fig. 2). Mineral compositions are shown in Figure 3.

The poikilitic lithology is composed of pigeonite oikocrysts surrounding chadacrysts and clasts of plagioclase, olivine and opaques. Mineral compositions are shown in Figure 3. Coexisting Fe-metal and schreibersite compositions are given by Gooley et al. (1973) and are reproduced here as Table 1.
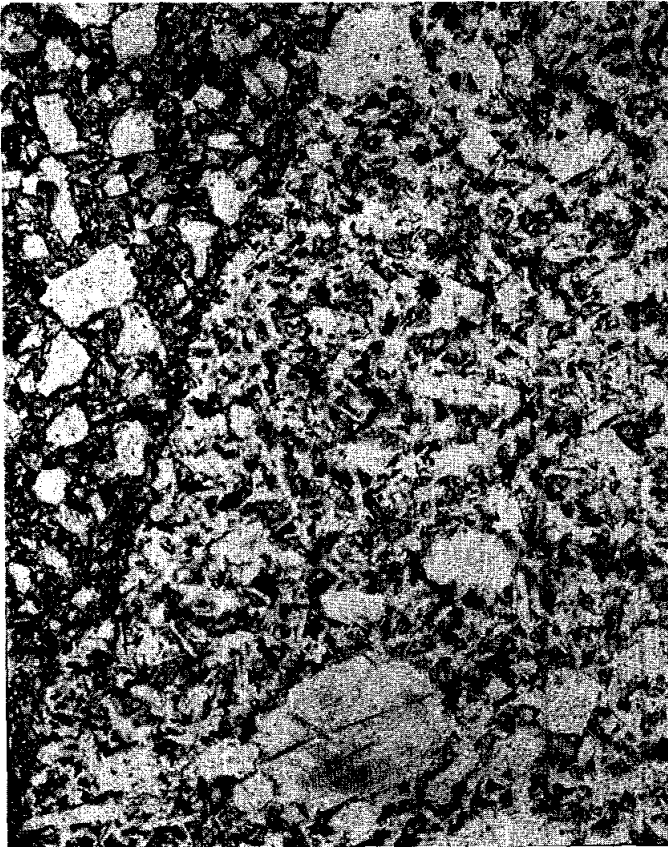


Figure 2. 61568,4, general view, ppl. width 2mm.

TABLE 1. Coexisting metal and schreibersite compositions (wt%)

|   |   | Ni | Co | Fe | P | S |
|---|---|---|---|---|---|---|
| a) | Metal | 6.9 | 0.4 | 92.4 | 0.01 | 0.02 |
|   | Schreibersite | 47.3 | 0.05 | 38.1 | 15.2 | 0.07 |
| b) | Metal | 4.1 | 0.5 | 95.8 | 0.04 | 0.02 |
|   | Schreibersite | 32.7 | 0.1 | 50.9 | 15.4 | 0.06 |
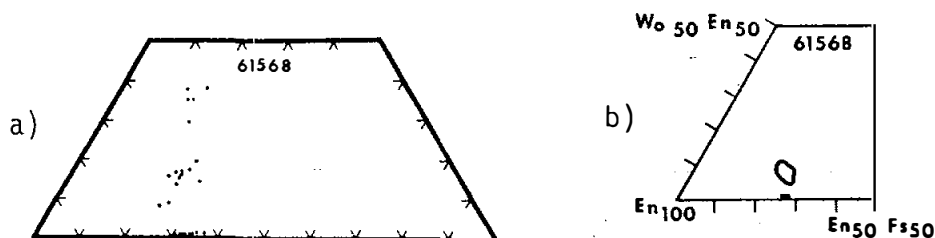


Figure 3. Mafic mineral compositions, olivine plotted along base; a) basaltic melt, from Warner et al. (1973); b) poikilitic melt, from Simonds et al. (1973).

PHYSICAL PROPERTIES: Pearce and Simonds (1974) report the results of a room temperature hysteresis curve determination on 61568. The very low saturation remanence to saturation magnetization ratio ($J_{RS}/J_S$ = 0.0021) indicates that most of the ferromagnetic phases in 61568 occur as >300 Å multidomain particles. The total Fe° is 0.26 wt% and Fe°/Fe$^{2+}$ is 0.0921 (Pearce and Simonds, 1974).

PROCESSING AND SUBDIVISIONS: In 1972 a small chip (,1) was allocated to Phinney for thin sectioning and petrography. The magnetic studies were done on the potted butt made from ,1.

INTRODUCTION:   61569 is a medium gray, coherent, poikilitic impact melt (Fig. 1).
It is angular with ∿5% vesicles, and was collected ∿45 m northeast of Plum Crater.
Zap pits are absent.



Figure 1. S-72-55317, smallest scale subdivision 0.5mm.

PETROLOGY: A petrographic description is given by Simonds et al. (1973). 61569 differs from most other Apollo 16 poikilitic rocks in that olivine is the major oikocryst phase. Rounded olivine oikocrysts (up to 1.5 mm across) enclose equant to tabular plagioclase chadacrysts and rare augite chadacrysts (Fig. 2). Plagioclase clasts are concentrated between the olivines and are surrounded by oikocrysts of pigeonite. Simonds et al. (1973) give a mode of 68% plagioclase + mesostasis, 22% olivine, 6% pigeonite, 2% augite and 2% opaques. Mineral compositions are shown in Figure 3.

CHEMISTRY: Major and trace element data are given by Wasson et al. (1977) and summarized here as Table 1.

PROCESSING AND SUBDIVISIONS: In 1972 a small chip (,1) was removed and allocated to Phinney for thin sectioning and petrography. In 1977 another small piece (,5) was allocated to Wasson for chemistry.



Figure 2. 61569,4, general view, xpl. width 2mm.

TABLE 1.  Summary chemistry of 61569

| | | |
|---|---|---|
| $SiO_2$ | | |
| $TiO_2$ | 1.00 | |
| $Al_2O_3$ | 21.9 | |
| $Cr_2O_3$ | 0.16 | |
| FeO | 7.4 | |
| MnO | 0.09 | |
| MgO | 10.0 | |
| CaO | 12.9 | |
| $Na_2O$ | 0.467 | |
| $K_2O$ | 0.186 | |
| $P_2O_5$ | | |
| Sr | | |
| La | 18.1 | |
| Lu | 0.82 | |
| Rb | | |
| Sc | 12.4 | |
| Ni | 1000 | |
| Co | 54 | |
| Ir | ppb | 20 |
| Au | ppb | 18 |
| C | | |
| N | | |
| S | | |
| Zn | | |
| Cu | | |

Oxides in wt%; others in ppm except as noted.
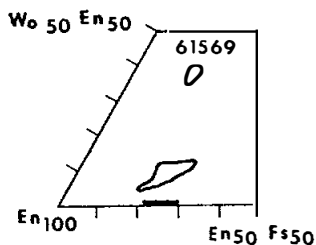


Figure 3. Mafic mineral compositions, olivine plotted along base, from Simonds et al. (1973).

INTRODUCTION:  61575 is a coherent, medium gray, crystalline rock with several large white clasts (Fig. 1).  It is a rake sample collected ∿45 m northeast of Plum Crater.
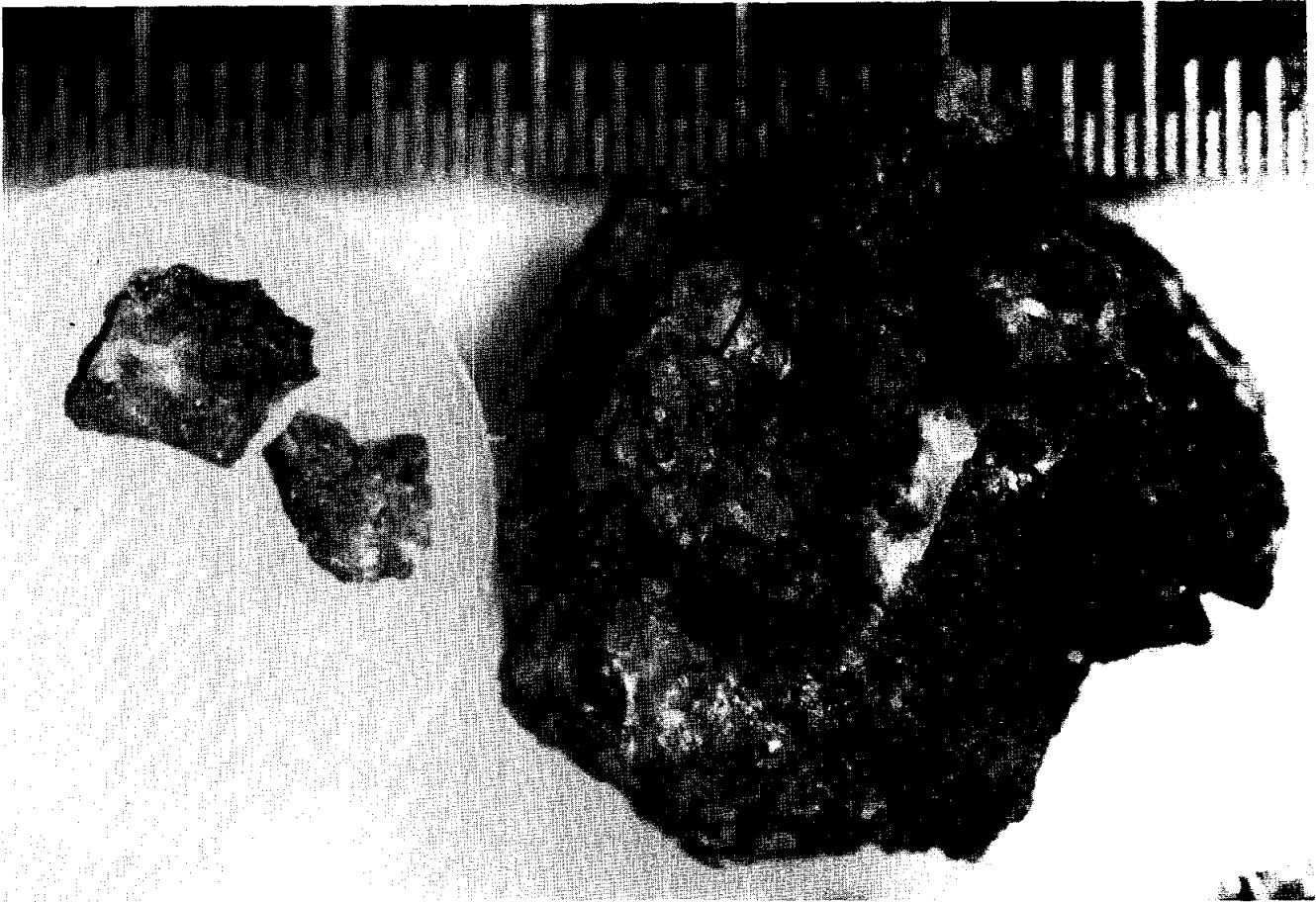


Figure 1. S-72-55323, smallest scale subdivision 0.5mm.

PETROLOGY:  Warner et al. (1973) include this rock in a general petrographic discussion of Apollo 16 rake samples.  The only thin section consists entirely of a single grain of severely shocked plagioclase (∿8 mm) with a few small, rounded inclusions of a mafic mineral (Fig. 2).  Phinney and Lofgren (1973, p. 19) state that this rock is "probably ... a coarse-grained plagioclase rock that has been partially melted and shocked ..."  Warner et al. (1973) classify it as "devitrified glass (?) with large clear plagioclase clasts".
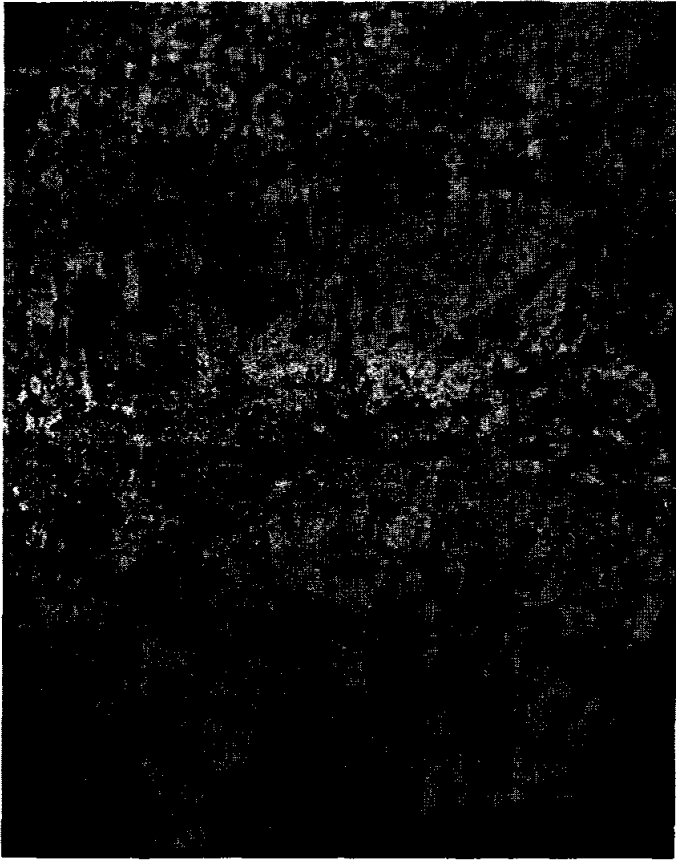
Figure 2. 61575,4, plagioclase grain, xpl. width 4mm.

PROCESSING AND SUBDIVISIONS:  In 1972 two small pieces were removed from the rock and one of them (,1) allocated to Phinney for thin sectioning and petrography.

INTRODUCTION:  61576 is a coherent, white fragment composed almost entirely of plagioclase (Fig. 1).  The continuous cleavage suggests that it is a single crystal.  A dark, vesicular, glassy coating occurs on one surface.  It is a rake sample collected ~45 m northeast of Plum Crater.  Zap pits are present on one surface.

PETROLOGY:  Bell and Mao (1975) report that 61576 is very homogeneous in composition and contains abundant inclusions.  No analyses are given.

PROCESSING AND SUBDIVISIONS:  In 1975 three small chips (,1) were removed and allocated to Bell.
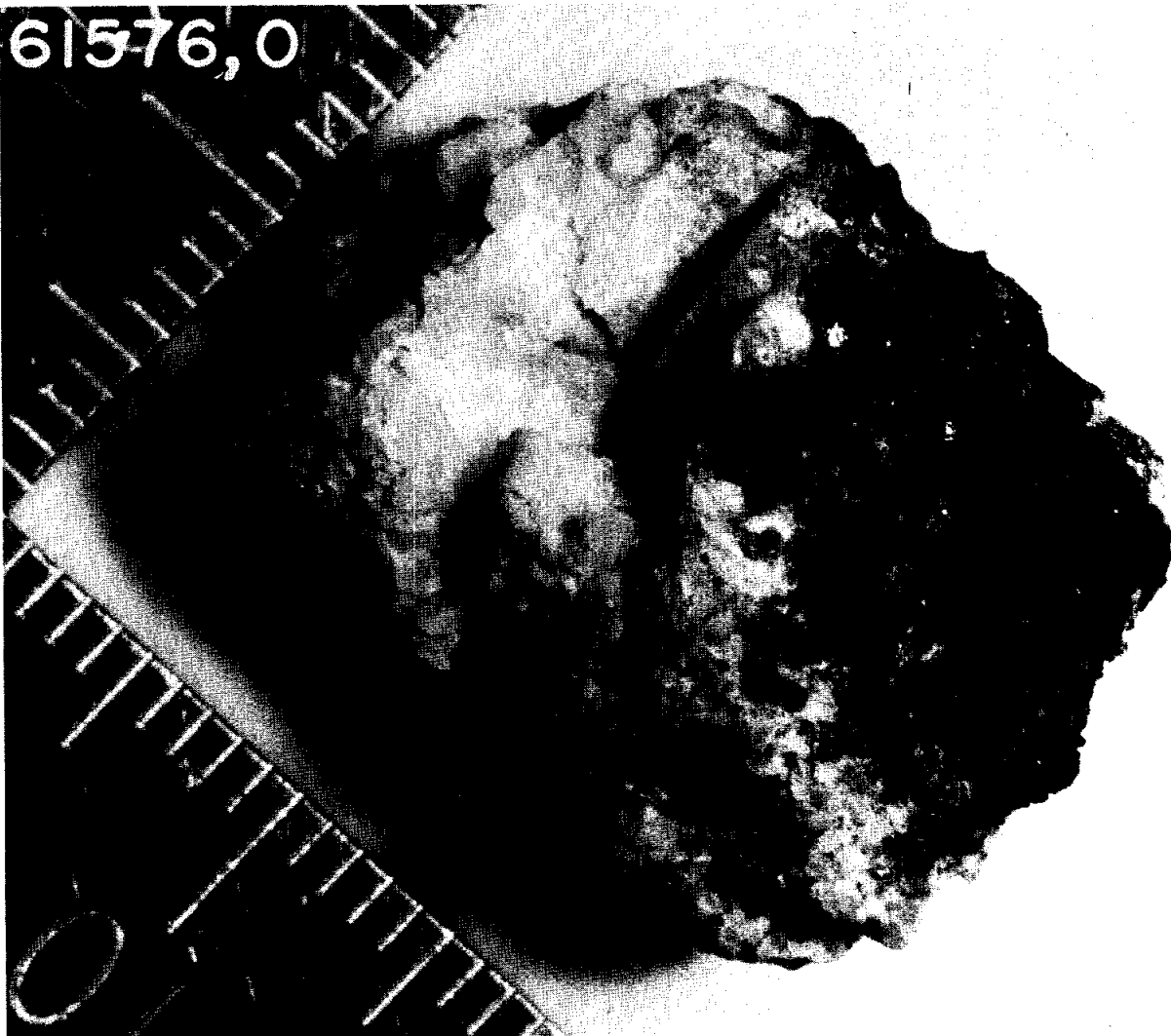
Figure 1. S-73-17117, mm scale.

INTRODUCTION:   61577 is a friable, white anorthositic rock with a partial coating of dark glass (Fig. 1).   It is a rake sample collected ∿45 m northeast of Plum Crater.  Zap pits are abundant on all surfaces.

PETROLOGY:   Tiny, anhedral mafic minerals are interstitial to blocky, anhedral plagioclase grains (Fig. 2).   A crust of clast-rich, glassy breccia is present.

PROCESSING AND SUBDIVISIONS:   In 1973 four small chips (,1) were removed and allocated to Phinney for petrography.
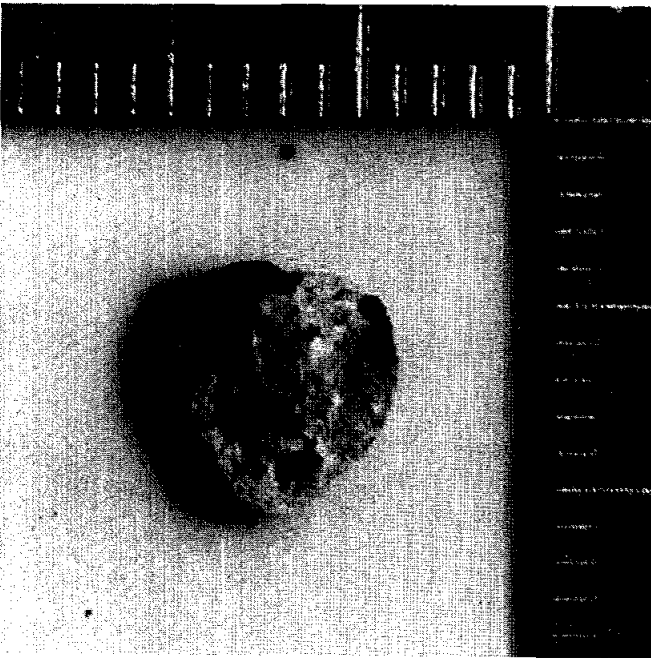


Figure 1. S-73-17118, mm scale.
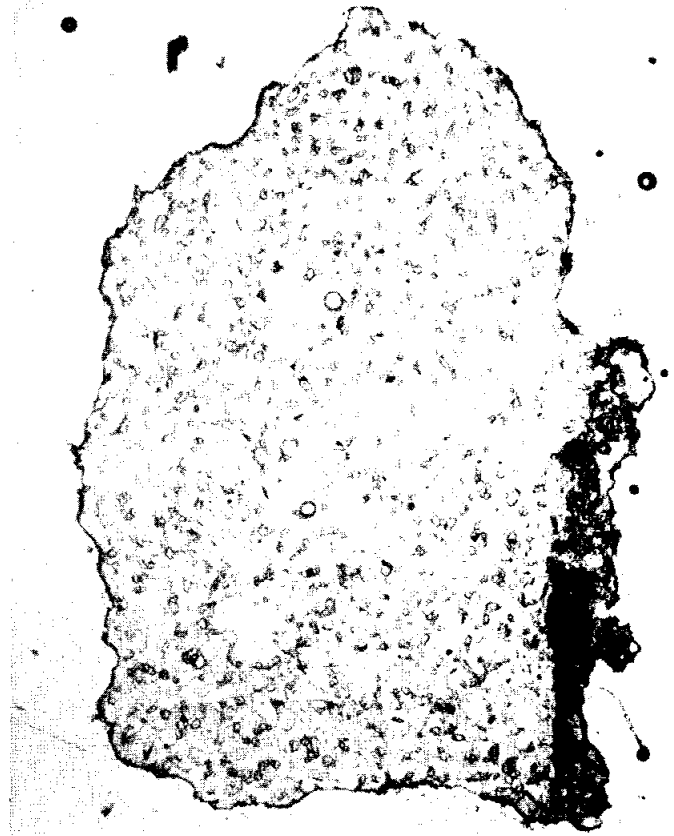


Figure 2. 61577,4, general view ppl. width 2mm.

INTRODUCTION:   62235 is a homogeneous, coherent block (Fig. 1) composed of
poikilitic, KREEP-rich melt with a few clasts and small vesicles.  It was col-
lected from the rim of Buster Crater where it was perched and its orientation
documented.  Zap pits are irregularly distributed with many on one side and
few on the others.
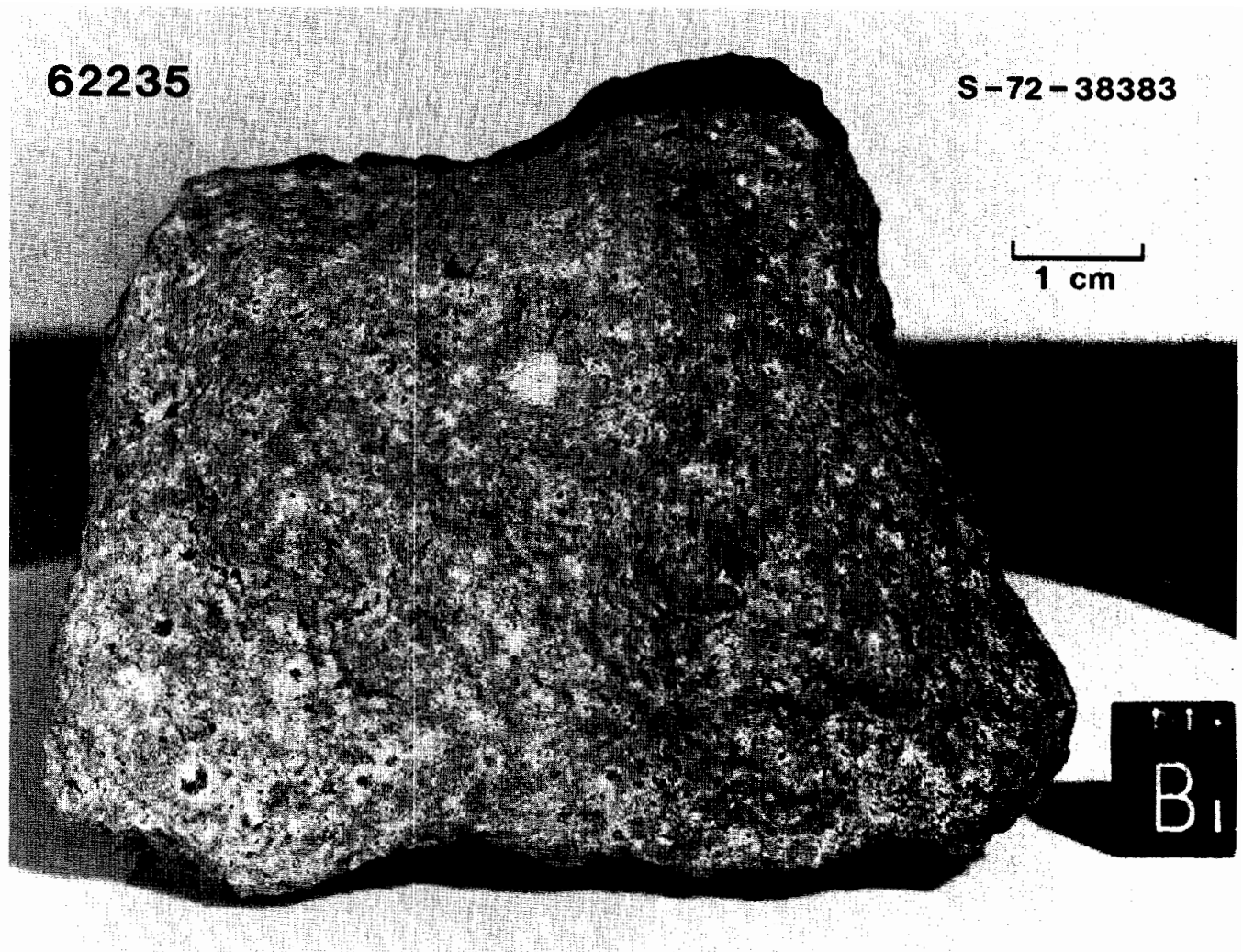


FIGURE 1.

PETROLOGY:   Crawford and Hollister (1974) give a detailed petrographic descrip-
tion with mineral analyses.  Vaniman and Papike (1981) include 62235 in a study
of highland melt rocks.  The rock is composed of ~57% calcic plagioclase with
the remainder mainly elongate oikocrysts of hypersthene (Fig. 2).  The oiko-
crysts are up to ~1 mm long and are often cored with unzoned olivine and over-
grown with pigeonite.  Some lamellae and patches of augite are also present
within the oikocrysts.  Mineral compositions are shown in Figure 3; the

a

b
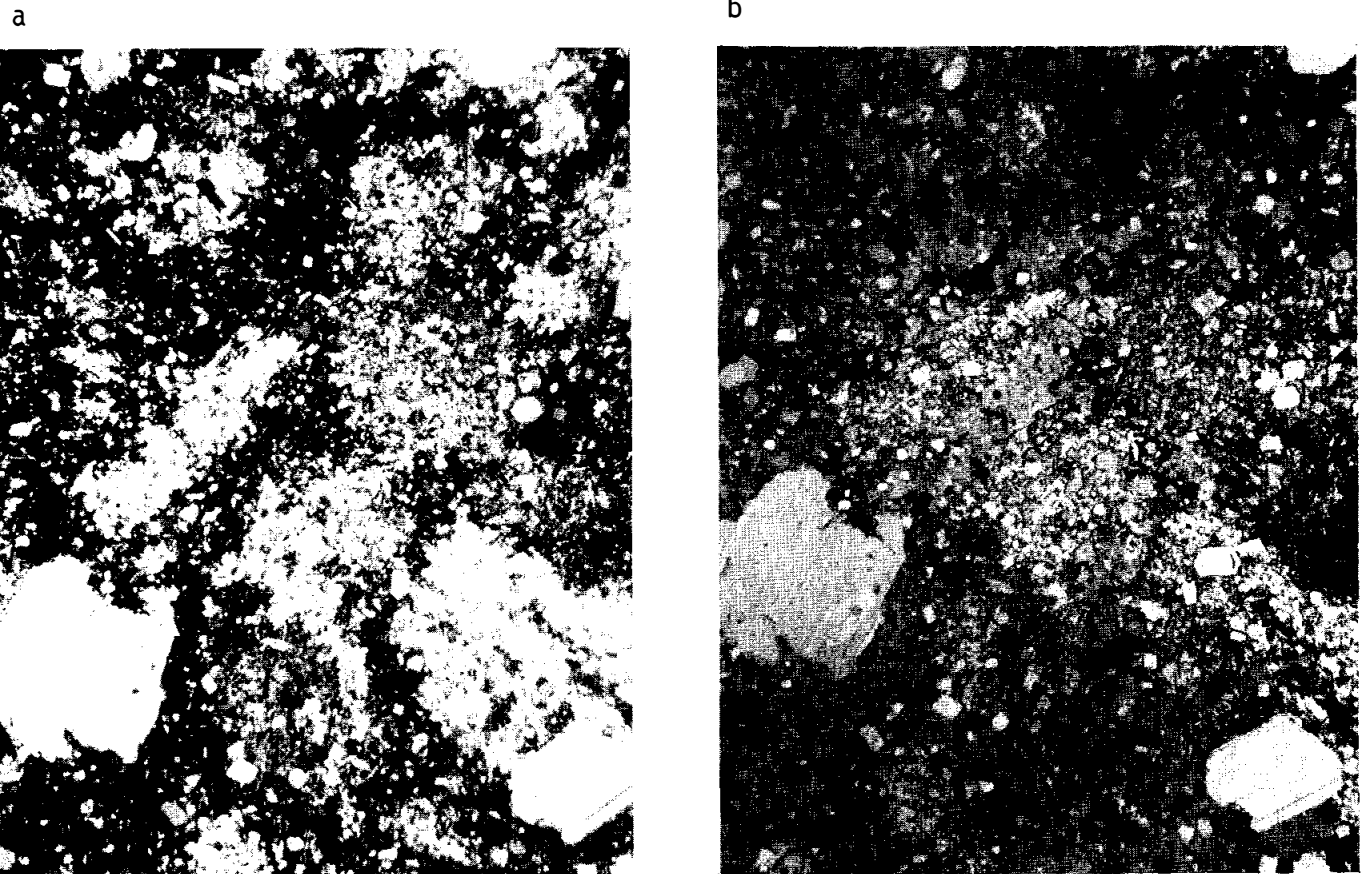


FIGURE 2. 62235,65. general view. width 2mm. a) xpl. b) ppl with reflector in.

early hypersthene is aluminous ($\sim$3% $Al_2O_3$). Interoikocryst areas are composed mainly of plagioclase, glass, ilmenite (or armalcolite?) and Fe-metal/troilite (Fig. 2). Pearce et al. (1976) show that Fe-metal composes 1.1% of the rock and has compositions within the meteoritic range (Fig. 4). A crystallization sequence of plagioclase → pyroxene → ilmenite was deduced by Engelhardt (1978, 1979).

Plagioclase occurs in several forms: (i) as large, shocked or polygonal clasts ($An_{94-96}$), (ii) as small, euhedral, blocky grains ($An_{98}$) with visible, more sodic (<$An_{90}$) rims, (iii) as a second group of blocky grains ($An_{84}$), (iv) as small, rectangular chadacrysts and laths in the interoikocryst areas ($An_{92-93}$). All of the coarser blocky grains show reverse zoning in their outer rims to $An_{92-93}$, the same composition as the chadacrysts and interoikocryst laths. Crawford and Hollister (1974) give Fe/Mg data for plagioclase.

Simonds et al. (1976) find that 62235 contains 9% total clasts larger than 50 μm, and that 95% of these clasts are plagioclase. Meyer et al. (1974) analyzed minor elements in plagioclase using the ion microprobe (Table 1) and found that the Ba contents of plagioclases larger than 50 μm are much too low for the plagioclases to be in equilibrium with the melt. These low-Ba plagioclases are $\sim$10% of 62235.

TABLE 1.  Minor elements in 62235 plagioclase (Meyer et al. (1974) (ppm except Na$_2$O, wt %)

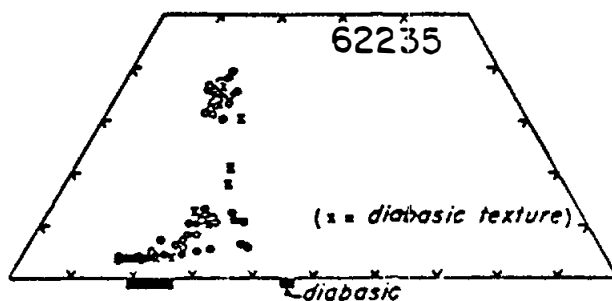|  | Na$_2$O | Li | Mg | K | Ti | Sr | Ba |
|---|---|---|---|---|---|---|---|
| 6 xenocrysts | 0.42 | 5 | 600 | 240 | 97 | 162 | 9 |
| 1 small grain | 0.76 | 10 | 360 | 500 | 130 | 270 | 30 |
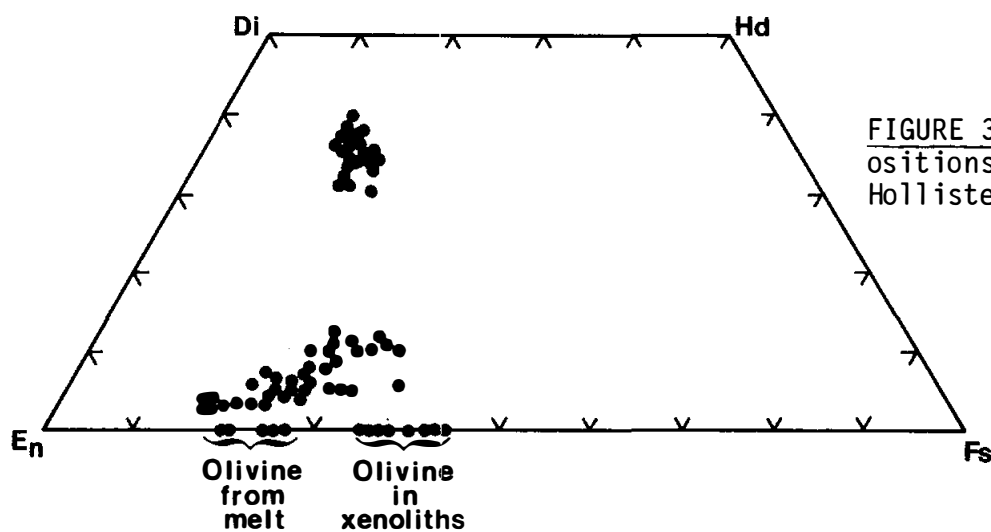
FIGURE 3a.  Mineral compositions; from Crawford and Hollister (1974).

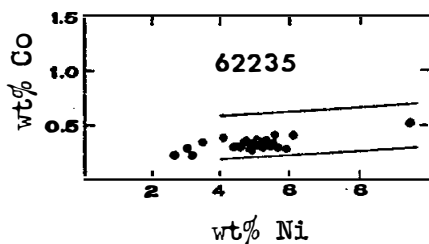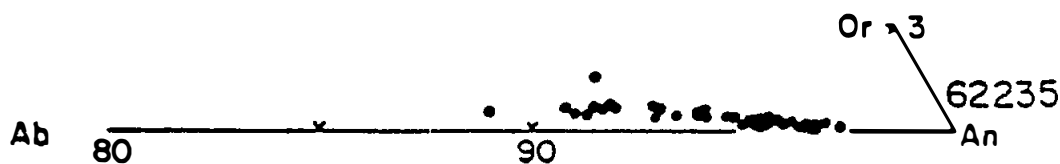FIGURE 3b.  Mineral compositions; from Vaniman and Papike (1981).

FIGURE 4. Metals; from Pearce et al.(1976).

The characteristics of the rock require that most of it crystallized from a silicate melt, the rest being fragmental. Crawford and Hollister (1974) interpret all but the coarsest shocked plagioclases as having crystallized from the melt and cite several features as suggesting crystallization at depth. They infer a volcanic origin with a source at $\sim$200 km. These interpretations are not unique and the evidence of Meyer et al. (1974) suggests that more of the plagioclase is fragmental and that some of the featured cited by Crawford and Hollister (1974) are due to clast-matrix interactions. The rock is very similar to the other poikilitic samples interpreted as impact melts.

CHEMISTRY: Major and trace element analyses are presented, with little specific comment, by Brunfelt et al. (1973), Hubbard et al. (1973), LSPET (1973), Laul et al. (1974) and Wanke et al. (1976). Moore et al. (1973) provide C data and Clark and Keith (1973) radionuclide data.

Chemically 62235 is a KREEP-rich, siderophile-rich rock (Table 1, Fig. 5) similar to several other poikilitic rocks. Crawford and Hollister (1974) suggest that the siderophiles are indigenous, but high contents are usually interpreted as meteoritic contamination (Laul et al. 1974). The carbon content of 2 ppm (Moore et al. 1973) is extremely low.

TABLE 2. Summary chemistry of 62235

| | |
|---|---|
| $SiO_2$ | 47.0 |
| $TiO_2$ | 1.2 |
| $Al_2O_3$ | 18.6 |
| $Cr_2O_3$ | 0.19 |
| FeO | 9.5 |
| MnO | 0.11 |
| MgO | 10.3 |
| CaO | 11.5 |
| $Na_2O$ | 0.48 |
| $K_2O$ | 0.34 |
| $P_2O_5$ | 0.40 |
| Sr | 160 |
| La | 60 |
| Lu | 2.7 |
| Rb | 9 |
| Sc | 16 |
| Ni | 700 |
| Co | 50 |
| Ir ppb | 19 |
| Au ppb | 17 |
| C | 2 |
| N | |
| S | 1000 |
| Zn | 2.2-11 |
| Cu | 3.9-11 |

Oxides in wt%; others in ppm except as noted.
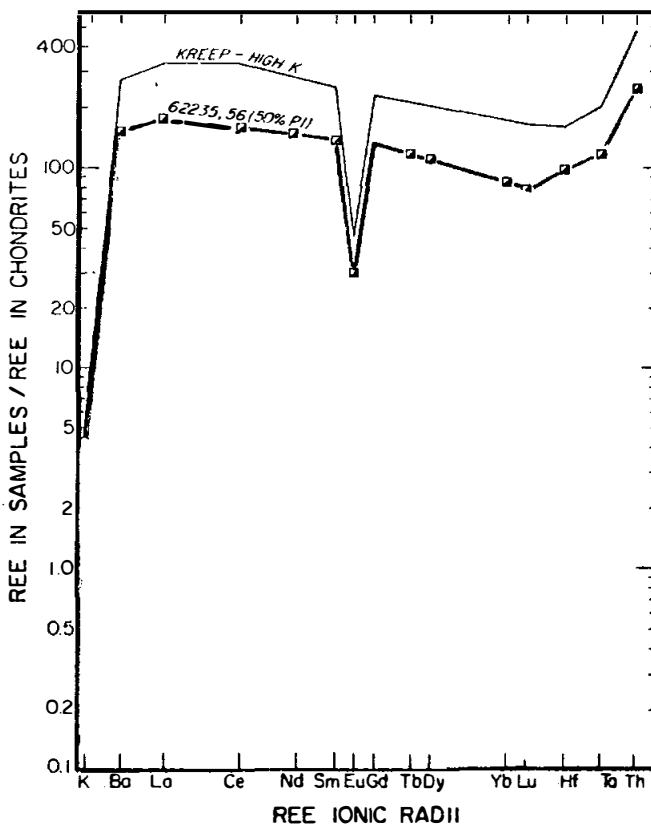


FIGURE 5. Incompatible elements; from Laul et al. (1974).

RADIOGENIC ISOTOPES AND GEOCHRONOLOGY: No internal isochron or $^{40}Ar$-$^{39}Ar$ data have been published. Nyquist et al. (1973) and Tera et al. (1974) provide whole-rock Rb-Sr isotopic data giving $T_{BABI}$ ages of ~4.5 b.y. (Table 3).

TABLE 3. Rb-Sr data for 62235

| Rb ppm | Sr ppm | $^{87}Sr/^{86}Sr$ | $^{87}Sr/^{86}Sr$* | $T_{BABI}$(b.y.) | Reference |
|---|---|---|---|---|---|
| 9.32 | 161 | 0.70989±7 | 0.70042 | 4.48 | Nyquist et al.(1973) |
| 9.03 | 162 | 0.70944±9 | 0.70042 | 4.50 | Tera et al.(1974) |

*Calculated for 3.9 b.y., corrected for interlaboratory bias to Caltech data.

Tera et al. (1974) provide U, Th, Pb isotopic data demonstrating the presence of much in situ radiogenic lead, as with many other KREEP samples. The sample falls on the U-Pb discord formed by most highland total rock samples, corresponding to a metamorphism age of ~3.9 b.y.

RARE GASES/EXPOSURE AGES: Drozd et al. (1974) provide $^{81}Kr$-Kr, $^{21}Ne$, and $^{38}Ar$ exposure ages of 153.9 ± 2.9, 104 ± 54 and 163.0 ± 54 m.y., respectively. However, the sample did not spend its entire 153 m.y. apparent exposure age at its surface location and it must have been lightly shielded. Pepin et al. (1974) show that the $^{21}Ne$ and $^{38}Ar$ ages (which depend on spallation production rates) agree with the $^{81}Kr$-Kr age if the effective irradiation depth was 90 g/cm$^2$. Crozaz et al. (1974) use cosmic tracks to give a maximum exposure age (single point method) of 4 m.y. and a "true" suntan age(track density/depth method) of 2 m.y. There are large grain-to-grain track density variations. Morrison et al. (1973) use microcrater densities to suggest an exposure age of 2-3 m.y.

Lightner and Marti(1974b) provide xenon concentration and isotopic data without a specific interpretation.

MICROCRATERS: Morrison et al. (1973) and Neukum et al. (1973) provide frequency distribution diagrams for microcraters (Fig. 6). Only about half the surface has microcraters and the rock was not continually tumbled. Morrison et al. (1973) conclude that the surface is well below steady-state for craters <0.08 cm in diameter. Neukum et al. (1973) conclude that 62235 has an equilibrium population. McDonnell et al. (1976) and Flavill et al. (1978) experimentally produced microcraters on a sample of 62235 by bombarding it with iron particles. They emphasize the importance of secondary ejecta.

PHYSICAL PROPERTIES: Collinson et al. (1973) provide NRM data for 62235 (Fig. 7) which they discuss further in Stephenson et al. (1974,1975) and Stephenson and Collinson (1974). They find two components of stable magnetization, one of which is extremely hard and of unusually high intensity. Investigation of paleointensity using the Thellier method suggests a field of 1.2 Oe, and using the anhysteretic remanent magnetization (ARM) method suggests a field of 1.4 Oe. Cisowski et al. (1975) used the data to give a field of 0.3 Oe using the IRM$_s$ method, later revised to 1.0 Oe (Cisowski et al., 1977). These results have been questioned: Brecher (1975) attributes the data to "textural remanance", not to any lunar field, and Pearce et al. (1976) performed heating experiments
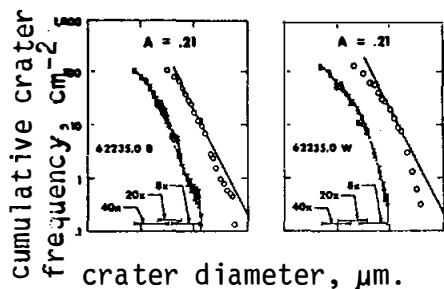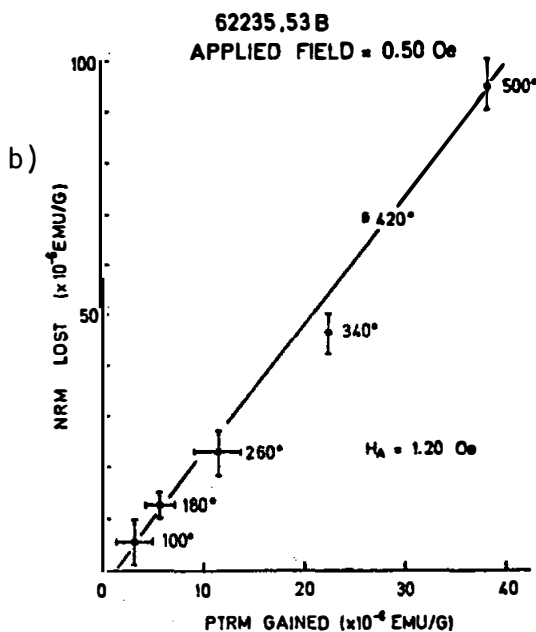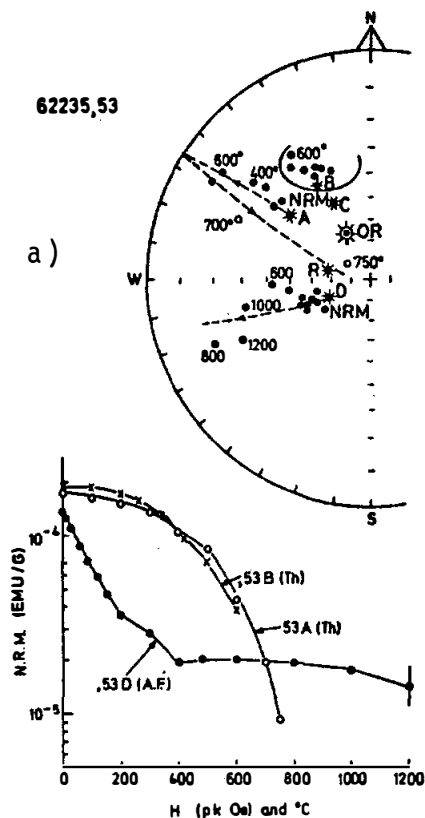
FIGURE 6. Microcraters; from Neukum et al. (1973).



FIGURE 7. Magnetic data; from Collinson et al. (1973) a) Alternating field and thermal demagnetization. b) Field intensity determination.

showing that complexities introduced by Fe-metal and troilite grains make the definition of paleointensity extremely difficult. Contrarily, Hargraves and Dorety (1976) interpret the small variation of NRM and IRM with alternating field demagnetization of 62235 to show that it is a good sample for paleointensity determinations.

Chung and Westphal (1973) provide dielectric constants, dielectric losses, and electrical conductivities for 62235 as functions of frequency and temperature (Fig. 8)
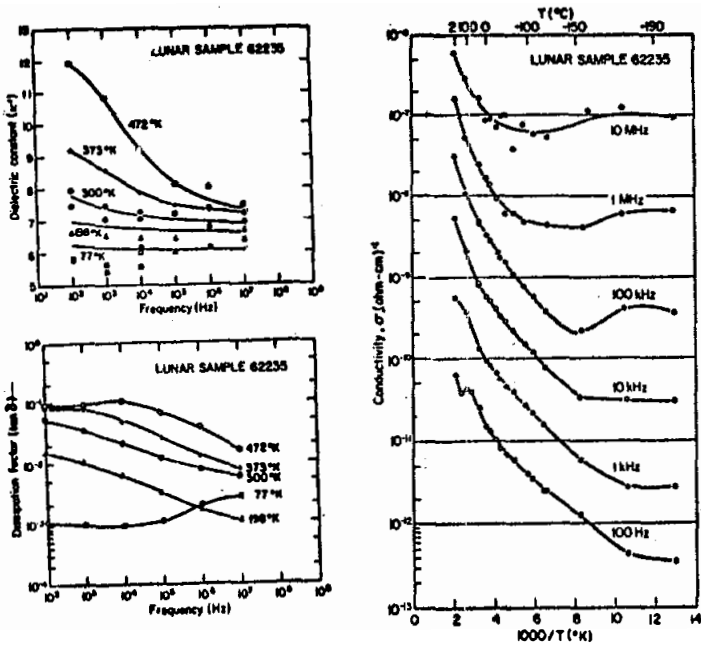
FIGURE 8. Electrical data; from Chung and Westphal (1973).
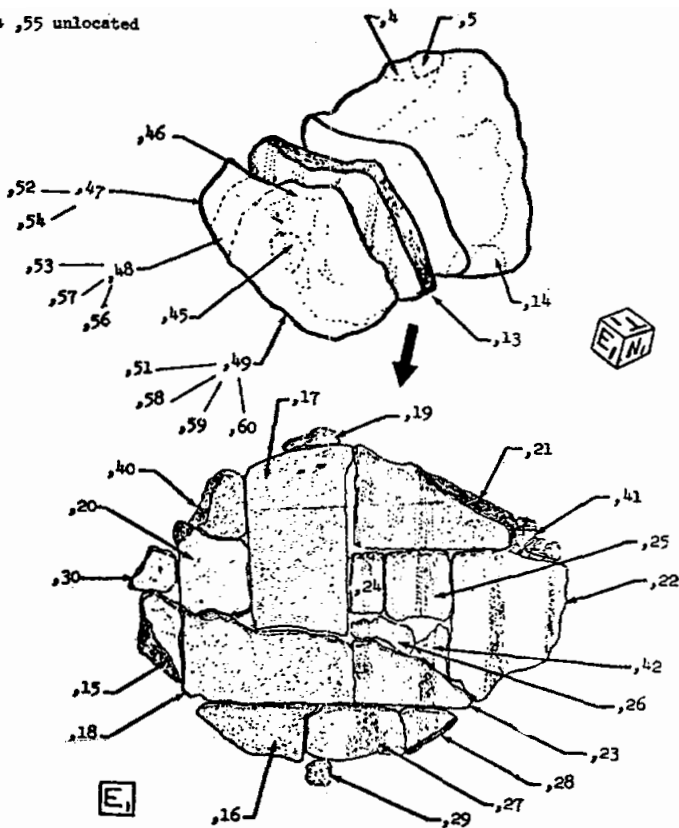


FIGURE 9. Cutting diagram.

PROCESSING AND SUBDIVISIONS:   In 1972, 62235 was sawn to produce a slab and two end-pieces (Fig. 9).   End piece ,12 and the slab ,13 were split and sub-stantially allocated (Figs.9,10).   A few splits are from the ,11 end piece.
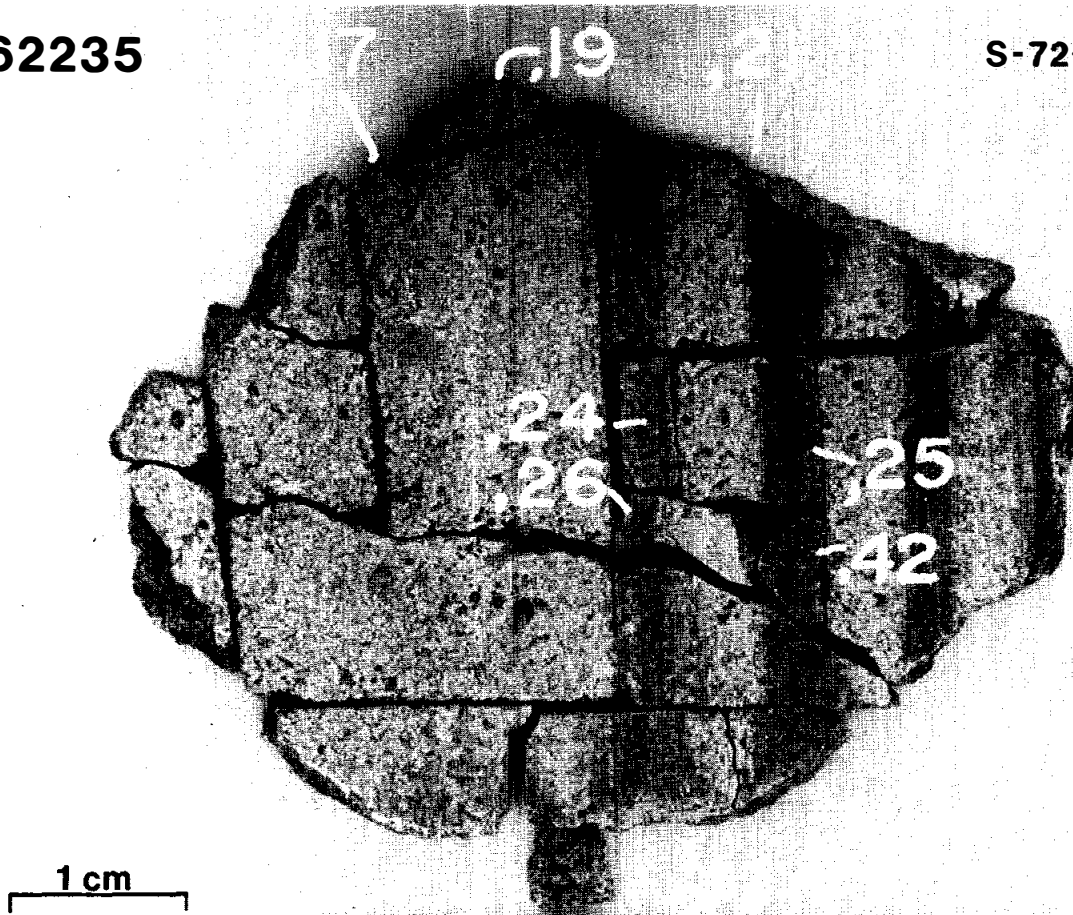


FIGURE 10.   Slab subdivision.

INTRODUCTION:   62236 is a monomict breccia, uncontaminated by meteoritic
siderophiles, and with mineral compositions indicating an affinity with ferroan
anorthosites.  These mineral compositions are similar to those in 62237 and,
like 62237, it contains more mafic minerals (10-15%) than ferroan anorthosites
sensu stricto.  The sample is very light gray, angular, and fairly coherent
but fractured (Fig. 1).

62236 was collected from the rim of Buster Crater, adjacent to 62235 and 62237,
and its orientation is known.  A few zap pits and a patina are present on all
surfaces.
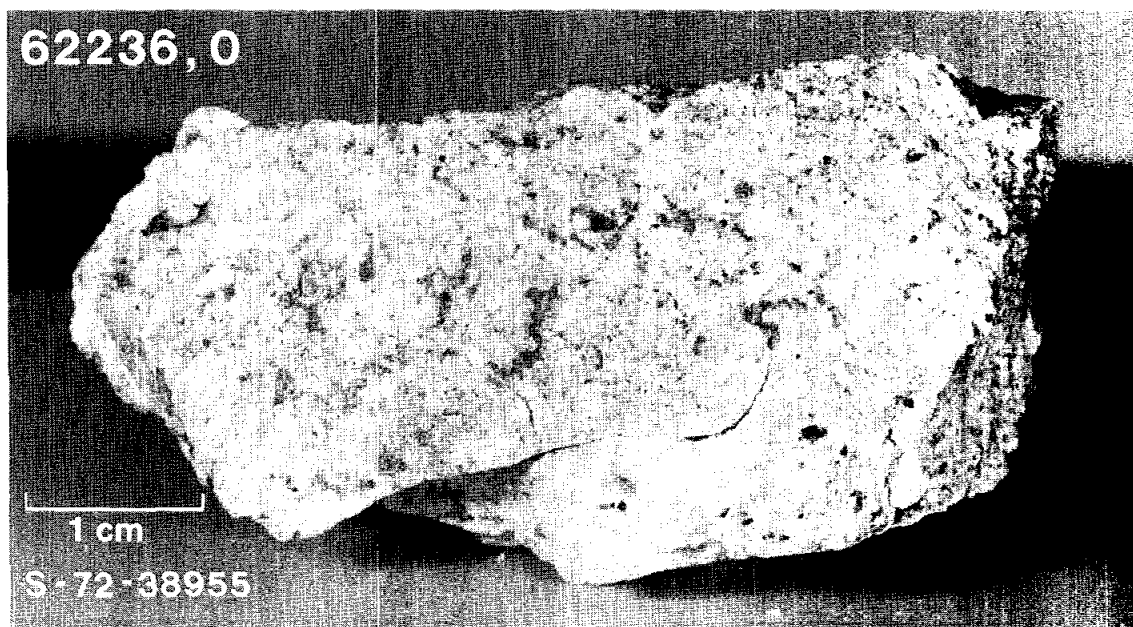


FIGURE 1.

PETROLOGY:   Warren and Wasson (1978, 1979) provide a petrographic description of
the pristine anorthosite with microprobe mineral analyses.  Takeda et al. (1979)
report microprobe data on olivines, plagioclases, and exsolved pyroxenes, with
x-ray information on the pyroxenes.

62236 is monomict and brecciated (Fig. 2).  Original plagioclase and pyroxene
grains appear to include at least some larger than 1 mm.  The mode is variable
on a small scale, but in general the sample is ∿ 85% plagioclase, and ortho-
pyroxene dominates over olivine and clinopyroxene.  (In 62237, in contrast,
olivine dominates over pyroxene.)  Cr-spinel, ilmenite (∿ 3% MgO) and troilite
are also present.  The phase compositions (Fig. 3) are homogeneous, identical
with those of 62237 and are in the field of ferroan anorthosites.  Takeda
et al. (1979) note that exsolved pyroxene is not common.  X-ray data suggest
that the orthopyroxene forms by pigeonite inversion.  The exsolved augite has
M-shaped Ca-profiles, the only ones so far reported from lunar samples.  Cool-
ing rate calculations from the exsolution lamellae suggest a depth of 6.7 km

(22 µm blebs) for the origin of 62236.

CHEMISTRY: Warren and Wasson (1978, 1979) provide major and trace (including siderophile) element abundances for the sample. Clark and Keith (1973) report K, U, Th and radionuclide abundances for the rock, derived from γ-ray spectroscopy.

62236 is extremely low in siderophile and incompatible elements indicating that it is a pristine lunar rock (Table 1, Fig. 4). Although it is more mafic than most other ferroan anorthosites, its rare-earth abundances are similar to pristine ferroan anorthosites and much lower than pristine troctolites and norites.



FIGURE 2. 62236,6. ppl. width 1.5mm.
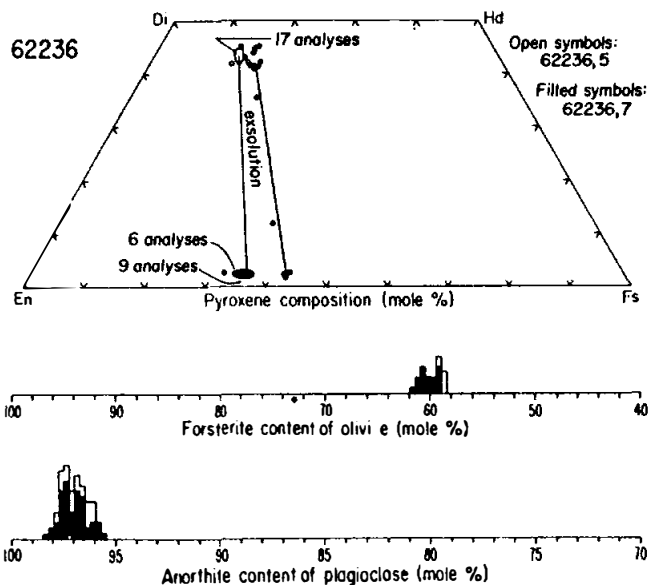


FIGURE 3a. Mineral compositions; from Warren and Wasson (1979).
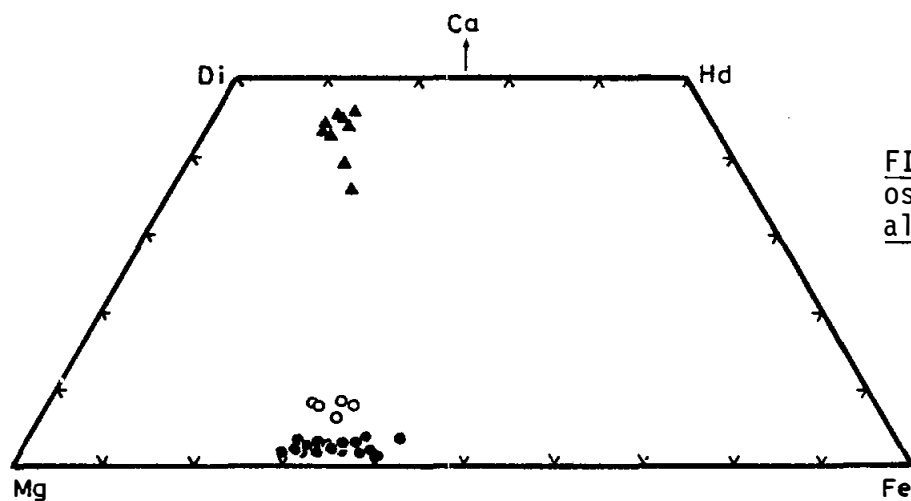
FIGURE 3b. Pyroxene comp-
ositions; from Takeda et
al. (1979).

TABLE 1    Summary chemistry of 62236

| | |
|---|---|
| SiO$_2$ | 44.2 |
| TiO$_2$ | |
| Al$_2$O$_3$ | 30.1 |
| Cr$_2$O$_3$ | 0.07 |
| FeO | 3.7 |
| MnO | 0.05 |
| MgO | 3.5 |
| CaO | 17.6 |
| Na$_2$O | 0.215 |
| K$_2$O | 0.013 |
| P$_2$O$_5$ | |
| Sr | |
| La | 0.18 |
| Lu | 0.021 |
| Rb | |
| Sc | 5.8 |
| Ni | 4.0 |
| Co | 7.9 |
| Ir ppb | <0.028 |
| Au ppb | <0.008 |
| C | |
| N | |
| S | |
| Zn | 2.0 |
| Cu | |

Oxides in wt %; others in ppm except as noted.

62236
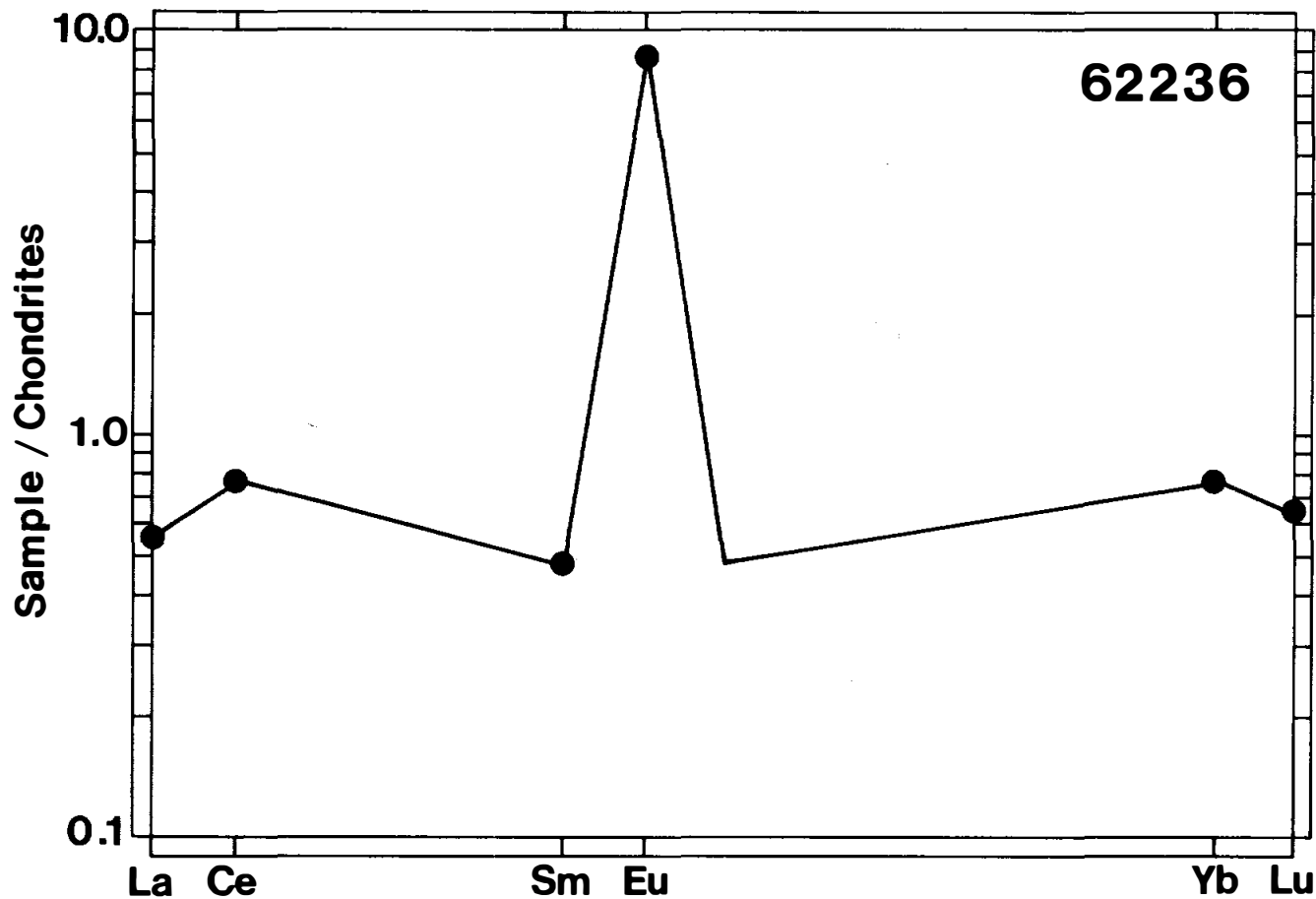


FIGURE 4. Rare earth elements; from Warren and Wasson (1979).

PROCESSING AND SUBDIVISIONS: The sample has not been sawn and only a few chips have been removed from ,0.

INTRODUCTION:   62237 is a monomict breccia, uncontaminated by meteoritic
siderophiles.   Olivine compositions indicate an affinity with ferroan anortho-
sites but like 62236 it is less feldspathic ($\sim$ 85% plagioclase).   Also like
62236, the sample is very light gray, subangular, and fairly coherent but
with several penetrative fractures (Fig. 1).

62237 was collected from the rim of Buster Crater, adjacent to 62235 and 62236
and its orientation is known.   Patina and a few zap pits occur on two faces.
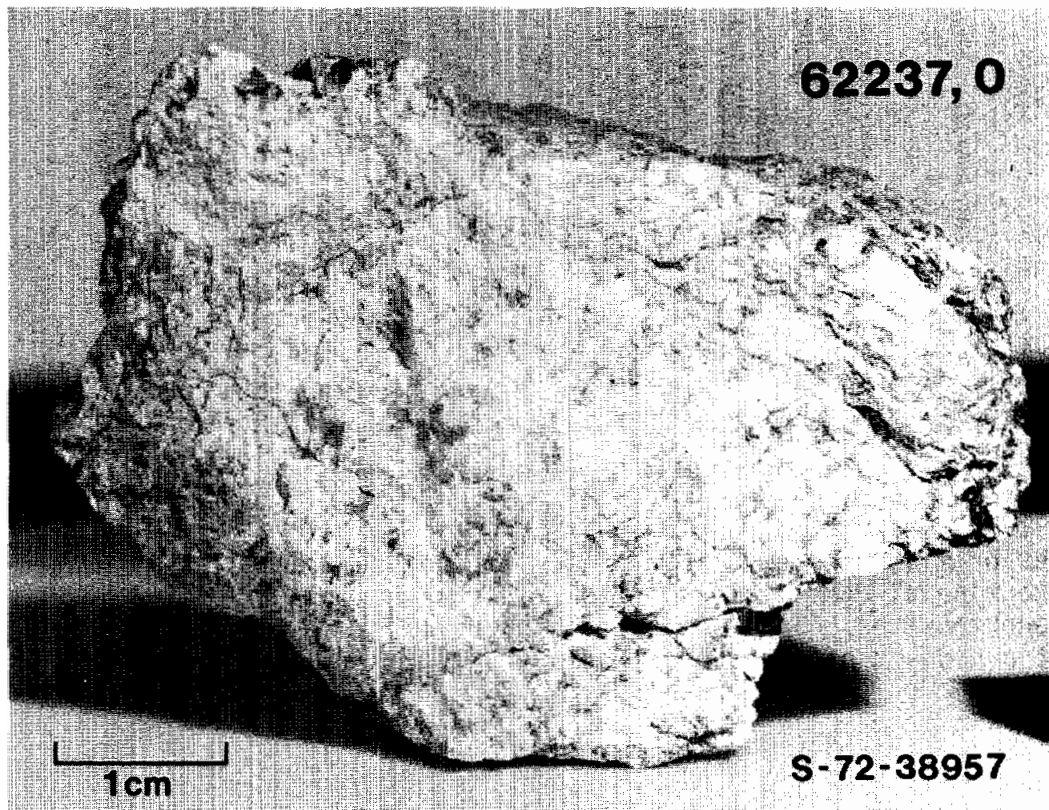


FIGURE 1.

PETROLOGY:   Petrographic descriptions with phase analyses and interpretation
are presented by Dymek et al. (1975) and Warren and Wasson (1977).   Meyer (1979)
reports minor element abundances in plagioclases (Table 1) and McKay et al.
(1978) calculate the possible range of Ti/Sm of the parent liquid.

62237 is brecciated (Fig. 2) and texturally inhomogeneous, with the original
coarse (> 1 mm) grain size locally preserved.   A mode by Dymek et al. (1975) has
83% plagioclase, 16% olivine, minor pyroxene, and small amounts of Cr-spinel,
ilmenite, and troilite; Warren and Wasson (1977) estimate 89% plagioclase and
10% olivine.   The mineral compositions reported by Dymek et al. (1975) (Fig. 3)
are confirmed by Warren and Wasson (1977).   Plagioclases and olivines have low
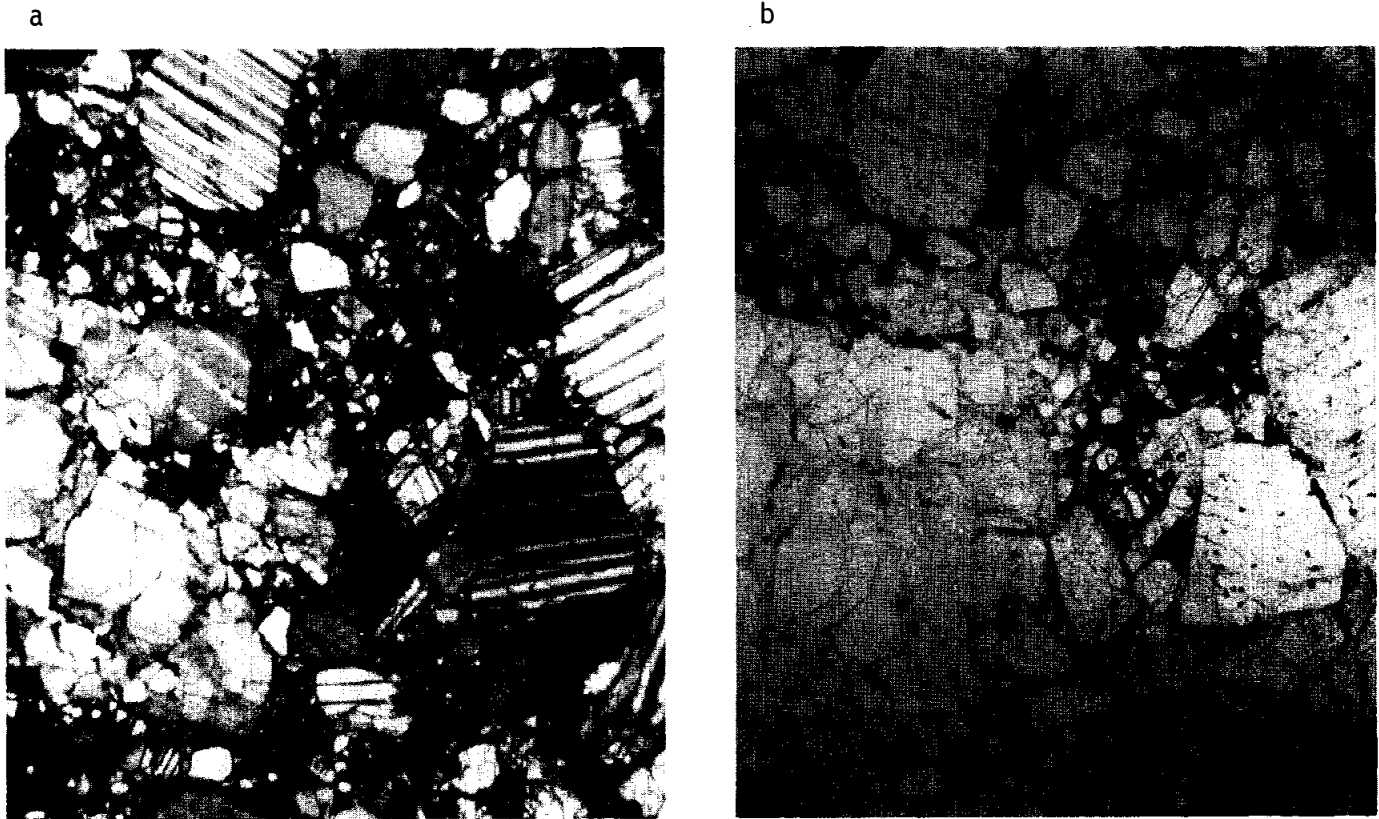
311

a

b



FIGURE 2. 62237,31. general view. width 2mm. a) xpl. b) same field, ppl.

abundances of minor elements. Pyroxenes include some complex, exsolved pigeon-
ites. The mineral compositions are similar to those in 62236 and less mafic
ferroan anorthosites. Dymek et al. (1975) stress that the olivine must be cumu-
late, not a product of a trapped liquid.

TABLE 1.

Ion probe analyses for minor elements (ppm)

in 62237 plagioclase (Meyer, 1979)

|  | Li | Mg | Ti | Sr | Ba |
|---|---|---|---|---|---|
| grain a) | 4 | 700 |  |  |  |
| grain b) | 2.7 | 370 | 75 | 203 | 10 |
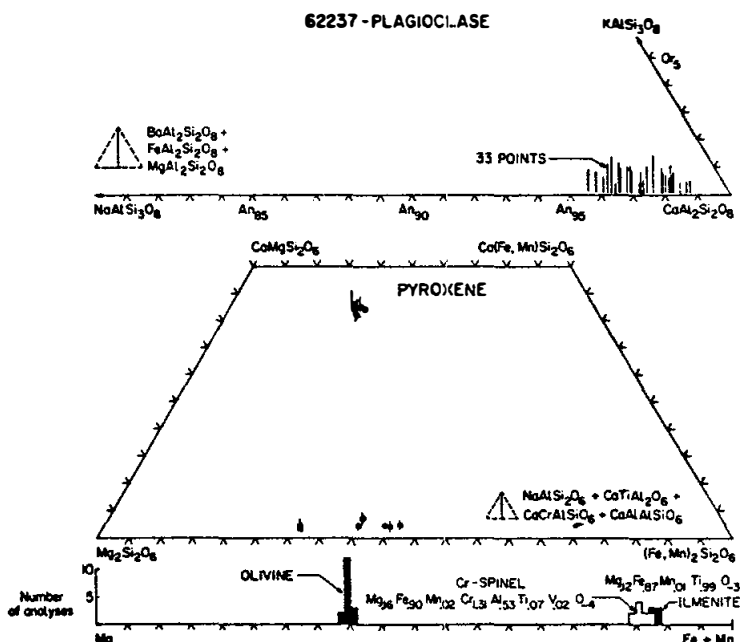
FIGURE 3. Mineral composit-
ions; from Dymek et al.(1975).

CHEMISTRY: Warren and Wasson (1978) report two analyses for major and trace (in-
cluding siderophile) elements for a split of 62237, and Dymek et al. (1975) re-
construct the chemical composition from the mode and mineral analyses. K, U,
Th and radionuclide abundance data are presented by Clark and Keith (1973) from
γ-ray spectroscopy, and Schaeffer and Schaeffer (1977) report K and Ca abundances.

The chemistry (Table 2, Fig. 4) confirms the affinity with pristine ferroan anor-
thosites. The rare-earth abundances are similar to 62236 and much lower than
pristine noritic and troctolitic rocks.

TABLE 2

Summary chemistry of 62237 (from Warren and Wasson,1978)

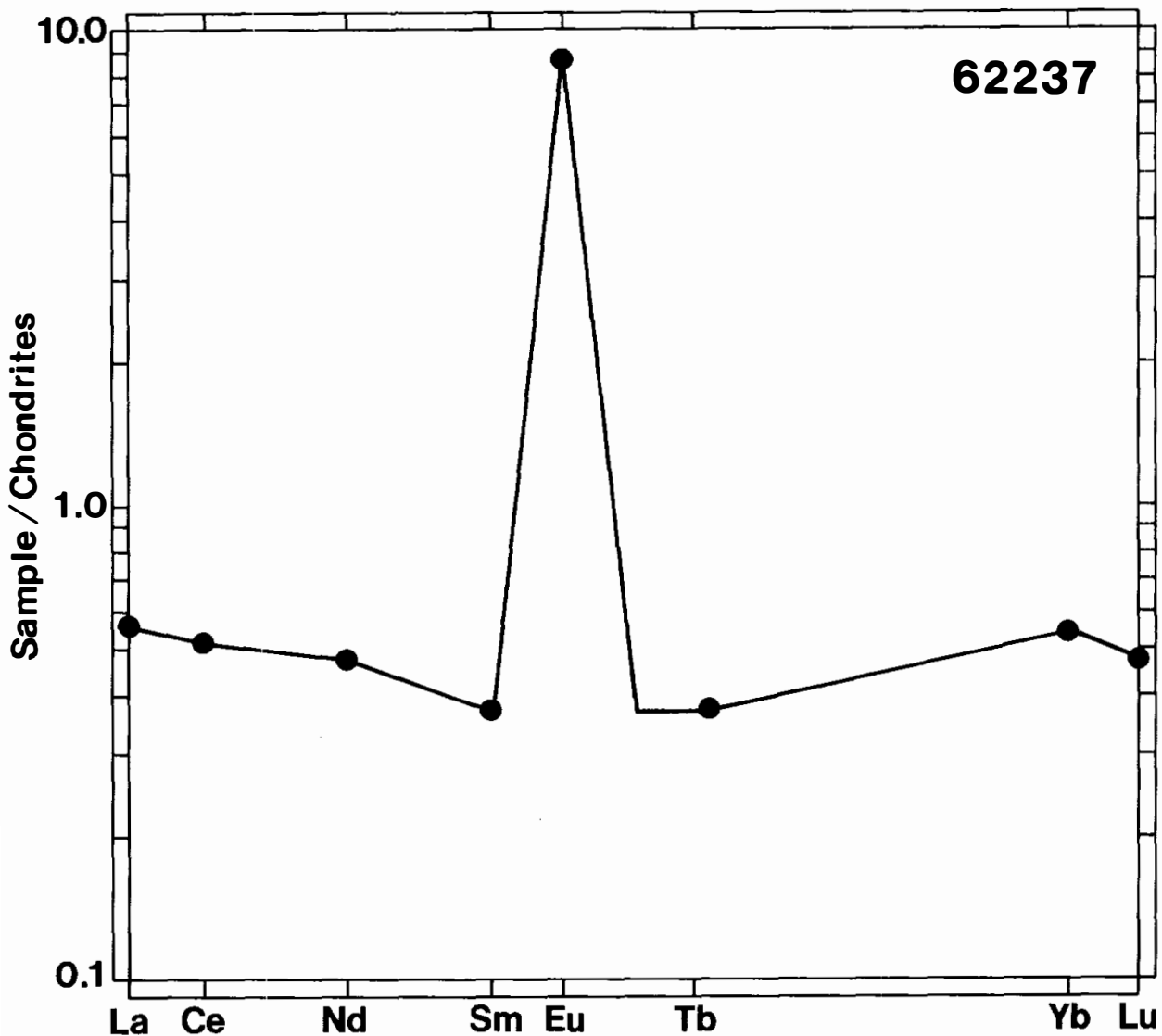| | | | | |
|---|---|---|---|---|
| $SiO_2$ | | Sr | | |
| $TiO_2$ | 0.02 ? | La | 0.19 | |
| $Al_2O_3$ | 31.1 | Lu | 0.015 | |
| $Cr_2O_3$ | 0.06 | Rb | | |
| FeO | 4.8 | Sc | 4.4 | |
| MnO | 0.05 | Ni | 5.8 | |
| MgO | 4.2 | Co | 11.1 | |
| CaO | 17.0 | Ir ppb | 0.015 ? | |
| $Na_2O$ | 0.21 | Au ppb | 0.017 | |
| $K_2O$ | 0.013 | C | | |
| $P_2O_5$ | | N | | |
| | | S | | |
| Oxides in wt%; others in ppm | | Zn | 1.6 | |
| except as noted | | Cu | | |

FIGURE 4. Rare earth elements; from Warren and Wasson (1978).

GEOCHRONOLOGY: Schaeffer and Schaeffer (1977) present Ar isotopic data. No plateau was obtained and the argon system is clearly extremely disturbed, with more than one trapped component. Individual releases give ages ranging from 2.49-5.68 b.y. with a total K-Ar "age" of 3.59 $\pm$ 0.05 b.y.

EXPOSURE AGES: Schaeffer and Schaeffer (1977) calculate $^{38}$Ar-Ca ages ranging from 24 to 2385 m.y. with an average of 32.9 m.y. The disturbed argon system makes the ages extremely unreliable.

PROCESSING AND SUBDIVISIONS: No saw cuts have been made, and most of the sample is preserved in two larger chips ,0 (37.9 g) and ,1 (8.9 g). A number of small chips in the range 0.5 - 2.0 g exist. The current thin sections are from a single potted butt ( ,4).

INTRODUCTION:  62238 is an angular, coherent, white sample (Fig. 1).  It con-
tains rare yellow minerals and is probably a cataclastic anorthosite.  It has
some adhering soil.  It was taken from a soil sample collected on the south
rim of Buster Crater, and lacks zap pits.



FIGURE 1. Smallest scale divisions in 0.5mm.

INTRODUCTION:  62245 is a coherent, medium gray, crystalline rock that is probably an impact melt (Fig. 1).  The N surface appears fresh and lacks zap pits whereas the other surfaces have patina and abundant zap pits.  This rock was taken from the soil sample from the southeast rim of Buster Crater.



FIGURE 1. Sample is about 2 cm. wide.
S-72-41308

INTRODUCTION:  62246 appears to be a coherent, white, cataclastic anorthosite coated by dark, vesicular glass (Fig. 1).  Considerable soil adheres to the glass and several white clasts are suspended in the glass.  This rock was taken from the soil sample from the southeast rim of Buster Crater.  A few zap pits are present on the glass coat.



FIGURE 1. Sample is about 3 cm. long.

S-72-41308

INTRODUCTION:  62247 is a friable, olive gray, clastic breccia (Fig. 1).  It was taken from the soil sample from the southeast rim of Buster Crater.  Zap pits are rare.
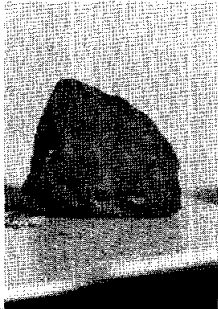


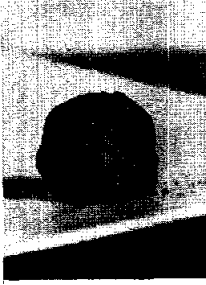FIGURE 1.  Sample is about 2 cm. wide
S-72-41308

INTRODUCTION:  62248 is a friable, olive gray, clastic breccia (Fig. 1).  A
small amount of splash glass is present on one surface.  Traces of metal or
glass spheres and granular aggregates of white material (cataclastic anorthosite ?)
are visible macroscopically.  This rock was taken from the soil sample from the
southeast rim of Buster Crater.  Zap pits are either absent or completely
covered by dust.



FIGURE 1. Sample is about 1.5 cm. wide.

S-72-41308

62255  DILITHOLOGIC (PRISTINE ANORTHOSITE AND IMPACT MELT) BRECCIA,  1239 g
PARTLY GLASS-COATED

INTRODUCTION:  62255 consists of ∿65% ferroan anorthosite and 35% dark, finely crystalline melt (Fig. 1).  Two sides are coated with black vesicular glass (Fig. 1) apparently distinct from the crystalline melt phase.  The anorthosite is chemically pristine but enriched in some volatiles.  The sample is blocky, and moderately coherent but fractured.

62255 was collected at the south rim of Buster Crater and its orientation is known.  It was apparently perched.  Patina and zap pits are present on most faces.
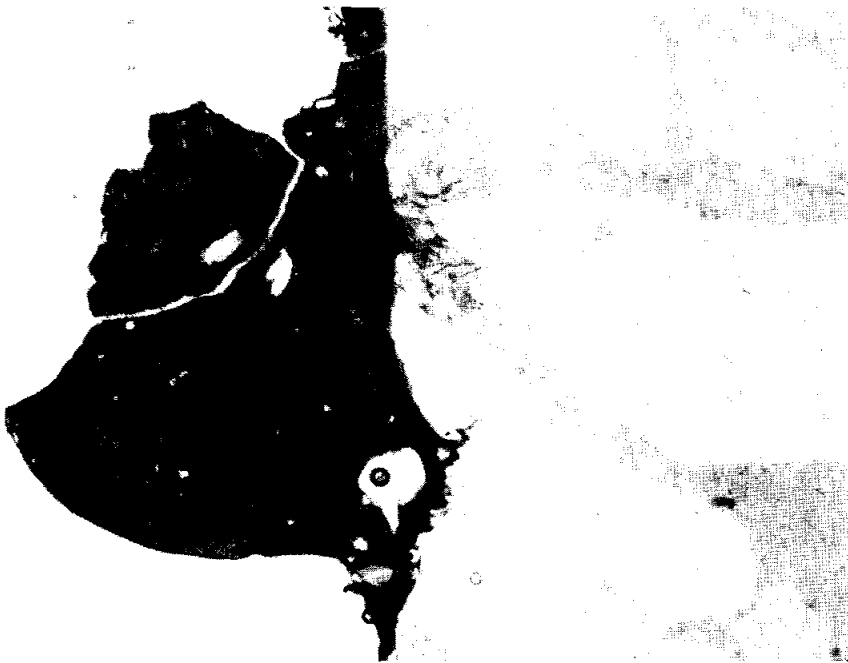


FIGURE 1a.

321

FIGURE 1b.



FIGURE 2. 62255,44. glass coat (left) and anorthosite (right), partly xpl. width 3mm.

PETROLOGY: Little petrographic work on 62255 has been published. Schaal et al. (1976) report on studies of microcraters in the anorthosite and provide some information on the anorthosite itself. Ryder and Norman (1978) provide a brief petrographic description of the anorthosite with mineral compositions and Meyer (1979) tabulates data for minor elements in plagioclase from ion microprobe studies.

The anorthosite (Fig. 2) is cataclastic and consists of plagioclase ($An_{92-97}$) with minor amounts of two pyroxenes ($En_{50-45}Wo_{4-8}$) (Ryder and Norman, 1979; Schaal et al., 1976). Low-calcium pyroxene occurs mainly as discrete grains (rarely up to 2 mm), but some plagioclases contain numerous tiny pyroxene grains. Some of the pyroxenes contain exsolution lamellae. Plagioclase grains are up to 4 mm in diameter and relict grain boundaries are visible in places. Ilmenite and troilite are rare. The minor element data for plagioclase from Meyer (1979) are presented in Table 1.

TABLE 1. Ion microprobe data for minor elements (ppm) in plagioclase (Meyer, 1979)

|  | Li | Mg | Ti | Sr | Ba |
|---|---|---|---|---|---|
| grain a) | 2.6 | 500 | | | |
| grain b) | 2.3 | 534 | 214 | 181 | 22 |

Schaal et al. (1976) note that glass in microcraters on the anorthosite consists entirely of plagioclase and even next to a pyroxene grain is not enriched in Mg, Fe, or Ca. In contrast, Brownlee et al. (1975) did note a slight enrichment of Mg and Fe in glass craters as compared with the underlying feldspar grain. This enrichment might be meteoritic.

The melt phase has a finely crystalline, "salt and pepper" texture which varies greatly. It contains 1-2% metal fragments. The contacts with the white are sharp but the relationship is unknown--the melt is not present in thin sections. The macroscopic features are consistent with the melt being a basaltic-textured impact melt.

In thin section, the glass coat (Fig. 2) is vesicular and contains anorthosite fragments and tiny metal blebs. It is brown and partly crystallized into spherulites of plagioclase. The contact with the anorthosite is generally sharp but in a few places the anorthosite is melted and in others tiny apophyses (200-300 μm) of glass intrude the anorthosite.

CHEMISTRY: All published chemical data are for the anorthosite. S.R. Taylor et al. (1974) present major and trace element analyses and Taylor and Bence (1975) diagram rare-earth abundances for the anorthosite and a plagioclase separate from it. Cripe and Moore (1974) and Moore and Lewis (1977) present S, and C and N data respectively. Hertogen et al. (1977) tabulate and discuss meteoritic siderophile and volatile element abundances. Ca and K data are presented by Jessberger et al. (1977) but the chip is described as pyroxene-rich.

The data are summarized in Table 2 and Figure 3. The siderophiles demonstrate that the ferroan anorthosite is free of meteoritic contamination but abundances of Tl (etc.) (not tabulated) demonstrate an enrichment in volatiles.

62255

| | |
|---|---|
| $SiO_2$ | 44.1 |
| $TiO_2$ | |
| $Al_2O_3$ | 35.3 |
| $Cr_2O_3$ | 0.002 |
| FeO | 0.20 |
| MnO | |
| MgO | 0.37 |
| CaO | 19.1 |
| $Na_2O$ | 0.49 |
| $K_2O$ | 0.09 |
| $P_2O_5$ | |
| Sr | |
| La | 0.46 |
| Lu | |
| Rb | 0.025 |
| Sc | |
| Ni | 1.6 |
| Co | |
| Ir  ppb | 0.016 |
| Au  ppb | 0.062 |
| C | 20 |
| N | 9 |
| S | 90 |
| Zn | 0.31 |
| Cu | <1 |

Oxides in wt%; others in ppm
except as noted.
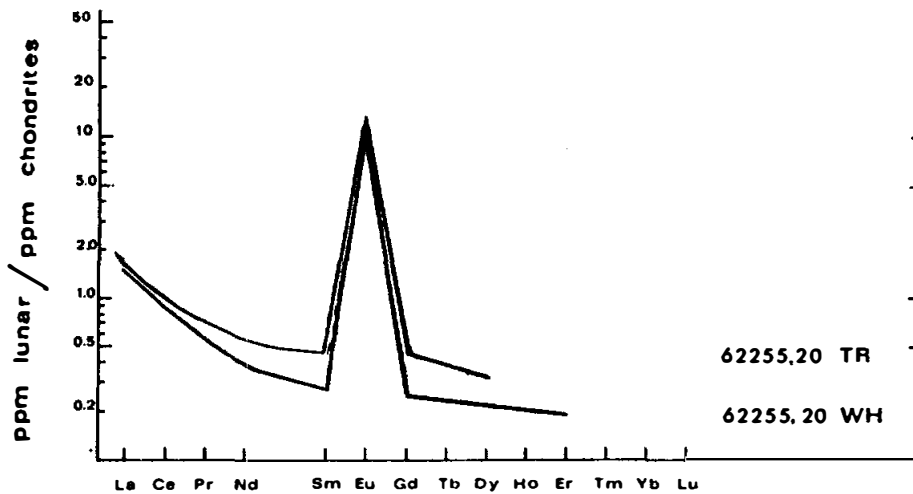


FIGURE 3. Rare earth data for 62255.  TR= whole rock anorthosite. WH=plagioclase separate from anorthosite; from Taylor and Bence (1975).

62255,20 TR

62255,20 WH

324

GEOCHRONOLOGY: Jessberger et al. (1977) found no plateau in $^{39}Ar$-$^{40}Ar$ studies and state that the sample is not datable. Thus the total K-Ar "age" of 3.66± .08 b.y. is unreliable.

RARE GASES AND EXPOSURE AGES: Jessberger et al. (1977) list an argon exposure age of 3 ± 1 m.y., Lightner and Marti (1974a) state that the exposure age is 2 m.y., and Drozd et al. (1977) quote (Marti, 1975, pers. comm.) an age of 1.9 m.y. The method for the study which gave the latter two ages is $^{81}Kr$-Kr (Marti, 1980, pers. comm.).

Lightner and Marti (1974a) present xenon isotopic data for an interior chip of anorthosite. The spallation component is small because the sample has both low incompatible element abundances and a short exposure age. As expected, no fissionogenic xenon was found. Trapped xenon is isotopically similar to terrestrial xenon but Lightner and Marti (1974a) argue that it is not terrestrial in origin. However, as discussed by Hertogen et al. (1977), contamination is possible, as Niemeyer and Leich (1976) found that terrestrial xenon could be strongly adsorbed on surfaces. Hertogen et al. (1977) suggest that the lunar volatile enrichment might somehow make the surface conducive to later xenon adsorption.

MICROCRATERS AND SURFACES: Schaal et al. (1976) report physical and chemical characteristics of microcraters on the anorthosite and Brownlee et al. (1975) report chemical data for such craters.

Padawer et al. (1974) determined the abundances of C and Fl with depth in exterior and interior chips of the anorthosite, but the abundances derived from both are considered to be contamination from Teflon packaging and other sources.

PHYSICAL PROPERTIES: Housley et al. (1976) show a FMR (ferromagnetic resonance) derivative spectrum and a corresponding absorption spectrum for an anorthosite chip. The FMR is very weak.

PROCESSING AND SUBDIVISIONS: Several large chips were taken from the sample and subdivided prior to sawing of the rock in October, 1975. The single saw-cut produced four large pieces--,0 (694 g); ,64 (53 g); ,80 (251 g); and ,81 (101 g) in addition to many smaller pieces (Fig. 4).
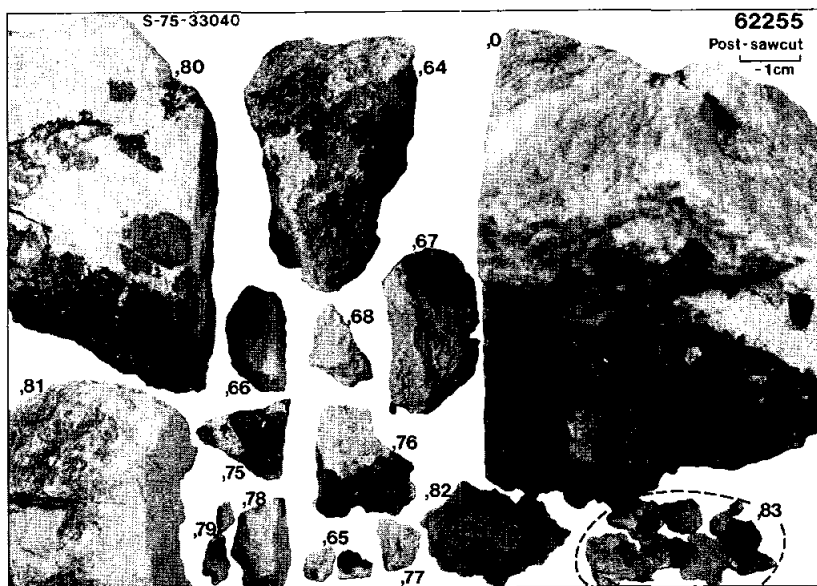


FIGURE 4. Sawn subdivisions of 62255.

325

INTRODUCTION:  62275 is a white, very friable, cataclastic anorthosite.
Mineral compositions and limited chemical data suggest that the rock is
monomict.  Macroscopically it has a chalky to sugary texture and a locally
streaked appearance.  There is no glass coat but a thin layer of patina is
present on some surfaces.  Zap pits are rare to absent on all surfaces but
the rock's friable nature is not amenable to the preservation of surface
features.  The sample was collected ∿ 25 m southeast of Buster Crater as a
single specimen but has since disintegrated (Fig. 1).  Lunar orientation
is known.
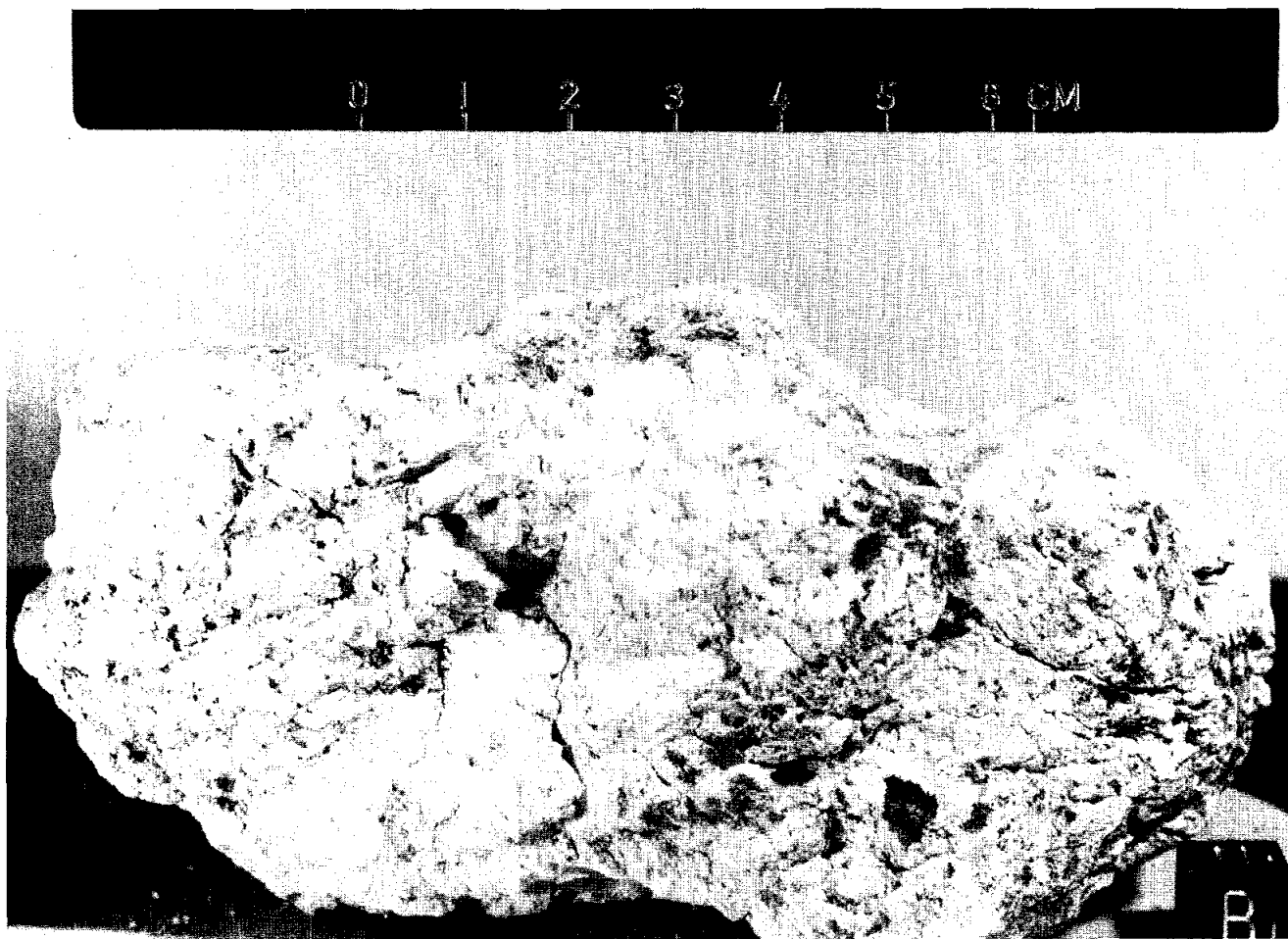


FIGURE 1. S-72-38386

PETROLOGY:  Prinz et al. (1973) and Dowty et al. (1974a) provide petrograph-
ic information.  The rock is an extremely shocked and cataclasized anorthosite
(Fig. 2).  Isolated clasts of plagioclase ($An_{97-99}$) and a brownish micro-
crystalline material (up to 2 mm long) rest in a finely comminuted anortho-
sitic matrix.  Modal data are given in Table 1.  The brownish clasts are not
simply recrystallized plagioclase but are enriched in Fe and Mg relative to
both pure plagioclase and the bulk rock (Table 2).  From the data available
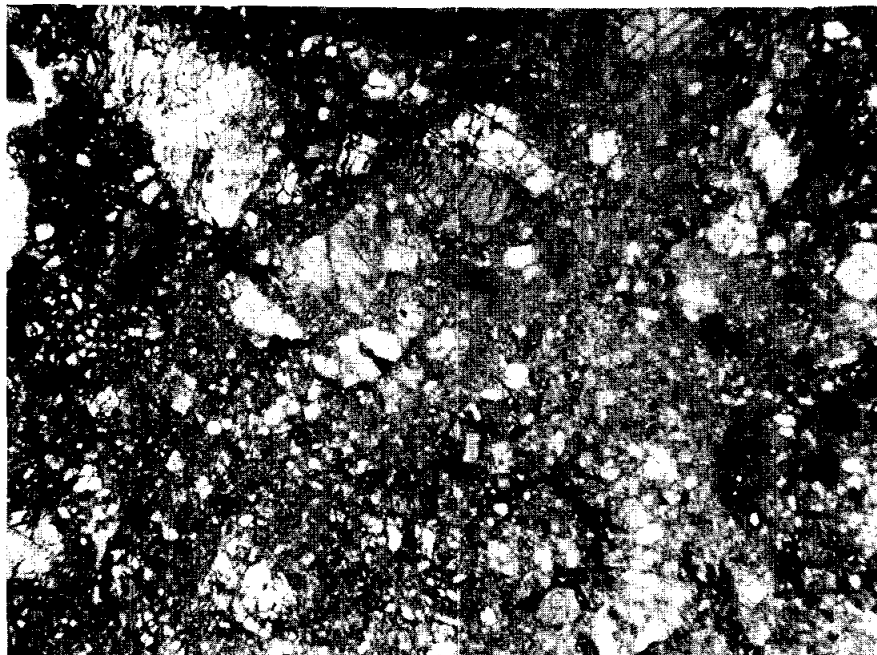it is not possible to tell if these clasts represent foreign material or

FIGURE 2. 62275,4.
general view, partly
xpl. width 3mm.

were formed more or less in situ. Mafic minerals are concentrated in highly
crushed zones. Despite extensive cataclasis, a relict cumulate texture is
discernable in some areas and a few mafic-plagioclase grain boundaries have
survived. Mineralogically 62275 is similar to known pristine anorthosites.
Mafics are ferroan and largely equilibrated (Fig. 3). The small range of
mineral compositions indicate that the rock may be monomict. Chromite-rich
spinel ($FeCr_2O_4$ $\sim$ 60 mol%), rare Fe-metal and troilite are accessory
minerals.

From the composition of the olivine-2 pyroxene-plagioclase assemblage, Herz-
berg (1979) calculates a temperature of equilibration of $\sim$ 780-980°C and a
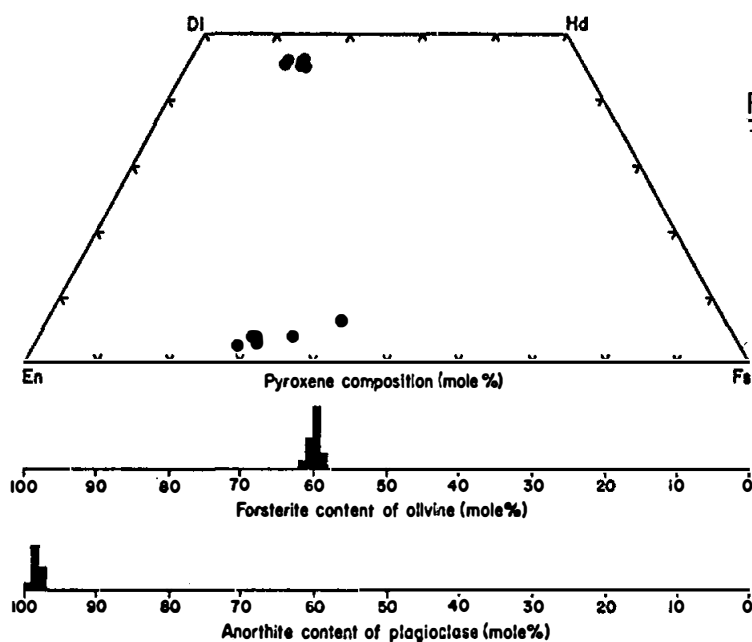pressure of equilibration of $\sim$ 1.3 - 3.2 kb.



FIGURE 3. Mineral compositions;
from R. Warner et al. (1976b).

TABLE 1  Mode of 62275 (Prinz et al., 1973)

|                                      | vol % |
|--------------------------------------|-------|
| feldspathic glass<br>and plagioclase | 93    |
| olivine                              | 6     |
| orthopyroxene                        | 1     |
| clinopyroxene                        | tr    |
| chromite                             | tr    |

TABLE 2  Summary chemistry of 62275 (DBAs from Prinz et al., 1973)

|                | Bulk Rock | Brownish clasts |
|----------------|-----------|-----------------|
| $SiO_2$        | 43.7      | 44.3            |
| $TiO_2$        | 0.04      | 0.13            |
| $Al_2O_3$      | 33.1      | 30.2            |
| $Cr_2O_3$      | 0.29      | 0.06            |
| $FeO$          | 2.20      | 3.4             |
| $MnO$          | <0.01     | 0.04            |
| $MgO$          | 1.91      | 3.1             |
| $CaO$          | 18.4      | 18.6            |
| $Na_2O$        | 0.30      | 0.34            |
| $K_2O$         | 0.06      | 0.03            |
| $P_2O_5$       |           |                 |

Oxides in wt%

CHEMISTRY:  A "bulk rock" defocussed electron beam analysis (DBA) of a thin section is presented by Prinz et al. (1973) and reproduced in Dowty et al. (1974a) and here as Table 2 with an average microprobe analysis of the brownish clasts.  The high Fe/Mg of the rock is comparable to that of other ferroan anorthosites.

Clark and Keith (1973) provide natural and cosmogenic radionuclide abundance data.  The very low K (119 ppm), Th (0.009 ppm) and U (<0.006 ppm) indicate very little, if any, contamination by KREEP.

EXPOSURE AGES:  Cosmogenic radionuclide data are reported by Clark and Keith (1973).  The rock is probably saturated in $^{26}Al$ relative to $^{22}Na$ ($^{26}Al/^{22}Na$ = 3.4)

FIGURE 4. Most of 62275,0. Largest piece is
about 5 cm. across.


PROCESSING AND SUBDIVISIONS: Although returned as one piece, from which ,1
was chipped to produce thin sections ,3 and ,4, 62275 has disintegrated into
numerous pieces and powder (Fig. 4 ).

INTRODUCTION:  62285 is a brown, extremely friable sample, most of which has disintegrated to powder (Fig. 1).  It is a loosely lithified soil clod.  It was taken from a soil sample collected about 30 m south of Buster Crater.



FIGURE 1. Smallest scale division in 0.5mm.

INTRODUCTION:  62286 is a brown, extremely friable sample, most of which has disintegrated to powder (Fig. 1).  It is a loosely lithified soil clod.  It was taken from a soil sample collected about 30 m south of Buster Crater.



FIGURE 1. Smallest scale division in 0.5mm.

INTRODUCTION: 62287 is an angular, coherent, medium dark gray fragment (Fig. 1). It contains rare, small white and black clasts, and has conchoidal fracture in places. It is probably a fine-grained or glassy impact melt. It was taken from a soil sample collected about 30 m south of Buster Crater and lacks zap pits.



FIGURE 1. Smallest scale division in 0.5mm.

INTRODUCTION:   62238 is a coherent, pale to medium gray breccia containing a variety of small light and dark clasts (Fig. 1).  The matrix is coherent and the fragment population varies from angular to rounded.  It was taken from a soil sample collected 30 m south of Buster Crater and lacks zap pits.



FIGURE 1. Smallest scale division in 0.5mm.

INTRODUCTION:  62289 is a brown, almost totally disaggregated soil clod (Fig. 1). It was taken from a soil sample collected about 30 m south of Buster Crater.
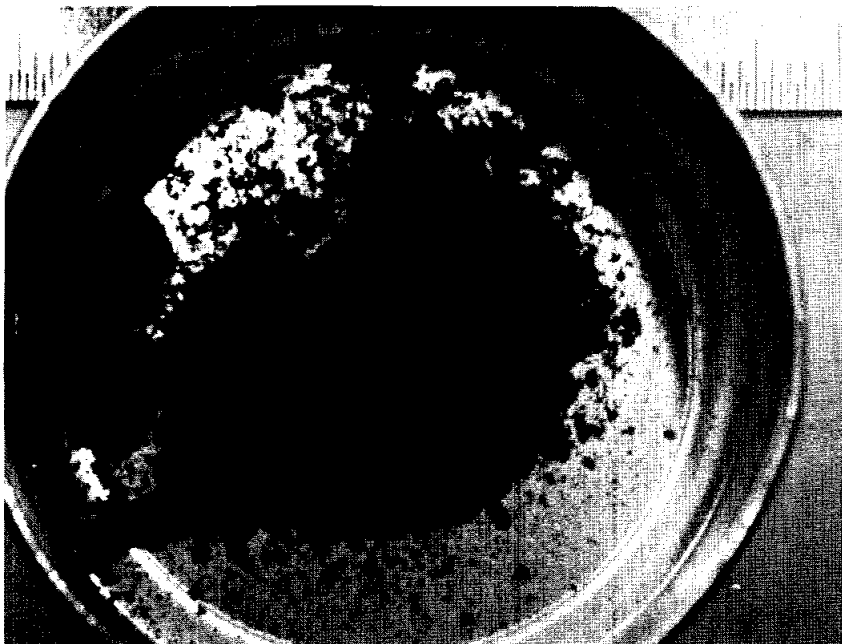


FIGURE 1. Smallest scale division in 0.5mm.

INTRODUCTION:   62295 is a mesostasis-rich, basaltic impact melt that is unique in being very magnesian and rich in olivine and spinel.  Macroscopically it is greenish-gray in color and quite tough (Fig. 1).  It was collected ∿ 35 m southwest of Buster Crater.  Zap pits are abundant on the "lunar top" surface, rare to absent on other surfaces.
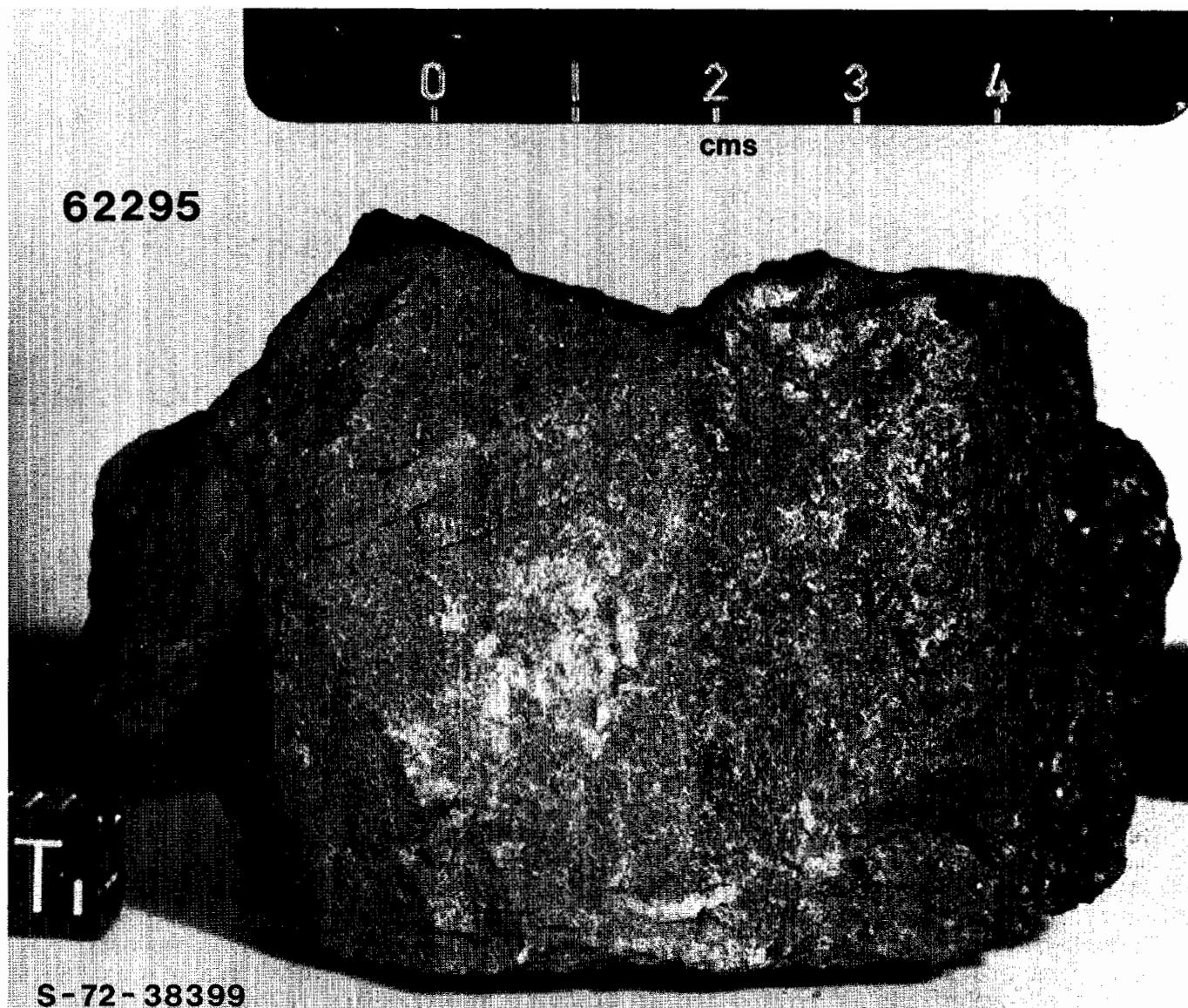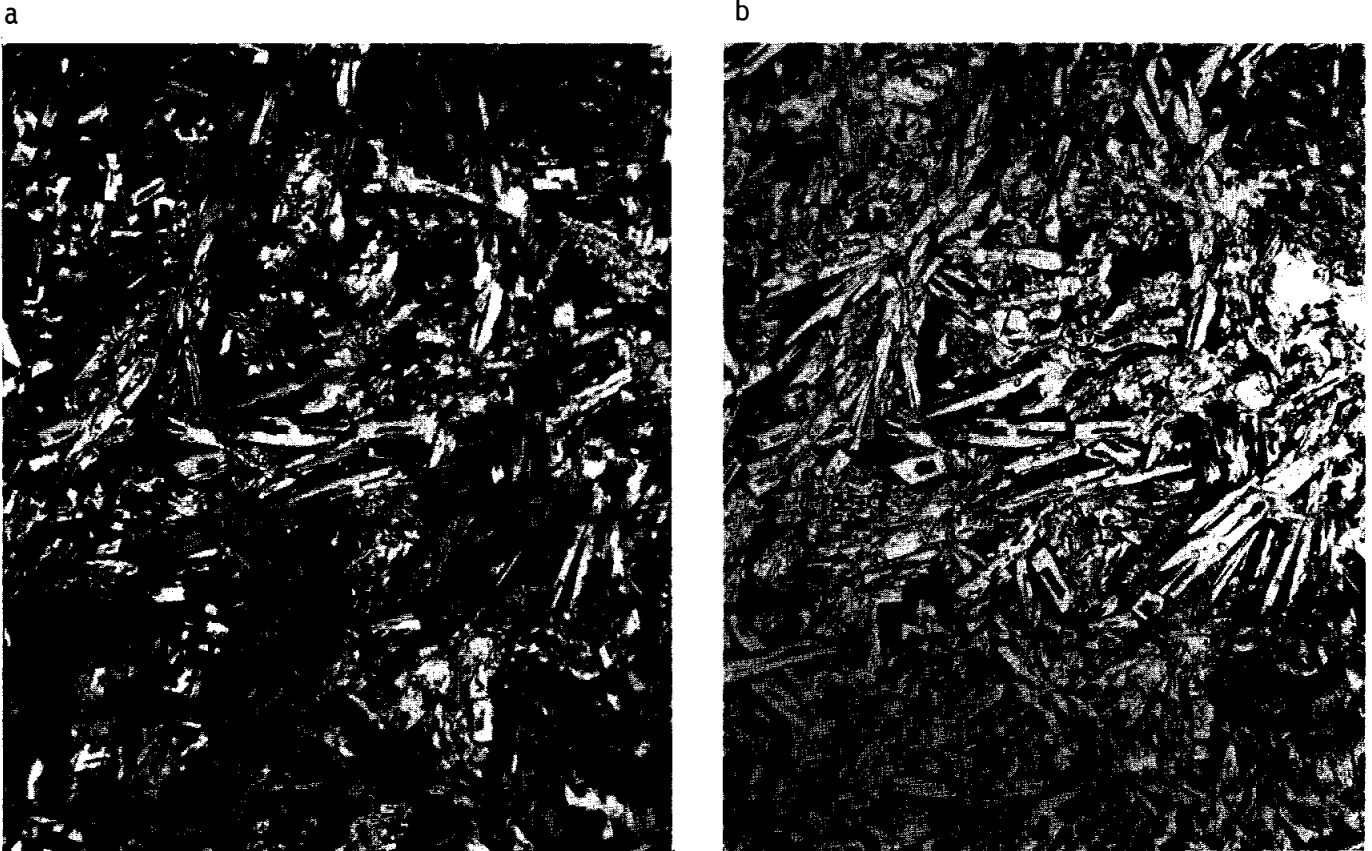


FIGURE 1.

62295



F IGURE 2.    62295,69.  general view.  width 2mm.  a )xpl.  b) ppl.


PETROLOGY:  General petrographic descriptions are given by Agrell et al. (1973),
Brown et al. (1973), Hodges and Kushiro (1973), Walker et al. (1973), Nord et al.
(1973), Weiblen and Roedder (1973), McGee et al. (1979) and Vaniman and Papike
(1981).  Steele and Smith (1975) provide data on minor elements in olivines.
Nord et al. (1973) studied mineral structures using high-voltage transmission
electron spectroscopy (HVTEM).  Misra and Taylor (1975) report metal compositions.
Melt inclusions were studied by Weiblen and Roedder (1973).

62295 is a fine-grained, mesostasis-rich basaltic impact melt with the mineral-
ogy of a spinel troctolite (Fig. 2).  It is somewhat heterogeneous on the thin
section scale, an approximate mode being 55% plagioclase, 25% olivine, 15%
mesostasis and 5% spinel.  Xenocrysts (up to 1.5 mm) of olivine ($Fo_{90-95}$),
plagioclase ($An_{94-99}$), pink spinel (9-16 mol% chromite) and metal are preserved
in a finer-grained matrix (<1 mm) characterized by a variety of quench textures.
Normally-zoned olivine ($Fo_{78-92}$) and plagioclase ($An_{90-96}$) are the principal
matrix minerals and occur as hollow, euhedral laths and skeletal grains, as vari-
olitic to graphic intergrowths and as clots with a feathery to spinifex texture.
Inclusions of a colorless to pale yellow spinel (2-4 mol% chromite) are abundant
in both matrix olivine and plagioclase.  These spinels are metastable and their
existence implies rapid cooling and crystal growth rates.  A complex, cryptocrys-
talline mesostasis of plagioclase, olivine, clinopyroxene, metal, troilite,
schreibersite and a fluor-phosphate fills interstices and hollow crystals.  The

336

pyroxenes are ferroaugites (Fig. 3) and occur only in the mesostasis. Metal shows a large range in composition (Fig. 4). Co-existing schreibersite is unusually rich in Ni (∿ 42% Ni) (see Misra and Taylor, 1975; Brown et al., 1973; Weiblen and Roedder, 1973 for other metal data).

The xenocrysts are inhomogeneously distributed through the rock and often core the radiate intergrowths mentioned above; all are mantled by fine-grained re-action rims. Several authors note that the xenocryst population is mineralogi-cally similar to the pink spinel troctolite (PST) clast in 67435. Steele and Smith (1975) find the xenocryst olivines to be poor in minor elements (except Cr) compared to matrix olivines (Table 1). Roedder and Weiblen (1977b) describe
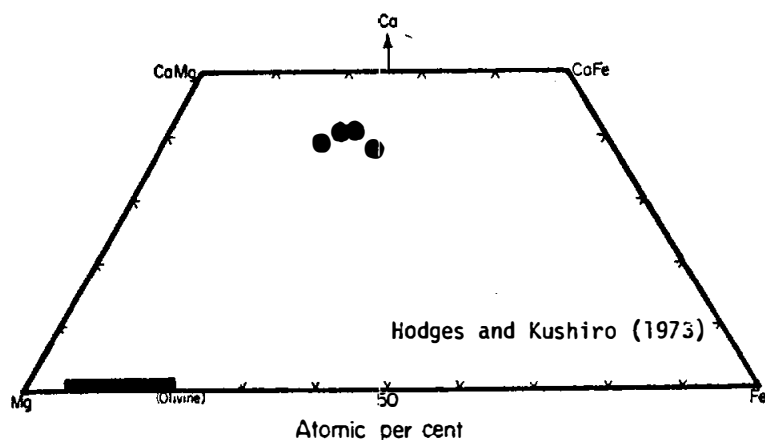


FIGURE 3a. Mafic mineral compositions.
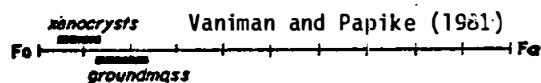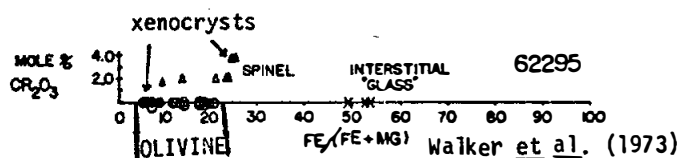
an unusual chondrule-like particle consisting of a single crystal of barred olivine with thin stringers of plagioclase and opaques separating the bars. The olivine shows reverse zoning with an intermediate area more magnesian ($Fo_{92}$) than either the core or rim (both ∿ $Fo_{88}$). The plagioclase stringers bear no crystallographic relation to the olivine and thus are not exsolution lamellae.
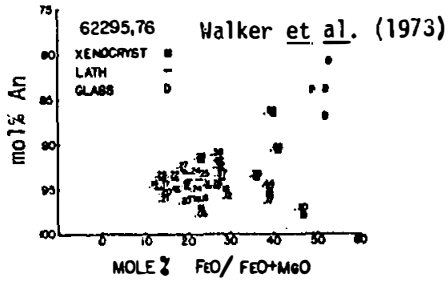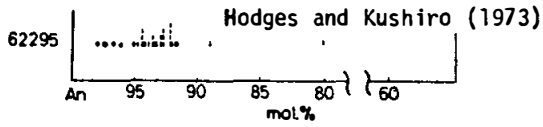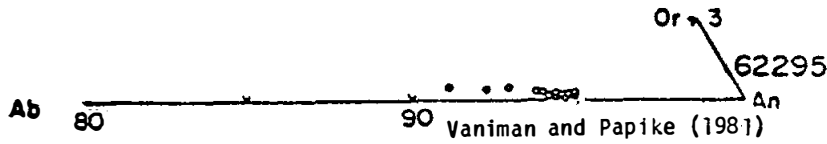
15

McGee et al. (1979)

Ab'

A

62295 | Hodges and Kushiro (1973)

An  95  90  85  80  60
mol %

62295,76  Walker et al. (1973)
XENOCRYST
LATH
GLASS

mol % An

MOLE % FeO/ FeO+MgO

FIGURE 3b. Plagioclase compositions.

Or 3

62295

Ab  80  90  An
Vaniman and Papike (1981)

TABLE 1. Minor elements in 62295 olivine (Steele and Smith, 1975)

|  | CaO | $TiO_2$ | MnO | $Al_2O_3$ | $Cr_2O_3$ |
|---|---|---|---|---|---|
| Matrix | 0.250 | 0.017 | 0.092 | 0.130 | 0.087 |
| Xenocryst | 0.060 | 0.009 | 0.045 | 0.048 | 0.124 |

Oxides in wt%

Melt
62295

Wt. % Cobolt

2.0
1.5
1.0
0.5

2  6  10  14  18
Wt. % Nickel
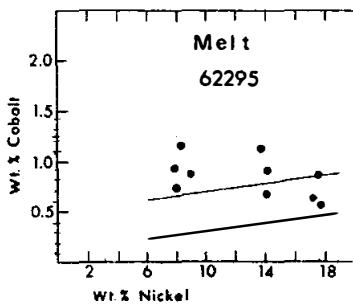
FIGURE 4. Metals; from Misra and Taylor (1975).

EXPERIMENTAL PETROLOGY:  Crystallization experiments on the 62295 composition are reported by Walker et al. (1973), Hodges and Kushiro (1973) and Ford et al. (1974).  All authors find spinel to be the liquidus phase at all pressures.  At low pressure spinel is followed by olivine, plagioclase and pyroxene with de- creasing temperature.  Below ∿ 1250°C and at low pressure, spinel reacts with the liquid to form olivine- and plagioclase.  At progressively higher pressures the spinel field expands and olivine is replaced by pyroxene.  There is no approach to multiply saturated conditions with increasing pressure (Figs. 5,6).

This crystallization sequence (spinel, olivine, plagioclase, pyroxene) is con- sistent with that predicted by low pressure phase diagrams (Fig. 7) and deter- mined by textural studies (e.g. Engelhardt, 1978).  Data from silicate melt inclusions (Weiblen and Roedder, 1973) are in basic agreement with this sequence except for apparently requiring a minor amount of a Ti-rich phase to follow olivine and preceed plagioclase (Fig. 8).

L. A. Taylor et al. (1976) performed subsolidus heating experiments on natural rock chips to observe changes in metal composition and morphology.  Their re- sults are summarized in Figure 9.
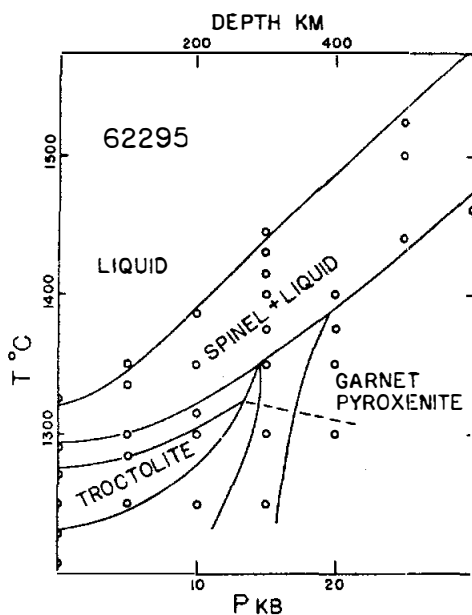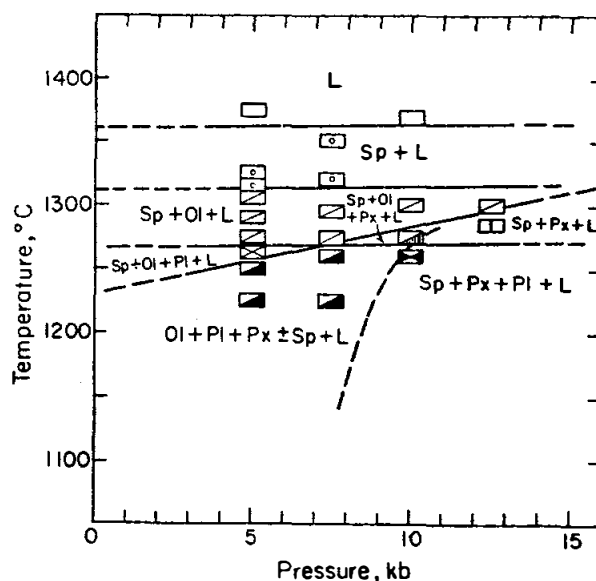


FIGURE 5. from Walker et al. (1973).
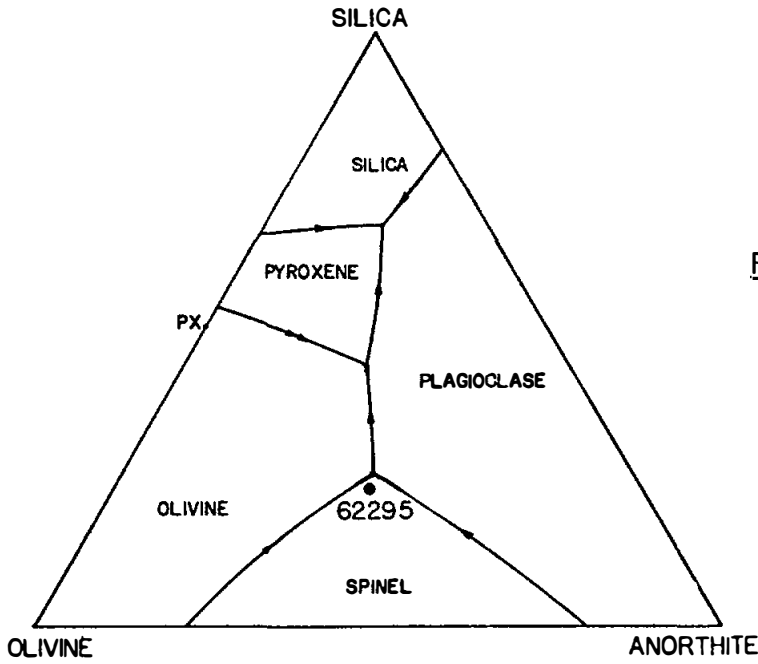


FIGURE 6. from Hodges and Kushiro (1973).

SILICA

SILICA

PYROXENE

PX

PLAGIOCLASE

OLIVINE

62295

SPINEL

OLIVINE                                    ANORTHITE

FIGURE 7. from Walker et al.(1973).
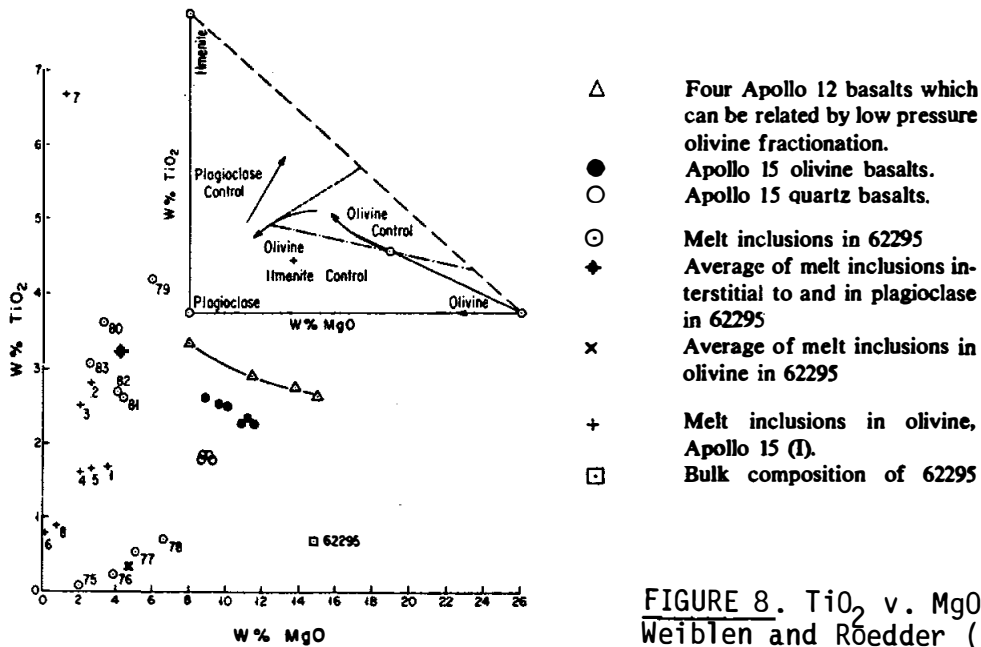


FIGURE 8. TiO$_2$ v. MgO; from Weiblen and Roedder (1973).

△   Four Apollo 12 basalts which can be related by low pressure olivine fractionation.

●   Apollo 15 olivine basalts.

○   Apollo 15 quartz basalts.

⊙   Melt inclusions in 62295

✦   Average of melt inclusions interstitial to and in plagioclase in 62295

×   Average of melt inclusions in olivine in 62295

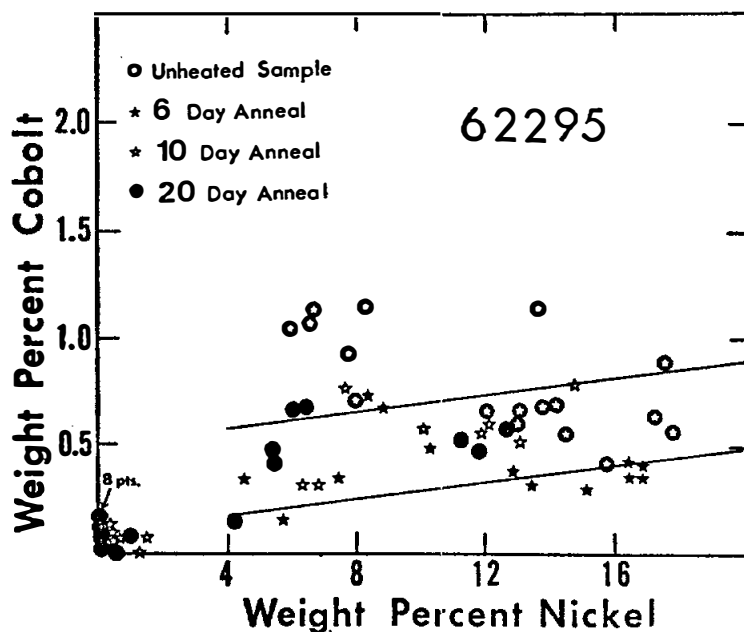+   Melt inclusions in olivine, Apollo 15 (I).

⊡   Bulk composition of 62295

FIGURE 9. from L.A. Taylor
et al.(1976).

CHEMISTRY: Major and trace element analyses are provided by Hubbard et al.
(1973), Rose et al. (1973) and Wänke et al. (1976). Krähenbühl et al. (1973)
give siderophile and volatile element data and Eldridge et al. (1973) report
natural and cosmogenic radionuclide abundances. Walker et al. (1973) present
major elements obtained by electron microprobe analyses of natural rock powder
fused to a glass. Other chemical data are found in the work of geochronologists
(referenced below).

62295 is among the most magnesian, and has one of the highest Mg/Fe (Mg/Mg+Fe
molar = 0.81), of any lunar impact melt analyzed (Table 2). Nonetheless it is
chemically distinct from the ultramafic PST clast in 67435 which contains $\sim$ 34%
MgO. Lithophile elements (Fig. 10) are slightly enriched over local soils and
are dominated by KREEP. Eldridge et al. (1973) note the low K/U ratio (770);
Th/U is typical of lunar rocks (3.9). The siderophile elements indicate a
meteoritic component (Table 2). Ganapathy et al. (1973) mention the high Ge
content (642 ppb) but do not consider it indicative of fumarolic volatiles due
to the normal volatile to involatile ratios (e.g. Tl/Cs and Tl/U) of the rock.
Hertogen et al. (1977) assign this sample to meteoritic group 1H, a group
largely restricted to Apollo 16.

STABLE ISOTOPES: Taylor and Epstein (1973) report whole rock $\delta O^{18}$ and $\delta Si^{30}$
values of +5.81 and -0.27 $^{o}/oo$ respectively.

TABLE 2. Summary chemistry of 62295

| | | | |
|---|---|---|---|
| $SiO_2$ | 45.3 | Sr | 131 |
| $TiO_2$ | 0.72 | La | 19 |
| $Al_2O_3$ | 20.5 | Lu | 0.88 |
| $Cr_2O_3$ | 0.17 | Rb | 5.2 |
| FeO | 6.2 | Sc | 10 |
| MnO | 0.09 | Ni | 285 |
| MgO | 14.7 | Co | 25 |
| CaO | 11.6 | Ir ppb | 4.3 |
| $Na_2O$ | 0.45 | Au ppb | 5.1 |
| $K_2O$ | 0.08 | C | |
| $P_2O_5$ | 0.14 | N | |
| | | S | 700 |
| Oxides in wt%, others in ppm except as noted. | | Zn | 18.9 |
| | | Cu | 14.1 |
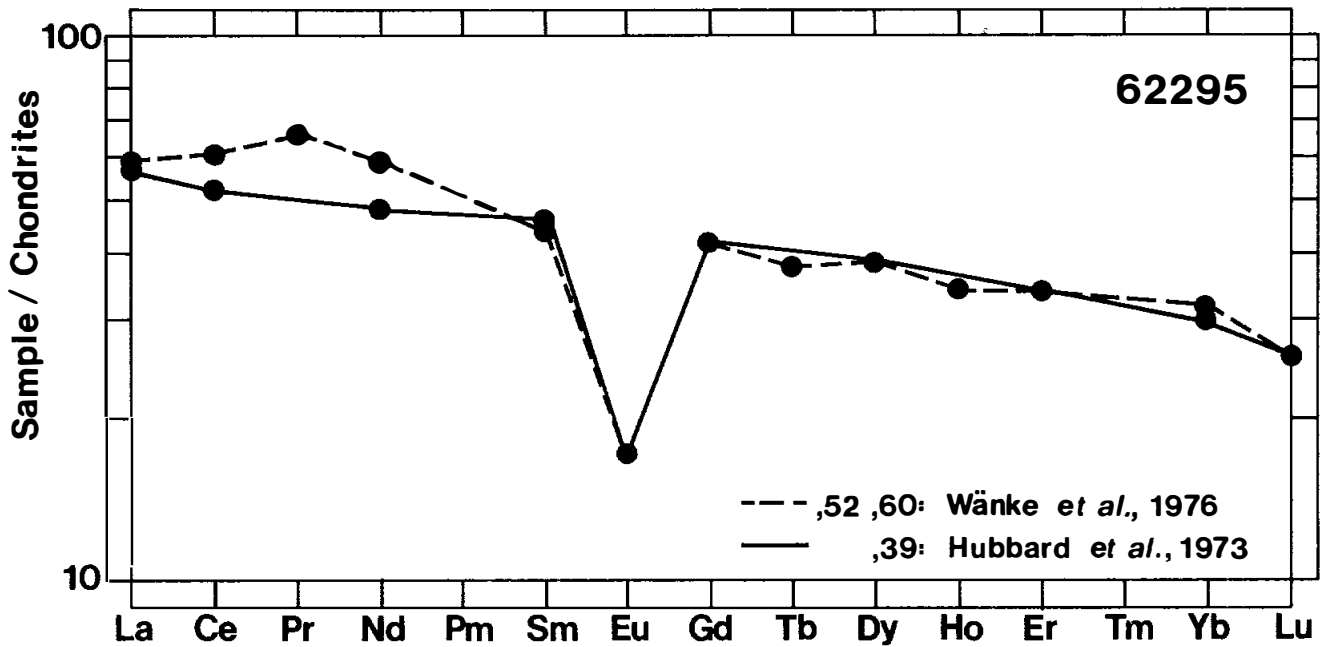


FIGURE 10. Rare earth elements.

RADIOGENIC ISOTOPES AND GEOCHRONOLOGY:   An Rb-Sr internal isochron age of 4.00 ± 0.06 b.y. with an initial $^{87}Sr/^{86}Sr$ of 0.69956 ± 6 (Fig. 11) was reported by Mark et al. (1974).  The age is interpreted as the crystallization age of the impact melt.

The isochron is not simply a mixing line because one fraction (H) falls off such a line (Fig. 11).  Mark et al. (1974) and Nyquist et al.(1973) provide whole-rock Rb-Sr data, summarized in Table 3.
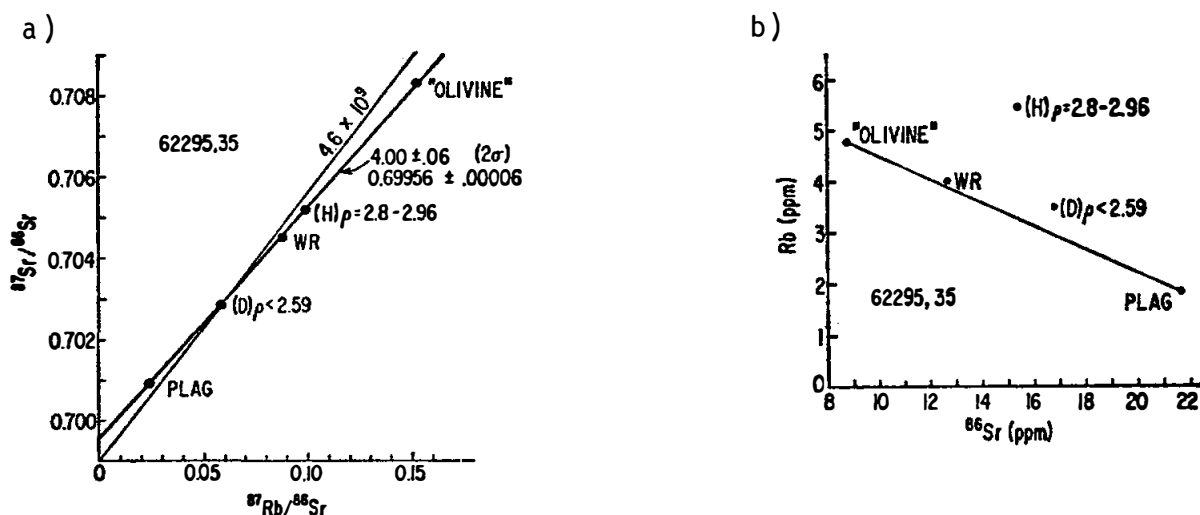
a)

b)



FIGURE 11.   Rb-Sr data.  a) isochron.  b) Rb v. $^{86}Sr$; from Mark et al.(1974).

TABLE 3  Summary of whole rock Rb-Sr data for 62295

| | $\dfrac{^{87}Rb}{^{86}Rb}$ | $^{87}Sr/^{86}Sr$ measured | $^{87}Sr/^{86}Sr$ at 4.6 b.y.* | $T_{BABI}$ (b.y.) | $T_{LUNI}$ (b.Y.) | Reference |
|---|---|---|---|---|---|---|
| 62295,34 | 0.0958 | 0.70501 | 0.69955 | 4.31 | 4.38 | Nyquist et al. (1973) |
| ,34 II | 0.0994 | 0.70519 | 0.69946 | 4.28 | 4.35 | Nyquist et al. (1973) |
| ,35 | 0.0877 | 0.70452 | 0.69956 | 4.39 | 4.46 | Mark et al. (1974) |

*corrected for interlaboratory bias by Nyquist (1977)

62295

Turner et al. (1973) could not obtain a good $^{39}Ar$-$^{40}Ar$ plateau due to equipment problems during the low temperature release, but an age of 3.89 ± 0.05 b.y. was inferred from the 900° and 1000° release data. A maximum age of 3.91 ± 0.05 b.y. was also calculated (Fig.12). The total Ar release age is 3.31 b.y.
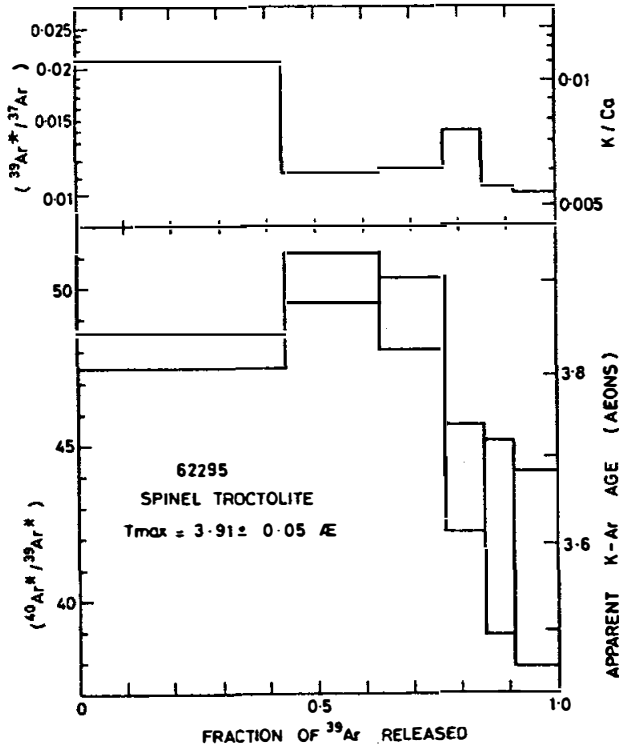
FIGURE 12. Ar release; from Turner et al. (1973).

RARE GAS/EXPOSURE HISTORY: From fossil track analyses Bhandari et al. (1973) infer that 62295 had a simple exposure history without shallow burial exposure in the regolith. A surface exposure age of 2.7 m.y. was calculated. Turner et al. (1973) report cosmogenic Ar isotope ratios and calculate an Ar exposure age of 310 m.y. Marti (1974, pers. comm., referenced in Hörz et al., 1975) determined a Kr exposure age of 235 m.y. Eldridge et al. (1973) provide short-lived cosmogenic radionuclide abundances and Lightner and Marti (1974b) report various Xe isotope concentrations.

MICROCRATERS: Morrison et al. (1973) and Neukum et al. (1973) provide size-frequency data. Microcraters occur on only one surface indicating a simple exposure history. The cratered surface is probably still in production.

PHYSICAL PROPERTIES: Magnetic and mossbauer studies by Brecher et al. (1973) indicate that 62295 contains 0.37 wt% metal, predominantly as coarse, multi-domain particles. There is also a small but significant fraction of single domain grains which are capable of carrying a relatively stable component of natural remanence (Figs. 13,14). Remanent properties of different chips scatter over an order of magnitude due to the inhomogeneous distribution of metal and the ability of the chips to acquire a viscous remanence. Cyclical heating experiments produced irreversible changes in the magnetic properties through the subsolidus reduction of $Fe^{2+}$ to produce new metal grains and the coalescence of preexisting metal grains.
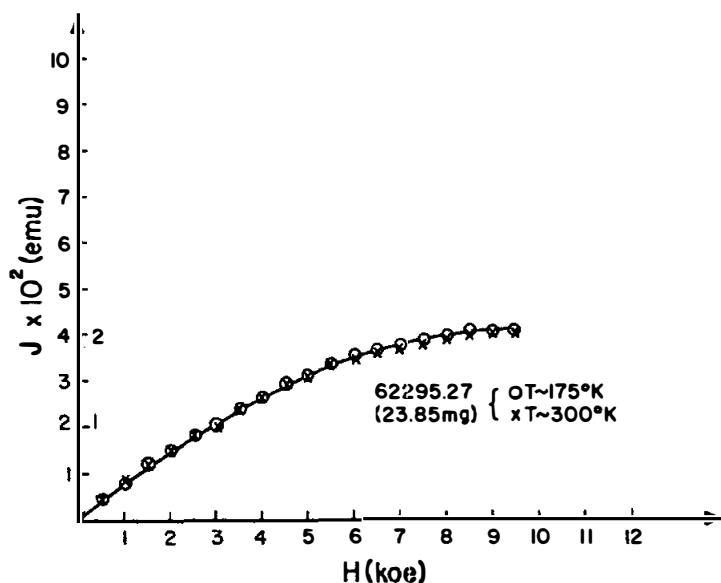
## MAGNETIZATION CURVE



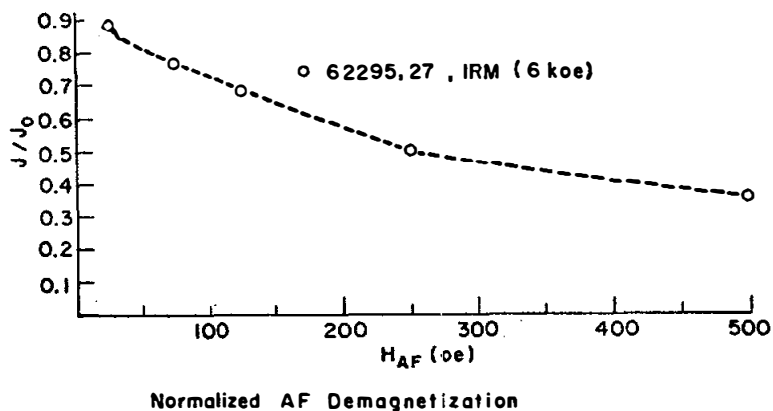FIGURE 13. Magnetic behaviour; from Brecher et al. (1973)



FIGURE 14. IRM stability; from Brecher et al. (1973).

Normalized AF Demagnetization

Todd et al. (1973) and Wang et al. (1973) report elastic property measurements under confining pressures of 1-5000 bars (Fig.15). Todd et al. (1973) also calculate and measure values of the mean volume thermal expansion coefficient over the range 25-200°C. The calculated value ($16.9°C^{-1}$) was an order of magnitude greater than the measured value ($6.8°C^{-1}$) apparently due to the presence of void space in the rock into which the minerals were able to expand.

Katsube and Collett (1973a,b) present and discuss measurements of the electrical characteristics of the rock (Fig.16).
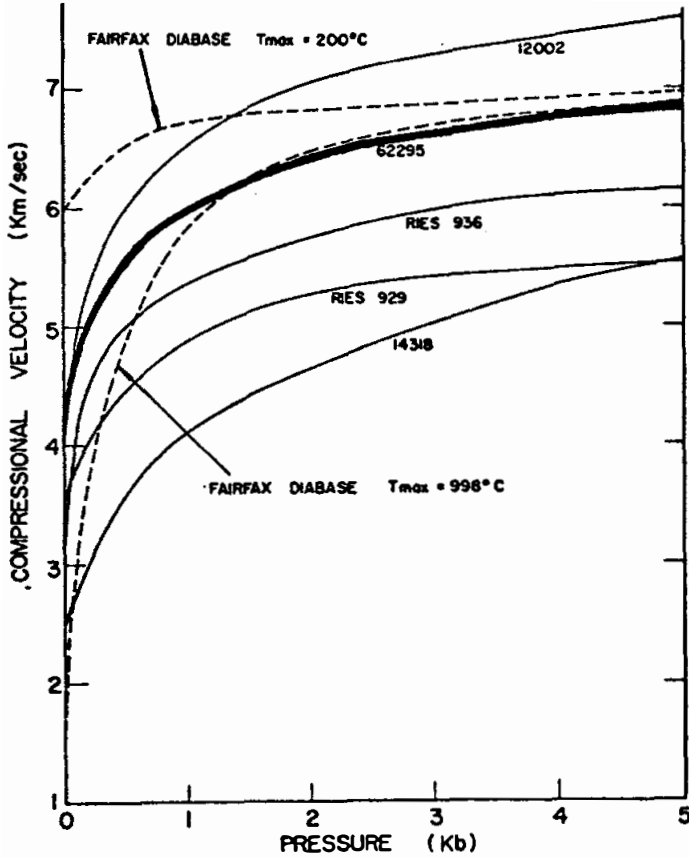
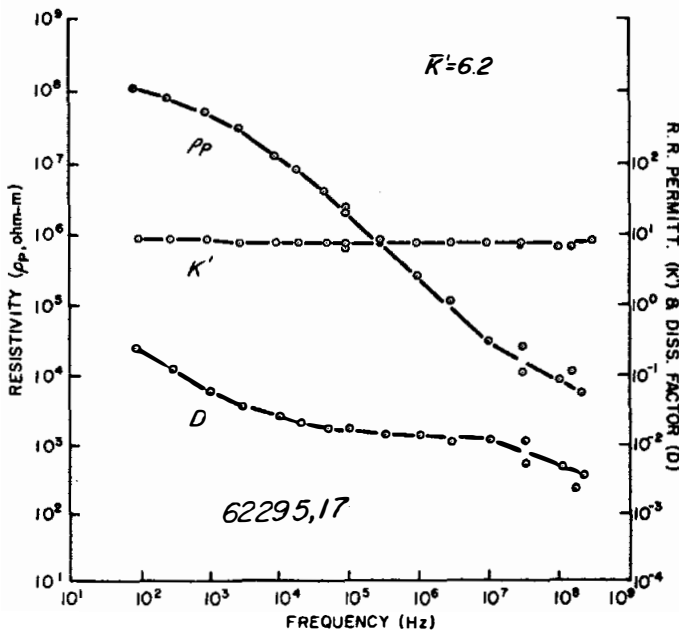FIGURE 15. Elastic properties; from Todd et al. (1973).

FIGURE 16. Electrical character-istics; from Katsube and Collett (1973a,b).

PROCESSING AND SUBDIVISIONS: In 1972, 62295 was broken along a natural fracture into three main pieces (,4 ,5 and ,6). That same year ,5 was sawn into many pieces (Fig. 17) and widely allocated. ,6 was cut into two pieces and then broken up into smaller chips for allocation and storage. In 1975 ,4 was sawn into two pieces (,4 and ,122) and the smaller of these (,122) sent to the Brooks remote storage vault. Most of the thin sections were made from ,12 (a portion of ,5) and ,45 (a portion of ,6). ,46 (a 5.41g split of ,6) was homogenized to a 100 mesh powder for 0.5g allocations to the experimental petrologists. 2.17g of this powder remains. The largest single pieces remaining today are ,4 (108.5g) at JSC and ,122 (48.1g) at Brooks.
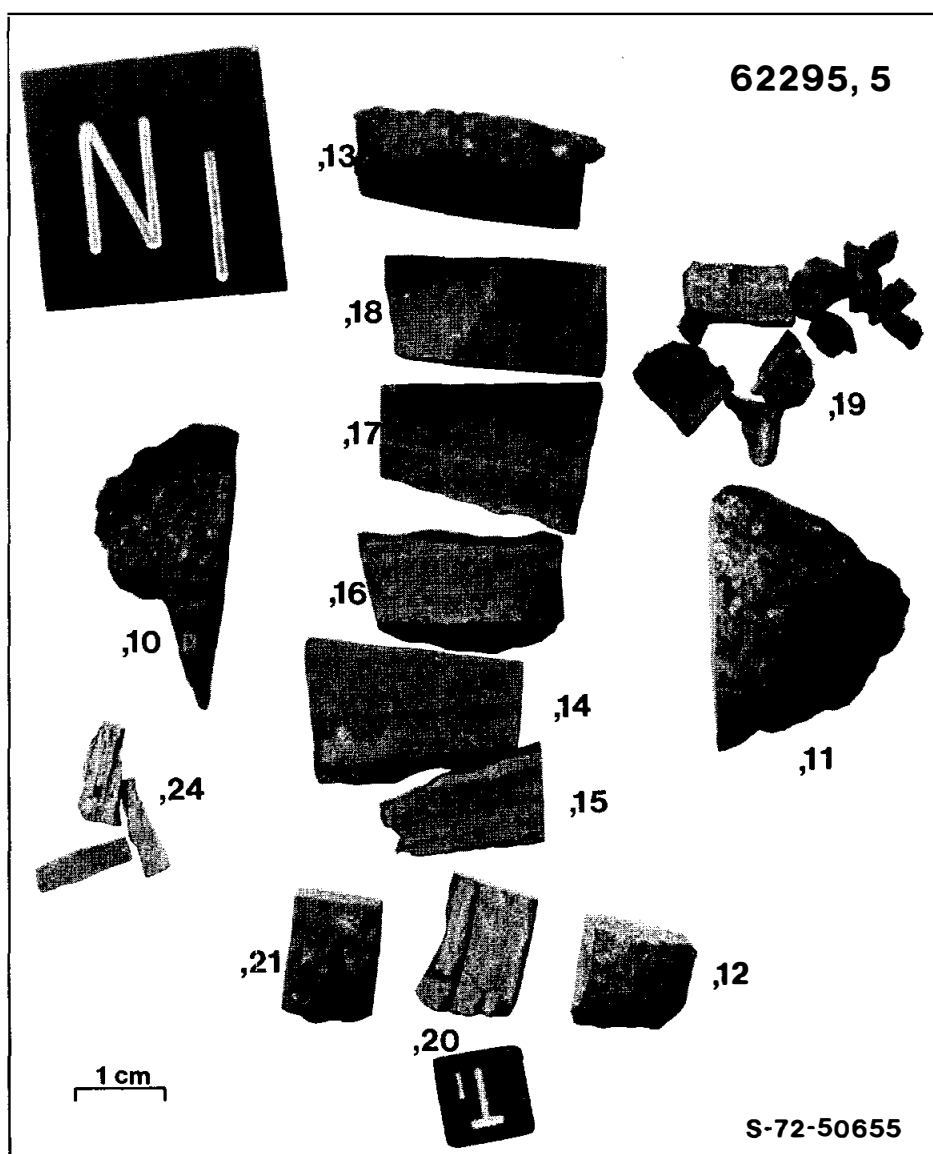


FIGURE 17. Subdivisions following sawing.

INTRODUCTION: 62305 is an extremely friable, gray breccia (Fig. 1). It contains a few small white clasts. It was taken from a soil sample collected 30 m south of Buster Crater and lacks zap pits.



FIGURE 1. Smallest scale division 0.5mm.

INTRODUCTION:  62315 is a friable, olive gray, clastic breccia (Fig. 1).  It is rounded with smooth, hummocky surfaces.  This rock was taken from the soil sample from the southeast rim of Buster Crater (62240).  Zap pits are absent.



FIGURE 1. Sample is about 1 cm. across.
S-72-41308